United States Department of Agriculture

Agricultural Research Service

Plum Island Animal Disease Center

Foreign Animal Disease Research Unit

Research Publications 2010

United States Department of Agriculture

Research, Education, and Economics
Agricultural Research Service

TABLE OF CONTENTS

North Atlantic Area • Plum Island Animal Disease Center
P.O. Box 848 • Greenport, NY 11944-0848
Voice: (631) 323-3000 • Fax: (631) 323-3006

TABLE OF CONTENTS

United States Department of Agriculture
Research, Education, and Economics
Agricultural Research Service
Foreign Animal Disease Research Unit
Plum Island Animal Disease Center
Luis L. Rodriguez, Research Leader

Foreword

"Facts are the air of scientists. Without them you can never fly."
-Linus Pauling

Foreign animal diseases such as foot-and-mouth disease, classical swine fever and African swine fever pose a major burden on the livelihoods of millions of people around the world, mostly in impoverished areas without adequate means to control them. Further, when these diseases incur into disease-free countries their economic and social impacts are immense and their control and eradication often involves the destruction of millions of animals, most of which may not even be infected. The mission of the USDA-ARS Foreign Animal Disease Research Unit (FADRU) at Plum Island is to carry out the research needed to understand the pathogenesis and the host response to foreign animal disease agents, and to translate this knowledge into useful interventions such as new diagnostic tools and vaccines for effective outbreak response, control and eradication.

This mission is accomplished by carrying out basic and applied research directed toward:

- understanding the genomic structure, viral factors determining virulence
- determining the pathogenesis and mechanism of defense and host resistance in livestock
- understanding the evolution and field epidemiology of Foreign Animal Disease (FAD) agents
- developing effective disease control strategies including novel agent detection methods, better vaccines, antiviral drugs and biotherapeutics

The collection of scientific publications presented here represents the product of FADRU scientist's research efforts over the past year (2010). This scientific knowledge is needed to develop better and more effective tools to prevent and control FAD. Other products include patents for inventions and funded research grants obtained by several FADRU researchers. Over the last year the FADRU also had a strong presence in international meetings and expert forums on FAD, vaccines and animal health. Our international presence is also strong with ongoing research collaborations with over a dozen countries including Argentina, Australia, Cameroon, India, Israel, Mexico, Pakistan, R. Georgia, Russia, Spain, South Africa, Uganda,

UK, and Vietnam. This is the result of increased effort to connect our scientific program to the rest of the world, increase our international presence, leverage our resources and increase opportunities to apply our research to provide solutions to real-world situations.

One of the most important components of the PIADC mission is technology transfer; that is, translating our research into usable technologies that are adopted by the vaccine industry, diagnostic labs and agencies responsible for disease control (e.g. APHIS). On this front, we are very proud that two of our vaccines are now under advanced development in close collaboration with Industry partners: the Ad5-FMD vaccine that is about to undergo field testing in US cattle in three states with DHS leading this effort with ARS support; and the Flag-T4 CSF vaccine starting advanced development with ARS leading and with DHS support. It is our hope that in the next 2-3 years we will have two new licensed vaccines available for the National Veterinary Stockpile for prevention and control of the two major foreign animal diseases.

As we look toward the future, I see amazing opportunities ahead. The FADRU have attained great successes in 2010 in the form of patents, scientific manuscripts, vaccines, diagnostics, training but most importantly new scientific knowledge that will help not only to protect our Country's agriculture and food security, but will also help rid the world from devastating diseases that impose a huge burden particularly to those areas most vulnerable to poverty and hunger.

2010 Research Highlights

- **The Early Pathogenesis of Foot-and-Mouth Disease in Cattle after Aerosol Inoculation: Identification of the Nasopharynx as the Primary Site of Infection.** The purpose of this study was to characterize the important steps in virus-host interaction associated with foot-and-mouth disease virus (FMDV) infection of cattle. The most important findings were that the primary sites of infection are the mucosa associated lymphoid regions of the nasopharynx (3-6 hours after inoculation) and that the lungs become infected at somewhat later times (12-24 hours after inoculation). Additionally, it was found that at still later times (24-48 hours after inoculation), FMDV enters the blood stream and causes disseminated disease. This information will guide the development of more effective countermeasures such as vaccines that can prevent primary infection and dissemination of FMDV.

- **Porcine Type I Interferon Rapidly Protects Swine against Challenge with Multiple Serotypes of Foot-and-Mouth Disease Virus.** In the event of an FMD outbreak in a disease-free country such as the US, it is necessary to induce immediate protection in order to limit or inhibit disease spread prior to induction of vaccine induced immunity. Vaccines can take up to seven days to induce protective immune responses. We have previously shown that an adenovirus vector containing the gene for type I interferon (Ad5-pIFN alpha) can protect swine from FMDV serotype A infection as early as 1 day after vaccination. In this study, we have extended our experiments to show that Ad5-pIFN alpha induces protection in swine that are challenged with two additional serotypes (O and Asia) and by contact exposure to infected animals, which is the natural route of FMDV infection. We also showed that intramuscular inoculation at 4 sites in the neck induced protection with a 10-fold lower dose as compared to intramuscular inoculation at 1 site, our previous method of inoculation. These results demonstrate the utility of interferon pretreatment of swine as an approach to rapidly protect against FMDV infection in an emergency outbreak situation.

- **Mutations in Classical Swine Fever Virus NS4B Affect Virulence in Swine. Finding virulence determinants for Classical Swine** Fever Virus (CSFV) is important not only in understanding disease mechanisms, but also in devising better vaccines. NS4B is one of the non-structural proteins of CSFV, a virus causing a severe disease in swine. Knowledge of NS4B function is very limited. We discovered a particular amino acid sequence in NS4B (called TIR) that is present in Toll-like-receptor (TLR) proteins. TLRs are host cell proteins that play a critical role in the induction of early immune response. We showed mutation of the TIR sequence in NS4B resulted in complete attenuation of CSFV in swine. This attenuated virus could be used as an experimental vaccine, protecting pigs against the challenge with virulent wild type virus. Additional results indicated that CSFV NS4B is able to down regulate the host production of important cytokines, which regulates early events of the anti-viral immune response, or chemokines, which regulate cell migration during the inflammatory process. This mechanism may facilitate the spread of the virus during the infection in swine.

- **Loss of Plasmacytoid Dendritic Cell Function Coincides with Lymphopenia and Viremia During Foot-and-Mouth Disease Virus Infection.** The pathogenesis of any infection plays a key role in designing the most effective intervention to combat th**e** disease. In the case of foot-and-mouth disease (FMD), the causative virus, FMDV, has evolved to be very contagious and induce a highly acute infection resulting in rapid onset of disease and quick resolution. This new data, and a series of studies we have already published, clearly indicate that the virus induces cellular responses that block cells from producing hormones, called cytokines. An important class of these cytokines are the interferon proteins that are so named because they interfere with viral infections. Interferons are nonspecific, antiviral hormones that induce cellular responses making the cell resistant to infection. These hormones are usually produced early in an infection and have a second role in addition to interfering with viral replication, that of initiating the activation of cells involved in the adaptive immune response. An important blood cell mediating this response, i.e. producing IFN**'**, is the plasmacytoid dendritic cell (pDC). Here we report an analysis of the function of this important population isolated from the blood of animals infected with FMDV. Infection in pigs leads to a block of the pDCs ability to produce interferon alpha. The paper discusses the critical balance between interferon induction blocking virus replication and cellular responses to viral infection that inhibit the animal's interferon response. The information is useful for further development of effective interventions for FMD.

- **Differential Gene Expression in Bovine Cells Infected with Wild Type and Leaderless Foot-and-Mouth Disease Virus. To develop strat**egies necessary to control foot-and-mouth disease (FMD), it is important to understand how the virus (FMDV) **a**nd the animal host interact. Identification of mechanisms that the host can utilize to rapidly control and contain virus replication may result in disease control approaches that are able to augment current and potential new vaccine strategies. We have developed a weakened version of FMDV, lacking an important virus protein (leader) involved in inhibition of host antiviral response. This leaderless virus is highly attenuated when inoculated into cattle or swine and remains localized and, in contrast to virulent virus, does not spread and cause disease. To gain a more comprehensive understanding of the L protein role in inhibition of the host antiviral response, we used a microarray analysis of bovine cells infected with wild type or leaderless virus. We identified 39 genes that were selectively up-regulated in leaderless vs. wild type virus infection. Most of the up-regulated genes corresponded to genes that mediate antiviral responses such as interferons, chemokines or transcription factors. Understanding the mechanism of FMDV inhibition of the host antiviral response at the molecular level should be helpful in the development of specific antiviral strategies that can rapidly inhibit or limit virus spread.

- **Spatial and Phylogenetic Analysis of Vesicular Stomatitis Virus Over-Wintering in the United States. Vesicular stomatitis is an i**mportant disease of livestock caused by an insect-transmitted virus; vesicular stomatitis virus (VSV) with t**w**o serotypes: New Jersey and Indiana. From 2004 through to 2006, 751 outbreaks caused by vesicular stomatitis virus (New Jersey serotype) (VSNJV) were reported in nine Southwestern U.S. states. Outbreaks occurred during late spring and summer and it has been hypothesized that over-wintering VSNJV strains that were introduced in 2004 from endemic areas of Mexico caused the 2005 and 2006 epidemics. Our analysis indicated that clusters of cases were centered in Colorado and Wyoming, respectively. Genetic analysis of the samples provide support to our hypothesis. This information provides a useful tool for tracing VSNJV outbreaks**.**

- **The Region between the Two Polyprotein Initiation Codons of Foot-and-Mouth Disease Virus is Critical for Virulence in Cattle.** There is limited understanding of the genetic sequences in FMDV that determine virulence. In this research, we describe the role of a region of the viral genome where viral protein synthesis is initiated (Inter AUG region). Mutant viruses containing mutations in the inter-AUG region did not cause disease in cattle or spread to their blood or other organs. In summary, changes in the inter-AUG region of FMDV result in decreased growth and attenuation in cattle. These findings can be applied to further the understanding of disease mechanisms and rational development of more effective vaccines against FMDV.

- **Effects of the Interactions of Classical Swine Fever Virus Core Protein with Proteins of the SUMOylation Pathway on Virulence in Swine.** Core is one of the four structural proteins of Classical Swine Fever Virus (CSFV), a virus causing a severe disease in swine. Knowledge of Core function is very limited. We identified two swine proteins that interact with CSFV Core during the virus infection. The sites of the Core protein which actually interact with the host proteins were also identified. CSFV harboring alteration of these Core regions resulted completely attenuated in swine. Therefore, CSFV Core protein specifically interacts with swine host protein during the cycle of virus replication and this interaction appears to be critical in the mechanism of virus virulence. These results will be useful in vaccine development against this important disease.

- **Mapping of Amino Acid Residues Responsible for Adhesion of Cell Culture-Adapted Foot-and-Mouth Disease SAT Type Viruses. In this report** novel amino acid residues within the capsid proteins of Foot-and-Mouth Disease Virus (FMDV) South African Territories (SAT) serotype 1 and SAT serotype 2 viruses were identified that affect virus host range in cell culture and plaque phenotype. We demonstrated that cell culture adaptation phenotype is acquired following repeated passages of the field strains in cell cultures. Furthermore, we illustrated that this phenotype can be transferred to an infectious copy DNA (cDNA) clone of FMDV field strains from which viable cell culture adapted viruses were recovered. This information is valuable for understanding the mechanism of FMDV adaptation to the host cell in vitro and the identification of amino acid in the outer capsid region responsible for binding to heparan sulfate psoteoglycan (HSPG).

- **Specific Detection of Rinderpest Virus by Real-Time Reverse Transcription-PCR in Preclinical and Clinical Samples of Experimentally Infected Cattle.** Rinderpest is a devastating disease of cattle that until recently caused serious economic hardship to various parts of the world, especially in Africa. Through a global vaccination effort we are at the brink of eradicating the disease from the world. It is very important to have rapid and sensitive diagnostic methods to detect any accidental or deliberate reintroduction of this disease. Here we report the development and validation in the laboratory of a highly sensitive detection test for Rinderpest virus (RPV), based on a real-time reverse transcription-PCR (RT-PCR). The test was able to detect all 16 RPV strains representing the genetic and geographic diversity of this virus. No cross-reactivity was detected with closely related viruses or viruses that cause similar disease. In samples from experimentally infected cattle, our test was able to detect the virus 2 to 4 days prior to the appearance of clinical disease. This portable and rapid real-time RT-PCR has the capability of detecting RPV before clinical disease is evident and provides differential diagnosis from look-alike diseases of cattle. As RPV is declared globally eradicated, this test provides an important rapid virus detection tool that does not require the use of infectious virus and allows the processing of a large number of samples.

Veterinary Pathology
47(1) 15-27

DOI: 10.1177/0300985809354350
http://vet.sagepub.com

Agricultural Diseases on the Move Early in the Third Millennium

J. Arzt,[1] W. R. White,[2] B. V. Thomsen,[3] and C. C. Brown[4]

Abstract

With few exceptions, the diseases that present the greatest risk to food animal production have been largely similar throughout the modern era of veterinary medicine. The current trend regarding the ever-increasing globalization of the trade of animals and animal products ensures that agricultural diseases will continue to follow legal and illegal trade patterns with increasing rapidity. Global climate changes have already had profound effects on the distribution of animal diseases, and it is an inevitable reality that continually evolving climatic parameters will further transform the ecology of numerous pathogens. In recent years, many agricultural diseases have given cause for concern regarding changes in distribution or severity. Foot-and-mouth disease, avian influenza, and African swine fever continue to cause serious problems. The expected announcement of the global eradication of rinderpest is one of the greatest successes of veterinary preventative medicine, yet the closely related disease peste des petits ruminants still spreads throughout the Middle East and Asia. The spread of novel strains of bluetongue virus across Europe is an ominous indicator that climate change is sure to influence trends in movement of agricultural diseases. Overall, veterinary practitioners and investigators are advised to not only maintain vigilance against the staple disease threats but to always be sufficiently broad-minded to expect the unexpected.

Keywords

agriculture, climate change, disease, epidemiology, globalization, trends, transboundary, foot-and-mouth disease

International animal health is a public good.

—Dr. Bernard Vallat, Director General of the OIE

Infectious diseases of animals have constrained agricultural endeavors for as long as humans have maintained animals for food, fiber, and draft. Sheep are believed to have been first domesticated in the 10th century BCE in Iraq, and in the 4th century BCE, Aristotle wrote extensively on the subject of veterinary diseases.[49] In the Old Testament, the fifth plague brought upon the pharaoh of Egypt was pestilence of cattle (most similar to rinderpest), as sandwiched between beasts and boils and contextually in the league of severity of death of first-born sons, thus clearly indicating familiarity with agricultural diseases as part of the early human experience. Changes in the distribution and severity of the effect of such diseases have surely occurred throughout the human agricultural experience and may be broadly separated as occurring owing to four main influences: environmental or ecological change, changes in movements of humans and their domesticated animals, evolution of hosts and/or pathogens, and changes in wildlife or vector distribution. These four influences upon agriculture were as relevant in prehistory as today. However, in the present era, profound environmental changes in the form of climate change and pan-societal globalization are occurring with such rapidity that the impact upon abilities to feed the world may be affected with similar severity. The discussion that follows is not an all-inclusive list of relevant agricultural diseases, nor is it a thorough treatment of any disease. Rather, it is a brief guide to the agricultural diseases that at present have indicated distributional changes that are noteworthy for potential impact on animal health, global food production, and commerce.

In the interest of presenting the most current status of changes in disease distributions, we cite selected, frequently updating public databases, as indicated. These include ProMED-mail* (from the International Society for Infectious Diseases), the WAHID† interface (from the World Organization for Animal

[1] Foreign Animal Disease Research Unit, Agricultural Research Service, Plum Island Animal Disease Center, USDA, Greenport, NY
[2] Foreign Animal Disease Diagnostic Laboratory, APHIS, Plum Island Animal Disease Center, USDA, Greenport, NY
[3] National Veterinary Services Laboratories, APHIS, USDA, Ames, IA
[4] Department of Veterinary Pathology, College of Veterinary Medicine, University of Georgia, Athens, GA

Corresponding Author:
Dr Jonathan Arzt, PO Box 848, Plum Island Animal Disease Center, Foreign Animal Disease Research Unit, Agricultural Research Service, USDA, Greenport, NY 11944
Email: jonathan.arzt@ars.usda.gov

Health, or OIE), Global Alert and Response[‡] (from the World Health Organization), and EMPRES[§] (from the Food and Agriculture Organization; FAO). Although such sources are not refereed in the manner of scientific literature, they do offer the advantage of more expedient availability of data on rapidly changing disease situations.

Foot-and-Mouth Disease

Foot-and-mouth disease (FMD) has for decades been, and continues to be, the exclusively agriculture-associated disease[‖] that poses the greatest economic threat to developed FMD-free nations. The cost of the 2001 epizootic in the United Kingdom has been estimated at $11 billion,[87] and estimated costs of an incursion in the United States have been projected at $20 billion to $60 billion.[58,63] Intense vigilance against FMD incursion is justified by this extreme expense, the ease with which the disease could be introduced (accidentally or intentionally), and the substantial difficulties associated with successful eradication. Current challenges in control of FMD are multifactorial and include the extreme contagiousness of the virus, the ability to spread over vast distances on wind-borne aerosols, the ability of the virus to infect numerous domestic and wild species, and the multiple serotypes of the virus that (at present) require distinct vaccine products. The significance of the last point is that when an outbreak is suspected, FMD virus must not just be confirmed but also serotyped and subtyped before an appropriate, type-specific vaccine can be disseminated in the field. The complexities surrounding the global control of FMD are reflected in the fact that even the most ambitious mitigation plans project programs of at least 30 years' duration.[73]

The disease itself is generally a syndrome of high morbidity and low mortality, although, rarely, some viral strains cause high mortality among certain hosts.[39] All domestic cloven-hoofed livestock are susceptible, and several studies have characterized susceptibility of American[68] and African[94] wildlife to infection.[88] FMD gets its name from the hallmark vesicular lesions most frequently occurring on the oral and pedal epithelium. Upon observation of such lesions, confirmatory diagnosis is necessary because several other conditions may manifest with indistinguishable clinical characteristics.

Although many FMD viruses have retained their established geographic ranges, there are noteworthy exceptions over recent years that serve as reminders that this disease may cause events with great surprise as well as mundane predictability.

The most significant FMD occurrence over the last decade has been the spread of the serotype O, PanAsia lineages of FMD virus across Asia and Europe.[34,48,92] The PanAsia strains have replaced previously enzootic viruses in numerous nations but have also caused incursions into several FMD-free nations, including Taiwan, the United Kingdom, Ireland, South Korea, Russia, Japan, France, and the Netherlands. The economic impact from these events has tallied well into the billions of dollars (US) from the depopulation of millions of infected and susceptible animals, trade losses, vaccine deployment, and lost tourism revenues.[47,48] Collectively, these outbreaks serve as a stark reminder of the true transboundary nature of FMD and the transcontinental impact that may occur subsequent to minimal (and initially regional) viral genomic changes. The spread of FMD virus serotype O (PanAsia) reinforces the general trend indicating that changes in distribution of FMD in enzootic regions typically follows legal and illegal movement of infected animals, whereas incursions into FMD-free regions is more commonly associated with illegal movement of animal products.[74,92]

In August–September 2007, the United Kingdom suffered another outbreak of FMD that was determined to have originated at the Pirbright laboratories for FMD research and vaccine development.[20,75] Rapid diagnosis and implementation of mitigation plans made the management of this event a great success, requiring the culling of only 1,578 animals[75] and the total cost of just £100 million.[20] Compared to the costs of other FMD outbreaks, this really was quite inexpensive. Overall, the event must serve as a reminder to FMD-free nations that regardless of the quality of biocontainment facilities, the risk of working on exotic agents within domestic terrain is never completely eliminated.

In the first 6 months of 2009, there were 122 FMD outbreaks reported to OIE.[100] These incidents span Asia, Africa, and the Middle East and include reintroduction to Taiwan, which had been FMD-free since at least 2001 (ProMED, archive 20090219.0689). FMD is also known to be enzootic or sporadically occurring in at least 9 South American nations,[82] and it is enzootic in the Republic of Turkey. These statistics clearly indicate that FMD is an agricultural disease of substantial importance that requires continued vigilant surveillance and preparedness.

Novel countermeasures to protect livestock against FMD are currently under development and over the next decade will likely improve the control and potential eradication of FMD virus.[38] Most notably, recombinant vaccine products offer several advantages over the conventional, inactivated virus preparations that are currently available. The holy grail of FMD vaccinology is a rapid-protecting, multivalent, long-duration, single-administration vaccine that allows differentiation of vaccinated and infected animals. This panacea is still many years away, however; but with the new approaches already in motion, at least such a product can be envisioned.

Avian Influenza

The attention and concern of the general public regarding the Asian-based highly pathogenic avian influenza (HPAI) H5N1 virus, causing human fatalities, transcontinental disease, and the potential emergence as a human pandemic virus, has put avian influenza at the forefront of transboundary diseases. This concern is understandable because avian influenza viruses are believed to have played a significant role in the emergence of the last three human influenza pandemics.[16,90] As Asian HPAI H5N1 virus continues to circulate within domestic poultry, there is continued human exposure and continued risk that the virus may become more readily transmissible from human

to human.[90] Between 2003 and July 2009 Asian HPAI H5N1 has resulted in 262 laboratory-confirmed human deaths, with 65% of the fatalities occurring in Indonesia and Vietnam.[37] During the first 6 months of 2009, Egypt reported 30 human cases of disease with 4 fatalities, and there have been 8 human deaths in Vietnam and China (4 each).[37] A silver lining of this awareness is that (1) the philosophy of one medicine has moved forward and (2) veterinary and public health infrastructure across the world has been strengthened, all of which has made the international community more prepared for the next disease threat—the 2009 pandemic influenza virus (H1N1), for instance.[41] However, the human health risks associated with H5N1 should not diminish the fact that HPAI is foremost a disease of poultry; as such, controlling the disease in poultry is key to preventing human disease.[16,90]

Avian influenza viruses are segmented, single-stranded, negative-sense RNA, enveloped type A influenza viruses that are further subtyped by their major surface glycoproteins, which may be any combination of the 16 hemagglutinin antigens and 9 neuraminidase antigens.[81] Aquatic birds worldwide are the reservoir hosts for influenza A viruses, and subclinical infections are especially common in the orders of Anseriformes (ducks, geese, and swans) and Charadriiformes (shore birds and gulls).[81] In poultry, the viruses are classified by the OIE as *high* or *low pathogenicity* based on intravenous inoculations of chickens; for H5 and H7 viruses, the amino acid sequence at the hemagglutinin cleavage site is a second method to evaluate the potential virulence of these viruses.[59] The majority of AI viruses from any of the H1 through H16 subtypes cause subclinical or mild disease, with a limited few H5 and H7 viruses being highly pathogenic.[85] When identified in poultry, all HPAI viruses are reportable to OIE and so termed *highly pathogenic notifiable avian influenza*.[59] All low-pathogenicity H5 and H7 subtypes, termed *low-pathogenicity notifiable avian influenza*, are also reportable, because these viruses may evolve into highly pathogenic strains if allowed to circulate in poultry.[59,85]

The number of HPAI outbreaks appears to be increasing. Thirteen of the 24 HPAI outbreaks since 1959 have occurred in the last 15 years.[15] In addition to the ongoing Asian HPAI H5N1 outbreak, there have been numerous other developments around the world. For example there was an H7N7 outbreak in England during 2008, two unrelated H7N3 outbreaks in Canada in 2004 and 2007, a H7N7 outbreak in North Korea during 2005, two unrelated H5N2 outbreaks primarily involving ostriches in South Africa during 2004 and 2006, and an H5N2 outbreak in the United States during 2004.[2,35,85,91] A notable large H7N7 outbreak during 2003 started in the Netherlands and spread to Germany and Belgium, and it resulted in the destruction of over 25 million birds.[5]

The ongoing Asian HPAI H5N1 outbreak in which hundred of millions of birds have died or been euthanized has spread across Asia, Europe, and Africa, illustrating how HPAI moves around the world regardless of political borders.[5] The virus was first identified in mainland China in 1996, then later in 1997 after causing mortality in poultry and humans in the Hong Kong Special Autonomous Region.[78,79] Between 1998 and 2002, new reassortant HPAI H5N1 viruses were identified in the region that caused clinical and subclinical disease in domestic ducks, which significantly changed the dynamics of disease transmission.[79] The rapid expansion of disease in nine countries in Southeast Asia during 2003–2004 was likely due to movement of asymptomatic domestic ducks shedding high levels of virus, in conjunction with ongoing legal and illegal movements of domestic poultry and poultry products.[79] After their initial introduction into a geographical area, these viruses were readily dispersed by live bird markets and by movement of contaminated poultry equipment, vehicles, and clothing.[85]

The following year, Asian HPAI H5N1 moved westward across Asia possibly by a different, less common route of transmission—namely, wild waterfowl. The role of wild waterfowl in the spread of Asian HPAI H5N1 is incompletely understood and controversial, but evidence suggests that wild waterfowl were involved in the spread of the virus along migratory flyways to countries in Eurasia in 2005 and in western Europe in 2006.[36] Also in 2006, Asian HPAI H5N1 was first identified in eight countries in Africa. Epidemiology and phylogenetic analysis of the African isolates suggests that there were three distinct introductions of the virus into Africa and that the viruses may have initially been introduced by wild migratory birds and then spread further by domestic poultry.[19] Meat products may have also played a role in dissemination. Recently, disease transmission via commercially processed duck purchased from grocery stores was the suspected cause of three outbreaks of Asian HPAI H5N1 in backyard chicken flocks in Germany.[40] Asian HPAI H5N1 virus has been isolated from duck meat imported into Japan and South Korea (from China); experimentally, disease transmission occurs when chickens are fed breast meat from previously inoculated chickens.[53,84,89] Through these different mechanisms, the virus has been spread to and reported by a total of 62 countries between 2003 and 2009.[99] So far, in the first half of 2009, 10 countries in Asia and Africa had identified the disease in poultry, with Egypt and Indonesia disease status listed as *endemic*.[101] During this period, isolated cases limited to wild birds have been identified in Russia, Mongolia, and Germany.[101]

Avian influenza viruses pose a major challenge because of their ability to cause disease in poultry, their inherent genetic instability and worldwide distribution, and their ability to infect many avian and mammalian species. These challenges and solutions are examined in detail in several publications, including *The Global Strategy for Prevention and Control of H5N1 Highly Pathogenic Avian Influenza*, by the Food and Agriculture Organization of the United Nations and the World Organization of Animal Health, in collaboration with the World Health Organization.[18,32,83] In well developed countries, robust biosecurity based on scientific advances and control methods has assisted in excluding the virus from commercial poultry production, and these countries also have the resources to rapidly identify and depopulate facilities should HPAI occur.[85] Current control methods have been less successful in poorly developed production systems such as those in villages and

backyards around the world.[21] Antigenic drift via point mutations and antigenic shift via genetic reassortment produce an ever-changing array of viruses, each with its own unique characteristics.[95] This genetic instability magnifies the difficulties of understanding the pathogenesis and epidemiology in each of the many susceptible species.[26]

Rift Valley Fever

Rift Valley fever (RVF) may be the most neglected of the important agricultural diseases. As a disease historically limited to Africa, it has been insufficiently addressed by the scientific communities of the developed world for decades. However, the expansion of the range of RVF beyond historical limits, into the Middle East and North and West Africa, indicates that this disease is a substantial international concern in the current era of globalization and climate change.

The RVF virus (RVFV) is a segmented, enveloped, single-stranded RNA virus in the genus *Phlebovirus*, Bunyaviridae family. Disease in ruminants appears most frequently as abortion storms or deaths of neonates. The classic primary lesion is massive hepatic necrosis owing to infection of hepatocytes; hemorrhagic syndromes and lesions of other organs are uncommon sequelae. RVF is zoonotic, and although many humans are infected asymptomatically, there are cases of severe liver disease as well as other complications, mostly vascular. Human case fatality rate with RVF is usually low, on the order of 1 to 5%, but it can be higher. Cases of the disease in humans occur when there is a high level of RVFV in the vector population, which would occur only if there are infected ruminants in the vicinity. Serologic evidence of infection exists for a range of animal species. It is likely that the virus is maintained in the vector and possibly subclinically in various hosts, only to emerge in epizootic (and/or epidemic) form after a heavy rainfall, which allows for an increase of the mosquito vector. Subsequently, infection of ruminants, which develop high viremias, would amplify within the vector populations and spill over to humans. For those unfamiliar with the disease ecology of RVF, West Nile fever provides a suitable parallel. Substitute crows for sheep and goats and the situation becomes similar.

At least 30 species of mosquitoes in eight genera can effectively carry RVFV from one mammalian species to another. Transovarial transmission occurs and the virus can remain dormant for years in eggs oviposited in dry areas. With rainfall, eggs hatch and mosquitoes can transmit the disease. Endemicity becomes thoroughly established, but episodic outbreaks of disease are decidedly sporadic, infrequent, and dependent on the increases in rainfall.

RVF was first recognized in 1930 in an outbreak among sheep on a farm near Lake Naivasha in Kenya's Rift Valley.[23] For more than 40 years thereafter, there were recurring reports of isolated outbreaks in Africa but all restricted to the geographic zone for which it is named, the Great Rift Valley, a 6,000-mile fissure in the earth's crust stretching along the eastern border of Africa.

In 1977, RVF was documented for the first time in a location outside of the Rift Valley, when the disease was diagnosed in Egypt in an extensive outbreak involving thousands of human and animal cases.[54] How it traveled across the Sahara to become established in the Nile Delta is uncertain, but most likely it was due to animal movement from Sudan.[1] However, the Aswan Dam was built in the years before this outbreak to allow for controlled flooding of agricultural lands, and this resulted in an increase in the mosquito population, which proved to be an important facilitating factor in the disease outbreak. Ten years later, an outbreak of RVF occurred again outside the Rift Valley, this time in Mauritania, in West Africa. Here, factors pointed to construction of the Diama Dam on the Senegal River.[25] These two human endeavors of dam building, creating increased water availability for vector expansion, were followed decades later by climatic events with the same result. Excessive rainfall, largely brought about by El Niño–Southern Oscillation effect, engendered moist, mosquito-enhancing conditions that contributed to outbreaks in East Africa in 1997–1998 and again in 2006–2007.[8] RVF was recognized for the first time outside of Africa in 2000, when reports surfaced almost simultaneously from the Kingdom of Saudi Arabia and from Yemen.[51,57] In this Arabian Peninsula outbreak, the human case fatality rate was an alarming 14%. The source of the virus, as determined from genetic analysis of causative strains, was most likely animals transported across the Red Sea from the Horn of Africa.[77] Annually, the religious festivals in the Arabian Peninsula utilize 7 to 10 million live animals for sacrifice, a number supplied primarily by East Africa, creating concerns for recurring transmission of RVFV[24] as well as other agricultural diseases.[¶] The greatest threat from RVF is that animal movements and changes in virus–vector–host dynamics will facilitate extension of the disease's range into Europe and beyond, with calamitous veterinary and human public health consequences. As has already occurred with bluetongue virus (BTV) vectors, evolving climatic conditions may allow expansion of the ranges of historical RVFV vectors and so promote the development of competence of new vectors in new regions.[52]

RVF could serve as the poster child to represent (1) disease threats associated with climate change and globalization and (2) benefits achievable through the one-medicine philosophy. Long neglected by the human and veterinary medical communities, the disease is now on the move through animal trade and in facilitated transmission mode owing to climatic changes. In many of the documented outbreaks, humans have been the sentinels of infection; that is, activity of the virus is first noted as a result of clinically ill humans presenting at medical facilities, even though the disease in animals always precedes that in humans.[10,25] This scenario is a clear indication of the potential advantages from the enhancement of veterinary infrastructure and disease surveillance in developing regions. Without amplification in agricultural animals, the disease in humans does not occur, because only ruminants have a sufficiently high viremia to infect enough mosquito vectors for extensive transmission. The limited capacity for diagnosis in the animal sector in many

of the regions in which RVF occurs contributes to lack of an early warning system for public health. However, even when the disease has been documented in animal populations and in humans, invariably the literature that follows the outbreak is unequivocally stovepiped, with rare articles addressing the outbreak in true ecologic and one-health fashion.

Countermeasures for RVF exist, but none are adequate. Once a herd or flock of ruminants experiences disease, the virus is readily amplified and spreads extensively through mosquito vectors. Controlling an outbreak in animals requires rapid depopulation and stringent insect control. Various vaccine formulations are available for livestock, but each has benefits and deficits, and none are approved for use in North America or Europe. For humans, a formalin-inactivated vaccine, TSI-GSD-200, has been used extensively to protect laboratory workers and has excellent safety and efficacy.[66]

The RVFV is classified between the Centers for Disease Control and Prevention and the US Department of Agriculture as a category A overlap select agent.[14] This means that any work with the agent has to be closely regulated and monitored, thereby making investigative work challenging. However, the designation may be warranted, given that intentional introduction into a geographic area that has ruminants and a competent mosquito vector could lead to establishment of the disease with immediate and long-term agricultural and public health concerns. Overall, RVF is a disease for which sustained global investment in improved surveillance, diagnostics, and countermeasures is well justified. Although RVF is still largely a disease of developing regions, developed nations should recognize the importance of investing in preparedness against this potentially catastrophic zoonotic disease.

African Swine Fever

African swine fever (ASF) and classical swine fever (CSF) have historically been the two most important transboundary diseases of pigs. Although CSF is a more important disease globally, ASF is treated in greater detail in this review owing to the first-ever incursion into the Caucasus region[#] of Central Asia in May 2007 and subsequent westward progression.

ASF was first documented in Kenya in 1921 as a cause of a high-mortality disease syndrome among populations of domestic pigs that had been exposed to wild suids;[56] the disease was subsequently recognized as enzootic in wild and domestic pigs in most countries of sub-Saharan Africa. ASF virus (ASFV) is the only known DNA arbovirus, and it is the sole member of the genus *Asfivirus*, Asfarviridae family. Domestic pigs and wild suids are the only species naturally infected with ASFV. ASF is a serious threat to domestic pig populations worldwide because of its high morbidity and mortality, high viral loads shed into all secretions (therefore contagious and infectious), extreme environmental resistance of the virus, and lack of any commercial or experimental vaccine. In addition, ASF is an important transboundary animal disease given the presence of globally distributed argasid tick vectors of the *Ornithodoros* genus and sizable naïve domestic and wild pig populations in most countries.

There are three distinct ASFV transmission cycles: an ancient and recurring sylvatic cycle involving *Ornithodoros* ticks and wild suids, including warthogs (*Phacochoerus* spp) and bushpigs (*Potamochoerus* spp); an *Ornithodoros* tick and domestic pig cycle; and a highly contagious domestic pig cycle with direct horizontal transmission. Warthogs have low blood and tissue titers and are rarely contagious to domestic pigs, but they are important in maintaining the sylvatic cycle. However, *Ornithodoros* ticks amplify and transmit the virus to wild or domestic pigs and remain infectious for years through transstadial, transovarial, and sexual transmission.

The most common route of incursion of ASFV into previously free countries or regions is through feeding uncooked or partially cooked contaminated pork products. ASFV remains infectious for 3 to 6 months in uncooked products, such as sausage, chorizo, and dry hams.[45] Once introduced, the virus is usually maintained horizontally by direct or indirect contact through infectious excretions and secretions. However, the virus may also enter the tick–domestic pig or sylvatic cycles if competent vectors are present. For example, in the 1960s during the Spanish epizootic, 50 to 55% of the ASF outbreaks were allegedly caused by *O erraticus* ticks.[30]

ASF attracted international attention when it left Africa for the first time in 1957, appearing in Lisbon, Portugal, causing nearly 100% mortality.[69] The disease persisted in Portugal and Spain until 1995, when it was finally eradicated at great effort and expense. This arrival of ASFV into Europe stimulated considerable research, including unsuccessful attempts to develop a vaccine and the discovery that *Ornithodoros* ticks maintained the virus for long periods and were capable vectors of the disease.[65] Attempts to vaccinate with an attenuated vaccine probably led to emergence of low-virulence strains and corresponding subacute and chronic forms of the disease that have higher survival rates.

ASF again left Africa to infect pigs in Malta, Sardinia (Italy), Brazil, and the Dominican Republic in 1978; in Haiti in 1979; and in Cuba in 1980. ASF has since been eradicated from these countries and has remained enzootic only in sub-Saharan Africa and Sardinia. In Malta, the entire population of 80,000 pigs died or were slaughtered within 12 months of diagnosis; this was the first time that any country had slaughtered all members of a species of domestic animal to eliminate a disease.[96] In 1998, ASF was reported in Madagascar for the first time and is now considered to be enzootic in domestic pigs; at the end of 2007, ASF was introduced onto a second Indian Ocean island, Mauritius.[72]

The unforeseen incursion and subsequent spread of ASF into the Caucasus in 2007 was a major event in the disease's epizootology. This was the first appearance of ASF north of Spain, and various factors led to the failure to contain the disease. ASFV likely entered the Caucasus at the Port of Poti, Republic of Georgia, through ship waste containing contaminated pork products that were disposed in local municipal dumps. Molecular analysis has shown that the Georgia strain

is most similar to isolates from Madagascar, which further reinforces the transboundary nature of this virus.[72]

Nearly all pigs in the Republic of Georgia are family-owned, free-range backyard animals that scavenge for food. Once ASFV entered the Georgian pig population, this husbandry system facilitated the rapid spread of the virus eastward: Approximately 60 days after the first cases were documented, 52 of 65 districts had been affected; more than 30,000 pigs had died; and 3,900 pigs had been euthanized.[28] This incursion led to cross-border spread to all of Georgia's neighbors—Armenia, Azerbaijian, and Russia. ASF entered Russia in November 2007 (ProMED, archive 20070607.1845) and has now been reported to affect Chechnya, North Ossetia-Alania, Ingushetia, Orenburg, the Stavropolskiy Kray (Stavropol), and the Krasnodarskiy Kray (Krasnodar). Most recently, ASFV has spread further westward into the Rostovskaya Oblast, which has common borders with Ukraine (ProMED, archive 20090410.1376) and puts ASFV in an excellent staging field for further westward expansion into eastern Europe. ASF is moving rapidly within Russia in areas bordering the Caucasus, and it will require more than a modified stamping-out approach for eradication, given that wild boar may be affected.

Socioeconomic aspects of ASF are disparate across nations and largely defined by the regional presence of ASFV and the economic role of swine production. Africa accounts for less than 1% of the world's pork supply. Nevertheless, in this part of the world, pigs are invaluable at the village level, especially in forested regions where cattle production is difficult. In these areas, swine provide large supplies of high-quality protein from low-grade nutritional sources.[65] In addition, in Africa, pigs often serve as a "piggy bank," with the sale of an animal providing for school fees, medical expenses, and clothing for special occasions. Traditional pig farming and ASF have coexisted for centuries in Africa, and the establishment of ASF-resistant pig populations has occurred in areas where introduction of naïve pigs would result in 100% mortality.[64] ASF still remains the most important constraint to pig production in much of Africa. By contrast, exporting countries are concerned with maintaining or expanding market share and with protecting their domestic livestock population from disastrous introduction of a transboundary animal disease. When first introduced, ASF-associated mortality can be nearly 100% in naïve herds, and near-permanent loss of export markets can be expected.

ASFV entered Spain in 1960 when the Spanish economy was relatively undeveloped and its swine industry was predominated by family holdings and outdoor pig raising (similar to the current era of swine rearing in the Caucasus). When introduced to Spain in 1960, clinical disease was acute and mortality approached 100%. However, by 1985, when Spain's eradication program began, the economy had changed markedly, and swine production had become industrial and intensive.[9] Through the years, ASF had become endemic, and the disease had changed to mild and subclinical forms, with less than 5% mortality. In addition, Spain's pig population continued to increase from 6.0 million to 16.7 million animals in 1960 and 1989, respectively. Although eradication took 10 years (1985–1995) and occurred at great economic cost, it was successfully completed without a vaccine, in the presence of infected soft tick vectors (*O erraticus*), and with relatively simple diagnostic serological tools. This disease eradication model might be applicable to the Caucasus and certain regions of sub-Saharan Africa with substantial technical and financial support from the international community. Eradication from such regions is unlikely to be successful without restructuring of swine industries, as proved to be an essential component of eradication in Spain.

Classical Swine Fever

CSF is more important globally than ASF because of its much wider geographic distribution and greater cumulative economic impact, causing disease outbreaks on all the major continents. CSF virus (CSFV) is a member of the *Pestivirus* genus of Flaviviridae family and thus belongs to a genus of important viruses that cross-react on diagnostic tests, including bovine viral diarrhea virus and border disease virus. CSF has some similarities to ASF, including high- and low-virulence forms and high degree of contagion. Both CSFV and ASFV are environmentally stable and are found in all secretions, excretions, and tissues, including meat. There are also important differences: The highly virulent viruses of CSF seldom circulate; effective vaccines are available for CSF but not for ASF; and there is no tick transmission of CSF.[22] Moderate- to low-virulence strains of CSF predominate globally, with most epizootics today caused by moderately virulent strains of virus.[46]

Because of the prevalence of low-virulence strains, in which animals may not appear clinically ill but still carry and transmit the virus, it is easy for CSFV to enter a free country or region and spread before the establishment of a diagnosis. Such a scenario resulted in the severe consequences of the epizootic in the Netherlands in 1997–1998, which resulted in losses of $2 billion.[55] In such instances, clinical surveillance is unreliable because the mild or subclinical disease course (when it does occur) can resemble many other common diseases of swine. When CSF returned to the United Kingdom in 2000 after a 14-year absence, diagnosis was complicated by lack of "typical" clinical signs and by clinical similarities to porcine dermatitis and nephropathy syndrome, which had become a serious problem in Great Britain one year earlier.[62]

In addition, because CSFV is immunosuppressive, antibodies form late (2 to 3 weeks postinfection); thus, serological surveillance has drawbacks in detecting early infection. Tissue surveillance by swabbing tonsils and testing with real-time reverse-transcription polymerase chain reaction is the most sensitive system for detecting early infection; however, implementation of this surveillance strategy on a sufficiently large scale is an expensive and time-consuming process that would require implementation of robotic high-throughput techniques. Overall, owing to the widespread distribution of CSF and abundance of low-virulence strains, this disease can readily cause unexpected incursions into disease-free regions.

Peste Des Petits Ruminants and Rinderpest

Peste des petits ruminants (PPR) is a severe viral disease of goats and sheep with variable but usually high morbidity and mortality. It is considered the most economically important viral disease of these species in enzootic regions.[71] Given that sheep and goats are more economically important than cattle in many regions of the world that rely on pastoralism, PPR has a major impact on the food supply in these regions.[12] Since the disease was first described in 1942, the distribution has steadily expanded to include large regions of Africa, the Middle East, and Asia. PPR is a high-priority disease for the FAO Emergency Preventive System, and mitigation of the disease's impact is considered an important step to help alleviate poverty in enzootic regions.[33] The disease readily crosses national boundaries, and it is now considered the most constraining disease of small ruminant production in sub-Saharan Africa and the Indian subcontinent.[86] Additionally, the eradication of rinderpest (RP) in Africa and Asia has elevated the relative economic importance of PPR.

PPR occurs in acute and subacute forms characterized by variable extents of fever, conjunctivitis, erosive stomatitis, enterocolitis, and pneumonia. It closely resembles RP clinically and pathologically except for the frequent occurrence of pneumonia with PPR. PPR virus (PPRV) is a distinct member of the Paramyxoviridae family, *Morbillivirus* genus, which includes RP virus (RPV), canine distemper virus, measles virus, phocine distemper virus, and cetacean morbillivirus of dolphins and porpoises. Each of these viruses has only one serotype, and they are all closely related phylogenetically, which generally facilitates vaccination strategies. Transmission of PPR is mainly by oronasal contact with secretions from infected animals, with nearly all outbreaks traced to movement of livestock.

There are four known phylogenetic lineages of PPRV. Lineage IV is a more recently emerged group of viruses occurring in Asia and the Middle East, in contrast to the other three PPRV lineages, which are of African origin. Lineage I and II viruses have been found exclusively in West Africa, whereas lineage III viruses occur in East Africa, Arabia, and southern India. The source of the "new" lineage IV virus is unknown, although it is most closely related to African lineage I.[86]

PPR was first discovered in the Ivory Coast in 1942; further investigations led to knowledge of its widespread occurrence in sub-Saharan and Sahelian Africa, including Egypt, Sudan, and Ethiopia. For over three decades, there was no clinical evidence that PPR had extended south of the line from Cameroon to Ethiopia, although such a transgression had been widely predicted. In Asia, PPR was first discovered in southern India in 1987. Subsequently, epizootic PPR spread across the Arabian Peninsula, the Middle East, and the remaining parts of the Indian subcontinent in 1993–1995, where it has since remained endemic. The last three decades have seen a considerable extension in worldwide distribution of PPR. This trend is likely multifactorial, with indeterminate contributions from increased transportation of live animals, better diagnostic tests, increased vigilance of surveillance systems, and greater awareness of PPR after eradication of RP. The recent spread of PPR can be correlated with the increase of animal movement for commercial and trade purposes (eg, the massive imports of small ruminants to the Middle East), transhumance and nomadic customs, and the extensive farming practices in the Saharan regions.[29] In recent years, PPR has expanded across international borders and has been repeatedly diagnosed in known enzootic regions. More recently in Asia—specifically, 2007—Tibet (China), Nepal, and Tajikistan reported their first cases of PPR. In Africa, PPR has now spread south of the equator to Gabon (1996), the Congo (2006), Kenya (2006), and Uganda (2007) and has now spread north of the Sahara to Morocco (2007) (ProMED, archive 20090314.1056).

The chronological spread of PPRV, as recorded by detection in previously unaffected countries, gives the impression that the geographical spread of PPR occurred eastward, from West Africa to Bangladesh. However, this does not necessarily mean that PPR originated in West Africa. Sequence analyses and lineage typing of historical and new PPRV isolates have provided interesting perspectives on the origin of the virus. For example, PPRV probably originated in Eurasia (as did RPV) and spread to Africa on multiple occasions via trade of livestock (ProMED, archive 20081016.3282). In addition, there is reasonable molecular evidence that PPR existed in India before being "discovered" in West Africa. In Asia, diagnosis may have been delayed owing to misdiagnoses of RP (oral erosions and diarrhea), contagious caprine pleuropneumonia, or pasteurellosis (bronchopneumonia), which is a common superinfection associated with primary PPR-induced pneumonia. Thus, PPR might have been transported to West Africa by sailing ship from India long ago. This would mean that lineage IV or a precursor was the parental lineage of PPR and that each time PPRV was transported to a new continent, a new lineage arose.

The Moroccan outbreak may illustrate the same fundamental pathway—that is, the movement of lineage IV out of Asia Minor to Africa. Preliminary results of sequencing the nucleocapsid N gene of viruses from this outbreak indicate that the PPR isolate is a lineage IV virus that is closely related to the Saudi Arabian and Iranian strains. This suggests that the virus entered Morocco from the Middle East by trade in live infected animals and not by nomadic movement across its open borders, as originally speculated. Considering the evidence that the emergence of new lineages of PPRV has historically been correlated with intercontinental movements of the virus, it has been proposed that the birth of a new African lineage may presently be occurring in Morocco (ProMED, archive 20081016.3282).

The continuing outbreaks of PPR in Morocco (as of this writing) should be of great concern for neighboring countries, especially Algeria, in which there are approximately 19 million sheep and 3 million goats. The risk is also high for southern European countries that historically have had substantial trade with Morocco. Of these countries, Spain seems to be particularly vulnerable, given its geographic proximity and the

importance of its vulnerable livestock of 23 million sheep and 3 million goats.[29]

Enhanced surveillance for PPR is justified for all African and Asian countries; vigilance is indicated in PPRV-free regions as well. When outbreaks occur, regional PPR eradication is a complex task leading to the need for mass vaccinations. The homologous live-attenuated PPR vaccine is commercially available; it is efficacious; and it creates long-lasting immunity. Perhaps with the imminent global eradication of RP, a renewed interest in PPR control and eradication will follow. A macroeconomic study in Niger found that control of PPR by vaccination was highly beneficial to the national goat industry.[80] In addition, the FAO believes that eradication of PPR is achievable with education of local governments and stakeholders, creation of sound global and regional strategies, understanding of PPR epidemiology and ecology, and use of thorough vaccination campaigns.[33] However, socioeconomic factors will ultimately dictate if eradication is pursued, and the lesser relative importance of small ruminant production to many developed nations may foster a degree of apathy. International funding and support will surely be necessary to control and possibly eradicate PPR and alleviate the immense economic and social problems it causes.

In contrast to PPR, there is convincing surveillance evidence in cattle and wildlife that the last remaining focus of RP, the Somali Pastoral Ecosystem, is free of clinical disease and the etiologic agent.[31] Declaration of global eradication in 2010 is expected to occur as planned. As of early 2009, the FAO's Global Rinderpest Eradication Program indicated that RPV has been eliminated from Europe, Asia, Middle East, Arabian Peninsula, and all of Africa; in effect, it has been eradicated globally.[31] This is an exceptional accomplishment for a disease that may have been circulating since the time of Aristotle (384–322 BCE) and has been described as the most dreaded of all animal diseases, causing terrible destruction of cattle and wildlife and bringing famine to rural human populations.[61] The notion that the last focus of RP has been eradicated is supported by the fact that (1) the last definitive detection of RPV occurred in 2001,[70] (2) all subsequent investigations of a possible "mild form" of circulating RPV in cattle have not been positive (by either virus detection or serology), and (3) repeated serological testing of wildlife in the region has been negative since 2002. Final declaration of RP freedom will be jointly declared by the FAO and OIE once remaining countries have completed the "OIE rinderpest pathway" (described in the OIE's Terrestrial Animal Health Code[**]) and been officially declared disease-free by the OIE.

Bluetongue

Bluetongue (BT) is a disease of ruminants caused by BTV and transmitted predominantly through feeding of biting midges of the genus *Culicoides*.[93] BT is enzootic in the United States[50,93] and many other nations and it has made occasional incursions into southern Europe[97] through much of the 20th century. However, recent changes in BT epizootology indicate that this disease is very much on the move.[67,97] The changes in Europe are most noteworthy in that since 1998 at least seven distinct strains of BTV have been detected across 12 nations, causing the deaths of millions of sheep and cattle.[67] Most significantly, in 2006 BTV serotype 8 caused the first outbreaks of BT ever detected in northern Europe. The virus was first identified in the Netherlands, and it subsequently spread across most northern European nations. The northernmost detection thus far has been within Vest-Agder county of Norway in February 2009 (ProMED, archive 20090402.1278).

Although the deaths of millions of animals are always of great concern, this situation is noteworthy because it is the most convincing example of a substantial change in the distribution of a veterinary disease attributed to the current, ongoing global climate changes. The spread of BTV in Europe is closely linked to the northern expansion of *Culicoides imicola*, the most important vector of BTV in Africa and Asia, and it is the warming temperatures and changes in humidity across Europe that have allowed this expansion.[67] Furthermore, these same climatic alterations have allowed indigenous European *Culicoides* spp to serve as competent BTV vectors. The situation in the United States has some similarities in that BTV-1 was first detected in Louisiana in 2004 and was suspected to be associated with a novel *Culicoides* spp vector.[43] Overall, this scenario provides a practical indication that climate change is already substantially affecting the host–vector–pathogen dynamics of veterinary diseases. It would be profoundly shortsighted to view this as an isolated set of circumstances rather than as a preview of additional climate-driven changes in agricultural disease distributions, some of which likely have already occurred but have not yet been detected.

Newcastle Disease

Newcastle disease, caused by avian paramyxovirus type 1, is one of the most significant diseases for poultry producers around the world.[6] Most birds are susceptible to infection, with the outcome varying from subclinical to severe, depending on the strain of the virus, the species of the bird, and other factors.[4] For international trading purposes, strains of virulent Newcastle disease virus (vNDV) are reportable to the OIE.[60] The definition of vNDV is based on intracerebral pathogenicity testing of the virus in day-old chicks and/or the presence of multiple basic amino acids at the cleavage site of the fusion protein.[60] The disease is widely distributed throughout the world; in 2008, 73 countries reported presence of the disease to the OIE.[98] Additionally, numerous nations in Asia, Africa, Central America, and South America have endemic or frequent outbreaks caused by vNDV, and there are sporadic outbreaks of the virus worldwide.[63] Disease transmission between countries occurs through a variety of methods, such as the movement of poultry, pet birds, and fomites and, to a much lesser extent, via wild birds such as double-crested cormorants (*Phalacrocorax auritus*) and Columbiforme birds (pigeons and doves).[4,17,42,44]

Virulent Newcastle disease virus causes significant losses in highly developed commercial production systems and in

village poultry, a major reservoir of the virus. During the 2002–2003 US outbreak in which backyard and commercial poultry were infected, disease eradication efforts cost an estimated $180 million, in addition to loss of export markets.[7] The negative effects of disease on income and food security provided by village poultry production are substantial, and vNDV is considered one of the major limiting factors in raising poultry in small flocks within developing countries.[3,11] Newcastle disease outbreaks, which cause regular episodes of 50 to 100% mortality in village poultry, confound the identification of HPAI outbreaks because both diseases have similar clinical signs and high mortality.[3] Greater research into methods of disease control are needed not only to decrease worldwide disease prevalence and thus risk of transboundary transmission but also to combat poverty and hunger in developing nations.

Ebola Reston in Pigs

In October 2008, during an investigation of unexplained increased mortality among pigs in the Philippines, researchers discovered that in addition to being infected with porcine respiratory and reproductive syndrome virus, some pigs were positive for Ebola-Reston virus (ERV).[13,27] Subsequently, humans with histories of direct contact with ERV-infected pigs were found to be positive for anti-ERV antibodies (ProMED, archive 20090203.0482).[13] Unlike other strains of Ebola virus, ERV may cause fatal infection in monkeys, but it has been known to cause only mild flu-like illness in humans. None of the serologically ERV-positive humans reported any significant illness, and there was no evidence of human-to-human transmission. Although it is unclear if there is any significance to these discoveries for pigs or humans, it is clear that this is a novel pathogen–host combination that merits further observation.

Conclusions

The continuously increasing population of the earth, combined with the commensurate progressive decrease of land available for agriculture, ensures that the balance of available and necessary food for human consumption will be tenuous in decades to come. This balance will be most precarious in developing nations, whereas richer, developed nations will undoubtedly be involved in the moral decisions regarding how to mitigate regional deficits in the developing world. Although politicians will ultimately be making such decisions, veterinary scientists will surely be tasked to generate some of the data that will form the basis for these decisions. The most important role for veterinary scientists in this scheme will be to monitor, assess, predict, and prevent (when feasible) the movements of diseases of food animals. Numerous subdisciplines of veterinary medicine and investigative science are crucial to the multidisciplinary understanding and control of transboundary diseases. However, in the context of this topic, emphasis must be placed on the importance of the roles of pathologists and regulatory field veterinarians, who often are the first individuals exposed to novel disease incursions.

That this "top 10" list of agricultural diseases on the move includes, exclusively, conditions of viral etiology is not coincidental. Viruses have the most rapid mutation rates and, as such, are generally expected to adapt most rapidly to changing environments. Clearly, other classes of diseases with direct or indirect effect on agriculture are on the move. Among bacterial diseases, bovine tuberculosis is on the rise in North America and Europe, and since 2005 there has been a sustained and unprecedented increase in Q fever cases in the Netherlands among goats and humans, which has resulted in regional mandatory vaccination of small ruminants.[76] Decimation of amphibians worldwide by chytridiomycosis may presently be serving as the prototype of the spread of fungal diseases associated with global climate change. And the still idiopathic conditions of colony collapse disorder and white nose syndrome are depleting populations of honey bees and bats, respectively. This only scratches the surface of the full complement of diseases on the move.

New, previously unknown diseases will surely continue to emerge. And, it is nearly certain that the trends described for the diseases discussed herein will progress, thus ensuring that FMD, ASF, HPAI, BT, RVF, and other catastrophic diseases are all but a stone's throw away from our doorsteps. It is also true that certain types of key events (or scenarios) that facilitate the movement of pathogens will always be unstoppable. This is a reality for human-initiated events, such as the presumed single action of swill feeding that brought ASF to the Caucasus and beyond. But it is just as relevant in considering the effect of waterfowl migration on HPAI or the effect of climate change on BT spreading through Europe. How the world will respond to these challenges is uncertain. Nations and international organizations that proactively invest in preparedness will be more successful and economical than reactive strategies that simply hope a new disease incursion will not occur. Reactive approaches often seem economical in the short term but in the long run may be far more expensive and may lead to irreparable consequences, such as enzootic establishment of previously exotic diseases.

The extreme consequences associated with the 2001 epizootic of FMD in the United Kingdom led to the increased awareness, diagnostic throughput capacity, and availability of first responders, which minimized the impact when the disease appeared again in 2007. Similarly, the profuse media attention given to the pandemic potential of HPAI contributed to a transboundary influenza preparedness that has helped to monitor and mitigate the current, ongoing H1N1 pandemic. Clearly, policy makers will have to pick and choose how to best invest in control of agricultural diseases; but, ultimately, it is the combinatorial breadth of that investment that will determine the global community's capacity to deal with the inevitable breaches of integrity. Globalization and global climate change make it evermore likely that agricultural diseases will emerge in new locations with greater frequency. Whether the resurgence of a historical disease such as tuberculosis or a novel discovery such as Ebola in swine, the agricultural, veterinary, and political communities are well advised to be prepared.

Notes

*ProMED-mail is a global electronic reporting system for outbreaks of emerging infectious diseases and toxins (http://www.promedmail.org).
†World Animal Health Information Database Interface provides access to all data within OIE's animal health database (http://www.oie.int/wahis/public.php?page=country).
‡Global Alert and Response is an integrated global alert and response system for epidemics of disease in humans and other public health emergencies (http://www.who.int/csr/en/).
§Emergency Prevention System for Transboundary Animal and Plant Pests and Diseases livestock program seeks to promote the effective containment and control of the most serious epidemic livestock diseases and transbounday animal diseases (http://empres-i.fao.org/empres-i/home).
‖*Exclusively agriculture-associated disease* is a distinction from disease that affects agriculture but has substantial impact on human public health, such as avian influenza or Rift Valley fever.
¶Numerous diseases could be spread in this manner, but in the context of the current review, transmission of foot-and-mouth disease virus, bluetongue virus, and peste des petits ruminants virus should be considered.
#The region between the Black and Caspian seas, divided by the Caucasus Mountains along the border between the Russian Federation, Georgia, and Azerbaijan.
**See http://www.oie.int/eng/normes/Mcode/en_sommaire.htm (accessed October 26, 2009).

Acknowledgements

We would like to thank Mr Dennis Senne and Dr Marvin Grubman for their thoughtful review of the manuscript.

References

1. Abd el-Rahim IH, Abd el-Hakim U, Hussein M: An epizootic of Rift Valley fever in Egypt in 1997. Rev Sci Tech **18:**741–748, 1999.
2. Abolnik C: Molecular characterization of H5N2 avian influenza viruses isolated from South African ostriches in 2006. Avian Dis **51:**873–879, 2007.
3. Alders RG, Pym RAE: Village poultry: still important to millions, eight thousand years after domestication. Worlds Poult Sci J **65:**181–190, 2009.
4. Alexander DJ: Newcastle disease and other avian paramyxoviruses. Rev Sci Tech **19:**443–462, 2000.
5. Alexander DJ: Summary of avian influenza activity in Europe, Asia, Africa, and Australasia, 2002–2006. Avian Dis **51:**161–166, 2007.
6. Alexander DJ, Senne DA. Newcastle disease, other avian paramyxoviruses, and pneumovirus infections. *In*: Diseases of Poultry, ed. Saif YM, Fadly AM, Glisson JR, McDougald LR, Nolan LK, and Swayne DE, 12th ed., pp. 75–115. Blackwell Publishing Professional, Ames, IA, 2008.
7. Anonymous: USDA outreach program targets noncommercial-bird-owning public. J Am Vet Med Assoc **224:**1898, 2004.
8. Anyamba A, Chretien JP, Small J, Tucker CJ, Formenty PB, Richardson JH, Britch SC, Schnabel DC, Erickson RL, Linthicum KJ: Prediction of a Rift Valley fever outbreak. Proc Natl Acad Sci U S A **106:**955–959, 2009.
9. Arias M, Sanchez-Vizcaino J: African swine fever eradication: the Spanish model. *In*: Trends in Emerging Viral Infections of Swine, pp. 133–139. Iowa State University Press, Ames, IA, 2002.
10. Arthur RR, el-Sharkawy MS, Cope SE, Botros BA, Oun S, Morrill JC, Shope RE, Hibbs RG, Darwish MA, Imam IZ: Recurrence of Rift Valley fever in Egypt. Lancet **342:**1149–1150, 1993.
11. Awan MA, Otte MJ, James AD: The epidemiology of Newcastle disease in rural poultry: a review. Avian Pathol **23:**405–423, 1994.
12. Banyard A, Rima B, Barrett T: Peste des petits ruminants virus. *In*: Rinderpest and Peste des Petits Ruminants, Virus Plagues of Large and Small Ruminants, ed. Barrett G, Pastoret P, and Taylor W, pp. 15–16. Elsevier, London, UK, 2006.
13. Barrette RW, Metwally SA, Rowland JM, Xu L, Zaki SR, Nichol ST, Rollin PE, Towner JS, Shieh WJ, Batten B, Sealy TK, Carrillo C, Moran KE, Bracht AJ, Mayr GA, Sirios-Cruz M, Catbagan DP, Lautner EA, Ksiazek TG, White WR, McIntosh MT: Discovery of swine as a host for the Reston ebolavirus. Science **325:**204–206, 2009.
14. Bird BH, Ksiazek TG, Nichol ST, Maclachlan NJ: Rift Valley fever virus. J Am Vet Med Assoc **234:**883–893, 2009.
15. Capua I, Alexander DJ: Avian influenza infection in birds: a challenge and opportunity for the poultry veterinarian. Poult Sci **88:**842–846, 2009.
16. Capua I, Alexander DJ: Ecology, epidemiology and human health implications of avian influenza viruses: why do we need to share genetic data? Zoonoses Public Health **55:**2–15, 2008.
17. Capua I, Dalla PM, Mutinelli F, Marangon S, Terregino C: Newcastle disease outbreaks in Italy during 2000. Vet Rec **150:**565–568, 2002.
18. Capua I, Marangon S: Control of avian influenza in poultry. Emerg Infect Dis **12:**1319–1324, 2006.
19. Cattoli G, Monne I, Fusaro A, Joannis TM, Lombin LH, Aly MM, Arafa AS, Sturm-Ramirez KM, Couacy-Hymann E, Awuni JA, Batawui KB, Awoume KA, Aplogan GL, Sow A, Ngangnou AC, El Nasri Hamza IM, Gamatie D, Dauphin G, Domenech JM, Capua I: Highly pathogenic avian influenza virus subtype H5N1 in Africa: a comprehensive phylogenetic analysis and molecular characterization of isolates. PLoS One **4:**e4842, 2009.
20. Cottam EM, Wadsworth J, Shaw AE, Rowlands RJ, Goatley L, Maan S, Maan NS, Mertens PP, Ebert K, Li Y, Ryan ED, Juleff N, Ferris NP, Wilesmith JW, Haydon DT, King DP, Paton DJ, Knowles NJ: Transmission pathways of foot-and-mouth disease virus in the United Kingdom in 2007. PLoS Pathog **4:**e1000050, 2008.
21. Cristalli A, Capua I: Practical problems in controlling H5N1 high pathogenicity avian influenza at village level in Vietnam and introduction of biosecurity measures. Avian Dis **51:**461–462, 2007.
22. Dahle J, Liess B: A review on classical swine fever infections in pigs: epizootiology, clinical disease and pathology. Comp Immunol Microbiol Infect Dis **15:**203–211, 1992.
23. Daubney RHJ, Garnham PC: Enzootic hepatitis or Rift Valley fever: an undescribed virus disease of sheep, cattle and man from East Africa. J Pathol Bacteriol **34:**545–579, 1931.

24. Davies FG: Risk of a rift valley fever epidemic at the haj in Mecca, Saudi Arabia. Rev Sci Tech **25:**137–147, 2006.
25. Digoutte JP, Peters CJ: General aspects of the 1987 Rift Valley fever epidemic in Mauritania. Res Virol **140:**27–30, 1989.
26. Ducatez MF, Webster RG, Webby RJ: Animal influenza epidemiology. Vaccine **26**(Suppl 4):D67–D69, 2008.
27. Editorial team: Ebola Reston virus detected pigs in the Philippines. Euro Surveill **14**(4):Art. 4, 2009. http://www.eurosurveillance.org/ViewArticle.aspx?ArticleId=19105. Accessed October 25, 2009.
28. Food and Agriculture Organization, United Nations: EMPRES Watch: African Swine Fever in the Caucasus (April 2008). ftp://ftp.fao.org/docrep/fao/011/aj214e/aj214e00.pdf. Accessed July 31, 2009.
29. Food and Agriculture Organization, United Nations: EMPRES Watch: Peste des Petits Ruminants (PPR) in Morocco (August 2008). ftp://ftp.fao.org/docrep/fao/011/aj120e/aj120e00.pdf. Accessed July 31, 2009.
30. Food and Agriculture Organization, United Nations: Eradication of Hog Cholera and African Swine Fever. http://www.fao.org/docrep/004/X6501E/X6501E00.HTM. Accessed July 31, 2009.
31. Food and Agriculture Organization, United Nations: The Global Rinderpest Eradication Programme: Status Report on Progress Made to Date in Eradication of Rinderpest: Highlighting Success Story and Action Require Till Global Declaration in 2010. http://www.fao.org/Ag/againfo/resources/documents/AH/GREP_flyer.pdf. Accessed July 31, 2009.
32. Food and Agriculture Organization, United Nations: The Global Strategy for Prevention and Control of H5N1 Highly Pathogenic Avian Influenza. http://un-influenza.org/files/aj134e00.pdf. Accessed July 31, 2009.
33. Food and Agriculture Organization, United Nations: Peste des Petits Ruminants (PPR): A Challenge for Small Ruminant Production. http://www.fao.org/ag/AGAinfo/resources/documents/AH/PPR_flyer.pdf. Accessed July 31, 2009.
34. Garabed RB, Johnson WO, Thurmond MC: Analytical epidemiology of genomic variation among Pan Asia strains of foot-and-mouth disease virus. Transbound Emerg Dis **56:**142–156, 2009.
35. Gibbens N: Avian influenza outbreak in Oxfordshire. Vet Rec **162:**795, 2008.
36. Gilbert M, Xiao X, Domenech J, Lubroth J, Martin V, Slingenbergh J: Anatidae migration in the western Palearctic and spread of highly pathogenic avian influenza H5NI virus. Emerg Infect Dis **12:**1650–1656, 2006.
37. Global Alert and Response, World Health Organization: Cumulative Number of Confirmed Human Cases of Avian Influenza A/(H5N1) Reported to WHO. http://www.who.int/csr/disease/avian_influenza/country/cases_table_2009_07_01/en/index.html. Accessed July 31, 2009.
38. Grubman MJ: Development of novel strategies to control foot-and-mouth disease: marker vaccines and antivirals. Biologicals **33:**227–234, 2005.
39. Grubman MJ, Baxt B: Foot-and-mouth disease. Clin Microbiol Rev **17:**465–493, 2004.
40. Harder TC, Teuffert J, Starick E, Gethmann J, Grund C, Fereidouni S, Durban M, Bogner KH, Neubauer-Juric A, Repper R, Hlinak A, Engelhardt A, Nockler A, Smietanka K, Minta Z, Kramer M, Globig A, Mettenleiter TC, Conraths FJ, Beer M: Highly pathogenic avian influenza virus (H5N1) in frozen duck carcasses, Germany, 2007. Emerg Infect Dis **15:**272–279, 2009.
41. Hayden EC: Avian influenza aided readiness for swine flu. Nature **459:**756–757, 2009.
42. Heckert RA, Collins MS, Manvell RJ, Strong I, Pearson JE, Alexander DJ: Comparison of Newcastle disease viruses isolated from cormorants in Canada and the USA in 1975, 1990 and 1992. Can J Vet Res **60:**50–54, 1996.
43. Johnson DJ, Ostlund EN, Stallknecht DE, Goekjian VH, Jenkins-Moore M, Harris SC: First report of bluetongue virus serotype 1 isolated from a white-tailed deer in the United States. J Vet Diagn Invest **18:**398–401, 2006.
44. Kim LM, King DJ, Guzman H, Tesh RB, da Rosa APAT, Bueno R Jr, Dennett JA, Afonso CL: Biological and phylogenetic characterization of pigeon paramyxovirus serotype 1 circulating in wild North American pigeons and doves. J Clin Microbiol **46:**3303–3310, 2008.
45. Kleiboeker S: African swine fever. *In*: USAHA Foreign Animal Diseases, pp. 117–123. Boca Publications Group, Boca Raton, FL, 2008.
46. Kleiboeker SB: Swine fever: classical swine fever and African swine fever. Vet Clin North Am Food Anim Pract **18:**431–451, 2002.
47. Knowles NJ, Samuel AR, Davies PR, Kitching RP, Donaldson AI: Outbreak of foot-and-mouth disease virus serotype O in the UK caused by a pandemic strain. Vet Rec **148:**258–259, 2001.
48. Knowles NJ, Samuel AR, Davies PR, Midgley RJ, Valarcher JF: Pandemic strain of foot-and-mouth disease virus serotype O. Emerg Infect Dis **11:**1887–1893, 2005.
49. Krebs RE, Krebs CA: Groundbreaking Scientific Experiments, Inventions and Discoveries of the Ancient World. Greenwood Press, Westport, CT, 2003.
50. Maclachlan NJ, Drew CP, Darpel KE, Worwa G: The pathology and pathogenesis of bluetongue. J Comp Pathol **141:**1–16, 2009.
51. Madani TA, Al-Mazrou YY, Al-Jeffri MH, Mishkhas AA, Al-Rabeah AM, Turkistani AM, Al-Sayed MO, Abodahish AA, Khan AS, Ksiazek TG, Shobokshi O: Rift Valley fever epidemic in Saudi Arabia: epidemiological, clinical, and laboratory characteristics. Clin Infect Dis **37:**1084–1092, 2003.
52. Martin V, Chevalier V, Ceccato P, Anyamba A, De Simone L, Lubroth J, de La Rocque S, Domenech J: The impact of climate change on the epidemiology and control of Rift Valley fever. Rev Sci Tech **27:**413–426, 2008.
53. Mase M, Eto M, Tanimura N, Imai K, Tsukamoto K, Horimoto T, Kawaoka Y, Yamaguchi S: Isolation of a genotypically unique H5N1 influenza virus from duck meat imported into Japan from China. Virology **339:**101–109, 2005.
54. Meegan JM, Hoogstraal H, Moussa MI: An epizootic of Rift Valley fever in Egypt in 1977. Vet Rec **105:**124–125, 1979.
55. Moennig V, Floegel-Niesmann G, Greiser-Wilke I: Clinical signs and epidemiology of classical swine fever: a review of new knowledge. Vet J **165:**11–20, 2003.
56. Montgomery RE: On a form of swine fever occurring in British East Africa (Kenya Colony). J Comp Pathol **34:**159–191, 1921.

57. Nasher AAW SA, Al Eriyani M, Bourgy AA, Al Kohlani AH, Benbrake M, El Mktary W, Al Selwy K, Kader AA, Abby MO, Amran GG, El Wasaby D, Zabarah A, Sabet A, Azy M, Header M, Header HR, Amin M, Wareth YA, Ramadany M, Al Bagali AS, Al-Arashi AM, Al-Ariyani G, Al Hamadi N, Al-Fosail H, Al-Qadsasi M, Said K, Hadi A, Al-Jouffi A, Omer AT, Al-Busaidi S, Ismalili S, Al-Sohby AA, Hady S, Shabana AA, Al-Salmi K, El-Zein HA, Khalifa M, El-Samani F, Hallaj Z, Klauke D, El-Kholy AA, Ibrahim IM, Naguib W, Salman D, Lewis S, Dykstra E, El-Sakka H, Graham R, Mahoney F: Outbreak of Rift Valley fever—Yemen, August–October 2000. MMWR Morb Mortal Wkly Rep **49:**1065–1066, 2000.
58. Office of Risk Analysis and Cost Benefit Analysis: Economic Impact of a Foreign Animal Disease (FAD) Outbreak Across the United States. Office of the Chief Economist, US Department of Agriculture, Washington, DC, 2005.
59. OIE: Avian influenza. *In*: Manual of Diagnostic Tests and Vaccines for Terrestrial Animals, 6th ed., pp. 465–481. Office International Des Epizooties, Paris, France, 2008.
60. OIE: Newcastle disease. *In*: Manual of Diagnostic Tests and Vaccines for Terrestrial Animals, 6th ed., pp. 576–589. Office International Des Epizooties, Paris, France, 2008.
61. Pastoret P, Yamanouchi K, Mueller-Doblies U, Rweyemamu MM, Horzinek M, Barrett T: Rinderpest—an old and worldwide story: history to c. 1902. *In*: Rinderpest and Peste des Petits Ruminants, Virus Plagues of Large and Small Ruminants, ed. Barrett G, Pastoret P, and Taylor W, pp. 87–88. Elsevier, London, UK, 2006.
62. Paton D: The reappearance of classical swine fever in England in 2000. *In*: Trends in Emerging Viral Infections of Swine, ed. Morilla A, Yoon K-J, and Zimmerman J, pp. 153–158. Iowa State Press, Ames, IA, 2002.
63. Pendell DL, Leatherman J, Schroeder TC, Alward GS: The economic impacts of a foot-and-mouth disease outbreak: a regional analysis. J Agric Appl Econ **39:**13–33, 2007.
64. Penrith ML, Lopes Pereira C, Lopes da Silva MM, Quembo C, Nhamusso A, Banze J: African swine fever in Mozambique: review, risk factors and considerations for control. Onderstepoort J Vet Res **74:**149–160, 2007.
65. Penrith M, Thomson G, Bastos A: African swine fever. *In*: Infectious Diseases of Livestock, ed. Coetzer JAW, 2nd ed., pp. 568–599. Oxford University Press, Oxford, UK, 2004.
66. Pittman PR, Liu CT, Cannon TL, Makuch RS, Mangiafico JA, Gibbs PH, Peters CJ: Immunogenicity of an inactivated Rift Valley fever vaccine in humans: a 12-year experience. Vaccine **18:**181–189, 1999.
67. Purse BV, Brown HE, Harrup L, Mertens PP, Rogers DJ: Invasion of bluetongue and other orbivirus infections into Europe: the role of biological and climatic processes. Rev Sci Tech **27:**427–442, 2008.
68. Rhyan J, Deng M, Wang H, Ward G, Gidlewski T, McCollum M, Metwally S, McKenna T, Wainwright S, Ramirez A, Mebus C, Salman M: Foot-and-mouth disease in North American bison (Bison bison) and elk (Cervus elaphus nelsoni): susceptibility, intra- and interspecies transmission, clinical signs, and lesions. J Wildl Dis **44:**269–279, 2008.
69. Ribeiro JM, Azevedo R, Teixeira J: An atypical strain of swine fever virus in Portugal. OIE Bull **50:**516–534, 1958.
70. Roeder P, Taylor WP, Rweyemamu MM. Rinderpest in the twentieth and twenty-first centuries. *In*: Rinderpest and Peste des Petits Ruminants, Virus Plagues of Large and Small Ruminants, ed. Barrett G, Pastoret PR, and Taylor WP, pp. 137–138. Elsevier, London, UK, 2006.
71. Rossiter P: Peste des petits ruminants. *In*: Infectious Diseases of Livestock, ed. Coetzer JAW, 2nd ed., pp. 660–672. Oxford University Press, Oxford, UK, 2004.
72. Rowlands RJ, Michaud V, Heath L, Hutchings G, Oura C, Vosloo W, Dwarka R, Onashvili T, Albina E, Dixon LK: African swine fever virus isolate, Georgia, 2007. Emerg Infect Dis **14:**1870–1874, 2008.
73. Rweyemamu M, Roeder P, MacKay D, Sumption K, Brownlie J, Leforban Y: Planning for the progressive control of foot-and-mouth disease worldwide. Transbound Emerg Dis **55:**73–87, 2008.
74. Rweyemamu M, Roeder P, MacKay D, Sumption K, Brownlie J, Leforban Y, Valarcher JF, Knowles NJ, Saraiva V: Epidemiological patterns of foot-and-mouth disease worldwide. Transbound Emerg Dis **55:**57–72, 2008.
75. Ryan E, Gloster J, Reid SM, Li Y, Ferris NP, Waters R, Juleff N, Charleston B, Bankowski B, Gubbins S, Wilesmith JW, King DP, Paton DJ: Clinical and laboratory investigations of the outbreaks of foot-and-mouth disease in southern England in 2007. Vet Rec **163:**139–147, 2008.
76. Schimmer B, Dijkstra F, Vellema P, Schneeberger PM, Hackert V, ter Schegget R, Wijkmans C, van Duynhoven Y, van der Hoek W: Sustained intensive transmission of Q fever in the south of the Netherlands, 2009. Euro Surveill **14**(19):Art. 5, 2009. http://www.eurosurveillance.org/ViewArticle.aspx?ArticleId=19210. Accessed October 25, 2009.
77. Shoemaker T, Boulianne C, Vincent MJ, Pezzanite L, Al-Qahtani MM, Al-Mazrou Y, Khan AS, Rollin PE, Swanepoel R, Ksiazek TG, Nichol ST: Genetic analysis of viruses associated with emergence of Rift Valley fever in Saudi Arabia and Yemen, 2000–01. Emerg Infect Dis **8:**1415–1420, 2002.
78. Shortridge KF: Poultry and the influenza H5N1 outbreak in Hong Kong, 1997: abridged chronology and virus isolation. Vaccine **17**(Suppl 1):S26–S29, 1999.
79. Sims LD, Domenech J, Benigno C, Kahn S, Kamata A, Lubroth J, Martin V, Roeder P: Origin and evolution of highly pathogenic H5N1 avian influenza in Asia. Vet Rec **157:**159–164, 2005.
80. Stem C: An economic analysis of the prevention of peste des petits ruminants in Nigerian goats. Prev Vet Med **16:**141–150, 1993.
81. Suarez DL: Influenza A virus. *In*: Avian Influenza, ed. Swayne DE, pp. 3–22. Blackwell Publishing Professional, Ames, IA, 2008.
82. Sumption K, Rweyemamu M, Wint W: Incidence and distribution of foot-and-mouth disease in Asia, Africa and South America: combining expert opinion, official disease information and livestock populations to assist risk assessment. Transbound Emerg Dis **55:**5–13, 2008.
83. Swayne DE: Avian influenza control strategies. *In*: Avian Influenza, ed. Swayne DE, pp. 287–297. Blackwell Publishing Professional, Ames, IA, 2008.

84. Swayne DE, Beck JR: Experimental study to determine if low-pathogenicity and high-pathogenicity avian influenza viruses can be present in chicken breast and thigh meat following intranasal virus inoculation. Avian Dis **49:**81–85, 2005.
85. Swayne DE, Halvorson DA: Influenza. *In*: Diseases of Poultry, ed. Saif YM, Fadly AM, Glisson JR, McDougald LR, Nolan LK, and Swayne DE, 12th ed., pp. 153–184. Blackwell Publishing Professional, Ames, IA, 2008.
86. Taylor W, Barrett T: Rinderpest and peste des petits ruminants. *In*: Diseases of Sheep, ed. Aitken I, 4th ed., pp. 460–469. Blackwell Publishing, Ames, IA, 2007.
87. Thompson D, Muriel P, Russell D, Osborne P, Bromley A, Rowland M, Creigh-Tyte S, Brown C: Economic costs of the foot and mouth disease outbreak in the United Kingdom in 2001. Rev Sci Tech **21:**675–687, 2002.
88. Thomson GR, Vosloo W, Bastos AD: Foot and mouth disease in wildlife. Virus Res **91:**145–161, 2003.
89. Tumpey TM, Suarez DL, Perkins LE, Senne DA, Lee JG, Lee YJ, Mo IP, Sung HW, Swayne DE: Characterization of a highly pathogenic H5N1 avian influenza A virus isolated from duck meat. J Virol **76:**6344–6355, 2002.
90. Uyeki TM: Global epidemiology of human infections with highly pathogenic avian influenza A (H5N1) viruses. Respirology **13**(Suppl 1):S2–S9, 2008.
91. Vaillancourt JP: Canadian experiences with avian influenza: a look at regional disease control—past, present, and future. Poult Sci **88:**885–891, 2009.
92. Valarcher JF, Leforban Y, Rweyemamu M, Roeder PL, Gerbier G, Mackay DK, Sumption KJ, Paton DJ, Knowles NJ: Incursions of foot-and-mouth disease virus into Europe between 1985 and 2006. Transbound Emerg Dis **55:**14–34, 2008.
93. Verwoerd D, Erasmus B: Bluetongue. *In*: Infectious Diseases of Livestock, ed. Coetzer JAW, 2nd ed., pp. 1201–1220. Oxford University Press, Oxford, UK, 2004.
94. Vosloo W, Bastos AD, Sangare O, Hargreaves SK, Thomson GR: Review of the status and control of foot and mouth disease in sub-Saharan Africa. Rev Sci Tech **21:**437–449, 2002.
95. Webster RG, Hulse DJ: Microbial adaptation and change: avian influenza. Rev Sci Tech **23:**453–465, 2004.
96. Wilkinson PJ, Lawman MJ, Johnston RS: African swine fever in Malta, 1978. Vet Rec **106:**94–97, 1980.
97. Wilson A, Mellor P: Bluetongue in Europe: vectors, epidemiology and climate change. Parasitol Res **103**(Suppl 1):S69–S77, 2008.
98. World Organization for Animal Health: Disease Timelines: Newcastle Disease. http://www.oie.int/wahis/public.php?page=disease_timelines&disease_type=Terrestrial&disease_id=16. Accessed July 31, 2009.
99. World Organization for Animal Health: Facts and Figures: Avian Influenza. http://www.oie.int/eng/info_ev/en_AI_factoids_2.htm. Accessed July 31, 2009.
100. World Organization for Animal Health: Summary of Immediate Notifications and Follow-Ups—2009: Foot and Mouth Disease. http://www.oie.int/wahis/public.php?page=disease_immediate_summary&disease_type=Terrestrial&disease_id=1. Accessed July 31, 2009.
101. World Organization for Animal Health: Summary of Immediate Notifications and Follow-Ups—2009: Highly Pathogenic Avian Influenza. http://www.oie.int/wahis/public.php?page=disease_immediate_summary&disease_type=Terrestrial&disease_id=15. Accessed July 31, 2009.

Return to Table of Contents

The Picornaviruses
Edited by Ellie Ehrenfeld, Esteban Domingo, and Raymond P. Roos

Chapter 25

Foot-and-Mouth Disease

MARVIN J. GRUBMAN, LUIS L. RODRIGUEZ, AND TERESA DE LOS SANTOS

INTRODUCTION

The Agent

Foot-and-mouth disease (FMD) is a highly infectious viral disease of domestic cloven-hoofed animals, including cattle, swine, goats, and sheep, as well as some species of wild animals (6). The viral agent, FMD virus (FMDV), is the type species of the *Aphthovirus* genus of the *Picornaviridae* family. FMDV is an antigenically variable virus consisting of seven serotypes (A, O, C, Asia 1, and South African Territories 1, 2, and 3 [SAT 1 to 3]) and multiple subtypes. Recently, two new members of the *Aphthovirus* genus, equine rhinitis A virus and bovine rhinovirus type 2, were identified (72, 73). FMDV contains a single-stranded, positive-sense RNA genome that codes for four structural and 10 nonstructural (NS) proteins (Fig. 1). The viral mRNA is translated into a polyprotein that is processed by virus-encoded proteinases L^{pro} and $3C^{pro}$, as well as the 18-amino-acid 2A peptide, into the mature structural and NS proteins (36, 80, 101, 138, 156). In addition, L^{pro} and $3C^{pro}$ also cleave a number of host cell proteins (19, 46, 54, 63, 154).

While all picornaviruses follow the same general replication strategy, each has a number of unique genomic features. Aphthoviruses and cardioviruses are the only members that contain an NS leader protein-coding region, L, which is located upstream of the capsid protein-coding region (Fig. 1). In addition, only aphthoviruses contain two in-frame AUG codons at the beginning of the polyprotein, potentially coding for two L proteins, Lab and Lb (beginning at the first or second AUG, respectively) (37, 72, 73), but studies by Cao et al. (29) suggest that the Lb protein of FMDV is the predominant form synthesized in vivo. The FMDV L^{pro} autocatalytically cleaves itself from the growing polypeptide, cleaves the translation initiation factor eukaryotic initiation factor 4G (eIF4G) (46, 80, 146), and either directly or indirectly cleaves the transcription factor nuclear factor κB (NF-κB) (44), while the cardiovirus L protein has no known proteolytic activity (120). Nevertheless, both of these L proteins play a significant role in evasion of the host cell innate immune response (66, 82,158) (see "Virulence Factors," below). Another major difference in the genome of FMDV compared to the other picornaviruses is the presence of multiple, nonidentical but highly conserved 3B-coding regions. Protein 3B, also termed VPg, is a small 23- to 24-amino-acid protein that is covalently linked to the 5′ end of virion RNA and plays a role in the initiation of RNA synthesis (64, 160).

The Disease

FMD is present in many areas of the world, including large parts of Africa and Asia and some countries in South America. The disease can be spread by direct animal contact, indirect contact via airborne transmission, or by contaminated material, including contaminated personnel, vehicles, and fomites (2). Infection mainly occurs by the respiratory tract through aerosolized virus but also through abrasions on the skin or in the mucous membranes. Airborne transmission can occasionally occur over long distances when climatic and meteorological conditions are appropriate (2). Studies have demonstrated that ruminants are more susceptible than pigs to infection by the respiratory route, while pigs excrete larger amounts of virus than cattle or sheep (2). Virus is also excreted in semen, urine, and feces, as well as the milk of lactating cows (6, 27). After slaughter the virus can remain infectious for quite some time in various tissues of the body, including bone marrow and lymph nodes if refrigerated, and in muscle if the fresh meat is rapidly frozen (6, 24). However, virus is inactivated during the process of postmortem acidification in meat (41).

Marvin J. Grubman, Luis L. Rodriguez, and Teresa de los Santos • Plum Island Animal Disease Center, North Atlantic Area, Agricultural Research Service, U.S. Department of Agriculture, Greenport, NY 11944.

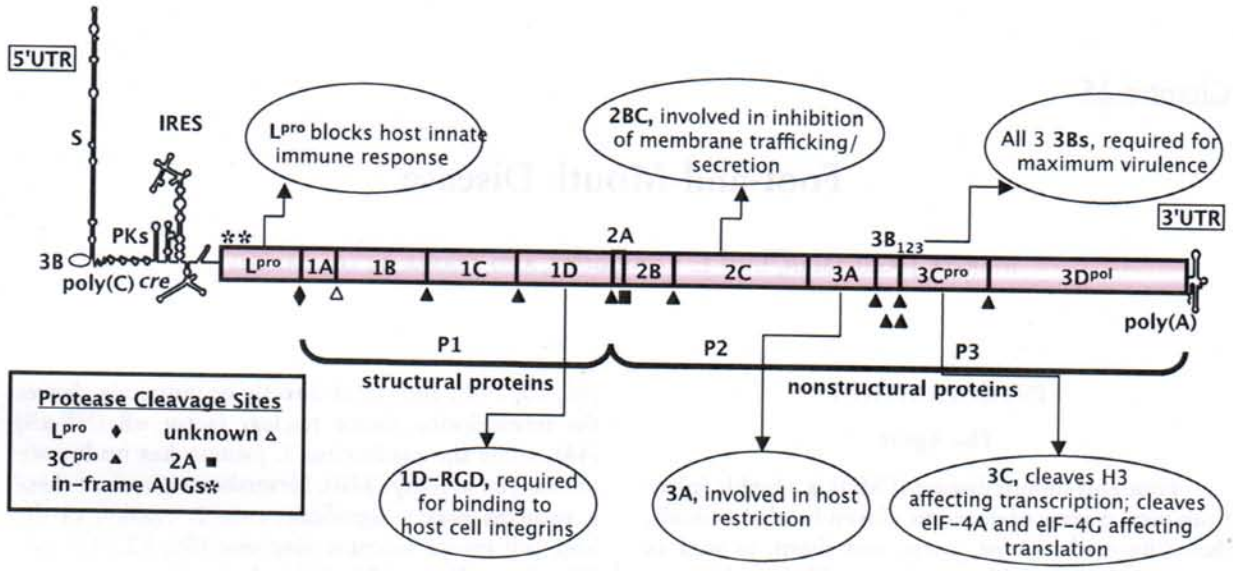

Figure 1. Schematic representation of the FMDV genome. The coding region of the genome is represented by shaded rectangles. Proteins that have been shown to be involved in the inhibition of host response, required for host receptor binding, and necessary for maximum virulence are indicated; their roles are further discussed in various sections of the text. PKs, pseudoknots.

FMDV rapidly replicates and spreads, and disease signs can appear within 2 to 3 days after exposure and can last for 7 to 10 days (65). The major consequence of FMD is a high degree of morbidity, including fever, lameness, and vesicular lesions on the tongue, feet, snout, and teats, but there is generally low mortality in infected animals except when the disease affects the young. For example, in the initial phase of the 1997 FMD outbreak in Taiwan, the fatality rate in suckling pigs was almost 100% (162). The disease has considerable debilitating effects, including weight loss, reduction in milk production, and loss of draught power, resulting in a loss of productivity. While cattle and pigs show overt clinical signs of disease, in sheep the disease may be mild and if lesions occur they are small and heal quickly, making it difficult to distinguish FMD from other common conditions (61). In goats the disease may even be milder (11). In addition, other vesicular diseases, including swine vesicular disease, vesicular stomatitis, and vesicular exanthema of swine, present very similar clinical disease signs, so that differential diagnosis may be challenging (6).

An important aspect of FMD is that following the acute phase of disease or after subclinical infection ruminants can become persistently infected, i.e., the carrier state, with no clinical signs (1, 142, 143). In addition, vaccinated ruminants exposed to live virus can also become persistently infected. The role of carrier animals in the spread of disease is controversial, but the presence of carrier animals has had a significant negative impact on the use of vaccination as part of the disease control strategy (see "Carrier State," below, and Chapter 20).

The initial site of infection is still somewhat unclear. Most studies suggest that the pharyngeal area, more specifically the dorsal soft palate, is the initial site of replication (2, 28), but other studies, including experiments using an attenuated strain of FMDV, have suggested that the lungs can also serve as a primary replication site after aerosol infection of cattle (25, 150) (see "Dissemination in the Host," below).

Disease Control

To control FMD outbreaks, countries initiate a number of measures, including culling of infected and in-contact susceptible animals, restriction of susceptible animal movement, and vaccination with a chemically inactivated whole virus. However, countries that had previously been FMD-free often hesitate to use vaccination to control an outbreak because of the difficulty in differentiating infected from vaccinated animals. To participate in international trade the World Organization for Animal Health requires countries to document serological evidence demonstrating the absence of FMDV-seropositive animals for 6 months after vaccination, but only for 3 months after slaughter. Therefore, the economic incentive for meat-exporting countries is not to vaccinate but to slaughter or to vaccinate and slaughter all vaccinated animals.

DISSEMINATION IN THE HOST

FMD affects a wide variety of cloven-hoofed animals, both domesticated and wild. Cattle, swine, sheep, and goats are the most economically important susceptible species, but over 70 species of wild animals, including deer, elk, antelope, impala, camel, llama, giraffe, and elephant, can also be affected (6).

Viral Entry

There have been extensive studies of the mechanism of FMDV entry into cells (see reference 65 and references therein). In tissue culture FMDV binds to four members of the α_v subgroup of cellular integrins, $\alpha_v\beta_1$, $\alpha_v\beta_3$, $\alpha_v\beta_6$, and $\alpha_v\beta_8$, via a highly conserved RGD motif located on the βG-βH loop of 1D (VP1) (Table 1) (14, 21, 22, 53, 76, 77, 107, 112). In addition to cellular integrins, FMDV is able to utilize other membrane-bound receptors. Antibody-complexed virus can bind to Fc receptors on macrophages, followed by internalization and viral replication (15, 93, 96). A recombinant artificial receptor expressing a single-chain monoclonal antibody against FMDV fused to the intracellular domain of intercellular adhesion molecule 1 can also be used by FMDV to attach, enter, and replicate in cells (128). However, the biological importance of the utilization of these alternative receptors remains to be determined. Some FMDV serotypes can be adapted to tissue culture by acquiring the ability of using cell surface heparan sulfate (HS) as a receptor (9, 75, 90, 107). Interestingly, these viruses display reduced virulence in host species (139). With respect to the mechanism of viral entry, studies in cells in culture expressing $\alpha_v\beta_6$ integrins have demonstrated that FMDV serotypes A, O, and C use clathrin-dependent endocytosis followed by acidification of endosomes that leads to capsid disassembly and release of viral RNA (22, 89, 112). O'Donnell et al. (111) showed that internalization of FMDV bound to the HS receptor involves caveola-mediated endocytosis, indicating that the mechanism of entry of FMDV into cells depends on specificity of receptor usage.

In vivo studies have demonstrated that in naïve cattle the $\alpha_v\beta_6$ integrin is expressed constitutively at high levels on the surface of epithelial cells in tissues susceptible to FMDV infection (26, 105, 113). Furthermore, this integrin is also expressed on the surface of FMDV-infected epithelial cells, suggesting that it acts as the major viral receptor and might be one of the determinants for viral tropism (105, 113). Monaghan et al. (105) did not detect expression of $\alpha_v\beta_3$ in epithelial cells at sites of lesion formation, while O'Donnell et al. (113) detected expression of this integrin in the epithelium of most FMDV-susceptible tissues except for the tongue. Both groups detected $\alpha_v\beta_3$ in endothelial cells of blood vessels, suggesting that this integrin may also play a role but as a secondary receptor, probably contributing to viral spread to secondary sites of infection (107, 113).

Early Events in Pathogenesis

In cattle the main route of infection is through the respiratory tract, while pigs are less susceptible to aerosol infection but are readily infected by direct contact with infected animals (2). A hallmark of most FMDV strains is the establishment of a viremia that follows replication at the primary site(s) and allows viral spread to selected tissues and development of clinical disease. A clear understanding of early events preceding the onset of viremia is relevant to development of effective preventive methods. However, despite many studies, consensus has not been reached as to the location of the primary sites(s) of replication. To attempt to simulate natural infection, investigators have used various methods of experimental exposure, including contact exposure, inoculation into the

Table 1. Integrin receptors for FMDV

Integrin	Recognition motif(s)	Tissue and cell distribution	FMDV receptor references	
			In vitro	In vivo
$\alpha_v\beta_1$	RGD	Malignant cells, smooth muscle, central nervous system	53, 76	
$\alpha_v\beta_3$	RGD, RLD/KRLDGS	Vascular endothelium, smooth muscle, osteoclasts, epithelial cells	21, 53, 107	107, 113
$\alpha_v\beta_6$	RGD	Epithelial cells	22, 53, 89, 112	26, 105, 113
$\alpha_v\beta_8$	RGD	Epithelial cells, human airways, central nervous system	77	

nasal cavity, aerosol exposure via a nebulizer within a chamber covering the head, direct nasal nebulization with a mask, etc. A significant factor in these studies is the size of the aerosol particles generated. Particles smaller than 3 μm in diameter are deposited in the lower respiratory tract, while particles of 3 to 6 μm in diameter are deposited in the middle and upper respiratory tracts (2, 118). Brown et al. (25) infected cattle by aerosol with a nebulizer (the authors did not mention the size of the particles generated) and found that within 24 h virus was detected in areas of the lung by in situ hybridization.

More recently Pacheco et al. (118) used aerosol exposure with a jet nebulizer (average size of particles, 5 μm in diameter) to infect cattle. At 24 h postinfection these authors found, by virus isolation, real-time reverse transcription-PCR, and immunohistochemistry, that the dorsal soft palate, the nasopharynx, and to a lesser extent the lungs are implicated as sites of early virus infection. The conflicting observations of these two studies may reflect the virus strain used, the size of the aerosols generated, etc. In recent experiments it was shown that in cattle exposed to infectious aerosols with a jet nebulizer, FMDV was first detected, by real-time reverse transcription-PCR and immunohistochemistry, in the nasopharynx at 6 h postexposure , followed by lung infection at 12 h and onset of viremia by 24 h postexposure (Color Plate 27) (4a). After 24 to 48 h postexposure the virus is distributed throughout the body, and although virus reaches all organs and tissues through the bloodstream, high-titer viral replication occurs only at sites where lesions appear, namely, the coronary bands of the hooves, the mouth (lips, tongue, and gums), the heart muscle, and the adrenal glands (137).

HOST IMMUNE RESPONSE

Immunosuppression

FMDV infection of susceptible animals results in an acute disease with a rapid induction of viremia by 1 to 3 days after infection that is correlated with a transient lymphopenia (12, 49). In swine most T-cell subsets as well as B cells are affected, and the functional capacity of T cells is significantly reduced in blood (12, 49) and secondary lymphoid organs (49). Similarly, Joshi et al. (78) recently reported that bovine T-cell subsets infected in vitro with FMDV serotypes A, O, or Asia are functionally impaired. Thus, FMDV infection rapidly induces a transient immune-depressed state in pigs and cattle, potentially providing favorable conditions for the virus to spread systemically and to be shed into the environment. T-cell numbers and function begin to return to normal levels 4 to 7 days postinfection. Evidence suggests that virus is cleared by phagocytosis of opsonized virus by 5 to 7 days postinfection (97, 98).

The mechanism of lymphocyte depletion is still unclear, but it is not the result of apoptosis. Bautista et al. (12), using three strains of FMDV serotype O, did not detect direct infection of swine T-cell subsets, while Diaz-San Segundo et al. (49) used FMDV serotype C and detected both the presence of viral NS proteins as well as active virus replication both in lymphocytes from infected pigs and in cell culture with peripheral blood mononuclear cells from naïve pigs. Joshi et al. (78) also found FMDV RNA and NS protein 3A after in vitro infection of lymphocytes isolated from naïve cattle with serotypes A, O, and Asia. It has been proposed that interleukin-10 (IL-10), a cytokine that has potent immunosuppressive functions in vivo, may be involved in the impaired activation of T cells in FMDV-infected swine (48, 116).

In spite of the lymphopenia, FMDV infection results in a rapid humoral response. An FMDV-specific neutralizing antibody response is detectable as early as 4 days postinfection and increases at 7 to 14 days. In general, protection induced by vaccination (50, 97) correlates with high levels of neutralizing antibodies and is serotype specific, although animals with low levels of neutralizing antibody can sometimes be protected (10). Borca et al. (23) and Ostrowski et al. (116, 117), using an adult mouse model system, demonstrated a rapid thymus-independent production of neutralizing antibody after infection with FMDV serotype O1 Campos. They reported that innate-like B cells located in the spleen were the main B-cell subset involved in the rapid production of protective antibodies (117). Additional research with naturally susceptible animals is necessary to understand the mechanism of immunosuppression FMDV has developed and to identify the viral protein(s) that participates in this process (see "Virulence Factors," below).

Interaction with Dendritic and Natural Killer Cells

As already mentioned, some vaccinated animals are protected from FMDV challenge even in the presence of low levels of neutralizing antibody, suggesting a role for cell-mediated immunity in protection. Until the past few years, however, very little was known about the interaction of FMDV with cells of the host innate immune system, except for reports of abortive in vitro infection of swine macrophages, especially in

the presence of antibodies (15, 131, 147). Recently a number of groups have examined the effect of FMDV infection on swine dendritic cells (DCs), which are the major antigen-presenting cells (13, 48, 70, 109). There are contradictory results regarding the ability of FMDV to infect DCs. Summerfield et al. (147) and Diaz-San Segundo et al. (48) demonstrated that in vitro FMDV can infect swine monocyte-derived DCs (MoDCs), but the infection is abortive. However, Nfon et al. (109) and Bautista et al. (13) did not detect infection of monocyte-derived or skin DCs in vitro, but virus exposure induced a strong alpha interferon (IFN-α) response.

In contrast, FMDV infection in vivo modulated the innate response by decreasing the secretion of IFN-α by both skin and MoDCs, but it did not affect the adaptive response, so that antigen uptake and processing were not compromised and expression of major histocompatibility complex (MHC) class II molecules and costimulatory molecules were maintained (48, 109). Diaz-San Segundo et al. (48) reported productive replication of FMDV serotype C in immature MoDCs in vitro and an increase in IL-10 production. While this cytokine has been shown to induce immunosuppression in vivo, it stimulates B-cell activation and proliferation (7). Cocultivation of MoDCs derived from FMDV-infected swine with T cells resulted in an inhibition of T-cell proliferation which could be reversed with antibody against IL-10. Furthermore, sera from FMDV-infected animals had increased levels of IL-10 compared to naïve animals (48). These authors suggested that IL-10 plays a critical role in impairing activation of T cells during acute infection and, in addition, promotes the activation and proliferation of virus-specific B cells and the production of neutralizing antibodies.

In vitro infection of plasmacytoid DCs, a class of DCs that can produce high levels of IFN-α, with FMDV was only detectable when complexed with FMDV-specific immune serum (70). The infection was abortive but resulted in the production of IFN-α.

Natural killer (NK) cells play an important role in the innate response against viral infections, but only recently have swine and bovine NK cells been partially characterized. The ability of FMDV to infect NK cells has not been examined, but the swine NK cell response declines soon after infection (58). In vitro studies by Toka et al. (155) demonstrated that swine NK cells stimulated with inflammatory cytokines induced efficient lysis of FMDV-infected target cells. Furthermore, they showed that cocultivation of NK cells with accessory cells, consisting of DCs as well as other cells, enhanced the killing activity of NK cells.

CARRIER STATE

History

FMDV, like several other vertebrate viruses, has developed mechanisms for long-term persistence in its natural hosts (see Chapter 20). Following the acute phase of infection in ruminants, some animals experience a long asymptomatic persistent infection, which can occur following clinical or subclinical infection in both vaccinated and nonvaccinated animals (1). Carrier animals are defined as those from which infectious virus can be recovered from the esophageal-pharyngeal fluids at 28 days or later after infection (151). For many years field observations suggested virus persistence in animals that had recovered from FMD, but it was not until 1959 that the presence of infectious virus was detected in saliva and esophageal-pharyngeal fluid from cattle that had recovered from FMD (157). Since then it has been widely demonstrated that a large proportion of ruminants continue to harbor infectious FMDV in their pharyngeal tissues for long periods of time and become chronic carriers. Whether these animals are infectious to others or not and the mechanisms mediating the establishment and maintenance of the persistent infection remain unclear and have been the subjects of much debate and extensive reviews (1, 106, 142, 148, 149 161).

Some authors have pointed out the need to make a distinction between persistently infected carriers, whose role as a source of infection to other animals remains unclear, and subclinically infected animals that show little or no clinical disease yet shed virus and have been clearly shown to be capable of transmission to susceptible animals (149). Here we only discuss carriers as the result of persistent infections. The carrier state has been well documented for cattle, African buffalo, and water buffalo and to a lesser extent in sheep and goats as well as a few other wild ruminant species (148). Pigs, however, clear the infection in 3 to 4 weeks, and virus is no longer detectable (1), except in one study in which viral RNA was detected in serum samples after 28 days postinfection (102).

Location of Persistent Virus

In cattle and buffalo, viral infection during persistence is associated with the nasopharyngeal region (38, 39, 47, 164). In cattle after aerosol or indirect contact exposure the virus initially replicates in the nasopharynx and lungs and subsequently generalizes through the bloodstream and increases to high titers at lesion sites in the feet and mouth (28, 150). After 2 weeks virus has cleared from blood and all

affected sites and infectious virus is only found in the nasopharynx associated with the basal layers of the epithelia (164). A recent study suggested that FMDV persists in the light zones of germinal centers in lymph nodes associated with the pharyngeal region (79). The authors proposed that FMDV maintained in a nonreplicating form at these sites serves as a source for the persistent infection. Further studies, utilizing new techniques, such as laser-capture microdissection, are needed to localize and characterize the cells associated with persistent infections.

Mechanism of Establishment and Maintenance of Carriers

Despite many years of research effort there is little conclusive evidence about the mechanisms mediating the establishment and maintenance of FMDV persistence. In contrast to other viruses for which well-defined mechanisms for establishing persistence have been described, such as herpes viruses and human immunodeficiency virus (115), no such mechanism has been identified for FMDV. Immune responses, both cellular and humoral, and cytokine responses have been suggested as critical components of the mechanisms of persistence. However, a recent study could not detect a difference in type I or type II IFNs in pharyngeal tissues of persistently or nonpersistently infected cattle (163). Alexandersen et al. (1) suggested that the immune status of the animal probably controls the level of virus replication, and those investigators have proposed two mechanisms for the development of persistence in the pharynx. One mechanism suggests that FMDV can infect immune system cells, such as macrophages, or other immunologically privileged sites, leading to evasion of the immune response. The second mechanism proposes that the virus exploits the host response to provide favorable intracellular conditions for long-term persistence, possibly by utilizing cytokine signaling.

Many hypotheses have been proposed about the clearance of persistent virus, but evidence suggests that cell-mediated immunity may be involved (32) (see Chapter 19). Studies on the innate immune response should help to define the mechanisms involved in persistence and possibly help develop methods to aid in its elimination (see Chapter 18).

Role of Carriers in Disease Spread, Control, and Eradication

The carrier state is characterized by asymptomatic low-level excretion of virus from the pharyngeal fluids. These fluids also contain neutralizing antibodies that attach to the virus and make virus isolation problematic (20). Therefore, it is difficult to envision persistently infected animals as sources of infection. In fact, transmission from persistently infected to naïve domestic animals has never been demonstrated under experimental conditions despite multiple attempts, including some with prolonged times of direct contact and immunosuppression of the carrier animals (100, 151). Only the African buffalo when infected with SAT virus has been shown to serve as a source of infection to naïve contact animals (3, 42, 159). The risk of transmission from carrier animals is difficult to estimate. However, the failure of multiple experiments to show transmission to susceptible animals suggests that carrier animals do not play a major role in FMDV transmission. On the other hand, inapparent or subclinical infections have played major roles in the dissemination of FMDV during outbreaks (148).

VIRULENCE FACTORS

Like many other viruses, FMDV must evoke multiple evasion mechanisms to overcome the nonspecific innate and the highly specific adaptive immune responses activated in the host upon viral infection. In addition to the high genetic variation (51), other mechanisms involving interaction of specific viral proteins or interactions of 5′ and 3′ untranslated regions (UTRs) with cellular targets have been shown to contribute to its virulence. With the exception of capsid protein 1A (VP4), which is not exposed on the virion surface, all the structural proteins are involved in interacting with the cellular receptor and are critical determinants of antigenicity (16). The NS proteins are involved in proteolytic processing as well as in other aspects of the replication cycle. A summary addressing the role of individual products or their precursors in virulence is discussed below (a synopsis is provided in Table 2).

L Protein

L^{pro} is encoded at the 5′ end of the viral polyprotein (132). Viral translation starts at two in-frame AUG codons separated by a stretch of 75 to 84 nucleotides (inter-AUG region), thus resulting in two forms of L^{pro}, Lab and Lb, that differ in length by 25 to 28 amino acids (37). It has been demonstrated that L^{pro} is a papain-like proteinase that cleaves itself, at the C terminus, from the growing polypeptide chain (62, 67, 81, 123, 146). Although Lab and Lb display similar activities in vitro (29, 101), Lb is the predominant protein synthesized in vivo, suggesting that this form of the protein is necessary and sufficient

Table 2. Summary of FMDV proteins that affect the host immune response

FMDV protein	Affected process	Mechanism
L^{pro}	Translation	Cleaves eIF4G
	Transcription	Directly or indirectly cleaves NF-κB
2B + 2C and/or 2BC	Secretion, membrane trafficking	May inhibit MHC class I surface expression and secretion of antiviral cytokines (no direct evidence)
3A	host tropism	Unknown
3B	Viral RNA replication	Primer for RNA synthesis
$3C^{pro}$	Transcription	Cleaves histone H3
VP1 (1D)[a]	Apoptosis	Deactivation of AKT pathway

[a] Overexpressed recombinant VP1 is responsible for this effect, but virus infection in vitro does not induce apoptosis.

for its function. Studies in vitro have proposed that the RNA sequence of the inter-AUG region, which is highly variable among all FMDV serotypes (31), may be an extension of the 5′ UTR and could be involved in start codon recognition possibly mediated by interaction with cellular factors (4, 29). A recent study has shown that insertion of 57 nucleotides within the inter-AUG sequence results in a virus variant that is attenuated in cattle, indicating that this region is an important determinant of virulence (121a).

L^{pro}-dependent inhibition of translation

L^{pro} is responsible for shutting off host protein synthesis, while viral internal ribosome entry site (IRES)-dependent mRNA translation is not affected (18, 46). The importance of this protein in virulence was demonstrated by studies of Mason et al. (95) and Chinsangaram et al. (34), which showed that an FMDV mutant lacking the L^{pro}-coding region (leaderless virus) (123) is highly attenuated in both cattle and swine. Leaderless FMDV does not spread from the initial site of inoculation and remains localized in the lungs when administered by aerosol (25). Furthermore, the reduced virulence of the leaderless virus correlates with the inability of this virus to block the host response to infection, in particular the synthesis of IFN protein (33, 35). In vitro studies have shown that after FMDV infection of BHK cells several proteins, including poly(A)-binding protein, polypyrimidine tract-binding protein (PTBP), and two subunits of the translation factor eIF3 (eIF3a and -b) undergo proteolytic cleavage (133). Although no direct involvement of L^{pro} has been demonstrated, cleavage of these factors may contribute to the shutoff of cellular translation observed during FMDV infection.

L^{pro}-dependent inhibition of transcription

L^{pro} affects transcription of IFN-β at early stages of FMDV infection (43). Transcription of IFN-β depends on the activation and assembly of specific transcription factors at the IFN-β promoter/enhancer in response to multiple stimuli, including viral infection (74). Among these transcription factors, NF-κB is activated by FMDV infection but subsequently degraded (44). Intact and active L^{pro} forms are required for this function (45) (Color Plate 28). Bioinformatic analysis revealed that L^{pro} contains a conserved protein domain, SAP, which is required for nuclear retention; mutation of the SAP domain results in viral attenuation with no NF-κB degradation (45) (Color Plate 29). Preliminary studies show that, in swine, the SAP mutant virus is attenuated but able to induce a significant neutralizing antibody response (F. Diaz-San Segundo et al., unpublished data).

2A, 2B, and 2C

In contrast to most picornaviruses, the P2 region of FMDV is processed into only two mature products, 2B and 2C, while 2A remains associated with the P1 structural protein precursor after autocatalytic processing (52, 138, 156). 2B and 2C are involved in inducing cytopathic effects and have been related to pathogenicity. It has been demonstrated that FMDV 2B and 2C, acting together, disrupt the secretory pathway and block the endoplasmic reticulum-to-Golgi complex transport, thereby affecting the delivery of proteins to the cell surface or the extracellular space (103, 104). This mechanism could explain the downregulation of surface expression of the major histocompatibility complex class I molecules observed in FMDV-infected epithelial cells (144). A decreased number of these molecules on the cell surface could prevent or limit viral peptide presentation and presumably delay the clearance of infected cells.

3A, 3B, and 3C

FMDV 3A encodes a protein of 153 amino acids, almost twice the size of its enteroviral counterpart. Attenuated strains containing deletions in the C-terminal region of 3A can be obtained by repeated passage of FMDV in chicken embryos (59, 60, 140).

A similar deletion was observed in the FMDV isolate (O/TAW/97) that caused a devastating FMD outbreak in Taiwan in 1997 in swine (17) but displayed reduced virulence in cattle and bovine-derived cells. Studies in vitro with bovine cells showed that infection with this mutant virus results in decreased amounts of viral RNA, while normal levels are obtained in swine cells, suggesting that 3A is involved in FMDV RNA replication (114). Involvement of 3A in the host range has also been shown by Nunez et al. (110), who reported that a single amino acid change in the 3A protein conferred adaptation to guinea pigs.

The FMDV 3B protein is unique in comparison to other picornaviruses because there are three copies in the viral genome (56). Viruses genetically manipulated to contain a reduced number of 3B-coding regions or altered amino acid sequences show lower levels of viral RNA replication with subsequent reduction of infective particle formation in cell culture (55). Moreover, viruses encoding only one copy of 3B have impaired replication in porcine and bovine cells and only cause mild disease in swine, suggesting that multiple copies of this protein are required for full virulence (119).

The 3C product is a viral proteinase ($3C^{pro}$) that is responsible for most of the cleavage of the viral polyprotein (5, 156). Grigera and Tisminetzky (66) reported that histone H3 was cleaved during FMDV infection; later, Falk et al. (54) and Tesar and Marquardt (154) showed that $3C^{pro}$ was involved in this process, thus constituting a virulence factor. Cleavage of histone H3 is consistent with the inhibition of host RNA synthesis during FMDV infection reported by Falk et al. (54). Although it is not clear how $3C^{pro}$, which is a cytoplasmic protein, can process a nuclear target, reports showing that the precursor 3ABC localizes to the perinuclear region (30) and that the precursor 3CD is found in the nucleus of infected cells (57) support this observation. $3C^{pro}$ has also been implicated in the cleavage of translation factors eIF4A and eIF4G, factors required for cap-dependent and IRES-dependent translation (19). Because cleavage is only partial, translation is not severely affected by this process.

Capsid Proteins

The capsid component 1D (VP1) mediates the interaction between FMDV and the primary cellular receptors, mainly integrins (see "Dissemination in the Host"). The highly conserved RGD amino acid sequence contained in the βG-βH loop of 1D determines viral binding to the integrin receptor, and mutation of this sequence results in viral particles that do not bind to permissive cultured cells nor cause disease in susceptible animals (86, 96, 99). There have been reports of viable type C viruses containing the RGGD sequence in the βG-βH loop that were isolated after challenging bovines previously immunized with a peptide vaccine (152, 153) and of viruses genetically engineered to contain an RGG sequence in the βG-βH loop that could infect cells with or without integrins or HS receptors; however, the abilities of these viruses to cause disease in susceptible animals have not been tested (8, 9). Viruses containing the SGD sequence in the cell receptor-binding site have been obtained after serial passages with a type A24 Cruzeiro virus by tongue inoculation of bovines (130). Inoculation of animals with the SGD virus resulted in clinical signs of FMD, with transmission to naïve steers and stability of the mutation. However, passage of this virus in tissue culture generated revertant viruses containing the RGD sequence that is present in wild-type viruses. These results indicated that FMDV could evolve with mutations in the RGD sequence of 1D as long as the mutation did not interfere with binding to the integrin receptor. Interestingly, an FMDV isolate adapted to utilize HS as the receptor contained a change, H56R, in the viral protein 1C (VP3) (75). However, there is no evidence that use of HS is involved in viral pathogenesis in the susceptible host, since no or only mild disease is observed after inoculation of cattle with this variant. Moreover, reversion to virulence correlates with compensatory mutations that remove the positive charge from the virion particle, and the mutants lose their ability to interact with HS in vitro and regain the ability to use integrins as the receptor (107, 139).

Expression of recombinant soluble FMDV capsid protein 1D has been associated with induction of apoptosis upon binding to the integrin receptor and signaling via the Akt pathway in cell culture (121). However, only limited evidence supports a role of apoptotic cell death in FMDV pathogenesis in swine (83). Induction of apoptosis in some tissues (spleen, lymph nodes, and heart) has been proposed as a secondary effect caused by the release of apoptogenic cytokines in response to FMDV infection and could explain the FMDV-induced myocarditis manifested particularly in young animals (68).

5′ and 3′ UTRs

The 5′ UTR of the FMDV genome is particularly long in comparison with other picornaviruses, containing more than 1,300 nucleotides and five functional elements (Fig. 1). The S fragment of approximately 360 nucleotides is capable of folding

into a long stem-loop (108). Although very limited information is available on the role of this fragment in virulence, by analogy with other picornaviruses it is predicted to be involved in viral replication (124). Recently, Lawrence and Rieder (85) reported that the cellular RNA helicase A (RHA) is part of a ribonucleoprotein complex that includes $3C^{pro}$ and specifically binds to the S fragment, suggesting that RHA plays a role in replication. Furthermore, RHA was shown to interact with viral NS proteins 3A and 2C. It is therefore expected that mutations of the S fragment region will affect FMDV virulence.

With respect to the poly(C) tract, some reports have suggested that the length of this region is important for viral pathogenesis (71), while other studies have demonstrated the opposite (40). Rieder et al. (129) were able to obtain viruses with essentially no poly(C) tract (containing only 2C residues), but the particle/PFU ratio was much higher than for viruses containing longer poly(C) tracts. Essentially no difference in the virulence of these viruses was found in inoculated mice (129); however, studies have not been performed in the natural host. Downstream of the poly(C) tract there is a pseudoknot region of unknown function (65), followed by a stem-loop structure likely to be the FMDV *cis*-acting replicative element (CRE). Mutation of the conserved AAACA motif in the FMDV CRE severely inhibits replication (94), but no studies have been performed in vivo to establish the role of CRE in viral pathogenesis.

The IRES element for aphthoviruses is similar to the cardiovirus IRES (group 2 IRESs) (18, 84) and comprises approximately 450 nucleotides that have been modeled into a five-domain structure (124). There is a polypyrimidine-rich region at the 3′ end, preceding the AUG initiation codon in the open reading frame. The PTBP interacts with at least two regions of the IRES (87, 126, 136), and deletion of this region abolished binding of PTBP and translation in vitro (88). It is known that the IRES-specific *trans*-acting factor 45 along with PTBP are required for translation of the FMDV genome (91, 126). Little is known about the role of the IRES in FMDV virulence; however, a virus with two mutations in the IRES region was rescued after repeated passage of a persistently infected BHK cell culture. This observation suggested that IRES modifications could affect virulence (92).

The 3′ UTR of FMDV contains about 100 nucleotides, folds into a specific stem-loop structure followed by a poly(A) tract of variable length (125), and appears important for genome replication (69, 127, 135). Deletion of the FMDV 3′ UTR reduces the efficiency of in vitro translation and blocks the ability to recover viable virus from transfected cells (141). Recent studies have proposed that the FMDV 3′ UTR folds into two stem-loops, SL1 and SL2 (145). Mutational analysis of this region showed that while deletion of SL1 was tolerated, resulting in viruses with slower growth kinetics and impaired negative-strand RNA synthesis, no virus could be recovered with genomes lacking SL2 (134). Nevertheless, insertion mutations within this region are tolerated, provided that the structures of SL1 and SL2 are maintained (122). These results suggested that the 3′ UTR of FMDV might contain a molecular determinant for virulence.

FUTURE DIRECTIONS

In the past few years a major emphasis in our attempt to understand the mechanisms of virus pathogenesis has been to study virus-host interactions at both the cellular and molecular levels. This has certainly been the case for FMDV, in which interactions of the virus with various components of the host innate and adaptive immune systems are being critically studied for the first time, and the role of viral proteins in the evasion of the host protective responses is being examined. However, as a result of the paucity of reagents for swine and bovine as well as the requirement of high-containment facilities to work with FMDV, the pace of investigation has not been as rapid as for other picornaviruses. As additional reagents become available, a number of areas will be examined in detail, including the initial interaction of the virus with the naturally susceptible host, a more comprehensive analysis of the mechanisms of immune evasion, the development and maintenance of the carrier state in ruminants, etc. At present, carrier animals still constitute one of the major obstacles hindering the use of vaccination by FMD-free countries to control an outbreak. Preventing or eliminating the carrier state should encourage countries to adopt a policy termed "vaccination-to-live." Additionally, despite recent advances in our understanding of FMDV immunopathogenesis, major challenges remain regarding the roles that different components of the immune response play in controlling viral infection. Finally, it is hoped that new information obtained from comprehensive viral pathogenesis studies will enable researchers to develop more effective disease control strategies, including induction of rapid protective responses to inhibit or at least limit the spread of this disease.

Acknowledgments. We thank Jonathan Arzt and Fayna Diaz-San Segundo for providing Color Plates 27 to 29 and also Fayna Diaz-San Segundo for critical reading of the manuscript.

REFERENCES

1. **Alexandersen, S., Z. Zhang, and A. I. Donaldson.** 2002. Aspects of persistence of foot-and-mouth disease virus in animals: the carrier problem. *Microbes Infect.* 4:1099–1110.
2. **Alexandersen, S., Z. Zhang, A. I. Donaldson, and A. J. M. Garland.** 2003. The pathogenesis and diagnosis of foot-and-mouth disease. *J. Comp. Pathol.* 129:1–36.
3. **Anderson, E. C.** 1986. Potential for the transmission of foot-and-mouth disease virus from African buffalo (*Syncerus caffer*) to cattle. *Res. Vet. Sci.* 40:278–280.
4. **Andreev, D. E., O. Fernandez-Miragall, J. Ramajo, S. E. Dmitriev, I. M. Terenin, E. Martinez-Salas, and I. N. Shatsky.** 2007. Differential factor requirement to assemble translation initiation complexes at the alternative start codons of foot-and-mouth disease virus. *RNA* 13:1–9.

4a. **Arzt, J., J. M. Pacheco, and L. L. Rodriguez.** The early pathogenesis of foot-and-mouth disease in cattle after aerosol inoculation: identification of the nasopharynx as the primary site of infection. *Vet. Pathol.*, in press.

5. **Bablanian, G. M., and M. J. Grubman.** 1993. Characterization of the foot-and-mouth disease virus 3C protease expressed in *Escherichia coli*. *Virology* 197:320–327.
6. **Bachrach, H. L.** 1968. Foot-and-mouth disease. *Annu. Rev. Microbiol.* 22:201–244.
7. **Balabanian, K., A. Foussat, L. Bouchet-Delbos, J. Couderc, R. Krzysiek, A. Amara, F. Baleux, A. Portier, P. Galanaud, and D. Emilie.** 2002. Interleukin-10 modulates the sensitivity of peritoneal B lymphocytes to chemokines with opposite effects on stromal cell-derived factor-1 and B-lymphocyte chemoattractant. *Blood* 99:427–436.
8. **Baranowski, E., C. M. Ruiz-Jarabo, N. Sevilla, D. Andreu, E. Beck, and E. Domingo.** 2000. Cell recognition by foot-and-mouth disease virus that lacks the RGD integrin-binding motif: flexibility in aphthovirus receptor usage. *J. Virol.* 74: 1641–1647.
9. **Baranowski, E., N. Sevilla, N. Verdaguer, C. M. Ruiz-Jarabo, E. Beck, and E. Domingo.** 1998. Multiple virulence determinants of foot-and-mouth disease virus in cell culture. *J. Virol.* 72:6362–6372.
10. **Barnett, P. V., and H. Carabin.** 2002. A review of emergency foot-and-mouth disease (FMD) vaccines. *Vaccine* 20:1505–1514.
11. **Barnett, P. V., and S. J. Cox.** 1999. The role of small ruminants in the epidemiology and transmission of foot-and-mouth disease. *Vet. J.* 158:6–13.
12. **Bautista, E. M., G. S. Ferman, and W. T. Golde.** 2003. Induction of lymphopenia and inhibition of T cell function during acute infection of swine with foot-and-mouth disease virus (FMDV). *Vet. Immunol. Immunopathol.* 92:61–73.
13. **Bautista, E. M., G. S. Ferman, D. Gregg, M. C. S. Brum, M. J. Grubman, and W. T. Golde.** 2005. Constitutive expression of alpha interferon by skin dendritic cells confers resistance to infection by foot-and-mouth disease virus. *J. Virol.* 79:4838–4847.
14. **Baxt, B., and Y. Becker.** 1990. The effect of peptides containing the arginine-glycine-aspartic acid sequence on the adsorption of foot-and-mouth disease virus to tissue culture cells. *Virus Genes* 4:73–83.
15. **Baxt, B., and P. W. Mason.** 1995. Foot-and-mouth disease virus undergoes restricted replication in macrophage cell cultures following Fc receptor-mediated endocytosis. *Virology* 207:503–509.
16. **Baxt, B., and E. Rieder.** 2004. Molecular aspects of foot-and-mouth disease virus virulence and host range: role of host cell receptors and viral factors, p. 145–172. *In* F. Sobrino and E. Domingo (ed.), *Foot and Mouth Disease: Current Perspectives*. Horizon Bioscience, Norfolk, England.
17. **Beard, C. W., and P. W. Mason.** 2000. Genetic determinants of altered virulence of Taiwanese foot-and-mouth disease virus. *J. Virol.* 74:987–991.
18. **Belsham, G. J., and J. K. Brangwyn.** 1990. A region of the 5′ noncoding region of foot-and-mouth disease virus RNA directs efficient internal initiation of protein synthesis within cells: involvement with the role of L protease in translational control. *J. Virol.* 64:5389–5395.
19. **Belsham, G. J., G. M. McInerney, and N. Ross-Smith.** 2000. Foot-and-mouth disease virus 3C protease induces cleavage of translation initiation factors eIF4A and eIF4G within U8 infected cells. *J. Virol.* 74:272–280.
20. **Bergmann, I. E., V. Malirat, P. Auge de Mello, and I. Gomes.** 1996. Detection of foot-and-mouth disease viral sequences in various fluids and tissues during persistence of the virus in cattle. *Am. J. Vet. Res.* 57:134–137.
21. **Berinstein, A., M. Roivainen, T. Hovi, P. W. Mason, and B. Baxt.** 1995. Antibodies to the vitronectin receptor (integrin αVβ3) inhibit binding and infection of foot-and-mouth disease virus to cultured cells. *J. Virol.* 69:2664–2666.
22. **Berryman, S., S. Clark, P. Monaghan, and T. Jackson.** 2005. Early events in integrin αVβ6-mediated cell entry of foot-and-mouth disease virus. *J. Virol.* 79:8519–8534.
23. **Borca, M. V., F. M. Fernandez, A. M. Sadir, M. Braun, and A. A. Schudel.** 1986. Immune response to foot-and-mouth disease virus in a murine experimental model: effective thymus-independent primary and secondary reaction. *Immunology* 59:261–267.
24. **Brooksby, J. B.** 1982. Portraits of viruses: foot-and-mouth disease virus. *Intervirology* 18:1–23.
25. **Brown, C. C., M. E. Piccone, P. W. Mason, T. S. McKenna, and M. J. Grubman.** 1996. Pathogenesis of wild-type and leaderless foot-and-mouth disease virus in cattle. *J. Virol.* 70:5638–5641.
26. **Brown, J. K., S. M. McAleese, E. M. Thornton, J. A. Pate, A. Schock, A. I. Macrae, P. R. Scott, H. R. Miller, and D. D. Collie.** 2006. Integrin-αvβ6, a putative receptor for foot-and-mouth disease virus, is constitutively expressed in ruminant airways. *J. Histochem. Cytochem.* 54:807–816.
27. **Burrows, R.** 1968. Excretion of foot-and-mouth disease prior to the development of lesions. *Vet. Rec.* 82:387–388.
28. **Burrows, R., J. A. Mann, A. J. Garland, A. Greig, and D. Goodridge.** 1981. The pathogenesis of natural and simulated natural foot-and-mouth disease infection in cattle. *J. Comp. Pathol.* 91:599–609.
29. **Cao, X., I. E. Bergmann, R. Fullkrug, and E. Beck.** 1995. Functional analysis of the two alternative translation initiation sites of foot-and-mouth disease virus. *J. Virol.* 69:560–563.
30. **Capozzo A. V., D. J. Burke, J. W. Fox, I. E. Bergmann, J. L. La Torre, and P. R. Grigera.** 2002. Expression of foot and mouth disease virus non-structural polypeptide 3ABC induces histone H3 cleavage in BHK21 cells. *Virus Res.* 90:91–99.
31. **Carrillo, C., E. R. Tulman, G. Delhon, Z. Lu, A. Carreno, A. Vagnozzi, G. F. Kutish, and D. L. Rock.** 2005. Comparative genomics of foot-and-mouth disease virus. *J. Virol.* 9:6487–6504.
32. **Childerstone, A. J., L. Cedillo-Baron, M. Foster-Cuevas, and R. M. Parkhouse.** 1999. Demonstration of bovine $CD8^+$ T-cell responses to foot-and-mouth disease virus. *J. Gen. Virol.* 80: 663–669.
33. **Chinsangaram, J., M. Koster, and M. J. Grubman.** 2001. Inhibition of L-deleted foot-and-mouth disease virus replication by alpha/beta interferon involves double-stranded RNA-dependent protein kinase. *J. Virol.* 12:5498–5503.

34. **Chinsangaram, J., P. W. Mason, and M. J. Grubman.** 1998. Protection of swine by live and inactivated vaccines prepared from a leader proteinase-deficient serotype A12 foot-and-mouth disease virus. *Vaccine* **16**:1516–1522.
35. **Chinsangaram, J., M. E. Piccone, and M. J. Grubman.** 1999. Ability of foot-and-mouth disease virus to form plaques in cell culture is associated with suppression of alpha/beta interferon. *J. Virol.* **73**:9891–9898.
36. **Clarke, B. E., and D. V. Sangar.** 1988. Processing and assembly of foot-and-mouth disease virus proteins using subgenomic RNA. *J. Gen. Virol.* **69**:2313–2325.
37. **Clarke, B. E., D. V. Sangar, J. N. Burroughs, S. E. Newton, A. R. Carroll, and D. J. Rowlands.** 1985. Two initiation sites for foot-and-mouth disease virus polyprotein in vivo. *J. Gen. Virol.* **66**:2615–2626.
38. **Condy, J. B., and R. S. Hedger.** 1974. The survival of foot-and-mouth disease virus in African buffalo with non-transference of infection to domestic cattle. *Res. Vet. Sci.* **16**:182–185.
39. **Condy, J. B., R. S. Hedger, C. Hamblin, and I. T. Barnett.** 1985. The duration of the foot-and-mouth disease virus carrier state in African buffalo (i) in the individual animal and (ii) in a free-living herd. *Comp. Immunol. Microbiol. Infect. Dis.* **8**: 259–265.
40. **Costa Giomi, M. P., I. E. Bergmann, E. A. Scodeller, P. Auge de Mello, L. Gomez, and J. L. La Torre.** 1984. Heterogeneity of the polyribocytidylic acid tract in aphthovirus: biochemical and biological studies of viruses carrying polyribocytidylic acid tracts of different lengths. *J. Virol.* **51**:799–805.
41. **Cottral, G. E., B. F. Cox, and D. E. Baldwin.** 1960. The survival of FMDV in cured and uncured meat. *Am. J. Vet. Res.* **21**: 288–297.
42. **Dawe, P. S., K. Sorensen, N. P. Ferris, I. T. Barnett, R. M. Armstrong, and N. J. Knowles.** 1994. Experimental transmission of foot-and-mouth disease virus from carrier African buffalo (*Syncerus caffer*) to cattle in Zimbabwe. *Vet. Rec.* **134**:211–215.
43. **de los Santos, T., S. de Avila Botton, R. Weiblen, and M. J. Grubman.** 2006. The leader proteinase of foot-and-mouth disease virus inhibits the induction of beta interferon mRNA and blocks the host innate immune response. *J. Virol.* **80**:1906–1914.
44. **de los Santos, T., F. Diaz-San Segundo, and M. J. Grubman.** 2007. Degradation of nuclear factor kappa B during foot-and-mouth disease virus infection. *J. Virol.* **81**:12803–12815.
45. **de los Santos, T., F. Diaz-San Segundo, J. Zhu, M. Koster, C. C. Dias, and M. J. Grubman.** 2009. A conserved domain in the leader proteinase of foot-and-mouth disease virus is required for proper subcellular localization and function. *J. Virol.* **83**: 1800–1810.
46. **Devaney, M. A., V. N. Vakharia, R. E. Lloyd, E. Ehrenfeld, and M. J. Grubman.** 1988. Leader protein of foot-and-mouth disease virus is required for cleavage of the p220 component of the cap-binding protein complex. *J. Virol.* **62**:4407–4409.
47. **Dhennin, L., G. Gayot, and L. Dhennin.** 1967. Test of the pharyngeal curette in the study of carriers of aphthae virus. *Bull. Acad. Vet. Fr.* **40**:59–65. (In Italian.)
48. **Diaz-San Segundo, F., T. Rodriguez-Calvo, A. de Avila, and N. Sevilla.** 2009. Immunosuppression during acute infection with foot-and-mouth disease virus in swine is mediated by IL-10. *PLoS One* **4**:e5659.
49. **Diaz-San Segundo, F., F. J. Salguero, A. de Avila, M. M. de Marco, M. A. Sanchez-Martin, and N. Sevilla.** 2006. Selective lymphocyte depletion during the early stage of the immune response to foot-and-mouth disease virus infection in swine. *J. Virol.* **80**:2369–2379.
50. **Doel, T. R.** 2005. Natural and vaccine induced immunity to FMD. *Curr. Top. Microbiol. Immunol.* **288**:103–131.
51. **Domingo, E., C. Escarmis, E. Baronowski, C. M. Ruiz-Jarabo, E. Carrillo, J. I. Nuñez, and F. Sobrino.** 2003. Evolution of foot-and-mouth disease virus. *Virus Res.* **91**:47–63.
52. **Donnelly, M. L., G. Luke, A. Mehrotra, X. Li, L. E. Hughes, D. Gani, and M. D. Ryan.** 2001. Analysis of the aphthovirus 2A/2B polyprotein 'cleavage' mechanism indicates not a proteolytic reaction, but a novel translational effect: a putative ribosomal 'skip.' *J. Gen. Virol.* **82**:1013–1025.
53. **Duque, H., and B. Baxt.** 2003. Foot-and-mouth disease virus receptors: comparison of bovine α_v integrin utilization by type A and O viruses. *J. Virol.* **77**:2500–2511.
54. **Falk, M. M., P. R. Grigera, I. E. Bergmann, A. Zibert, G. Multhaup, and E. Beck.** 1990. Foot-and-mouth disease virus protease 3C induces specific proteolytic cleavage of host cell histone H3. *J. Virol.* **64**:748–756.
55. **Falk, M. M., F. Sobrino, and E. Beck.** 1992. VPg gene amplification correlates with infective particle formation in foot-and-mouth disease virus. *J. Virol.* **66**:2251–2260.
56. **Forss, S., and H. Schaller.** 1982. A tandem repeat gene in a picornavirus. *Nucleic Acids Res.* **10**:6441–6450.
57. **García-Briones, M., M. F. Rosas, M. González-Magaldi, M. A. Martín-Acebes, F. Sobrino, and R. Arma-Portela.** 2006. Differential distribution of non-structural proteins of foot-and-mouth disease virus in BHK-21 cells. *Virology* **349**:409–421.
58. **Geering, W. A.** 1967. Foot and mouth disease in sheep. *Aust. Vet. J.* **43**:485–489.
59. **Giraudo, A. T., E. Beck, K. Strebel, P. A. de Mello, J. L. La Torre, E. A. Scodeller, and I. E. Bergmann.** 1990. Identification of a nucleotide deletion in parts of polypeptide 3A in two independent attenuated aphthovirus strains. *Virology* **177**: 780–783.
60. **Giraudo, A. T., A. Sagedahl, I. E. Bergmann, J. L. La Torre, and E. A. Scodeller.** 1987. Isolation and characterization of recombinants between attenuated and virulent aphthovirus strains. *J. Virol.* **61**:419–425.
61. **Golde, W. T., C. K. Nfon, and F. N. Toka.** 2008. Immune evasion during foot-and-mouth disease virus infection of swine. *Immunol. Rev.* **225**:85–95.
62. **Gorbalenya, A. E., E. V. Koonin, and M. M. Lai.** 1991. Putative papain related thiol proteases of positive-strand RNA viruses. Identification of rubi- and aphthovirus proteases and delineation of a novel conserved domain associated with proteases of rubi-, alpha- and coronaviruses. *FEBS Lett.* **288**:201–205.
63. **Grigera, P. R., and S. G. Tisminetzky.** 1984. Histone H3 modification in BHK cells infected with foot-and-mouth disease virus. *Virology* **136**:10–19.
64. **Grubman, M. J.** 1980. The 5′ end of foot-and-mouth disease virion RNA contains a protein covalently linked to the nucleotide pUp. *Arch. Virol.* **63**:311–315.
65. **Grubman, M. J., and B. Baxt.** 2004. Foot-and-mouth disease. *Clin. Microbiol. Rev.* **17**:465–493.
66. **Grubman, M. J., M. P. Moraes, F. Diaz-San Segundo, L. Pena, and T. de los Santos.** 2008. Evading the host immune response: how foot-and-mouth disease virus has become an effective pathogen. *FEMS Immunol. Med. Microbiol.* **53**:8–17.
67. **Guarne, A., J. Tormo, R. Kirchweger, D. Pfistermueller, I. Fita, and T. Skern.** 1998. Structure of the foot-and-mouth disease virus leader protease: a papain-like fold adapted for self-processing and eIF4G recognition. *EMBO J.* **17**:7469–7479.
68. **Gulbahar, M. Y., W. C. Davis, T. Guvenc, M. Yarim, U. Parlak, and Y. B. Kabak.** 2007. Myocarditis associated with foot-and-mouth disease virus type O in lambs. *Vet. Pathol.* **44**:589–599.

69. **Gutierrez, A., E. Martinez-Salas, B. Pintado, and F. Sobrino.** 1994. Specific inhibition of aphthovirus infection by RNAs transcribed from both the 5′ and the 3′ noncoding regions. *J. Virol.* **68**:7426–7432.
70. **Guzylack-Piriou, L., F. Bergamin, M. Gerber, K. C. MuCullough, and A. Summerfield.** 2006. Plasmacytoid dendritic cell activation by foot-and-mouth disease virus requires immune complexes. *Eur. J. Immunol.* **36**:1674–1683.
71. **Harris, T. J., and F. Brown.** 1977. Biochemical analysis of a virulent and an avirulent strain of foot-and-mouth disease virus. *J. Gen. Virol.* **34**:87–105.
72. **Hinton, T. M., F. Li, and B. S. Crabb.** 2000. Internal entry site-mediated translation initiation in equine rhinitis A virus: similarities to and differences from that of foot-and-mouth disease virus. *J. Virol.* **74**:11708–11716.
73. **Hollister, J. R., A. Vagnozzi, N. J. Knowles, and E. Rieder.** 2008. Molecular and phylogenetic analysis of bovine rhinovirus type 2 shows it is closely related to foot-and-mouth disease virus. *Virology* **373**:411–425.
74. **Honda, K., H. Yanai, A. Takaoka, and T. Taniguchi.** 2006. Regulation of the type I IFN induction: a current view. *Int. Immunol.* **17**:1367–1378.
75. **Jackson, T., F. M. Ellard, R. A. Ghazaleh, S. M. Brookes, W. E. Blakemore, A. H. Corteyn, D. I. Stuart, J. W. Newman, and A. M. King.** 1996. Efficient infection of cells in culture by type O foot-and-mouth disease virus requires binding to cell surface heparan sulfate. *J. Virol.* **70**:5282–5287.
76. **Jackson, T., A. P. Mould, D. Sheppard, and A. M. King.** 2002. Integrin αVβ1 is a receptor for foot-and-mouth disease virus. *J. Virol.* **76**:935–941.
77. **Jackson, T., S. Clark, S. Berryman, A. Burman, S. Cambier, D. Mu, S. Nishimura, and A. M. King.** 2004. Integrin αVβ8 functions as a receptor for foot-and-mouth disease virus: role of the β-chain cytodomain in integrin-mediated infection. *J. Virol.* **78**:4533–4540.
78. **Joshi, G., R. Sharma, and N. K. Kakker.** 2009. Phenotypic and functional characterization of T cells and in vitro replication of FMDV serotypes in bovine lymphocytes. *Vaccine* **27**:6656–6661.
79. **Juleff, N., M. Windsor, E. Reid, J. Seago, Z. Zhang, P. Monaghan, I. W. Morrison, and B. Charleston.** 2008. Foot-and-mouth disease virus persists in the light zone of germinal centres. *PLoS One* **3**:e3434.
80. **Kirchweger, R., E. Ziegler, B. J. Lamphear, D. Waters, H. D. Liebig, W. Sommergruber, F. Sobrino, C. Hohenadl, D. Blaas, R. E. Rhoads, and T. Skern.** 1994. Foot-and-mouth disease virus leader proteinase: purification of the Lb form and determination of its cleavage site on eIF-4 gamma. *J. Virol.* **68**:5677–5684.
81. **Kleina, L. G., and M. J. Grubman.** 1992. Antiviral effects of a thiol protease inhibitor on foot-and-mouth disease virus. *J. Virol.* **66**:7168–7175.
82. **Kong, W.-P., G. D. Ghadge, and R. P. Roos.** 1994. Involvement of cardiovirus leader in host cell-restricted virus expression. *Proc. Natl. Acad. Sci. USA* **91**:1796–1800.
83. **Ku, B. K., S. B. Kim, O. K. Moon, S. J. Lee, J. H. Lee, Y. S. Lyoo, H. J. Kim, and J. H. Sur.** 2005. Role of apoptosis in the pathogenesis of Asian and South American foot-and-mouth disease viruses in swine. *J. Vet. Med. Sci.* **67**:1081–1088.
84. **Kuhn, R., N. Luz, and E. Beck.** 1990. Functional analysis of the internal translation initiation site of foot-and-mouth disease virus. *J. Virol.* **64**:4625–4631.
85. **Lawrence, P., and E. Rieder.** 2009. Identification of RNA helicase A (RHA) as a new host factor in the replication cycle of foot-and-mouth disease virus. *J. Virol.* **83**:11356–11366.
86. **Leippert, M., E. Beck, F. Weiland, and E. Pfaff.** 1997. Point mutations within the βG-βH loop of foot-and-mouth disease virus O1K affect virus attachment to target cells. *J. Virol.* **71**:1046–1051.
87. **Luz, N., and E. Beck.** 1990. A cellular 57 kDa protein binds to two regions of the internal translation site of foot-and-mouth disease virus. *FEBS Lett.* **269**:311–314.
88. **Luz, N., and E. Beck.** 1991. Interaction of a cellular 57-kilodalton protein with the internal translation initiation site of foot-and-mouth disease virus. *J. Virol.* **65**:6486–6494.
89. **Martin-Acebes, M. A., M. Gonzalez-Magaldi, K. Sandvig, F. Sobrino, and R. Armas-Portela.** 2007. Productive entry of type C foot-and-mouth disease virus into susceptible cultured cells requires clathrin and is dependent on the presence of plasma membrane cholesterol. *Virology* **369**:105–118.
90. **Martinez, M. A., N. Verdaguer, M. G. Mateu, and E. Domingo.** 1997. Evolution subverting essentiality: dispensability of the cell attachment Arg-Gly-Asp motif in multiply passaged foot-and-mouth disease virus. *Proc. Natl. Acad. Sci. USA* **94**:6798–6802.
91. **Martinez-Salas, E., R. Ramos, E. Lafuente, and S. Lopez de Quinto.** 2001. Functional interactions in internal translation initiation directed by viral and cellular IRES elements. *J. Gen. Virol.* **82**:973–984.
92. **Martinez-Salas, E., J. C. Saiz, M. Davila, G. J. Belsham, and E. Domingo.** 1993. A single nucleotide substitution in the internal ribosome entry site of foot-and-mouth disease virus leads to enhanced cap-independent translation in vivo. *J. Virol.* **67**:3748–3755.
93. **Mason, P. W., B. Baxt, F. Brown, J. Harber, A. Murdin, and E. Wimmer.** 1993. Antibody-complexed foot-and-mouth disease virus, but not poliovirus, can infect normally insusceptible cells via the Fc receptor. *Virology* **192**:568–577.
94. **Mason, P. W., S. V. Bezborodova, and T. M. Henry.** 2002. Identification and characterization of a *cis* -acting replication element (cre) adjacent to the internal ribosome entry site of foot-and-mouth disease virus. *J. Virol.* **76**:9686–9694.
95. **Mason, P. W., M. E. Piccone, T. S. McKenna, J. Chinsangaram, and M. J. Grubman.** 1997. Evaluation of a live-attenuated foot-and-mouth disease virus as a vaccine candidate. *Virology* **227**:96–102.
96. **Mason, P. W., E. Rieder, and B. Baxt.** 1994. RGD sequence of foot-and-mouth disease virus is essential for infecting cells via the natural receptor but can by bypassed by an antibody-dependent enhancement pathway. *Proc. Natl. Acad. Sci. USA* **91**:1932–1936.
97. **McCullough, K. C., F. de Simone, E. Brocchi, L. Capucci, J. R. Crowther, and U. Kihm.** 1992. Protective immune response against foot-and-mouth disease. *J. Virol.* **66**:1835–1840.
98. **McCullough, K. C., D. Parkinson, and J. R. Crowther.** 1988. Opsonization-enhanced phagocytosis of foot-and-mouth disease virus. *Immunology* **65**:187–191.
99. **McKenna, T. S., J. Lubroth, E. Rieder, B. Baxt, and P. W. Mason.** 1995. Receptor binding site-deleted foot-and-mouth disease (FMD) virus protects cattle from FMD. *J. Virol.* **69**:5787–5790.
100. **McVicar, J. W., and P. Sutmoller.** 1969. The epizootiological importance of foot-and-mouth disease carriers. II. The carrier status of cattle exposed to foot-and-mouth disease following vaccination with an oil adjuvant inactivated virus vaccine. *Arch. Gesamte Virusforsch.* **26**:217–224.
101. **Medina, M., E. Domingo, J. K. Brangwyn, and G. J. Belsham.** 1993. The two species of the foot-and-mouth disease virus leader protein, expressed individually, exhibit the same activities. *Virology* **194**:355–359.

102. **Mezencio, J. M., G. D. Babcock, E. Kramer, and F. Brown.** 1999. Evidence for the persistence of foot-and-mouth disease virus in pigs. *Vet. J.* **157**:213–217.
103. **Moffat, K., G. Howell, C. Knox, G. J. Belsham, P. Monaghan, M. D. Ryan, and T. Wileman.** 2005. Effects of foot-and-mouth disease virus nonstructural proteins on the structure and function of the early secretory pathway: 2BC but not 3A blocks endoplasmic reticulum-to-Golgi transport. *J. Virol.* **79**:4382–4395.
104. **Moffat, K., C. Knox, G. Howell, S. J. Clark, H. Yang, G. J. Belsham, M. Ryan, and T. Wileman.** 2007. Inhibition of the secretory pathway by foot-and-mouth disease virus 2BC protein is reproduced by coexpression of 2BC with 2C, and the site of inhibition is determined by the subcellular location of 2C. *J. Virol.* **81**:1129–1139.
105. **Monaghan, P., S. Gold, J. Simpson, Z. Zhang, P. H. Weinreb, S. M. Violette, S. Alexandersen, and T. Jackson.** 2005. The $\alpha_v\beta_6$ integrin receptor for foot-and-mouth disease virus is expressed constitutively on the epithelial cells targeted in cattle. *J. Gen. Virol.* **86**:2769–2780.
106. **Moonen, P., and R. Schrijver.** 2000. Carriers of foot-and-mouth disease virus: a review. *Vet. Q.* **22**:193–197.
107. **Neff, S., D. Sa-Carvalho, E. Rieder, P. W. Mason, S. D. Blystone, E. J. Brown, and B. Baxt.** 1998. Foot-and-mouth disease virus virulent for cattle utilizes the integrin $\alpha_v\beta_3$ as its receptor. *J. Virol.* **72**:3587–3594.
108. **Newton, S. E., A. R. Carroll, R. O. Campbell, B. E. Clarke, and D. J. Rowlands.** 1985. The sequence of foot-and-mouth disease virus RNA to the 5′ side of the poly(C) tract. *Gene* **40**:331–336.
109. **Nfon, C. K., G. S. Ferman, F. N. Toka, D. A. Gregg, and W. T. Golde.** 2008. Interferon-α production by swine dendritic cells is inhibited during acute infection with foot-and-mouth disease virus. *Viral Immunol.* **21**:68–77.
110. **Nunez, J. I., E. Baranowski, N. Molina, C. M. Ruiz-Jarabo, C. Sanchez, E. Domingo, and F. Sobrino.** 2001. A single amino acid substitution in nonstructural protein 3A can mediate adaptation of foot-and-mouth disease virus to the guinea pig. *J. Virol.* **75**:3977–3983.
111. **O'Donnell, V., M. LaRocco, and B. Baxt.** 2008. Heparan sulfate-binding foot-and-mouth disease virus enters cells via caveola-mediated endocytosis. *J. Virol.* **82**:9075–9085.
112. **O'Donnell, V., M. LaRocco, H. Duque, and B. Baxt.** 2005. Analysis of foot-and-mouth disease virus internalization events in cultured cells. *J. Virol.* **79**:8506–8518.
113. **O'Donnell, V., J. M. Pacheco, D. Gregg, and B. Baxt.** 2009. Analysis of foot-and-mouth disease virus integrin receptor expression in tissues from naïve and infected cattle. *J. Comp. Pathol.* **141**:98–112.
114. **O'Donnell, V. K., J. M. Pacheco, T. M. Henry, and P. W. Mason.** 2001. Subcellular distribution of the foot-and-mouth disease virus 3A protein in cells infected with viruses encoding wild-type and bovine-attenuated forms of 3A. *Virology* **287**:151–162.
115. **Oldstone, M. B. A.** 1991. Molecular anatomy of viral persistence. *J. Virol.* **65**:6381–6386.
116. **Ostrowski, M., M. Vermeulen, O. Zabal, J. R. Geffner, A. M. Sadir, and O. J. Lopez.** 2005. Impairment of thymus-dependent responses by murine dendritic cells infected with foot-and-mouth disease virus. *J. Immunol.* **175**:3971–3979.
117. **Ostrowski, M., M. Vermeulen, O. Zabal, P. I. Zamorano, A. M. Sadir, J. R. Geffner, and O. J. Lopez.** 2007. The early protective thymus-independent antibody response to foot-and-mouth disease virus is mediated by splenic $CD9^+$ B lymphocytes. *J. Virol.* **81**:9357–9367.
118. **Pacheco, J. M., J. Arzt, and L. L. Rodriguez.** 2010. Early events in the pathogenesis of foot-and-mouth disease in cattle after controlled aerosol exposure. *Vet. J.* **183**:46–53.
119. **Pacheco, J. M., T. M. Henry, V. K. O'Donnell, J. B. Gregory, and P. W. Mason.** 2003. Role of nonstructural proteins 3A and 3B in host range and pathogenicity of foot-and-mouth disease virus. *J. Virol.* **77**:13017–13027.
120. **Parks, G. D., G. M. Duke, and A. C. Palmenberg.** 1986. Encephalomyocarditis virus 3C protease: efficient cell-free expression from clones which link viral 5′ noncoding sequences to the P3 region. *J. Virol.* **60**:376–384.
121. **Peng, J. M., S. M. Liang, and C. M. Liang.** 2004. VP1 of foot-and-mouth disease virus induces apoptosis via the Akt signaling pathway. *J. Biol. Chem.* **279**:52168–52174.
121a. **Piccone, M. E., J. M. Pacheco, S. J. Pauszek, E. Kramer, E. Rieder, M. V. Borca, and L. L. Rodriguez.** 2009. The region between the two polyprotein initiation codons of foot-and-mouth disease virus is critical for virulence in cattle. *Virology* **396**:152–159.
122. **Piccone, M. E., S. Pauszek, J. Pacheco, E. Rieder, E. Kramer, and L. L. Rodriguez.** 2009. Molecular characterization of a foot-and-mouth disease virus containing a 57-nucleotide insertion in the 3′ untranslated region. *Arch. Virol.* **154**:671–676.
123. **Piccone, M. E., E. Rieder, P. W. Mason, and M. J. Grubman.** 1995. The foot-and-mouth disease virus leader proteinase gene is not required for viral replication. *J. Virol.* **69**:5376–5382.
124. **Pilipenko, E. V., V. M. Blinov, B. K. Chernov, T. M. Dmitrieva, and V. I. Agol.** 1989. Conservation of the secondary structure elements of the 5′-untranslated region of cardio- and aphthovirus RNAs. *Nucleic Acids Res.* **17**:5701–5711.
125. **Pilipenko, E. V., S. V. Maslova, A. N. Sinyakov, and V. I. Agol.** 1992. Towards identification of *cis*-acting elements involved in the replication of enterovirus and rhinovirus RNAs: a proposal for the existence of tRNA-like terminal structures. *Nucleic Acids Res.* **20**:1739–1745.
126. **Pilipenko, E. V., T. V. Pestova, V. G. Kolupaeva, E. V. Khitrina, A. N. Poperechnaya, V. I. Agol, and C. U. Hellen.** 2000. A cell cycle-dependent protein serves as a template-specific translation initiation factor. *Genes Dev.* **14**:2028–2045.
127. **Pilipenko, E. V., K. V. Poperechny, S. V. Maslova, W. J. Melchers, H. J. Slot, and V. I. Agol.** 1996. *cis*-element, oriR, involved in the initiation of (-) strand poliovirus RNA: a quasi-globular multi-domain RNA structure maintained by tertiary ('kissing') interactions. *EMBO J.* **15**:5428–5436.
128. **Rieder, E., A. Berinstein, B. Baxt, A. Kang, and P. W. Mason.** 1996. Propagation of an attenuated virus by design: engineering a novel receptor for a noninfectious foot-and-mouth disease virus. *Proc. Natl. Acad. Sci. USA* **93**:10428–10433.
129. **Rieder, E., T. Bunch, F. Brown, and P. W. Mason.** 1993. Genetically engineered foot-and-mouth disease viruses with poly(C) tracts of two nucleotides are virulent in mice. *J. Virol.* **67**:5139–5145.
130. **Rieder, E., T. Henry, H. Duque, and B. Baxt.** 2005. Analysis of a foot-and-mouth disease virus type A24 isolate containing an SGD receptor recognition site in vitro and its pathogenesis in cattle. *J. Virol.* **79**:12989–12998.
131. **Rigden, R. C., C. P. Carrasco, A. Summerfield, and K. C. McCullough.** 2002. Macrophage phagocytosis of foot-and-mouth disease virus may create infectious carriers. *Immunology* **106**:537–548.
132. **Robertson, B. H., M. J. Grubman, G. N. Weddell, D. M. Moore, J. D. Welsh, T. Fischer, D. J. Dowbenko, D. G. Yansura, B. Small, and D. G. Kleid.** 1985. Nucleotide and amino

acid sequence coding for polypeptides of foot-and-mouth disease virus type A12. *J. Virol.* **54**:651–660.

133. **Rodríguez Pulido, M., P. Serrano, M. Sáiz, and E. Martínez-Salas.** 2007. Foot-and-mouth disease virus infection induces proteolytic cleavage of PTB, eIF3a,b, and PABP RNA-binding proteins. *Virology* **364**:466–474.
134. **Rodríguez Pulido, M., F. Sobrino, B. Borrego, and M. Sáiz.** 2009. Attenuated foot-and-mouth disease virus RNA carrying a deletion in the 3′ noncoding region can elicit immunity in swine. *J. Virol.* **83**:3475–3485.
135. **Rohll, J. B., D. H. Moon, D. J. Evans, and J. W. Almond.** 1995. The 3′ untranslated region of picornavirus RNA: features required for efficient genome replication. *J. Virol.* **69**: 7835–7844.
136. **Rust, R. C., K. Ochs, K. Meyer, E. Beck, and M. Niepmann.** 1999. Interaction of eukaryotic initiation factor eIF4B with the internal ribosome entry site of foot-and-mouth disease virus is independent of the polypyrimidine tract-binding protein. *J. Virol.* **73**:6111–6113.
137. **Ryan, E., D. Mackay, and A. Donaldson.** 2008. Foot-and-mouth disease virus concentrations in products of animal origin. *Transbound. Emerg. Dis.* **55**:89–98.
138. **Ryan, M. D., A. M. King, and G. P. Thomas.** 1991. Cleavage of foot-and-mouth disease virus polyprotein is mediated by residues located within a 19 amino acid sequence. *J. Gen. Virol.* **72**:2727–2732.
139. **Sa-Carvalho, D., E. Rieder, B. Baxt, R. Rodarte, A. Tanuri, and P. W. Mason.** 1997. Tissue culture adaptation of foot-and-mouth disease virus selects viruses that bind to heparin and are attenuated in cattle. *J. Virol.* **71**:5115–5123.
140. **Sagedahl, A., A. T. Giraudo, P. A. De Mello, I. E. Bergmann, J. L. La Torre, and E. A. Scodeller.** 1987. Biochemical characterization of an aphthovirus type C3 strain Resende attenuated for cattle by serial passages in chicken embryos. *Virology* **157**:366–374.
141. **Saiz, M., S. Gomez, E. Martínez-Salas, and F. Sobrino.** 2001. Deletion or substitution of the aphthovirus 3′ NCR abrogates infectivity and virus replication. *J. Gen. Virol.* **82**:93–101.
142. **Salt, J. S.** 1993. The carrier state in foot and mouth disease: an immunological review. *Br. Vet. J.* **149**:207–223.
143. **Salt, J. S.** 1998. Persistent infection with foot-and-mouth disease virus. *Top. Trop. Virol.* **1**:77–128.
144. **Sanz-Parra, A., F. Sobrino, and V. Ley.** 1998. Infection with foot-and-mouth disease virus results in a rapid reduction in MHC class I surface expression. *J. Gen. Virol.* **79**:433–436.
145. **Serrano, P., M. Rodríguez Pulido, M. Saiz, and E. Martínez-Salas.** 2006. The 3′ end of the foot-and-mouth disease virus genome establishes two distinct long-range RNA-RNA interactions with the 5′ end region. *J. Gen. Virol.* **87**:3013–3022.
146. **Strebel, K., and E. Beck.** 1986. A second protease of foot-and-mouth disease virus. *J. Virol.* **58**:893–899.
147. **Summerfield, A., L. Guzylack-Piriou, L. Harwood, and K. C. McCullough.** 2009. Innate immune responses against foot-and-mouth disease virus: current understanding and future directions. *Vet. Immunol. Immunopathol.* **128**:205–210.
148. **Sutmoller, P., and O. R. Casas.** 2002. Unapparent foot and mouth disease infection (sub-clinical infections and carriers): implications for control. *Rev. Sci. Tech.* **21**:519–529.
149. **Sutmoller, P., and A. Gaggero.** 1965. Foot-and mouth diseases carriers. *Vet. Rec.* **77**:968–969.
150. **Sutmoller, P., and J. W. McVicar.** 1976. Pathogenesis of foot-and-mouth disease: the lung as an additional portal of entry of the virus. *J. Hyg.* (London) **77**:235–243.
151. **Sutmoller, P., J. W. McVicar, and G. E. Cottral.** 1968. The epizootiological importance of foot-and-mouth disease carriers. I. Experimentally produced foot-and-mouth disease carriers in susceptible and immune cattle. *Arch. Gesamte Virusforsch.* **23**:227–235.
152. **Taboga, O., C. Tami, E. Carrillo, J. I. Nunez, A. Rodriguez, J. C. Saiz, E. Blanco, M. L. Valero, X. Roig, J. A. Camarero, D. Andrue, M. G. Mateu, E. Giralt, E. Domingo, F. Sobrino, and E. L. Palma.** 1997. A large-scale evaluation of peptide vaccines against foot-and-mouth disease: lack of solid protection in cattle and isolation of escape mutants. *J. Virol.* **71**: 2606–2614.
153. **Tami, C., O. Taboga, A. Berinstein, J. I. Nunez, E. L. Palma, E. Domingo, F. Sobrino, and E. Carrillo.** 2003. Evidence of coevolution of antigenicity and host cell tropism of foot-and-mouth disease virus in vivo. *J. Virol.* **77**:1219–1226.
154. **Tesar, M., and O. Marquardt.** 1990. Foot-and-mouth disease virus protease 3C inhibits cellular transcription and mediates cleavage of histone H3. *Virology* **174**:364–374.
155. **Toka, F. N., C. K. Nfon, H. Dawson, D. M. Estes, and W. T. Golde.** 2009. Activation of porcine natural killer (NK) cells and lysis of foot-and-mouth disease virus (FMDV) infected cells. *J. Interferon Cytokine Res.* **29**:47–60.
156. **Vakharia, V. N., M. A. Devaney, D. M. Moore, J. J. Dunn, and M. J. Grubman.** 1987. Proteolytic processing of foot-and-mouth disease virus polyproteins expressed in a cell free system from clone-derived transcripts. *J. Virol.* **61**:3199–3207.
157. **van Bekkum J. G., H. S. Frenkel, H. H. J. Frederiks, and S. Frenkel.** 1959. Observations on the carrier state of cattle exposed to foot-and-mouth disease virus. *Tijdschr. Diergeneeskd.* **84**:1159–1164.
158. **van Pesch, V., O. van Eyll, and T. Michiels.** 2001. The leader protein of Theiler's virus inhibits immediate-early alpha/beta interferon production. *J. Virol.* **75**:7811–7817.
159. **Vosloo, W., A. D. Bastos, E. Kirkbride, J. J. Esterhuysen, D. J. van Rensburg, R. G. Bengis, D. W. Keet, and G. R. Thomson.** 1996. Persistent infection of African buffalo (*Syncerus caffer*) with SAT-type foot-and-mouth disease viruses: rate of fixation of mutations, antigenic change and interspecies transmission. *J. Gen. Virol.* **77**:1457–1467.
160. **Wimmer, E.** 1982. Genome-linked proteins of viruses. *Cell* **28**:199–201.
161. **Woodbury, E. L.** 1995. A review of the possible mechanisms for the persistence of foot-and-mouth disease virus. *Epidemiol. Infect.* **114**:1–13.
162. **Yang, P. C., R. M. Chu, W. B. Chung, and H. T. Sung.** 1999. Epidemiological characteristics and financial costs of the 1997 foot-and-mouth disease epidemic in Taiwan. *Vet. Rec.* **145**:731–734.
163. **Zhang, Z., J. B. Bashiruddin, C. Doel, J. Horsington, S. Durand, and S. Alexandersen.** 2006. Cytokine and Toll-like receptor mRNAs in the nasal-associated lymphoid tissues of cattle during foot-and-mouth disease virus infection. *J. Comp. Pathol.* **134**:56–62.
164. **Zhang, Z. D., and R. P. Kitching.** 2001. The localization of persistent foot and mouth disease virus in the epithelial cells of the soft palate and pharynx. *J. Comp. Pathol.* **124**:89–94.

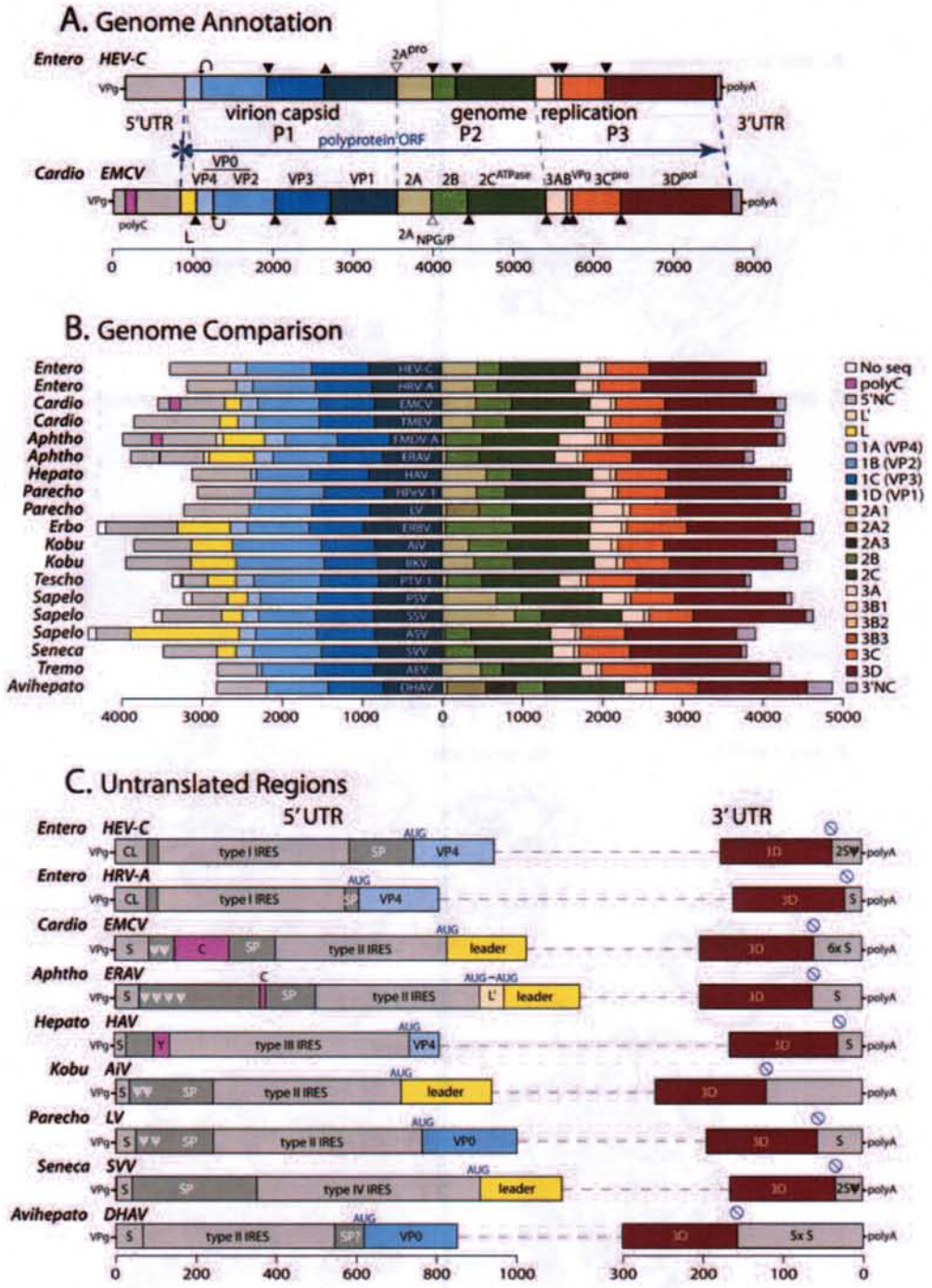

Color Plate 1 (Chapter 1). Comparative genome organization. (A) The genomes of HEV-C and EMCV are drawn to scale (RNA base length), aligned at the 1D/2A junction, to illustrate relative features. The primary cleavage site (open triangle), $3C^{pro}$-dependent secondary cleavage sites (closed triangle), and maturation cleavage site (downward-turned arrow) are highlighted. (B) Full genome sequences for isolates of representative genera and species are shown to scale, colored according to coding features, and aligned relative to the junction of 1D/2A1. Missing 5′-terminal data (No seq) are estimated in each case as 100 bases. The 3′ poly(A) tail (40 to 100 bases) is not shown. Reference GenBank accession numbers for included sequences are as follows: enterovirus HEV-C (j02281); enterovirus HRV-A (x02316); cardiovirus EMCV (m81861); cardiovirus Theiler's murine encephalomyelitis virus (m20562); aphthovirus FMDV-A (m14409, x00429); aphthovirus ERAV (dq268580); hepatovirus HAV (m14707); parechovirus HPev-1 (l02971); parechovirus LV (ef202833); ERBV (x96871); kobuvirus AiV (ab010145); bovine kobuvirus (ab084788); teschovirus PTV-1 (nc_003985); porcine sapelovirus (af406813); SSV (ay064708); avian sapelovirus (ay563023); SVV (dq641257); tremovirus avian encephalomyelitis virus (nc_003990); avihepatovirus DHAV (dq249299). (C) Key features of representative 5′ and 3′ UTRs are drawn to scale. Known RNA structure elements include terminal cloverleafs (CL), terminal stems (S), type 1 pseudoknots (ψ), poly(C) tracts (C), oligo pyrimidine tracts (Y), spacer segments (SP), IRESs (type I, II, III, or IV), ORF initiation codons (AUG), and ORF termination codons (circle with slash). A supplemental table listing the known start/stop positions for each RNA and/or ORF feature in this figure is available at http://virology.wisc.edu/acp.

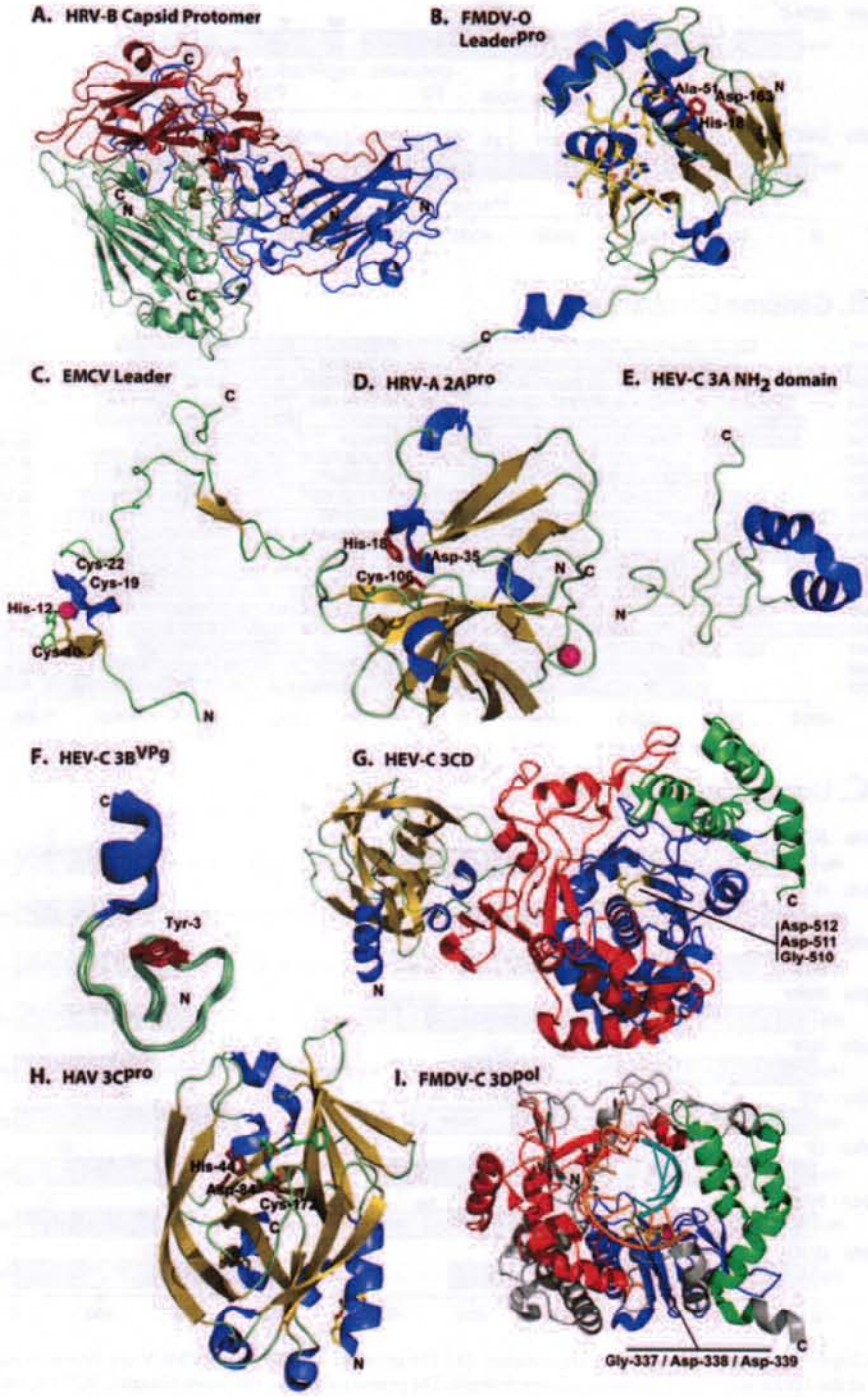

Color Plate 2 (Chapter 1). Structures of picornavirus proteins. (A) The four virion proteins comprising a capsid assembly protomer are derived from a single (enterovirus HRV-B or HRV-14) P1 polyprotein precursor. For visual distinction, this illustration of an X-ray structure (PDB no. 4HRV) assigns individual proteins their historical color referents of blue (VP1), green (VP2), red (VP3), and gold (VP4). VP1, VP2, and VP3 each have similar wedge-shaped, eight-stranded β-barrel configurations. VP4 is on the inside of the virion and can be considered an NH_2 extension of VP2. During particle assembly, 5 protomers combine into a pentamer, and then 12 pentamers coalesce around the viral RNA to form a completed virion. (B to I) Structures are depicted as cartoon models with α-helices in blue, β-strands in gold, and loops in green, except for 3D^{pol} and 3CD^{pro}, which are colored using the standard conventions for the major functional domains (the "palm" in blue, "fingers" in red, and "thumb" in green). The protein termini are labeled. (B) The X-ray structure of the aphthovirus FMDV-O leader protease Lb^{pro} (PDB no. 1QOL) includes the last nine residues of the COOH-terminal extension of a (crystallographic) neighboring Lb^{pro} molecule bound within the active site (yellow sticks). (C) NMR structure of the cardiovirus EMCV mengovirus leader

ED:
Continuation of Color Plate 2 on facing page OK?

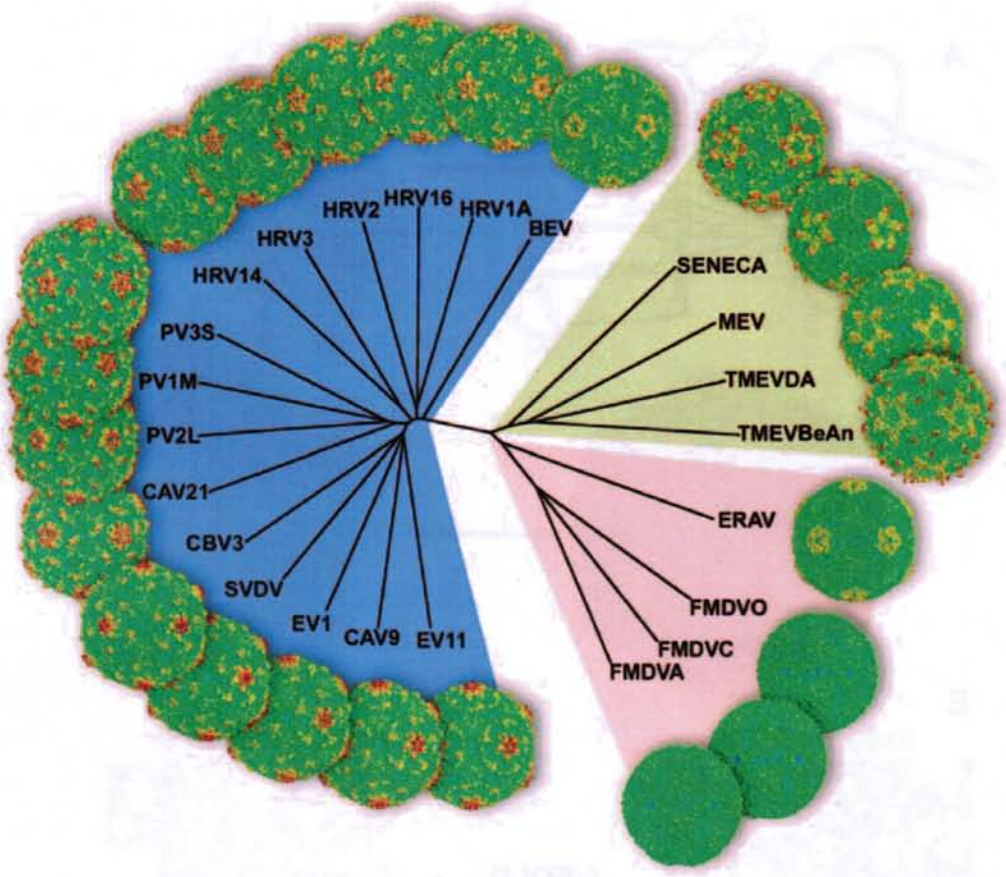

Color Plate 3 (Chapter 4). Structure-based phylogenetic tree, calculated using the protomeric subunits of all the intact native picornavirus structures in the protein data bank as of October 2009 (9) (listed in Table 1). The virus structures are shown oriented such that the view is looking down an icosahedral two-fold axis of symmetry. Atoms are drawn as spheres colored according to their distance from the particle center, ranging from blue (at 120-Å radius) to red (at 170-Å radius). Enteroviruses are shown against a blue background, aphthoviruses are against a pink background, and cardioviruses and closely related viruses are against a green background. The method of calculating evolutionary distance is described in reference 64, and the tree was calculated and plotted using the PHYLIP package (20).

Query 1

protein (PDB no. 2BAI). Three Cys residues and one His residue coordinate Zn^{2+} (pink sphere) in a CHCC zinc-finger motif. (D) X-ray structure of the enterovirus HRV-A and HRV-02) protease $2A^{pro}$ (PDB no. 2HRV). The COOH-terminal domain coordinates a tightly bound Zn^{2+} ion (pink sphere). The catalytic triad is highlighted (red). (E) NMR structure of the soluble NH_2-terminal domain of the enterovirus HEV-C and poliovirus 1 3A protein (PDB no. 1NG7). (F) Bundle of the 10 best-resolved NMR structures of the poliovirus 1 $3B^{VPg}$ (PDB no. 2BBL). Tyr-3 (red) is a strongly conserved residue used to link this protein to the 5′ end of the genome. (G) X-ray structure of the poliovirus 1 $3CD^{pro}$ precursor (PDB no. 2IJD). The $3D^{pol}$ active site displays a Gly-Asp-Asp (GDD) motif, which is universally conserved in all RNA-dependent RNA polymerases (yellow). (H) X-ray structure of the HAV protease $3C^{pro}$ (PDB no. 2A4O), including a covalently bound inhibitor (acetyl-Val-Phe-amide; green sticks). The catalytic triad is highlighted (red). (I) X-ray structure of the aphthovirus FMDV-C S8c1 polymerase $3D^{pol}$ shows the protein complexed with a template-primer RNA (PDB no. 1WNE). The GDD motif (yellow), a coordinated Mg^{2+} ion (pink sphere), template RNA (orange), and primer strand (turquoise) are highlighted.

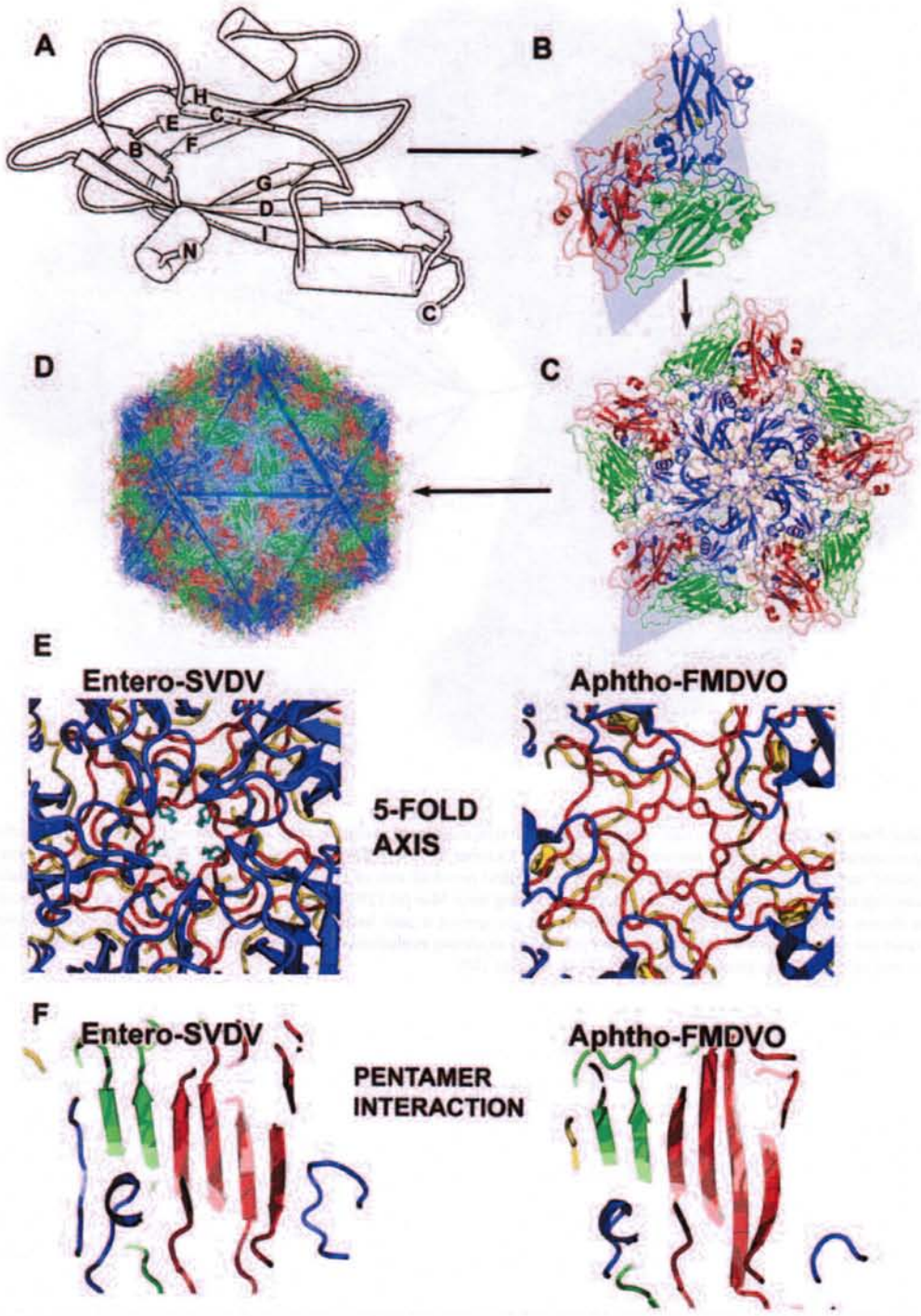

Color Plate 4 (Chapter 4). Architecture. (A) Ribbon outline showing the core β-barrel architecture based loosely on FMDV VP3. The nomenclature for the eight strands comprising the two β-sheets and hence the loops joining the strands is introduced. (B) Ribbon depiction of an SVDV biological protomeric subunit (1OOP [9]) color coded as follows: VP1, blue; VP2, green; VP3, red; VP4, yellow. The background blue kite shape is used to delineate this subunit within the pentameric subunit shown in panel C. (C) Ribbon depiction of a complete capsid (SVDV), with blue lines superimposed to highlight the icosahedral symmetry. (D) Close-ups of the five-fold symmetry axes in SVDV (enterovirus) and FMDV (1BBT [9]) (aphthovirus). The proteins are color coded as for panel B, and the myristate is shown in cyan. (E) β-Strands color coded according to the protein contributing to a sheet spanning the two-fold pentamer interface for SVDV (left) and FMDV (right) (colors are as defined for panel B).

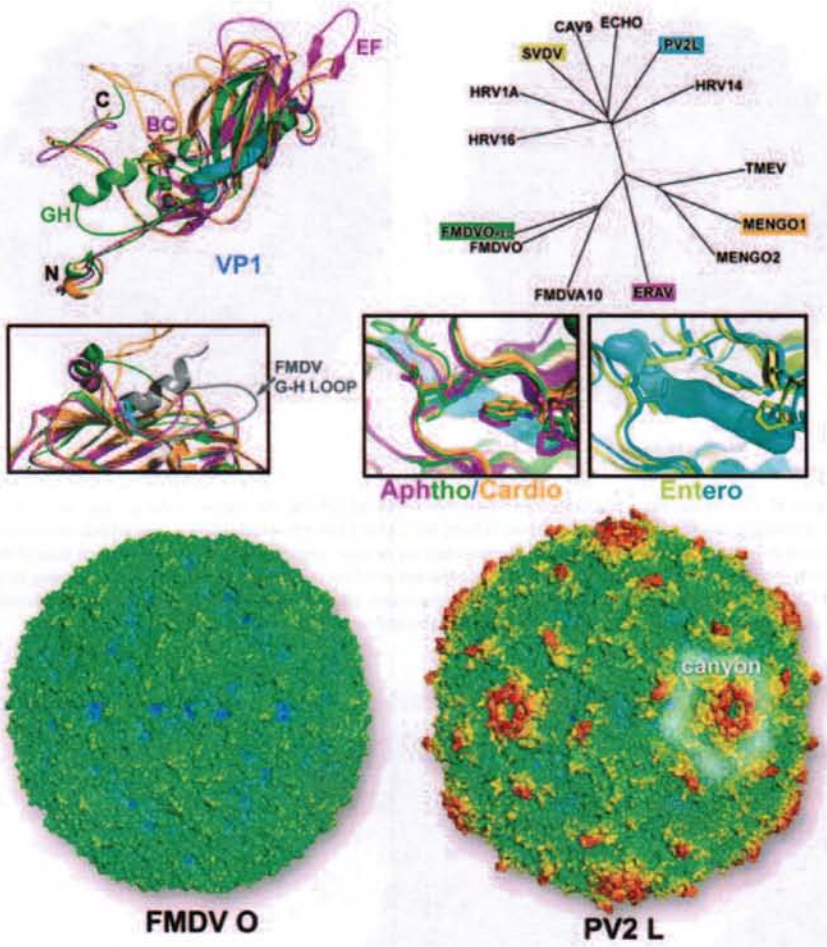

Color Plate 5 (Chapter 4). Structural features. (Top left) Overlay of ribbon depictions of VP1 for FMDV O (dark green), ERAV (magenta), and mengovirus (orange) (aphthoviruses and cardioviruses). For ease of identification the top left panel shows the same viruses highlighted in the corresponding colors on a structure based the phylogenetic tree calculated for VP1 (using the method described for Color Plate 3). (Center panels) The left panel is a close-up view of the ERAV, mengovirus, and FMDV VP1s overlaid together with the reduced FMDV O1BFS VP1 G-H loop structure (grey), while the two panels to the right show close-ups of the pocket in the VP1 β-barrel are for these same viruses and, in addition for means of comparison, for the enteroviruses PV2L (cyan) and SVDV (lime green). A surface-rendered pocket factor is shown in cyan in both of these close-ups but can only fit in the enterovirus pocket (in aphtho- and cardioviruses, side chains fill the pocket). (Bottom panels) Color depth-cued surface renditions of FMDV O (left) and PV2L (right) (both colored using the radius-dependent scheme defined for Color Plate 3). One of the canyons circling the five-fold axes of enteroviruses is highlighted. Note the relatively smooth surface of FMDV.

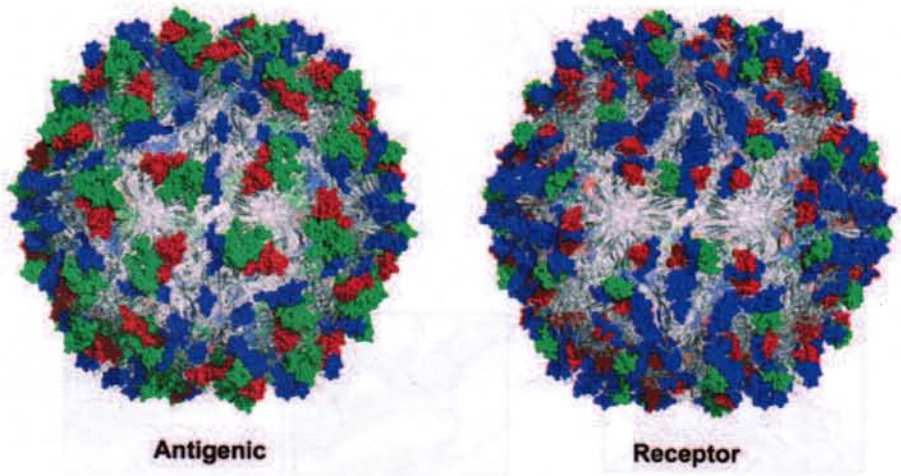

Color Plate 6 (Chapter 4). Consensus sites. (A) Consensus antigenic sites highlighting the atoms of the relevant secondary structure using spheres color coded according to protein (using the scheme defined for Color Plate 4B) overlaid on a grey ribbon depiction of CVA21 (data from MAb escape mutants; sites are considered to be consensus when six or more serotypes of the viruses studied shared the same site [54]). (B) Consensus receptor-binding sites shown by highlighting the relevant residues using spheres color coded according to protein on a grey ribbon depiction of CVA21 (data are from footprints of complex structures, aligned with CVA21 and considered consensus when three or more serotypes use the same site). The atomic data include all the relevant structures listed in Table 1.

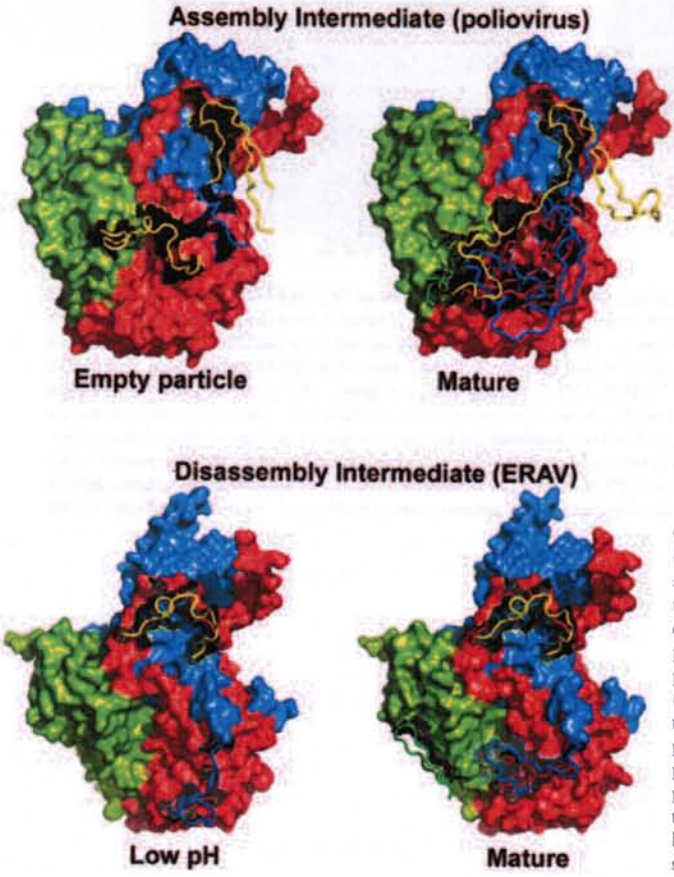

Color Plate 7 (Chapter 4). Intermediate structures. (Top) Comparison of protomers of poliovirus mature and empty (assembly intermediate) structures. The protomeric subunits are viewed from the inside, and the common structures on the surface are color coded by protein. The VP1 and VP2 N termini and VP4 (mature particle) are shown as tubes in standard protein colors (as defined for Color Plate 4B); for the empty particle, the VP0 N terminus is shown in yellow. (Bottom) Comparison of protomers of mature ERAV and the low-pH structure (likely disassembly intermediate). The protomeric subunits are viewed from the inside, and the common structures on the surface are color coded by protein. The VP1 and VP2 N termini and VP4 are shown as tubes in the standard protein colors.

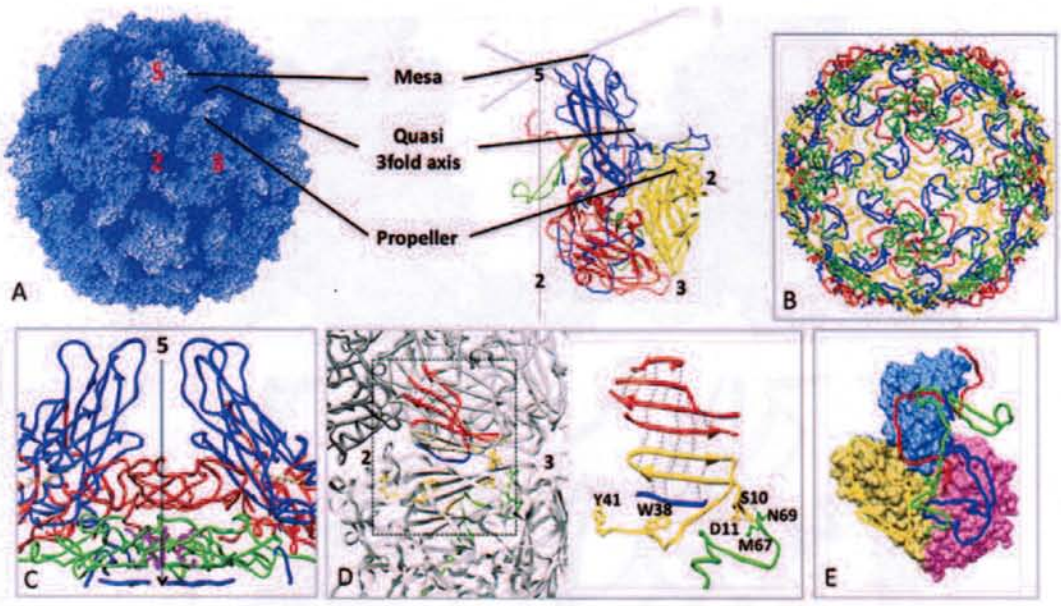

Color Plate 8 (Chapter 6). Structure of PV. (A) Depth-cued view of the intact particle with a ribbon model of a protomer, showing the prominent surface features, including star-shaped mesas at the five-fold axes, three-bladed propellers at the three-fold axes, deep canyons surrounding the five-fold mesas, and saddle-shaped depressions crossing the two-fold axes. A five-fold axis, two-fold axis, and three-fold axis are indicated in red for reference. To the right of the depth-cued virion, the ribbon diagram shows the structure of the four coat protein molecules from a single protomer, with VP1 in blue, VP2 in yellow, VP3 in red, and VP4 in green. An icosahedral framework with five-fold, two-fold, and three-fold axes is provided for reference. VP1, VP2, and VP3 share a common core structure (an eight-stranded β-barrel). Each of the proteins has unique loops, carboxy-terminal extensions on the outer surface, and a long amino-terminal extension on the inner surface. (B) The amino-terminal extensions of VP1, VP2, and VP3 together with VP4 form an elaborate network on the inner surface of the capsid shell that stabilizes the virus particle. The network is viewed from the inside here. (C) The network includes a number of prominent intraprotomer interactions, including those contributed by the amino-terminal extension of VP3 as it wraps underneath the surface of VP1 and by the amino-terminal extension of VP1 as it wraps underneath the surface of VP3. The portions of VP4 and VP3 that extend beyond the protomer at top right and a β-hairpin from the amino-terminal extension of VP2 that extends beyond the protomer at the lower left contribute to interprotomer interactions are shown. (D) The β-tube formed as five copies of the amino terminus of VP3 intertwine around the five-fold axes forms a plug which blocks an otherwise-open channel connecting the outer surface (top) and inner surface (bottom) of the virus. The β-tube is flanked by a three-stranded β-sheet formed by the hairpin from the amino terminus of VP4 and a strand from the extreme amino terminus of VP1. The myristoyl substituent at the amino terminus of VP4 (purple) mediates the interaction between the VP3 β-tube and the flanking β-sheet. This structure stabilizes the interprotomer interactions linking protomers in a pentameric subassembly. (E) A seven-stranded β-sheet formed by four strands from the β-barrel of VP3 from one pentamer, a β-hairpin from the amino terminus of VP2 from a two-fold related pentamer, and a β-strand from the amino-terminal extension of VP1 from the original pentamer. This interaction stabilizes interactions between two-fold related pentamers in the intact virion.

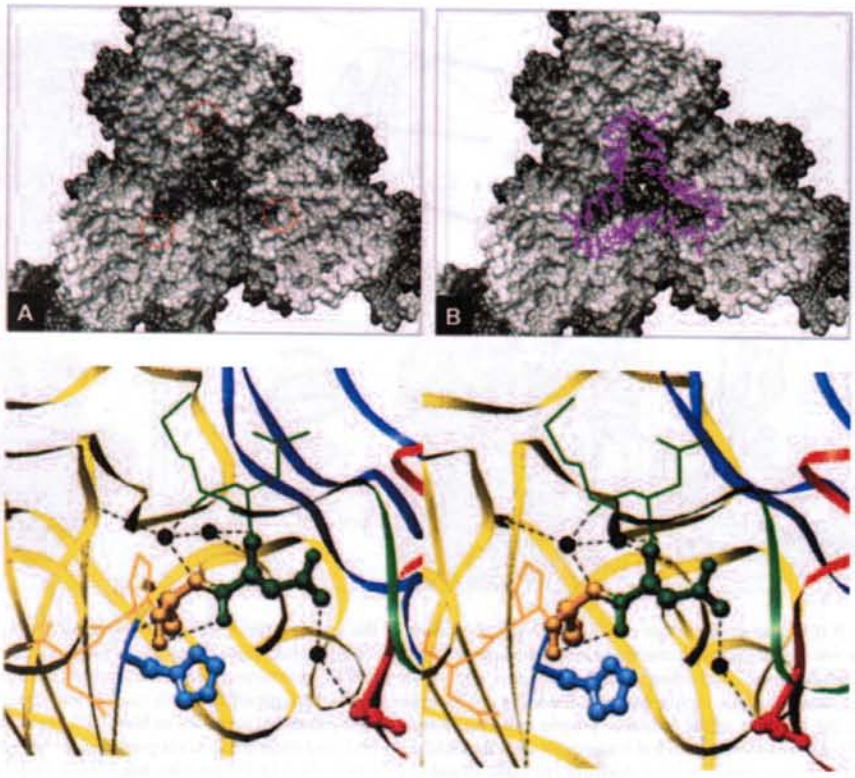

Color Plate 9 (Chapter 6). The inner surface of the 73 empty capsids provides some clues about the mechanism of VP0 cleavage. (A) The stretch of peptide containing the scissile bond of VP0 is located at the tips of a trefoil-shaped depression in the inner surface of the empty capsid structure. Three protomers of the capsid protein are shown, surrounding a three-fold axis viewed from the inside of the capsid looking out. The depression is filled by the amino terminus of VP1 in the mature virion. (B) Stereo representation of the atomic model, showing the peptide containing the scissile bond (green/yellow boundary) with a neighboring histidine and network of water. Mutations of this histidine are impaired for VP0 cleavage. (C) The trefoil-shaped depression with the ordered RNA from Cowpea chlorotic mottle virus docked into the depression. RNA binding to this site could participate in autocatalyic cleavage of VP0.

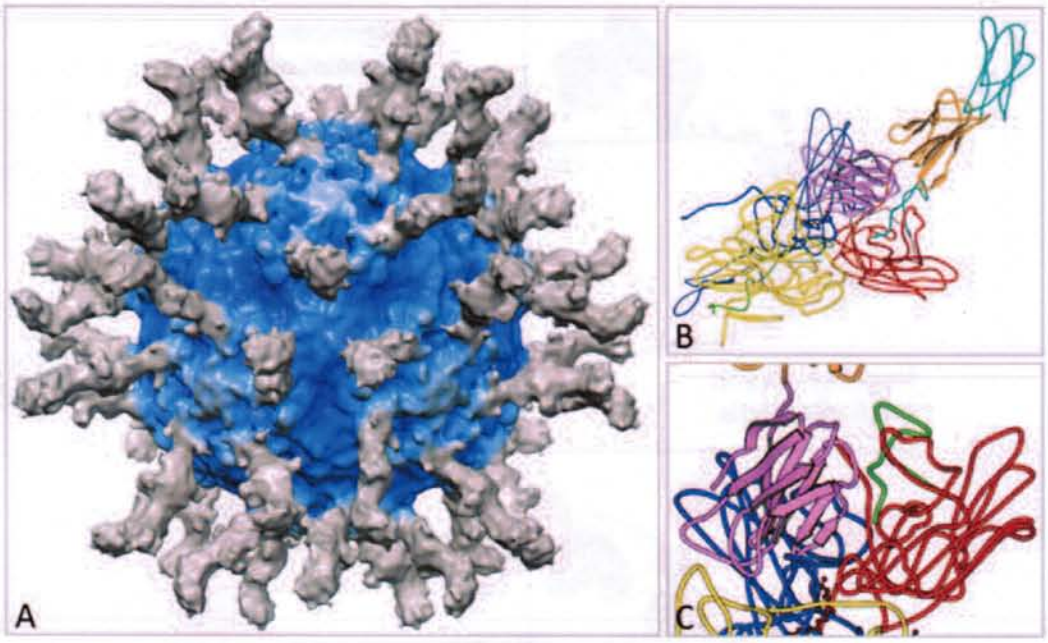

Color Plate 10 (Chapter 6). Structure of the virus-receptor complex. (A) Cryo-EM structure of the complex of PV with the fully glycosylated ectodomain of its receptor, PVR. The structure has been colored to show the density corresponding to the virus (blue) and the density for the receptor (grey). (B) Ribbon diagram showing a model for the receptor and the virus, built into the cryo-EM density. (C) Close-up view of the interaction of the amino-terminal domain of the receptor with the virus. The complementarity of the fit is excellent, with the receptor containing several surface features of the virus that are known to be rearranged in cell entry intermediates, including the GH loop of VP1, the EF loops of VP2 and VP3, and the carboxy termini of VP1, VP2, and VP3.

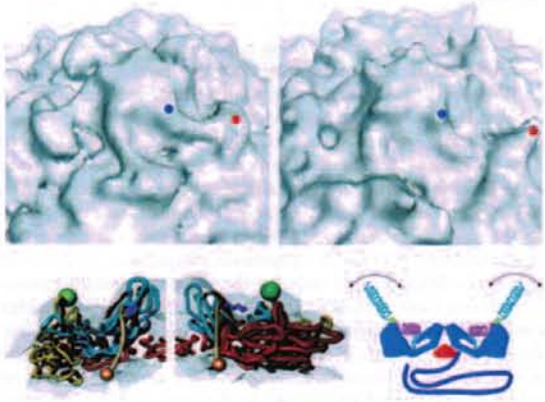

Query 2

Color Plate 11 (Chapter 6). Structure of the 135S particle. (Top left) Cryo-EM reconstruction of the 135S particle at 10 Å revealed prominent ridges of density connecting the tips of the five-fold mesa (blue dot) with the tips of the propeller-like feature surrounding the three-fold axes (red dot). This ridge, which is missing in the structure of the mature virion (top right), can be modeled as an α-helix. (Bottom left and middle) The cryo-EM density (grey) and models for the capsid proteins that were fit and refined into the density map (colors). In this view, five-fold-related protomers have been butterflied to show the surfaces that normally interact in the interprotomer interface. The first well-ordered residue in the β-barrel of VP1 is shown as an orange sphere, and the course of the amino-terminal extension of VP1 as it exits through the interface at the base of the canyon is shown as a gold tube. The helix fit into the ridge of density (tentatively assigned as residues 41 to 53 of VP1) is shown in purple, and the site of a prominent difference in the density for the intact 135S particle and the density for 135S particles in which residues 1 to 31 of VP1 are proteolytically removed are shown in green. In the left panel these features come from the neighboring subunit. (Bottom right) Cartoon representation of the model, showing the RNA inside the particle (dark blue), the VP3 plug (red), and the exiting VP1 peptide (cyan), with the helix of residues 41 to 53 (magenta). The arrows indicate that the amino-terminal amphipathic helix of VP1 residues 1 to 30 is flexibly linked to the capsid and is therefore not visible in the cryo-EM reconstruction.

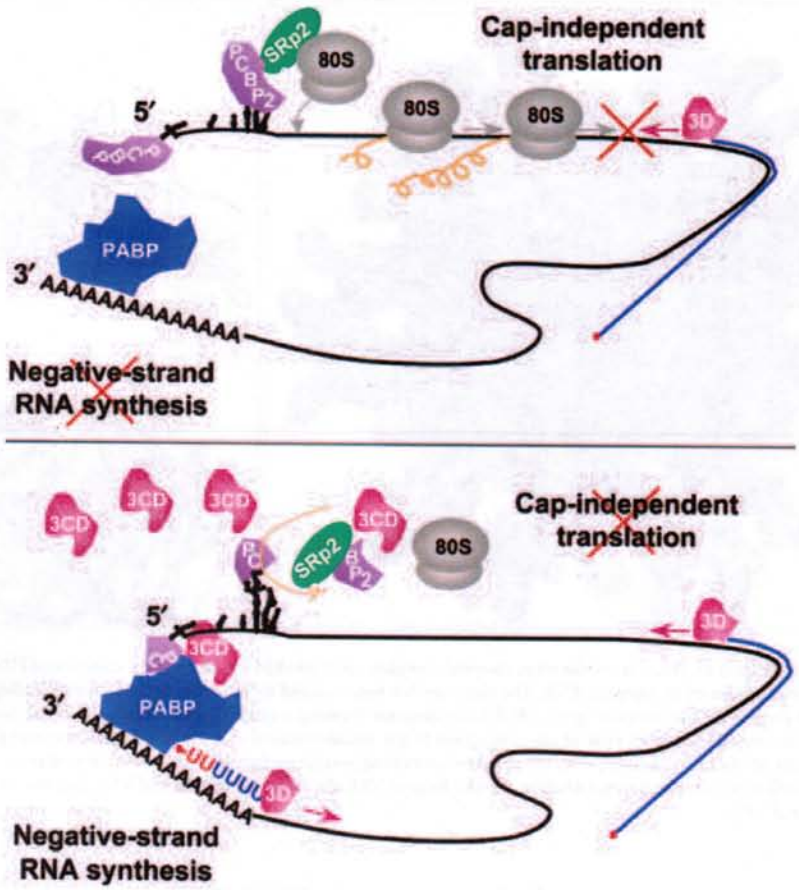

Color Plate 12 (Chapter 8). Model for template selection during poliovirus translation and viral RNA replication. The figure depicts poliovirus positive strand RNA (black line) under conditions that favor cap-independent translation (top panel) or those that favor negative-strand RNA synthesis (bottom panel). Under conditions that favor translation early during the infectious cycle (top panel), the RNA is bound by ribosomes (denoted by 80S on the gray spheres) continuously initiating and elongating nascent viral polypeptide chains (depicted by orange curly lines). Initiation of translation is facilitated by the binding of cellular protein PCBP2 to the poliovirus IRES in the 5′ noncoding region of positive-strand RNA (secondary structures with thickened black lines) and the possible bridging of RNA to the ribosome by the cellular protein, SRp20. The presence of multiple ribosomes on viral RNA may preclude the viral RNA polymerase (3D) from elongating any newly initiated negative strand RNAs. Under conditions that favor negative-strand RNA synthesis later during the infectious cycle (bottom panel), PCBP2 has been cleaved by the accumulated 3CD (or 3C) proteinase polypeptides (as indicated by the orange arrow). This inhibits the binding of ribosomes to the IRES, thereby reducing the levels of translation initiation complex formation and releasing SRp20 from PCBP2. The cleaved form of PCBP2 can still participate in ternary complex formation with the 5′ stem-loop I structure and 3CD. This may facilitate the interaction of the 5′ ribonucleoprotein complex with the 3′ poly(A) tract via a bridging interaction with poly(A)-binding protein. This latter interaction would lead to initiation of negative-strand RNA synthesis on templates that are now cleared of translating ribosomes. The gray arrows indicate the direction of ribosomes traversing the RNA during translation, while the red arrows indicate the direction of the 3D RNA polymerase during negative-strand RNA synthesis. The blue lines represent nascent negative-strand RNAs with a VPg (small solid red circle) at their 5′ ends. The UUUUUU represents the 5′ oligo(U) tract that is templated by the 3′ poly(A) tract on genomic positive-strand RNAs. The separation of the two processes is shown for illustration purposes only, since it is likely that the viral replication cycle is a dynamic process with both activities occurring simultaneously (but not on the same template RNA). (From reference 66, with permission of the publisher.)

Query 3

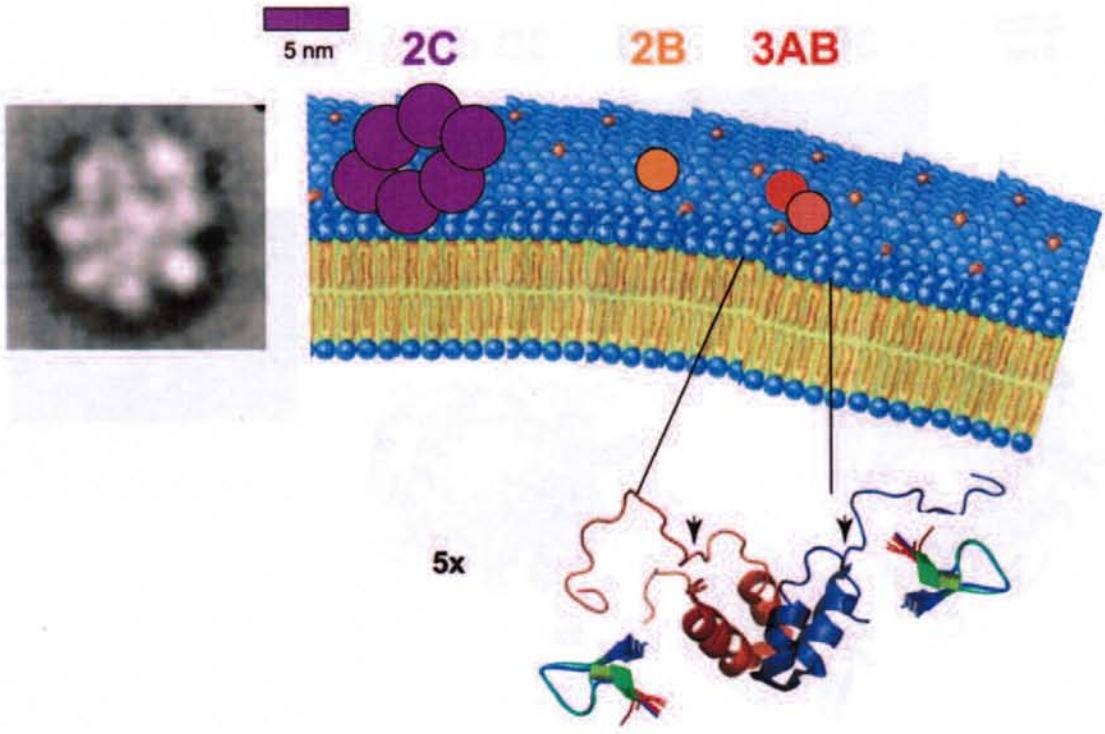

Color Plate 13 (Chapter 8). Schematic of the surface of a PV-induced vesicle, with known membrane-associated proteins of the RNA replication complex shown to scale. A cutaway section of the outer bilayer of a PV-induced membranous vesicle is shown with lipids and proteins shown to scale, and the appropriate curvature for this 400-nm vesicle is indicated. The 8- to 10-nm width of the lipid bilayer is shown, and proteins are represented as abstract shapes that indicate their relative sizes and published oligomeric forms. For PV protein 2C, an electron microscopic image of an oligomeric form has been published (1); this image is shown to scale. Although evidence has been presented that 2B proteins are oligomeric, no structural image is yet available. For poliovirus protein 3A, the NMR structure of a dimeric form of the soluble N-terminal domain has been published (73); this structure is shown at a 5× increase in scale below the bilayer. Arrows indicate the amino termini of the 3A proteins that are natively unfolded; the carboxyl termini are connected to the membrane-associated hydrophobic region.

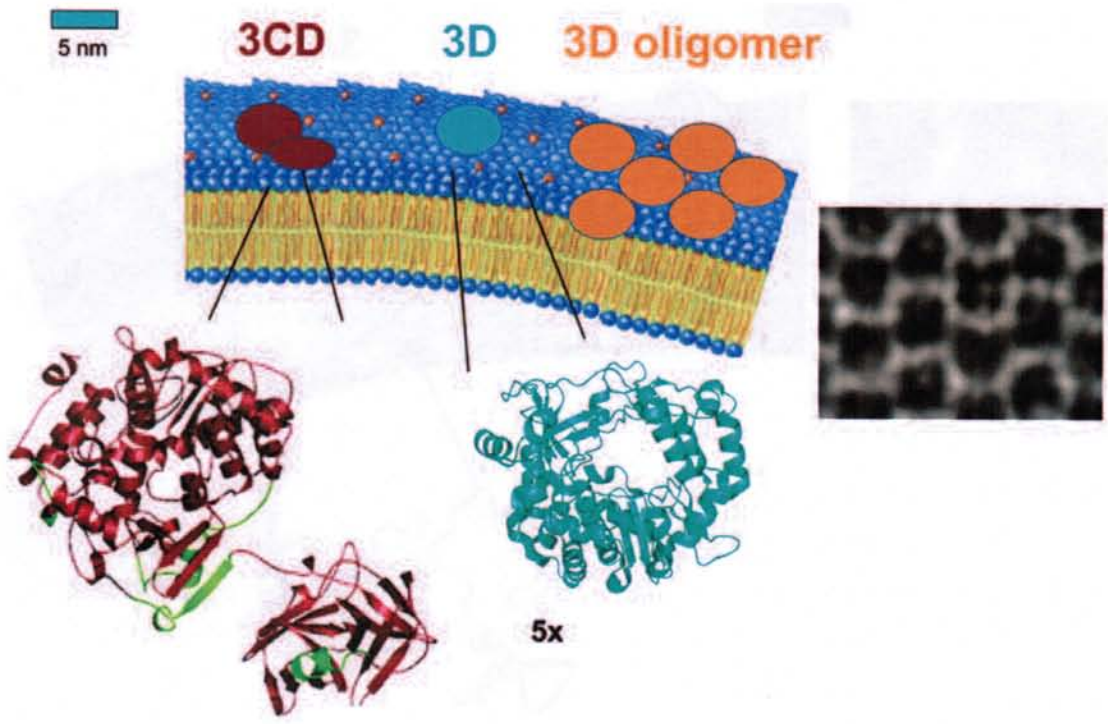

Color Plate 14 (Chapter 8). Schematic of the surface of a PV-induced vesicle, with known polymerase-containing complexes shown to scale. A cutaway section of the outer bilayer of a membranous vesicle, 400 nm in diameter, induced during PV infection is indicated. One-sixth of the circumference of the bisected vesicle is shown, with the appropriate curvature. The 8- to 10-nm width of the lipid bilayer is indicated, with approximately 150 lipids in each leaflet of the portion of the membrane shown. Bar, 5 nm (may be used to estimate the relative sizes of the PV proteins and complexes known or suggested to be involved in RNA replication). For those proteins for which electron microscopic images of oligomeric forms are available, those images are provided and shown to scale, with permission from the original references. Proteins, their relative sizes, and any oligomeric forms that have been observed by electron microscopy or NMR, are shown as abstract shapes. For those proteins whose monomeric structures have been solved, the structures are shown at 5× magnification. In the 3CD structure, the green sequences indicate those that are most changed from those of the 3C and 3D structures.

Query 4

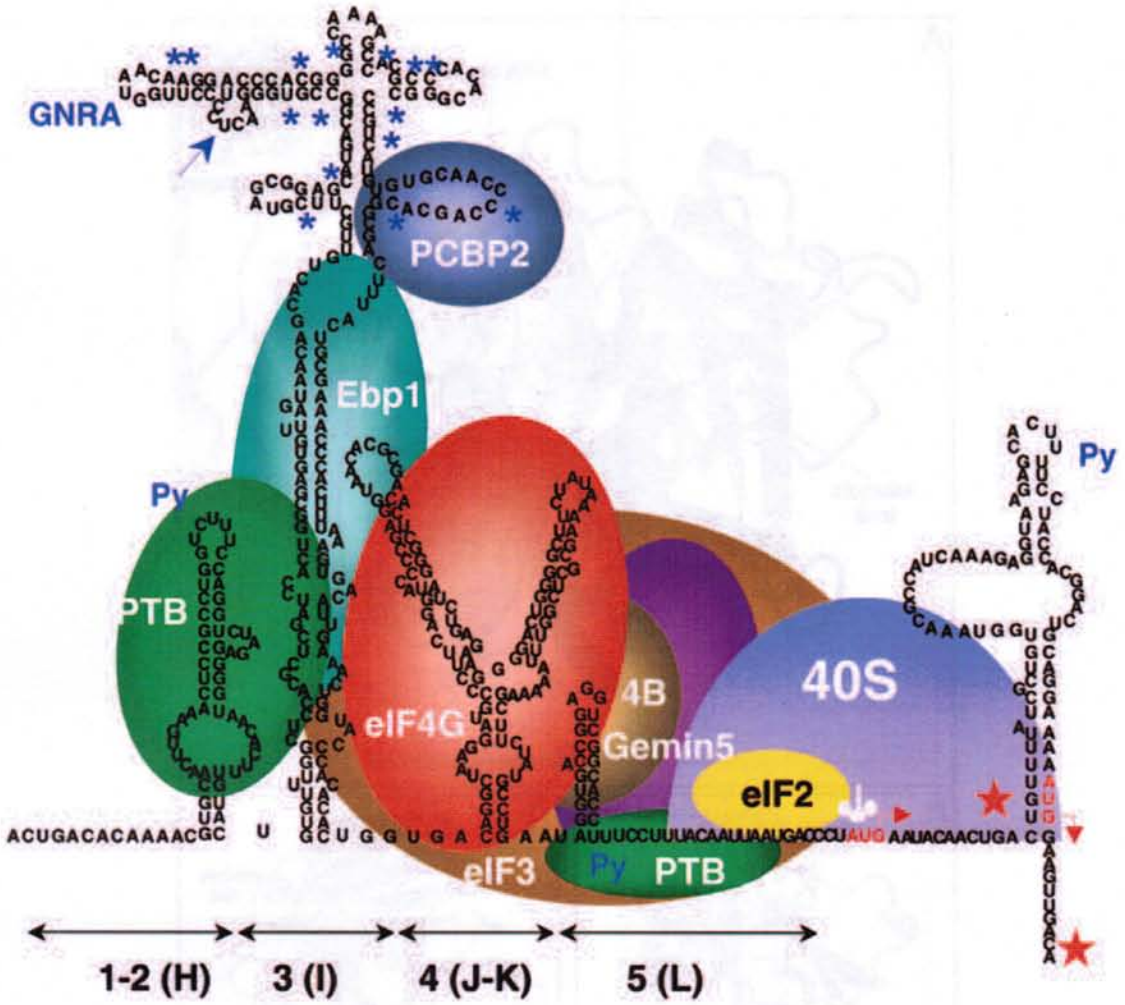

Color Plate 15 (Chapter 9). Map of RNA-protein binding of the FMDV IRES. The schematic shows the factors required for IRES activity, depicted on the secondary structure derived from RNA probing of the entire FMDV IRES. The positions of domains 1 to 5 (or H to L) are shown at the bottom. For simplicity, only proteins whose binding site and functional involvement in IRES activity have been analyzed in detail are represented. Blue asterisks surrounding the GNRA motif mark changes in RNA accessibility to DMS in vivo relative to naked RNA in vitro. An arrow points to the RNase P cleavage site in vitro. Py denotes the position of a conserved polypyrimidine tract. Initiator codons, with the corresponding toeprints (depicted by stars), are highlighted in red in the sequence.

Query 5

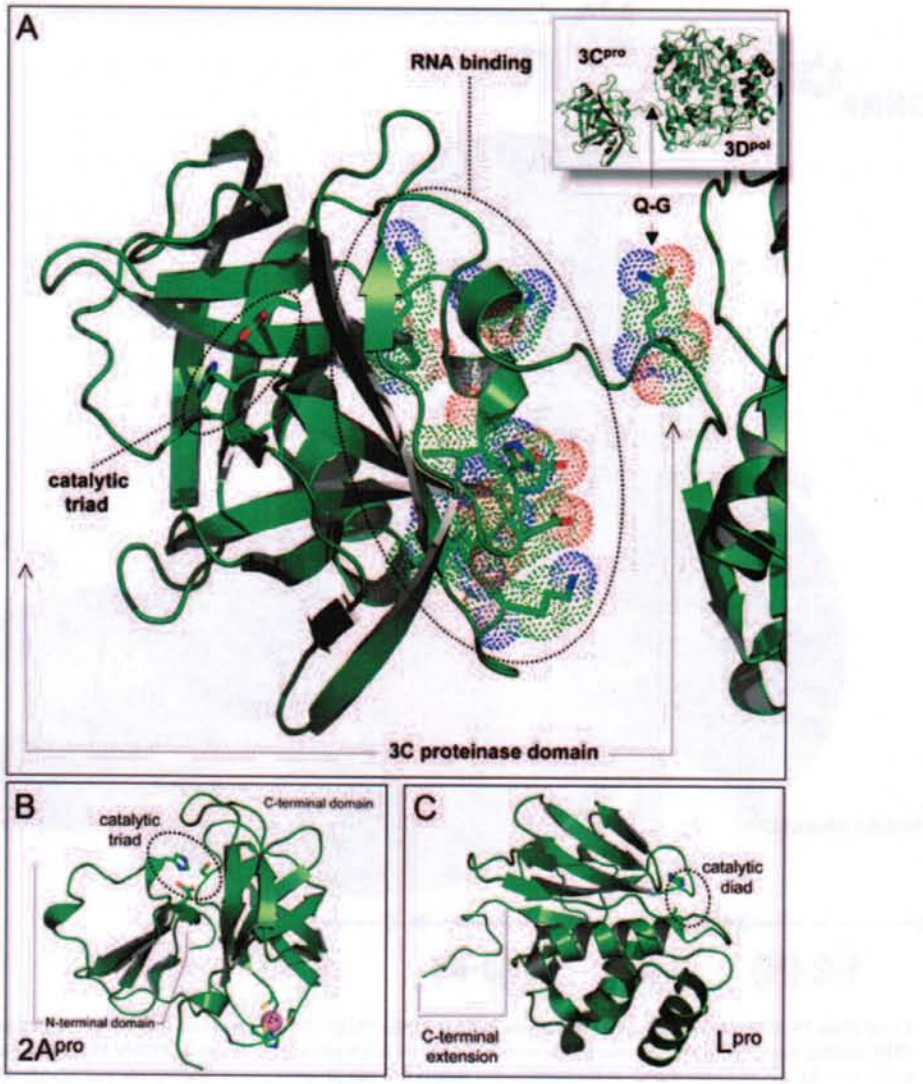

Color Plate 16 (Chapter 9). Atomic structures of picornavirus proteinases. Structures were rendered using PyMol (DeLano Scientific). (A) Structure of PV 3CD^{pro} (2IJD) is shown in the inset (upper right) with the proteinase domain enlarged. The 3C proteinase domain is structurally related to the large subclass of serine proteinases. The position of the catalytic triad (H^{40}, E^{71}, and C^{147}, the latter mutated to alanine for purposes of structural determination) is shown. The RNA-binding site on the opposite face of the 3C^{pro} domain, close to the 3C/3D glutamine/glycine (Q-G) cleavage site, is shown. (B) The structure of rhinovirus 2A^{pro} (2HRV) reveals a bilobal structure similar to the small subclass of serine proteinases. The position of the active site is shown (H^{18}, D^{35}, and C^{106}) together with the position of the zinc atom, which performs a structural, and not catalytic, role. (C) The structure of L^{pro} (1QOL) is related to thiol (papain-like) proteinases, and the position of the catalytic diad (C^{51} and H^{148}, the former mutated to alanine for purposes of structural determination) and the protruding C-terminal extension on the opposite face are shown.

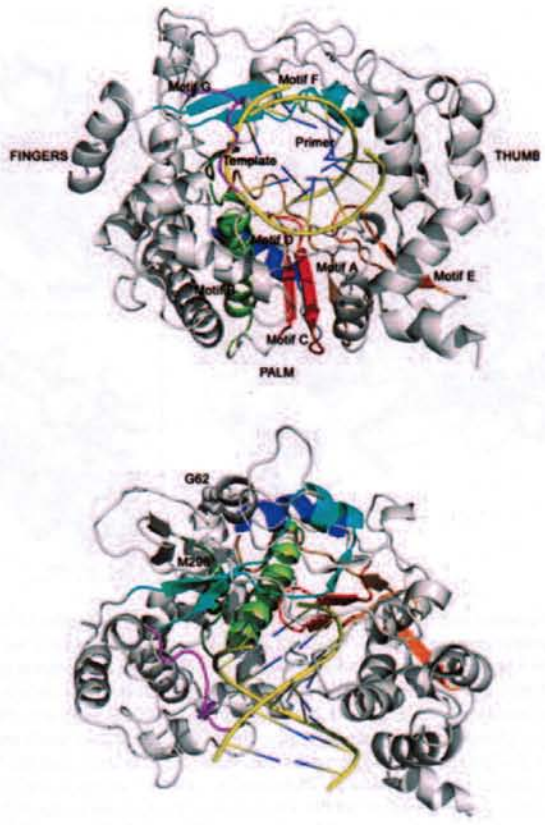

Color Plate 17 (Chapter 12). Ribbon diagrams of the structure of FMDV 3D polymerase in complex with an RNA template primer (PDB ID 1WNE), shown in different views. (Top) Conventional orientation displaying the right-hand confirmation. The polymerase is depicted in gray, with the fingers, palm, and thumb subdomains specifically labeled. The six different conserved structural motifs of the palm and fingers domains are colored as follows: A, brown; B, green; C, red; D, blue; E, orange; F, cyan; G, magenta. (Bottom) Top-down view (90° upward rotation relative to the structure shown at the top), with the same color codes. Amino acids G62 and M296, involved in resistance of picornaviruses to R, are indicated. (Based on reference 62 and C. Ferrer-Orta et al., submitted for publication.)

Query 6

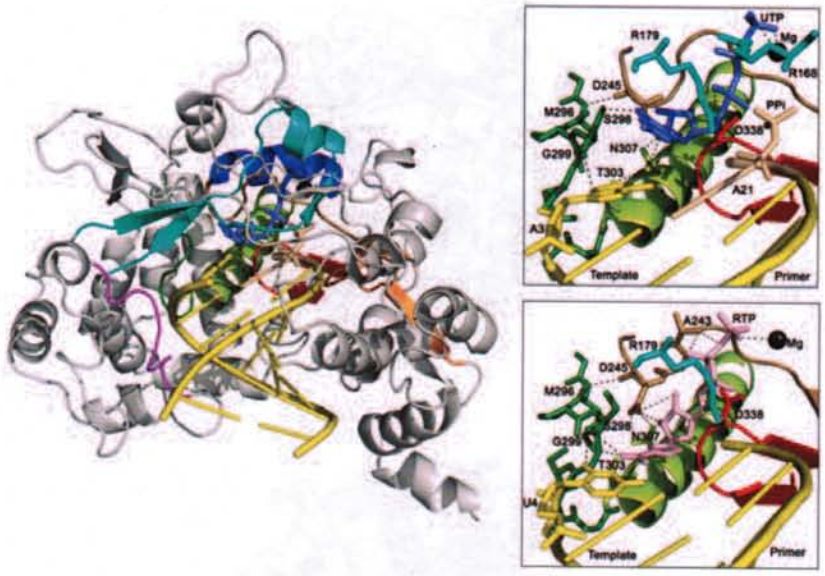

Color Plate 18 (Chapter 12). Structure and interactions of the FMDV 3D-VPg-UMP complex (PDB ID 2F8E). The FMDV polymerase is shown in grey, the primer protein VPg in yellow, and the UMP in purple. VPg lines the RNA-binding cleft of the 3D polymerase, positioning its Tyr-3 hydroxyl group as a molecular mimic of the free 3′-hydroxyl group of a nucleic acid primer at the active site for nucleotidylylation. The two insets on the right side show close-ups of the interactions established between VPg and different polymerase residues. In the active site, the hydroxyl group of the Tyr-3 side chain was found covalently attached to a UMP molecule by a phosphodiester linkage. (Upper inset) Two metal ions (dark grey spheres) participate in the uridylylation reaction. Metal 1 bridges the catalytic aspartate, Asp338 of motif C (red), and the O^- of the tyrosine side chain, now covalently bound to phosphate α of UMP. Metal 2 coordinates the carboxyl group of Asp245 of motif A (brown), the O1 oxygen of phosphate α, and the hydroxyl group of Ser298 within loop β9-α11, next to motif B (dark green). The conserved Tyr336 of motif C and the positively charged residues K164, R168, K172, and R179 of motif F (cyan) also participate in the uridylylation process. (Lower inset) In addition to the interactions in the polymerase active site, the lower inset shows the different residues of motifs F (R168; cyan) and E (K387 and R388; orange) that together with residues within the first helix of the thumb subdomain (amino acids from T407 to I411; grey) interact with the central part of VPg. Finally, the FMDV 3D residues Gly216 and Cys217 (grey), in the fingers subdomain, establish hydrophobic contacts with VPg at the exit of the polymerase cavity. (Based on references 59 and 60 with publisher permission.)

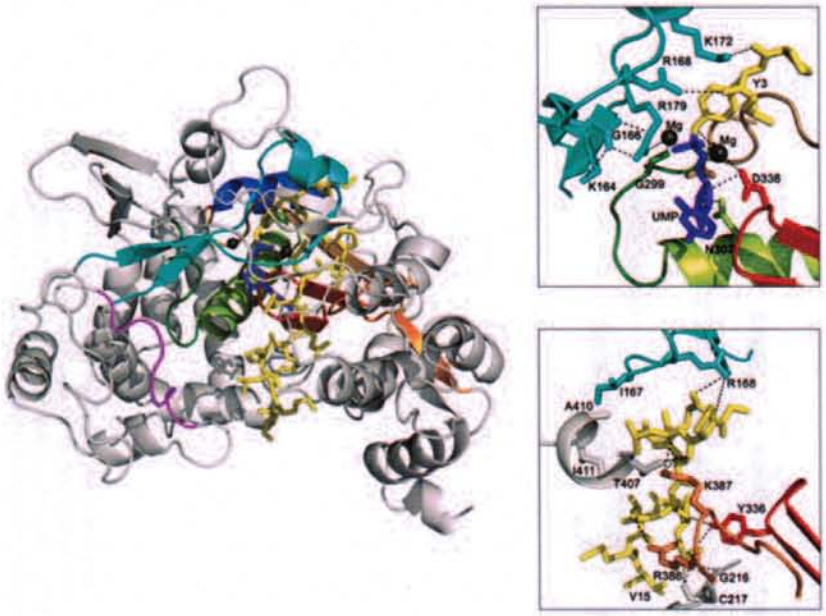

Color Plate 19 (Chapter 12). Structure and interactions of the FMDV polymerase, RNA template primer, and rNTP substrates. The polymerase is shown in grey in the central panel, with the conserved motifs, involved in contacts with the RNA molecule, highlighted in different colors. The template and primer strands of the RNA molecule are shown in yellow. The upper inset on the right side shows a close-up of the interactions in the polymerase active site after AMP incorporation, PPi release (sand), and the positioning of the new incoming UTP (blue) close to the active site, as seen in the structure of the FMDV 3D-RNA-ATP/UTP complex (PDB ID 2E9Z). The residues that establish contacts are shown as sticks and the hydrogen bonds as dashed lines, in black. The UTP is located close to the nucleotide-binding pocket bound to the polymerase/template/primer complex through a metal ion and the basic residues of motif F (cyan). The ribose and base moieties of UTP establish additional contacts with Asn307 of motif B (lime green) and Ser298 of the β9-α11 loop (dark green). The ribose-binding pocket is partially occluded by the side chains of Asp245, Thr303, and Asn307, which are connected by hydrogen bonds. The lower inset on the right side shows a close-up of the interactions in the polymerase active site with RTP (PDB ID 2E9R). The incoming nucleotide analog (pink) is located adjacent to the 3′ terminus of the primer and is base-paired to the template acceptor base. The position of the RTP base is further stabilized by interactions with residues of motifs A (brown) and B (lime green) and the loop β9-α11 (dark green). The triphosphate moiety is hydrogen bonded to different residues of motifs A and F (cyan) and interacts with one metal ion (dark green sphere). (Based on reference 61.)

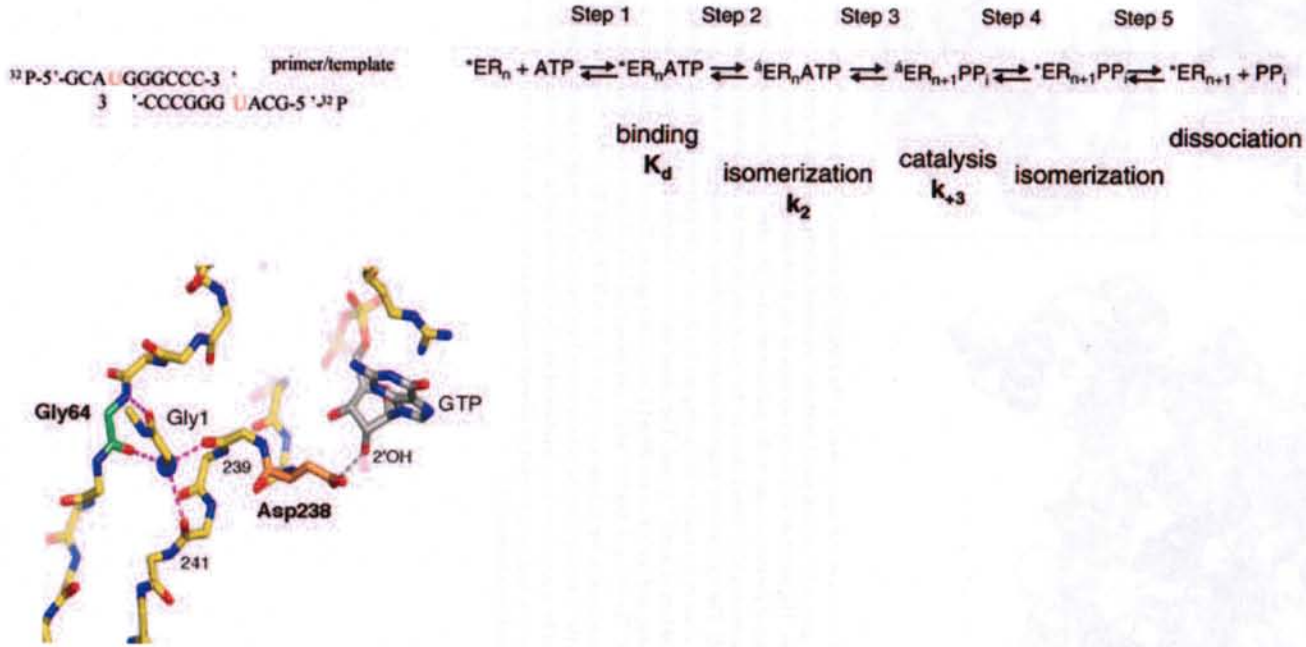

Query 7

Color Plate 20 (Chapter 13). In vitro and structural analyses of picornavirus RdRp fidelity. An in vitro biochemical assay, developed by the Cameron lab, uses a symmetrical, RNA primer-template that permits the measure of incorporation kinetics and fidelity of purified polymerase enzyme. This system permits the dissection of polymerase activity into five steps. Studies with the wild-type and G64S enzymes showed that step 2 is a critical step in determining RdRp fidelity. The crystal structure of the poliovirus RdRp revealed that a hydrogen bond network in which residue 64 participates is altered by the G64S change. (Adapted from references 4, 6, and 92.)

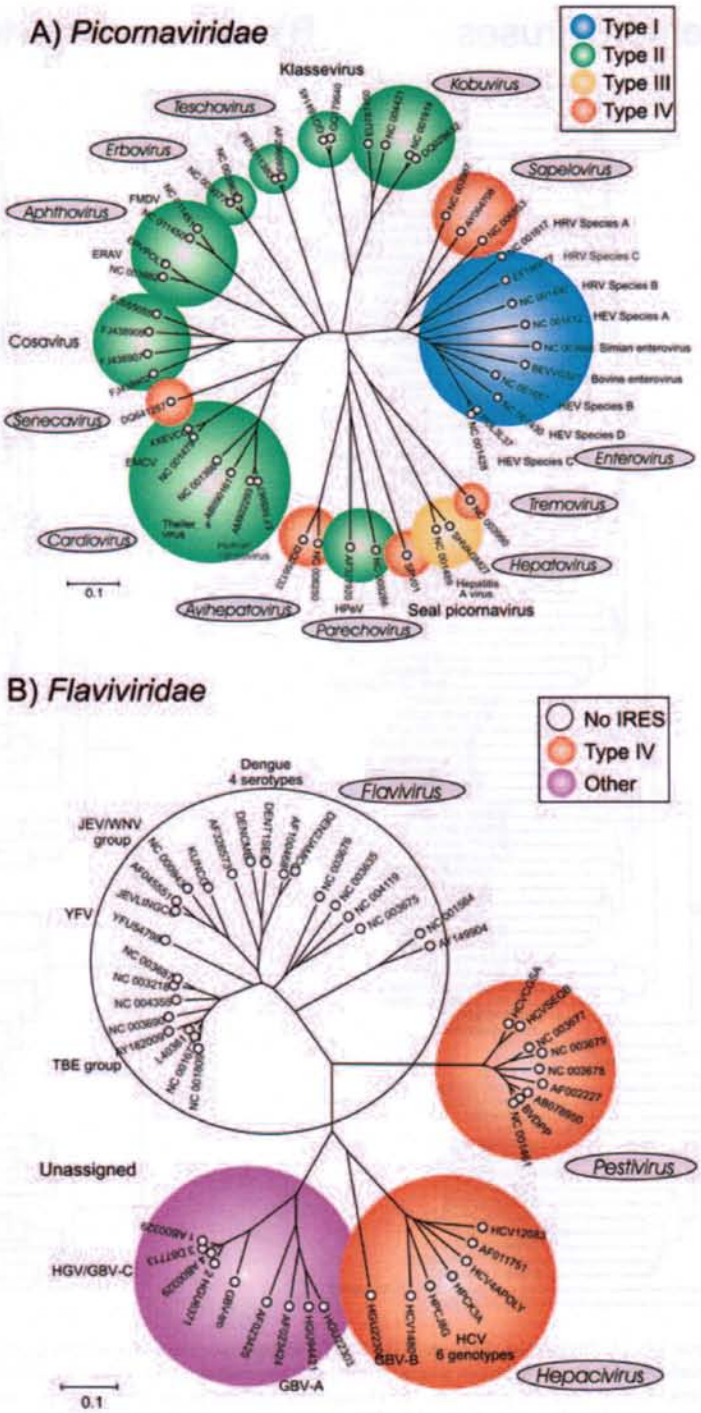

Color Plate 21 (Chapter 14). IRES types of the 12 classified (names in grey ovals) and 3 likely further genera within the *Picornaviridae* (A) and the 4 genera within the *Flaviviridae* (B). The distribution of the type IV IRESs shows several inconsistencies with the branching order of the different picornavirus genera. A structurally similar and likely evolutionarily related type IV IRES is also found in the flavivirus genera *Hepacivirus* (containing the human pathogen hepatitis C virus) and *Pestivirus*. The *Picornaviridae* tree was constructed by neighbor joining using amino acid sequence distances between sequences in the $3D^{pol}$ regions (positions 5862 to 7365, as numbered in the poliovirus Leon strain [accession number K01392]) from representative members of each species and genus. The *Flaviviridae* tree is based on the region of identifiable homology in the RNA-dependent RNA polymerase (NS5[B]) between positions 8395 and 8759 (numbered as in the hepatitis C virus type 1 prototype sequence H77 [accession number AF011751]). (Panel A is an update of a previous analysis [31].)

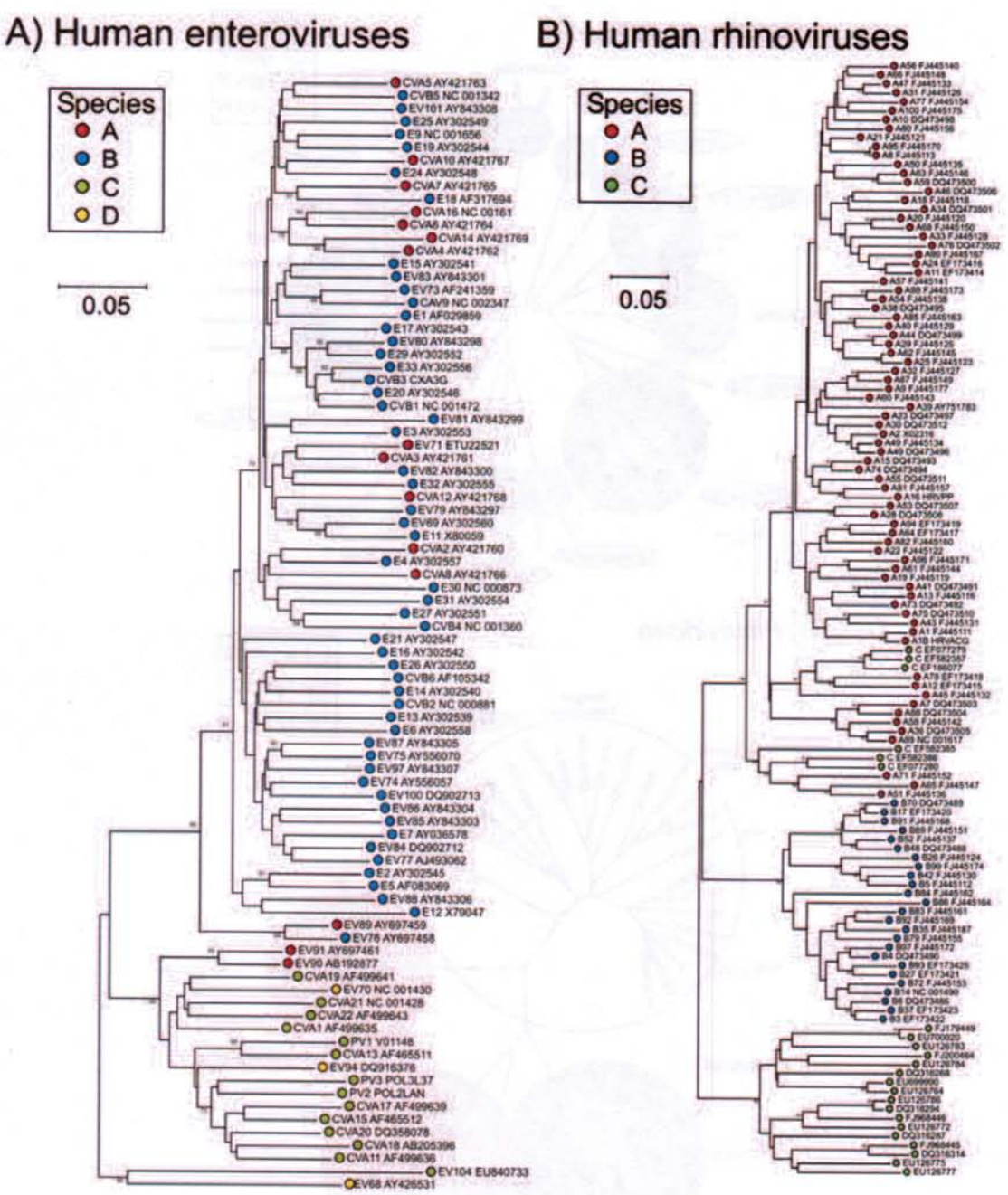

Color Plate 22 (Chapter 14). (A) Phylogenetic analysis of the 5′ UTR of prototype sequences of HEVs, color coded by species (A to D). Sequence labels indicate the serotype and accession number. Abbreviations: CVA, coxsackie A virus; CVB, coxsackie B virus; EV, enterovirus; E, echovirus; PV, poliovirus. (B) Phylogenetic analysis of the 5′ UTR of prototypic and available complete genome sequences of HRV-A to -C and partial 5′ UTR sequences representing the divergent species C 5′ UTR group. The trees were constructed by neighbor joining using uncorrected nucleotide sequence distances from the whole 5′ UTR (A) or between positions 291 and 616 for HRV (positions numbered according to the NC_001490 reference sequence [serotype 14]). Bootstrap resampling was used to determine robustness of the groupings; values of ≥70% are shown.

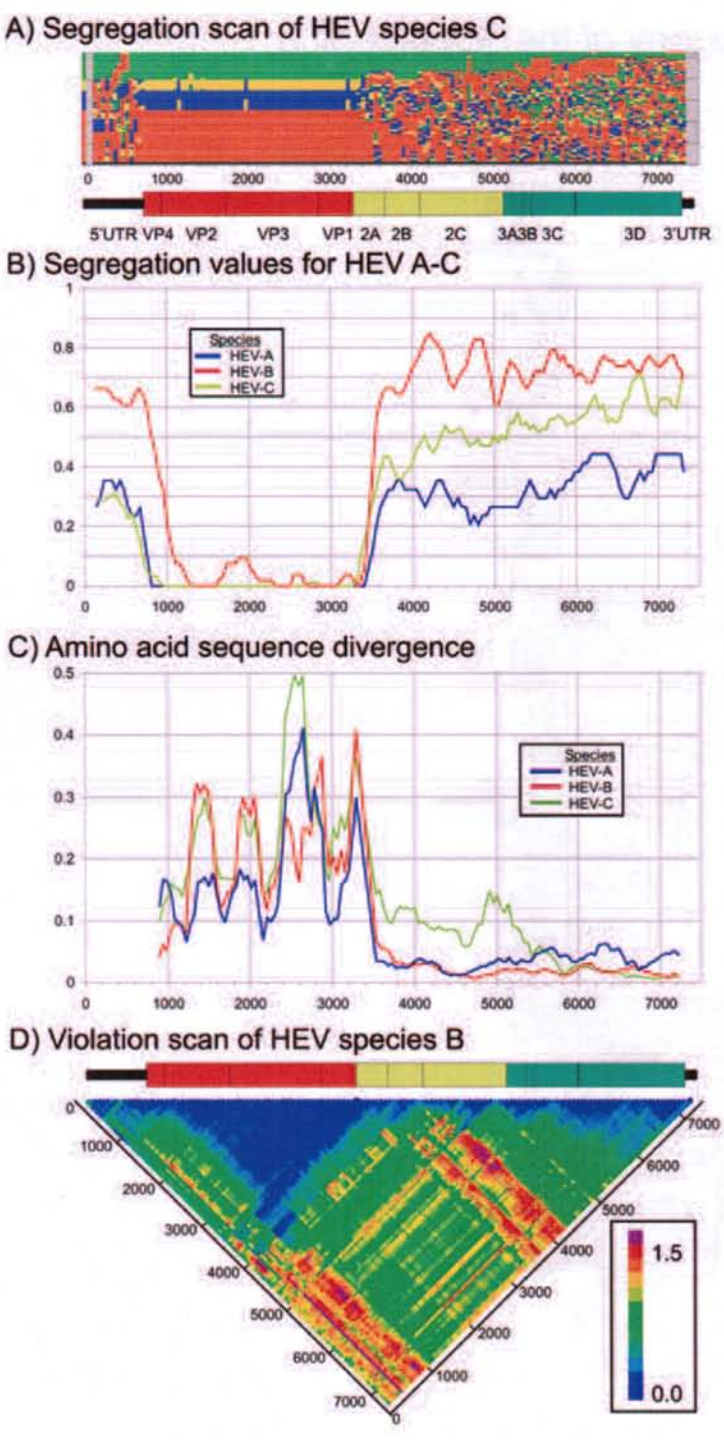

Color Plate 23 (Chapter 14). (A) Phylogenetic grouping of isolates of different serotypes of HEV species C (including poliovirus serotypes 1 to 3) in a series of phylogenetic trees generated from consecutive 300-base fragments across the genome. Below the map is a genome diagram of HEVs, drawn to scale and numbered according to the poliovirus P3/Leon/37 sequence (accession number K01392). (B) Segregation scores for consecutive fragments across genomes of HEV-A to -C, where zero (*y* axis) represents perfect phylogenetic segregation by assigned group (serotypes) and 1 represents the calculated value with no association between phylogeny and group assignment. (C) Mean pairwise amino acid sequence distances between sequences in consecutive 300-base fragments across the genome; values were averaged over a window size of 3 for the three enterovirus species. (D) Phylogenetic compatibility matrix between trees generated from different genomic regions of HEV-B. The matrix shows phylogenetic compatibility scores between trees generated from consecutive 300-base fragments of genome alignments of each virus group, color coded according to the key (compatibility scores from 0.0 to 1.5). Phylogenetically compatible regions are shown in deep blue. (The components of this figure are modified from illustrations in reference 66.)

Query 8

Query 9

A) Phylogeny of the 3Dpol region

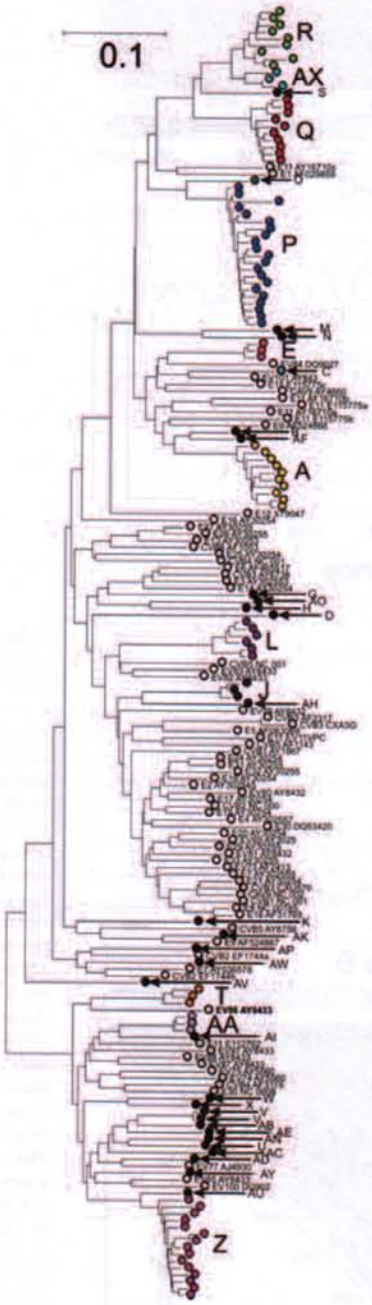

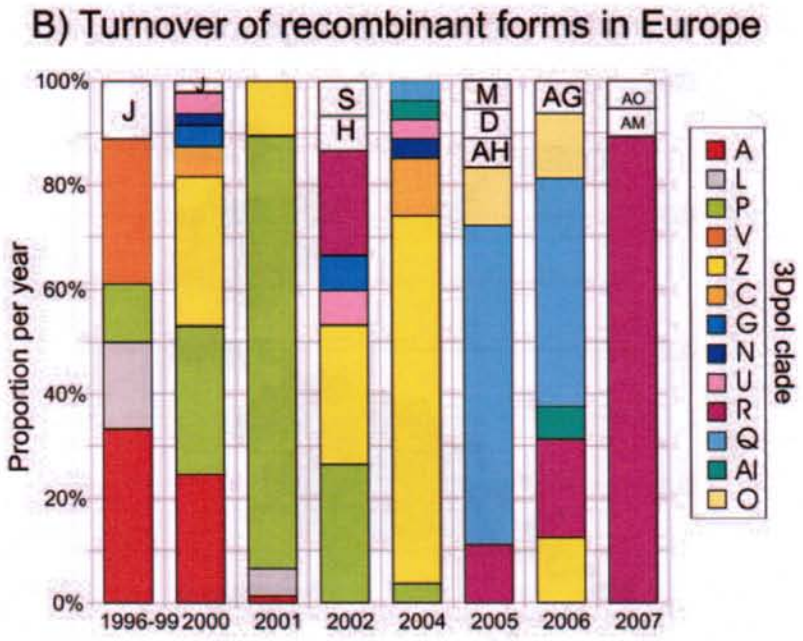

Color Plate 24 (Chapter 14). (A) Phylogenetic tree of a region in the $3D^{Pol}$ gene (representative of the NS region) of isolates of echovirus 30 collected worldwide between 2001 and 2007. Echovirus 30 sequences were resolved into a total of 38 phylogenetically distinct lineages, with the main clades color coded (those with >3 members are shown in black). Echovirus 30 clades were highly interspersed with those of other species B serotypes (unfilled circles, labeled by serotype designation and accession number, as for Color Plate 22). (B) Turnover of echovirus 30 in Europe over the last decade (240 isolates), showing the relative abundances of isolates with different $3D^{Pol}$ sequences (color coded as for the phylogenetic tree in panel A). Isolates with rarer $3D^{Pol}$ clades (two or fewer occurrences) are individually labeled. The tree was constructed by neighbor joining using maximum composite likelihood nucleotide sequence distances from the $3D^{Pol}$ gene (positions 6968 to 7151, numbered as for the poliovirus P3/Leon/37 strain [accession number K01392]). Bootstrap resampling was used to determine robustness of the groupings; values of ≥70% are shown. The components in this illustration are modified from reference 44.

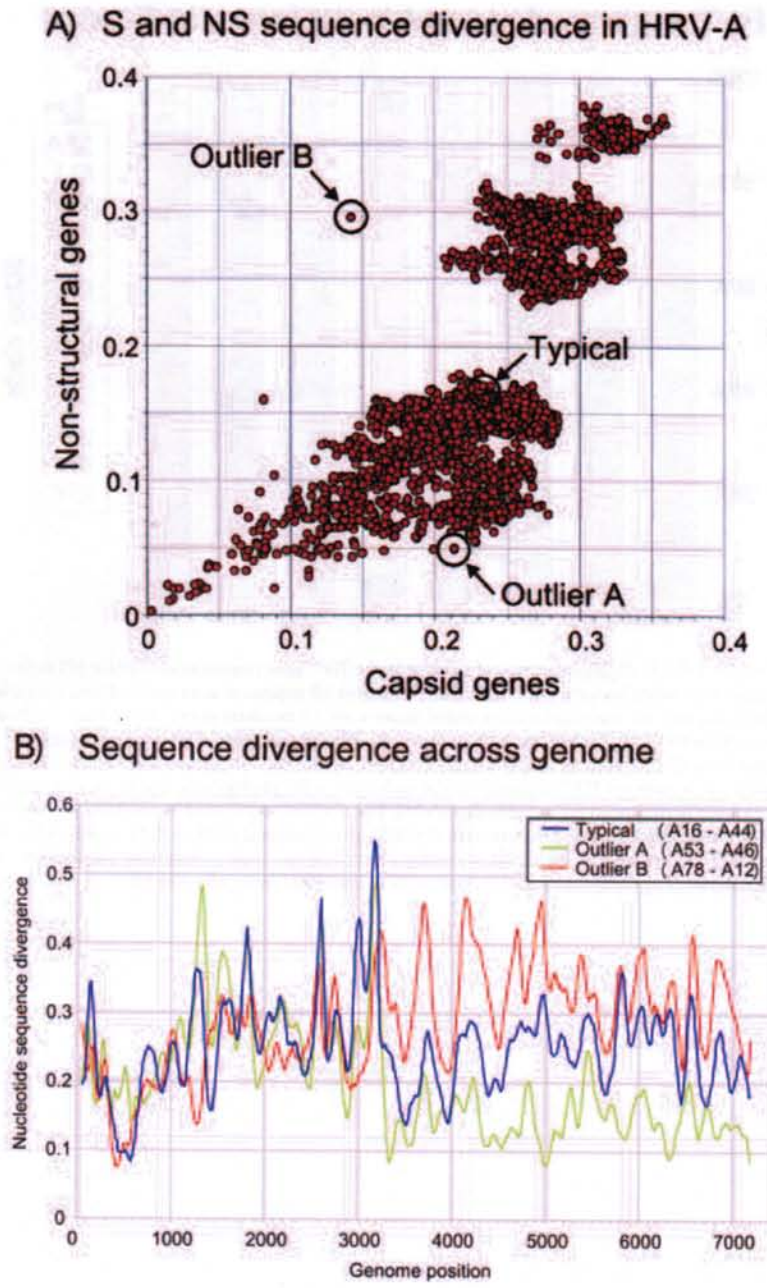

Color Plate 25 (Chapter 14). (A) Sequence divergence in the capsid and NS gene regions between the 74 serotypes of HRV-A (each of the 3,321 pairwise comparisons is individually plotted). (B) Nucleotide sequence divergence scan between two representative HRV-A serotypes (types 16 and 44) falling within the main group, representing the typical degrees of divergence in S and NS regions between picornavirus serotypes. Also shown are two selected outliers with similar degrees of sequence divergence in the capsid region but different variabilities in the NS region, indicative of past recombination.

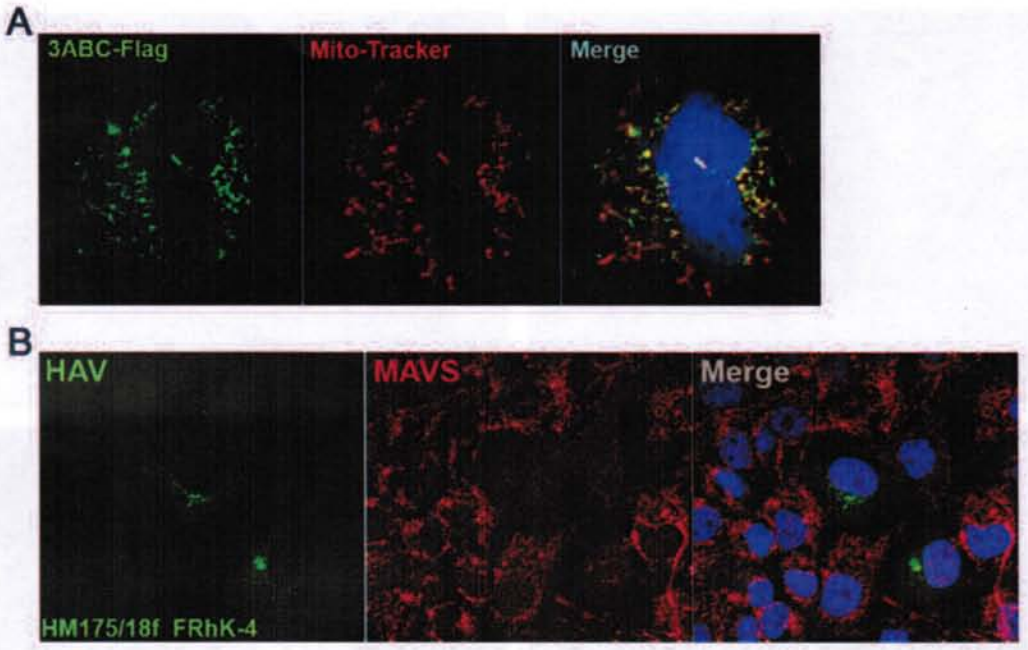

Color Plate 26 (Chapter 24). 3ABC mediates cleavage of the IFN-signaling adaptor protein MAVS (106). (A) Laser-scanning confocal microscopy images showing colocalization of ectopically expressed 3ABC-Flag and MitoTracker, a mitochondrial marker. (B) Confocal microscopy images demonstrating that HM175/18f infection of FRhK-4 (fetal rhesus kidney) cells abolishes expression of the adaptor protein MAVS. (Reproduced from Yang et al. [106] with permission of the publisher.)

Query 10

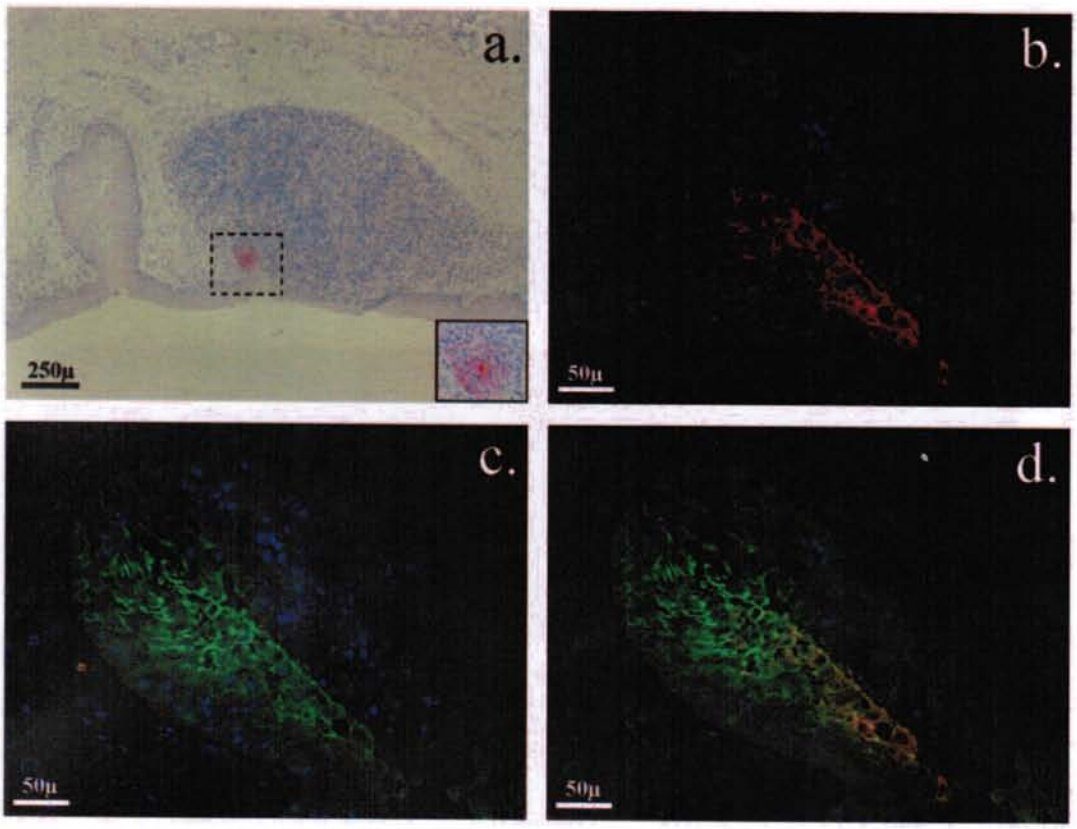

Color Plate 27 (Chapter 25). Earliest detection of FMDV in vivo. Localization of FMDV strain O1 Manisa in the nasopharyngeal mucosa-associated lymphoid tissue (MALT) of a bovine 6 h after aerosol exposure. (a) Immunohistochemical detection of FMDV capsid antigen within superficial MALT. Magnification, ×4. The insert (magnification, ×40) shows a higher magnification of the region of interest (dashed line). (b, c, and d) Simultaneous immunofluorescent localization of FMDV capsid (red) and cytokeratin (green) with nuclear counterstain (blue) on a serial section of the tissue shown in panel a. In the merged image (d), FMDV colocalizes with cytokeratin in nasopharyngeal epithelial cells (yellow/orange), indicating that these are the primary infection sites in cattle. Magnification, ×40. (Images courtesy of Jonathan Arzt.)

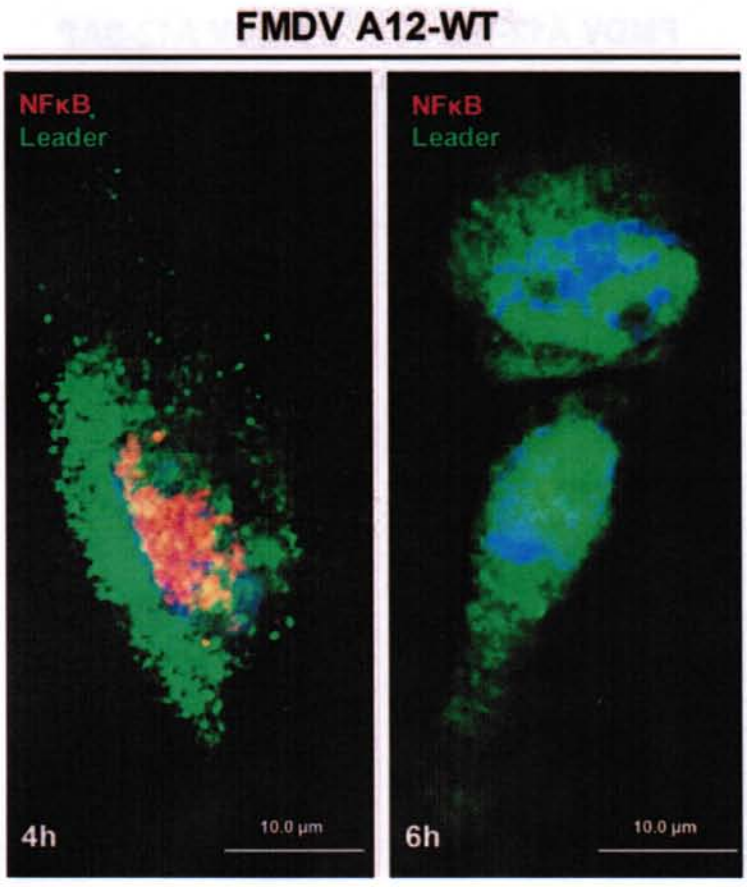

Color Plate 28 (Chapter 25). FMDV induces degradation of NF-κB. (Left) Bovine epithelial cells infected with FMDV serotype A12 wild-type show that by 4 h postinfection, L^{pro} (green) is present in the cytoplasm and the nucleus of an infected cell while activated NF-κB (red) is concentrated in the nucleus. (Right) Progression of the infection leads to a complete disappearance of NF-κB concurrent with an increased presence of L^{pro} in the nuclei of infected cells. Nuclei were stained with 4′,6-diamidino-2-phenylindole. (Images courtesy of Fayna Diaz-San Segundo.)

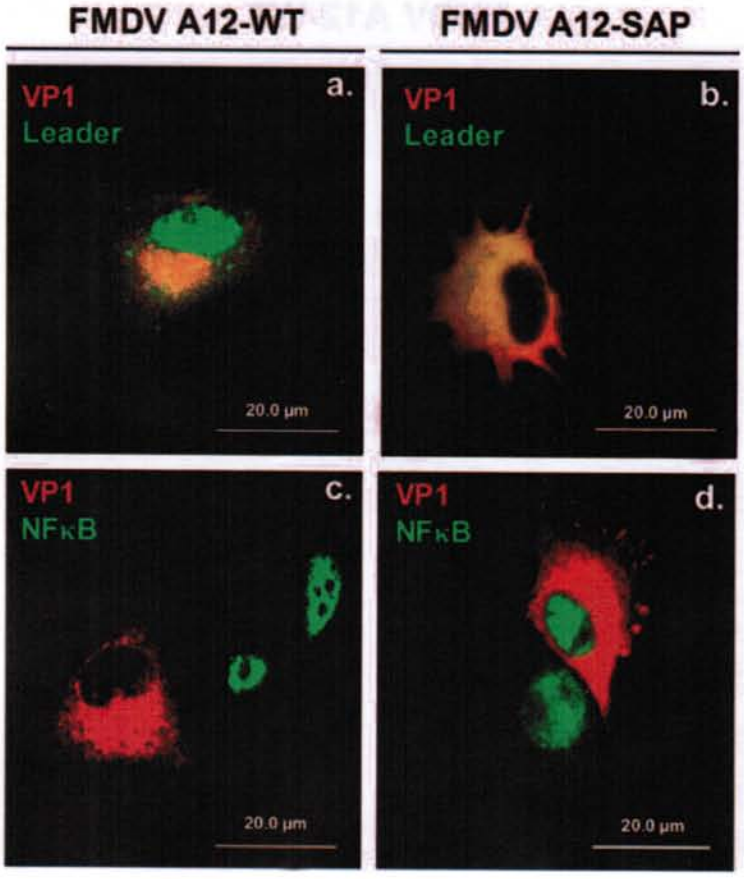

Color Plate 29 (Chapter 25). Mutation of the L^{pro} SAP domain affects nuclear retention and degradation of NF-κB. (a) By 6 h postinfection, L^{pro} (green) is present in the cytoplasm and nucleus of FMDV wild-type -infected bovine epithelial cells. FMDV-infected cells are indicated by the presence of VP1 (1D) (red). (b) NF-κB (green) staining is not detected in infected cells but is detected in the nuclei of bystander cells. (c and d) At the same time point, L^{pro} of the FMDV SAP mutant is only localized to the cytoplasm of the infected cell (c), with no degradation of NF-κB (d). (Images courtesy of Fayna Diaz-San Segundo.)

Return to Table of Contents

Review
Future Virology

Adenovirus serotype 5-vectored foot-and-mouth disease subunit vaccines: the first decade

Marvin J Grubman†, Mauro P Moraes, Christopher Schutta, Jose Barrera, John Neilan, Damodar Ettyreddy, Bryan T Butman, Douglas E Brough & David A Brake

†Author for correspondence: USDA, ARS, NAA, Plum Island Animal Disease Center, PO Box 848, Greenport, NY 11944, USA ■ Tel.: +1 631 323 3329 ■ Fax: +1 631 323 3006 ■ marvin.grubman@ars.usda.gov

The results of the first decade of the development of a replication-defective human adenovirus serotype 5 (Ad5) containing the capsid- and 3C protease-coding regions of foot-and-mouth disease (FMD) virus as a vaccine candidate are presented. In proof-of-concept studies, it was demonstrated that a single inoculation with this vaccine vector containing the capsid of FMD virus A24 Cruzeiro protected both swine and cattle following homologous challenge by direct inoculation 1 week postvaccination. We have expanded these studies in cattle with larger numbers of animals and by testing the vaccine in direct-contact challenge studies, including its ability to prevent FMD virus shedding and transmission. Furthermore, we have developed manufacturing protocols to allow the scalable production of these FMD molecular vaccine products for US Department of Agriculture licensure approval and availability for inclusion in the US National Veterinary Stockpile. We have also constructed and initiated cattle efficacy testing of Ad5 vectors containing the capsid-coding regions from other FMD virus serotypes and subtypes, as well as initiated studies to improve FMD molecular vaccine potency.

Foot-and-mouth disease (FMD) is a highly contagious disease of domestic and wild cloven-hoofed animals including cattle, swine, sheep, goats, deer and buffalo. The disease results in vesicular lesions on the tongue, feet and teats, but causes low mortality, except in young animals. However, infection has a severe adverse impact on animal production and productivity. Furthermore, FMD is a reportable disease and countries in which the disease is present cannot trade susceptible animals or their products with FMD-free countries. Thus, FMD can have a significant economic impact on affected countries, especially those that have a considerable investment in export of susceptible animal species and their products [1].

The disease is caused by the FMD virus (FMDV), a member of the *Picornavirus* family, genus *Aphthovirus*. FMDV is a positive-sense RNA virus with a genome of approximately 8500 bp surrounded by an icosahedral capsid containing 60 copies each of four structural proteins. The viral mRNA is translated into a polyprotein that is processed, mainly by the viral encoded nonstructural (NS) protein, 3C protease ($3C^{pro}$), into the four capsid proteins and ten NS proteins (Figure 1) [1]. FMDV is highly antigenically variable and is composed of seven serotypes, A, O, C, Asia-1, South African Territories types 1, 2 and 3 and multiple subtypes within each serotype.

The steps to control FMD outbreaks include restriction of susceptible animal movement, slaughter of infected and in-contact susceptible animals, decontamination of infected premises and, in countries in which the disease is enzootic, vaccination with an inactivated whole virus vaccine. However, some FMD-free countries hesitate to use the current vaccine in outbreak situations. Thus, during the FMD outbreaks in the UK in 2001 and 2007, the government considered but did not implement vaccination programs and, instead, slaughtered millions of animals. The 2001 outbreak spread to The Netherlands, which vaccinated hundreds of thousands of animals but, nevertheless, the government also slaughtered these animals. By contrast, in the 1997 FMD outbreak in Taiwan, the first in 68 years, the government vaccinated animals and did not slaughter them. These different approaches are the result of a number of considerations, but perhaps the major factor is the time required to regain FMD-free status. The World Organization of Animal Health (OIE) policy mandates that countries that either slaughter infected or in-contact animals or vaccinate and then slaughter these animals can regain FMD-free status by documenting absence of disease for 3 months after the last case, while countries that vaccinate susceptible animals must wait 6 months to regain this

Keywords
foot-and-mouth disease virus ■ replication-defective adenovirus ■ subunit vaccines

future medicine part of fsg

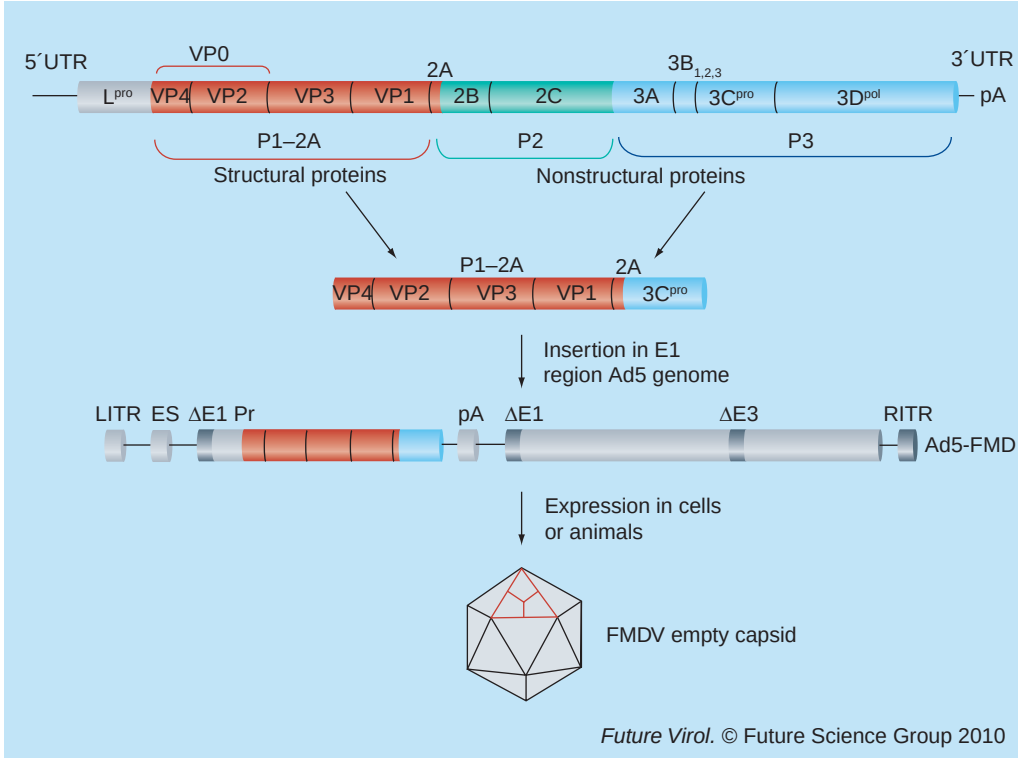

Figure 1. Map of the foot-and-mouth disease virus genome and construction of the adenovirus serotype 5–foot-and-mouth disease vector. The functional elements in the genome that are indicated include the 5′ untranslated region (5′UTR), the coding region for all the viral-encoded proteins, the 3′ end of the genome (3′UTR) and the polyadenylic acid (pA) tract. The viral mRNA is translated into a polyprotein that is processed by viral enzymes including $3C^{pro}$. Processing of capsid protein VP0 into VP4 and VP2 occurs by an unknown mechanism. The structural protein precursor, P1–2A, and the $3C^{pro}$-coding regions were cloned by recombinant DNA techniques and inserted into the E1 region of the Ad5 vector to create Ad5–FMD. The Ad5–FMD virus was used to infect tissue culture cells or inoculated into animals and FMDV capsid proteins were synthesized. ΔE1: Deletion in the E1 region; ΔE3: Deletion in the E3 region; $3C^{pro}$: 3C protease; $3D^{pol}$: 3D polymerase; Ad5: Adenovirus serotype 5; ES: Encapsidation signal; FMD: Foot-and-mouth disease; FMDV: Foot-and-mouth disease virus; LITR: Left internal terminal repeat; pA: Polyadenylic acid tract; Pr: Promoter; RITR: Right internal terminal repeat; UTR: Untranslated region.

status. Thus, there is a significant economic incentive for countries that export cattle and swine, as well as their products, to regain FMD-free status as quickly as possible.

Both the OIE and FMD-free countries have raised concerns over the use of the current inactivated vaccine. This vaccine is produced in suspension cultures of FMDV-infected baby hamster kidney cells and is obtained from cell-free supernatants. The supernatants contain not only virus particles, but also viral NS proteins, which are produced during virus infection and depending on the concentration/purification protocols of the vaccine manufacturer these NS proteins contaminate the vaccine preparation to varying degrees. As a result, it can be difficult to distinguish vaccinated from infected animals using currently approved OIE diagnostic assays. In addition, if vaccinated animals are exposed to live virus they can become persistently infected, but are often asymptomatic. Evidence suggests that the level of infection does not induce detectable amounts of antibodies to NS proteins, making persistently infected animals difficult to identify [2].

Furthermore, there is growing concern over the accidental or intentional introduction of OIE list A agricultural pathogens that adversely affect a country's livelihood, such as FMDV, into FMD-free countries. Thus, these countries are very interested in developing novel FMD vaccines that address the limitations of the current inactivated vaccine. Some of the key limitations or disadvantages of the current inactivated vaccines that need to be addressed include thermostability and requirement to maintain frozen product, relatively short-lived duration of immunity and inadequate protection amongst subtypes in a major serotype (e.g., types A and O). With regard to this, higher-potency vaccines developed for emergency use and national

stockpiles can be effective in providing adequate protection against new, emerging subtypes in some instances.

We have developed a subunit vaccine strategy that uses the coding information for an immunogen that contains the entire FMDV capsid polyprotein-coding region (P1–2A), as well as the viral $3C^{pro}$ required for polyprotein processing, but lacks the information for most of the other viral NS proteins (Figure 1). Thus far, the most efficient delivery system is a replication-defective human adenovirus serotype 5 (Ad5) vector [1,3,4]. Thus, this vaccine is a marked differentiation of infected from vaccinated animals (DIVA) vaccine, since it lacks the coding regions for a number of viral NS proteins, and vaccinated herds can be distinguished from infected herds in a manner similar to that used with current, highly purified, inactivated vaccines and FMDV NS protein 3ABC diagnostic tests. Expression and processing of the capsid polyprotein allows for assembly of these proteins into a virus particle lacking viral nucleic acid; that is, an empty capsid (Figure 1). This approach does not require infectious FMDV and, therefore, eliminates some of the concerns regarding the manufacture of the current inactivated FMD vaccine, including incomplete inactivation, escape of live virus from vaccine manufacturing facilities, as well as the ability to produce this vaccine in the USA without the need for expensive high-containment facilities.

As it is 10 years since the publication of our initial study using this approach [3], this article summarizes our proof-of-concept studies and presents feasibility experiments in cattle with the FMD A24 Cruzeiro subunit vaccine candidate (Figure 1). Further information on the clinical, manufacturing and regulatory development activities of this first FMD subunit vaccine also is provided, as well as a brief overview on the early development of Ad5–FMD vaccine candidates against other FMDV serotypes and subtypes. Future perspectives for utilizing this strategy to combat the disease in FMD-free countries as well as countries in which the disease is enzootic are discussed.

Development of novel vaccines

Empty viral capsids are natural products of FMDV infection of cell cultures and are as immunogenic as virions when inoculated into animals [5–7]. We have used rDNA procedures to construct this immunogen and have examined a number of approaches to deliver it to animals [4]. As previously mentioned, to date, the most efficient delivery system is the replication-defective human Ad5 vector [1,3,4]. The vector we have used in our proof-of-concept studies has a deletion in the E1 region in which we have inserted the FMDV P1–2A and $3C^{pro}$-coding regions under the control of a cytomegalovirus promoter (Figure 1) [3]. Some of the advantages of this delivery system include the ability to infect cells of several animal species, including cattle and swine, the effective induction of a transgene-specific immune response in animals transduced with recombinant Ad5 vectors [8], their low pathogenicity in humans and animals, their ability to only grow in cell lines containing the missing portion of the Ad5 genome [9,10] and their capacity to incorporate up to 11 kbp of foreign genes.

Potency & efficacy of Ad5–FMD vaccines

In our initial studies in cell culture, we demonstrated that the capsid polyprotein of a laboratory strain of FMDV was synthesized and processed by $3C^{pro}$ into the capsid proteins VP0 (the precursor of VP4 and VP2), VP3 and VP1 [3]. Furthermore, assembly of the capsid proteins occurred since they were all immunoprecipitated with monospecific polyclonal or monoclonal antibodies. Studies in swine with this vector as well as a vector containing an inactive $3C^{pro}$ demonstrated that after two intramuscular (im.) inoculations of 1×10^8 followed by 5×10^8 plaque-forming units (PFU)/animal, generation of an FMDV-specific neutralizing antibody response and protection from contact challenge was induced only by the vector containing the active $3C^{pro}$ [11]. Additional analysis of the Ad5 vector-expressed FMDV antigen has confirmed that the antigen is presented as a multiepitope empty capsid-like structure. Co-immunoprecipitation studies directed at each of the capsid proteins expressed in Ad5–A24-infected cells confirmed the earlier published studies. Furthermore, biochemical evaluation by both reverse-phase HPLC and light scattering of the purified FMDV antigen has shown that the particle size that is generated approximates that of an FMDV capsid [Brough DE *et al.*, Manuscript in Preparation].

Since only one vaccination will be possible in a program to rapidly control an FMD outbreak in a disease-free country, we examined the potency and efficacy of a tenfold higher dose of Ad5–FMD, specifically, 5×10^9 PFU. An Ad5–A24 Cruzeiro vector was used to inoculate swine and the animals were challenged by direct inoculation of homologous virus at 42,

14 and 7 days postvaccination [12]. Animals in all the vaccinated groups were protected from clinical disease. To demonstrate the efficacy of this vaccine in cattle – the most economically important animals susceptible to FMDV – five animals were vaccinated im. with one dose of 5×10^9 PFU/animal and challenged 7 days later by intradermalingual (IDL) inoculation with 2×10^4 bovine infectious dose 50, a twofold higher challenge dose than recommended by the OIE [13]. All vaccinated animals were protected against disseminated disease.

Approaches to improve vaccine potency

While our first-generation Ad5–FMD vector has successfully protected both swine and cattle, the dose required is relatively high. In addition, the same dose resulted in only partial protection in swine vaccinated with another South American vaccine strain, O1 Campos (Ad5–O1C) [14]. This serotype is known to require larger amounts of antigenic mass in the traditional inactivated vaccines [15,16]. As a result, we have attempted to enhance the potency of the FMDV immunogen using a variety of approaches.

As a first approach, we inoculated swine with the Ad5–O1C vector as well as a second vector expressing porcine granulocyte–macrophage colony-stimulating factor, a successful adjuvant for DNA vaccines (see citations in [14]). In swine, the combination of those vectors, despite the induction of an early increase in neutralizing antibodies, did not result in improved protection compared with the vaccine alone [14].

It has been demonstrated that type I interferon (IFN-α/β) can act as an adjuvant and boost the immune response to antigens when coadministered with soluble protein [17], a chemically inactivated vaccine [18] or DNA encoding a transgene [19]. As a second approach we demonstrated – in agreement with the previously mentioned studies – that swine inoculated with an Ad5 vector containing the gene for porcine, *IFN*-α, administered with either a low or high dose of Ad5–A24 vaccine, enhanced both the long-term adaptive immune response, that is, 42 days postvaccination, and protection of animals in both groups as compared with swine inoculated with only Ad5–A24 [20].

The addition of the *3D*^{pol} coding region may actually reduce vaccine potency, because a recombinant Ad5-expressing serotype O capsid (O/China/99) required three doses to protect guinea pigs against homologous challenge [21].

Utilizing a different approach, we hypothesized that since FMDV genome replication occurs on internal cellular membranes that are altered by virus infection, the induction of similar membrane rearrangements in Ad5–FMD transduced cells may enhance FMDV capsid formation and stability, allowing for a more potent immune response.

Recently, we have included the coding regions for FMDV NS proteins 2B and 2C in the Ad5–A24 vaccine [22]. There were remarkable changes in the arrangement of cellular membranes in bovine cells transduced with the new vectors as observed by electron microscopy. Furthermore, the addition of only the *NS 2B* coding region resulted in an increased number of smooth cytoplasmic vesicles as compared with the original vector and the *NS 2B*- and *2C*-expressing vector. In animals, the vaccine expressing NS protein 2B, but not the original vaccine or the *NS 2B*- and *2C*-containing vaccine, induced a more rapid FMDV-specific neutralizing antibody response (detectable 4 days postvaccination) and resulted in a more efficacious vaccine. We are now focusing efforts to determine the nature of the morphologic changes induced by NS protein 2B in transduced cells in order to understand the mechanism of the adjuvant activity of this new vaccine. In addition, the inclusion of *NS 2B* coding region into serotype O1C Ad5-vectored vaccine candidate was tested in bovines. There were an increased number of animals protected in the group that was inoculated with the *NS 2B* coding region-containing construct as compared with the construct lacking the complete *NS 2B* coding region and this correlated with the increased presence of an antigen-specific $CD8^+$ T-cell response after homologous challenge [Moraes MP *et al.*, Manuscript in Preparation].

Ad5–A24 vaccine candidate

Early development studies

The US Department of Agriculture (USDA) Agricultural Research Service (ARS) proof-of-concept cattle safety and efficacy results using the prototype Ad5–A24 vaccine met the predefined criteria for US Department of Homeland Security (DHS) Science and Technology to initiate a vaccine development plan for regulatory licensure through the USDA Center for Veterinary Biologics (CVB). USDA ARS identified a biotechnology company, GenVec, Inc., which had proprietary technology centered on replication-deficient Ad5 vectors that are incapable of generating replication-competent wild-type adenovirus owing to the additional deletion of the adenovirus E4 domain.

The P1–2A and $3C^{pro}$ coding regions from FMDV A24 Cruzeiro and A12, respectively, were used to construct the FMD A24 Cruzeiro vaccine development vector Adt.A24.11D (Ad5–A24), which was produced in an E1/E4 complementing cell line, 293-ORF6 (M2A) [10,23]. Since then, several other FMDV transgenes have been constructed using this technology, demonstrating the robustness of this technology for future applications. GenVec's M2A cell line/vector technology provides robust, consistent construction and production of Ad5–FMDV vectors. FMDV inserts as transgenes are highly toxic to production cells and the M2A platform allows for efficient vector construction and production by suppressing transgene expression [24]. A new manufacturing process using serum-free suspension culture for upstream production of the Ad5 vector and streamlined purification processes has been developed to provide a means to scale-up to the necessary levels for vaccine production. Using this system, we have shown that the production of the Ad5–A24 vector is robust, reproducible and of consistent yield and quality with each batch produced. In addition, Ad5 vectors expressing FMDV transgenes are genetically stable after serial passaging of the Ad5 vector. The expected sequence of the FMDV transgene and Ad5 vector is unchanged after ten serial passages and the level of FMDV protein expression elicited from the molecular vaccine is consistent after serial passaging. This provides a significant technology advance for these molecular FMDV vaccines over existing vaccine manufacture, wherein batch failures due to genetic divergence during production can occur [25].

An initial efficacy study in a 7-day postvaccination IDL homologous bovine challenge model demonstrated 100% seroconversion in Ad5–A24 vaccinates on the day of challenge and 100% protection against generalized disease, results that were similar to those previously observed using the USDA ARS Ad5–A24 prototype vaccine [13]. Based on these results, initial development efforts focused on the identification of a manufacturing-compatible downstream processing method that did not require cesium chloride (CsCl) purification of the Ad5–A24 vaccine. Following Ad5–A24 production in a 10 l bioreactor, downstream processing steps involving column chromatography were completed to generate three vaccine preparations with increasing levels of purity, identified as downstream fraction (DS)5, DS7 and DS9/10. On day 0, groups of cattle (n = 6) were immunized im. with Ad5–A24 DS5 (treatment [T]01), DS7 (T02), DS9/10 (T03) vaccine. Positive and negative control groups (n = 4) were immunized with CsCl gradient triple purified Ad5–A24 or vaccine final formulation buffer, respectively. No adverse local or systemic reactions were observed in vaccinates during the 72 h postvaccination observation period. The Ad5–A24 vaccine preparations were antigenic in cattle as demonstrated by the presence of significant serum virus neutralization (SVN) titers to A24 Cruzeiro at the time of FMDV challenge (7 days postvaccination) in 100, 83 and 67% of DS5, DS7 and DS9/10 treatment groups, respectively (Table 2). Following IDL direct challenge with FMDV A24 Cruzeiro, the incidence of generalized disease, for example, foot lesions, was 75% in sham-immunized naive cattle and 0% in Ad5–A24 CsCl-vaccinated cattle (Table 2). Importantly, all cattle in all Ad5–A24 vaccinated treatment groups were completely protected against generalized disease, including three vaccinated cattle (#7121, 7126 and 7127) that were seronegative on the day of the challenge. Collectively, these results demonstrated for the first time that Ad5–A24 experimental vaccines prepared using scalable manufacturing processes are safe, antigenic and confer solid protection against generalized disease following FMDV direct inoculation.

Based on these results, the Ad5–A24 DS5 vaccine preparation was downselected for further development and evaluated for efficacy in a FMDV direct contact challenge model previously developed by DHS scientists (Table 3). On day 7, groups of cattle (n = 6) were immunized im. with Ad5–A24 DS5 high (T01; 5.0×10^{10} total particle units [PU]), medium (T02; 1.25×10^{10} total PU) or low (T03; 3.12×10^{9} total PU) dose vaccine. A negative control group (T04; n = 4) was immunized with vaccine final formulation buffer. An HPLC assay is used for Ad5–A24 DS5 vaccine dose quantification based on total PU. This assay employs a reference that is derived from Ad5–A24 vaccine used to demonstrate efficacy. In addition, a focus-forming unit assay (similar to the conventional PFU assay) was performed in order to determine vaccine particle infectivity. In this particular study, the PU:focus-forming unit ratio was 16.

On day 0, eight naive cattle were IDL challenged with FMDV A24 Cruzeiro and then co-mingled with Ad5–A24 vaccinates (T01–T03) and sham-immunized cattle (T04). All cattle (n = 30) were co-mingled for 2 weeks and cattle were examined for lesions at four timepoints postcontact challenge. In addition to pedal lesion scoring, direct contact challenge cattle were also assessed for oral lesions (tongue and dental pad). The maximum clinical score for each animal at each time point was six (e.g., four feet positive,

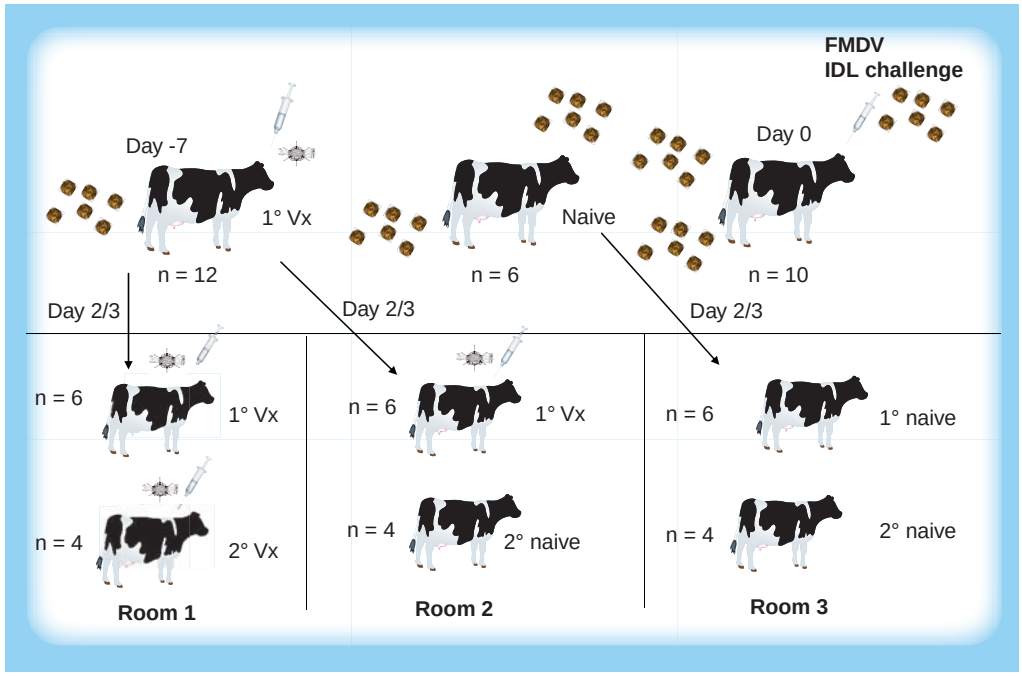

Figure 2. Adenovirus serotype 5–A24 vaccine prevention of foot-and-mouth disease virus transmission study (experimental design). For the primary direct contact challenge phase, 12 cattle were immunized with Ad5–A24 1 week prior to co-mingling on day 0 with six naive cattle and ten cattle infected with FMDV by IDL challenge. On day 2, a total of six Ad5–A24 primary vaccinates and three naive cattle were moved into separate rooms housing Ad5–A24 secondary vaccinates (room 1) or secondary-naive cattle (rooms 2 or 3). On day 3, the same procedure was repeated with the remaining Ad5–A24 primary vaccinates and primary-naive cattle. For the secondary direct-contact challenge phase, ten cattle in each of the three rooms were monitored for a total for 43 days.
Ad5: Adenovirus serotype 5; FMDV: Foot-and-mouth disease virus; IDL: Intradermalingual; Vx: Vaccinate.

tongue positive and dental pad positive). In some vaccinated animals, dental pad lesions subsequently resolved and were no longer apparent at the last time point scored (day 14).

Foot-and-mouth disease virus-specific SVN titers in Ad5–A24-immunized cattle were vaccine dose dependent. At 1 week postvaccination,, the incidence of seroconversion (SVN titer ≥ 0.9 $\log_{10}$) was 100% (6/6), 100% (6/6) and 67% (4/6) in Ad5–A24 DS5 treatment groups that received high (T01), medium (T02) and low (T03) dose Ad5–A24, respectively (Table 3). Following direct-contact challenge on day 0, none of the sham-vaccinated cattle (T04) were protected against generalized disease and 100% of these cattle showed tongue and pedal lesions on all four feet by day 7 (Table 3). Based on the most stringent criteria of protection against disease (e.g., absence of any lesions) at 14 days postchallenge, the overall protection in Ad5–A24 vaccinates was 61% (11/18); the Ad5–A24 DS5 vaccine at the high (T01), medium (T02) and low (T03) doses conferred 67, 83 and 33% protection, respectively. In the high-dose group (T01), there was no correlation between SVN titer on day 0 (day of contact challenge exposure) and protection. For example, one of the high-dose vaccinates (#826) had the highest SVN titer, yet developed a tongue lesion on day 7, whereas three other vaccinates (#816, 818 and 840) showed completed protection against FMDV disease. The absence of an association between SVN titer and complete protection was also observed in the other two Ad5–A24-vaccinated groups. Based on the OIE criteria of protection against disease (absence of pedal lesions), the overall protection in Ad5–A24 vaccinates at 14 days postchallenge was 83% (15/18); Ad5–A24 DS5 vaccine at the high (T01), medium (T02) and low (T03) doses conferred 83, 100 and 66% protection, respectively. These results demonstrate for the first time that the Ad5–A24 DS5 vaccine can confer a high level of protection against generalized disease using a direct contact challenge model. A direct contact challenge model is believed by some FMDV experts to more closely represent a natural FMDV outbreak versus the IDL challenge model that is recommended by OIE for the serial release of inactivated FMD vaccines.

The ideal product profile for any FMD vaccine is the ability to prevent FMDV shedding in vaccinates and subsequent transmission to naive cattle. Thus, the Ad5–A24 DS5 vaccine was tested for the ability to prevent FMDV shedding and disease transmission to other Ad5–A24 vaccinates or to naive (nonvaccinated) cattle. As shown in Figure 2, on day 7, cattle were immunized im. with Ad5–A24 vaccine (n = 12; 5×10^{10} PU; primary vaccinates) or vaccine formulation buffer (n = 6; primary naive). At 7 days postvaccination (day 0) all Ad5–A24-vaccinated and sham-immunized cattle were co-mingled with FMDV donor or 'seeder' cattle (n = 10) that had been challenged earlier the same day. On day 2, a total of six Ad5–A24 primary vaccinates were moved into separate rooms (three per room) housing either Ad5–A24-immunized cattle (n = 4; secondary vaccinates; room 1) or sham-immunized cattle (n = 4; secondary naive; room 2). Also on day 2, three primary-naive cattle were moved into a separate room housing sham-vaccinated cattle (n = 4; secondary naive; room 3). On day 3, the procedure was repeated with the remaining Ad5–A24 primary vaccinates and primary-naive cattle. The ten cattle in each room (total of three rooms) were allowed to freely co-mingle within each room for a total of 43 days. During this period, cattle were inspected for signs of generalized disease (pedal and oral lesions) and daily air samples were collected and tested by real-time PCR to detect the presence of FMDV nucleic acid.

Results show that in room 1, 100% of Ad5–A24 primary vaccinates and 100% of Ad5–A24 secondary vaccinates were protected against generalized disease (Table 4). All air-sampling results from room 1 were negative throughout the 6-week postcontact challenge co-mingling period, with the exception of a single, weakly positive sample on day 4. Similarly, room 2 results show that 100% of Ad5–A24 primary vaccinates and, most importantly, 100% of secondary naive cattle were protected against FMDV-induced generalized disease. Air-sampling results from room 2 were consistent with the clinical results, and not a single air sample tested positive for FMDV by real-time PCR. Consistent with these results, none of the secondary-naive cattle developed detectable FMDV A24-specific SVN titers, and were seronegative after 14 days co-mingling with Ad5–A24 primary vaccinates exposed to FMDV. The FMDV shed and transmission model employed was effective, based on the results obtained from room 3. All secondary-naive cattle exposed to primary-naive cattle developed generalized disease and numerous, strongly positive air samples were found through day 12 of co-mingling, followed by sporadic positive samples through day 23. Interestingly, in room 3 no positive air samples were found after

Table 1. Milestones in the development of the replication-defective human adenovirus vectored foot-and-mouth disease subunit vaccines.

Year	Milestones	Ref.
1999	First publication, proof of concept. Characterization of expression and processing of the FMDV capsid of laboratory strain serotype A12 in an Ad5 vector. The $3C^{pro}$ activity is essential for production of neutralizing antibodies in mice. Early studies in swine.	[3]
2001	Characterization of the response against A12 in swine. The $3C^{pro}$ activity is essential for protection of pigs. Evidence of Th1/Th2 immune response.	[11]
2002	Introduction of FMDV capsid from a field strain (A24 Cruzeiro). Protection of swine with a single dose as early as 7 days postvaccination.	[12]
2003	Strategic utilization of the vaccine in combination with type 1 interferon. Protection of swine as early as 1 day after vaccination. Coexpression of capsids from two FMDV serotypes in one Ad5 vector (A24 and O1 Campos).	[27,28]
2004	DHS and Genvec, Inc. join ARS for development of a commercial product.	
2005	Introduction of Ad5–A24 vaccine in bovine: protection at 7 days postvaccination. Introduction of O1 Campos capsid with partial protection of pigs. Expression of pGM-CSF in combination with Ad5–O1 Campos produce a short adjuvant effect.	[13,14]
2006	Type 1 interferon induces a lasting adjuvant effect with increased production of IgG1 antibodies. Early animal experiments with a commercial Ad5 vector.	[20]
2006–2009	Potency and safety studies and scalable production. Production of adenovirus-expressing O/China/99 vaccine. Introduction of additional nonstructural protein (NS) 2B improves protection in pigs.	[21,22]
2008	Completed first USDA Center for Veterinary Biologics regulatory approved FMD vaccine trial on the USA mainland.	GenVec, Inc. regulatory dossier

$3C^{pro}$: 3C protease; Ad5: Adenovirus serotype 5; ARS: Agricultural Research Service; DHS: US Department of Homeland Security; FMDV: Foot-and-mouth disease virus; Th1: T-helper cell 1; Th2: T-helper cell 2; USDA: US Department of Agriculture.

Table 2. Adenovirus serotype 5–A24 vaccine preparations: immunogenicity and vaccine efficacy.

Group	Animal (#)	Days postvaccination (SVN titer)		Days postdirect challenge (clinical score)			
		-7	*0*	*3*	*6*	*9*	*14*
Ad5–A24 DS5	7111	0.6	1.2	0	0	0	0
	7112	0.6	0.9	0	0	0	0
	7113	0.6	1.2	0	0	0	0
	7114	0.6	1.2	0	0	0	0
	7115	0.6	0.9	0	0	0	0
	7116	0.6	1.2	0	0	0	0
GMT		0.6	1.1				
SD		0.0	0.2				
Ad5–A24 DS7	7117	0.6	1.2	0	0	0	0
	7118	0.6	1.2	0	0	0	0
	7119	0.6	0.9	0	0	0	0
	7120	0.6	0.9	0	0	0	0
	7121	0.6	0.6	0	0	0	0
	7122	0.6	1.2	0	0	0	0
GMT		0.6	1.0				
SD		0.0	0.2				
Ad5–A24 DS9/10	7123	0.6	1.2	0	0	0	0
	7124	0.6	1.5	0	0	0	0
	7125	0.6	1.2	0	0	0	0
	7126	0.6	0.6	0	0	0	0
	7127	0.6	0.6	0	0	0	0
	7128	0.6	1.2	0	0	0	0
GMT		0.6	1.1				
SD		0.0	0.4				
Ad5–A24 CsCl	7129	0.6	1.5	0	0	0	0
	7130	0.6	1.2	0	0	0	0
	7131	0.6	0.9	0	0	0	0
	7132	0.6	1.5	0	0	0	0
	7133	0.6	1.2	0	0	0	0
	7134	0.6	1.2	0	0	0	0
GMT		0.6	1.3				
SD		0.0	0.2				
FFB (sham)	7135	0.6	0.6	3	4	4	4
	7136	0.6	0.6	0	0	0	0
	7137	0.6	0.6	4	4	4	4
	7138	0.6	0.6	4	4	4	4
GMT		0.6	0.6				
SD		0.0	0.0				

Ad5: Adenovirus serotype 5; CsCl: Cesium chloride; DS: Downstream fraction; FFB: Final formilation buffer; GMT: General mean titer; SD: Standard deviation; SVN: Serum virus neutralization.

day 23, suggesting that FMDV-infected cattle do not shed virus into the air following resolution of primary disease (data not shown). Future studies will evaluate the ability of the Ad5–A24 vaccine to prevent or significantly reduce viral persistence following direct or contact FMDV challenge and will include probang sampling, since these results will provide information on FMD control strategies for trade.

The results from these early development safety and efficacy studies on the Ad5–A24 vaccine candidate fulfilled the criteria to transition

Ad5–A24 to a full development program comprised of the clinical, manufacturing and regulatory elements necessary to meet requirements for product licensure.

Full development studies

The Ad5–A24 vaccine is considered to be a category 3 recombinant vaccine according to USDA CVB guidelines [101]. Although Ad5–A24 vaccine virus is incapable of replicating in host cells that lack E1 and E4 complementation, the vaccine candidate is considered to be a modified live virus. Thus, Summary Information Format (SIF) guidelines state that safety studies related to vaccine reversion to virulence (backpassage) and vaccine shed–spread into the environment should be conducted as part of the overall risk assessment for the recombinant vaccine. Therefore, there was a need for these studies to be conducted with a master seed vaccine virus produced on the master seed manufacturing cell line. Hence, the Ad5–A24 master seed vaccine virus was produced on the M2A master seed cell line and satisfactorily tested for purity and absence of extraneous agents.

For the backpassage (reversion to virulence) study, the vaccine virus must be administered using the route most likely to allow for reisolation of vaccine virus. Since human adenovirus

Table 3. Adenovirus serotype 5–A24 DS5: dose titration immunogenicity and vaccine efficacy.

Group	Animal (#)	Days postvaccination (SVN titer)		Days postcontact challenge* (clinical score‡)			
		-7	*0*	*3*	*7*	*10*	*14*
Ad5–A24 high dose (T01)	816	0.6	2.4	0	0	0	0
	818	0.6	1.8	0	0	0	0
	826	0.6	2.4	0	1 (T)	1 (T)	1 (T)
	837	0.6	2.1	1 (T)	2 (T, F)	2 (T, F)	2 (T, F)
	838	0.6	2.1	0	0	1 (DP)	0
	840	0.6	2.1	0	0	0	0
GMT or mean Lesion		0.6	2.2	0.2	0.5	0.7	0.5
SD		0.0	0.2	0.4	0.8	0.8	0.8
Ad5–A24 medium dose (T02)	815	0.6	2.1	0	1 (D3)	1 (DP)	0
	819	0.6	1.5	0	1 (D3)	2 (T, DP)	1 (T)
	820	0.6	1.5	0	0	0	0
	823	0.6	0.9	0	0	0	0
	824	0.6	2.1	0	1 (DP)	1 (DP)	0
	825	0.6	0.9	0	0	0	0
GMT or mean lesion		0.6	1.5	0.0	0.5	0.7	0.2
SD		0.0	0.5	0.0	0.5	0.8	0.4
Ad5–A24 low dose (T03)	814	0.6	0.6	1 (T)	1 (T)	1(T)	1 (T)
	822	0.6	1.8	0	4 (F, DP)	4 (F, DP)	3 (F)
	833	0.6	0.6	5 (T, F)	5 (T, F)	5 (T, F)	5 (T, F)
	834	0.6	1.5	0	1 (DP)	1 (DP)	0
	836	0.6	0.9	0	0	1 (T)	1 (T)
	839	0.6	1.2	0	1 (DP)	1 (DP)	0
GMT or mean lesion		0.6	1.1	1.0	2.0	2.2	1.7
SD		0.0	0.5	2.0	2.0	1.8	2.0
FFB (sham; T04)	817	0.6	0.6	2 (F)	5 (T, F)	5 (T, F)	5 (T, F)
	827	0.6	0.6	0	5 (T, F)	5 (T, F)	5 (T, F)
	828	0.6	0.6	5 (T, F)	5 (T, F)	5 (T, F)	5 (T, F)
	831	0.6	0.6	0	5 (T, F)	5 (T, F)	5 (T, F)
GMT or mean lesion		0.6	0.6	1.8	5.0	5.0	5.0
SD		0.0	0.0	2.4	0.0	0.0	0.0

**Challenge at 7 days postvaccination by direct contact.*
‡Clinical score is sum of pedal and oral (tongue and dental pad) lesions; maximum score/animal/day = 6.
Ad5: Adenovirus serotype 5; DP: Dental pad lesion; F: Foot lesion; FFB: Final formulation buffer; GMT: General mean titer; SD: Standard deviation; SVN: Serum virus neutralization; T: Tongue lesion.

Table 4. Adenovirus serotype 5–A24 DS5: prevention against foot-and-mouth disease virus shedding and transmission.

Treatment	Co-mingling room (n)	Protection against generalized disease (%)	A24 SVN titers (% positive)	Air sampling (real-time PCR; % positive)
Ad5–A24 primary vaccinate (n = 6)	1	100	100	3.6
Ad5–A24 secondary vaccinate (n = 4)		100	100	
Ad5–A24 primary vaccinate (n = 6)	2	100	100	0
Secondary naive (n = 4)		100	0	
Primary naive (n = 6)	3	0	100	39.3
Secondary naive (n = 4)		0	100	

Ad5: Adenovirus serotype 5.

is a respiratory mucosal pathogen, Ad5–A24 was inoculated intranasally in a total 2 ml dose of 5×10^{10} PU into ten healthy commercial 5–6-month-old cross-bred calves to determine whether the Ad5–A24 vaccine virus could be recovered from the animals subsequent to inoculation. Animals were observed daily for 14 days postinoculation, and serum samples were tested to detect any evidence of seroconversion to FMDV and/or Ad5 vaccine vector. Swab samples of nasal and oral secretions were collected on days 0, 1, 2, 3, 7 and 14 postinoculation, and virus isolation was attempted on each sample.

Table 5. Adenovirus serotype 5–A24 vaccine shed–spread study: serum virus neutralization titers to foot-and-mouth disease virus A24 Cruzeiro.

Treatment group	Animal (#)	Days postvaccination of SVN titer (log_{10}) to A24 Cruzerio*				
		0	*7*	*14*	*21*	*35*
Ad5–A24 (cattle)	101	0.6	1.5	1.2	1.8	1.5
	104	0.6	1.8	1.2	1.5	2.1
	107	0.6	1.8	1.8	2.1	2.1
	109	0.6	1.5	2.4	2.4	2.4
	110	0.6	0.9	0.6	1.2	1.2
None (cattle, co-mingled)	102	0.6	0.6	0.6	0.6	0.6
	103	0.6	0.6	0.6	0.6	0.6
	105	0.6	0.6	0.6	0.6	0.6
	106	0.6	0.6	0.6	0.6	0.6
	108	0.6	0.6	0.6	0.6	0.6
Ad5–A24 (pig)	3	0.6	0.6	1.8	0.9	1.2
	4	0.6	0.6	1.8	1.2	1.2
	5	0.6	0.9	1.8	1.5	1.5
	6	0.6	0.6	0.9	1.5	1.2
	8	0.6	0.6	1.2	1.2	1.2
None (pig, co-mingled)	1	0.6	0.6	0.6	0.6	0.6
	7	0.6	0.6	0.6	0.6	0.6
	10	0.6	0.6	0.6	0.6	0.6
	11	0.6	0.6	0.6	0.6	0.6
	12	0.6	0.6	0.6	0.6	0.6

**SVN titers to foot-and-mouth disease virus A24 >0.9 log_{10} are considered to be positive.*
Ad5: Adenovirus serotype 5; SVN: Serum virus neutralization.

The Ad5 vector was recovered from nasal swabs collected from 40% (4/10) of cattle at the 24-h sampling point; however, the oral swabs of all ten animals at this time point were negative, indicating the virus vector recovered from the four positive calves did not disseminate beyond the original (nasal) inoculation site (data not shown). The PCR testing of the recovered vaccine virus indicated that its genotype was not altered as a result of bovine passage, and the vaccine virus recovered was undoubtedly a residual of the intranasal Ad5–A24 inoculum collected from the site of inoculation. Detection of residual inoculum at the earliest samples taken from the inoculation site was not unexpected and is consistent with a previously published report that evaluated a replication-defective human Ad5 vaccine expressing bovine herpes virus type 1 glycoproteins [26]. Importantly, all vaccine virus isolation tests carried out on all sample types at all time points later than 24 h postinoculation were negative. The lack of any later isolations of vaccine virus from any test samples was considered to be consistent with the known replication-deficient genotype of the Ad5–A24 vaccine virus. None of the Ad5–A24-vaccinated cattle seroconverted to FMDV A24 Cruzeiro or to the Ad5 vaccine vector, suggesting that intranasal administration of Ad5–A24 vaccine fails to induce systemic SVN antibodies.

For the shed–spread study, the vaccine virus must be administered using the route intended for the product label. The study was conducted in both cattle and pigs (Tables 5 & 6). A total of ten healthy 5–6-month-old cattle and ten healthy 5-week-old weaned pigs were divided randomly into two groups of five animals each. Each calf (#101, 104, 107, 109 and 110) or pig (#3, 4, 5, 6 and 8) in the vaccinated group was immunized im. in a 2 ml dose with 5×10^{10} PU Ad5–A24. An equal number of calves (#102, 103, 105, 106 and 108) and pigs (#1, 7, 10, 11 and 12) served as co-mingled controls. The two groups of cattle were

Table 6. Adenovirus serotype 5–A24 vaccine shed–spread study: serum virus neutralization titers to human Ad5 (vaccine vector).

Treatment group	Animal (#)	Days postvaccination of SVN titer (log_{10}) to human Ad5*				
		0	*7*	*14*	*21*	*35*
Ad5–A24 (cattle)	101	0.6	1.5	1.8	2.1	1.8
	104	0.6	0.9	1.5	1.2	1.2
	107	0.6	2.1	2.1	2.1	2.4
	109	0.6	1.8	2.7	2.7	1.8
	110	0.6	1.5	1.5	2.1	1.5
None (cattle, co-mingled)	102	0.6	0.6	0.6	0.6	0.6
	103	0.6	0.6	0.6	0.6	0.6
	105	0.6	0.6	0.6	0.6	0.6
	106	0.6	0.6	0.6	0.6	0.6
	108	0.6	0.6	0.6	0.6	0.6
Ad5–A24 (pig)	3	0.6	0.9	0.9	0.9	0.9
	4	0.6	0.6	0.9	1.2	1.2
	5	0.6	1.5	1.2	1.5	1.2
	6	0.6	1.5	1.2	0.9	0.6
	8	0.6	0.9	1.2	1.2	1.8
None (pig, co-mingled)	1	0.6	0.6	0.6	0.6	0.6
	7	0.6	0.6	0.6	0.6	0.6
	10	0.6	0.6	0.6	0.6	0.6
	11	0.6	0.6	0.6	0.6	0.6
	12	0.6	0.6	0.6	0.6	0.6

**SVN titers to human Ad5 >1.2 log_{10} are considered to be positive.*
Ad5: Adenovirus serotype 5; SVN: Serum virus neutralization.

co-mingled within a single room and the two groups of swine were co-mingled within a second room for 35 days. Swab samples of nasal secretions were collected on day 0 (prevaccination) and on days 7, 14, 21 and 35 postvaccination. Vaccine virus isolation was attempted on each sample. Blood was also drawn and serum samples prepared from each animal on days 0 (prevaccination), 7, 14, 21 and 35. Serum samples were assayed, and the titers of human Ad5-neutralizing antibodies and FMDV A24 Cruzeiro-neutralizing antibodies were determined. Titers above 1.2 log_{10} were considered positive in the human Ad5 SVN assay, while titers above 0.9 log_{10} were considered positive in the FMDV A24 SVN assay.

Results demonstrated that all vaccinated cattle seroconverted to FMDV A24 Cruzeiro by day 7 postvaccination, while all the vaccinated swine were seropositive by day 14 (Table 5). Peak FMDV A24 SVN titers among individual vaccinated cattle ranged from 1.2 to 2.4 log_{10}, and the peak among individual vaccinated swine ranged from 1.2 to 1.8 log_{10}. Similarly, all vaccinated cattle had seroconverted to human Ad5 by day 14 postvaccination (Table 6). Four of five vaccinated swine were found to have positive human Ad5 titers at one or more time points during the study. Most importantly, all the placebo-treated cattle and swine that were co-mingled with vaccinated animals remained seronegative to both FMDV A24 Cruzeiro and human Ad5 at all sampling time points. These data, combined with the results that demonstrated all samples were negative for vaccine virus isolation (data not shown), provides strong evidence that Ad5–A24 vaccinates fail to replicate, shed or spread vaccine virus following im. administration.

Ad5–FMD vaccine: additional serotypes & subtypes

The Ad5-based FMD vaccines for other major serotypes and subtypes are currently in early development. Several serotype- and subtype-specific Ad5–FMD vaccine candidates have been produced at the premaster seed level and a laboratory-scale downstream process similar to the process used for manufacturing Ad5–A24 has been identified. Vaccine candidates are initially evaluated for the ability to induce SVN titers and to protect cattle following IDL challenge at 3 weeks postvaccination. Candidates that confer 100% efficacy are subsequently evaluated for the ability to provide protection against generalized disease, viremia and fever at 1 week postvaccination. Several vaccine candidates have successfully completed these feasibility efficacy studies and are

currently in various stages of further development. It is anticipated that a similar regulatory pathway for product licensure will be employed for these Ad5–FMD vaccine candidates as has been employed for the Ad5–A24 vaccine, since the only difference is the specific FMDV transgene carried by the Ad5 vaccine vector.

Ad5–A24 vaccine candidate: status & future perspective

Several important USDA CVB regulatory requirements have been successfully completed for the Ad5–A24 vaccine candidate, including:

- Master seed virus production and characterization;
- Master cell line production and characterization;
- Establishment of a scaleable manufacturing process;
- Technology transfer to a CVB licensed manufacturing facility;
- Regulatory approval of an outline of production;
- Production of prelicensing serials;
- Submission of SIF and risk assessment (including vaccine backpassage and shed–spread study results).

Additional USDA CVB regulatory requirements still need to be achieved to obtain product licensure, including:

- Approval of the minimum immunizing dose and vaccine dose required for product release and outdating
- Approval of SIF and risk assessment
- Completion of the field safety study in cattle

Approval of Ad5–A24 will represent the first molecular-based FMD vaccine that is DIVA compatible, safe for manufacture and safe for use in meat and milk-producing livestock. In the future, Ad5–A24 vaccine safety and efficacy studies will be completed in swine and small ruminants (e.g., sheep and goats) to collect further information on these species. In addition, a real-time vaccine stability program will be implemented to monitor vaccine potency. Preliminary information suggests that FMD vaccines made in the Ad5 vaccine platform will be very stable for long periods of time (years) in the frozen state. In addition, preliminary data indicate that Ad5–FMD vaccines are very likely to remain potent for several weeks following thawing and refrigeration storage, or for several days following thawing and storage at ambient temperatures. Moreover, Ad5–FMD vaccine potency does not appear to significantly decrease following repeated freezing and thawing. Outside the USA, the Ad5–A24 vaccine will probably be further developed for commercial use in FMD vaccine markets, particularly in South America where it could be used in FMDV A24 Cruzeiro eradication programs.

Concurrently with the DHS development program, a variety of approaches will be examined to enhance the potency of this first-generation FMD molecular vaccine platform, including the use of traditional (e.g., synthetic emulsions) or cytokine-based adjuvants. Alternative routes of vaccine delivery, including transdermal inoculation with needle-free vaccine injection devices, are also being pursued. The use of other human or simian adenovirus vector serotypes to improve vaccine potency and reduce the effective or minimum protective vaccine dose also will be evaluated. We believe that this comprehensive approach will enable the discovery and subsequent development of improved FMD molecular vaccine platforms that can be applied for several of the additional important FMDV serotypes and subtypes.

Acknowledgements

We would like to thank the past and present members of the Grubman laboratory who have been involved in this project from its onset, Ethan Hartwig for real-time PCR air sampling, as well as members of the DHS, Science and Technology Directorate at Plum Island and GenVec, Inc. for their dedication and Teresa de los Santos for preparation of Figure 1. *We also thank the animal care staff at the Plum Island Animal Disease Center for their professional support and assistance.*

Financial & competing interests disclosure

This research was supported in part by Current Research Information System (CRIS) project number 1940-32000-32053-00D, ARS, US Department of Agriculture (Marvin J Grubman) and by funding from DHS Science and Technology. David A Brake is the founder of BioQuest Associates LLC. Damodar Ettyreddy, Bryan T Butman and Douglas E Brough are employees of GenVec, Inc., which is working on commercialization of the adenovirus serotype 5–foot-and-mouth disease vector. The authors have no other relevant affiliations or financial involvement with any organization or entity with a financial interest in or financial conflict with the subject matter or materials discussed in the manuscript apart from those disclosed.

No writing assistance was utilized in the production of this manuscript.

Executive summary

Potency & efficacy of adenovirus serotype 5–foot-and-mouth disease vaccines

- The adenovirus serotype 5 (Ad5)– foot-and-mouth disease (FMD)-vectored vaccine requires inclusion of the viral 3C protease, as well as the capsid precursor polyprotein coding region, P1–2A, to allow capsid protein processing and induction of a neutralizing and protective immune response in swine and cattle.
- One dose (5×10^{10} total particle unit) of the Ad5–A24 vectored vaccine can protect both swine and cattle from homologous virus challenge as early as 7 days postadministration.

Ad5–A24 vaccine candidates: early development studies

- This vectored vaccine can protect cattle against either intradermalingual inoculation or direct contact FMD virus (FMDV) challenge.
- A new manufacturing process using serum-free suspension cultures and a streamlined purification process has been developed.
- The Ad5–A24 vector is genetically stable and the level of FMDV protein expressed is consistent after ten serial passages.

Ad5–A24 vaccine candidate: full development studies

- The Ad5–A24 vectored vaccine effectively prevents FMDV shedding and transmission to secondary vaccinates or sham-immunized cattle.
- In a shed–spread study, placebo-treated cattle and swine co-mingled with vaccinated cattle and swine remained seronegative to both FMDV and human Ad5.

Ad5–FMD vaccine: additional serotypes & subtypes

- The development of Ad5–FMD vectors for other major FMDV serotypes and subtypes is currently ongoing.

Ad5–A24 vaccine candidates: status & future perspective

- To enhance the potency and reduce the minimum protective vaccine dose of the Ad5–FMD vectors, we are currently examining a number of approaches to:
  - Include traditional adjuvants
  - Include cytokine-based adjuvants
  - Utilize alternative vaccine delivery routes
  - Use alternate adenovirus vectors
- Several US Department of Agriculture Center for Veterinary Biologics regulatory requirements still need to be met in order to obtain product licensure.

Bibliography

Papers of special note have been highlighted as:
- ▪ of interest
- ▪▪ of considerable interest

1. Grubman MJ, Baxt B: Foot-and-mouth disease. *Clin. Microbiol. Rev.* 17, 465–493 (2004).
   - ▪▪ **Describes the disease, its pathogenesis and molecular biology of foot-and-mouth disease virus (FMDV).**
2. Kitching RP: A recent history of foot-and-mouth disease. *J. Comp. Pathol.* 118, 89–108 (1998).
3. Mayr GA, Chinsangaram J, Grubman MJ: Development of replication-defective adenovirus serotype 5 containing the capsid and 3C protease coding regions of foot-and-mouth disease virus as a vaccine candidate. *Virology* 263, 496–506 (1999).
4. Grubman MJ, Morgan DO, Kendall J, Baxt B: Capsid intermediates assembled in a foot-and-mouth disease virus genome RNA-programmed cell-free translation system and in infected cells. *J. Virol.* 56, 120–126 (1985).
5. Rowlands DJ, Sangar DV, Brown F: A comparative chemical and serological study of the full and empty particles of foot-and-mouth disease virus. *J. Gen. Virol.* 26, 227–238 (1974).
6. Rweyemamu MM, Terry G, Pay TW: Stability and immunogenicity of empty particles of foot-and-mouth disease virus. *Arch. Virol.* 59, 69–79 (1979).
7. Grubman MJ: Development of novel strategies to control foot-and-mouth disease: marker vaccines and antivirals. *Biologicals* 33, 227–234 (2005).
8. Prevec L, Schneider M, Rosenthal KL, Belbeck LW, Derbyshire JB, Graham FL: Use of human adenovirus-based vectors for antigen expression in animals. *J. Gen. Virol.* 70(Pt 2), 429–434 (1989).
9. Graham FL, Smiley J, Russell WC, Nairn R: Characteristics of a human cell line transformed by DNA from human adenovirus type 5. *J. Gen. Virol.* 36, 59–74 (1977).
10. Brough DE, Lizonova A, Hsu C, Kulesa VA, Kovesdi I: A gene transfer vector-cell line system for complete functional complementation of adenovirus early regions E1 and E4. *J. Virol.* 70, 6497–6501 (1996).
11. Mayr GA, O'Donnell VO, Chinsangaram J, Mason PW, Grubman MJ: Immune responses and protection against foot-and-mouth disease virus (FMDV) challenge in swine vaccinated with adenovirus–FMDV constructs. *Vaccine* 2152–2162 (2001).
12. Moraes MP, Mayr GA, Mason PW, Grubman MJ: Early protection against homologous challenge after a single dose of replication-defective human adenovirus type 5 expressing capsid proteins of foot-and-mouth disease virus (FMDV) strain A24. *Vaccine* 20, 1631–1639 (2002).
    - ▪ **Presents the first demonstration that one dose of adenovirus serotype 5 (Ad5)–A24 vector can protect swine when challenged 7 days later.**
13. Pacheco JM, Brum MC, Moraes MP, Golde WT, Grubman MJ: Rapid protection of cattle from direct challenge with foot-and-mouth disease virus (FMDV) by a single inoculation with an adenovirus-vectored FMDV subunit vaccine. *Virology* 337, 205–209 (2005).
    - ▪ **Presents the first demonstration that one dose of Ad5–A24 vector can protect cattle when challenged 7 days later.**
14. Caron L, Brum MCS, Moraes MP, Golde WT, Arns CW, Grubman MJ: Granulocyte-machrophage colony-stimulating factor does not increase the potency or efficacy of a foot-and-mouth disease virus subunit vaccine. *Pesqui. Vet. Bras.* 23, 150–158 (2005).

15. Pay TW, Hingley PJ: Correlation of 140S antigen dose with the serum neutralizing antibody response and the level of protection induced in cattle by foot-and-mouth disease vaccines. *Vaccine* 5, 60–64 (1987).
16. Doel TR, Williams L, Barnett PV: Emergency vaccination against foot-and-mouth disease: rate of development of immunity and its implications for the carrier state. *Vaccine* 12, 592–600 (1994).
17. Le Bon A, Schiavoni G, D'Agostino G, Gresser I, Belardelli F, Tough DF: Type I interferons potently enhance humoral immunity and can promote isotype switching by stimulating dendritic cells *in vivo*. *Immunity* 14, 461–470 (2001).
18. Proietti E, Bracci L, Puzelli S *et al.*: Type I IFN as a natural adjuvant for a protective immune response: lessons from the influenza vaccine model. *J. Immunol.* 169, 375–383 (2002).
19. Cull VS, Broomfield S, Bartlett EJ, Brekalo NL, James CM: Coimmunisation with type I IFN genes enhances protective immunity against cytomegalovirus and myocarditis in gB DNA-vaccinated mice. *Gene Ther.* 9, 1369–1378 (2002).
20. de Avila Botton S, Brum MC, Bautista E *et al.*: Immunopotentiation of a foot-and-mouth disease virus subunit vaccine by interferon α. *Vaccine* 24, 3446–3456 (2006).
21. Lu Z, Bao H, Cao Y *et al.*: Protection of guinea pigs and swine by a recombinant adenovirus expressing *O* serotype of foot-and-mouth disease virus whole capsid and 3C protease. *Vaccine* 26(Suppl. 6), G48–G53 (2008).
22. Pena L, Moraes MP, Koster M *et al.*: Delivery of a foot-and-mouth disease virus empty capsid subunit antigen with nonstructural protein 2B improves protection of swine. *Vaccine* 26, 5689–5699 (2008).
23. Gall JG, Crystal RG, Falck-Pedersen E: Construction and characterization of hexon-chimeric adenoviruses: specification of adenovirus serotype. *J. Virol.* 72, 10260–10264 (98).
24. Gall JG, Lizonova A, EttyReddy D *et al.*: Rescue and production of vaccine and therapeutic adenovirus vectors expressing inhibitory transgenes. *Mol. Biotechnol.* 35, 263–273 (2007).

▪▪ **Describes the construction and production of adenovirus-based vaccines and therapeutics, which express transgene products that are inhibitory to the growth of adenovectors.**

25. Boldwell C, Brown AL, Barnett PV *et al.*: Host cell selection of antigenic variants of foot-and-mouth disease virus. *J. Gen. Virol.* 70, 45–57 (1989).
26. Gogev S, Vanderheijden N, Lemaire M *et al.*: Induction of protective immunity to bovine herpesvirus type 1 in cattle by intranasal administration of replication-defective human adenovirus type 5 expressing glycoprotein gC or gD. *Vaccine* 20, 1451–1465 (2002).
27. Moraes MP, Chinsangaram J, Brum MC, Grubman MJ: Immediate protection of swine from foot-and-mouth disease: a combination of adenoviruses expressing interferon α and a foot-and-mouth disease virus subunit vaccine. *Vaccine* 22, 268–279 (2003).
28. Wu Q, Moraes MP, Grubman MJ: Recombinant adenovirus co-expressing capsid proteins of two serotypes of foot-and-mouth disease virus (FMDV): *in vitro* characterization and induction of neutralizing antibodies against FMDV in swine. *Virus Res.* 93, 211–219 (2003).

Website

101. US Department of Agriculture Center for Veterinary Biologics (2008). www.aphis.usda.gov/animal_health/vet_biologics/vb_sifs.shtml

Affiliations

- Marvin J Grubman, USDA, ARS, NAA, Plum Island Animal Disease Center, PO Box 848, Greenport, NY 11944, USA
Tel.: +1 631 323 3329
Fax: +1 631 323 3006
marvin.grubman@ars.usda.gov
- Mauro P Moraes
Plum Island Animal Disease Center, North Atlantic Area, Agricultural Research Service, US Department of Agriculture, Greenport, NY 11944, USA
Tel.: +1 631 323 3016
Fax: +1 631 323 3006
mauro.moraes@ars.usda.gov
- Christopher Schutta
Plum Island Animal Disease Center, Department of Homeland Security, Science & Technology Directorate, Greenport, NY 11944, USA
Tel.: +1 631 323 3182
Fax: +1 631 323 3097
christopher.schutta@dhs.gov
- Jose Barrera
The McConnell Group, Inc., Dublin, PA 18917, USA
Tel.: +1 632 323 3049
Fax: +1 631 323 3097
jose.barrera@associates.dhs.gov
- John Nielan
Plum Island Animal Disease Center, Department of Homeland Security, Science & Technology Directorate, Greenport, NY 11944, USA
Tel.: +1 631 323 3025
Fax: +1 631 323 3097
john.neilan@dhs.gov
- Damodar Ettyreddy
GenVec, Inc., Gaithersburg, MD 20878, USA
Tel.: +1 240 632 0740
Fax: +1 301 944 1938
dreddy@genvec.com
- Bryan T Butman
GenVec, Inc., Gaithersburg, MD 20878, USA
Tel.: +1 240 632 5554
Fax: +1 301 944 1938
bbutman@genvec.com
- Douglas E Brough
GenVec, Inc., Gaithersburg, MD 20878, USA
Tel.: +1 240 632 5540
Fax: +1 301 944 1938
dbrough@genvec.com
- David A Brake
BioQuest Associates LLC, East Lyme, CT 06333, USA
Tel.: +1 631 323 3042
Fax: +1 631 323 3097
david.brake@associates.dhs.gov

JOURNAL OF VIROLOGY, Feb. 2010, p. 1536–1549 Vol. 84, No. 3
0022-538X/10/$12.00 doi:10.1128/JVI.02050-09

Mutations in Classical Swine Fever Virus NS4B Affect Virulence in Swine[▽]

I. Fernandez-Sainz,[1] D. P. Gladue,[1] L. G. Holinka,[1] V. O'Donnell,[1,2] I. Gudmundsdottir,[2] M. V. Prarat,[1] J. R. Patch,[1] W. T. Golde,[1] Z. Lu,[3] J. Zhu,[1] C. Carrillo,[4] G. R. Risatti,[2] and M. V. Borca[1]*

Plum Island Animal Disease Center, ARS, USDA,[1] Plum Island Animal Disease Center, DHS,[3] and Plum Island Animal Disease Center, APHIS, USDA,[4] Greenport, New York 11944, and Department of Pathobiology and Veterinary Science, University of Connecticut, Storrs, Connecticut 06269[2]

Received 29 September 2009/Accepted 2 November 2009

NS4B is one of the nonstructural proteins of classical swine fever virus (CSFV), the etiological agent of a severe, highly lethal disease of swine. Protein domain analysis of the predicted amino acid sequence of the NS4B protein of highly pathogenic CSFV strain Brescia (BICv) identified a putative Toll/interleukin-1 receptor (TIR)-like domain. This TIR-like motif harbors two conserved domains, box 1 and box 2, also observed in other members of the TIR superfamily, including Toll-like receptors (TLRs). Mutations within the BICv NS4B box 2 domain (V2566A, G2567A, I2568A) produced recombinant virus NS4B.VGIv, with an altered phenotype displaying enhanced transcriptional activation of TLR-7-induced genes in swine macrophages, including a significant sustained accumulation of interleukin-6 (IL-6) mRNA. Transfection of swine macrophages with the wild-type NS4B gene partially blocked the TLR-7-activating effect of imiquimod (R837), while transfection with the NS4B gene harboring mutations in either of the putative boxes displayed decreased blocking activity. NS4B.VGIv showed an attenuated phenotype in swine, displaying reduced replication in the oronasal cavity and limited spread from the inoculation site to secondary target organs. Furthermore, the level and duration of IL-6 production in the tonsils of pigs intranasally inoculated with NS4B.VGIv were significantly higher than those for animals infected with BICv. The peak of IL-6 production in infected animals paralleled the ability of animals infected with NS4B.VGIv to resist challenge with virulent BICv. Interestingly, treatment of peripheral blood mononuclear cell cultures with recombinant porcine IL-6 results in a significant decrease in BICv replication.

Classical swine fever (CSF) is a highly contagious lethal disease of swine. The etiological agent, CSF virus (CSFV), is a small enveloped virus with a positive single-stranded RNA (ssRNA) genome. Along with bovine viral diarrhea virus (BVDV) and border disease virus (BDV), CSFV is classified as a member of the genus *Pestivirus* within the family *Flaviviridae* (2). The 12.5-kb CSFV genome contains a single open reading frame that encodes a 3,898-amino-acid polyprotein and ultimately yields 11 to 12 final cleavage products (NH_2-Npro-C-E^{rns}-E1-E2-p7-NS2-NS3-NS4A-NS4B-NS5A-NS5B-COOH) through co- and posttranslational processing of the polyprotein by cellular and viral proteases (36, 46). NS4B is one of the nonstructural proteins of CSFV, and its function has not been clearly characterized.

Several studies of other flaviviruses, including hepatitis C virus (HCV), have revealed that NS4B is an endoplasmic reticulum (ER)-associated integral membrane protein that contains four putative transmembrane domains flanked by cytoplasmic N- and C-terminal regions (16, 25, 26, 34). The N-terminal region contains a conserved amphipathic helix that can become a transmembrane domain upon NS4B cleavage (10, 26), while the C-terminal region contains two predicted helical domains (17). *In vitro* studies have shown that NS4B is involved in HCV RNA replication (3, 8, 24, 47). NS4B itself is sufficient to induce the formation of a membranous web, a specific membrane alteration that serves as a scaffold to facilitate HCV RNA replication (7). A recent study demonstrated that amino acids (aa) 40 to 69 in the N-terminal portion of NS4B are essential in the formation of a functional replication complex (13).

Additionally, NS4B interacts with other HCV nonstructural proteins during the viral replication cycle. Physical interaction between NS4B and nonstructural protein 3 (NS3) has been implicated in productive replication of HCV RNAs (32, 33). In studies of BVDV replication, NS3, NS4B, and NS5A have been associated as components of a multiprotein complex that serves a critical role in viral RNA synthesis (34). Further, it has been shown that NS4B not only functions in RNA replication but also plays an important role in virus assembly and release (17).

Interaction of flavivirus NS4B with molecular components of the immune system has also been reported. The double-stranded RNA-triggered, interferon regulatory factor 3 (IRF-3)-mediated antiviral interferon (IFN) expression pathway is suppressed in the presence of HCV NS4B protein (43). Expression of dengue virus NS4B strongly blocks the IFN-induced signal transduction cascade by interfering with STAT1 phosphorylation (31), an observation extended to West Nile and yellow fever viruses (30).

* Corresponding author. Mailing address: Plum Island Animal Disease Center, USDA/ARS/NAA, P.O. Box 848, Greenport, NY 11944-0848. Phone: (631) 323-3135. Fax: (631) 323-3006. E-mail: manuel.borca@ars.usda.gov.

▽ Published ahead of print on 18 November 2009.

In BVDV, cytopathogenicity in infected cell cultures has been linked to a single residue in NS4B. A mutation in residue 15 of NS4B (Y to C) conferred a noncytopathic phenotype in cell culture (34). Interestingly, only one study has provided *in vivo* evidence of a direct involvement of NS4B in virus virulence. Replacement of cysteine 102 with a serine in the West Nile virus NS4B protein rendered the virus temperature sensitive, with attenuated neuroinvasive and neurovirulence phenotypes in mice (50).

Investigation of the identity of CSFV NS4B with the NS4B proteins of members of the *Flaviviridae*, such as HCV, shows only a negligible resemblance (http://www.ebi.ac.uk/clustalw/). Despite this divergence, the topology of NS4B is similar among members of the *Flaviviridae* (26); it contains several ER and cytoplasmic domains separated by transmembrane regions (22, 26).

Using sequence analysis, we have identified a predicted Toll–interleukin-1 receptor (TIR)-like domain within CSFV NS4B. This predicted TIR domain is unique to CSFV and BVDV; it is not present in other pestiviruses or flaviviruses. TIR domains are known to participate in the signal transduction of Toll-like receptors (TLRs). TLRs constitute a large family of proteins that play essential roles in recognizing various microbial components, activating the innate immune system, and inducing cytokines needed for the adaptive immune response (1, 18, 19, 42). The signal transduction of TLRs is based on homotypic domain interactions, or TIR-to-TIR interactions, with TIR-containing adaptor proteins, such as MyD88, TIRAP/MAL, TRIF, and TRAM (1, 18). This signal transduction leads to the activation of many transcription factors, such as NF-κBs and IRFs, that translocate to the nucleus and regulate the transcription of genes involved in the immune response (1, 15, 19).

TIR domains contain three conserved motifs, named boxes 1, 2, and 3, which have been identified by multisequence alignments (39). Alanine substitutions in box 1 and 2 motifs within the TIR domain of the human interleukin-1 (IL-1) receptor inhibited its signaling, whereas mutations in box 3 had no effect (40). Based on those observations, we targeted box 1 and 2 motifs in CSFV NS4B for mutagenesis, replaced the wild-type sequence with alanines, and examined the phenotypic changes incurred with the mutant viruses. We report here that the substitutions in box 2 of the NS4B protein of highly virulent CSFV Brescia (BICv) produced an attenuated virus (NS4B.VGIv), with localized replication in the tonsils and limited dissemination during the infection. Regardless of its limited *in vivo* replication, animals infected with NS4B.VGIv were completely protected against virulent challenge with BICv as early as 3 days postinoculation. Cellular gene expression analyses of primary swine macrophage cultures infected with NS4B.VGIv showed significantly higher levels of activation of several genes, particularly IL-6, than those in cultures infected with the parental virus, BICv. Interestingly, most of the genes showing increased transcriptional activation upon NS4B.VGIv infection are also induced by activated TLR-7 (1, 18, 19), suggesting NS4B-mediated interference with TLR-7 activity during infection with virulent wild-type virus. The transient expression of wild-type NS4B, but not of the NS4B gene harboring mutations in either of the putative boxes, interfered with the transcriptional activation of TLR-7-induced immune-regulatory genes (e.g., IL-6) in swine macrophages treated with a TLR-7 activator, imiquimod R837 (I-R837) (5, 11, 15, 21, 45, 49). *In vivo* analyses demonstrated significantly higher levels of IL-6 that were maintained in the tonsils of swine experimentally infected with NS4B.VGIv than in those of swine infected with BICv. Furthermore, treatment of swine peripheral blood mononuclear cell (PBMC) cultures with recombinant porcine IL-6 resulted in a significant reduction in BICv replication.

MATERIALS AND METHODS

Domain annotation of CSFV NS4B. The NS4B amino acid sequence (CSFV strain Brescia polyprotein amino acid residues 2337 to 2683) was used for domain annotations utilizing the SMART (simple modular architecture research tool) software program. This program identifies protein domains in sequence databases that share sequence homology with query sequences and outputs multiple sequence alignments of the query sequences with sequences of domain families. The porcine TIR domains of TLRs (1, 18) were also identified utilizing the SMART program software (39), along with human TLR1 and human TLR2, and were manually aligned together. The crystal structure for human TLR1 (RCSB PDB no. 11081518) was used as a template for modeling the NS4B structure, as viewed on the SWISS-MODEL program (http://www.expasy.org/spdbv/) (14), to compare NS4B residues to the crystallized human TLR1.

Viruses and cells. Swine kidney cells (SK6) (44), free of BVDV, were cultured in Dulbecco's minimal essential medium (DMEM) (Gibco, Grand Island, NY) with 10% fetal calf serum (FCS) (Atlas Biologicals, Fort Collins, CO). CSFV strain Brescia was propagated in SK6 cells and was used for the construction of an infectious cDNA clone (37). Growth kinetics was assessed using primary swine macrophage cell cultures prepared as described by Zsak et al. (51). Titration of CSFV from clinical samples was performed using SK6 cells in 96-well plates (Costar, Cambridge, MA). After 4 days in culture, viral infectivity was assessed using an immunoperoxidase assay utilizing the anti-CSFV monoclonal antibody (MAb) WH303 (6) and the Vectastain ABC kit (Vector Laboratories, Burlingame, CA). Titers were calculated according to the method of Reed and Muench (35) and were expressed as 50% tissue culture infective doses ($TCID_{50}$) per milliliter. The sensitivity of the test, as performed, was $\geq \log_{10} 1.8$ $TCID_{50}$/ml. Plaque assays were performed using SK6 cells in 6-well plates (Costar). SK6 monolayers were infected, overlaid with 0.5% agarose, and incubated at 37°C for 3 days. Plates were fixed with 50% (vol/vol) ethanol-acetone and were stained by immunohistochemistry with MAb WH303 (6).

Construction of CSFV mutants. A full-length infectious clone (IC) of the virulent strain Brescia (pBIC) (37) was used as a template in which putative TIR motifs $I_{2531}Y_{2532}K_{2533}$ (box 1) and $V_{2566}G_{2567}I_{2568}$ (box 2) were replaced with alanine triplets (see Fig. 2). Mutations were introduced by site-directed mutagenesis, using the QuikChange XL site-directed mutagenesis kit (Stratagene, Cedar Creek, TX), performed per manufacturer's instructions and using the following primers (only 5′→3′ forward primer sequences are shown; mutations producing amino acid substitutions are italicized): for the IYK mutant, GTCATACTGAGTACCGCA*GCCGCCGCA*ACCTACCTATCAA TCAGG; for the VGI mutant, TCACAAAACCCAGTATCT*GCGGCTGCA* GCGGTCATGCTAGGGGTG. An IYK-VGI mutant was produced by sequential mutagenesis using the pIYK construct as a template with VGI primers.

Recombinant NS4B was expressed in swine macrophages as an N-terminal fusion of human green fluorescent protein II (hGFP II) into the Vitality phrGFP II-N mammalian expression vector (Stratagene, La Jolla, CA). Each version of NS4B (wild-type NS4B, NS4B.IYK, NS4B.IYK.VGI, or NS4B.VGI) was PCR amplified from a corresponding CSFV full-length infectious clone using primers F (5′-GAATTCCGCTCAGGGGGATGTGCAGAGAT-3′) and R (5′-GTCGA CTTATAGCTG GCGGATCTTTCCTT-3′), followed by cloning into the vector using EcoRI and SalI restriction sites.

***In vitro* rescue of CSFV Brescia and NS4B mutants.** Full-length genomic clones were linearized with SrfI and were *in vitro* transcribed using the T7 Megascript system (Ambion, Austin, TX). RNA was precipitated with LiCl and was transfected into SK6 cells by electroporation at 500 V, 720 Ω, and 100 W with a BTX 630 electroporator (BTX, San Diego, CA). SK6 cells were seeded in 12-well plates and incubated for 4 days at 37°C under 5% CO_2. Virus was detected by immunoperoxidase staining as described above, and stocks of rescued viruses were stored at −70°C.

DNA sequencing and analysis. Full-length clones and *in vitro*-rescued virus were completely sequenced with CSFV-specific primers by the dideoxynucleotide

chain termination method (38). Viruses recovered from infected animals were sequenced in the region of the genome that contained the desired mutations. Sequencing reactions were prepared with the Dye Terminator cycle sequencing kit (Applied Biosystems, Foster City, CA). Reaction products were sequenced on a Prism 3730xl automated DNA sequencer (Applied Biosystems). Sequence data were assembled using Sequencher 4.7 software (Gene Codes Corporation, Ann Arbor, MI). The final DNA consensus sequence represented, on average, five redundancies at each base position.

Animal infections. The virulence of NS4B.VGIv relative to that of BICv was initially assessed in 10- to 12-week-old, 40-lb commercial-breed pigs inoculated intranasally (i.n.) with 10^5 $TCID_{50}$ of each virus. Fourteen pigs were randomly allocated into 2 groups of 8 and 6 animals and were inoculated with NS4B.VGIv or BICv, respectively. Clinical signs (anorexia, depression, purple skin discoloration, staggering gait, diarrhea, and coughing) and changes in body temperature (fever defined as a rectal temperature of >104°F) were recorded daily throughout the experiment and were scored as previously described (28).

The effects of NS4B mutations on CSFV shedding and tissue distribution within the host were assessed in pigs i.n. inoculated with recombinant NS4B.VGIv ($n = 8$) or BICv ($n = 8$). To determine the distribution of the virus in tissues, one pig per group was sacrificed at 1, 2, 3, 4, 7, and 9 days postinfection (dpi), and tissue samples were collected. Tonsils, mandibular lymph nodes, spleens, and kidneys were removed from each pig and were either snap-frozen in liquid nitrogen for subsequent virus titration or mounted on polystyrene blocks for immunofluorescence analysis (see below). Blood, nasal swabs, and tonsil scraping samples were also obtained from each pig before necropsy and were used to assess virus shedding. The remaining 2 pigs in each group were monitored to check for the appearance of clinical signs during a 21-day observation period.

For infection-challenge studies, 12 pigs were randomly allocated into 3 groups containing 4 animals each. Pigs in groups 1 and 2 were i.n. inoculated with NS4B.VGIv, and pigs in group 3 were mock infected. At 3 dpi (group 1) or 28 dpi (group 2), animals were challenged with BICv along with animals in group 3. Clinical signs and body temperature were recorded daily throughout the experiment as described above. Blood, serum, nasal swabs, and tonsil scrapings were collected at various times postchallenge, with blood obtained from the anterior vena cava in EDTA-containing tubes (Vacutainer) for total and differential white blood cell counts. Total and differential white blood cell and platelet counts were obtained using a Beckman Coulter ACT (Beckman Coulter, CA).

Sample collection, immunofluorescence, and confocal microscopy. Triplicate samples were collected postmortem from palatine tonsils of infected-challenged animals. The tissues were mounted on polystyrene blocks using optimal cutting temperature (OCT) compound (Tissue-Tek Sakura, Torrance, CA), promptly frozen in liquid nitrogen, and stored at −70°C.

To assess the presence of VGIv and BICv, and to study the expression of IL-6, sections (thickness, 4 μm) were obtained from each of the triplicate cryopreserved tissue samples and were fixed with acetone for 10 min at −20°C. After fixation, tissue sections were incubated at room temperature (RT) for 90 min in blocking buffer containing 2% (wt/vol) bovine serum albumin (Sigma, St. Louis, MO) and 20% (vol/vol) normal bovine serum (Gibco-Invitrogen, Carlsbad, CA) in phosphate-buffered saline (PBS). Either primary MAb WH303 against CSFV E2 (6) or an anti-swine IL-6 MAb (R&D Systems, Minneapolis, MN) was diluted in blocking buffer and incubated with tissue sections overnight at 4°C in a humid chamber. After five washes with PBS at RT, tissue sections were incubated for 90 min at 37°C with the appropriate secondary antibodies, goat anti-mouse isotype-specific IgG labeled with either Alexa Fluor 488 or Alexa Fluor 594 (Molecular Probes-Invitrogen, Carlsbad, CA), diluted in blocking buffer. Following this incubation, tissue sections were washed five times with PBS at RT, counterstained with TOPRO-iodide 642/661 (Molecular Probes) for 5 min at RT, washed as before, mounted, and examined in a Leica scanning confocal microscope (TCS2; Leica Microsystems, Bannockburn, IL). Data were collected utilizing an appropriate control lacking incubation with primary antibodies in order to determine channel crossover settings and negative background levels. The captured images were adjusted for contrast and brightness using Adobe Photoshop software (Adobe, San José, CA).

Quantitative real-time PCR (qrt-PCR). Swine macrophage primary cell cultures were infected at a multiplicity of infection (MOI) of 1, and total cellular RNA was extracted at 24 and 48 h postinfection/posttreatment using a RNeasy minikit (Qiagen). Contaminant genomic DNA was removed by DNase treatment using Turbo DNA-*free* (Ambion). After DNase treatment, genomic DNA contamination of RNA stocks was assessed by real-time PCR amplification targeting the porcine β-actin gene. Total RNA was quantified and cDNA synthesized with random primers using a High Capacity cDNA reverse transcription kit (Applied Biosystems, Foster City, CA) in 100-μl reaction mixtures containing 2,500 ng of total RNA. For gene expression quantification, first-strand cDNA was amplified by real-time PCR using *Power* SYBR green PCR master mix (Applied Biosystems) with primer pairs described in reference 4. A 50-μl reaction mixture contained 25 μl of *Power* SYBR green PCR master mix, 5 μl of cDNA, and 400 nmol/liter of each primer. Cycling conditions were as follows: activation of the AmpliTaq Gold polymerase at 95°C for 10 min, 40 cycles of denaturation at 95°C for 15 s followed by annealing and extension at 60°C for 1 min, and a melting curve analysis performed at the end of the PCR. Real-time PCRs were run using the ABI 7500 Real-Time PCR system platform (Applied Biosystems). Gene expression data were normalized by assessing mRNA accumulation of a housekeeping gene (β-actin) in infected and mock-infected cell cultures. Relative quantities (RQ) of mRNAs were then calculated using the $2^{-\Delta\Delta CT}$ method (described in ABI Prism 7700 sequence detection system User Bulletin 2 [PN 4303859]). The normalized mRNA expression level of a cellular gene in infected cells was considered significant when it departed from its level in uninfected cells 3-fold in either direction (4).

Effect of NS4B on swine macrophages treated with imiquimod R837. Primary blood-derived swine macrophage cultures were transfected with 5 μg of phrGFP, phrGFP/NS4B, phrGFP/NS4B.IYK, phrGFP/NS4B.IYK.VGI, or phrGFP/NS4B.VGI plasmid DNA by using Lipofectamine (Invitrogen, Carlsbad, California) according to the manufacturer's protocol. Twenty-four hours after transfection, cells were treated with 20 μg/ml imiquimod R837 (Invitrogen, San Diego, CA), and RNA was collected 24 h posttreatment using QIAshredder columns (Qiagen), followed by RNA isolation using an RNeasy kit (Qiagen). The RNA was treated to remove genomic DNA contamination, reverse transcribed, and processed by real-time PCR. Gene expression was quantified by qrt-PCR as described above.

Development of a recombinant adenovirus expressing swine IL-6. A replication-defective human adenovirus type 5 (Ad5) containing the porcine IL-6 gene was developed (29). Briefly, the IL-6 gene (GenBank accession no. DQ832259) was synthesized (Bio Basic Inc., Ontario, Canada), flanked by ClaI and XbaI restriction sites (pIL-6). The pIL-6 fragment was subsequently cloned into pAd5Blue (29), which was also digested with ClaI and XbaI (pAd5pIL6). The Ad5pIL6 plasmid was then linearized with PacI and transfected into human embryonic kidney 293 (HEK 293) cells using Lipofectamine 2000 (Invitrogen, Carlsbad, CA). Recombinant virus was harvested 4 days posttransfection, further amplified in HEK 293 cells, and purified using a discontinuous followed by a continuous CsCl gradient centrifugation procedure. Recombinant IL-6 was generated by infecting nonpermissive SK6 cells with Ad5pIL6v. At 24 h postinfection (hpi), the culture medium containing secreted IL-6 was harvested and used in subsequent experiments.

Effect of IL-6 treatment on swine PBMC cultures infected with CSFV. Primary swine macrophage or PBMC cultures were prepared as described by Zsak et al. (51) in 24-well plates (Primaria, Falcon; Becton Dickinson, Franklin Lakes, NY). Cultures were treated with either Ad5-derived IL-6 (at a concentration of approximately 85 ng/ml, as quantified by an enzyme-linked immunosorbent assay specific for swine IL-6 [Quantikine IL-6 immunoassay; R&D Research, MN]) or the supernatant obtained from SK6 cells infected with Ad5Blue virus, or they were mock treated. Twenty-four hours later, cultures were infected with BICv at an MOI of 0.1. Virus yield was assessed at 24 hpi. Additionally, a dose-response experiment was performed using 10-fold-decreasing concentrations of IL-6 (85 through 0.085 ng/ml) under conditions similar to those described above.

Effect of treatment with imiquimod R837 in swine macrophage cultures infected with CSFV. Primary swine macrophage cultures were prepared as described previously (51) in 24-well plates. Cultures were treated with 20 μg/ml imiquimod R837 either 24 h before the virus infection or at 6, 18, or 24 h after virus infection. Cultures were infected with either BICv or NS4B.VGIv at an MOI of 0.1. Virus yield was assessed at 24 hpi by determining the titers of samples in SK6 cells.

RESULTS

NS4B contains a putative TIR domain. Utilizing SMART program analysis software (39) for wide genome screening of CSFV strain Brescia, we observed that NS4B has a putative TIR domain located between amino acids 195 and 328 (residues 2531 to 2664 of the CSFV polyprotein). In general, TIR domains lack a specific amino acid sequence and show only 20 to 30% identity (data not shown) (http://www.cellsignal.com/reference/domain/tir.html). To identify TIR domains, the

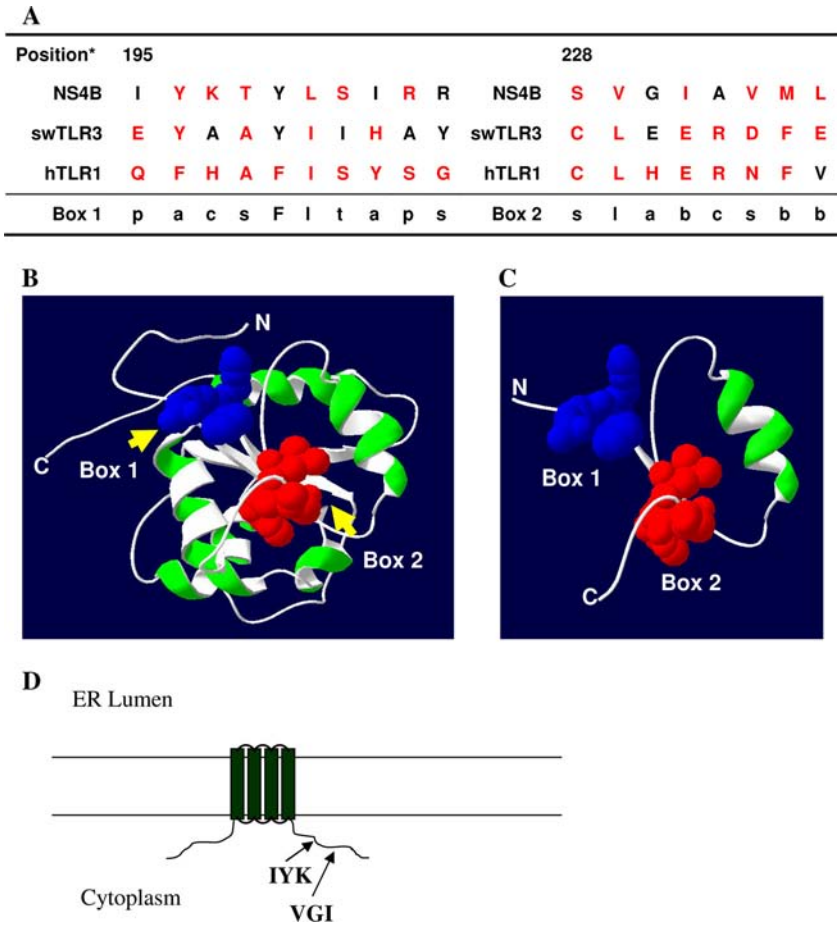

FIG. 1. (A) Alignment of the CSFV NS4B TIR domain against *Sus scrofa* Toll-like receptor TIR domains (swTLR3) and human TLR1 (hTLR1). Shown are amino acid sequences between positions 195 and 204 (box 1) and between positions 228 and 235 (box 2) of the CSFV NS4B protein. "Position *" indicates the residue position in the CSFV NS4B protein. The consensus sequence is composed of residues in 60% of TIR domains for box 1 and box 2. Amino acid consensus: a, aromatic amino acids (F, H, W, Y); b, big amino acids (E, F, H, I, K, L, M, Q, R, W, Y); c, charged amino acids (D, E, H, K, R); h, hydrophobic amino acids (A, C, F, G, H, I, L, M, T, V, W, Y); l, aliphatic amino acids (I, L, V); p, polar amino acids (C, D, E, H, K, N, Q, R, S, T); s, small amino acids (A, C, D, G, N, P, S, T, V); t, tiny amino acids (A, G, S). (B) Human TLR1 TIR domain crystal structure, with the corresponding residues of the CSFV NS4B IYK mutant highlighted in blue and those of the VGI mutant highlighted in red. The crystal structure was viewed using Swiss-PDB Viewer (http://www.expasy.org/spdbv/). (C) Simplified human TLR1 TIR domain crystal structure containing only residues 634 to 676, colored and modeled as in panel B. (D) Schematic representation of CSFV NS4B protein topology (based on the structure predicted from HCV [25, 26]). Predicted positions for boxes 1 and 2 are indicated.

SMART program utilizes areas of similar amino acid properties that are specific to known TIR domains. A TIR domain consists of three boxes (termed boxes 1, 2, and 3 by Slack et al. [40]); box 1 and box 2 are the most critical for function. These boxes of conserved residues are set in a core sequence ranging from 135 to 160 amino acids. In NS4B, both boxes 1 and 2 display high similarity to the consensus sequence profile of the TIR domain family. This consensus sequence, (particularly compared with swine TLR3 and human TLR1) is shown in Fig. 1A.

To avoid abolishing the putative essential function of NS4B, we determined areas in the predicted TIR domain that would be suitable for disrupting potential TIR-TIR domain interactions without completely altering the putative secondary structure of NS4B. To do this, we used the crystal structure of human Toll-like receptor 1 as a model and determined that residues IYK in box 1 and VGI in box 2 are potential protein contact sites in the TIR domain of CSFV NS4B that, if modified, would not affect the protein secondary structure (Fig. 1B and C).

Construction of CSFV NS4B mutant viruses. Mutagenesis of box 1 and 2 motifs of NS4B was conducted according to the report by Slack et al. (40). Infectious RNA was *in vitro* transcribed from a full-length IC of CSFV Brescia containing mutations at the desired amino acid positions (Fig. 1A and 2A) that was subsequently used to transfect SK6 cells. Infectious clone mutants, referred to as pNS4B.IYK, pNS4B.VGI, and double mutant pNS4B.IYK.VGI, contained putative TIR-like motifs partially replaced by alanine residues (Fig. 2A). Infectious virus was rescued from transfected cells by day 4 after transfection with the pNS4B.VGI construct. In contrast, after four independent transfection procedures, the pNS4B.IYK and pNS4B.IYK.VGI constructs did not produce infectious viruses. NS4B.IYK and NS4B.IYK.VGI RNA transcripts used in transfections were completely sequenced to verify fidelity during the *in vitro*

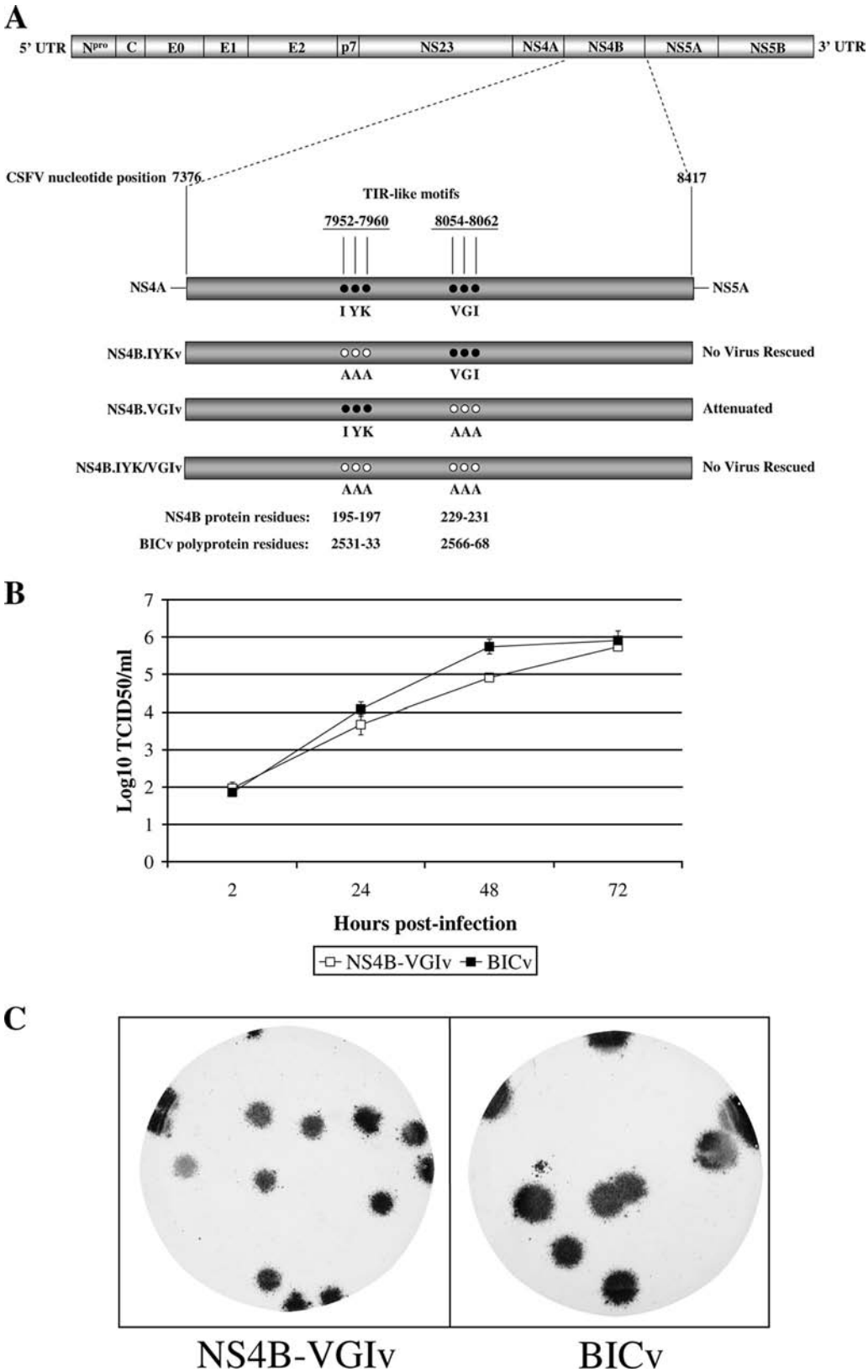

FIG. 2. (A) Schematic representation of substitutions at box 1 and box 2 of classical swine fever virus NS4B protein, generated by site-directed mutagenesis of the full-length cDNA clone pBIC. Wild-type NS4B is shown at the top: box 1 (IYK) and box 2 (VGI) are depicted, along with their positions in the CSFV nucleotide sequence, CSFV polypeptide, and NS4B amino acid sequence. Mutants are designated by the mutated residues. (B) *In vitro* growth characteristics of CSFV NS4B.VGIv and the parental virus, BICv. Primary swine macrophage cell cultures were infected

TABLE 1. Swine survival and fever response following infection with CSFV mutant NS4B.VGIv or the parental strain, BICv

Virus	Survival		Fever[a]		
	No. of survivors/ total no.	Time to death (days)[a]	No. of days to onset	Duration (no. of days)	Maximum daily temp (°F)
NS4B.VGIv	8/8	No	No	No	103.8 (0.4)
BICv	0/6	11 (0.82)	3 (0)	6.75 (1.71)	106.5 (0.6)

[a] Values are means (standard deviations).

transcription reaction. The complete nucleotide sequence of the rescued NS4B.VGI virus (NS4B.VGIv) genome was identical to that of the parental DNA plasmid, confirming that only mutations at predicted motif sites were present in the rescued virus.

Replication of the CSFV NS4B.VGIv mutant *in vitro*. The *in vitro* growth characteristics of the mutant virus NS4B.VGIv relative to those of the parental virus, BICv, were evaluated in a multistep growth curve. Primary swine macrophage cell cultures were infected at an MOI of 0.01 $TCID_{50}$ per cell. Virus was adsorbed for 1 h (time zero), and samples were collected at various times postinfection through 72 h. NS4B.VGIv exhibited growth characteristics similar to those of BICv (Fig. 2B). Similar results were obtained when growth kinetics was assessed in SK6 cells (data not shown). Additionally, when NS4B.VGIv was tested for its plaque size in SK6 cells, it exhibited a reduction in plaque size of approximately 50% relative to the parental virus, BICv (Fig. 2C).

Virulence of CSFV NS4B.VGIv mutants *in vivo*. To examine whether the mutations in residues 2566 to 2568 of the CSFV polypeptide (residues 229, 230, and 231 of the NS4B protein) affected virulence, pigs were intranasally inoculated with 10^5 $TCID_{50}$ of the NS4B.VGIv mutant (Table 1) and were monitored for clinical disease, evaluated relative to that with the parental virus BICv. While BICv exhibited a characteristic lethal phenotype, animals infected with NS4B.VGIv survived the infection and remained clinically normal throughout the observation period (21 days). All animals infected with BICv presented clinical signs of CSF starting 4 to 6 dpi, developing classical symptoms of the disease and dying around day 11 postinfection. White blood cell and platelet counts dropped by 4 to 6 dpi in animals inoculated with BICv and kept declining until death, while only a transient decrease was observed in animals inoculated with NS4B.VGIv (data not shown).

Viremia in NS4B.VGIv-inoculated animals was transient (Tables 2 and 3) and was significantly reduced, by 10^4 to 10^5, from that observed in BICv-infected swine. Similar patterns were observed for nasal and tonsil samples (Table 2). In all cases, nucleotide sequences of the NS4B gene from viruses recovered from infected animals were identical to those of stock viruses used for inoculation (data not shown).

TABLE 2. Titers of virus in clinical samples after intranasal inoculation with mutant NS4B.VGIv or the parental strain, BICv

Virus (dpi)	No. of animals with virus/total no. of inoculated animals per group (avg viral titer from positive infected animals [$\log_{10}$ $TCID_{50}$/ml])		
	Blood	Nasal swabs	Tonsil scrapings
NS4B.VGIv			
4	0/4	1/4 (1.9)	0/4
6	3/4 (2.2)	1/4 (2.4)	0/4
8	1/4 (2.0)	0/4	1/4 (1.90)
12	0/4	0/4	0/4
BICv			
4	4/4 (4.5)	0/4	4/4 (2.0)
6	4/4 (7.2)	4/4 (4.5)	4/4 (4.1)
8	4/4 (7.6)	4/4 (5.0)	4/4 (4.8)
12	D[a]	D	D

[a] D, all animals in this group were dead by this time point.

The ability of NS4B.VGIv to establish a systemic infection in intranasally inoculated animals was compared with that of the virulent parental virus, BICv. Randomly selected animals were euthanized at 1, 2, 3, 4, 7, and 9 dpi (one animal/time point/group), and virus titration was performed in collected tissues (tonsils, mandibular and retropharyngeal lymph nodes, kidneys, spleen, and blood). The titers measured in those tissue samples are shown in Table 3. *In vivo* replication of NS4B.VGIv was transient in tonsils, with titers 10^2 to 10^5 lower than those of BICv depending on the time postinfection. Differences between NS4B.VGIv and BICv titers were also observed in mandibular and retropharyngeal lymph nodes, and no mutant virus was detected in blood, spleen, or kidneys, indicating a severely limited ability of NS4B.VGIv to spread within the host.

NS4B.VGIv protects pigs against lethal CSFV challenge. The limited *in vivo* replication kinetics of NS4B.VGIv is similar to that observed with CSICv, a CSFV vaccine strain (37). However, restricted viral *in vivo* replication could also impair protection against wild-type virus infection. Thus, the ability of NS4B.VGIv to induce protection against virulent BICv was assessed in early and late vaccination-exposure experiments. Groups of pigs ($n = 4$) were intranasally inoculated with NS4B.VGIv and were challenged at 3 or 28 dpi. Mock-vaccinated control pigs receiving BICv ($n = 4$) developed anorexia, depression, and fever by 4 days postchallenge (dpc), as well as marked reductions in circulating leukocytes and platelets by 4 dpc (data not shown), and died or were euthanized *in extremis* by 10 dpc. Notably, infection with NS4B.VGIv (under the conditions described in this report) induced protection when pigs were challenged with the virulent parental virus at 3 and 28 dpi, as evidenced by the absence of clinical signs (Table 4). All pigs survived the BICv challenge and remained clinically

(MOI, 0.01) with the mutant or BICv, and virus yields were titrated at different times postinfection in SK6 cells. Data are means and standard deviations from two independent experiments. Sensitivity of virus detection, $\geq \log_{10}$ 1.8 $TCID_{50}$/ml. (C) Plaque formation by the CSFV NS4B.VGIv mutant and BICv. SK6 monolayers were infected, overlaid with 0.5% agarose, and incubated at 37°C for 3 days. Plates were fixed with 50% (vol/vol) ethanol-acetone and were stained by immunohistochemistry with MAb WH303 (6).

TABLE 3. Titers of virus in tissues after intranasal inoculation with mutant NS4B.VGIv or the parental strain, BICv

Virus (dpi)	Viral titer[a] ($TCID_{50}$/ml) in:						Virus detection[b]
	Tonsils	MLN	RFLN	Spleen	Kidneys	Blood	
NS4B.VGIv							
1	Neg	Neg	Neg	Neg	Neg	Neg	Neg
2	Neg	Neg	Neg	Neg	Neg	Neg	Neg
3	Neg	1.97	2.1	Neg	Neg	Neg	Neg
4	Neg	1.97	2.2	Neg	Neg	Neg	+
7	3.2	Neg	3.2	Neg	Neg	Neg	++
9	Neg	Neg	Neg	Neg	Neg	Neg	ND
BICv							
1	Neg	Neg	Neg	Neg	Neg	Neg	Neg
2	1.97	2.3	Neg	Neg	Neg	Neg	Neg
3	3.8	3.8	2.9	2.3	Neg	2.0	+++
4	4.2	3.6	5.0	3.8	2.8	4.2	+++
7	5.0	4.5	4.8	5.6	2.6	5.8	+++
9	5	5.1	4.6	4.6	4.1	6.5	ND

[a] Neg, viral titer of ≤ 1.8 $TICD_{50}$/ml. MLN, mandibular lymph nodes; RFLN, retropharyngeal lymph nodes.
[b] Immunofluorescence was performed on tonsil tissues obtained from one animal per time point using anti-E2 MAb WH303. Neg, negative. Positive reactivity was estimated from low (+) to strong (+++). ND, not determined.

normal, without significant changes in their hematological values (data not shown). Viremia and virus shedding of vaccinated-exposed animals were examined at 4, 6, 8, 12, 14, and 21 dpc (Table 5). As expected, in mock-vaccinated control animals, viremia was observed by 4 dpc, with virus titers remaining high by 8 dpc ($10^{7.8}$ $TCID_{50}$/ml) in the surviving pigs. Furthermore, virus was detected in the nasal swabs and tonsil scrapings of these animals after 4 to 6 dpc. In contrast, no challenge virus was detected in any clinical sample obtained from animals previously inoculated with NS4B.VGIv. Thus, even though NS4B.VGIv showed limited *in vivo* growth, solid protection was induced shortly after vaccination.

Transcriptional activation profile of immunologically relevant genes in swine macrophages infected with NS4B.VGIv. To further understand possible mechanisms responsible for NS4B.VGIv attenuation, the pattern of activation of immunologically relevant genes in swine macrophages infected with mutant and parental viruses was analyzed using quantitative real-time PCR (4) followed by melting curve analysis. To assess changes in cellular gene expression upon infection, primary porcine macrophage cell cultures were infected at an MOI of 1 $TCID_{50}$ per cell with either NS4B.VGIv or BICv. Total cellular RNA was extracted from infected and mock-infected cells at 24 hpi (exponential growth) and 48 hpi (growth plateau). Prior to synthesis of cDNA, total RNA was treated with DNase and tested for genomic DNA contamination by means of real-time PCR (see Materials and Methods). Steady-state levels of mRNA accumulation were determined for 58 swine immunomodulatory genes as described elsewhere (4). This approach identified 8 genes differentially expressed in primary porcine macrophages infected with NS4B.VGIv or BICv (Fig. 3): AMCF-1 (also known as IL-8), AMCF-2, IFN-α, IL-1α, IL-1β, IL-6, MCP2 (also known as CCL8), and NCP-1. Expression of AMCF-1, AMCF-2, IFN-α, IL-1α, and NCP-1 was slightly augmented at 24 hpi. Expression of IL-1β was significantly increased at 24 hpi, and increased levels of MCP-2 were detected at 48 hpi. Notably, levels of IL-6 were significantly increased (>10-fold) both at 24 and at 48 hpi in cultures infected with NS4B.VGIv (Fig. 3A and B).

TABLE 4. Swine survival and fever response after challenge of NS4B.VGIv-infected animals with virulent BICv

Vaccine (challenge time)	Survival[a]		Fever[a]	
	No. of survivors/ total no.	CSFV symptoms/time to death (days)	Mean time to onset (days)	Duration (days)
NS4B.VGI (3 dpi)	4/4	No	No	No
NS4B.VGI (28 dpi)	4/4	No	No	No
Mock	0/4	Yes/9.5 (1.2)	4.5 (0.7)	9.5 (0.7)

[a] Values in parentheses are standard deviations.

IL-6 expression in tonsils of pigs infected with NS4B.VGIv or BICv. Since NS4B.VGIv induces a higher level of IL-6 expression than BICv in swine cells *in vitro* (Fig. 3), it was important to investigate whether these changes in expression also occur *in vivo* during CSFV infection. Two groups containing six animals each were infected intranasally with 10^5 $TCID_{50}$ of either NS4B.VGIv or BICv. One animal from each group was euthanized at 6 h and 1, 2, 3, 4, and 7 days postinfection, and their tonsils were removed in order to assess the presence of cells producing IL-6 by means of immunofluorescence and detection of cells harboring viral antigen (as described in Materials and Methods). The results demonstrated abundant expression of IL-6 in tonsils, which could be detected as early as 1 dpi in NS4B.VGIv-infected animals and was sustained until 3 dpi, with some cells expressing IL-6 at 4 dpi (Fig. 4). In contrast, IL-6-producing cells were detected in the tonsils of BICv-infected pigs only at days 2 and 3 postinfection, and their numbers were significantly lower than those in NS4B.VGIv-infected animals at the same time points (Fig. 4). Interestingly, viral titers and the presence of viral antigen in tonsils appear to have an inverse relationship with the extent and abundance of IL-6 expression. A significant number of infected cells were observed in the tonsils of animals infected with BICv, starting at 3 dpi and lasting until the animals died. Mean-

TABLE 5. Detection of virus in nasal swabs, tonsil scrapings, and blood samples obtained after challenge of NS4B.VGIv-infected animals with virulent BICv

Challenge group and sample	No. of animals from whom virus was isolated/total no. of animals challenged (avg virus titer from positive infected animals [$\log_{10}$ $TCID_{50}$/ml]) at the following time:						
	Day of challenge	4 dpc	6 dpc	8 dpc	12 dpc	14 dpc	21 dpc
3 dpi							
Nasal	0/4	0/4	0/4	0/4	0/4	0/4	0/4
Tonsil	0/4	0/4	0/4	0/4	0/4	0/4	0/4
Blood	0/4	0/4	0/4	0/4	0/4	0/4	0/4
28 dpi							
Nasal	0/4	0/4	0/4	0/4	0/4	0/4	0/4
Tonsil	0/4	0/4	0/4	0/4	0/4	0/4	0/4
Blood	0/4	0/4	0/4	0/4	0/4	0/4	0/4
Control							
Nasal	0/4	0/4	4/4 (4.4)	4/4 (4.9)	D[a]	D	D
Tonsil	0/4	1/4 (2.0)	4/4 (4.1)	4/4 (4.8)	D	D	D
Blood	0/4	4/4 (4.5)	4/4 (7.4)	4/4 (7.8)	D	D	D

[a] D, animals died or were euthanized.

while, NS4B.VGIv was poorly and transiently detected in the tonsils of infected animals between 4 and 7 dpi only (Table 3). Thus, it appears that both *in vitro* and *in vivo*, NS4B.VGIv infection consistently induced a stronger IL-6 response than that observed during BICv infection, and the expression of IL-6 *in vivo* seems to be inversely related to the ability of the virus to replicate in the tonsils of infected animals.

Effect of IL-6 treatment of swine PBMC cultures on the replication of CSFV. The possible effect of IL-6 on the replication of CSFV was analyzed in swine PBMC and macrophage cultures. Swine primary cell cultures of PBMCs and macrophages were pretreated with approximately 85 ng/ml of adenovirus-derived swine IL-6 24 h before infection with BICv (MOI, 0.1). The presence of IL-6 had no effect on virus replication in macrophage cell cultures. Virus titers in the supernatants harvested at 24 h from IL-6 treated cultures, mock-treated cultures, or cultures containing Ad5Blue virus were practically undistinguishable (Fig. 5A). However, PBMC cultures treated with IL-6 showed a drastic decrease (by $\log_{10}$ 3.15 $TCID_{50}$/ml, with a standard deviation [SD] of 0.2) in virus yield from that for mock-treated or untreated cultures (Fig. 5A). A dose-response experiment performed using different concentrations of IL-6 showed that the detrimental effect of this cytokine on BICv replication is dose dependent (Fig. 5B).

CSFV NS4B blocks the effect of imiquimod R837, a TLR-7 activator, in swine macrophage cultures. The differential pattern of immunologically relevant genes activated in macrophages during infection with NS4B.VGIv and BICv resembled that induced by a well-characterized compound that stimulates macrophage activity, imiquimod R837 (I-R837) (5, 11, 12, 21, 45, 49). I-R837, an imidazoquinoline amine analog to guanosine, is an immune response modifier with potent indirect antiviral activity (5). This low-molecular-weight synthetic drug induces the activation of TLR-7 (12, 15, 21), leading to expression of several cytokines, such as type I IFN, IL-1, IL-6, IL-8, IL-10, MCP-1, and tumor necrosis factor (TNF) (5, 11, 12, 15, 21, 45, 49). The similarity between the pattern of gene activation in macrophages stimulated with I-R837 and by infection with NS4B.VGIv suggests the possibility of interference by CSFV NS4B with TLR-7 function (Fig. 3). First, in order to analyze this possibility, primary swine macrophage cultures were transfected with either phrGFP.NS4B or phrGFP constructs, followed 24 h later by stimulation with 20 μg/ml of I-R387. Blockage of increased transcription of the marker genes IFN-β, IL-1β, IL-6, and TNF-α in swine macrophage cultures treated with I-R387 was assessed as an indication of suppressed TLR-7 activity. Transfection with pGFP.NS4B provokes a blockage of the transcriptional activation of the IFN-β, IL-1β, IL-6, and TNF-α genes compared with the level of activation detected in macrophages transfected with pGFP. Thus, CSFV NS4B appears to obstruct the TLR-7 function induced by I-R837 (Fig. 6A, B, C, and D). Second, the abilities of mutant forms of NS4B protein (the IYK and VGI mutants and the IYK VGI double mutant) to block I-R837-induced TLR-7 activation were assessed by an experiment similar to that described above. Macrophage cultures were transfected with either phrGFP.NS4B, phrGFP.NS4B.IYK, phrGFP.NS4B.VGI, or phrGFP.NS4B.IYK.VGI and were stimulated with 20 μg/ml of I-R837 at 24 h posttransfection. The transcriptional activation of the IL-6 gene (used as a marker for TLR-7 activation) was then assessed 24 h after I-R837 treatment. Transcriptional activation of the IL-6 gene was blocked in cells transfected with wild-type phrGFP.NS4B. However, cells transfected with mutant forms of NS4B, phrGFP.NS4B.IYK or phrGFP.NS4B.IYK.VGI, failed to block the transcription of the IL-6 gene. A partial block of IL-6 transcription was observed in cells transfected with mutant phrGFP.NS4B.VGI. Therefore, alterations of both the IYK and the VGI motif in NS4B appear to affect its ability to block the TLR-7 activity induced by I-R837 (Fig. 6E).

Effect of I-R837 treatment of swine macrophage cultures on the replication of CSFV. I-R837 is known to possess antiviral activity (5). Thus, the effect of I-R837 on the replication of BICv or NS4B.VGIv was analyzed using swine macrophage

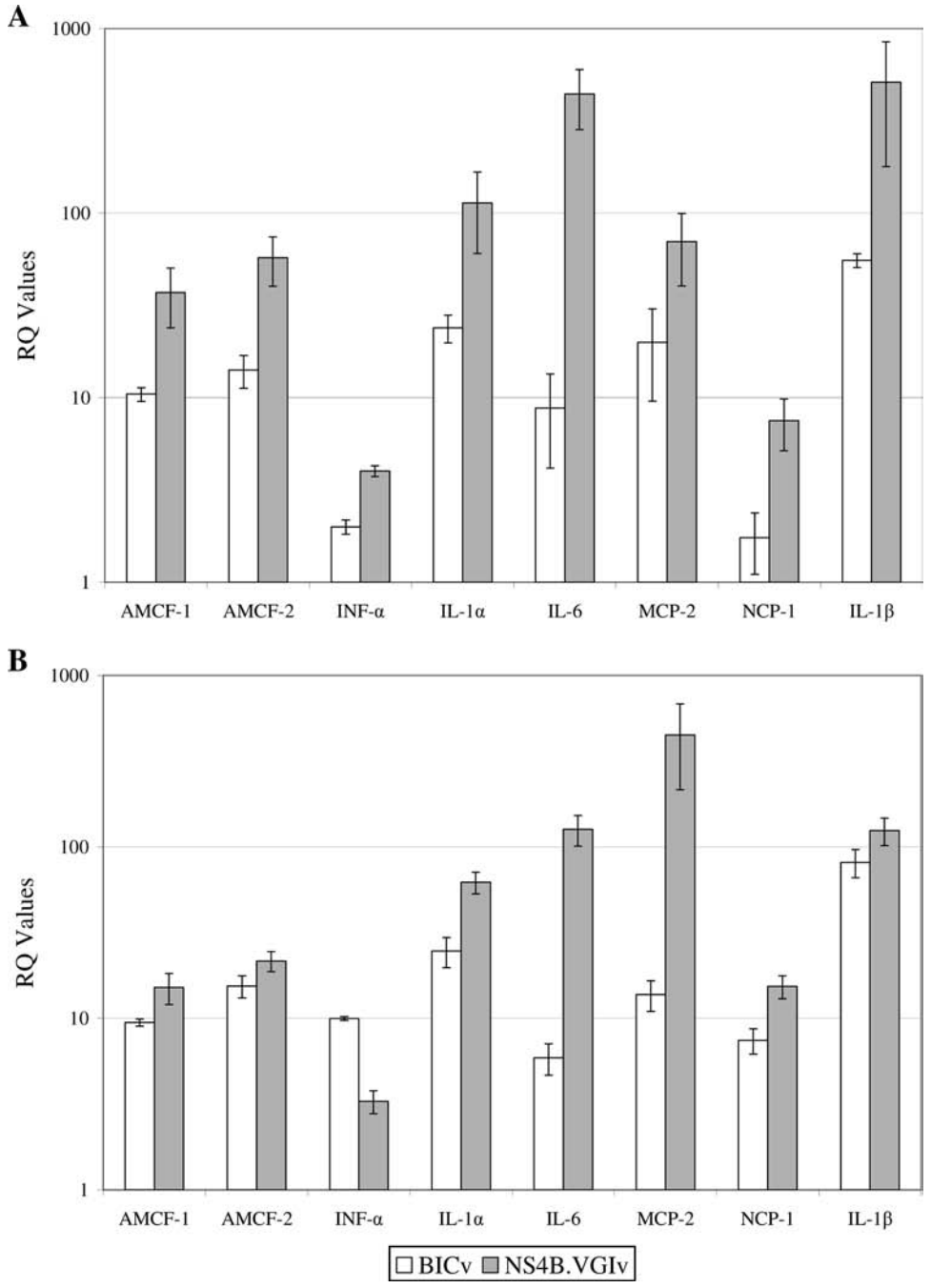

FIG. 3. Gene expression changes in peripheral blood-derived macrophages at 24 h (A) and 48 h (B) after infection with CSFV NS4B.VGIv or BICv. Gene expression was quantified by qrt-PCR. Values are expressed as RQ of mRNA accumulation (estimated by the $2^{-\Delta\Delta CT}$ method) with standard deviations.

cultures. Swine primary macrophage cell cultures were pretreated with 20 μg/ml of I-R837 24 h before infection with either BICv or NS4B.VGIv (MOI, 0.1). The presence of I-R837 clearly reduces the yield of BICv at 24 hpi (by $\log_{10}$ 3.17 $TCID_{50}$/ml [SD, 0.5]) from that for the untreated culture. Interestingly, I-R837 treatment seems to be less effective in cultures infected with NS4B.VGIv (reduction, $\log_{10}$ 1.86 $TCID_{50}$/ml [SD, 0.15]) (Fig. 7A).

Additionally, the effect of I-R837 on CSFV progeny yield was assessed in cells treated after infection. Macrophage cell cultures were infected with either the parental virus, BICv, or mutant NS4B.VGIv (MOI, 0.1) and were then treated with 20 μg/ml of I-R837 at 6, 12, or 18 h postinfection. The presence of I-R837 clearly reduced NS4B.VGIv yields in macrophage cultures treated at 6 h postinfection (by $\log_{10}$ 2.7 $TCID_{50}$/ml [SD, 0.2]). The observed effect on virus progeny yield progressively disappeared when macrophage cultures were treated at 6, 18, and 24 h postinfection. BICv

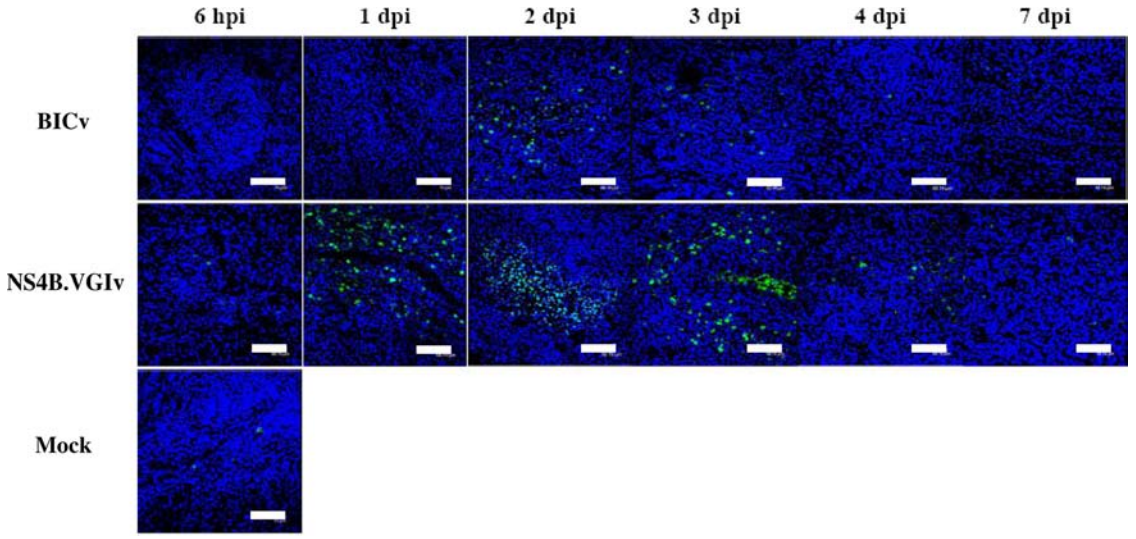

FIG. 4. Detection of IL-6-producing cells in the tonsils of animals infected i.n. with either NS4B.VGIv or BICv at 10^5 $TCID_{50}$/ml. The presence of IL-6 was detected by immunofluorescence.

progeny yields were not affected by treatment of macrophage cultures with I-R837 (Fig. 7B).

DISCUSSION

It has been demonstrated that the NS4B protein of flaviviruses, an endoplasmic reticulum-associated integral membrane protein (10, 16, 17, 25, 26, 34), is involved in several viral functions including RNA replication (3, 7, 8, 9, 13, 24, 47), interacting closely with other viral nonstructural proteins during the cycle of replication (32, 33, 34), and in the process of virus assembly and release (17). Although direct involvement of NS4B in flavivirus virulence has been reported infrequently (50), its role in the modulation of interferon response has been described (30, 31, 43). However, although the topology of NS4B is similar among members of the *Flaviviridae* (17, 25, 26, 27), and it contains several ER and cytoplasmic domains separated by transmembrane regions (Fig. 1D), the CSFV NS4B protein exhibits only a negligible resemblance (http://www.ebi.ac.uk/clustalw/) to those of other members of the *Flaviviridae*, such as HCV NS4B. This feature hampers the prediction of shared motifs or putative functional activities between the CSFV NS4B protein and those of other members of the *Flaviviridae*. For instance, in flaviviruses, motifs located toward the N-terminal cytoplasmic portion of the proteins are associated with NS4B functions, while the predicted TIR motifs found in CSFV NS4B are located toward the C-terminal cytoplasmic portion of the protein (Fig. 1D).

The data presented in this report suggest that the CSFV NS4B protein contains a region showing similarities to the TIR domain of Toll-like receptors/IL-1, including the motifs in boxes 1 and 2, shown to be critical for TIR function (40). Here we observed that alterations in NS4B box 1 are lethal for viral viability, while substitutions in box 2 (NS4B.VGIv) lead to complete virus attenuation in swine. TIR domains participate in the signal transduction of Toll-like receptors (TLRs), based on homotypic domain interaction or TIR-to-TIR interaction with TIR-containing adaptor proteins, which in turn lead to the activation of many transcription factors, such as NF-κBs and IRFs (1, 18, 19, 42). These activated transcription factors translocate to the nucleus, regulating gene transcription and the cellular immune response.

TLR-7 is normally activated by ssRNA as a mechanism of host defense against ssRNA viruses (1, 15, 18, 19). TLR-7 activation subsequently leads to increased transcription levels of several immunologically relevant genes, such as type I IFN, IL-1, IL-6, IL-8, IL-10, MCP-1, and TNF (5, 11, 12, 15, 21, 45, 49). The pattern of gene activation observed in macrophages infected with BICv suggests that viral mechanisms would block the activation of TLR-7. In contrast, infection with NS4B.VGIv would allow the activation of TLR-7, suggesting that NS4B may indeed prevent the activation of TLR-7 during infection with BICv. This mechanism of inhibition in turn might be disrupted during infection with mutant NS4B.VGIv. It is possible that during BICv infection of macrophages, NS4B interferes with the activation of TLR-7, either through direct TIR-to-TIR interaction with TLR-7 or possibly by competition for MyD88. This would explain the activation of TLR-7 signaling during infection with NS4B.VGIv, which leads to cytokine production, facilitating host control of the viral infection. Indirect evidence that this may happen is provided by the observation that transfection of macrophages with wild-type NS4B reduces the responsiveness of TLR-7 to a well characterized activator, I-R837 (Fig. 6A, B, C, and D). Interestingly, transfection with an NS4B gene harboring a mutation in either the putative box 1 (IYK) or box 2 (VGI), or mutations in both box 1 and box 2 (IYK and VGI), was less efficient at mediating this reduction (Fig. 6E). Additionally, when I-R837 was added after the infection, its antiviral activity did not affect BICv replication as it affected NS4B.VGIv replication. Perhaps BICv is able to block the effect of I-R837, while NS4B.VGIv is not (Fig. 7B). To our knowledge, this mechanism of evading TLR activation has not been observed with ssRNA viruses, but it has been described for vaccinia virus (VV), a double-stranded DNA virus (41). VV expresses an early protein, A46R, which

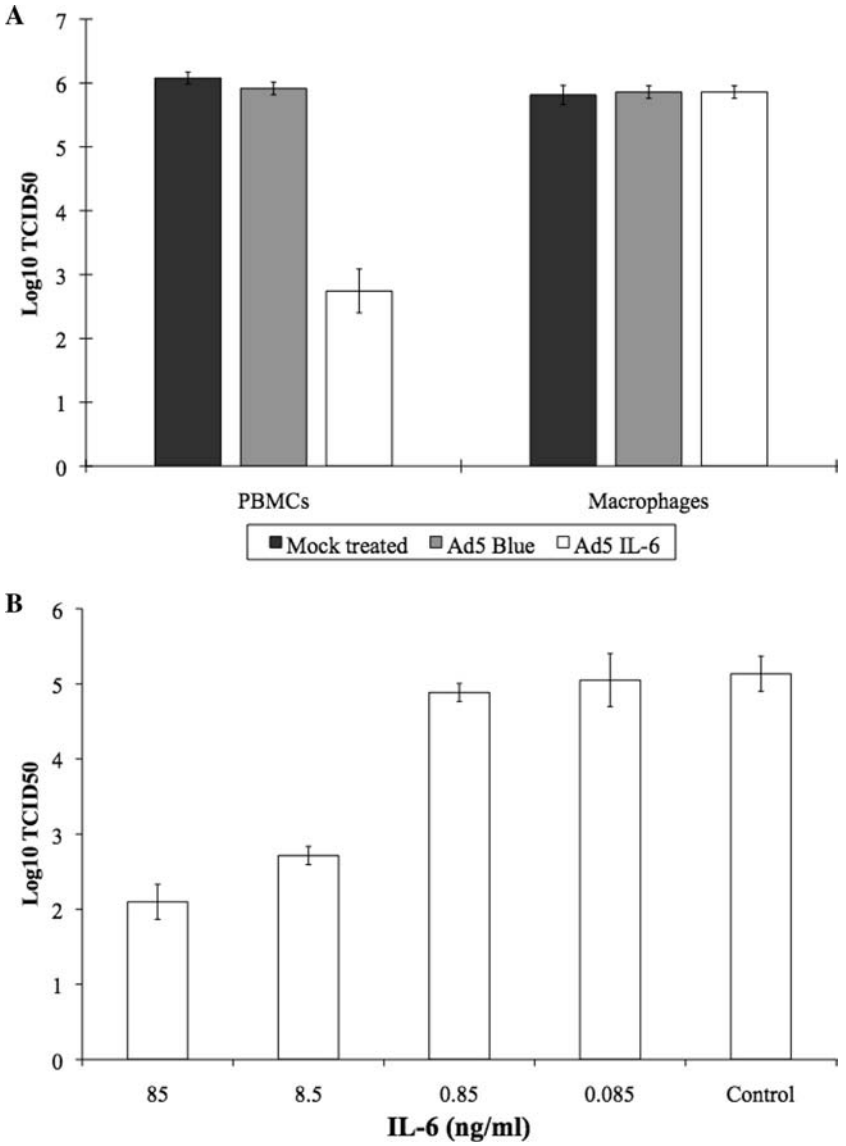

FIG. 5. Effects of IL-6 treatment on swine PBMC and macrophage cell cultures infected with CSFV. (A) Primary swine macrophage or PBMC cultures were either treated with Ad5-derived IL-6, mock treated, or treated with the Ad5-Blue culture supernatant; 24 h later, cultures were infected with BICv. (B) PBMC cultures were treated either with different IL-6 concentrations or with the Ad5Blue culture supernatant (control) Twenty-four hours later, cultures were infected with BICv. Infections were performed at an MOI of 0.1, and virus yield was assessed 24 hpi.

contains a TIR domain that interferes with host signal transduction of TLRs via interaction with the TIR domains of Toll-like receptors and TIR-containing adaptor proteins (41). Our results suggest that CSFV NS4B interferes with TLR signaling in a related manner, via its TIR-like domain.

IL-6, a cytokine produced primarily by cells of the monocyte/macrophage lineage, has been shown to be critically involved in several aspects of the acute-phase response and the development of the acquired immune response (23, 48). IL-6 plays an important role as a cofactor both in early events of cytotoxic T-lymphocyte (CTL) activation and in the process of B-cell late differentiation (48). Furthermore, it has been shown that IL-6 serves an important role during the development of an efficient immune response to viral infections. Interleukin-6-deficient mice have an impaired T-cell-dependent antibody response to vesicular stomatitis virus infection as well as a decreased CTL response to VV (20). IL-6 significantly inhibited the replication of CSFV *in vitro*. Swine PBMCs pretreated with adenovirus-derived porcine IL-6 24 h before infection with BICv displayed a significant reduction in virus yield (Fig. 5). This ability is not restricted to BICv, since similar results were obtained with NS4B.VGIv (data not shown). Although the mechanism mediating this reduction is not known, it is clear that it requires the involvement of nonadherent PBMCs, since this effect was not seen with adherent primary swine macrophages alone. It is possible that nonadherent PBMCs pretreated with IL-6 release soluble molecules that are not released in adherent macrophages alone, and that these soluble molecules ultimately mediate the inhibition of CSFV replication

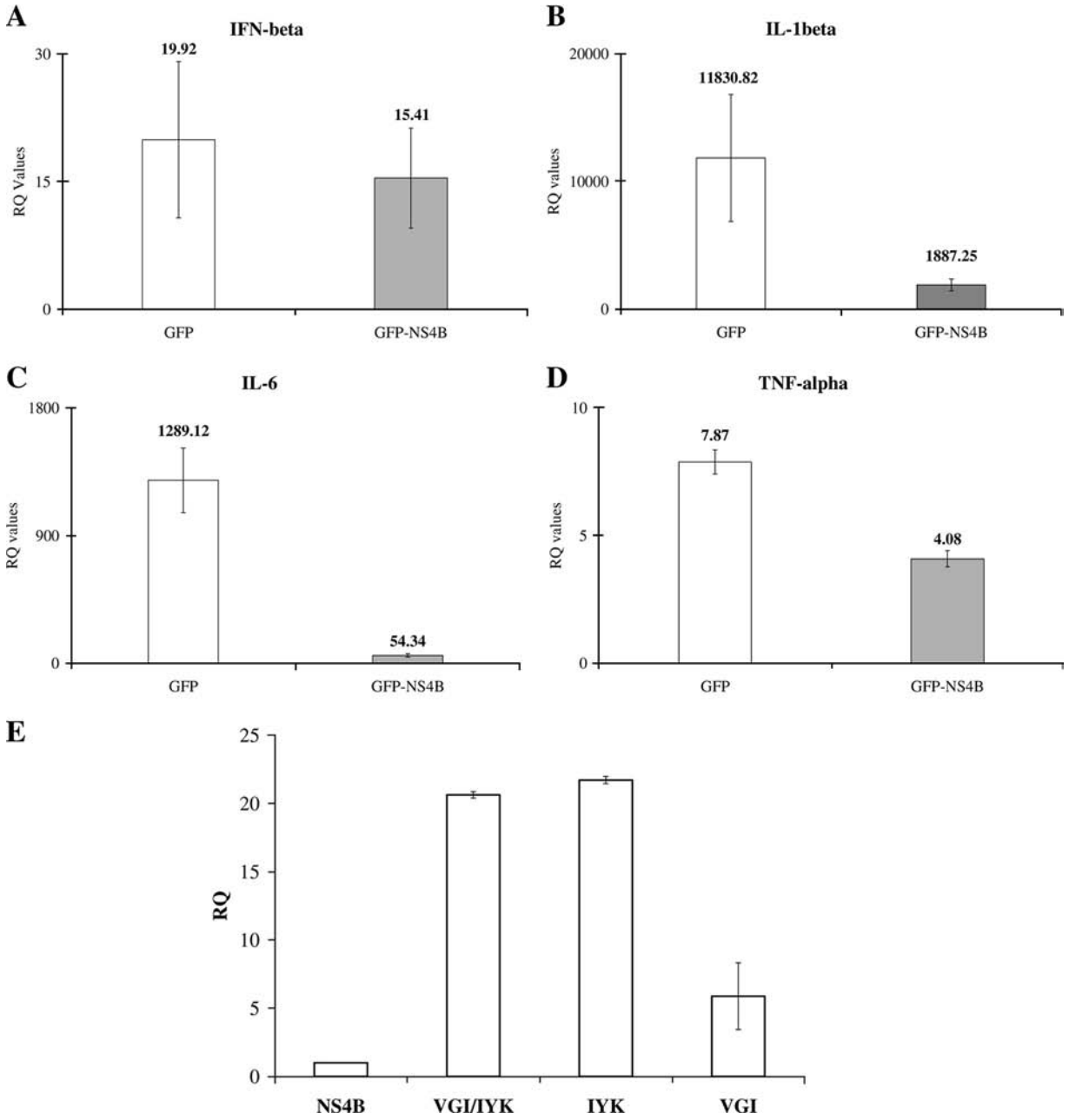

FIG. 6. Effect of CSFV NS4B protein on I-R837 activity in swine macrophages. Primary swine macrophage cultures were transfected with phrGFP or phrGFP/NS4B (A, B, C, and D) or with the phrGFP/NS4B, phrGFP/NS4B.IYK, phrGFP/NS4B.VGI, or phrGFP/NS4.IYK.VGI construct (E), and 24 h later, the cultures were stimulated with 20 μg/ml of I-R387. Blockage of increased transcription of the marker genes IFN-β (A), IL-1β (B), IL-6 (C and E), and TNF (D) in swine macrophage cultures treated with I-387 was assessed as an indication of the suppression of TLR-7 activity. RNA quantification was performed as described for Fig. 3. The results in panels A, B, C, and D are expressed as RQ, while in panel E, the results are expressed as RQ relative to NS4B, which is arbitrarily assigned the value of 1 unit.

in adherent macrophages. The *in vivo* studies have provided indirect support suggesting that IL-6 plays a significant role during CSFV infection (Fig. 5). In this study, the intensity and duration of IL-6 expression suggest an inverse relationship with levels of viral antigen and titers in the tonsils of animals infected with either BICv or NS4B.VGIv. This implies that expression levels of IL-6 are inversely related to the ability of the virus to replicate in the tonsils of infected animals. Of particular note from this study, it was shown that peak cellular IL-6 levels at 3 dpi coincided with protection when pigs were challenged with the highly virulent parental virus, suggesting that IL-6 can play an early protective role against CSFV infection.

In summary, we report here that the nonstructural NS4B protein of CSFV strain Brescia has similarities to the TLR family with regard to protein structure and motifs present in boxes 1 and 2. Alterations in box 1 are lethal for virus viability, while substitutions in box 2 (NS4B.VGIv) lead to

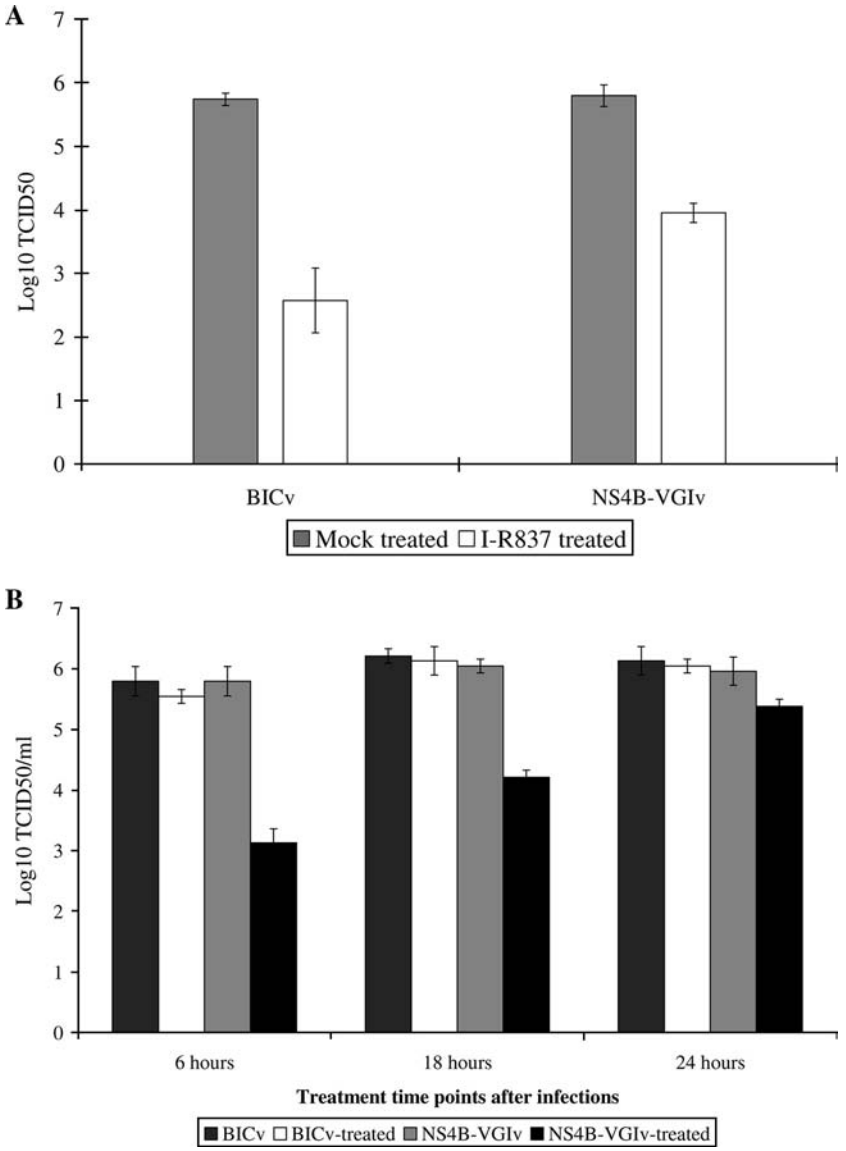

FIG. 7. Effect of imiquimod R837 (I-R837) treatment on swine primary macrophage cell cultures infected with CSFV. (A) Macrophages were either treated with I-R837 or mock treated, and 24 h later, cultures were infected with either NS4B.VGIv or BICv. (B) Macrophages were treated with I-R837 at 6, 12, or 18 h after virus infection. Infections were performed at an MOI of 0.1, and virus yields were assessed at 24 hpi.

complete virus attenuation in swine. A direct link between reduced virulence *in vivo* and alteration of the activation profile of immunologically relevant genes could not be determined. However, it is possible that disruption of the TIR domain in NS4B led to increased production of host innate immune response mediators, potentially altering the outcome of infection in the porcine host. In addition to the disruption of the TIR domain, the increased levels of IL-6 observed during *in vivo* NS4B.VGIv infection could also aid in controlling the infection, contributing to the attenuated phenotype of NS4B.VGIv. The rapid protective immunity elicited by NS4B.VGIv suggests that the VGI residues could be modified for the development of a live-attenuated CSFV vaccine that would provide rapid protection against CSF disease. An improved understanding of the underlying genetic basis of viral virulence and the host immune response will permit future rational design of efficacious biological tools for controlling CSF disease.

ACKNOWLEDGMENT

We thank the Plum Island Animal Disease Center Animal Care Unit staff for excellent technical assistance.

REFERENCES

1. **Akira, S., and K. Takeda.** 2004. Toll-like receptor signalling. Nat. Rev. Immunol. **4:**499–511.
2. **Becher, P., R. Avalos Ramirez, M. Orlich, S. Cedillo Rosales, M. Konig, M. Schweizer, H. Stalder, H. Schirrmeier, and H. J. Thiel.** 2003. Genetic and antigenic characterization of novel pestivirus genotypes: implications for classification. Virology **311:**96–104.
3. **Blight, K. J.** 2007. Allelic variation in the hepatitis C virus NS4B protein dramatically influences RNA replication. J. Virol. **81:**5724–5736.
4. **Borca, M. V., I. Gudmundsdottir, I. J. Fernandez-Sainz, L. G. Holinka, and G. R. Risatti.** 2008. Patterns of cellular gene expression in swine macrophages infected with highly virulent classical swine fever virus strain Brescia. Virus Res. **138:**89–96.

5. **Dockrell, D. H., and G. R. Kinghorn.** 2001. Imiquimod and resiquimod as novel immunomodulators. J. Antimicrob. Chemother. **48:**751–755.
6. **Edwards, S., V. Moennig, and G. Wensvoort.** 1991. The development of an international reference panel of monoclonal antibodies for the differentiation of hog cholera virus from other pestiviruses. Vet. Microbiol. **29:**101–108.
7. **Egger, D., B. Wolk, R. Gosert, L. Bianchi, H. E. Blum, D. Moradpour, and K. Bienz.** 2002. Expression of hepatitis C virus proteins induces distinct membrane alterations including a candidate viral replication complex. J. Virol. **76:**5974–5984.
8. **Einav, S., M. Elazar, T. Danieli, and J. S. Glenn.** 2004. A nucleotide binding motif in hepatitis C virus (HCV) NS4B mediates HCV RNA replication. J. Virol. **78:**11288–11295.
9. **Einav, S., D. Gerber, P. D. Bryson, E. H. Sklan, M. Elazar, S. J. Maerkl, J. S. Glenn, and S. R. Quake.** 2008. Discovery of a hepatitis C target and its pharmacological inhibitors by microfluidic affinity analysis. Nat. Biotechnol. **26:**1019–1027.
10. **Elazar, M., P. Liu, C. M. Rice, and J. S. Glenn.** 2004. An N-terminal amphipathic helix in hepatitis C virus (HCV) NS4B mediates membrane association, correct localization of replication complex proteins, and HCV RNA replication. J. Virol. **78:**11393–11400.
11. **Gibson, S. J., L. M. Imbertson, T. L. Wagner, T. L. Testerman, M. J. Reiter, R. L. Miller, and M. A. Tomai.** 1995. Cellular requirements for cytokine production in response to the immunomodulators imiquimod and S-27609. J. Interferon Cytokine Res. **15:**537–545.
12. **Gibson, S. J., J. M. Lindh, T. R. Riter, R. M. Gleason, L. M. Rogers, A. E. Fuller, J. L. Oesterich, K. B. Gorden, X. Qiu, S. W. McKane, R. J. Noelle, R. L. Miller, R. M. Kedl, P. Fitzgerald-Bocarsly, M. A. Tomai, and J. P. Vasilakos.** 2002. Plasmacytoid dendritic cells produce cytokines and mature in response to the TLR7 agonists, imiquimod and resiquimod. Cell. Immunol. **218:**74–86.
13. **Gouttenoire, J., V. Castet, R. Montserret, N. Arora, V. Raussens, J. M. Ruysschaert, E. Diesis, H. E. Blum, F. Penin, and D. Moradpour.** 2009. Identification of a novel determinant for membrane association in hepatitis C virus nonstructural protein 4B. J. Virol. **83:**6257–6268.
14. **Guex, N., and M. C. Peitsch.** 1997. SWISS-MODEL and the Swiss-Pdb-Viewer: an environment for comparative protein modeling. Electrophoresis **18:**2714–2723.
15. **Hemmi, H., T. Kaisho, O. Takeuchi, S. Sato, H. Sanjo, K. Hoshino, T. Horiuchi, H. Tomizawa, K. Takeda, and S. Akira.** 2002. Small anti-viral compounds activate immune cells via the TLR7 MyD88-dependent signaling pathway. Nat. Immunol. **3:**196–200.
16. **Hügle, T., F. Fehrmann, E. Bieck, M. Kohara, H. G. Krausslich, C. M. Rice, H. E. Blum, and D. Moradpour.** 2001. The hepatitis C virus nonstructural protein 4B is an integral endoplasmic reticulum membrane protein. Virology **284:**70–81.
17. **Jones, D. M., A. H. Patel, P. Targett-Adams, and J. McLauchlan.** 2009. The hepatitis C virus NS4B protein can trans-complement viral RNA replication and modulates production of infectious virus. J. Virol. **83:**2163–2177.
18. **Kanzler, H., F. J. Barrat, E. M. Hessel, and R. L. Coffman.** 2007. Therapeutic targeting of innate immunity with Toll-like receptor agonists and antagonists. Nat. Med. **13:**552–559.
19. **Kawai, T., and S. Akira.** 2009. The roles of TLRs, RLRs and NLRs in pathogen recognition. Int. Immunol. **21:**317–337.
20. **Kopf, M., H. Baumann, G. Freer, M. Freudenberg, M. Lamers, T. Kishimoto, R. Zinkernagel, H. Bluethmann, and G. Kohler.** 1994. Impaired immune and acute-phase responses in interleukin-6-deficient mice. Nature **368:**339–342.
21. **Lee, J., T. H. Chuang, V. Redecke, L. She, P. M. Pitha, D. A. Carson, E. Raz, and H. B. Cottam.** 2003. Molecular basis for the immunostimulatory activity of guanine nucleoside analogs: activation of Toll-like receptor 7. Proc. Natl. Acad. Sci. U. S. A. **100:**6646–6651.
22. **Li, S., L. Ye, X. Yu, B. Xu, K. Li, X. Zhu, H. Liu, X. Wu, and L. Kong.** 2009. Hepatitis C virus NS4B induces unfolded protein response and endoplasmic reticulum overload response-dependent NF-κB activation. Virology **391:** 257–264.
23. **Libermann, T. A., and D. Baltimore.** 1990. Activation of interleukin-6 gene expression through the NF-κB transcription factor. Mol. Cell. Biol. **10:**2327–2334.
24. **Lindström, H., M. Lundin, S. Haggstrom, and M. A. Persson.** 2006. Mutations of the hepatitis C virus protein NS4B on either side of the ER membrane affect the efficiency of subgenomic replicons. Virus Res. **121:**169–178.
25. **Lundin, M., H. Lindstrom, C. Gronwall, and M. A. Persson.** 2006. Dual topology of the processed hepatitis C virus protein NS4B is influenced by the NS5A protein. J. Gen. Virol. **87:**3263–3272.
26. **Lundin, M., M. Monne, A. Widell, G. Von Heijne, and M. A. Persson.** 2003. Topology of the membrane-associated hepatitis C virus protein NS4B. J. Virol. **77:**5428–5438.
27. **Miller, S., S. Sparacio, and R. Bartenschlager.** 2006. Subcellular localization and membrane topology of the Dengue virus type 2 non-structural protein 4B. J. Biol. Chem. **281:**8854–8863.
28. **Mittelholzer, C., C. Moser, J. D. Tratschin, and M. A. Hofmann.** 2000. Analysis of classical swine fever virus replication kinetics allows differentiation of highly virulent from avirulent strains. Vet. Microbiol. **74:**293–308.
29. **Moraes, M. P., G. A. Mayr, P. W. Mason, and M. J. Grubman.** 2002. Early protection against homologous challenge after a single dose of replication-defective human adenovirus type 5 expressing capsid proteins of foot-and-mouth disease virus (FMDV) strain A24. Vaccine **20:**1631–1639.
30. **Muñoz-Jordan, J. L., M. Laurent-Rolle, J. Ashour, L. Martinez-Sobrido, M. Ashok, W. I. Lipkin, and A. Garcia-Sastre.** 2005. Inhibition of alpha/beta interferon signaling by the NS4B protein of flaviviruses. J. Virol. **79:**8004–8013.
31. **Muñoz-Jordan, J. L., G. G. Sanchez-Burgos, M. Laurent-Rolle, and A. Garcia-Sastre.** 2003. Inhibition of interferon signaling by dengue virus. Proc. Natl. Acad. Sci. U. S. A. **100:**14333–14338.
32. **Paredes, A. M., and K. J. Blight.** 2008. A genetic interaction between hepatitis C virus NS4B and NS3 is important for RNA replication. J. Virol. **82:**10671–10683.
33. **Piccininni, S., A. Varaklioti, M. Nardelli, B. Dave, K. D. Raney, and J. E. McCarthy.** 2002. Modulation of the hepatitis C virus RNA-dependent RNA polymerase activity by the non-structural (NS) 3 helicase and the NS4B membrane protein. J. Biol. Chem. **277:**45670–45679.
34. **Qu, L., L. K. McMullan, and C. M. Rice.** 2001. Isolation and characterization of noncytopathic pestivirus mutants reveals a role for nonstructural protein NS4B in viral cytopathogenicity. J. Virol. **75:**10651–10662.
35. **Reed, L. J., and H. A. Muench.** 1938. A simple method of estimating fifty per cent endpoints. Am. J. Hyg. **27:**493–497.
36. **Rice, C. M.** 1996. Flaviviridae: the viruses and their replication, p. 931–959. *In* B. N. Fields, D. M. Knipe, and P. Howley (ed.), Fundamental virology, 3rd ed. Lippincott-Raven, Philadelphia, PA.
37. **Risatti, G. R., M. V. Borca, G. F. Kutish, Z. Lu, L. G. Holinka, R. A. French, E. R. Tulman, and D. L. Rock.** 2005. The E2 glycoprotein of classical swine fever virus is a virulence determinant in swine. J. Virol. **79:**3787–3796.
38. **Sanger, F., S. Nicklen, and A. R. Coulson.** 1977. DNA sequencing with chain-terminating inhibitors. Proc. Natl. Acad. Sci. U. S. A. **74:**5463–5467.
39. **Schultz, J., F. Milpetz, P. Bork, and C. P. Ponting.** 1998. SMART, a simple modular architecture research tool: identification of signaling domains. Proc. Natl. Acad. Sci. U. S. A. **95:**5857–5864.
40. **Slack, J. L., K. Schooley, T. P. Bonnert, J. L. Mitcham, E. E. Qwarnstrom, J. E. Sims, and S. K. Dower.** 2000. Identification of two major sites in the type I interleukin-1 receptor cytoplasmic region responsible for coupling to pro-inflammatory signaling pathways. J. Biol. Chem. **275:**4670–4678.
41. **Stack, J., I. R. Haga, M. Schroder, N. W. Bartlett, G. Maloney, P. C. Reading, K. A. Fitzgerald, G. L. Smith, and A. G. Bowie.** 2005. Vaccinia virus protein A46R targets multiple Toll-like-interleukin-1 receptor adaptors and contributes to virulence. J. Exp. Med. **201:**1007–1018.
42. **Subramaniam, S., C. Stansberg, and C. Cunningham.** 2004. The interleukin 1 receptor family. Dev. Comp. Immunol. **28:**415–428.
43. **Tasaka, M., N. Sakamoto, Y. Itakura, M. Nakagawa, Y. Itsui, Y. Sekine-Osajima, Y. Nishimura-Sakurai, C. H. Chen, M. Yoneyama, T. Fujita, T. Wakita, S. Maekawa, N. Enomoto, and M. Watanabe.** 2007. Hepatitis C virus non-structural proteins responsible for suppression of the RIG-I/Cardif-induced interferon response. J. Gen. Virol. **88:**3323–3333.
44. **Terpstra, C., R. Woortmeyer, and S. J. Barteling.** 1990. Development and properties of a cell culture produced vaccine for hog cholera based on the Chinese strain. Dtsch. Tierarztl. Wochenschr. **97:**77–79.
45. **Testerman, T. L., J. F. Gerster, L. M. Imbertson, M. J. Reiter, R. L. Miller, S. J. Gibson, T. L. Wagner, and M. A. Tomai.** 1995. Cytokine induction by the immunomodulators imiquimod and S-27609. J. Leukoc. Biol. **58:**365–372.
46. **Thiel, H. J., R. Stark, E. Weiland, T. Rumenapf, and G. Meyers.** 1991. Hog cholera virus: molecular composition of virions from a pestivirus. J. Virol. **65:**4705–4712.
47. **Thompson, A. A., A. Zou, J. Yan, R. Duggal, W. Hao, D. Molina, C. N. Cronin, and P. A. Wells.** 2009. Biochemical characterization of recombinant hepatitis C virus nonstructural protein 4B: evidence for ATP/GTP hydrolysis and adenylate kinase activity. Biochemistry **48:**906–916.
48. **Van Snick, J.** 1990. Interleukin-6: an overview. Annu. Rev. Immunol. **8:**253–278.
49. **Wagner, T. L., V. L. Horton, G. L. Carlson, P. E. Myhre, S. J. Gibson, L. M. Imbertson, and M. A. Tomai.** 1997. Induction of cytokines in cynomolgus monkeys by the immune response modifiers, imiquimod, S-27609 and S-28463. Cytokine **9:**837–845.
50. **Wicker, J. A., M. C. Whiteman, D. W. Beasley, C. T. Davis, S. Zhang, B. S. Schneider, S. Higgs, R. M. Kinney, and A. D. Barrett.** 2006. A single amino acid substitution in the central portion of the West Nile virus NS4B protein confers a highly attenuated phenotype in mice. Virology **349:**245–253.
51. **Zsak, L., Z. Lu, G. F. Kutish, J. G. Neilan, and D. L. Rock.** 1996. An African swine fever virus virulence-associated gene NL-S with similarity to the herpes simplex virus ICP34.5 gene. J. Virol. **70:**8865–8871.

Return to Table of Contents

Veterinary Pathology
000(00) 1-16

DOI: 10.1177/0300985810372509
http://vet.sagepub.com

The Early Pathogenesis of Foot-and-Mouth Disease in Cattle After Aerosol Inoculation: Identification of the Nasopharynx as the Primary Site of Infection

J. Arzt[1,2], J. M. Pacheco[1], and L. L. Rodriguez[1]

Abstract

To characterize the early events of foot-and-mouth disease virus (FMDV) infection in cattle subsequent to simulated natural exposure, 16 steers were aerosol inoculated with FMDV and euthanized at various times. Samples were collected from each steer antemortem (serum, nasal swabs, and oral swabs) and postmortem (up to 40 tissues per animal) and screened for FMDV by virus isolation and for FMDV RNA by real-time reverse transcription polymerase chain reaction. Tissues that tested positive for FMDV or viral RNA were examined by immunohistochemistry and multichannel immunofluorescence microscopy. In previremic steers, FMDV was most consistently localized to nasopharyngeal tissues, thereby indicating this region as the most important site of primary viral replication. The earliest site of microscopic localization of FMDV antigens was the lymphoid follicle-associated epithelium of the pharyngeal mucosa-associated lymphoid tissue of the nasopharynx at 6 hours postaerosolization. At early time points after aerosol inoculation, viral antigens colocalized with cytokeratin-positive pharyngeal epithelial cells; intraepithelial FMDV-negative, MHCII/CD11c-double-positive dendritic cells were present in close proximity to FMDV-positive cells. Onset of viremia coincided with marked increase of viral loads in pulmonary tissues and with substantial decrease of viral detection in nasopharyngeal tissues. These data indicate that subsequent to aerogenous exposure to FMDV, the temporally defined critical pathogenesis events involve (1) primary replication in epithelial cells of the pharyngeal mucosa-associated lymphoid tissue crypts and (2) subsequent widespread replication in pneumocytes in the lungs, which coincides with (3) the establishment of sustained viremia.

Keywords

aerosol, bovine, cattle, foot-and-mouth disease, pathogenesis, virus

Foot-and-mouth disease (FMD) is a highly contagious picornaviral disease affecting domestic and wild cloven-hoofed animals.[2,13] Under natural transmission conditions, within and between herds of cattle, the etiologic agent, FMD virus (FMDV), is spread through inhalation of aerosolized virus, and under appropriate environmental conditions, virus-laden droplets may travel vast distances while maintaining infectivity.[1,13,22]

Numerous researchers have experimentally investigated the pathogenesis of FMD in cattle;[1,4,6,7,14,15] however, a consensus still does not exist regarding many basic aspects of the early stages of infection. Most notably, the anatomic sites and cellular events involved in primary infection and the establishment of viremia are not well defined. Elucidation of these critical events and improved understanding of virus–host interactions have high probability to favorably affect the goal of improving efficacy of vaccines and biotherapeutic countermeasures to protect domestic livestock against FMDV.

Early evidence that the respiratory tract was the natural route of infection implicated the nasal cavity[14] or lungs[10] as the sites of primary replication. Yet, as investigation proceeded, opinion on this subject diverged into 2 camps favoring either the nasopharynx[2,7] or lungs[4,6] as the primary infection site. A unique set of experiments performed in the 1970s effectively isolated the contributory roles of the upper and lower respiratory tract by

[1] Plum Island Animal Disease Center, Foreign Animal Disease Research Unit, Agricultural Research Service, US Department of Agriculture, Greenport, New York
[2] Department of Microbiology, Immunology, and Pathology, Colorado State University, Fort Collins, CO

Corresponding Author:
Jonathan Arzt, Foreign Animal Disease Research Unit, USDA/ARS Plum Island Animal Disease Center, PO Box 848, Greenport, NY 11944
Email: jonathan.arzt@ars.usda.gov

placement of indwelling tracheostomy tubes in cattle.[24] This work concluded that both the lungs and the pharynx could similarly serve as portals for the establishment of systemic infection. The only studies to microscopically localize FMDV in the early (previremic) stages of infection utilized in situ hybridization and concluded that lungs supported infection earlier than the pharynx.[4,6] In consideration of the disparate findings across FMD pathogenesis studies, it is necessary to remember that the various studies have utilized a broad range of serotypes and subtypes of FMDV, which may have substantial differences in virulence and tissue tropism. Additionally, heterogeneity of inoculation systems and differences in sensitivity and/or specificity of virus detection methods may account for some disparity among the published studies.

Recent reports from our laboratory have described a novel method for aerosol inoculation of cattle with FMDV and trimodal systems for detection of FMDV in bovine tissues during the early stages of infection.[3,18] In the current study, we utilized similar experimental systems to further characterize the distribution of FMDV in cattle during the previremic and early viremic phases of infection, with the overall conclusion that subsequent to aerogenous inoculation of cattle, infection initiates in the nasopharynx, it is promptly followed by pulmonary infection, and the onset of viremia is coincident with increased viral load in the lungs and decreased virus in the nasopharynx.

Materials and Methods

Experimental Animals, Virus, and Inoculation Systems

Sixteen 9- to 18-month-old Holstein steers weighing 400 to 500 kg were obtained from an experimental-livestock provider accredited by the Association for Assessment and Accreditation of Laboratory Animal Care (Thomas-Morris Inc, Reisterstown, MD). For all experiments, animals were individually housed in a biosafety level 3 animal facility from time of inoculation until time of euthanasia. Experiments were terminated by euthanasia via intravenous barbiturate overdose at predetermined end points at 0.1 hours post aerosol inoculation (hpa; steer No. 1), 3.0 hpa (steer Nos. 2, 3), 6.0 hpa (steer Nos. 4, 5), 12.0 hpa (steer Nos. 6, 7), 24.0 hpa (steer Nos. 8-13), 48.0 hpa (steer Nos. 14, 15), 240.0 hpa (steer No. 16).

Virus inoculum consisted of a clarified, macerate of tongue epithelium harvested from 2 steers experimentally infected with the FMDV strain O_1-Manisa as previously described.[12,18] The inoculum was quantitated as $BTID_{50}$ (bovine tongue infectious dose 50%). All steers were aerosol inoculated with 10^7 $BTID_{50}$ of FMDV-O_1-Manisa as previously described.[18] Briefly, each steer was sedated with xylazine and fitted with a commercially available aerosol delivery system (Aeromask-ES, Trudell Medical, London, Ontario, Canada), which was placed over the muzzle. The mask was attached to a jet nebulizer (Whisper Jet, Vital Signs Inc, Totowa, NJ), which was subsequently attached to an air compressor that generated 25 psi of pressure. Aerosolization proceeded until the complete inoculum was expelled from the nebulizer cup (10 to 15 minutes).

Sample Collection

Antemortem sampling consisted of collection of whole blood in serum separation tubes, oral swabs, and nasal swabs. All animals were sampled before inoculation to ensure FMDV-free status and at several time points throughout the duration of the experiment, which varied according to goals of the individual experiments. Swabs and serum tubes were transported from the animal room to the laboratory on ice and were immediately centrifuged for harvesting of serum, saliva, and nasal secretion. Samples were then stored at –70°C until time of processing.

Necropsies were performed immediately subsequent to euthanasia at predetermined time points, and tissue specimens were collected from oral cavity, nasal cavity, soft palate, pharynx, larynx, trachea, lungs, lymph nodes, and skin (Table 1). Tissues collected from each animal varied depending on the goals of individual experiments. Detailed descriptions of tissue designations and collection strategies has been published.[18] For each anatomically defined specimen, two 30-mg tissue samples were aliquoted into separate screw-cap 1.5-ml tubes and frozen immediately in liquid nitrogen for transfer within 2 hours to a –70°C freezer in which they were stored until the time of processing. An adjacent specimen from each tissue was placed in a cryomold, embedded in Optimal Cutting Temperature Compound (Sakura Finetek, Torrance, CA), frozen on a bath of liquid nitrogen, and stored at –70°C for immunohistochemistry (IHC).

FMDV RNA Detection

Two samples of each tissue listed in Table 1 per animal were thawed and immediately macerated in a TissueLyser bead beater (Qiagen, Valencia, CA) as previously described.[18] After maceration, 50 µl of each sample was transferred to a 96-well plate (Thermo Scientific, Waltham, MA) containing 150 µl of lysis/binding solution. RNA was then extracted with Ambion's MagMax-96 Viral RNA Isolation Kit (Ambion, Austin, TX) on a King Fisher-96 Magnetic Particle Processor (Thermo Scientific, Waltham, MA). RNA was eluted in a final volume of 25 µl. Once extracted, 2.5 µl of RNA was analyzed by real-time reverse transcription polymerase chain reaction (rRT-PCR) on the ABI 7000 system (Applied Biosystems, Austin, TX) as previously described.[8] Samples with cycle threshold values < 40 were considered positive. The remaining macerated tissue was clarified at 1,000 rpm for 2 minutes at 4°C, and the supernatant was cleared of bacterial contamination using centrifuge tube filters (Spin-X, Costar, Corning, NY). Clarified and cleared samples were stored at –70°C until virus isolation (VI) was performed.

To convert cycle threshold values generated by rRT-PCR from experimental samples to RNA genome copies per milligram, serial 10-fold dilutions of in vitro synthesized FMDV RNA of known RNA concentration were analyzed by the rRT-PCR protocol described above. The equation of the curve of RNA copy versus cycle threshold value, further adjusted for

Table 1. Tissue-Specific Distribution of FMDV in Steer Nos. 2-15 with Cumulative Percentage Positivity[a]

Sample Identification[b]	3 HPA		6 HPA		12 HPA		24 HPA						48 HPA		Previremic Cumulative Percentage Positivity[c]		
	2	3	4	5	6	7	8	9	10	11	12	13	14	15	rRT-PCR	VI	rRT-PCR or VI
Serum	NEG	NEG	NEG	NEG	NEG	NEG	NEG	NEG	NEG	4.67	3.94	**4.02**	**6.62**	**7.24**	18.2	0.0	18.2
Oral cavity / oropharynx																	
Lower lip					NEG		**NEG**	2.63	NEG				NEG	**3.66**	25.0	25.0	50.0
Tongue–R	NEG	NEG	NEG	NEG		NEG	NEG	2.81	NEG	2.41	NEG	NEG	NEG	**3.97**	20.0	0.0	20.0
Ventral soft palate–R	NEG	NEG	NEG	NEG	NEG	2.34	**2.39**	3.55	NEG				**4.54**	4.44	33.3	11.1	33.3
Ventral soft palate–C	NEG	NEG	2.27	NEG	2.98	3.34	**3.21**	2.50	NEG				4.54	**4.37**	55.6	11.1	55.6
Nasopharynx/larynx																	
Dorsal soft palate–R	NEG	NEG	**2.58**	NEG	**3.43**	**NEG**	**3.75**	7.30	**2.75**	**3.68**	**NEG**	**4.56**	NEG	NEG	54.5	63.6	72.7
Dorsal soft palate–C	2.92	NEG	**2.85**	NEG	**NEG**	**4.34**	**4.98**	**4.01**	**3.85**	**4.01**	**5.11**	**NEG**	2.99	**2.92**	72.7	72.7	81.8
Dorsal nasopharynx–R	2.33	2.78	**NEG**	2.90	**NEG**	**3.19**	**3.62**	**NEG**	**3.31**	**3.97**	**3.07**	3.34	NEG	**2.33**	72.7	72.7	100.0
Dorsal nasopharynx–C	2.95	NEG	NEG	2.30	**NEG**	**4.90**	**4.15**	**3.29**	**5.06**	**3.07**	**3.34**	**2.79**	**NEG**	**3.98**	72.7	63.6	81.8
Epiglottis–V	2.50	2.47	NEG	NEG	2.96	**3.56**	2.36	3.92	**NEG**	**3.88**	NEG	**3.76**	**NEG**	NEG	63.6	27.3	72.7
Larynx–V	NEG	NEG	3.35	NEG	**2.79**	**4.62**	**4.09**	**4.70**	3.53	**4.03**	**2.74**	**3.22**	**NEG**	**2.88**	72.7	54.5	72.7
Lungs/trachea																	
Trachea–aborad	NEG	2.44	NEG	2.29	NEG	2.37	NEG	NEG	NEG				3.55	3.45	33.3	0.0	33.3
Tracheal bifurcation	NEG	NEG	NEG	NEG	NEG	NEG	NEG	3.72	2.45				2.44	**4.95**	22.2	0.0	22.2
Proximal cranial lobe	NEG	NEG	NEG	3.18	NEG	**2.78**	3.38	2.89	NEG				NEG	**4.67**	44.4	11.1	44.4
Mid cranial lobe	NEG	NEG	NEG	**NEG**	NEG	3.60	**4.05**	NEG	NEG				NEG	3.44	22.2	22.2	33.3
Distal cranial lobe	NEG	NEG	NEG	**NEG**	NEG	**5.12**	**2.28**	NEG	NEG	**4.93**	NEG	**2.54**	NEG	**5.54**	27.3	36.4	36.4
Proximal mid lobe	NEG	NEG	NEG	2.75	NEG	NEG	**4.63**	2.63	NEG				5.04	**3.97**	33.3	11.1	33.3
Mid mid lobe	NEG	NEG	NEG	NEG	**2.52**	2.74	**5.22**	NEG	NEG				2.51	3.49	33.3	22.2	33.3
Distal mid lobe	NEG	NEG	NEG	NEG	2.80	NEG	**4.11**	3.83	NEG	**5.18**	**5.43**	**3.87**	5.03	**3.76**	45.5	27.3	45.5
Proximal caudal lobe	NEG	NEG	NEG	NEG	**2.76**	NEG	2.73	3.09	NEG				3.88	**3.65**	33.3	11.1	33.3
Mid caudal lobe	NEG	NEG	NEG	NEG	NEG	NEG	NEG	2.92	NEG				3.51	3.71	11.1	0.0	11.1
Distal caudal lobe	2.41	2.61	NEG	NEG	NEG	NEG	3.27	3.34	NEG	**2.94**	**3.25**	**4.50**	2.44	NEG	54.5	18.2	54.5
Additional tissues																	
Lingual tonsil	2.58	NEG	2.79	NEG	NEG	NEG	NEG	NEG	NEG	**3.10**	2.65	3.90	3.01	4.13	36.4	9.1	36.4
Palatine tonsil	NEG	NEG	NEG	NEG	**NEG**	NEG	NEG	NEG	NEG				**4.53**	**2.86**	11.1	0.0	11.1
Nasopharyngeal tonsil	NEG	2.82	NEG	NEG	NEG	NEG	2.57	NEG	NEG				NEG	NEG	22.2	0.0	22.2
Retropharyngeal LN	NEG	NEG	NEG	NEG	NEG	NEG				NEG	**NEG**	NEG	NEG	NEG	0.0	12.5	12.5
Hilar LN	NEG	NEG	NEG	NEG	NEG	NEG				**NEG**	NEG	NEG		**NEG**	0.0	12.5	12.5
Interdigital cleft	2.49	NEG	NEG	NEG	NEG	NEG				**NEG**	NEG	NEG	**7.70**	**7.96**	12.5	0.0	25.0
Alar fold	NEG						2.34	NEG	NEG				NEG	3.68	25.0	0.0	25.0
Turbinates–C					NEG	NEG	**NEG**	NEG	NEG				NEG	NEG	0.0	20.0	20.0
Thyroid	NEG	NEG		NEG		NEG				**2.61**	NEG				16.7	16.7	16.7

[a] HPA, hours post aerosol inoculation; rRT-PCR, real-time reverse transcription polymerase chain reaction; VI, virus isolation; R, rostral; C, caudal; V, ventral; LN, lymph node; NEG, rRT-PCR negative. Blank cells indicate *not examined*. Tabulated numerical data are $\log_{10}$ foot-and-mouth disease virus (FMDV) RNA genome copies per ml of serum or mg of tissue as determined by rRT-PCR. Negative tissues indicate that RNA quantity was below the detection threshold of 2.26 $\log_{10}$ FMDV genome copies per mg of tissue (corresponding to cycle threshold = 40.00). Entries in bold text were positive for FMDV by virus isolation; nonbold text indicates that virus isolation was negative.

[b] Additional tissues tested were negative for all previremic steers examined, as follows: dental pad, tongue (caudal), tongue (torus), hard palate (rostral), hard palate (caudal), nasal planum, turbinates (rostral), trachea (orad), trachea (mid).

[c] Previremia is defined as serum virus isolation negative at all times sampled, including the time of euthanasia. Percentage positivities for rRT-PCR and VI separately are defined as the number of positive results using one modality, divided by the number of steers for which a tissue type was examined by that modality. Percentage positivity for rRT-PCR or VI is defined as the number of times that a tissue was positive by either modality, divided by the number of steers for which that tissue type was examined by both modalities.

average mass of tissue samples and dilutions during processing, was used for subsequent conversions. The cycle threshold positivity cutoff of 40 corresponded to a detection threshold value of 2.26 $\log_{10}$ FMDV RNA copies per milligram (RNA/mg) of tissue. The rRT-PCR results reported in Table 1 are the higher RNA/mg value of the 2 samples processed per tissue per animal; the rRT-PCR results reported in Figure 1 are the mean $\log_{10}$ FMDV RNA copies per milliliter (RNA/ml) for all animals sampled at each time point.

FMDV Isolation

VI was performed separately on the duplicate samples of each tissue on LFBK cells as previously described.[18,25] Upon detection of cytopathic effect, FMDV positivity was confirmed by rRT-PCR on cell culture supernatants. Samples in which no cytopathic effect was observed were amplified through 3 blind passages and the supernatants were tested by rRT-PCR before they were deemed negative. Each VI result in Table 1 is reported positive if either or both duplicate samples per tissue were positive.

Immunohistochemical and Immunofluorescent Localization of FMDV Antigens

Microscopic localization of FMDV antigens was performed in cryosections as previously described.[3,18] Briefly, tissue sections were blocked for 2 hours at 20°C; primary antibodies were diluted in blocking buffer and applied to tissue sections for 18 hours at 4°C. For IHC, specific anti-FMDV immunoreactivity was detected with a micropolymer alkaline phosphatase kit (Biocare, Concord, CA). For multichannel immunofluorescent (MIF), detection was performed with goat, anti-rabbit, and isotype-specific anti-mouse secondary antibodies labeled with AlexaFluor dyes (AF 350, 488, 594, 647). Slides were examined with a wide-field, epifluorescent microscope, and images were captured with a cooled, monochromatic digital camera. Images of individual detection channels were adjusted for contrast and brightness and merged in commercially available software (Adobe Photoshop CS2). Mouse monoclonal anti-FMDV antibodies against viral structural proteins were 10GA4 and 12AF4;[23] anti–nonstructural protein antibodies were F19-6 and F19-51.[27] Antibodies used to label cell markers in MIF experiments were mouse monoclonal anti-pancytokeratin plus (Biocare No. CM162), anti-bovine cytokeratin (CK; Sigma No. C6909, Sigma-Aldrich, Inc, St. Louis, MO), anti-CD11c (VMRD No. BAQ153A, VMRD, Pullman, WA), anti-MHCII (VMRD No. CAT82A), and anti-vimentin (Dako No. M0725, Dako, Carpinteria, CA), and rabbit polyclonal anti–Von Willibrand factor (Dako No. A0082).

For each tissue screened by IHC, a duplicate negative-control serial section treated with a mouse monoclonal anti-VSV-Indiana antibody of similar concentration was prepared. Additional negative control tissue sections were prepared from a steer that received a virus-free aerosol inoculum and was euthanized 24 hours post aerosol inoculation (hpa). Immunohistochemical and MIF labeling were considered positive when there was an intense cell-associated signal within the experimental tissue, with the absence of such staining in the negative controls.

Results

Inoculum Detection Controls

For the purpose of determining if the FMDV screening techniques would detect residual inoculated virus, 1 aerosol-inoculated steer (No. 1) was euthanized immediately after inoculation (0.1 hpa) and was subjected to standard tissue collection and screening techniques as described for the other animals. All 28 tissues collected from this animal were VI negative, and only a single tissue, proximal cranial lung, was positive by rRT-PCR (2.56 RNA/mg). This information confirmed that the inoculum reached as far as the lungs and strongly affirmed that any rRT-PCR- and VI-positive findings at subsequent time points represent FMDV replicated de novo. Based on the positive rRT-PCR finding for proximal cranial lung from steer No. 1, the frozen Optimal Cutting Temperature Compound–embedded tissue specimen from this tissue was examined by IHC to similarly test for detection of inoculated virus. Forty serial sections were examined (alternating anti-FMDV capsid and anti-FMDV 3D [polymerase] primary antibodies) with no detection of FMDV antigens in any section, confirming that inoculum quantity was insufficient to be detected by IHC. Data generated from this animal are not included in subsequent analyses.

Antemortem Profiles of FMDV-Infected Cattle

Neither vesicles nor fever (rectal temperature $\geq$ 40°C) was observed in any previremic animals. The earliest detection of fever in any animal occurred at 60 hpa, in steer No. 16; this animal was febrile from 60 to 96 hpa, with maximum body temperature of 41°C detected at 60 hpa. The 3 steers euthanized as 48 hpa or later (viremic) all developed vesicles of 1 ($n = 2$) or 2 ($n = 1$) interdigital clefts at 48 hpa (Fig. 1). One steer (No. 15) had subtle blanching of the epithelium of the lingual torus at 48 hpa, which was subsequently determined histologically to be an early vesicle. The 1 steer that survived 240 hpa (No. 16) developed vesicles of tongue and all 4 interdigital clefts between 48 and 120 hpa. No other clinical signs of infection or gross lesions were detected in the animals that survived 0.1 to 48.0 hpa.

The aerosol inoculation system provided highly consistent patterns of viral shedding, viremia, and clinical signs across experimental animals; however, some interanimal variation was observed. Antemortem data are presented as cumulative average $\log_{10}$ FMDV genome copy numbers per milliliter (RNA/ml) for all animals at each time point (Fig. 1). For oral swab samples, the quantity of FMDV RNA (inoculum) progressively decreased from 0.1 to 8.0 hpa with de novo replicated virus first detected at 24 hpa and peaking at 72 hpa at 8.17 RNA/ml. Similarly, nasal swab samples showed gradual elimination of inoculum from 0.1 to 4.0 hpa with de novo replicated viral RNA beginning to increase at 6 hpa.

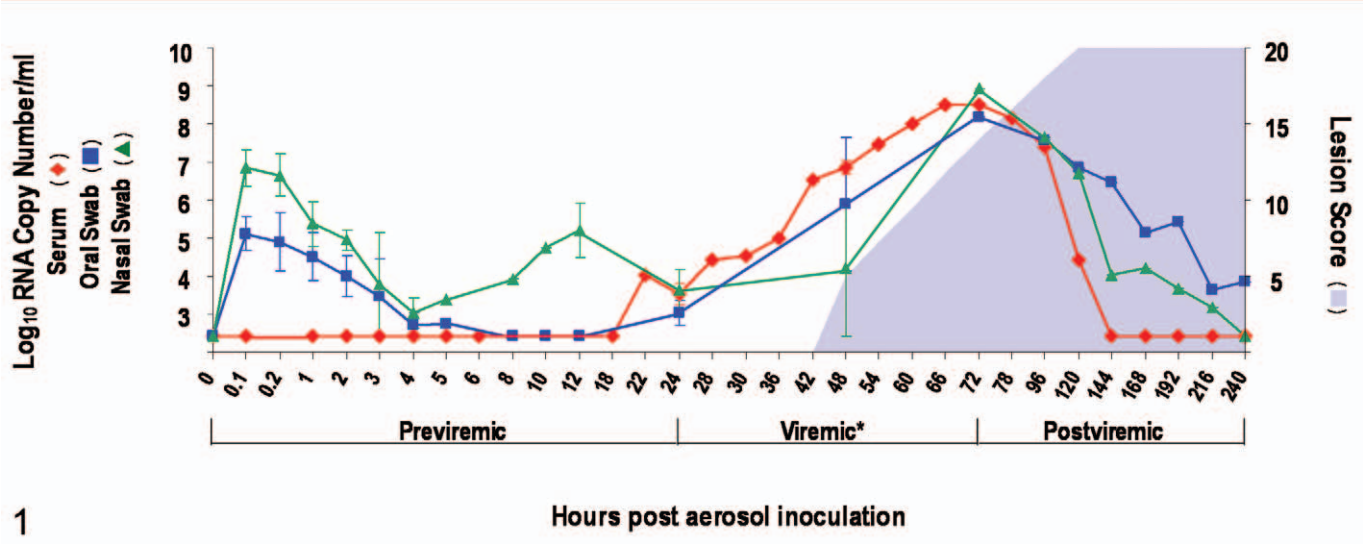

Figure 1. Time course of foot-and-mouth disease virus RNA quantity (log_{10} genome copy number / ml) determined by real-time reverse transcription polymerase chain reaction in serum (red), nasal swab samples (green), and oral swab samples (blue) collected from steers aerosol-inoculated with foot-and-mouth disease virus O_1-Manisa. Each data point represents the mean $\pm$ SE for all steers sampled at a given time (hours postaerosol inoculation). Lesion (vesicle) score was calculated by evaluating each foot and the head independently, with 2 points assigned for a small vesicle ($\leq$ 1.0cm) and 4 points for a large vesicle. Viremia (*) was defined by positive findings on serum virus isolation. *X*-axis calibration not to scale.

However, unlike oral swabs, the viral RNA quantity never dropped below detection threshold before de novo replication was detected (Fig. 1). Also unlike oral swabs, the nasal shedding pattern showed 2 peaks, at 12 and 72 hpa (5.22 and 8.92 RNA/ml, respectively) with an intervening trough. Maximum nasal and oral FMDV RNA/ml occurred coincidently at 72 hpa with the nasal detection peak being slightly higher but decreasing more precipitously relative to salivary samples.

The earliest detection of FMDV RNA in sera occurred at 22 hpa in 1 steer. At 24 hpa, 6 of 9 steers had RNA-positive sera, and at 48 hpa the sera of all 3 steers sampled were FMDV rRT-PCR positive (Fig. 1). Detection of infectious FMDV in sera was delayed relative to RNA, with a single VI-positive steer (1 of 9) at 24 hpa and with the remaining 3 steers (3 of 3) becoming serum VI positive by 48 hpa; viremia was defined by the detection of infectious virus in serum. Overall, FMDV RNA was detected in sera from 22 to 120 hpa, whereas viremia was detected from only 24 to 72 hpa.

Tissue-Specific Distribution of FMDV and Viral RNA

Steers were euthanized at predetermined time points regardless of clinical progression of disease in individual animals. Sample collection schemes were predetermined and standardized with minor variation among individual animals, based on the expected stage of disease at the time of euthanasia (Table 1). A maximum of 40 anatomically distinct tissue specimens were collected per animal. Both steers euthanized at 3 hpa had more FMDV RNA–positive tissues in the nasopharyngeal/laryngeal (NP/L) sites (6 of 12 tissues; 50.0%) than in other anatomic regions (2 of 18 pulmonary tissues; 11.1%) (Table 1). At this time point, FMDV RNA quantities were generally low, and no tissues contained infectious virus. The 2 highest quantities of FMDV RNA were detected in caudal dorsal soft palate (2.92 RNA/mg) and caudal dorsal nasopharynx (2.95 RNA/mg) of steer No. 2.

From 6 to 12 hpa, within the NP/L sites there was greater quantity of tissues positive for infectious FMDV (14 of 24; 58.3%) and viral RNA (13 of 24; 54.2%) relative to all other anatomic regions; at 12 hpa, every NP/L tissue examined was positive by VI, rRT-PCR, or both. Within this period, rRT-PCR and VI positivity percentages for pulmonary specimens were also increasing but to a lesser extent than that of NP/L tissues. At the individual tissue-specific level, the greatest quantities of FMDV RNA between 6 and 12 hpa were detected in distal cranial lung (5.12 RNA/mg) and caudodorsal nasopharynx (4.9 RNA/mg) of steer No. 7 (12 hpa).

At 24 hpa, 97.2% of NP/L samples (35 of 36 at tissue level) were positive for either FMDV RNA or infectious virus, with 72.2% double positive (VI and rRT-PCR). By contrast, 61.1% of pulmonary specimens (22 of 36 at tissue level) were VI or rRT-PCR positive, with 36.1% double positivity. The highest quantity of FMDV RNA at 24 hpa (7.3 RNA/mg) was detected within the rostral dorsal soft palate of steer No. 9. The only positive findings (rRT-PCR or VI) from lymph nodes of previremic steers in the study were the hilar lymph node of steer No. 11 and the medial retropharyngeal lymph node of steer No. 12, which were VI positive at 24 hpa.

Both steers euthanized at 48 hpa were viremic at the time of euthanasia; as such, infectious FMDV and FMDV RNA detected in the tissues of these animals may have been present within and/or exterior to blood vessels in these tissues. Viral

load was substantially decreased in the NP/L sites at 48 hpa relative to 24 hpa, with 66.6% positive by VI or rRT-PCR (8 of 12 tissues) and 33.3% double positive. By contrast, VI or rRT-PCR positivity of the lungs from 48-hpa steers was increased relative to 24 hpa, with 77.8% single positive (14 of 18 tissues) and 27.8% double positive. The greatest quantity of FMDV RNA detected in these animals was from the interdigital clefts of both steers (7.70 and 7.96 RNA/mg) and the lingual torus of steer No. 15 (6.19 RNA/mg), all of which had grossly detected vesicles. Among nonlesional tissues collected from the 48 hpa steers, the greatest quantity of FMDV RNA was obtained from the distal anterior lung of steer No. 15 (5.54 RNA/mg).

Given that the primary goal of these experiments was to characterize the involvement of various tissues as primary replication sites of FMDV, greater attention was focused on the animals that had VI-negative sera at the time of euthanasia (Table 1). For these animals (all except steer Nos. 13–16), tissue-specific cumulative positivity percentages (PPs) were calculated for each tissue for rRT-PCR, VI, and both. PP was defined as follows:

total positive results at tissue X by modality Y in previremic steers / total specimens of tissue X examined by modality Y in previremic steers.

Thus, PP served as an indicator of the relative frequency of involvement of each tissue in previremic FMD in these animals. The PP index demonstrated that among previremic animals, the specimens most frequently positive for infectious FMDV or FMDV RNA were the tissues of the NP/L sites. Specifically, the only 100% PP value occurred for rRT-PCR or VI positivity in rostrodorsal nasopharynx. The next-highest PP values (81.8%) were achieved in only caudodorsal soft palate and caudodorsal nasopharynx. Overall, 15 of 18 PP values from NP/L sites were greater than all PPs from other tissues. PP values from lung and ventral soft palate indicate lesser consistency of FMDV positivity relative to NP/L sites. PP values from lymphoid tissues were uniformly low, with lingual tonsil having the highest overall PP in this tissue category.

Microscopic Localization of FMDV Antigens and Phenotypic Characterizations of Associated Cells

Inoculation to 12 hpa. Despite numerous attempts, FMDV antigens could not be microscopically (immunohistochemically) identified in any of the rRT-PCR-positive tissues from the steers euthanized at 3 hpa. The earliest time point at which viral antigens were localized in situ was at 6 hpa, within the rostrodorsal nasopharynx of both steers (Nos. 4 and 5) euthanized at this time point. Viral antigens were not localized in any other tissues from these animals despite screening of more than 100 additional IHC slides from pulmonary and pharyngeal sites that were rRT-PCR or VI positive. In both steers, FMDV capsid antigen was similarly localized to microscopic epithelial crypts of the follicle-associated epithelium (FAE) overlying pharyngeal mucosa–associated lymphoid tissue (PALT; Figs. 2, 3). Although the epithelial crypts were vaguely discernable by IHC-light microscopy (Fig. 2), the MIF examination of a serial section clearly demonstrated that FMDV in these regions was intraepithelial rather than within subjacent lymphoid tissue (Fig. 3A). Furthermore, simultaneous labeling with CD11c and MHCII indicated that the FAE and subjacent lymphoid regions had diffuse distribution of cells positive for both these antigens individually and as CD11c–MHCII double positives (presumptive dendritic cells [DCs]); Fig. 3B–3D). Despite the presence of DCs in close proximity to FMDV antigens, virus colocalized exclusively with CK in these tissues. Individual cells containing FMDV antigens were rarely identified in the subepithelial dome region immediately subjacent to antigen-positive crypts (not shown); however, phenotypic characterization of these cells with various markers was not achieved.

At 12 hpa, the distribution of viral antigens in the nasopharynx was similar to that observed at 6 hpa with the exception that there was slightly greater intimacy of association between FMDV antigens and the DC markers CD11c and MHCII (not shown). However, colocalization of FMDV antigens with DC markers was not observed. The lungs of both steers euthanized at 12 hpa (Nos. 6, 7) had regional anti-FMDV immunoreactivity (Figs. 4–7). Steer No. 7 had numerous FMDV capsid and nonstructural antigen–positive cells within the distal segment of the cranial lung lobe (Figs. 5–7). In this animal, there were 2 distinct morphological variants of immunopositive cells when viewed by light microscopy: a squamous cell type associated with alveolar septa (type I pneumocyte; Fig. 5, Insert A), and a polygonal cell type variably associated with alveolar septa or lumina (type II pneumocyte or alveolar macrophage; Fig. 5, Insert B). MIF labeling of this tissue indicated that both morphologic categories of FMDV-positive cells were additionally CK positive (Figs. 6A, 7), von Willebrand factor (vWF) negative (Fig. 7), vimentin negative (Fig. 6B), confirming that infected cells were of epithelial histogenesis. However, throughout the alveolar parenchyma, vWF- and vimentin-positive cells were ubiquitously interspersed with CK-positive pneumocytes (Figs. 6B, 7). The other steer euthanized at 12 hpa (No. 6) had antigenically and morphologically distinct pulmonary viral distribution. The distal segment of the middle lung lobe of this animal had a single, small focus of immunopositivity for FMDV 3D protein (Fig. 4), which was negative for capsid antigens (not shown). Unlike steer No. 7, FMDV-positive cells in this region were exclusively squamous.

Twenty-four hpa. At 24 hpa, nasopharyngeal tissues had some of the same qualities described at 6 and 12 hpa but with variations. Viral immunopositivity was similarly localized to FAE of PALT regions but was less associated with crypt regions. Rather, FAE overlying large, expansive, cryptless regions were more commonly affected (Figs. 8–12). In such areas there were substantially greater quantities of FMDV-positive cells within the epithelium (Figs. 8–9) and the superficial and deep subepithelium (Figs. 9–12) relative to earlier time points. These cells were often positive for FMDV structural and nonstructural proteins (Fig. 12). Within subepithelial lymphoid

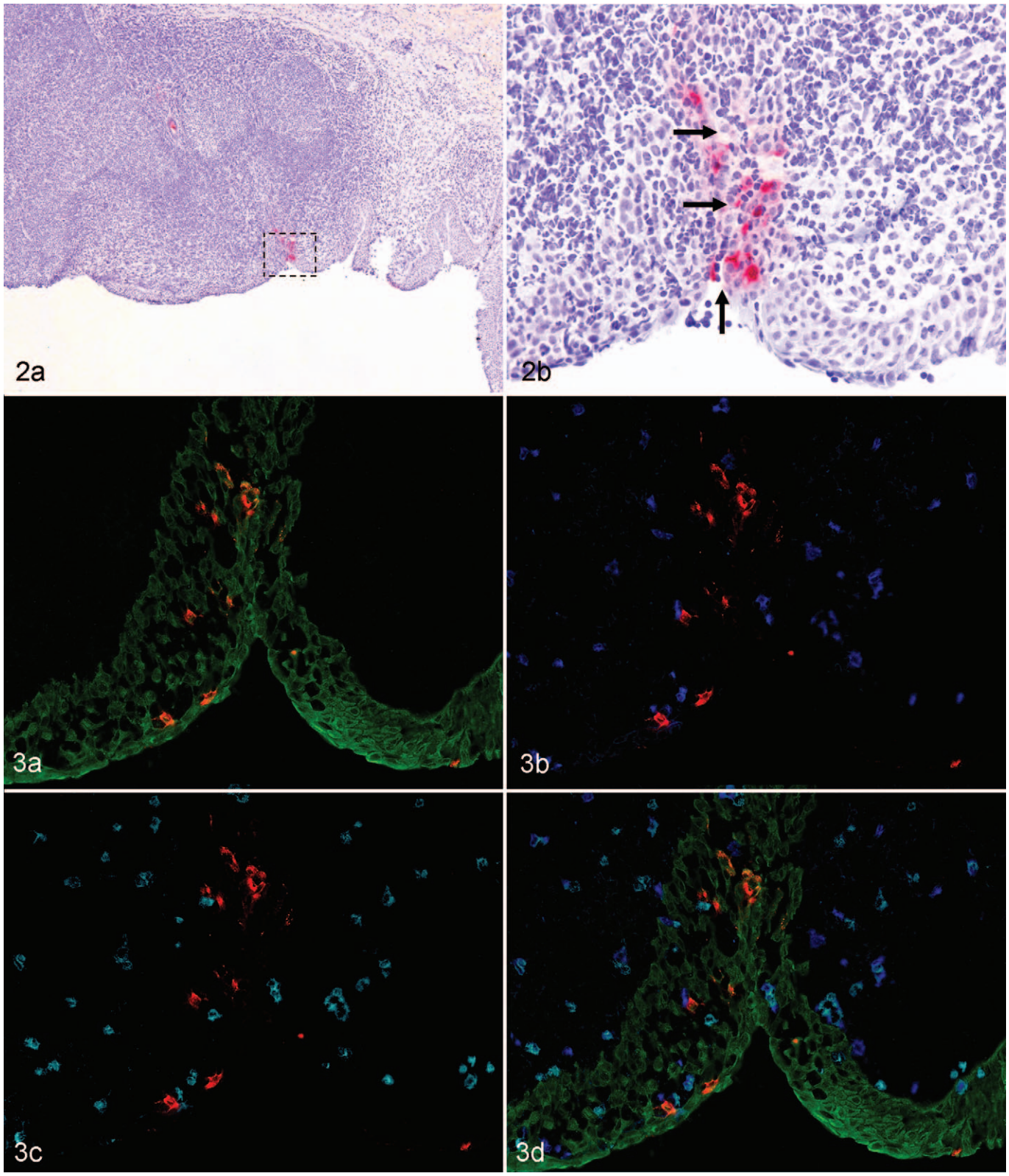

Figure 2. Rostrodorsal nasopharynx, steer No. 4. A, Immunohistochemical localization of FMDV to epithelial crypt of mucosa-associated lymphoid tissue. Anti-FMDV capsid monoclonal antibody. Micropolymer alkaline phosphatase. Gill s hematoxylin counterstain. B, higher magnification of region of interest from Figure 2A. FMDV antigens localize to crypt epithelium subjacent to crypt lumen (arrows). Anti-FMDV capsid monoclonal antibody. Micropolymer alkaline phosphatase. Gill s hematoxylin counterstain. **Figure 3.** Rostrodorsal nasopharynx, steer

regions, small quantities of FMDV structural and nonstructural protein–positive cells had morphologic and phenotypic (CK–, MHCII+, CD11c+) characteristics of DCs (Figs. 9–12). Additionally, concurrent labeling with anti-vWF antibody indicated that within lymphoid follicles, FMDV-positive DCs were occasionally present within 50 μm of capillary endothelia, but direct interaction between DCs and vascular cells was not observed in these areas. Microvesiculation (Figs. 8, 9) and erosion (Figs. 8–11A) of nasopharyngeal FAE were rarely observed; in such regions, capillary endothelia (vWF-positive cells) were present within the disrupted epithelium immediately adjacent to FMDV-positive epithelial cells and DCs (Figs. 8, 9). Intraepithelial vWF-positive cells were not observed in regions lacking erosion, suggesting that this was a response to viral disruption of epithelial integrity.

Compared to those at 12 hpa, the lungs at 24 hpa had more foci of immunopositive cells with a morphologic trend toward a greater quantity of polygonal versus squamous epithelial cell positivity (Fig. 13). Additionally, the CK/FMDV double-positive polygonal cells were often free within alveolar lumina with deterioration of surrounding CK architecture.

Forty-eight hpa. At 48 hpa there was a marked decrease of detection of FMDV immunopositive cells in the nasopharynx. Individual, and small clusters of, antigen-positive cells were present within the strata basale and spinosum of NP/L epithelia and lamina propria with no apparent predilection for FAE regions. A single cluster of FMDV-positive cells within the epiglottal epithelium of steer No. 14 was suggestive of a microvesicle. This steer was the only animal in which FMDV antigens were identified within the palatine tonsil (not shown).

In contrast to the lesser quantity of FMDV antigens localized to the upper respiratory tract (relative to steer euthanized at 6–24 hpa), at 48 hpa there was substantially increased quantity of structural and nonstructural FMDV antigens in pulmonary samples with multifocal, coalescing distribution (Figs. 14, 15). Several tissues had regionally extensive fields spanning up to 2.0 mm of FMDV antigen-positive cells within alveolar parenchyma. Within these regions, alveolar septa were expanded by infiltrates of mixed leukocytes and proteinaceous material (fibrin). Cells containing FMDV antigens were round to polygonal with eccentric nuclei and were more frequently free within alveolar lumina or loosely associated with alveolar septa when examined by IHC-light microscopy (Fig. 14). However, when examined by MIF, these cells were nearly exclusively strongly CK positive (Fig. 15). In these regions there were well-demarcated transitions from the normal CK latticework pattern in regions lacking FMDV positivity to disorganized CK clumping and dissociation of cells from septa in virus-positive regions. The pattern of MIF labelings also revealed that a subpopulation of FMDV-positive cells had somewhat greater association with alveolar septa than that detectable by light microscopy. Labelings for vimentin and vWF suggested that theses markers were present in a more normal architecture relative to the deterioration of the CK (pneumocytes) pattern. FMDV/CK double-positive cells were often directly adjacent to vWF-positive capillary endothelia (Fig. 15B). Overall, the pattern had strong similarities to the acantholytic degeneration seen in FMD vesicles.

Discussion

In considering the early pathogenesis of FMD in any species, 2 critical issues have substantial translational relevance to the development of vaccines and biotherapeutics. Identifying the primary site (or sites) of infection is foremost because blocking these sites is the only method of achieving complete sterile protection. Identifying the mechanism of the establishment of viremia is secondary but still substantial. In most cases, blocking (or impairing) this process would substantially decrease shedding, transmission, and severity of clinical signs. Previous investigations of the early pathogenesis of FMD in cattle have independently implicated the nasopharynx[7,15] and the lungs[4,6,10] as sites of primary infection. A single study indicated that upper or lower respiratory tract can similarly serve as sites of primary infection and portals for systemic generalization of FMD.[24] Recent reviews have suggested that subsequent to natural aerosol exposure, FMDV replicates in the pharynx and establishes viremia by draining through the lymphatic system, but after experimental aerosol inoculation, viremia is established directly through the lungs.[1,2] However, the primary experimental basis for these claims is not entirely clear. Another pathogenesis study implicated the nasal mucosa as the site of primary infection.[14] Overall, the published literature does not provide enough information to allow a clear interpretation of the critical virus–host interactions associated with early FMDV infection of cattle.

The current study provides a more thorough description of the early events of experimental FMD in cattle than that previously published. Additionally, the use of a controlled aerosol inoculation system has allowed a consistently repeatable method of exposure to virus while preserving the natural route of infection; high-throughput techniques have facilitated

Figure (continued). No. 4. A, multichannel immunofluorescence (MIF) of serial section of region of interest identified in Figure 2A. Colocalization (orange) of FMDV capsid antigens (red) with pancytokeratin-positive (green) crypt epithelial cells. Anti-FMDV capsid and anti-pancytokeratin monoclonal antibodies. B, simultaneous MIF of specimen in Figure 3A. MHCII-positive (blue) cells in close proximity to but not colocalized with FMDV capsid (red) antigen. Anti-FMDV capsid and anti-MHCII monoclonal antibodies. C, simultaneous MIF of specimen in Figure 3A and 3B. CD11c-positive (aqua) cells in close proximity to but not colocalized with FMDV capsid (red) antigens. Anti-FMDV capsid and anti-CD11c monoclonal antibodies. D, merge of simultaneous MIF images from Figure 3A to 3C. Intraepithelial MHCII-positive (blue) and CD11c-positive (aqua) cells (presumptive dendritic cells) are in close proximity to FMDV/pancytokeratin double-positive cells. Anti-FMDV capsid, anti-pancytokeratin, anti-CD11c, and anti-MHCII monoclonal antibodies

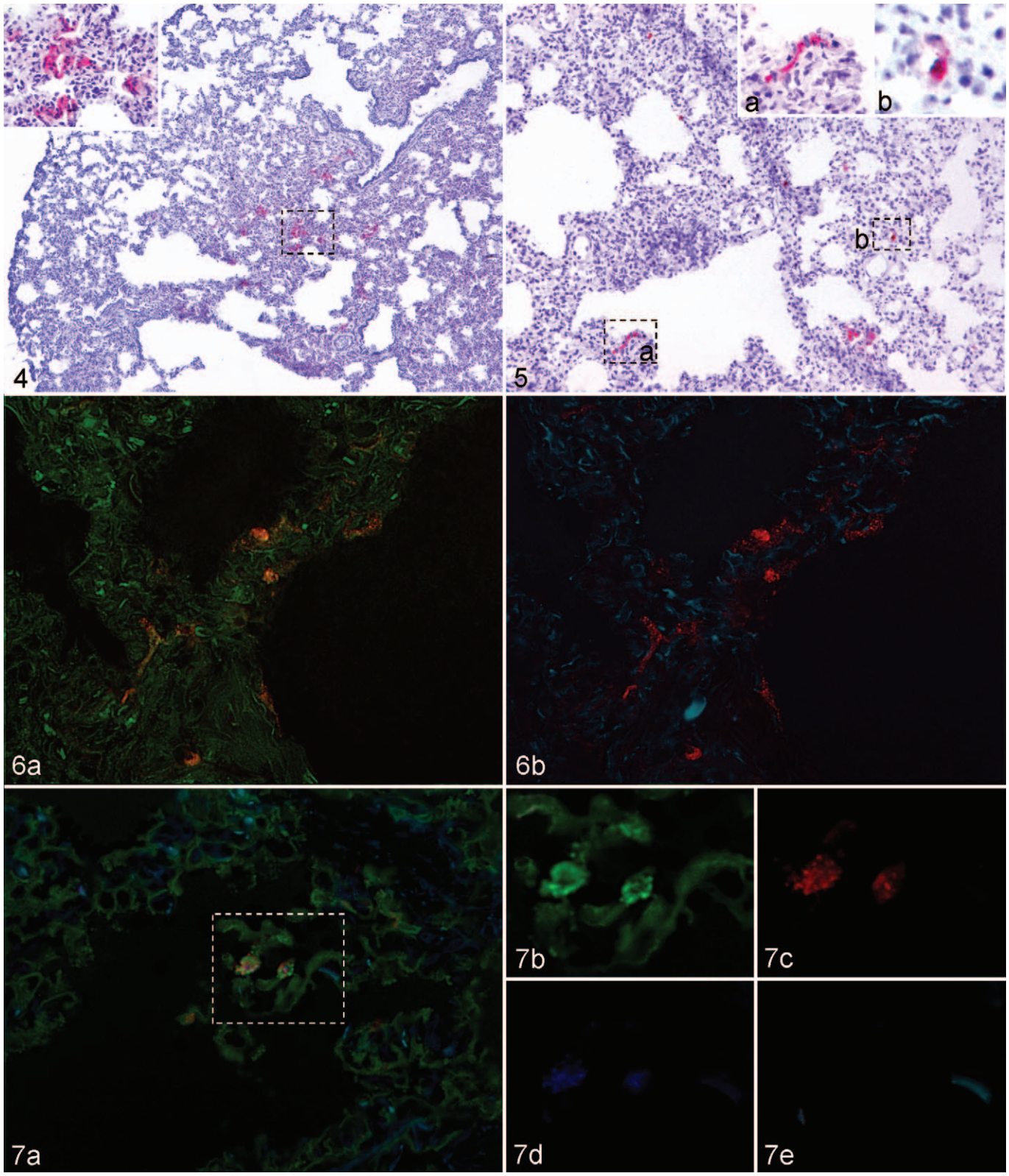

Figure 4. Distal middle lung lobe, steer No. 6. Focal region of anti-FMDV immunoreactivity with localization of antigen exclusively to alveolar septa (insert). AntiFMDV 3D protein monoclonal antibody. Micropolymer alkaline phosphatase. Gill s hematoxylin counterstain. **Figure 5.** Distal cranial lung lobe, steer No. 7. Immunohistochemical localization of FMDV antigen to squamous cells of alveolar septa (Insert A) and polygonal cells of alveolar lumina (Insert B). Anti-FMDV capsid monoclonal antibody. Micropolymer alkaline phosphatase. Gill s hematoxylin counterstain. **Figure 6.** A, Distal cranial lung lobe, steer No. 7. Multichannel immunofluorescence of serial section of tissue shown in Figure 5. Colocalization

screening of numerous tissues per animal and has thus provided a highly detailed mapping of FMDV distribution.

Screening of tissues and swab specimens by rRT-PCR and VI indicated that there are tissue-specific temporal trends regarding distribution of FMDV and viral RNA subsequent to aerosol inoculation. The period of 3 to 12 hpa was generally dominated by amplification of virus in the nasopharyngeal/laryngeal (NP/L) tissues, with a trend toward progressively higher levels of viral RNA and greater prevalence of VI positivity over time. Similarly, within the period of 4 to 12 hours, FMDV RNA detection from nasal swabs was increasing toward the first of 2 peaks. The temporal coincidence of these trends suggests that the RNA in nasal swabs in this period originated from FMDV replication in the NP/L tissues. At 24 hpa, FMDV and viral RNA were increasingly abundant in the pulmonary tissues, with minimal change in the NP/L sites indicating pan–respiratory distribution of virus associated with numerous foci of replication in both upper and lower respiratory tract. However, at 48 hpa, detection of FMDV by both screening tests was decreasing in NP/L tissues, with further increase in the lungs. This coincided with the onset of viremia and the approach to the second peak in nasal swab RNA detection. Interpretation of the 2 peaks of the nasal swab FMDV RNA detection curve in the context of the tissue-specific rRT-PCR data suggests that there are distinct pharyngeal and pulmonary phases of FMDV release into the respiratory tract. Overall, the tissue-specific prevalence values for all previremic animals collectively indicates NP/L sites as the most important sites of primary FMDV infection.

The rRT-PCR and VI data indicate that subsequent to aerosol inoculation, virus inoculum was distributed throughout the entire respiratory tract; yet, immunolocalization of FMDV antigens indicated that primary infection was limited to specific regions of the nasopharynx and, somewhat later, the lungs. At early time points, tissues that were positive for FMDV by VI or rRT-PCR but IHC–MIF negative were interpreted as having virus or viral RNA on their superficial surfaces but not active infection and replication. Thus, VI and rRT-PCR served as screening tests for infection at the tissue and cellular level (high sensitivity), whereas IHC–MIF functioned as a confirmatory procedures (high specificity). In the present study, the overall success of this screening and confirmation approach provided adequate efficacy of FMDV localization.

The similar localization of FMDV antigens to the lymphoid FAE of PALT crypts of the rostrodorsal nasopharynx in both steers euthanized at 6 hpa demonstrated the importance of this region in the establishment of primary infection. The colocalization of FMDV antigens with CK and lack of colocalization with MHCII or CD11c in these tissues demonstrated that the first cells infected with FMDV are of epithelial origin. This is the first microscopic documentation of localization of FMDV to the respiratory tract of any aerogenously infected animal earlier than 24 hpa. Two previous works have demonstrated nasopharyngeal intraepithelial FMDV RNA in cattle by in situ hybridization at 5 days after contact exposure;[20,26] however, at this later phase of infection, it is impossible to separate primary aerogenous from secondary hematogenous infection. The exclusive infection of PALT FAE cells in the context of pan–respiratory exposure to virus suggests that there are specific, intrinsic qualities of these cells that make them highly susceptible to infection. The caudal segment of the dorsal soft palate is anatomically aligned with the rostral dorsal nasopharynx, and these 2 tissues were determined to be largely similar morphologically, phenotypically, and with regard to FMD pathogenesis within this study. The laryngeal tissues (epiglottis and larynx) are morphologically similar to the nasopharyngeal sites but with less mucosa-associated lymphoid tissue, which might explain the slightly decreased detection of virus in the former.

Although the nature of the susceptibility of the NP/L tissues remains elusive, possibilities include cell-specific expression of virus-specific receptors (αV integrins or other) and expression of other presently unidentified cellular factors by the susceptible cells or by other cells in the immediate microenvironment. Although αVβ6 and αVβ3 expression has been characterized in these tissues from uninfected cattle,[16,17] simultaneous localization with FMDV has not been described. The nearly diffuse epithelial distribution of αVβ6 described in one study[17] combined with the multifocal distribution of primary FMDV infection (current work) suggests that the expression of integrins does not solely dictate cellular susceptibility to infection.

The FAE is an extremely active epithelium, and candidate cells that might affect the microenvironment include intraepithelial DCs, lymphocytes, and natural killer cells. Similarly, M cells in these regions may directly facilitate infection by providing nonspecific portals for entry of virus into the host via pinocytosis. Morphologic and phenotypic characterization of bovine PALT has indicated that such cells are present in the FAE to varying extents in FMDV-infected cattle and in the resting (naïve) state (J.A., unpublished data). Additionally, physical characteristics of the FAE crypts may influence susceptibility to infection; it is possible that pooling of secretions in these regions allows increased time for adsorption of virions

Figure (continued). (orange) of FMDV capsid antigens (red) with pancytokeratin-positive (green) cells of alveolar septa. Anti-FMDV capsid and anti-pancytokeratin monoclonal antibodies. B, cranial lung lobe, steer No. 7. Simultaneous multichannel immunofluorescence of specimen in Figure 6A. Vimentin positive (blue) cells in close proximity to but not colocalized with FMDV capsid antigen (red). Anti-FMDV capsid and anti-vimentin monoclonal antibodies. **Figure 7.** A, Distal cranial lung lobe, steer No. 7. Multichannel immunofluorescence of serial section of tissue shown in Figures 5 and 6. Triple colocalization of FMDV capsid (red) and FMDV3D protein (blue) antigens with cytokeratin (green) in pneumocytes. Von Willebrand factor positive capillary endothelial cells (aqua) are interspersed with pneumocytes and are negative for both FMDV antigens. B-E, higher-magnification single-channel views of region of interest identified in Figure 7A; individual channels: B, cytokeratin (green); C, FMDV capsid (red); D, FMDV 3D polymerase (blue); E, von Willebrand factor (aqua).

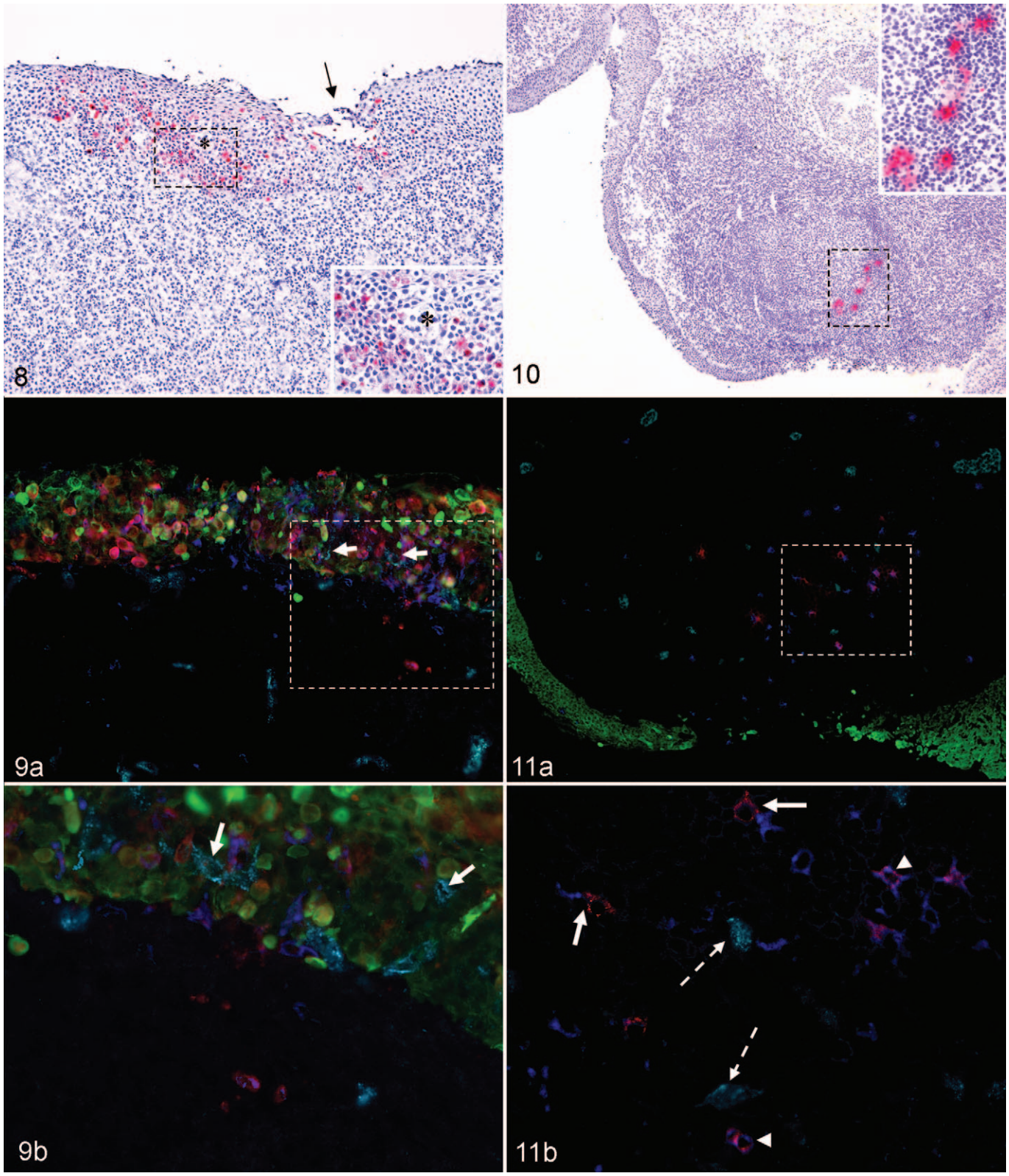

Figure 8. Caudodorsal soft palate, steer No. 11. Transepithelial immunohistochemical localization of FMDV to mucosa-associated lymphoid tissue epithelium and superficial lamina propria in a region of microvesiculation (*) and erosion (arrow). Anti-FMDV capsid monoclonal antibody. Micropolymer alkaline phosphatase. Gill s hematoxylin counterstain. **Figure 9.** A, Multichannel immunofluorescence of serial section of specimen in Figure 8. Intraepithelial and subepithelial colocalization (purple) of FMDV capsid antigens (red) with MHCII (blue) positive, presumptive dendritic cells. Colocalization (orange) of FMDV capsid antigens (red) with cytokeratin-positive (green) epithelial cells. Von

and thus increases efficiency of infection in a highly localized manner. Current efforts in our laboratory are directed toward investigating these mechanisms.

Determining the role of the lungs in early infection was less straightforward. Although viral RNA was detectable in pulmonary tissues at 3 hpa and infectious virus at 6 hpa (similar to NP/L sites), the prevalence of VI- and rRT-PCR-positive samples was low at these time points compared to that in the NP/L sites; additionally, viral antigens could not be detected in lungs until 12 hpa (ie, 6 hours later than the nasopharynx). At least 2 hypotheses are supported by this contrast in the data describing processes in the NP/L sites and lung. It is possible that the viral RNA and infectious virus detected in the lungs before 12 hpa represent foci that were in the process of establishing primary infection independent of infection of the nasopharynx but with a relative lag (eclipse) period. Alternatively, it is possible that primary infection of the NP/L sites serves as a requisite phase in the establishment of pulmonary infection presumably by dose amplification of inoculated virus. In this scenario, the nasopharyngeally amplified virus would serve as an endogenously generated secondary aerosol delivered to the lungs via normal respiration. It is also possible that under conditions of natural exposure (ie, direct or indirect contact), both infection scenarios are relevant with contributory roles determined by viral dose, aerosol droplet size, and various aspects of virus host interactions.

Regardless of the contributory roles of lungs versus nasopharynx in the early pathogenesis of FMD in cattle, it is clear that the pulmonary epithelia are permissive to FMDV replication. Our trimodal identification of FMDV in distal lung segments of both steers euthanized at 12 hpa (previremic) indicates the consistent role of the lungs in the early progression of FMD. This is consistent with previous works that localized FMDV RNA to alveolar septa in previremic FMD in aerosol inoculated cattle.[4,6] In the present study, the morphologic localization of FMDV to alveolar septa combined with exclusive colocalization with CK in these regions suggests that pneumocytes are the most relevant cells supporting viral replication in the lungs. The morphologic variation of FMDV-positive cells (squamous versus polygonal) seen in the lungs of steer No. 7 likely represents a temporal and pathologic continuum with the squamous variant (type I pneumocyte) representative of early cellular infection that progresses to infection of cells with polygonal morphology (type II pneumocytes). Thus, the single, small (type I pneumocyte morphology) focus of anti-FMDV immunopositivity in middle lung lobe of steer No. 6 (Fig. 4) is interpreted as an earlier stage relative to cranial lung specimen of steer No. 7 (Figs. 5–7). This concept is further supported by the increasing abundance of FMDV-immunopositive type II pnuemocytes at 24 and 48 hpa and by "conventional wisdom" on the subject of responses to insults by pulmonary epithelia.[9] At 12 hpa, colocalization of FMDV antigens and CK was rarely identified within terminal bronchiolar epithelia, indicating that these cells are also susceptible to infection but with apparently lesser efficiency compared to pneumocytes.

The question of how viremia is established in FMD has substantial implications for ongoing and future development of FMD prophylaxis. It has been suggested that in bovine FMD, the mechanism of the establishment of viremia is that virus drains from the pharynx to the regional lymph nodes from which viremia is established.[1,2] In the present study, the lack of detection of FMDV or viral RNA in lymph nodes draining the respiratory tract and oral cavity in the previremic and early viremic phases of FMD suggests that this is not the route of establishment of viremia within the current work's experimental conditions. A specific region's ability to serve as a portal for establishment of viremia depends on local presence of virus in immediate proximity to blood vessels and on a competent mechanism of movement of virions from the extravascular to intravascular space. The transfer mechanism is a complex subject that was not addressed by the current study but likely involves several molecular and cellular recognition events. However, in the current work, the requirement for intimate association of FMDV and blood vessels was shown to be met in previremic animals in tissues of the nasopharynx and lungs.

As early as 12 hpa, FMDV-positive type I pneumocytes were present within alveolar septa that contained abundant vWF- and vimentin-positive cells (ie, capillary endothelia). This suggests that in the lungs, FMDV would have a high likelihood of gaining access to the vasculature. However, at 24 hpa,

Figure (continued). Willebrand antigenpositive (aqua) capillary endothelial cells are present within epithelium (arrows) and lamina propria in close proximity to FMDV-positive cells. Anti-FMDV capsid, anti-MHCII, antivon Willebrand antigen, and anti-pancytokeratin monoclonal antibodies. B, Higher magnification of region of interest identified in Figure 9A, multichannel immunofluorescence of serial section of specimen in Figure 8. Von Willebrand antigenpositive (aqua) capillary endothelial cells are present within epithelium (arrows) and lamina propria in close proximity to FMDV-positive cells. FMDV/MHCII individual and double-positive cells are present within subepithelial lymphoid region. Anti-FMDV capsid, anti-MHCII, antivon Willebrand antigen, and anti-pancytokeratin monoclonal antibodies. **Figure 10.** Rostrodorsal nasopharynx, steer No. 12. Immunohistochemical localization of FMDV to lymphoid follicular dark zone of mucosa-associated lymphoid tissue. Anti-FMDV capsid monoclonal antibody. Micropolymer alkaline phosphatase. Gill s hematoxylin counterstain. **Figure 11.** A, Multichannel immunofluorescence of serial section of specimen in Fig. 10. Colocalization (purple) of FMDV capsid antigens (red) with MHCII-positive (blue) dendritic cells. FMDV does not colocalize with cytokeratin (green) or von Willebrand antigen (aqua). Anti-FMDV capsid, anti-MHCII, antivon Willebrand antigen, and anti-bovine cytokeratin monoclonal antibodies. B, Higher magnification of region of interest identified in Figure 11A. Multichannel immunofluorescence of serial section of specimen in Figure 10. Within a lymphoid follicle, FMDV antigens (red) are in close proximity to (arrows) and colocalize with (purple; arrowheads) MHCII-positive (blue) cells. FMDV does not colocalize with von Willebrand antigenpositive (aqua) endothelial cells (broken arrows). Anti-FMDV capsid, anti-MHCII, antivon Willebrand antigen, and anti-pancytokeratin monoclonal antibodies.

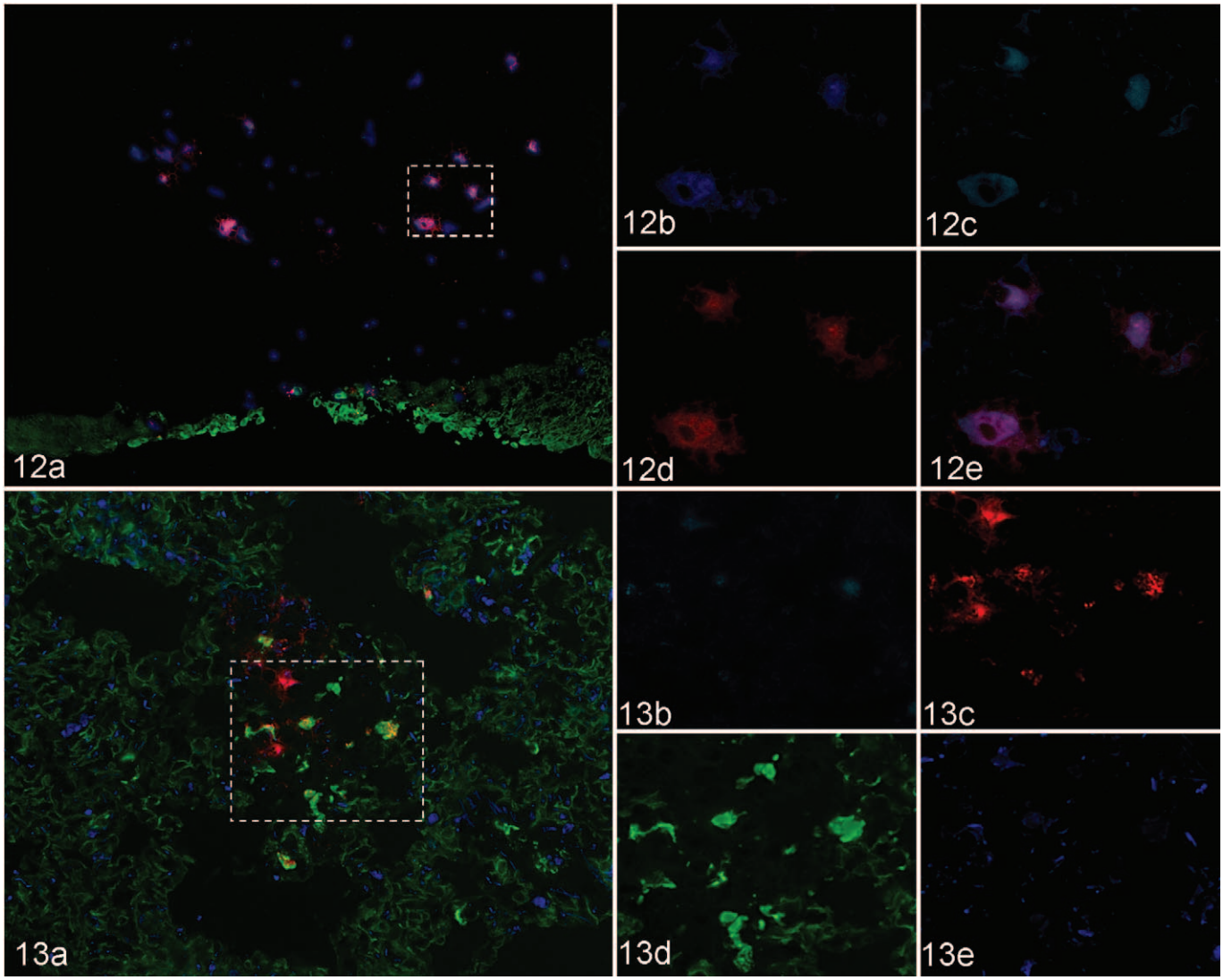

Figure 12. A, rostrodorsal nasopharynx, steer No. 12. Multichannel immunofluorescence of serial section of specimen in Figures 10 and 11. Triple colocalization (pink) of FMDV capsid antigen (red), FMDV 3D polymerase antigen (aqua), and CD11c (blue) in dendritic cells. Surface epithelium is cytokeratin positive (green). Anti-FMDV capsid, anti-FMDV 3D polymerase, anti-CD11c, and anti-pancytokeratin monoclonal antibodies. B-E, Higher-magnification, single-channel views of region of interest identified in Figure 12A: B, CD11c (blue); C, FMDV 3D polymerase (aqua); D, FMDV capsid (red); E, 4-channel merge. **Figure 13.** A, caudal lung lobe, steer No. 13. Multichannel immunofluorescence. Triple colocalization (yellow) of FMDV capsid antigen (red), FMDV 3D polymerase antigen (aqua), and cytokeratin (green) in degenerating (acantholytic) pneumocytes. Von Willebrand factor antigenpositive endothelial cells (blue) are interspersed with pneumocytes. Pneumocyte architecture is disrupted in focus of infection. Anti-FMDV capsid, anti-FMDV 3D polymerase, and anti-pancytokeratin monoclonal antibodies. Antivon Willebrand factor polyclonal antibody. B-E, higher-magnification single-channel views of region of interest identified in the multichannel immunofluorescent image: B, FMDV 3D polymerase (aqua); C, FMDV capsid (red); D, cytokeratin (green); E, von Willebrand factor (blue).

FMDV was also present in close proximity to vWF-positive (endothelial) cells within the PALT epithelium and lamina propria. The intraepithelial capillaries in regions of erosion may represent a neovascular response to ongoing FMDV-induced epithelial injury. Additionally, small caliber intraepithelial blood vessels have been demonstrated within the normal reticular epithelium (FAE) of the bovine palatine tonsil, which has many morphologic and phenotypic similarities to PALT.[19] The possibility that viremia may be established in the PALT is supported by the presence of these vessels associated with FMDV-positive epithelial cells and DCs. Overall, these findings are consistent with the earlier work demonstrating that the lungs or upper respiratory tract may independently serve as portals for systemic dissemination.[24]

An additional, salient consideration regarding the site of establishment of viremia is that in the period in which viremia was established (24–48 hpa), viral load in the NP/L sites was decreasing by all detection methods, whereas in the lungs, virus

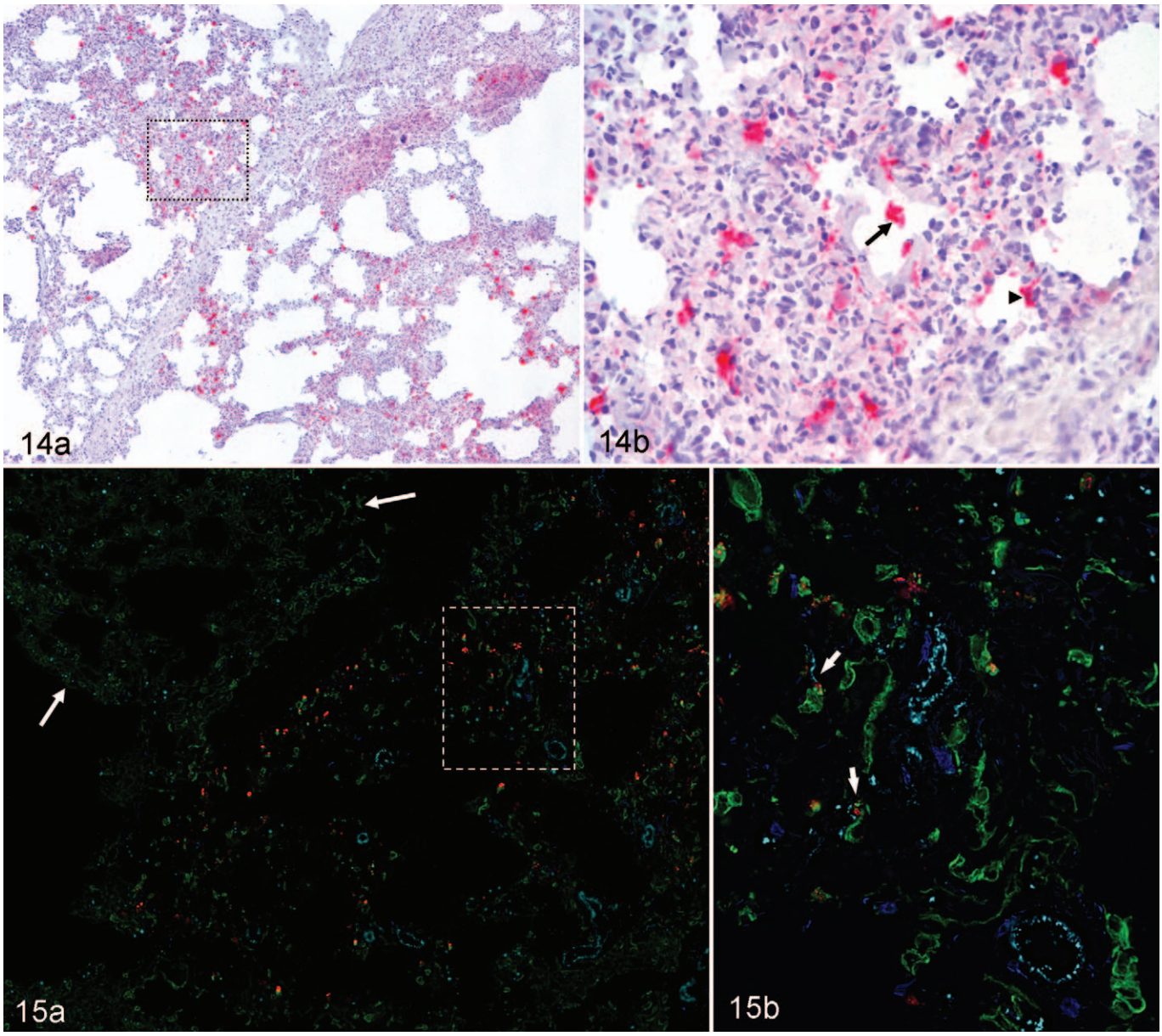

Figure 14. Distal middle lung lobe, steer No, 15. A, regionally extensive distribution of anti-FMDV immunoreactive cells in a region of distortion of alveolar architecture. Anti-FMDV 3D polymerase monoclonal antibody. Micropolymer alkaline phosphatase. Gill s hematoxylin counterstain. B, higher magnification of region of interest identified in Figure 14A. Anti-FMDV immunopositive cells are predominantly free within alveolar lumina (arrow) or adhered to septal walls (arrowhead). Alveolar septa are expanded and infiltrated by mixed leukocytes. Anti-FMDV 3D polymerase monoclonal antibody. Micropolymer alkaline phosphatase. Gill s hematoxylin counterstain. **Figure 15.** Distal middle lung lobe, steer No, 15. A, multichannel immunofluorescence of serial section of specimen in Figure 14. FMDV antigen (red) colocalizes with pancytokeratin-positive (green) cells. Within FMDV/pancytokeratin double-positive cells there is minimal subcellular colocalization. Normal pancytokeratin lattice pattern (between arrows) is extensively disrupted in FMDV-positive region and replaced by clumped pancytokeratin-positive cells with poorly defined intercellular associations. Anti-FMDV capsid, antivon Willebrand antigen, and anti-pancytokeratin monoclonal antibodies. B, higher magnification of region of interest identified in Figure 15A; multichannel immunofluorescence of serial section of specimen in Figure 14A. FMDV/pancytokeratin double-positive cells are in close proximity to von Willebrand factorpositive (aqua) capillaries (arrows) and vessels and MHCII-positive cells (blue). Anti-FMDV capsid, anti-MHCII, antivon Willebrand antigen, and anti-pancytokeratin monoclonal antibodies.

was replicating to high genome copy numbers in cells that are in direct association with capillary endothelia. At the time of establishment of viremia, pulmonary quantities of FMDV, viral RNA, and structural and nonstructural antigens were all increasing. Although these data do not conclusively establish a single responsible anatomic site for the establishment of

FMDV viremia in cattle, interaction between processes in upper and lower respiratory tract regions are likely, and current efforts in our laboratory are directed toward defining the relative contributory roles of these regions.

The FMDV-associated degenerative process observed in the lungs at 48 hpa has many microscopic similarities to the classic acantholytic degeneration described for vesicles caused by FMDV and other pathologic processes;[11,28] however, macroscopic lesions were not detected in the lungs. As is seen with keratinocytes in FMDV vesicles, the pneumocytes swell, lose association with adjacent structures, and dissociate into an expanding cavitary space.[21,28] However, unlike a classic vesicle in which the morphologic characteristics of acantholysis are well defined and recognizable, this pulmonary acantholytic-like degeneration could easily be mistaken for a histiocytic alveolitis. The morphology of the acantholytic pneumocytes is similar to that of alveolar macrophages, and it is only the CK positivity of these cells that confirms their epithelial histogenesis. An additional consideration on this subject is the relationship that this pulmonary process may have to the maintenance of high-titer viremia during acute FMD. Although it has been suggested that sustained FMDV viremia is maintained by viral replication in lesional and/or nonlesional skin,[1,5] this hypothesis has never been thoroughly elucidated. Several factors support the notion that the lungs may be important amplifiers of FMDV and may be responsible for maintaining high titer viremia, including (1) the relatively high FMDV RNA/mg and large quantities of FMDV structural and nonstructural antigens detected in the lungs of viremic cattle in this study, (2) the overall mass of the lungs, and (3) the extensive vascularity of lungs.

In conclusion, the data presented herein support a model for early FMDV infection of aerosol-inoculated cattle that includes the following key events: (1) primary replication in epithelial cells of the PALT crypts and (2) subsequent widespread replication in pneumocytes in the lung, which coincides with (3) the establishment of sustained viremia. Current work in our laboratory is directed toward similar investigation of additional serotypes and strains of FMDV and further elucidation of FMDV–host interactions in the early pathogenesis of FMD.

Acknowledgements

This research was funded by Agricultural Research Service–Current Research Information System project No. 1940-32000-052-00D. We wish to acknowledge Meghan Tucker for superb histotechnological support and Elizabeth Bishop, Ethan Hartwig, and George Smoliga for crucial assistance in collecting and processing samples. We also thank the animal resource unit personnel at the Plum Island Animal Disease Center for their patience and assistance in caring for and collecting samples from experimental animals. We thank Dr Manuel Borca and Dr Fawzi Mohammed for thoughtful review of the article.

Declaration of Conflicting Interests

The authors declared no potential conflicts of interests with respect to the authorship and/or publication of this article.

Funding

The authors are all salaried employees of the US federal government. The research described and the authorship of the manuscript was all conducted within the duties of the authors' job posts. There was no additional support.

References

1. Alexandersen S, Mowat N: Foot-and-mouth disease: host range and pathogenesis. Curr Top Microbiol Immunol **288:**9–42, 2005.
2. Alexandersen S, Zhang Z, Donaldson AI, Garland AJ: The pathogenesis and diagnosis of foot-and-mouth disease. J Comp Pathol **129:**1–36, 2003.
3. Arzt J, Gregg DA, Clavijo A, Rodriguez LL: Optimization of immunohistochemical and fluorescent antibody techniques for localization of foot-and-mouth disease virus in animal tissues. J Vet Diagn Invest **21:**779–792, 2009.
4. Brown CC, Meyer RF, Olander HJ, House C, Mebus CA: A pathogenesis study of foot-and-mouth disease in cattle, using in situ hybridization. Can J Vet Res **56:**189–193, 1992.
5. Brown CC, Olander HJ, Meyer RF: Pathogenesis of foot-and-mouth disease in swine, studied by in-situ hybridization. J Comp Pathol **113:**51–58, 1995.
6. Brown CC, Piccone ME, Mason PW, McKenna TS, Grubman MJ: Pathogenesis of wild-type and leaderless foot-and-mouth disease virus in cattle. J Virol **70:**5638–5641, 1996.
7. Burrows R, Mann JA, Garland AJ, Greig A, Goodridge D: The pathogenesis of natural and simulated natural foot-and-mouth disease infection in cattle. J Comp Pathol **91:**599–609, 1981.
8. Callahan JD, Brown F, Osorio FA, Sur JH, Kramer E, Long GW, Lubroth J, Ellis SJ, Shoulars KS, Gaffney KL, Rock DL, Nelson WM: Use of a portable real-time reverse transcriptase-polymerase chain reaction assay for rapid detection of foot-and-mouth disease virus. J Am Vet Med Assoc **220:**1636–1642, 2002.
9. Caswell J, Williams K. The respiratory system *In*: Jubb, Kennedy & Palmer's Pathology of Domestic Animals, ed. Maxie MG, 5th ed., pp. 523–653. Saunders, St. Louis, MO, 2007.
10. Eskildsen M: Experimental pulmonary infection of cattle with foot-and-mouth disease virus. Nord Vet Med **21:**86–91, 1969.
11. Frenkel HS: Histologic changes in explanted bovine epithelial tongue tissue infected with the virus of foot-and-mouth disease. Am J Vet Res **10:**142–145, 1949.
12. Golde WT, Pacheco JM, Duque H, Doel T, Penfold B, Ferman GS, Gregg DR, Rodriguez LL: Vaccination against foot-and-mouth disease virus confers complete clinical protection in 7 days and partial protection in 4 days: use in emergency outbreak response. Vaccine **23:**5775–5782, 2005.
13. Grubman MJ, Baxt B: Foot-and-mouth disease. Clin Microbiol Rev **17:**465–493, 2004.
14. Korn G: Experimentelle untersuchungen zum virusnachweis im inkubationsstadium der maul-und klauenseuche und zu ihrer pathogenese. Arch Exp Veterinarmed **11:**637–649, 1957.
15. McVicar JW, Graves JH, Sutmoller P: Growth of foot-and-mouth disease virus in the bovine pharynx. *In*: Proceedings of the 74th Annual Meeting of the United States Animal Health Association, pp. 230–234. United States Animal Health Association, St. Joseph, MO, 1970.

16. Monaghan P, Gold S, Simpson J, Zhang Z, Weinreb PH, Violette SM, Alexandersen S, Jackson T: The alpha(v)beta6 integrin receptor for foot-and-mouth disease virus is expressed constitutively on the epithelial cells targeted in cattle. J Gen Virol **86:**2769–2780, 2005.
17. O'Donnell V, Pacheco JM, Gregg D, Baxt B: Analysis of foot-and-mouth disease virus integrin receptor expression in tissues from naive and infected cattle. J Comp Pathol **141:**98–112, 2009.
18. Pacheco JM, Arzt J, Rodriguez LL: Early events in the pathogenesis of foot-and-mouth disease in cattle after controlled aerosol exposure. Vet J **183:**46–53, 2008.
19. Palmer MV, Thacker TC, Waters WR: Histology, immunohistochemistry and ultrastructure of the bovine palatine tonsil with special emphasis on reticular epithelium. Vet Immunol Immunopathol **127:**277–285, 2009.
20. Prato Murphy ML, Forsyth MA, Belsham GJ, Salt JS: Localization of foot-and-mouth disease virus RNA by in situ hybridization within bovine tissues. Virus Res **62:**67–76, 1999.
21. Seibold HR: A revised concept of the lingual lesions in cattle with foot-and-mouth disease. Am J Vet Res **24:**1123–1130, 1963.
22. Sellers RF, Parker J: Airborne excretion of foot-and-mouth disease virus. J Hyg (Lond) **67:**671–677, 1969.
23. Stave JW, Card JL, Morgan DO: Analysis of foot-and-mouth disease virus type O1 Brugge neutralization epitopes using monoclonal antibodies. J Gen Virol **67:**2083–2092, 1986.
24. Sutmoller P, McVicar JW: Pathogenesis of foot-and-mouth disease: the lung as an additional portal of entry of the virus. J Hyg (Lond) **77:**235–243, 1976.
25. Swaney LM: A continuous bovine kidney cell line for routine assays of foot-and-mouth disease virus. Vet Microbiol **18:**1–14, 1988.
26. Woodbury EL, Ilott MC, Brown CC, Salt JS: Optimization of an in situ hybridization technique for the detection of foot-and-mouth disease virus in bovine tissues using the digoxigenin system. J Virol Methods **51:**89–93, 1995.
27. Yang M, Clavijo A, Li M, Hole K, Holland H, Wang H, Deng MY: Identification of a major antibody binding epitope in the non-structural protein 3D of foot-and-mouth disease virus in cattle and the development of a monoclonal antibody with diagnostic applications. J Immunol Methods **321:**174–181, 2007.
28. Yilma T: Morphogenesis of vesiculation in foot-and-mouth disease. Am J Vet Res **41:**1537–1542, 1980.

Return to Table of Contents

CLINICAL AND VACCINE IMMUNOLOGY, Apr. 2010, p. 550–558 Vol. 17, No. 4
1556-6811/10/$12.00 doi:10.1128/CVI.00429-09

IgA Antibody Response of Swine to Foot-and-Mouth Disease Virus Infection and Vaccination▽#

Juan M. Pacheco,[1] John E. Butler,[2] Jessica Jew,[2] Geoffrey S. Ferman,[1] James Zhu,[1] and William T. Golde[1]*

Plum Island Animal Disease Center, Agricultural Research Service, USDA, Greenport, New York,[1] and Department of Microbiology, University of Iowa College of Medicine, Iowa City, Iowa[2]

Received 21 October 2009/Returned for modification 30 November 2009/Accepted 15 January 2010

Foot-and-mouth disease virus (FMDV) continues to be a significant economic problem worldwide. Control of the disease involves the use of killed-virus vaccines, a control measure developed decades ago. After natural infection, the primary site of replication of FMDV is the pharyngeal area, suggesting that a mucosal immune response is the most effective. Humoral immunity to killed-virus vaccination induces antibodies that can prevent the clinical disease but not local infection. Determining whether infection or vaccination stimulates IgA-mediated local immunity depends on the method of analysis. Different assays have been described to analyze the quality of antibody responses of cattle and swine to FMDV, including indirect double-antibody sandwich enzyme-linked immunosorbent assay (IDAS-ELISA) and antibody capture assay-ELISA (ACA-ELISA). We tested these assays on swine and show that vaccinated animals had FMDV-specific IgM and IgG but no IgA in either serum or saliva. After the infection, both assays detected FMDV-specific IgM, IgG, and IgA in serum. Notably, serum IgA was more readily detected using the ACA-ELISA, whereas IgA was not detected in saliva with this assay. FMDV-specific IgA antibodies were detected in saliva samples using the IDAS-ELISA. These data show that parenterally administered, killed-virus vaccine does not induce a mucosal antibody response to FMDV and illuminates limitations and appropriate applications of the two ELISAs used to measure FMDV-specific responses. Further, the presence of the IgA antivirus in serum correlates with the presence of such antibodies in saliva.

Foot-and-mouth disease virus (FMDV) continues to be a significant economic problem worldwide. In FMDV-free countries, an outbreak of the virus freezes the export of all animal products, causing significant loss of revenue to the livestock industry. Eradication of the disease from areas of endemicity involves the use of killed-virus vaccines, a control measure developed decades ago. The vaccine offers clinical protection against FMDV, but it does not prevent virus excretion or the establishment of latency after challenge infection (14). Recovery from FMDV and protection from reinfection are associated predominantly with the presence of circulating neutralizing antibody (20, 25, 32).

Transmission of FMDV between animals is primarily via oral-pharyngeal exposure from contaminated feed and aerosols emitted from infected animals. This has led to a particular interest in the local, mucosal immune response to FMDV infection in the pharynx since, following exposure, this region is the most common site for primary virus replication (30, 36). Unfortunately, analysis of mucosal immunity has essentially been limited to assessment of immunoglobulin A (IgA) responses to FMDV infection of swine. Alternatively, the virus can gain direct entry into the skin through cuts or abrasions, particularly during infection of swine, as reviewed by Alexandersen and colleagues (2). The latter route of viral entry is more common in swine than in other susceptible species.

The role of T cells in stimulating B cell proliferation and subsequent differentiation to high-affinity antibody production in the swine response to FMDV is of particular interest. In the response of other species to different pathogens, it has been clearly demonstrated that both Th1 and Th2 responses contribute to effective immunity and clearance of pathogens (4, 26, 28, 33, 34). Manipulating vaccine formulations to target immune responses will be useful for FMDV prophylactics in swine and cattle, but the present knowledge of immune responses in these species offers little insight into the importance of the Th1/Th2 paradigm in effective antiviral immunity. Thus, extrapolating the Th1/Th2 paradigm of mice to swine is problematic.

In mice, the B cell switch from IgM to IgG2b antibody secretion is mediated by Th1 cytokines, specifically, gamma interferon (IFN-γ), whereas Th2 cytokines, including interleuken-4 (IL-4), IL-5, IL-13, and transforming growth factor β (TGF-β), accompany class switch to IgG1, IgG3, IgE, and IgA. However, IgG1 and IgG2b are not homologous immunoglobulins among distantly related mammals since speciation preceded subclass diversification (13, 23).

Further complicating our understanding of antibody responses in pigs is the fact that there are six subclasses of porcine IgG, five of which occur in at least two allelic forms (13). IgG1 is transcribed predominately in fetal and adult swine but not in the ileal Peyer's patches and mesenteric lymph nodes of fetal and neonatal piglets, where IgG3 predominates (11). IgG2 is poorly transcribed in all tissues of fetal and

* Corresponding author. Mailing address: Plum Island Animal Disease Center, Agricultural Research Service, USDA, P.O. Box 848, Greenport, NY 11944-0848. Phone: (631) 323-3249. Fax: (631) 323-3006. E-mail: william.golde@ars.usda.gov.

Supplemental material for this article may be found at http://cvi.asm.org/.

▽ Published ahead of print on 27 January 2010.

neonatal piglets. IgG3, the primordial porcine IgG, is most 5′ in the CH locus and, based on sequences motifs, is best equipped to activate complement and bind to Fcγ receptors (13, 17a). Currently, only two monoclonal antibodies (MAbs) that are described as specific for IgG1 and IgG2 are available. Based on preliminary results, anti-IgG1 is quite likely IgG1 specific, whereas the anti-IgG2 MAb likely recognizes an infraclass group that includes IgG2, IgG4, and IgG6. Since purified forms of IgG4 and IgG6 are not yet available, this has yet to be tested.

There are other factors that complicate understanding antibody responses to viral infection of mucosal surfaces in swine. In their studies on the distribution of antibody-containing cells, Bianchi and colleagues recognized differential reactivities among anti-porcine IgA MAb, which they suggested might reflect different IgA subclasses, as in humans (3). At nearly the same time, the porcine Cα gene was cloned and was shown to occur in two allelic forms, one of which was missing 4 amino acids of the hinge due to a splice accepter site mutation (5, 6). Sera from swine homozygous for IgAa and IgAb were exchanged to show that the MAbs generated by Bianchi and colleagues differentially recognized the two allotypic variants (29). The distribution of the two allotypes appears to be founder and breed associated, with IgAa occurring in the highest frequency (29).

The study reported here focuses on the mucosal antibody response of swine and utilizes isotype-specific reagents in two different, sensitive enzyme-linked immunosorbent assays (ELISAs). The comparison of assays for determination of the quality of antibody responses to FMDV addresses the limitations of presently available reagents. We tested for antibody responses in serum and saliva at 7, 14, or 21 days postvaccination (dpv) with a single dose of vaccine and compared the responses to those resulting from direct inoculation of pigs or following contact transmission of infection. FMDV-specific IgA, IgM, and IgG antibodies were readily detected in serum after infection, and IgA was detected in the saliva of the same animals. However, following vaccination, there were IgM and IgG responses in serum but no IgA antibodies in serum or saliva. These results illuminate the need to develop alternative FMDV vaccines designed for more efficient mucosal delivery and the induction of a mucosal IgA response that is predicted to yield better control of FMDV in an outbreak.

MATERIALS AND METHODS

Experimental design and animals. All vaccine trials and live-virus challenges in pigs were reviewed and approved by the Plum Island Animal Disease Center's Animal Care and Use Committee before initiation of these studies. Eighteen Yorkshire pigs weighing 25 to 30 kg were used for the study and housed together in one room measuring 6 by 6 m. Vaccinated animals were inoculated with the inactivated, purified O1 Manisa strain of FMDV in a double-oil emulsion (provided by T. Doel, Merial Animal Health, Pirbright, Surrey, United Kingdom), previously described in a bovine vaccination/challenge study (18). The estimated potency was consistent with a vaccine consisting of three 50% protective doses (PD_{50}), and the vaccine was administered at the manufacturer's recommended dose of 1.0 ml per animal (half of a bovine dose), intramuscularly in the neck. Vaccinations were staggered to allow simultaneous challenge of all pigs. Five animals were vaccinated 21 days before challenge (animals 51, 52, 53, 54, and 55, named group −21), and five animals were vaccinated 7 days before challenge (animals 56, 57, 58, 59, and 60, named group −7). Three pigs were used as a source of direct-contact virus (pigs 61, 62, and 63, named the direct-inoculation [DI] group) by means of intradermal inoculation of 100,000 PFU of pig-derived O1 Manisa in two sites in the heel bulb. The five remaining animals were used as nonvaccinated controls (pigs 64, 65, 66, 67, and 68, named the direct-contact [DC] group). One animal (pig 61) was euthanized at 7 days postchallenge (dpc) due to severity of lesions; therefore, no results for antibodies are shown for this particular animal.

Sample collection. Serum and saliva were collected weekly from dpc −21 to 28 for antibody detection. Whole blood was collected in heparin at 0, 1, 2, 3, 4, 5, 6, and 7 dpc for virus isolation.

Clinical assessment. Records of the sites on the animals showing vesicles were prepared each day, and a vesicle score was calculated by summing the following: one point for each affected digit, one point for vesicles on the tongue, one point for vesicles on the snout, one point for vesicles on the lower lip, and one point for vesicles on the carpal or tarsal area of one or more legs. A maximum lesion score of 20 was possible. Once a vesicle appeared at a site, the site was scored "positive" on all subsequent days, even if the vesicles at that site had begun to heal.

Virus isolation and quantification. The presence of virus in whole-blood samples was measured by a standard plaque assay with BHK-21 cells (22).

FMDV-neutralizing antibodies from serum. Serum samples were heat inactivated (56°C, 30 min) and used for microtiter neutralization assay on BHK-21 cells. Serial dilutions of serum were incubated with a virus dose of 100 50% tissue culture infective doses ($TCID_{50}$) of FMDV O1 Manisa for 1 h at 37°C and then transferred to preformed monolayers of BHK-21 cells and incubated at 37°C for 48 to 72 h. Cytopathic effect (CPE) was used to determine the endpoint titers, which were calculated as the reciprocal of the last serum dilution to neutralize 100 $TCID_{50}$ of virus in 50% of the wells.

Specificity of antiporcine IgA antibodies. Porcine IgAa and IgAb were purified from late-phase colostrum samples obtained from sows homozygous for IgAa and IgAb, respectively, using previously described methods; their purity was confirmed by SDS-PAGE (8, 24). The protein concentration of each preparation was determined by absorbance at 280 nm using an absorbance coefficient of 1.36 (1 cm, 0.1%). The functional or active concentration was determined by the recognition of immobilized IgAa and IgAb by biotinylated polyclonal anti-IgA reagents. Within the titration range for both allotypic variants, two different concentrations of immobilized IgAa and IgAb (60 ng and 30 ng, respectively) were selected for all subsequent tests. These were then used as targets for detection by the various anti-porcine MAb and polyclonal antibodies (PAbs) listed in Table 1. The dilution of each MAb tested was optimized so that the activities of different MAbs could be compared on the same microtiter plates (Table 1).

MAbs bound to immobilized IgAa and IgAb were detected using goat anti-mouse IgG conjugated to alkaline phosphatase (AP; Sigma product number A2429) followed by *para*-nitrophenyl phosphate (AP substrate) at 1 mg/ml. The detection of immobilized IgAa and IgAb by various biotinylated PAbs to porcine IgA was visualized using ExtrAvidin AP (Sigma-Aldrich product number E2636). Biotinylation of the gamma globulin fraction of the polyclonal antisera was done using *N*-hydroxysuccinimide ester–polyethyleneoxide–biotin according to the instructions of the manufacturer (Pierce Chemical, Rockford, IL).

Isotype-specific antibody immunoassay for FMDV. The IgM, IgA, and total IgG responses to the virus were determined by two specific antibody immunoassays. The first of these uses a sandwich-based system in which FMDV was captured by a rabbit anti-FMDV O1 Manisa antiserum (Institute for Animal Health, Pirbright, United Kingdom), diluted to 1:4,000 in carbonate-bicarbonate buffer (pH 9.6) and adsorbed on Immulon 2 microtiter plates (Dynatech Corp., Chantilly, VA) at 50 μl/well (see Fig. S1A in the supplemental material). This procedure for virus immobilization avoids adsorption-induced conformational change and the adsorption of culture medium proteins along with the virus (21). After 4 washes with PBS-T (0.05% Tween 20 in phosphate-buffered saline [PBS]), plates were blocked for 1 h at 37°C with blocking buffer (10% normal horse serum [Sigma, St. Louis, MO] in PBS-T) in a shaking incubator. Preparations of inactivated FMDV from infected fibroblasts (BHK-21 cells) that were captured in this manner were then used as the solid-phase antigen. Serum/saliva samples were tested for FMDV-specific IgM, IgA, and total IgG antibodies. After incubation of the samples and appropriate washing steps, the bound swine antibodies were detected using either goat anti-swine IgM or goat anti-swine IgG directly conjugated to horseradish peroxidase (product number 04-14-03 or 04-14-02, respectively; KPL, Gaithersburg, MD) or a mouse monoclonal anti-swine IgA (clone K61 1B4, product number MCA638; Serotec, Raleigh, NC) that was subsequently detected using goat anti-mouse IgG directly conjugated with horseradish peroxidase (product number 04-18-02 from KPL). This ELISA format has been previously described as an isotype-specific indirect double-antibody sandwich ELISA (IDAS-ELISA) (35). In the interest of consistency with the published data, we have retained this nomenclature.

TABLE 1. Anti-porcine IgA MAbs and PAbs tested

Reagent	Species	Source	Dilution used	IgA concn (ng)	Specificity
M1459	Mouse	Klaus Nielsen	1:10,000	60	Neutral
				30	Neutral
M1450	Mouse	Klaus Nielsen	1:10,000	60	IgAa biased
				30	IgAa biased
M1457	Mouse	Klaus Nielsen	1:10,000	60	IgAb biased
				30	IgAb biased
MCA638	Mouse	Serotec	1:200	60	Neutral
				30	Neutral
28.8.1	Mouse	Andre Bianchi	1:2,000	60	IgAa biased
				30	IgAa biased
27.9.1	Mouse	Andre Bianchi	1:5,000	60	IgAa biased
				30	IgAa biased
KAK 5376	Rabbit	Francek Klobasa	1:40,000	60	Neutral
				30	Neutral
KAK 6272	Rabbit	Francek Klobasa	1:150	60	Neutral
				30	Neutral
ZAK 141	Goat	Francek Klobasa	1:5,000	60	Neutral
				30	Neutral
ZAK 71	Goat	Francek Klobasa	1:40,000	60	Neutral
				30	Neutral

The second assay used the same mouse MAb described above but in an assay configuration previously described by van Zaane and colleagues as the isotype-specific antibody capture assay-ELISA (ACA-ELISA) (35). In this configuration, Immulon 2 microtiter plates were coated with sheep anti-mouse IgG (product number AAC10P from Serotec) diluted 1:200 in coating buffer (carbonate-bicarbonate, pH 9.6) at 50 μl/well (see Fig. S1B in the supplemental material). After 4 washes with PBS-T, the plates were blocked as described above, washed, and subsequently incubated with monoclonal mouse anti-swine IgA (the same antibodies used above). After washing of the plates, the samples, serum or saliva, from vaccinated and/or infected swine were added. After appropriate washing steps, the virus was added and subsequently detected using rabbit anti-FMDV O1 Manisa hyperimmune antiserum (Institute for Animal Health, Pirbright, United Kingdom) diluted to 1:4,000. The rabbit antibody was detected using goat polyclonal anti-rabbit IgG conjugated with peroxidase.

An optical density at 450 nm (OD_{450})/OD_{570} ratio of 0.1 was selected as a background cutoff for both ELISAs based on analysis of negative controls and results from prevaccination/infection samples. Results for both ELISAs are expressed as OD_{450}/OD_{570} ratios at a single dilution: 1/100 for serum samples and 1/5 for saliva samples. These working dilutions were selected after titration assays were performed in parallel with both ELISAs, with dilutions from 1/25 to 1/400,000 for serum or 1/1 to 1/400,000 for saliva samples. When samples were analyzed by IDAS-ELISA, the OD_{450}/OD_{570} ratio of the selected dilutions was directly related with the titer (the last dilution that showed an OD_{450}/OD_{570} ratio above the cutoff). The ACA-ELISA did not yield endpoint values because the dilution curves had multiple slopes, possibly related to an intraisotype competition (see Fig. S1 in the supplemental material for a diagram of comparative ELISAs).

Statistical analysis. The general linear model of statistical analysis implemented in the SAS 9.1 package (SAS Institute Inc., Cary, NC) was used to test the significant differences among treatment groups. If the *P* value of the test was equal to or smaller than 0.05, the differences among the groups were declared significant and Tukey's Studentized range test was used to detect the differences between the groups.

RESULTS

Viremia and clinical signs. Naïve animals inoculated directly in the heel bulb with FMDV showed clear signs of disease by 1 dpc, characterized by formation of vesicles, with a peak clinical score of 19 to 20 out of a maximum of 20 (Table 2). Virus in blood was isolated at 1 dpc, and the peak of viremia for these animals was at 2 dpc (Table 3). A second cohort of animals became infected by direct contact with the directly inoculated, infected pigs. These animals also showed clear signs of FMD, with vesicles detected as early as 3 dpc, with a peak lesion score of 16 to 18 out of 20 by 4 to 6 dpc (Table 2). In these contact-infected animals, viremia followed the pattern of the needle-inoculated animals, with an expected delay of 48 h (Table 3).

Of the animals vaccinated 21 days before natural infection by contact as the challenge, 2 out of 5 animals (pigs 51 and 55) were protected, with no detectable clinical signs and no virus isolated from their blood for 7 days after contact. The 3 remaining animals (pigs 52, 53, and 54) did not show virus in their blood, and few lesions were detected (clinical scores were 3, 5, and 13, respectively). Of the animals challenged 7 dpv, only 1 of 5 animals (pig 60) was protected, having no clinical signs or viremia for 7 days after contact. The 4 remaining animals (pigs 56, 57, 58, and 59) had low clinical scores of 1, 2, 5, and 5, respectively (Table 2). As with the other vaccinated group, there was no virus isolated from the blood of any of these animals over the 7-day sampling period.

Serum neutralizing antibody response following vaccination and infection. Serum samples from animals vaccinated 21 days before challenge with killed-virus vaccine showed rising titers of neutralizing antibodies, peaking at 14 dpv (dpc −7 in Fig. 1). Within the group vaccinated 7 days before challenge, animal 57 did not show any neutralizing antibody titer, but the other 4 animals had detectable titers on the day of challenge. In other studies, samples were taken on days 1 through 4 postvaccination and were uniformly negative, as were samples from days 1 through 4 postchallenge from all naïve animals, regardless of whether they were directly inoculated or infected by contact. No correlation was detected between serum neutralizing titer and protection from clinical disease, and all animals showed increasing titers of neutralizing antibody after challenge, peaking at 14 dpc (Fig. 1). These data indicate that animals protected from the development of clinical disease were not protected from infection. The subclinical infection results in production of viral antigen, which boosts the serum neutralizing antibody response.

TABLE 2. Clinical score for FMD

Group	Pig	Clinical score at dpc[e]:							
		0	1	2	3	4	5	6	7
−21[a]	51	0	0	0	0	0	0	0	0
	52	0	0	1	1	1	4	5	5
	53	0	0	0	0	0	2	2	3
	54	0	0	0	0	2	7	10	13
	55	0	0	0	0	0	0	0	0
−7[b]	56	0	0	0	0	0	0	3	5
	57	0	0	0	0	0	2	4	5
	58	0	0	0	0	0	2	2	2
	59	0	0	0	0	0	0	1	1
	60	0	0	0	0	0	0	0	0
DI[c]	61	0	1	13	19	19	19	19	19
	62	0	1	15	20	20	20	20	20
	63	0	1	17	18	19	19	19	19
DC[d]	64	0	0	0	1	16	18	18	18
	65	0	0	0	6	18	18	18	18
	66	0	0	0	1	14	16	16	16
	67	0	0	0	3	13	17	18	18
	68	0	0	0	12	16	15	16	16

[a] Animals were vaccinated on dpc −21 (infected by direct contact with directly inoculated animals).
[b] Animals were vaccinated on dpc −7 (infected by direct contact with directly inoculated animals).
[c] Animals were directly inoculated on the day of challenge.
[d] Naïve animals infected by direct contact with directly inoculated animals.
[e] Clinical scores were calculated as numbers of vesicles on each toe (4 per foot, with a potential score of 16), in the mouth or on the lips, on the tongue, on the snout, and elsewhere, for a maximum score of 20, on the indicated day postchallenge of directly inoculated animals.

Specificity of Ig isotype ELISAs used in this study. A complicating factor in understanding the antibody response of swine to FMDV is the limitation of the reagents available to determine the quality of the antibody response. MAbs reactive with each of the six porcine IgG subclasses (12, 13) are not available; only two MAbs designated anti-IgG1 and anti-IgG2 are currently available. In addition, the analysis of the IgA antibody used required further analysis of specificity.

Before using the porcine IgG subclass-specific MAbs in studies of FMDV, we tested their specificity in several ways since in preliminary tests, inconsistent results in ACA-ELISA and IDAS-ELISA were obtained. First, we used three MAbs, anti-IgG1, anti-IgG2, and anti-IgA, to capture their target Igs from serum. Then we used the same MAbs as detection antibodies for the Igs that had been captured. We found that anti-IgG1 recognized Igs captured by all three MAbs, whereas anti-IgG2 appeared to be specific for the Ig that had been captured with anti-IgG2 antibody and did not recognize Igs

TABLE 3. Viremia

Group	Pig	No. of PFU/ml on dpc[e]:							
		0	1	2	3	4	5	6	7
−21[a]	51	<0.7	<0.7	<0.7	<0.7	<0.7	<0.7	<0.7	<0.7
	52	<0.7	<0.7	<0.7	<0.7	<0.7	<0.7	<0.7	<0.7
	53	<0.7	<0.7	<0.7	<0.7	<0.7	<0.7	<0.7	<0.7
	54	<0.7	<0.7	<0.7	<0.7	<0.7	<0.7	<0.7	<0.7
	55	<0.7	<0.7	<0.7	<0.7	<0.7	<0.7	<0.7	<0.7
−7[b]	56	<0.7	<0.7	<0.7	<0.7	<0.7	<0.7	<0.7	<0.7
	57	<0.7	<0.7	<0.7	<0.7	<0.7	<0.7	<0.7	<0.7
	58	<0.7	<0.7	<0.7	<0.7	<0.7	<0.7	<0.7	<0.7
	59	<0.7	<0.7	<0.7	<0.7	<0.7	<0.7	<0.7	<0.7
	60	<0.7	<0.7	<0.7	<0.7	<0.7	<0.7	<0.7	<0.7
DI[c]	61	<0.7	4.1	5.6	<0.7	<0.7	<0.7	ND	ND
	62	<0.7	4.2	5.8	<0.7	<0.7	<0.7	ND	ND
	63	<0.7	4.2	5.9	1.7	<0.7	<0.7	ND	ND
DC[d]	64	<0.7	<0.7	<0.7	3.5	5.7	2.4	<0.7	<0.7
	65	<0.7	<0.7	<0.7	2.2	4.0	2.2	<0.7	<0.7
	66	<0.7	<0.7	<0.7	2.1	4.5	<0.7	<0.7	<0.7
	67	<0.7	<0.7	<0.7	3.4	4.3	<0.7	<0.7	<0.7
	68	<0.7	<0.7	<0.7	4.5	2.3	<0.7	<0.7	<0.7

[a] Animals were vaccinated on dpc −21 (infected by direct contact with directly inoculated animals).
[b] Animals were vaccinated on dpc −7 (infected by direct contact with directly inoculated animals).
[c] Animals were directly inoculated on the day of challenge.
[d] Naïve animals were infected by direct contact with directly inoculated animals.
[e] Day postchallenge of directly inoculated animals. ND, not determined.

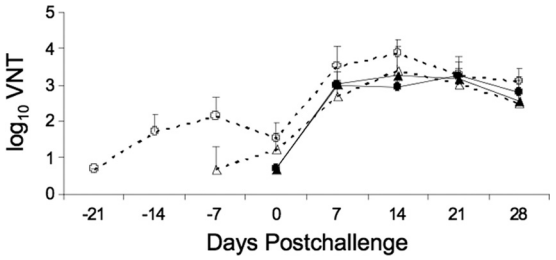

FIG. 1. Mean serum-neutralizing antibody responses in swine following vaccination and challenge with FMDV O Manisa. Three pigs were directly inoculated (closed circles) and used as donors for challenge of groups of 5 pigs that were vaccinated at −21(open circles) or −7 (open triangles) dpc and to 5 naïve pigs (contact inoculated, closed triangles). VNT, virus-neutralizing titer.

captured by anti-IgG1. Therefore, we did not use the monoclonal anti-IgG1 or anti-IgG2 antibodies in these analyses. Anti-IgA proved to be specific by the same criterion and when tested using purified pan porcine IgG and purified IgA.

In a separate study, these anti-porcine IgG MAbs were tested against porcine-camelid chimeric Igs constructed from the gene sequences of a number of the porcine IgG subclasses and allotypic variants (J. E. Butler, S. Muylderman, P. Boyd, and J. K. Lunney, unpublished). These tests confirmed that anti-IgG2 did not recognize any known IgG1 variant, whereas anti-IgG1 was weakly cross-reactive with several subclass chimeric Igs and was biased to the IgG1b allotype. However, since purified forms of all six subclasses and their allotypes are currently unavailable, the full specificity of these two MAbs to swine IgG remains unknown. Therefore, we relied on a polyclonal antibody (PAb) to IgG throughout the study.

Since anti-IgA proved to be specific in these tests of specificity, our concern was then for allotype bias. Further assessment of the specificity of IgA reagents confirmed evidence of allotype bias by MAbs and raised the possibility that data obtained in immunoassays might be biased by the particular MAbs and PAbs for porcine IgAa and IgAb used in our studies. Figure 2 compares the relative specificities of six anti-porcine MAb and four PAb reagents at two different concentrations of immobilized IgAa and IgAb. The reagents are described in Table 1. Allotype bias was evaluated by two-tailed Student *t* tests. Four MAbs to IgA (M1457, M1450, 27.9.1, and 28.8.1) were biased in one or the other direction, although 27.9.1 was not significantly biased when tested against IgAa and IgAb at 30 ng. The mean values shown in Fig. 2 are from independently prepared triplicate dilutions. Monoclonal antibodies M1459 from the Centre for Veterinary Biologics (CVB) at the National Veterinary Services Laboratory (NVSL), APHIS, U.S. Department of Agriculture (USDA) (Ames, IA), and MCA638 from Serotec (Raleigh, NC) show no allotype bias in their reactivities for two different concentrations of immobilized IgAa and IgAb. However, there was a 50-fold difference in useful concentration/dilution, indicating that the Serotec product is supplied in a highly diluted form (Table 1). The criterion for allotype bias is based on the premise that since PAbs are comprised of many antibodies that recognize different epitopes, bias will be reduced compared to that of MAbs that theoretically recognize only one epitope. This premise is supported by the empirical results obtained with four different PAbs (Table 1; Fig. 2). Based on these specificity tests, we analyzed the IgA anti-FMDV response of vaccinated and challenged animals using the Serotec monoclonal antibody to IgA (clone K61 1B4, Serotec product number MCA638).

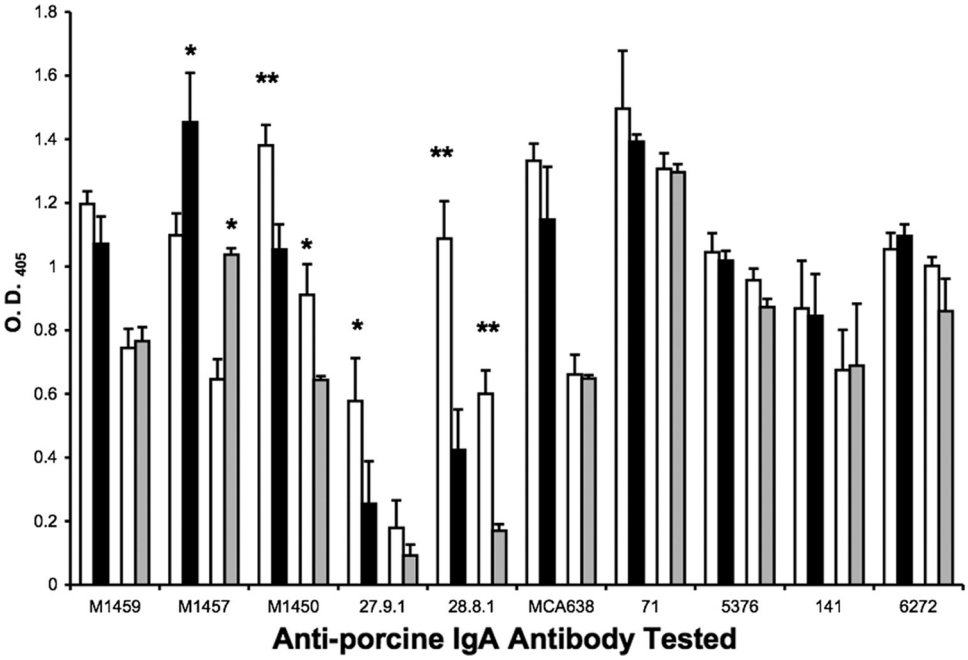

FIG. 2. The allotype specificity of six MAbs and four PAbs raised against porcine IgA tested against IgAa (open bars) and IgAb (black bars) immobilized at 60 ng per well or IgAa (open bars) and IgAb (gray bars) immobilized at 30 ng per well. *, $P < 0.04$; **, $P < 0.006$ (two-tailed Student *t* test results).

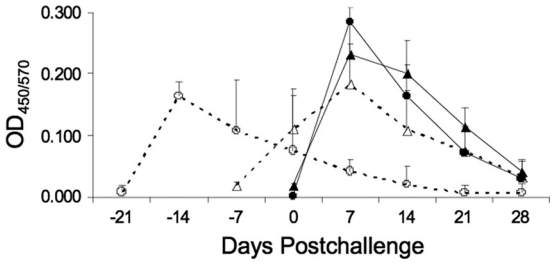

FIG. 3. Mean serum IgM antibody responses in swine following vaccination and challenge with FMDV O Manisa. Three pigs were directly inoculated (closed circles) and used as donors for challenge of groups of 5 pigs that were vaccinated at −21 (open circles) or −7 (open triangles) dpc and to 5 naïve pigs (contact inoculated; closed triangles).

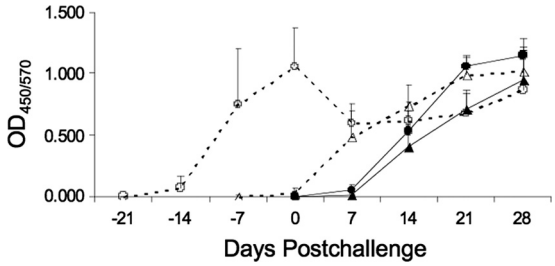

FIG. 4. Mean serum IgG antibody responses in swine following vaccination and challenge with FMDV O Manisa. Three pigs were directly inoculated (closed circles) and used as donors for challenge of groups of 5 pigs that were vaccinated at −21 (open circles) or −7 (open triangles) dpc and to 5 naïve pigs (contact inoculated; closed triangles).

Serum IgM and IgG responses to FMDV following infection or vaccination and challenge. Analysis of the serum IgM response to FMDV was carried out using the IDAS-ELISA. The data in Fig. 3 illustrate that IgM anti-FMDV peaked in all animals from all treatment groups at 7 dpv (day −14 relative to the live-virus challenge) as well as at 7 dpc in the naïve controls. As expected, the mean signal for IgM from serum samples taken from animals vaccinated 21 days before challenge decreased after 7 dpv and was not affected by exposure to virus, even though one of these animals exhibited clinical signs of disease. The boost in the IgM response in the animals challenged at day 7 was also expected, as the IgM response had yet to peak and there was a new exposure to FMDV antigens. By 28 dpc, IgM antibody was diminishing in a normal pattern in all groups.

Analysis of the serum IgG anti-FMDV antibody response shows that no animals had IgG at 7 dpv for vaccinated animals or 7 dpc for nonvaccinated controls (dpc −14, 0, or 7 in Fig. 4). Rising titers of IgG were detected by day 14 following inoculation or vaccination in animals not challenged at 7 dpv and continued rising at day 21 for all groups whether vaccinated, directly infected, or infected by contact with animals presenting with disease. Following challenge, the animals vaccinated 7 days previously showed a rising titer of IgG anti-FMDV. Contrarily, the animals challenged 21 dpv showed a flat IgG response pattern, indicating a lack of further exposure to antigen. This includes the three animals that showed clinical signs of disease (numbers 52, 53, and 54 in Table 2). This result is consistent with the observation that none of the vaccinated animals had detectable viremia and therefore little or no viral antigen to stimulate a boost in the antibody response.

IgA anti-FMDV antibody responses. The IgA response to FMDV vaccination and infection illustrates the complexity of analyzing these responses. Serum IgA was not detectable in the vaccinated groups by either ELISA methodology when samples taken before challenge were analyzed (Fig. 5A and B). Following virus exposure, the IgA anti-FMDV response was very low at 7 dpc in all groups regardless of the assay used (Fig. 5A and B). Contrarily, all nonvaccinated animals exhibited an IgA anti-FMDV response detectable in serum samples by 14 dpc using either assay. Interestingly, the difference in IgA levels reached statistical significance when vaccinated animals were compared at 21 dpv and both groups of naïve animals were compared at 21 dpc ($P = 0.001$) but only in the ACA-ELISA (Fig. 5A). Further, the same differential comparison of the day 14 samples was nearly significant ($P = 0.068$) (Fig. 5A) by the ACA-ELISA. When the same set of serum samples were assayed with the IDAS-ELISA, the results differed. Here, animals directly inoculated with FMDV had an IgA anti-FMDV response at both 14 and 21 dpc, significantly more than that of either contact-exposed or vaccinated animals ($P = 0.0026$ and 0.0001, respectively) (Fig. 5B). However, there were no significant differences between contact-exposed animals and vaccinated animals on either day 14 or day 21 (Fig. 5B).

Results with saliva samples add to the understanding of the antibody response using these different assays, both in previous reports and in the present study. As in the sera, no IgA anti-FMDV was detected in the saliva by either method of ELISA before the challenge (Fig. 5C and D). Unlike with the sera, the ACA-ELISA detected only minimal levels of IgA in the saliva of the infected animals (Fig. 5C). However, the IDAS-ELISA detected salivary IgA anti-FMDV starting at 7 or 14 dpc, regardless of whether animals were infected by direct inoculation or contact transmission. These animals produced more IgA in their saliva than the vaccinated animals at day 14, with differences being significant only between the contact and vaccinated groups. The difference in IgA levels reached statistical significance when we compared vaccinated animals at 21 dpv and both groups of naïve animals at 21 dpc ($P = 0.023$) (Fig. 5D).

Following the challenge of vaccinated animals, there was a barely detectable IgA anti-FMDV response in either serum or saliva. This was predicted, as both vaccinated groups had very mild disease and no detectable viremia following challenge. Therefore, there was very little antigen available in vaccinated animals to drive the switch to an IgA anti-FMDV response. The IgA anti-FMDV response was detected only in the naïve, infected animals. Detection in serum requires the ACA-ELISA format, whereas detection in saliva was seen only in the IDAS-ELISA format. Importantly, in all animals where IgA anti-FMDV was detected in saliva, it was also detected in serum.

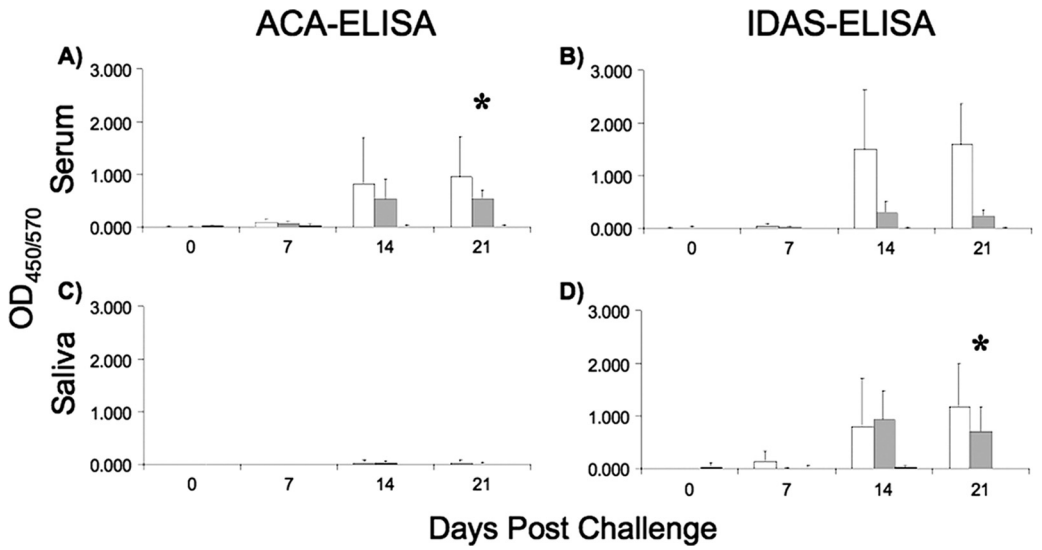

FIG. 5. Mean serum and saliva IgA antibody responses in swine following vaccination and challenge with FMDV O Manisa. Three pigs were directly inoculated (white bars) and used as donors for challenge of groups of 5 pigs (contact inoculated, gray bars) or vaccinated at −21 dpc (black bars). Porcine IgA was detected with mouse monoclonal anti-IgA (Serotec product number MCA638). * denotes differences with statistical significance when vaccinated animals were compared at 21 dpv and both groups of naïve animals were compared at 21 dpc ($P = 0.001$ for panel A and $P = 0.023$ for panel D).

DISCUSSION

Historically, the prediction of protection against infection with FMDV correlates with the presence of serum neutralizing antibody. Many exceptions to this have been reported, highlighting the need to understand more about the immune response to FMDV. Even within the more narrow analysis of the humoral response to the virus, there is still minimal understanding of the details of the development of anti-FMDV antibody responses in different lymphoid tissues and the circulation leading to control of the disease by antibodies. For example, neutralizing antibody titers are used to correlate humoral immune responses and protection against infection, but little is known about the role of nonneutralizing antibodies in the antiviral response. Further, the majority of available data derives from studies where animals are challenged with FMDV by needle inoculation. Certainly, this allows for control of the challenge dose and consistent induction of clinical disease, but natural infection is by contact with contaminated feed or bedding and, most often, actively infected animals shedding virus.

The results of the contact challenge of vaccinated pigs presented here show that vaccinated animals were only partially protected, as 3 of 5 animals in the group vaccinated 21 days prior to virus challenge and 4 of 5 animals in the group vaccinated 7 days prior to challenge developed clinical symptoms of disease. Clearly, all vaccinated animals showed delayed clinical signs, a reduced clinical score when disease developed, and no detection of virus in their blood. By comparison, naïve animals had a rapid onset of disease, high clinical scores, and high levels of viremia as a result of the same exposure to virus. Serum neutralizing antibodies were detected in all but one of the vaccinated animals before contact with infected animals, and it should be noted that relative levels of neutralizing antibody did not correlate with levels of clinical disease.

The lack of protection could be related to the severe challenge in our study, as the different vaccinated and naïve groups were housed together for the duration of the experiment. This resulted in an overwhelming challenge from the unprotected pigs rechallenging the vaccinated pigs, as these animals shed high levels of FMDV. For instance, a milliliter of vesicular fluid can contain 10^6 to 10^8 infectious viral particles. The concept of overwhelming challenge has been cited for swine (P. Barnett et al., unpublished) and cattle (15) and is particularly relevant with regard to high-density farming practices. The lack of protection may also be related to the insufficient immune response after vaccination, particularly at a mucosal level, as discussed by Eblé et al. (17). If natural introduction of virus is via oral infection in swine during a contact transmission, FMDV-specific antibody in oral secretions such as saliva should then be critical to protection against infection.

A central objective of this study was to develop a better understanding of the mucosal antibody response. Because of the limited reagents available to determine antibody isotypes, we did not analyze IgG subtypes and limited our analysis to the IgA response in serum and saliva.

Results presented here indicate that analysis of different samples, for at least the IgA isotype of the antibody, requires use of the appropriate assay. For IgA anti-FMDV in serum, the ACA-ELISA, which first captures all of a given isotype of an antibody, is the most accurate analysis. Saliva and likely nasal samples are most accurately assayed for IgA anti-FMDV by the IDAS-ELISA, capturing all of the FMDV-specific antibody and determining IgA in that population. Given what we know from analysis of human antibody responses relative to the presence of IgA in different fluids, these results are consistent. Small concentrations of IgA in serum require the capture of all the IgA first, followed by analysis for the FMDV-specific antibodies among those proteins. IgG interference in the detection of serum IgA antibodies in an IDAS-ELISA

format has been previously demonstrated (7). The dominance of IgA in mucosal secretions means that interisotype inhibition of IgA detection using an IDAS-ELISA format is inconsequential.

For this study, a very important result to be emphasized is that if there is a detectable IgA anti-FMDV response in serum, then there is also one in saliva, and if IgA anti-FMDV is detectable in saliva, it is also detectable in serum. Our data clearly show a strong correlation between the results of ACA-ELISA in sera and IDAS-ELISA in saliva (with an r^2 of 0.82). Therefore, these results indicate that collection of only serum samples and analysis by ACA-ELISA allow for a representative analysis of the IgA anti-FMDV response in pigs. This differs in part with previously published data for which investigators used only a single assay for IgA response and did not compare the two assays (1, 16, 27, 31). This is strong support for the idea that local IgA responses in swine also cause elevation of serum IgA responses. This has also been observed in colonized piglets (10) and more recently in isolator piglets infected with swine influenza (J. E. Butler, K. M. Lager, Z. Bergman, and X.-Z. Sun, unpublished). Similar results were also obtained with rabbits immunized through inhalation of ovalbumin (9) and by studies of sheep showing that IgA produced in the respiratory tract makes a major contribution to serum IgA levels (19).

Intramuscular vaccination with inactivated FMDV in double-oil emulsion induced no IgA response in serum or saliva regardless of the assay employed, making this result very clear. After infection, IgA was detected in serum with both ELISAs; however, only the assay that captured all IgA antibody and determined the anti-FMDV within that (the ACA-ELISA) yielded statistically significant differences. Saliva samples had a different result, with all saliva samples testing negative for IgA anti-FMDV. The assay that analyzes all anti-FMDV antibodies in a sample, the IDAS-ELISA, showed a strong IgA anti-FMDV response in infected animals and no IgA anti-FMDV in saliva of vaccinated animals. This is an example of the intraisotype competition due to the presence of larger amounts of IgA in saliva; since there is little antibody of other isotypes in the saliva, the interisotype competition does not affect the assay. In order to detect these antibodies, they need to be concentrated by reactivity with the virus as they are in the IDAS-ELISA, and then they can be detected with isotype-specific reagents. Capturing all IgA from a saliva sample creates a condition where only a diminishingly small part of the antibody present is reactive with FMDV.

As previously reported (16), our results show that intramuscular inoculation with killed-virus vaccine does not induce an IgA response. This highlights the need to further understand the development of the immune response to this virus as we confront the design of new, rapid-action vaccines for FMDV. As the primary component of countermeasures deployed in response to outbreaks of FMDV, vaccines targeting induction of a mucosal IgA response are predicted to be highly effective considering that the pharynx is the main site of primary replication for FMDV. Such vaccines are likely to yield better control of FMDV spread in an outbreak and increase the likelihood of using these vaccines and limiting the impact of future outbreaks.

ACKNOWLEDGMENTS

We thank Lindsey Banigan (University of Delaware) for assistance in the animal studies. We also thank Xiu Zhu Sun of the Department of Microbiology, University of Iowa College of Medicine, for his assistance in specificity analysis of the different anti-IgA reagents. Finally, we acknowledge the Laboratory Animal Resources group at Plum Island Animal Disease Center for their professional work.

This work was supported by grant CRIS 1940-32000-042, USDA (W.T.G.), and a reimbursable agreement with the Agricultural Research Service, USDA, and the Department of Homeland Security (agreement 60-1940-4-0027). J. M. Pacheco was the recipient of a Plum Island Animal Disease Center Research Participation Program fellowship, administered by the Oak Ridge Institute for Science and Education (ORISE) through an interagency agreement between the U.S. Department of Energy (DOE) and the USDA.

REFERENCES

1. **Abu Elzein, E. M., and J. R. Crowther.** 1981. Detection and quantification of IgM, IgA, IgG1 and IgG2 antibodies against foot-and-mouth disease virus from bovine sera using an enzyme-linked immunosorbent assay. J. Hyg. (Lond.) **86:**79–85.
2. **Alexandersen, S., Z. Zhang, A. I. Donaldson, and A. J. Garland.** 2003. The pathogenesis and diagnosis of foot-and-mouth disease. J. Comp. Pathol. **129:**1–36.
3. **Bianchi, A. T., H. W. Moonen-Leusen, P. J. van der Heijden, and B. A. Bokhout.** 1995. The use of a double antibody sandwich ELISA and monoclonal antibodies for the assessment of porcine IgM, IgG and IgA concentrations. Vet. Immunol. Immunopathol. **44:**309–317.
4. **Boom, W. H., L. Liebster, A. K. Abbas, and R. G. Titus.** 1990. Patterns of cytokine secretion in murine leishmaniasis: correlation with disease progression or resolution. Infect. Immun. **58:**3863–3870.
5. **Brown, W. R., and J. E. Butler.** 1994. Characterization of a C alpha gene of swine. Mol. Immunol. **31:**633–642.
6. **Brown, W. R., I. Kacskovics, B. A. Amendt, N. B. Blackmore, M. Rothschild, R. Shinde, and J. E. Butler.** 1995. The hinge deletion allelic variant of porcine IgA results from a mutation at the splice acceptor site in the first C alpha intron. J. Immunol. **154:**3836–3842.
7. **Butler, J. E., Y. Heo, P. Adams, and H. B. Richerson.** 1990. The antigen-limited nature of microtiter ELISAs requires partial depletion of IgG to permit reliable determination of rabbit serum IgA antibody activity. Mol. Immunol. **27:**319–325.
8. **Butler, J. E., F. Klobasa, and E. Werhahn.** 1981. The differential localization of IgA, IgM and IgG in the gut of suckled neonatal piglets. Vet. Immunol. Immunopathol. **2:**53–65.
9. **Butler, J. E., H. B. Richerson, P. A. Swanson, M. T. Suelzer, and W. C. Kopp.** 1983. Carrier requirement for development of acute experimental hypersensitivity pneumonitis in the rabbit. Int. Arch. Allergy Appl. Immunol. **71:**74–82.
10. **Butler, J. E., P. Weber, M. Sinkora, J. Sun, S. J. Ford, and R. K. Christenson.** 2000. Antibody repertoire development in fetal and neonatal piglets. II. Characterization of heavy chain complementarity-determining region 3 diversity in the developing fetus. J. Immunol. **165:**6999–7010.
11. **Butler, J. E., and N. Wertz.** 2006. Antibody repertoire development in fetal and neonatal piglets. XVII. IgG subclass transcription revisited with emphasis on new IgG3. J. Immunol. **177:**5480–5489.
12. **Butler, J. E., N. Wertz, N. Deschacht, and I. Kacskovics.** 2009. Porcine IgG: structure, genetics, and evolution. Immunogenetics **61:**209–230.
13. **Butler, J. E., Y. Zhao, M. Sinkora, N. Wertz, and I. Kacskovics.** 2009. Immunoglobulins, antibody repertoire and B cell development. Dev. Comp. Immunol. **33:**321–333.
14. **Doel, T. R.** 2003. FMD vaccines. Virus Res. **91:**81–99.
15. **Donaldson, A. I., and R. P. Kitching.** 1989. Transmission of foot-and-mouth disease by vaccinated cattle following natural challenge. Res. Vet. Sci. **46:**9–14.
16. **Eblé, P. L., A. Bouma, M. G. de Bruin, F. van Hemert-Kluitenberg, J. T. van Oirschot, and A. Dekker.** 2004. Vaccination of pigs two weeks before infection significantly reduces transmission of foot-and-mouth disease virus. Vaccine **22:**1372–1378.
17. **Eblé, P. L., A. Bouma, K. Weerdmeester, J. A. Stegeman, and A. Dekker.** 2007. Serological and mucosal immune responses after vaccination and infection with FMDV in pigs. Vaccine **25:**1043–1054.

17a. **Eguchi-Ogawa, T., X.-Z. Sun, N. Wertz, H. Uenishi, F. Puimi, P. Chardon, K. Wells, G. J. Tobin, and J. E. Butler.** Antibody repertoire development in fetal and neonatal piglets. XI. The relationship of VDJ usage and the genomic organization of the variable heavy chain locus. J. Immunol., in press.

18. **Golde, W. T., J. M. Pacheco, H. Duque, T. Doel, B. Penfold, G. S. Ferman, D. R. Gregg, and L. L. Rodriguez.** 2005. Vaccination against foot-and-mouth disease virus confers complete clinical protection in 7 days and partial pro-

tection in 4 days: use in emergency outbreak response. Vaccine **23:**5775–5782.
19. **Gorin, A. B., and J. Gould.** 1979. Immunoglobulin synthesis in the lungs and caudal mediastinal lymph node of sheep. J. Immunol. **123:**1339–1342.
20. **Graves, J. H., P. D. McKercher, and J. J. Callis.** 1972. Foot-and-mouth disease vaccine: influence of the vaccine virus subtype on neutralizing antibody and resistance to disease. Am. J. Vet. Res. **33:**765–768.
21. **Herrmann, J. E., R. M. Hendry, and M. F. Collins.** 1979. Factors involved in enzyme-linked immunoassay of viruses and evaluation of the method for identification of enteroviruses. J. Clin. Microbiol. **10:**210–217.
22. **Hierholzer, J. C., and R. A. Killington.** 1996. Virus isolation and quantitation, p. 25–46. *In* B. W. Mahy and H. O. Kangro (ed.), Virology methods manual. Academic Press, Inc., San Diego, CA.
23. **Kehoe, J. M., and J. D. Capra.** 1974. Nature and significance of immunoglobulin subclasses. N. Y. State J. Med. **74:**489–491.
24. **Klobasa, F., F. Habe, E. Werhahn, and J. E. Butler.** 1985. Changes in the concentrations of serum IgG, IgA and IgM of sows throughout the reproductive cycle. Vet. Immunol. Immunopathol. **10:**341–353.
25. **McCullough, K. C., F. De Simone, E. Brocchi, L. Capucci, J. R. Crowther, and U. Kihm.** 1992. Protective immune response against foot-and-mouth disease. J. Virol. **66:**1835–1840.
26. **Moran, T. M., H. Park, A. Fernandez-Sesma, and J. L. Schulman.** 1999. Th2 responses to inactivated influenza virus can be converted to Th1 responses and facilitate recovery from heterosubtypic virus infection. J. Infect. Dis. **180:**579–585.
27. **Mulcahy, G., C. Gale, P. Robertson, S. Iyisan, R. D. DiMarchi, and T. R. Doel.** 1990. Isotype responses of infected, virus-vaccinated and peptide-vaccinated cattle to foot-and-mouth disease virus. Vaccine **8:**249–256.
28. **Müller, I., J. A. Garcia-Sanz, R. Titus, R. Behin, and J. Louis.** 1989. Analysis of the cellular parameters of the immune responses contributing to resistance and susceptibility of mice to infection with the intracellular parasite, Leishmania major. Immunol. Rev. **112:**95–113.
29. **Navarro, P., R. K. Christensen, P. Weber, M. Rothschild, G. Ekhardt, and J. E. Butler.** 2000. Porcine IgA allotypes are not equally transcribed or expressed in heterozygous swine. Mol. Immunol. **37:**653–664.
30. **Pacheco, J. M., J. Arzt, and L. L. Rodriguez.** 2010. Early events in the pathogenesis of foot-and-mouth disease in cattle after controlled aerosol exposure. Vet. J. **183:**46–53.
31. **Parida, S., J. Anderson, S. J. Cox, P. V. Barnett, and D. J. Paton.** 2006. Secretory IgA as an indicator of oro-pharyngeal foot-and-mouth disease virus replication and as a tool for post vaccination surveillance. Vaccine **24:**1107–1116.
32. **Salt, J. S., G. Mulcahy, and R. P. Kitching.** 1996. Isotype-specific antibody responses to foot-and-mouth disease virus in sera and secretions of "carrier" and "non-carrier" cattle. Epidemiol. Infect. **117:**349–360.
33. **Sher, A., R. T. Gazzinelli, I. P. Oswald, M. Clerici, M. Kullberg, E. J. Pearce, J. A. Berzofsky, T. R. Mosmann, S. L. James, and H. C. Morse III.** 1992. Role of T-cell derived cytokines in the downregulation of immune responses in parasitic and retroviral infection. Immunol. Rev. **127:**183–204.
34. **Sieling, P. A., and R. L. Modlin.** 1994. Cytokine patterns at the site of mycobacterial infection. Immunobiology **191:**378–387.
35. **van Zaane, D., and J. Ijzerman.** 1984. Monoclonal antibodies against bovine immunoglobulins and their use in isotype-specific ELISAs for rotavirus antibody. J. Immunol. Methods **72:**427–441.
36. **Zhang, Z. D., and R. P. Kitching.** 2001. The localization of persistent foot and mouth disease virus in the epithelial cells of the soft palate and pharynx. J. Comp. Pathol. **124:**89–94.

Return to Table of Contents

JOURNAL OF VIROLOGY, Feb. 2010, p. 2063–2077 Vol. 84, No. 4
0022-538X/10/$12.00 doi:10.1128/JVI.01874-09

Interferon-Induced Protection against Foot-and-Mouth Disease Virus Infection Correlates with Enhanced Tissue-Specific Innate Immune Cell Infiltration and Interferon-Stimulated Gene Expression▽†

Fayna Diaz-San Segundo,[1,2] Mauro P. Moraes,[1] Teresa de los Santos,[1] Camila C. A. Dias,[1,2] and Marvin J. Grubman[1]*

Plum Island Animal Disease Center, North Atlantic Area, Agricultural Research Service, U.S. Department of Agriculture, Greenport, New York 11944,[1] and Oak Ridge Institute for Science and Education, PIADC Research Participation Program, Oak Ridge, Tennessee 37831[2]

Received 3 September 2009/Accepted 18 November 2009

Previously, we demonstrated that type I interferon (IFN-α/β) or a combination of IFN-α/β and type II IFN (IFN-γ) delivered by a replication-defective human adenovirus 5 (Ad5) vector protected swine when challenged 1 day later with foot-and-mouth disease virus (FMDV). To gain a more comprehensive understanding of the mechanism of protection induced by IFNs, we inoculated groups of six swine with Ad5-vectors containing these genes, challenged 1 day later and euthanized 2 animals from each group prior to (1 day postinoculation [dpi]) and at 1 (2 dpi) and 6 days postchallenge (7 dpi). Blood, skin, and lymphoid tissues were examined for IFN-stimulated gene (ISG) induction and infiltration by innate immune cells. All IFN-inoculated animals had delayed and decreased clinical signs and viremia compared to the controls, and one animal in the IFN-α treated group did not develop disease. At 1 and 2 dpi the groups inoculated with the IFNs had increased numbers of dendritic cells and natural killer cells in the skin and lymph nodes, respectively, as well as increased levels of several ISGs compared to the controls. In particular, all tissues examined from IFN-treated groups had significant upregulation of the chemokine 10-kDa IFN-γ-inducible protein 10, and preferential upregulation of 2′,5′-oligoadenylate synthetase, Mx1, and indoleamine 2,3-dioxygenase. There was also upregulation of monocyte chemotactic protein 1 and macrophage inflammatory protein 3α in the skin. These data suggest that there is a complex interplay between IFN-induced immunomodulatory and antiviral activities in protection of swine against FMDV.

Foot-and-mouth disease virus (FMDV) is the causative agent of one of the most contagious and economically devastating diseases affecting cloven-hoofed livestock worldwide. The virus, a member of the *Picornaviridae* family, rapidly replicates in the host and spreads via aerosol and by direct contact (3). Foot-and-mouth disease (FMD) is characterized by fever, lameness, lymphopenia, and the appearance of vesicular lesions on the mouth, tongue, nose, feet, and teats (19, 28) and is controlled by inhibition of susceptible animal movement, slaughter of infected animals, and possibly vaccination with an inactivated whole-virus vaccine. However, both the conventional inactivated vaccine and a replication-defective human adenovirus 5 (Ad5) FMDV subunit vaccine that we have recently developed require approximately 7 days to induce full protection in swine and cattle (25, 38, 44). In FMD outbreaks in disease-free countries the induction of rapid protection, prior to the development of vaccine-induced adaptive immunity, is necessary to inhibit or limit disease spread and thus potentially reduce the number of animals that have to be slaughtered.

Interferons (IFNs) are the first line of the host innate immune defense against viral infection (49), and it has been demonstrated that type I and type II IFN (IFN-α/β and IFN-γ, respectively) have antiviral activity against many viruses (5, 29). After the IFN pathway is stimulated transcriptional upregulation of hundreds of effector genes occurs (17, 52). Our group has demonstrated that pretreatment of cell cultures with type I and type II IFNs can dramatically inhibit FMDV replication (12, 14, 37), and at least two type I IFN-stimulated genes (ISGs), double-stranded-RNA-dependent protein kinase (PKR) and 2′,5′-oligoadenylate synthetase (OAS)/RNase L, are involved in this process (12, 16). Furthermore, swine pretreated with an Ad5 vector expressing porcine IFN-α (Ad5-pIFN-α) or porcine IFN-γ (Ad5-CI-pIFN-γ) are sterilely protected when challenged with FMDV 1 day later (13, 37) and protection lasted 3 to 5 days (36). Interestingly, the action of type I IFN in combination with type II IFN can synergistically block virus replication *in vivo* since swine inoculated with a combination of Ad5-CI-pIFN-α and Ad5-CI-pIFN-γ, at doses that alone do not protect against FMDV, are completely protected against clinical disease and do not develop viremia (37). The protection conferred in IFN-treated pigs correlated with an increase of the 10-kDa IFN-γ-inducible protein 10 (IP-10), indoleamine 2,3-dioxygenase (INDO), and OAS mRNA expression in peripheral blood mononuclear cells (PBMCs), and this upregulation was synergistic in the group of animals treated with the combination of Ad5-CI-pIFN-α and Ad5-CI-pIFN-γ. Nevertheless, this approach has only been partially successful in cattle, since Ad5-pIFN-α-treated animals devel-

* Corresponding author. Mailing address: Plum Island Animal Disease Center, USDA, ARS, NAA, P.O. Box 848, Greenport, NY 11944. Phone: (631) 323-3323. Fax: (631) 323-3006. E-mail: marvin.grubman@ars.usda.gov.

† Supplemental material for this article may be found at http://jvi.asm.org/.

▽ Published ahead of print on 2 December 2009.

oped clinical disease after FMDV challenge, although the disease was delayed and less severe compared to control animals (60).

Type I and type II IFNs have some overlapping biologic activities but unique functional roles in the innate and adaptive immune response. Type I IFNs, are primarily responsible for inducing direct antiviral responses in infected cells and do so with more potency than IFN-γ (53). IFN-γ is mainly produced by activated T lymphocytes and natural killer (NK) cells predominantly activating components of the cell-mediated immune system such as cytotoxic T lymphocytes, macrophages, and NK cells, and inducing Th1 differentiation, but it can also display antiviral activity (42). However, it has also been shown that type I IFNs can stimulate dendritic cell (DC) maturation and NK cell activation (56). Furthermore, other cytokines and chemokines, including IP-10 (35, 37), monocyte chemotactic protein 1 (MCP-1) (8), macrophage inflammatory protein 1α (MIP-1α) (31), and MIP-3α (50), that do not have direct antiviral activity but are involved in chemoattraction of various immune cells to the site of infection are also induced by IFNs.

DCs, professional antigen-presenting cells, and NK cells play a key role in the initiation and regulation of the immune response. After priming by pathogen-derived products, their reciprocal interactions may result in a potent activating cross talk that regulates both the quality and intensity of the innate immune response (15). Swine DCs include distinct subsets with specific biological functions (41, 51, 61). Langerhans cells (LCs) are DCs resident in the epithelium, particularly the epidermis. The skin and mucosa are the predilection sites of FMDV replication (3, 28). LCs migrate selectively to MIP-3α (via CCR6) (10), a chemokine that is regulated by the expression of IFN-γ (50) and is secreted by keratinocytes (10). Other IFN-γ-regulated chemokines, including MCP-1, MIP-1α, and IP-10, are involved in epidermal DC maturation (24) and NK cell recruitment and activation (54). Furthermore, upon maturation DCs are able to produce cytokines, including interleukin-12 (IL-12) (47), IL-15 (34), and IL-18 (4), that are involved in NK cell proliferation and activation (46, 57). It has also been shown that murine DCs produce IL-2, and this cytokine can activate NK cells (27). Recently, Pintaric et al. (46) and Toka et al. (57) demonstrated that human IL-2 can activate swine NK cells. Clearly there is a complex interplay between IFN-induced chemokine and cytokine activation of various immune cells and their possible role in protection against FMD.

In the present study we examined in more detail the effects of IFN treatment on induction of protective mechanisms against FMDV. Groups of animals were inoculated with either Ad5-CI-pIFN-α or Ad5-CI-pIFN-γ alone or in combination, challenged with FMDV 1 day later, and two animals from each group were euthanized 1 day postinoculation (dpi) and 1 and 6 days postchallenge (dpc). We examined ISGs in skin, the main site of virus replication, PBMCs, and lymphoid tissues and also evaluated possible immune cell recruitment to the skin and lymph nodes. We found that protection correlated with recruitment of DCs and NK cells to the skin and lymph nodes, respectively, and upregulation of a number of cytokines, some of which have been shown to block FMDV replication in cell culture (12), and chemokines that are involved in chemoattraction of DCs and NK cells. The chemokine IP-10 was significantly upregulated in all tissues examined, whereas MIP-3α, and MCP-1 were mainly induced in the skin. These data suggest that IFN-induced immunomodulatory, as well as antiviral, activities may be involved in protection of swine against FMD.

MATERIALS AND METHODS

Cells and viruses. Human 293 cells were used to generate, grow, and titer recombinant Ad5s (26, 38). Baby hamster kidney cells (BHK-21, clone 13) were used to measure FMDV titers in plaque assays. IBRS-2 cells (swine kidney) were used to measure antiviral activity in plasma from inoculated animals by a plaque reduction assay (12). The recombinant viruses Ad5-CI-pIFN-α and Ad5-CI-pIFN-γ were constructed as described by Moraes et al. (37). FMDV serotype A24 (strain Cruzeiro, Brazil, 1955) was isolated from vesicular lesions of an infected bovine.

Animal experiment. Twenty-eight circovirus-free Yorkshire gilts (ca. 40 to 60 lb) were housed in the secure disease agent isolation facilities at the Plum Island Animal Disease Center according to a protocol approved by the Institutional Animal Care and Use Committee. In this experiment, the animals were divided into five groups containing six animals per group (unless otherwise stated), and each group was housed in a separate room: one group inoculated with 2 ml of 10^9 PFU Ad5-CI-pIFN-α, one group inoculated with 2 ml of 10^{10} PFU Ad5-CI-pIFN-γ, one group inoculated with 2 ml of 10^9 PFU Ad5-CI-pIFN-α and 10^{10} PFU Ad5-CI-pIFN-γ, and two control groups, one inoculated with 2 ml of 10^{10} PFU Ad5-Blue (four animals; two animals in this group were euthanized prior to the start of the experiment because of health reasons) and one inoculated with 2 ml of phosphate-buffered saline (PBS). The animals were monitored clinically for adverse effects from Ad5-CI-pIFN-α and Ad5-CI-pIFN-γ administration, including fever and lethargy. One day postinoculation two animals in each group were slaughtered, and the remaining animals were challenged with 3.5×10^5 PFU of FMDV serotype A24, at two sites in the heel bulb of the right rear foot. One day postchallenge (or 2 dpi) another two animals from each group were slaughtered and the remainder of the pigs were monitored for clinical signs until 6 dpc (7 dpi) when they were also slaughtered. Lesion scores of the animals were determined as described in Moraes et al. (37).

Sample collection. Blood was obtained daily to assay for antiviral activity and the presence of pIFN-α and pIFN-γ by enzyme-linked immunosorbent assay (ELISA) and to extract PBMC (see below). Blood and nasal swab specimens were collected daily for the first 7 days after challenge for those animals that were kept alive until the end of the experiment. After euthanasia and exsanguination of the animals at set time points, tissue samples (three different anatomical locations of skin, as well as inguinal and popliteal lymph nodes, and tonsils) were taken and divided in two sets. One set was immersed in RNA later (Ambion, Austin, TX) and stored at −70°C for RNA extraction, and the other was snap-frozen in liquid nitrogen-chilled isopentane and placed in a cryomold embedded in optimal cutting temperature compound (OCT; Sakura Finetek, Torrance, CA) and stored at −70°C for analysis by histopathology and immunohistochemistry (IHC).

Virus titration, antiviral activity, and IFN detection in plasma. Viremia was determined by a standard plaque assay of total blood on BHK-21 cells. Plasma was obtained by centrifugation of heparinized blood at 2,500 rpm for 10 min and examined for antiviral activity by a plaque reduction assay (13). The level of pIFN-α and pIFN-γ in plasma was determined by ELISA (37). Nasal swab specimens were obtained on the day of challenge and daily for 7 days after challenge, and virus was isolated from the swab samples as previously described (37).

Immunohistochemical and histopathological analysis. Frozen 4-μm sections were mounted onto electrostatically charged glass slides (SuperFrost Plus; Fisher Scientific, Worcester, MA) and fixed for 10 min in acetone at −20°C. Thereafter, the slides were kept at −70°C for up to 8 weeks, until they were stained. For immunostaining, the slides were incubated with the following primary antibodies: mouse monoclonal antibody (MAb) anti-porcine SLA-II (AbD Serotec, Raleigh, NC), mouse MAb anti-porcine CD172 (Southern Biotech, Birmingham, AL), mouse MAb anti-porcine CD1 (Southern Biotech), mouse anti-human iNOS (BD Bioscience, Franklin Lakes, NJ), and mouse MAb anti-human Mx1 (kindly provided by Otto Haller, University of Freiburg), which labels porcine Mx1 protein (30). The bound primary antibodies were detected by the avidin-biotin-peroxidase complex technique (Vectastain ABC Kit Elite; Vector, Burlingame, CA) according to the manufacturer's instructions and developed either with 3,3′-diaminobenzidine (Dako, Glostrup, Denmark) or Fast Red TR/naphthol (Sigma, St. Louis, MO). Slides were counterstained with Harry's hematoxylin and coverslipped by using routine methods. To control the specificity of antibody binding, a duplicate negative control serial section treated with nonspecific pri-

mary antibody was used. The positive cells were counted in 10 consecutive fields of 1 mm^2 each per slide. Means and standard deviations of the numbers of labeled cells were calculated, and differences were tested for significance.

Indirect immunofluorescence analysis (IFA). Four percent paraformaldehyde fixed inguinal and popliteal lymph node and skin frozen sections were pretreated with 0.1% saponin (wt/vol) in PBS, blocked with blocking buffer (PBS, 2% fetal bovine serum, 10% porcine serum), and then incubated overnight at 4°C with the primary antibodies mouse MAb anti-porcine CD3 (Southern Biotech), anti-porcine-CD8 (Southern Biotech), rat MAb anti-porcine CD2 (Antigenix America, Huntington Station, NY), mouse anti-porcine CD1 (Southern Biotech), and mouse anti-human CD207/Langerin (Denritics, Dardilly, France). Alexa Fluor 488, Alexa Fluor 594, and Alexa Fluor 647 (Molecular Probes/Invitrogen, Carlsbad, CA)-conjugated secondary antibodies were used for detection. Nuclei were visualized by DAPI (4′,6′-diamidino-2-phenylindole) staining included in ProLong Gold Antifade mounting medium (Invitrogen). Sections were examined in a Nikon 90i fluorescence microscope, and the images were taken with a DSQi1Mc digital camera and NIS-Elements Software, version 3.0 (Nikon, Melville, NY).

The number of positive cells for CD2 and CD8 and negative for CD3 primary antibodies were counted in 10 consecutive fields of 34 mm^2 each per slide, and the percentage of these cells was calculated in relation to the total number of cells per field. Mean and standard deviation of the number of labeled cells were calculated, and differences were tested for significance.

Analysis of ISGs. Expression of several ISGs (see Table S1 in the supplemental material) was analyzed in PBMCs and different tissues isolated from IFN-treated animals. PBMCs were purified from heparinized blood with Lymphoprep (Axis-Shield, Oslo, Norway). RNA was extracted from $\sim 10^7$ cells by utilizing an RNeasy miniprep kit (Qiagen, Valencia, CA). RNA from skin was extracted by using an RNeasy miniprep kit with a modified protocol. Then, 4- to 8-mm^3 sections of skin were pulverized by cooling in liquid nitrogen and crushing. Pulverized tissue was transferred to a tube with RLT buffer (Qiagen), with β-mercaptoethanol (10 μl per ml of RLT buffer) and proteinase K (20 mg/ml), incubated for 10 min at 55°C, and then centrifuged at 10,000 × *g*. Supernatants were mixed with 100% ethanol and passed through an RNeasy minicolumn (Qiagen), and the extraction was completed according to the manufacturer's protocol. Lymphoid, spleen, and tonsils tissue RNA was extracted by mechanical homogenization with a Tissuemiser (Fisher Scientific) in RLT with β-mercaptoethanol. After a homogenate was obtained, the solution was passed through Qiashredder (Qiagen), and RNA was obtained by using an RNeasy extraction kit according to the manufacturer's instructions.

A quantitative real-time reverse transcription-PCR (RT-PCR) was used to evaluate the mRNA levels of several ISGs (16). 18S rRNA or porcine GAPDH (glyceraldehyde-3-phosphate dehydrogenase) were used as the internal control to normalize the values for each sample. The sequences of primers and probes that were used are listed in Table S1 in the supplemental material. Reactions were performed in an ABI Prism 7000 sequence detection system (Applied Biosystems). Relative mRNA levels were determined by comparative cycle threshold analysis (user bulletin 2; Applied Biosystems) utilizing as a reference the samples at 0 dpi from the control groups. We only considered genes upregulated if there was a twofold or greater induction in both animals.

Statistical analyses. Data handling, analysis, and graphic representation was performed by using Prism 2.01 (GraphPad Software, San Diego, CA) or Microsoft Excel. Statistical differences were determined by using a Student *t* test (*, $P < 0.05$; **, $P < 0.01$; ***, $P < 0.005$).

RESULTS

Effect of Ad5-CI-pIFNs on clinical response against FMDV. Based on previous experiments (13, 37), we inoculated animals with 10^9 PFU of Ad5-CI-pIFN-α, 10^{10} PFU of Ad5-CI-pIFN-γ, or a combination of 10^9 PFU of Ad5-CI-pIFN-α and 10^{10} PFU of Ad5-CI-pIFN-γ, respectively. We included two control groups, one inoculated with 10^{10} PFU of Ad5-Blue and one inoculated with PBS. In previous studies these doses of IFN were sufficient to sterilely protect all animals when challenged with 10^5 PFU of FMDV A24 (13, 38). In the present study, animals were challenged with a higher dose (3.5×10^5 PFU of FMDV A24). All of the control animals inoculated with PBS developed viremia at 1 dpc and clinical signs starting at 2 dpc with a significant lesion score by 3 to 4 dpc (Fig. 1a). Similarly, the other control animals inoculated with 10^{10} PFU of Ad5-Blue also developed viremia by 1 dpc (data not shown).

One of the IFN-α-treated pigs never showed clinical signs and only developed a low level viremia at 6 dpc, while the other animal showed a significant delay in both the onset of viremia and clinical disease. i.e., at 4 and 5 dpc, respectively, with a lower lesion score and 1,000- to 10,000-fold lower levels of viremia compared to the controls (Fig. 1b). Animals treated with Ad5-CI-pIFN-γ also showed a delay in the onset of clinical signs, i.e., 3 or 5 dpc, and in the development of viremia, i.e., 2 or 3 dpc, and the level of viremia was 10- to 20-fold lower than the controls (Fig. 1c). Finally, animals that were treated with the combination of Ad5 expressing IFN-α and IFN-γ showed a delay in the onset of the disease comparable to what was observed in the animals inoculated with Ad5-CI-pIFN-α and a lower lesion score compared to the controls and the IFN-γ-inoculated group. However, the levels of viremia were ~10-fold higher than in the IFN-α treated group (Fig. 1d). Although viremia correlated with FMDV in nasal swabs, virus shedding was significantly reduced and delayed in all of the animals treated with IFNs, especially in the Ad5-CI-pIFN-α group, which did not have detectable virus in nasal swabs until 5 dpc (data not shown).

When we analyzed the skin of these animals we observed that, 1 day after the challenge, all animals from the control groups had ballooning degeneration and increased cytoplasmic eosinophilic staining of the cells in the stratum spinosum with acantholysis and areas of necrosis at the site of inoculation, where we could identify the start of vesicle formation (Fig. 2i). Interestingly, in skin from the heel bulb of a foot other than the one inoculated (skin NIS) we also observed vacuolization of keratinocytes of the stratum spinosum of the epidermis and lymphocytic infiltration (Fig. 2e), although macroscopically we did not detect any lesions at this time point. On the other hand, none of the IFN-treated animals showed any microscopic lesions in skin at a site other than the inoculation site (Fig. 2f to h) 1 day after challenge. However, at this time point, IFN-treated animals showed microscopic lesions in the skin at the inoculation site, including cellular vacuolization and karyopyknosis of keratinocytes and the presence of acantholysis in the epidermis (Fig. 2j to l). One day after challenge we could detect the presence of virus by real-time RT-PCR at the inoculation site in all of the control animals, low levels of virus in both animals in the IFN combination group, and in one of two animals in the IFN-α and IFN-γ groups. However, only the control animals and the IFN combination group showed a virus-positive signal in skin at a different location than the inoculation site at 1 dpc (see Table S2 in the supplemental material).

IFN levels and antiviral activity in plasma. All of the animals were assayed for the presence of IFN-α, IFN-γ, and antiviral activity in plasma. Only plasma from the groups inoculated with Ad5-CI-pIFN-α or the combination had antiviral activity and the level was the highest in the Ad5-CI-pIFN-α group (data not shown). The levels of IFN-α detected in animals 1 day after treatment with Ad5-CI-pIFN-α were low (ca. 3.5×10^3 to 5.3×10^3 pg/ml) (Fig. 3) compared to previous experiments in which 1.1×10^5 to 3.0×10^5 pg of protein/ml was detected in the plasma of swine treated with the same dose of Ad5-pIFN-α (28). Surprisingly, animals from the combined

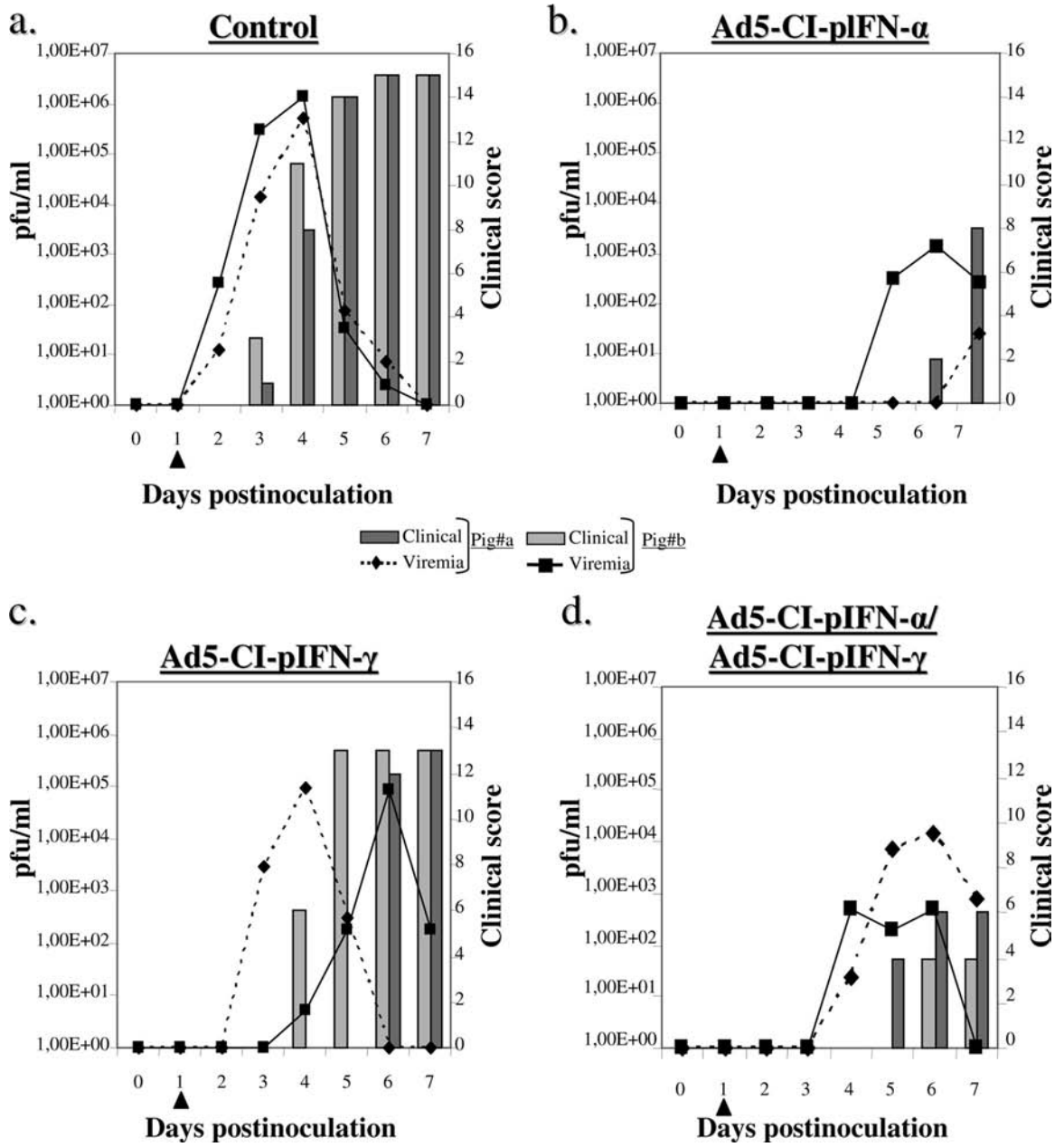

FIG. 1. Clinical outcome and viremia of swine inoculated with Ad5s and challenged with FMDV. Animals were treated with PBS (Control, panel a), Ad5-CI-pIFN-α (panel b), Ad5-CI-pIFN-γ (panel c), or Ad5-CI-pIFN-α/Ad5-CI-pIFN-γ (panel d) and 1 day later (1 dpi, arrowhead) were challenged with FMDV. Two animals from each group (animals a and b) were kept alive until 7 dpi and monitored for clinical disease and viremia. Blood samples were taken to detect viremia (lines, number of PFU/ml of whole blood), and the animals were physically monitored for lesion score (solid bars, number of toes with lesions plus the snout and tongue combined). Only the data from the two animals in each group euthanized at 7 dpi are presented individually in this figure.

treatment group expressed lower levels of IFN-α in plasma than the animals inoculated with Ad5-CI-pIFN-α alone (Fig. 3). Animals inoculated with Ad5-CI-pIFN-γ did not express significant levels of IFN-α protein in plasma (Fig. 3) or detectable levels of IFN-γ (data not shown). However, the levels of IFN detected seemed to be sufficient to produce a delay in the onset of the disease in a dose-dependent manner.

iNOS and Mx1 proteins are expressed in skin in response to IFN. As mentioned above, the level of IFN-γ was undetectable in plasma and IFN-α levels were very low compared to previous experiments. Therefore, we were concerned that we would not be able to detect the upregulation of ISGs induced by the IFN treatment. In order to confirm that the animals inoculated with Ad5-IFNs were systemically expressing and responding to the cytokines, we performed IHC in different tissues, including skin and various lymphoid organs, using iNOS and Mx1 as markers of IFN-γ and -α stimulation, respectively.

One day after inoculation (0 dpc), we observed the presence

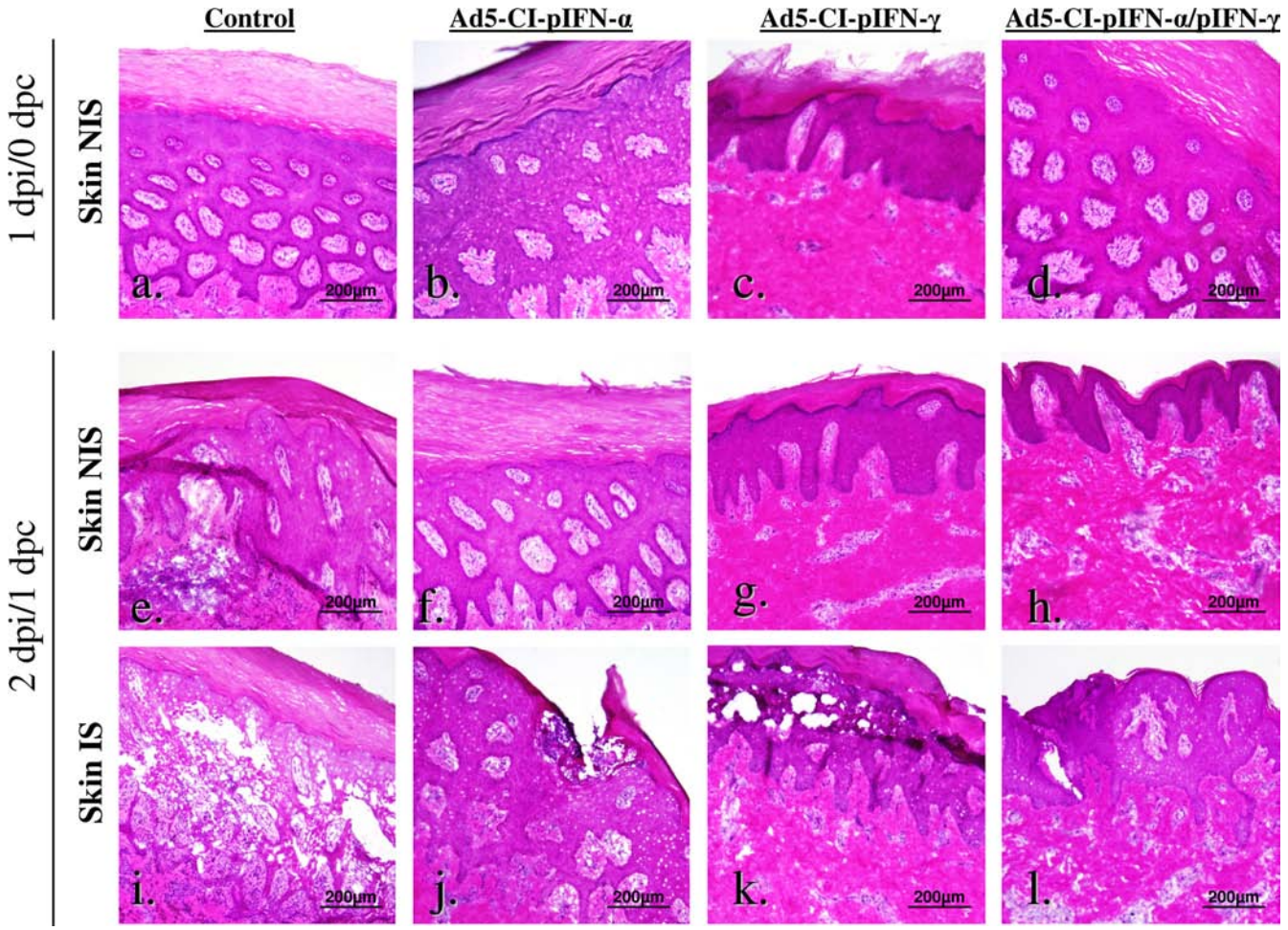

FIG. 2. Tissue sections from skin of swine treated with Ad5-IFNs and challenged 1 day later. Skin from the heel-bulb, at the inoculation site (IS) and noninoculation site on another foot (NIS), of IFN-treated animals (Ad5-CI-pIFN-α [panels b, f, and j], Ad5-CI-pIFN-γ [panels c, g, and k], or Ad5-CI-pIFN-α/Ad5-CI-pIFN-γ [panels d, h, and l]) or control animals (panels a, e, and i) were harvested 1 day after the IFN treatment (0 dpc) and 1 day after the challenge (1 dpc) and routinely stained for histopathologic analysis.

of positive cells for iNOS in the tonsils of all treated animals compared to controls (Fig. 4 compare panels e, i, and m to panel a). At the same time points, skin of treated animals also showed a diffuse iNOS positive signal in the stratum basale of the epidermis (Fig. 4f, j, and n). The tonsils of Ad5-CI-pIFN-α-treated animals, alone or in combination with Ad5-CI-pIFN-γ, were also reactive against anti-Mx1 MAb compared to control animals or animals inoculated with Ad5-CI-pIFN-γ (Fig. 4, compare panels g and o to panels c and k). In animals treated with Ad5-CI-pIFN-α the positive reaction was not only localized in the epithelium of the tonsils but also in the lymphoid follicles (Fig. 4g). Skin of animals inoculated with Ad5-CI-pIFN-α showed an increase in the Mx1 signal localized to the stratum basale and basal cells of the stratum spinosum (Fig. 4h). However, animals inoculated with Ad5-CI-pIFN-γ did not show any positive staining for Mx1 (Fig. 4l) and resembled the skin of control animals (Fig. 4d). Although Mx1 is not directly involved in the inhibition of FMDV replication (14), and we currently do not know whether iNOS has anti-FMDV activity, distribution of these proteins in the skin is indicative of systemic antiviral responses induced by type I and II IFNs.

Langerhans DCs increased in skin after IFN treatment. The major FMDV replication organ and the main site of macroscopic lesions in FMD is the skin (3). Although we have reported that either IFN-α or IFN-γ treatment can protect against FMDV replication, and their action is synergistic when inoculated in combination (13, 37), we have never examined the possible role of various immune cells in the IFN-induced FMDV-protective response. Swine DCs, including skin DCs, are $CD1^{+,}$ $SLAII^{+}$ and $CD172^{+}$ (6, 51) and skin DCs also express Langerin (41). To study the possible infiltration of DCs in the epidermis after IFN treatment, skin cross-sections were stained using different antibody combinations: CD1/SLAII, CD1/CD172, CD172/SLAII, or each antibody separately. Serial skin sections from a naive pig demonstrated that epidermal DCs, mainly localized in the stratum basale of the epidermis, were $CD1^{+}$, $SLAII^{+}$, and $CD172^{+}$. To facilitate the analysis of this cell population, we examined IHC staining against the CD1 cellular marker (Fig. 5), since the three antibodies hybridized to the same cell in the epidermis (data not shown). Skin from Ad5-CI-pIFN-α-treated animals had a higher number of $CD1^{+}$ cells at the time of challenge (1 dpi/0 dpc) (Fig.

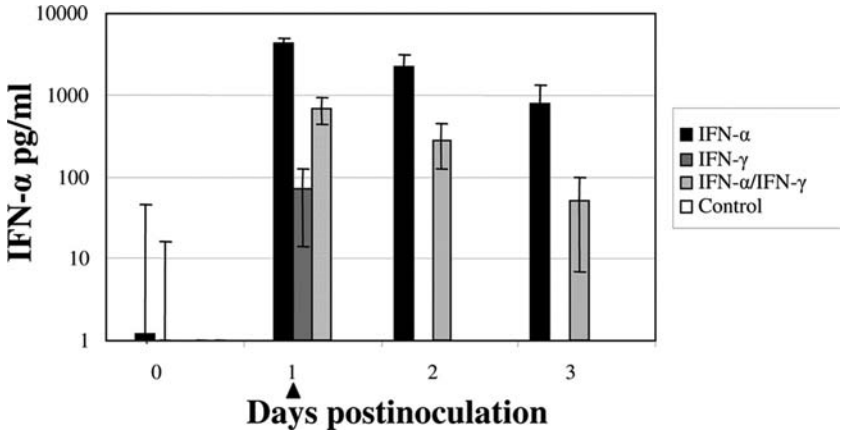

FIG. 3. IFN-α in plasma of Ad5-IFN-treated animals and control animals detected by ELISA. Plasma samples were collected at different times prior to and after administration of Ad5s or PBS, and the amounts of IFN-α were detected by ELISA. An arrowhead indicates the day of challenge.

5a, panel 3) compared to control animals (either the PBS [Fig. 5a, panel 1] or the Ad5-Blue-inoculated groups [data not shown]). LCs of animals inoculated with Ad5-CI-pIFN-α not only increased in number but also showed more dendrites, and they were spread throughout the stratum basale and stratum spinosum (Fig. 5a, panels 3 and 4, note the arrowheads). Similar findings were observed in animals inoculated with Ad5-CI-pIFN-γ at either 1 or 2 days after the treatment (0 dpc or 1 dpc) (Fig. 5a, panels 5 and 6), although the number of $CD1^+$ cells was slightly lower. Skin from animals treated with the combination of Ad5-CI-pIFN-α and Ad5-CI-pIFN-γ resembled the pattern of skin DC distribution in the two other treated groups (Fig. 5a, panels 7 and 8). When we double stained for CD1 and Langerin, we observed that all $CD1^+$ cells from the epidermis were Langerin-positive cells (Fig. 5b). In order to analyze the significance of these findings, $CD1^+$ cells from 10 consecutive 1-mm^2 fields were counted in the skin samples of each animal examined (see Materials and Methods). The difference between the control group and the IFN-treated animals was significant ($P < 0.05$) (Fig. 5c). Interestingly, ex vivo skin DCs from animals inoculated with Ad5-CI-pIFN-α and Ad5-CI-pIFN-γ showed upregulated expression of CD80/CD86, molecules that are directly correlated with the maturation of DCs (data not shown).

To determine whether NK cells might be infiltrating the skin, we also examined skin utilizing triple IFA. Porcine NK cells are included in the $CD2^+/CD8^+/CD3^-$ cell compartment (62). We could not detect any $CD2^+/CD8^+/CD3^-$ cells infiltrating the epidermis, nor in proximal areas of the dermis prior to (1 dpi/0 dpc) and after (2 dpi/1 dpc) challenge in IFN-treated animals (data not shown), suggesting that direct interaction between DCs and NK cells induced by IFN treatment, if any, does not occur in the skin.

Distribution of NK cells in lymphoid organs. Although we could not detect the presence of NK cells in the skin, we hypothesized that IFN treatment could induce upregulation of cytokine production by skin DCs that might stimulate the recruitment, proliferation or activation of NK cells into the draining lymph nodes. To test this hypothesis, we performed CD2/CD3/CD8 IFA in inguinal and popliteal lymph nodes (Fig. 6a and b). The majority of cells distributed in the paracortex of the inguinal and popliteal lymph nodes, either in the central or peripheral deep cortical units, were $CD3^+$ (Fig. 6a) but some $CD2^+/CD8^+/CD3^-$ cells (NK cells) could be observed (Fig. 6a, asterisks). Moreover, in agreement with previous data published by Ferlazzo et al. (22), naive animals showed a low percentage of NK cells present in peripheral lymph nodes, mainly colocalized with T cells in the paracortex (data not shown) (21). Quantification of the percentage of NK cells per 34-mm^2 field in inguinal and popliteal draining lymph nodes of IFN-treated animals and control pigs showed a statistically significant increase in the number of NK cells in all treated animals compared to the controls at 1 (0 dpc) and 2 dpi (1 dpc) (Fig. 6b).

Proinflammatory cytokine induction in skin and lymph nodes after IFN treatment. Upon activation, DCs secrete a number of cytokines, including IL-15, IL-18, and IL-12, which upregulate NK cell cytotoxicity (34). As explained above, we hypothesized that the increase of NK cells in lymph nodes would be a consequence of secretion of proinflammatory cytokines by DCs that could result in recruitment and proliferation/activation of NK cells in lymph nodes. To test this hypothesis, we examined skin and lymph nodes for the upregulation of IL-15, IL-18, and IL-12 mRNA and their receptors (IL-15R, IL-18R, and IL-12R) after IFN treatment. In the skin we found that IL-18 was induced in all IFN-treated groups by 1 dpi, but there was no or reduced induction by 2 dpi (Fig. 7a). In contrast, IL-15, which only slightly increased in the IFN-α/γ group by 1 dpi, showed higher expression levels in the IFN-α group by 2 dpi concomitant with enhanced IL-15R levels. The slightly increased levels of IL-15 and IL-15R were maintained in the IFN-α/γ group at 0 and 1 dpi (Fig. 7a). At the same time, there was an upregulation of IL-12R in all IFN-treated groups at 1 dpi, possibly induced by IL-15 or IL-18 (Fig, 7a), as previously described (20, 40). In correlation with the upregulation of mRNA levels of IL-15 and IL-18 in skin we observed upregulation of IL-15, IL-18, and IL-12 and IL-15R and IL-18R in the popliteal lymph node in the group inoculated with IFN-α and IL-15 and IL-15R in the combination group at 1 dpi, but the induction decreased by 2 dpi (Fig. 7b). In the inguinal lymph node we observed more consistent changes by 2 dpi, with

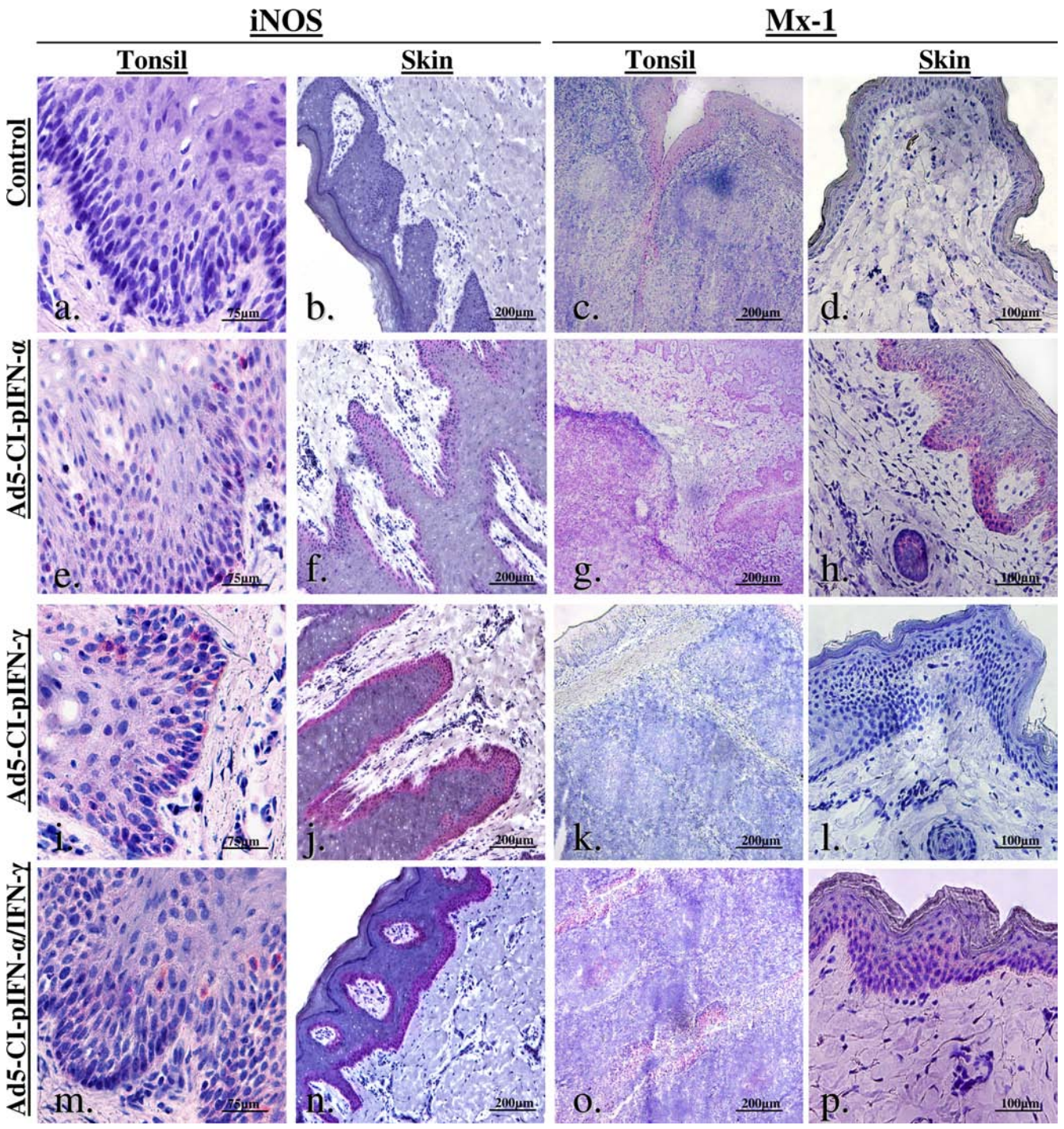

FIG. 4. IHC staining of iNOS- and Mx1-positive cells in the tonsils and skin of Ad5-IFN-treated animals. Tissues from the tonsils and skin of control swine (panels a to d), swine treated with Ad5-CI-pIFN-α (panels e to h), Ad5-CI-pIFN-γ (panels i to l), or Ad5-CI-pIFN-α/Ad5-CI-pIFN-γ (panels m to p) 1 day after the treatment (0 dpc) were harvested and stained to detect iNOS- or Mx1-positive cells. The bound primary antibody was detected by the avidin-biotin-peroxidase complex technique and developed with Fast Red TR/naphthol, and positivity is indicated in bright purple. Sections were counterstained with Harry's hematoxylin (blue).

upregulation of IL-18R in the IFN-α group; IL-18R and IL-12R in the IFN-γ group; and IL-15R, IL-18R, and IL-12R in the IFN-α/γ group (Fig. 7c). Although there is a variable effect among IFN treatments, the correlation between the upregulation of these cytokines and the increased presence of NK cells in the lymph nodes suggest that NK cell proliferation might be induced by these cytokines.

IFN-α and IFN-γ induce several genes in different organs. We also examined the effect of IFN treatment on the induction of a number of ISGs, including genes with direct antiviral

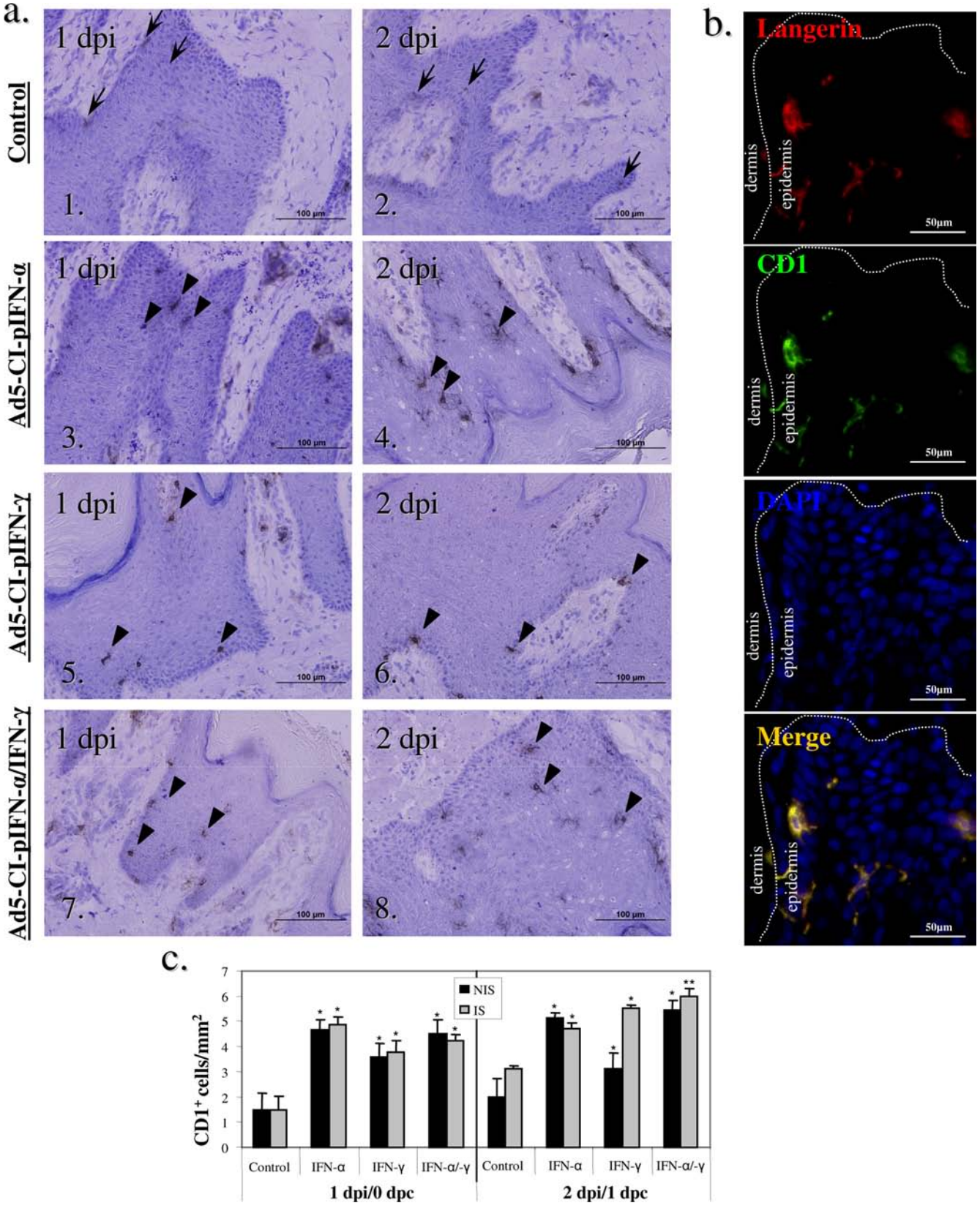

FIG. 5. IHC detection of DCs in skin from the heel-bulb of swine. (a) Skin from control animals or Ad5-IFN-treated swine was harvested 1 dpi (0 dpc; panels 1, 3, 5, and 7) and 2 dpi (1 dpc; panels 2, 4, 6, and 8) after Ad5 treatment, and positive cells were detected by IHC using the avidin-biotin-peroxidase complex technique and developed with 3,3′-diaminobenzidine, which gives a brown product where primary antibody binds (dark brown); sections were counterstained with Harry's hematoxylin. Arrows indicate the positive staining for DCs in control animals; these cells

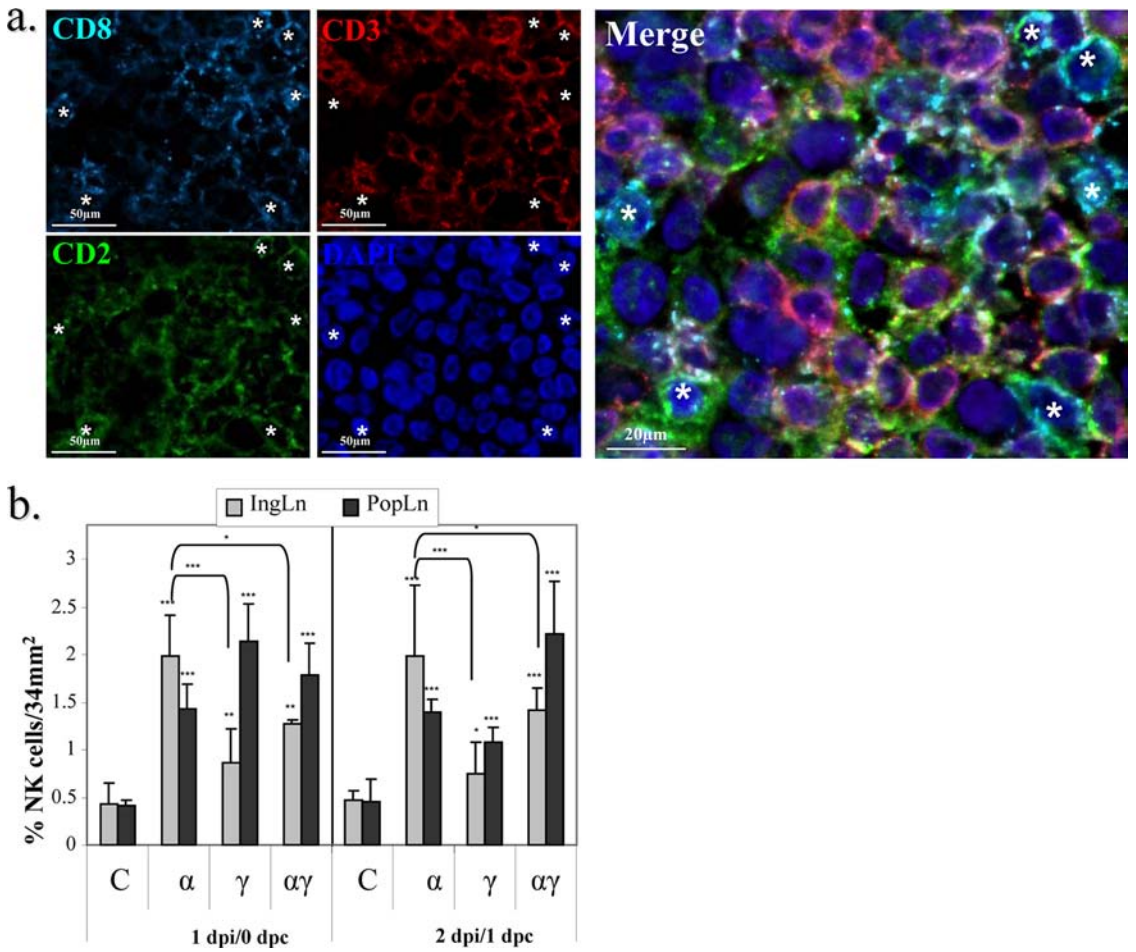

FIG. 6. Distribution of NK cells in lymph nodes. (a) IFA detection of CD2 (green), CD8 (light blue) and CD3 (red) cellular markers in popliteal lymph node cryostat sections of Ad5-CI-pIFN-α treated swine. The $CD2^+$ $CD8^+$ $CD3^-$ cell compartment contain porcine NK cells. $CD2^+$ $CD8^+$ $CD3^-$ cells are marked with an asterisk in the merge picture and in the individual color pictures showing positive signal for CD2 and CD8 and negative for CD3. Nuclei were stained with DAPI (dark blue). (b) The findings of semiquantitative analysis of the percentage of NK cells in areas of 34-mm^2 sections of inguinal (light gray) and popliteal (dark gray) lymph nodes of Ad5-CI-pIFN-α-, Ad5-CI-pIFN-γ -, or Ad5-CI-pIFN-α/Ad5-CI-pIFN-γ-treated animals and controls at 1 and 2 days after the treatment (0 and 1 dpc, respectively) are represented. Statistical analysis of the treated animals with the control group showed significant differences between the groups (*, $P < 0.05$; **, $P < 0.01$; ***, $P < 0.005$).

activity, as well as chemokines that are involved in attraction and activation of various immune cells (Fig. 8 and 9). Previously, we demonstrated that inoculation of pigs with Ad5-CI-pIFN-α in combination with Ad5-CI-pIFN-γ induced the synergistic upregulation of INDO and IP-10 in PBMCs (37). In the present study we observed similar results in PBMCs at both 1 dpi (Fig. 8 and 9a) and 2 dpi (Fig. 8 and 9b). Mx1 and OAS were upregulated in PBMCs upon IFN-α treatment, but there was also upregulation of INDO in the IFN-γ group (Fig. 8). In the inguinal lymph node we observed consistent upregulation of Mx1 and OAS induced by IFN-α, and synergistic upregulation of INDO by the combination of type I and II IFNs (Fig. 8). The popliteal lymph node showed a similar upregulation pattern as in the inguinal lymph node, but in addition there was an upregulation of iNOS (Fig. 8). Interestingly, we observed a slight upregulation of the chemokines, MIP-3α and MIP-1α in the inguinal and popliteal lymph nodes, respectively, which were not upregulated in the PBMCs (Fig. 8). In the skin, the effect of mRNA upregulation of chemokines involved in maturation/chemoattraction of DCs was evident, particularly in the heel bulb (skin IS and skin NIS), with MCP-1 upregulated by IFN treatment and MIP-3α synergistically upregulated at both 1 dpi and 2 dpi (Fig. 8). At the same time points skin showed upregulation of Mx1 and OAS by IFN-α and synergis-

appeared small and localized in the stratum basale of the epidermis. Arrowheads indicate the positive staining of DCs in treated animals; these cells appeared larger than positive cells in control animals, showed dendrites, and were localized along the stratum spinosum. (b) Double-IFA detection of CD207/Langerin (red) and CD1 (green) in the epidermis of the heel-bulb. Nuclei were stained with DAPI (blue). (c) Quantification of the number of positive cells in the tissue sections was performed as described in Materials and Methods. The number of positive cells is significantly higher in IFN-treated animals than in the control animals (*, $P < 0.05$; **, $P < 0.01$).

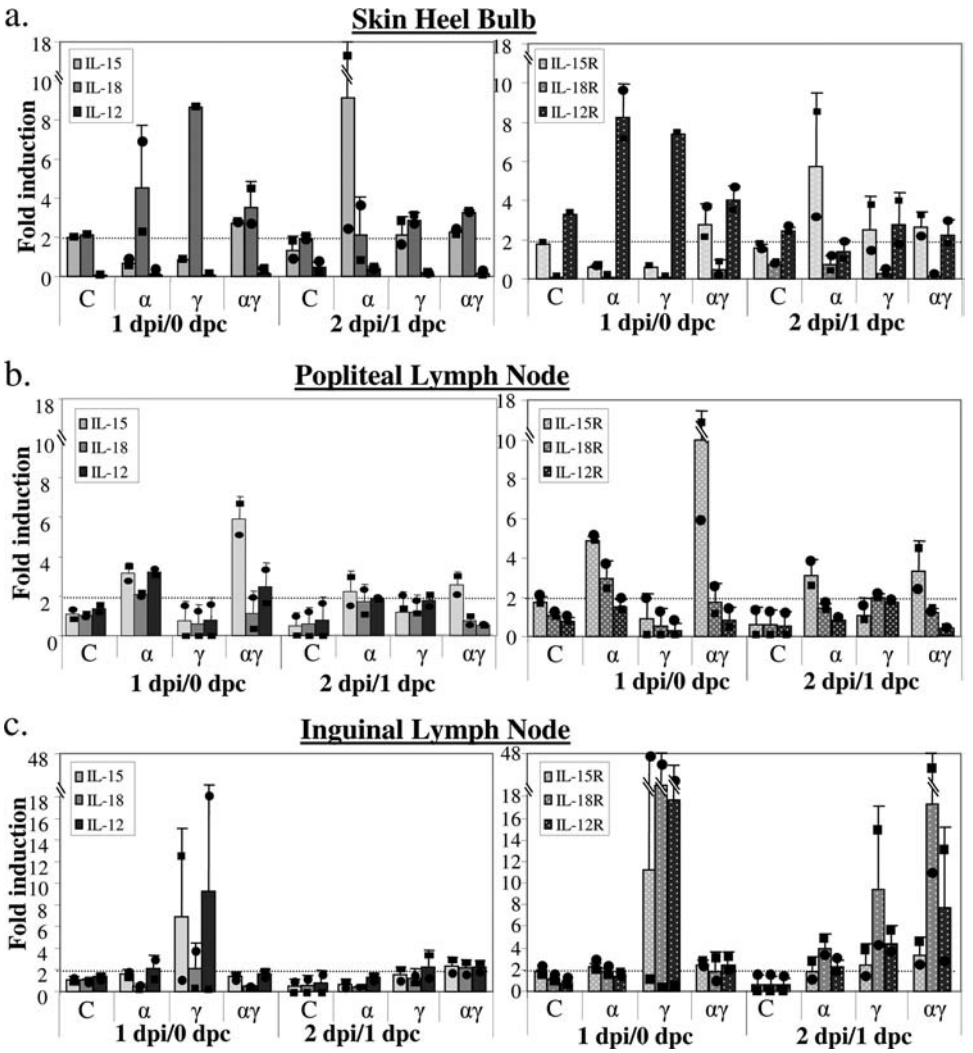

FIG. 7. NK-stimulating proinflammatory cytokines in skin and lymphoid organs. The proinflammatory cytokines IL-15, IL-18, and IL-12 and their receptors—IL-15R, IL-18R, and IL-12R—were analyzed by RT-PCR in skin (a) and in the popliteal (b) and inguinal (c) lymph nodes at 1 and 2 days after the treatment (1 and 2 dpi, respectively). We considered genes upregulated when both animals in the group showed values of ≥2 (dotted line).

tic upregulation of INDO by the combination treatment at 1 and 2 dpi (Fig. 8).

It has been shown that after IFN treatment, induced IP-10 has several roles in the innate immune response, including chemoattraction of NK cells and DCs (32, 58). One day after treatment, IP-10 was upregulated by type I and type II IFN or the combination in lymph nodes and all anatomical locations of skin examined and was synergistically upregulated in PBMCs (Fig. 9a), as previously described (37). Two days after treatment there was a similar induction of IP-10 in the IFN-α-treated group and synergistic upregulation in PBMCs (Fig. 9b). However, induction of IP-10 was reduced in lymph nodes from IFN-γ- and combination-treated animals compared to 1 dpi (Fig. 9b). At 6 days after challenge all control animals showed several genes induced in all organs examined but predominantly in the skin, probably due to the effect of viral replication (Fig. 8 and 9c). Interestingly, IP-10 was never upregulated in the control animals in any organ examined, but it was upregulated in all IFN-treated animals, with synergistic effects in PBMC and the popliteal lymph node at 7 dpi (Fig. 9c). These results suggest that the expression of IP-10 in response to IFN treatment, and its correlation with the increase in the number of cells from the innate immune system (DCs and NK cells) in the skin and lymph nodes, respectively, might be involved in the tissue-specific mechanism of protection against FMDV conferred by IFNs.

DISCUSSION

In this study we have attempted to gain a comprehensive understanding of the IFN-induced mechanisms that result in the rapid protection of swine against FMDV challenge. Previously, we described that protection of animals inoculated with Ad5-pIFN-α correlated with the level of IFN-α expression in plasma (13), while in animals inoculated with Ad5-pIFN-γ alone or with the combination of both IFNs protection corre-

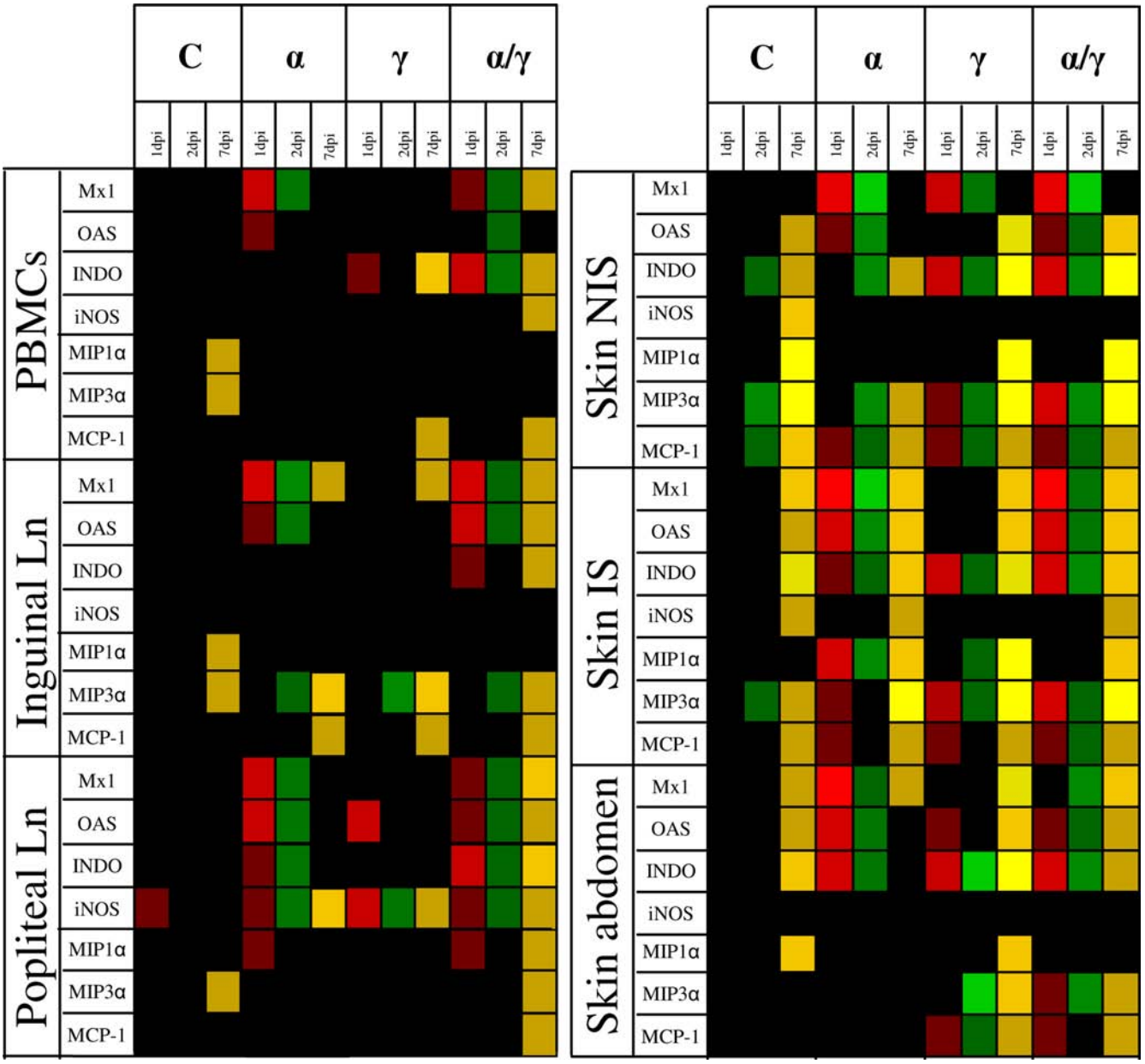

FIG. 8. Induction of ISGs in swine PBMC, inguinal lymph nodes, popliteal lymph nodes, and skin. RT-PCR was used to analyze the upregulation of ISGs in different organs. The relative mRNA levels were determined by comparative cycle threshold analysis, utilizing as a reference the samples at 0 dpi from the control group, and the upregulation of genes at different time points are represented as follows. At 1 dpi: light red, >50-fold; red, 30- to 50-fold; dark red, 10- to 30-fold; brown, 2- to 10-fold. At 2 dpi: lime green, >50-fold; green, 30- to 50-fold; forest green, 10- to 30-fold; dark green, 2- to 10-fold. At 7 dpi: bright yellow, >50-fold; yellow, 30- to 50-fold; orange, 10- to 30-fold; mustard, 2- to 10-fold. At all of the time points, a fold induction of <2 (black) was not considered upregulated.

lated with upregulation in the PBMC of ISGs that have either direct antiviral activity, INDO and OAS, or immunomodulatory roles, IP-10 (37). In the present study, we show for the first time proliferation/migration of immune cells (DCs and NK) to skin and lymphoid organs in response to IFN treatment. In addition, we confirm the IFN-induced upregulation in the PBMC of several ISGs involved in antiviral responses, as previously described, but we also show tissue-specific effects of IFN treatment in the skin and lymph nodes with increased expression of cytokines and chemokines involved in activation of the innate immune system.

Ad5 vectors containing porcine type I and II IFN alone or in combination were used to treat swine. Two animals in each group were euthanized prior to and at 1 and 6 dpc. Clinically, all animals in the IFN-inoculated groups had delayed and less severe disease compared to the control animals, and one animal in the IFN-α-treated group had no clinical disease at 6 dpc. These results appear to differ from our previous data since a dose of 10^9 PFU of Ad5-pIFN-α completely protected swine from FMDV challenge 1 to 3 days after administration (13, 36). However, in these earlier experiments the level of IFN-α expression in protected swine was 11 to 30,000 pg/ml, which is

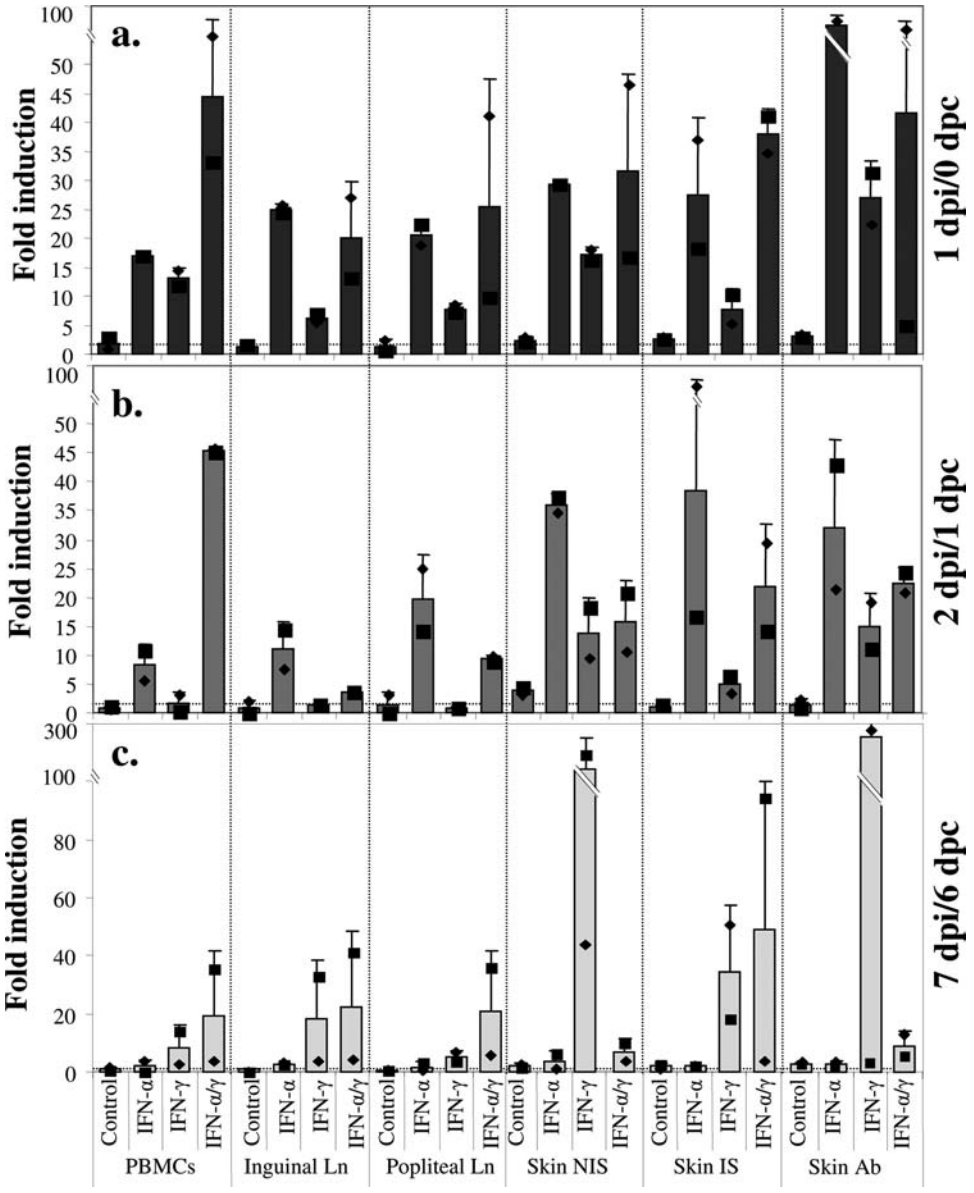

FIG. 9. IP-10 expression in different organs. One day after treatment (1 dpi/0 dpc) (a), 2 days after treatment (2 dpi/1 dpc) (b), and 7 days after treatment (7 dpi/6 dpc) (c) samples from blood, lymph nodes, and skin from the heel-bulb either in the noninoculation site (Skin NIS), in the inoculation site (Skin IS), or from the abdomen (Skin Ab) were taken and analyzed for the upregulation of mRNA levels of IP-10 compared to animals before treatment. Control animals were treated with Ad5-Blue or PBS. Values below 2 (dotted line) are not considered upregulated.

considerably higher than the ~5,000 pg/ml expressed in the Ad5-CI-pIFN-α-inoculated group in this experiment. At this lower level of IFN-α expression we previously found that swine have delayed and less severe clinical disease after challenge, similar to our present experiment. Furthermore, in this experiment the FMDV challenge dose is ~20-fold higher than recommended by the OIE and 3.5-fold higher than used previously (37). The relatively low levels of IFN-α detected in this experiment suggested that the Ad5 vector was not expressing the transgene as efficiently possibly because of the use of a cytomegalovirus (CMV) promoter with an enhancer (CI promoter [37]) compared to only the CMV promoter previously used (13, 36) or the use of a higher passage level of the Ad5 vectors, compared to the earlier study (13), may contain higher amounts of WT Ad5 lacking the pIFN genes.

Since the level of IFN-α was low and we could not detect IFN-γ expression in plasma after Ad5-CI-pIFN-γ administration, we examined whether ISG products could be detected. We demonstrated systemic expression of proteins induced by type I and type II IFNs. The detection of Mx1 and iNOS in tonsils and skin of IFN-treated animals indicates that, although expression of the delivered IFNs by Ad5 is low, especially IFN-γ, it is still sufficient to induce ISG expression.

We found that all animals inoculated with IFN have a statistically significant increase in the number of Langerhans DCs in the skin and NK cells in the lymph nodes. These changes

correlated with (i) the upregulation of mRNA levels of IL-15 and IL-18 in the skin, two cytokines that have been shown to be produced by activated DCs (4, 34) and that are involved in porcine NK cell proliferation and activation (46, 57); (ii) a slight increase of IL-15, IL-18, and IL-12 in the popliteal lymph node at 1 dpi and a upregulation of IL-15R and IL-18R at 1 dpi; (iii) the increase in the mRNA levels of IL-18R in the inguinal lymph node, the upstream draining lymph node, only at 2 dpi in all IFN-treated groups. It is important to mention the absence or low levels of IL-12 upregulation in these tissues, a cytokine involved in activation of NK cells (7). However, there is evidence that for other viral infections, such as lymphocytic choriomeningitis virus, there is no induction of IL-12-dependent IFN-γ production by NK cells (43). In the case of FMDV infection, this might be compensated for by the observed upregulation of IL-18, which has two IL-12-independent effects on NK cells, the stimulation of IFN-γ and production and enhancement of perforin-dependent cytotoxicity (2). On the other hand, IL-15, which was also upregulated in our study, stimulates NK cell activity against virus-infected cells (1), which may be physiologically relevant in the innate immune response during the course of FMDV infection. Whether the increase in the number of LCs in skin and NK cells in the lymph nodes is directly correlated with the upregulation of proinflammatory cytokines or whether these factors play a role in protection against FMDV requires further investigation. However, it has been demonstrated that NK cells are rapidly recruited to lymph nodes upon DC activation (33). Furthermore, preliminary data indicate that there is maturation of skin DCs in IFN-α- and IFN-γ-treated animals compared to controls, as measured by upregulation of CD80/CD86 molecules. In addition, preliminary studies showed that NK cell killing activity is activated in IFN-α- and IFN-α/γ-treated animals at 1 to 2 dpi, while there is a delay and a lower level of killing activity in IFN-γ-treated animals. Hence, the pathways involving NK cell cytokine responses due to possible cross talk with activated/mature DCs and the resultant induction of an FMDV-antiviral state are intricate and perhaps even more complex than currently appreciated. Nevertheless, the data presented here have yielded important findings that will presumably help focus our examination of the role of NK cell responses in protection against FMDV infection.

Concomitant with these effects, IFN treatment generated a significant upregulation of the chemokine IP-10 in PBMCs, lymph nodes, and skin. This chemokine is involved in the recruitment, proliferation, and activation of NK cells (54) and has been demonstrated to have a protective effect in mice infected with a number of viruses, including mouse hepatitis virus (58), coxsackievirus B3 (62), dengue virus (11), and respiratory syncytial virus (32), but not in Theiler's murine encephalomyelitis virus (TMEV) (59). It has also been shown that IP-10 is rapidly but transiently induced by Ad5 vectors delivered systemically or within the liver or lung (39, 54). Although we have noted that our control vector, Ad5-Blue, induces a rapid upregulation of IFN-α protein by 4 h after intramuscular administration (36) and induction of a number of cytokines/chemokines, including IP-10, by 6 h postinfection, these effects were not detectable by 24 h postinfection (36) (Fig. 8 and 9). Furthermore, we have shown that Ad5-Blue-inoculated swine are not protected from challenge with FMDV (13, 45). Thus, the rapid but transient induction of numerous genes by the Ad5 vector does not appear to be involved in the protection of swine against FMDV induced by Ad5-pIFN.

The chemokines MIP-3α and MCP-1 were also upregulated after IFN treatment, mainly in the skin. These chemokines are involved in the recruitment and proliferation of DCs and NK cells and have been shown to be coordinately induced after murine cytomegalovirus infection (48). In particular, MIP-3α has been described to control the migration of skin DCs (9). Therefore, the upregulation of these chemokines may be involved in the observed increase of DCs in IFN-treated animals which may have a role in the protection of the animals against FMDV.

Interestingly, we did not detect upregulation of IP-10 in control animals challenged with FMDV at any time or in any of the samples examined even at 7 dpi/6 dpc when numerous other genes, including MCP-1, MIP-3α, and MIP-1α, were induced. These results are in contrast to the significant induction of IP-10 observed in mice infected with a variety of viruses, including dengue virus (11), respiratory syncytial virus (32), and mouse hepatitis virus (58), as well as two members of the picornavirus family, coxsackievirus B3 and TMEV (59, 62). In a recent study, the cytokine IL-10 has been proposed as an immunosuppressive factor involved in the regulation of the adaptive response to FMDV infection (18). Increased amounts of IL-10 inhibit the action of monocytes, macrophages, and NK cells during the immune response to viral infection and inhibit the synthesis of proinflammatory cytokines (23, 55). Furthermore, it has been shown that IL-10 can suppress IP-10 gene transcription by inhibiting lipopolysaccharide-induced synthesis of type I IFNs (55). It will be interesting to examine whether the induction of IL-10 during FMDV infection plays a role in the suppression of IP-10 transcription.

Based on our results, we hypothesize that one or more of the above chemokines (or others not yet examined) may be involved in the recruitment/proliferation and activation of DCs and NK cells in IFN-treated animals and that the maturation of these cells has a role in the control of FMDV replication. However, at this time, we cannot confirm this hypothesis nor can we speculate about the sequence of events leading to the increased numbers of DCs and NK cells. To follow these events in more detail we plan to pursue several approaches, including examining earlier time points after Ad5-IFN administration to swine and utilizing model systems that will allow us to demonstrate direct involvement of various cytokines/chemokines in inhibition of FMDV replication.

It is possible that both the IFN-induced antiviral and immunomodulatory activities have roles in protection of swine against FMD. Therefore, it will be of interest to identify the specific players in these processes with the goal of developing a more robust strategy to induce rapid protection in both swine and cattle.

ACKNOWLEDGMENTS

This research was supported in part by the Plum Island Animal Disease Research Participation Program administered by the Oak Ridge Institute for Science and Education through an interagency agreement between the U.S. Department of Energy and the U.S. Department of Agriculture (appointment of Fayna Diaz-San Segundo and Camila C. A. Dias), by CRIS project number 1940-32000-053-00D, ARS, USDA (M. J. Grubman and T. de los Santos) and by reimburs-

able agreement 60-1940-7-047 with the Department of Homeland Security (M. J. Grubman).

We thank Noemi Sevilla, CISA-INIA, Valdeolmos, Madrid, Spain, for helpful discussions and suggestions. We also thank Harry Dawson, USDA, ARS, Nutrient Requirements and Function Laboratory, Beltsville, MD, for creating the PIN library with the recommendations of RT-PCR conditions for measuring swine gene expression. Finally, we thank the animal care staff at the Plum Island Animal Disease Center for their professional support and assistance.

REFERENCES

1. **Ahmad, A., E. Sharif-Askari, L. Fawaz, and J. Menezes.** 2000. Innate immune response of the human host to exposure with herpes simplex virus type 1: in vitro control of the virus infection by enhanced natural killer activity via interleukin-15 induction. J. Virol. **74:**7196–7203.
2. **Akira, S.** 2000. The role of IL-18 in innate immunity. Curr. Opin. Immunol. **12:**59–63.
3. **Alexandersen, S., Z. Zhang, A. I. Donaldson, and A. J. Garland.** 2003. The pathogenesis and diagnosis of foot-and-mouth disease. J. Comp. Pathol. **129:**1–36.
4. **Andoniou, C. E., S. L. H. van Dommelen, V. Voigt, D. M. Andrews, G. Brizard, C. Asselin-Paturel, T. Delale, K. J. Stacey, G. Trinchieri, and M. A. Degli-Esposti.** 2005. Interaction between conventional dendritic cells and natural killer cells is integral to the activation of effective antiviral immunity. Nature Immunol. **214:**331–341.
5. **Basler, C. F., and A. Garcia-Sastre.** 2002. Viruses and the type I interferon antiviral system: induction and evasion. Int. Rev. Immunol. **21:**305–337.
6. **Bautista, E. M., D. Gregg, and W. T. Golde.** 2002. Characterization and functional analysis of skin-derived dendritic cells from swine without a requirement for in vitro propagation. Vet. Immunol. Immunopathol. **88:**131–148.
7. **Biron, C. A., K. B. Nguyen, G. C. Pien, L. P. Cousens, and T. P. Salazar-Mather.** 1999. Natural killer cells in antiviral defense: function and regulation by innate cytokines. Annu. Rev. Immunol. **17:**189–220.
8. **Brown, Z., M. E. Gerritsen, W. W. Carley, R. M. Strieter, S. L. Kunkel, and J. Westwick.** 1994. Chemokine gene expression and secretion by cytokine-activated human microvascular endothelial cells. Differential regulation of monocyte chemoattractant protein-1 and interleukin-8 in response to interferon-gamma. Am. J. Pathol. **145:**913–921.
9. **Caberg, J. H., P. Hubert, L. Herman, M. Herfs, P. Roncarati, J. Boniver, and P. Delvenne.** 2008. Increased migration of Langerhans cells in response to HPV16 E6 and E7 oncogene silencing: role of CCL20. Cancer Immunol. Immunother. **58:**39–47.
10. **Charbonnier, A. S., N. Kohrgruber, E. Kriehuber, G. Stingl, A. Rot, and D. Maurer.** 1999. Macrophage inflammatory protein 3alpha is involved in the constitutive trafficking of epidermal Langerhans cells. J. Exp. Med. **190:**1755–1768.
11. **Chen, J. P., H. L. Lu, S. L. Lai, G. S. Campanella, J. M. Sung, M. Y. Lu, B. A. Wu-Hsieh, Y.-L. Lin, T. E. Lane, A. D. Luster, and F. Liao.** 2006. Dengue virus induces expression of CXC chemokine ligand 10/IFN-γ-inducible protein 10, which competitively inhibits viral binding to cell surface heparin sulfate. J. Immunol. **177:**3185–3192.
12. **Chinsangaram, J., M. Koster, and M. J. Grubman.** 2001. Inhibition of L-deleted foot-and-mouth disease virus replication by alpha/beta interferon involves double-stranded RNA-dependent protein kinase. J. Virol. **75:**5498–5503.
13. **Chinsangaram, J., M. P. Moraes, M. Koster, and M. J. Grubman.** 2003. Novel viral disease control strategy: adenovirus expressing alpha interferon rapidly protects swine from foot-and-mouth disease. J. Virol. **77:**1621–1625.
14. **Chinsangaram, J., M. E. Piccone, and M. J. Grubman.** 1999. Ability of foot-and-mouth disease virus to form plaques in cell culture is associated with suppression of alpha/beta interferon. J. Virol. **73:**9891–9898.
15. **Della Chiesa, M., S. Sivori, R. Castriconi, E. Marcenaro, and A. Moretta.** 2005. Pathogen-induced private conversations between natural killer and dendritic cells. Trends Microbiol. **13:**128–136.
16. **de los Santos, T., S. de Avila Botton, R. Weiblen, and M. J. Grubman.** 2006. The leader proteinase of foot-and-mouth disease virus inhibits the induction of beta interferon mRNA and blocks the host innate immune response. J. Virol. **80:**1906–1914.
17. **Der, S. D., A. Zhou, B. R. G. Williams, and R. H. Silverman.** 1998. Identification of genes differentially regulated by interferon α, β, or γ using oligonucleotide arrays. Proc. Natl. Acad. Sci. U. S. A. **95:**15623–15628.
18. **Diaz-San Segundo, F., T. Rodriguez-Calvo, A. de Avila, and N. Sevilla.** 2009. Immunosuppression during acute infection with foot-and-mouth disease virus in swine is mediated by IL-10. PLoS One **4**:1–11.
19. **Díaz-San Segundo, F., F. J. Salguero, A. de Avila, M. M. de Marco, M. A. Sanchez-Martín, and N. Sevilla.** 2006. Selective lymphocyte depletion during the early stage of the immune response to foot-and-mouth disease virus infection in swine. J. Virol. **80:**2369–2379.
20. **Fantuzzi, L., P. Puddu, B. Varano, M. Del Cornò, F. Belardelli, and S. Gessani.** 2000. IFN-alpha and IL-18 exert opposite regulatory effects on the IL-12 receptor expression and IL-12-induced IFN-gamma production in mouse macrophages: novel pathways in the regulation of the inflammatory response of macrophages. J. Leukoc. Biol. **68:**707–714.
21. **Fehniger, T. A., M. A. Cooper, G. J. Nuovo, M. Cella, F. Facchetti, M. Colonna, and M. A. Caligiuri.** 2003. $CD56^{bright}$ natural killer cells are present in human lymph nodes and are activated by T-cell derived IL-2: a potential new link between adaptive and innate immunity. Blood **101:**3052–3057.
22. **Ferlazzo, G., D. Thomas, S. L. Lin, K. Goodman, B. Morandi, W. A. Muller, A. Moretta, and D. Munz.** 2004. The abundant NK cells in human secondary lymphoid tissues require activation to express killer cell Ig-like receptors and become cytolytic. J. Immunol. **172:**1455–1462.
23. **Fiorentino, D. F., A. Zlotnik, T. R. Mosmann, M. Howard, and A. O'Garra.** 1991. IL-10 inhibits cytokine production by activated macrophages. J. Immunol. **147**:3815–3822.
24. **Fujita, H., A. Asahina, Y. Tada, H. Fujiwara, and K. Tamaki.** 2005. Type I interferons inhibit maturation and activation of mouse Langerhans cells. J. Invest. Dermatol. **125:**126–133.
25. **Golde, W. T., J. M. Pacheco, H. Duque, T. Doel, B. Penfold, G. S. Ferman, D. R. Gregg, and L. L. Rodriguez.** 2005. Vaccination against foot-and-mouth disease virus confers complete clinical protection in 7 days and partial protection in 4 days: use in emergency outbreak response. Vaccine **23:**5775–5782.
26. **Graham, F. L., J. Smiley, W. C. Russell, and R. Nairn.** 1977. Characteristics of a human cell line transformed by DNA from human adenovirus 5. J. Gen. Virol. **36:**59–72.
27. **Granucci, F., I. Zanoni, N. Pavelka, S. L. Van Dommelen, C. E. Andoniou, F. Belardelli, M. A. Degli Esposti, and P. Ricciardi-Castagnoli.** 2004. A contribution of mouse dendritic cell-derived IL-2 for NK cell activation. J. Exp. Med. **200:**287–295.
28. **Grubman, M. J., and B. Baxt.** 2004. Foot-and-mouth disease. Clin. Microbiol. Rev. **17:**465–493.
29. **Henke, A., R. Zell, G. Ehrlich, and A. Stelzner.** 2001. Expression of immunoregulatory cytokines by recombinant coxsackievirus B3 variants confers protection against virus-caused myocarditis. J. Virol. **75:**8187–8194.
30. **Jung, K., and C. Chae.** 2006. Expression of Mx protein and interferon-*a* in pigs experimentally infected with swine influenza virus. Vet. Pathol. **43:**161–167.
31. **Kasama, T., R. M. Strieter, T. J. Standiford, M. D. Burdick, and S. L. Kunkel.** 1993. Expression and regulation of human neutrophil-derived macrophage inflammatory protein 1 alpha. J. Exp. Med. **178:**63–72.
32. **Lindell, D. M., T. E. Lane, and N. W. Lukacs.** 2008. CXCL10/CXCR3-mediated responses promote immunity to respiratory syncytial virus infection by augmenting dendritic cell and $CD8^+$ T-cell efficiency. Eur. J. Immunol. **38:**2168–2179.
33. **Longhi, M. P., C. Trumpfheller, J. Idoyaga, M. Caskey, I. Matos, C. Kluger, A. M. Salazar, M. Colonna, and R. M. Steinman.** 2009. Dendritic cells require a systemic type I interferon response to mature and induce $CD4^+$ Th1 immunity with poly IC as adjuvant. J. Exp. Med. **206:**1589–1602.
34. **Lucas, M., W. Schachterle, K. Oberle, P. Aichele, and A. Diefenbach.** 2007. Natural killer cell-mediated control of infections requires production of interleukin 15 by type I IFN-triggered dendritic cells. Immunity **26:**503–517.
35. **Luster, A. D., J. C. Unkeless, and J. V. Ravetch.** 1985. Gamma-interferon transcriptionally regulates an early-response gene containing homology to platelet proteins. Nature **315:**672–676.
36. **Moraes, M. P., J. Chinsangaram, M. C. S. Brum, and M. J. Grubman.** 2003. Immediate protection of swine from foot-and-mouth disease: a combination of adenoviruses expressing interferon alpha and a foot-and-mouth disease virus subunit vaccine. Vaccine **22:**268–279.
37. **Moraes, M. P., T. de los Santos, M. Koster, T. Turecek, H. Wang, V. G. Andreyev, and M. J. Grubman.** 2007. Enhanced antiviral activity against foot-and-mouth disease virus by a combination of type I and II porcine interferons. J. Virol. **81:**7124–7135.
38. **Moraes, M. P., G. A. Mayr, P. W. Mason, and M. J. Grubman.** 2002. Early protection against homologous challenge after a single dose of replication-defective human adenovirus type 5 expressing capsid proteins of foot-and-mouth disease virus (FMDV) strain A24. Vaccine **20:**1631–1639.
39. **Muruve, D. A., M. J. Barnes, I. E. Stillman, and T. A. Libermann.** 1999. Adenoviral gene therapy leads to rapid induction of multiple chemokines and acute neutrophil-dependent hepatic injury in vivo. Hum. Gene Ther. **10:**965–976.
40. **Musikacharoen, T., A. Oguma, Y. Yoshikai, N. Chiba, A. Masuda, and T. Matsuguchi.** 2005. Interleukin-15 induces IL-12 receptor β1 gene expression through PU. 1 and IRF 3 by targeting chromatin remodeling. Blood **105:**711–720.
41. **Nfon, C. K., H. Dawson, F. N. Toka, and W. T. Golde.** 2008. Langerhans cells in porcine skin. Vet. Immunol. Immunopathol. **126:**236–247.
42. **Okuse, C., J. A. Rinaudo, K. Farrar, F. Wells, and B. E. Korba.** 2005. Enhancement of antiviral activity against hepatitis C virus in vitro by interferon combination therapy. Antivir. Res. **65:**23–34.
43. **Orange, J. S., and C. A. Biron.** 1996. Characterization of early IL-12, IFN-

α/β, and TNF effects on antiviral state and NK cell responses during murine cytomegalovirus infection. J. Immunol. **156:**4746–4756.
44. **Pacheco, J. M., M. C. S. Brum, M. P. Moraes, W. T. Golde, and M. J. Grubman.** 2005. Rapid protection of cattle from direct challenge with foot-and-mouth disease virus (FMDV) by a single inoculation with an adenovirus vectored FMDV subunit vaccine. Virology **337:**205–209.
45. **Pena, L., M. P. Moraes, M. Koster, T. Burrage, J. M. Pacheco, F. Diaz-San Segundo, and M. J. Grubman.** 2008. Delivery of a foot-and-mouth disease virus empty capsid subunit antigen with nonstructural protein 2B improves protection of swine. Vaccine **26:**5689–5699.
46. **Pintaric, M., W. Gerner, and A. Saalmuller.** 2008. Synergistic effects of IL-2, Il-12 and IL-18 on cytolytic activity, perforin expression and IFN-γ production of porcine natural killer cells. Vet. Immunol. Immunopathol. **121:**68–82.
47. **Raymond, C. R., and B. N. Wilkie.** 2005. Toll-like receptor, MHC II, B7 and cytokine expression by porcine monocytes and monocyte-derived dendritic cells in response to microbial pathogen-associated molecular patterns. Vet. Immunol. Immunopathol. **107:**235–247.
48. **Salazar-Mather, T. P., and K. L. Hokeness.** 2006. Cytokine and chemokine networks: pathways to antiviral defense. Curr. Top. Microbiol. Immunol. **303:**29–46.
49. **Samuel, C. E.** 2001. Antiviral actions of interferons. Clin. Microbiol. Rev. **14:**778–809.
50. **Scapini, P., C. Laudanna, C. Pinardi, P. Allavena, A. Mantovani, S. Sozzani, and M. A. Cassatella.** 2002. Neutrophils produce biologically active macrophage inflammatory protein-3α (MIP-3α)/CCL20 and MIP-3β/CCL19. Eur. J. Immunol. **31:**1981–1988.
51. **Summerfield, A., and K. C. McCullough.** 2009. The porcine dendritic cell family. Dev. Comp. Immunol. **33**:299–309.
52. **Takaoka, A., and H. Yanai.** 2006. Interferon signalling network in innate defense. Cell Microbiol. **8:**907–922.
53. **Tan, H., J. Derrick, J. Hong, C. Sanda, W. M. Grosse, H. J. Edenberg, M. Taylor, S. Seiwert, and L. M. Blatt.** 2005. Global transcriptional profiling demonstrates the combination of type I and type II interferon enhances antiviral and immune responses at clinically relevant doses. J. Interferon Cytokine Res. **25:**632–649.
54. **Taub, D. D., T. J. Sayers, C. R. D. Carter, and J. R. Ortaldo.** 1995. α and β chemokines induce NK cell migration and enhance NK-mediated cytolysis. J. Immunol. **155:**3877–3888.
55. **Tebo, J. M., H. S. Kim, J. Gao, D. A. Armstrong, and T. A. Hamilton.** 2009. Interleukin-10 suppresses IP-10 gene transcription by inhibiting the production of class I interferon. Blood **92:**4742–4749.
56. **Tilg, H.** 1997. New insights into the mechanisms of interferon alpha: an immunoregulatory and anti-inflammatory cytokine. Gastroenterology **112:** 1017–1021.
57. **Toka, F. N., C. K. Nfon, H. Dawson, and W. T. Golde.** 2009. Accessory-cell-mediated activation of porcine NK cells by Toll-like receptor 7 (TLR7) and TLR8 agonists. Clin. Vaccine Immunol. **16:**866–878.
58. **Trifilo, M. J., C. Montalto-Morrison, L. N. Stiles, K. R. Hurst, J. L. Hardison, J. E. Manning, P. S. Masters, and T. E. Lane.** 2004. CXC chemokine ligand 10 controls viral infection in the central nervous system: evidence for a role in innate immune response through recruitment and activation of natural killer cells. J. Virol. **78:**585–594.
59. **Tsunoda, I., T. E. Lane, J. Blackett, and R. S. Fujinami.** 2004. Distinct roles for IP-10/CXCL10 in three animal models, Theiler's virus infection, EAE, and MHV infection, for multiple sclerosis: implication of differing roles for IP-10. Multiple Sclerosis **10:**26–34.
60. **Wu, Q., M. C. S. Brum, L. Caron, M. Koster, and M. J. Grubman.** 2003. Adenovirus-mediated type I interferon expression partially protects cattle from foot-and-mouth disease. J. Interferon Cytokine Res. **23:**371–380.
61. **Yang, H., and M. E. Parkhouse.** 1996. Phetotypic classification of porcine lymphocyte subpopulations in blood and lymphoid tissues. Immunology **89**: 76–83.
62. **Yuan, J., Z. Liu, T. Lim, H. Zhang, J. He, E. Walker, C. Shier, Y. Wang, Y. Su, A. Sall, B. McManus, and D. Yang.** 2009. CXCL10 inhibits viral replication through recruitment of natural killer cells in coxsackievirus B3-induced myocarditis. Circ. Res. **104:**628–638.

Return to Table of Contents

JOURNAL OF INTERFERON & CYTOKINE RESEARCH
Volume 00, Number 00, 2010

DOI: 10.1089/jir.2010.0055

ORIGINAL ARTICLE

Porcine Type I Interferon Rapidly Protects Swine Against Challenge with Multiple Serotypes of Foot-and-Mouth Disease Virus

Camila C.A. Dias,[1,2] Mauro P. Moraes,[1] Fayna Diaz-San Segundo,[1,2] Teresa de los Santos,[1] and Marvin J. Grubman[1]

Foot-and-mouth disease virus (FMDV) causes a highly contagious disease of cloven-hoofed animals. Current inactivated vaccines require approximately 7 days to induce protection, but before this time vaccinated animals remain susceptible to disease. Previously, we demonstrated that intramuscular (IM) inoculation of a replication-defective human adenovirus type 5 (Ad5) vector containing a porcine interferon α gene (*pIFNα*) can protect swine challenged 1 day later by intradermal (ID) injection with FMDV A24 Cruzeiro from both clinical disease and virus replication. To extend these studies to other FMDV serotypes, we demonstrated the effectiveness of Ad5-pIFNα against ID challenge with O1 Manisa and Asia-1 and against A24 Cruzeiro in a direct contact challenge model. We also showed that an Ad5 vector containing the *pIFNβ* gene can protect swine against ID challenge with A24 Cruzeiro. Further, IM inoculation of a 10-fold lower dose of Ad5-pIFNα at 4 sites in the neck compared with 1 site in the hind limb can protect swine against ID challenge. These studies demonstrate the ability of Ad5-delivered type I IFN to rapidly protect swine against several FMDV serotypes and suggest that various modifications of this approach may enable this strategy to be successfully used in other FMD susceptible species.

Introduction

Foot-and-mouth disease (FMD) is a highly contagious viral disease of cloven-hoofed animals that has significant economic consequences in affected countries. The infectious agent, FMD virus (FMDV), is a member of the *Aphthovirus* genus of the Picornaviridae family, and contains a single-stranded positive-sense RNA genome of about 8,500 nucleotides encapsidated by 60 copies each of 4 structural proteins (Grubman and Baxt 2004). FMDV is an antigenically variable virus consisting of 7 serotypes (A, O, C, Asia-1, and South African territories 1–3) and multiple subtypes (Domingo and others 2003). Currently, the disease is controlled by restriction of animal movement, slaughter of infected and in-contact susceptible animals, and possibly vaccination with an inactivated whole virus vaccine (Grubman and Baxt 2004). Administration of this vaccine or an experimental vaccine based on a replication-defective human adenovirus type 5 (Ad5) vector containing the FMDV capsid and 3C proteinase coding regions requires approximately 7 days to induce protective immunity in animals (Moraes and others 2002; Golde and others 2005; Pacheco and others 2005). However, since FMDV infection results in rapid replication and spread within the host and shedding of virus into the environment, animals exposed to virus before 7 days postvaccination are still susceptible to the disease. As a result we have initiated a program to stimulate a rapid innate response to protect animals before vaccine-induced adaptive immunity. We anticipate that this approach would be used in combination with vaccination to induce both a rapid and specific long-lasting protective immune response (Grubman 2003, 2005; Moraes and others 2003; de Avila Botton and others 2006).

Type I interferon (IFNα/β) is the first line of host defense against viral infection and upon its induction and secretion it causes upregulation of hundreds of IFN-stimulated genes (ISGs) and their products (Der and others 1998; Takaoka and Yanai 2006; Fontana and others 2008). We and others have shown that replication of all FMDV serotypes is inhibited in cell culture by pretreatment with type I IFN (Ahl and Rump 1976; Chinsangaram and others 1999, 2001; Moraes and others 2007). More recently, we constructed an Ad5 vector containing porcine IFNα (Ad5-pIFNα) and demonstrated

[1]Plum Island Animal Disease Center, Agricultural Research Service, U.S. Department of Agriculture, Greenport, New York.
[2]Plum Island Animal Disease Center Research Participation Program, Oak Ridge Institute for Science and Education, Oak Ridge, Tennessee.

that swine inoculated with this vector intramuscularly (IM) at 1 site in the hind limb produce significant levels of pIFNα and are completely protected when challenged by intradermal (ID) inoculation with FMDV serotype A24 Cruzeiro 1 day later (Chinsangaram and others 2003). Further, protection lasts for 3–5 days and even treatment 1 day post-challenge reduces viremia and clinical disease (Moraes and others 2003). In preliminary studies we have demonstrated that Ad5-pIFNα can enhance the efficacy of our Ad5-FMD vaccine, indicating that IFN does not appear to adversely affect the adaptive immune response (de Avila Botton and others 2006). We have also initiated studies to understand the molecular mechanisms induced by IFN treatment that result in protection against FMDV challenge and found a correlation between protection and both, specific ISG upregulation and tissue specific infiltration of dendritic cells (DCs) and natural killer (NK) cells (Moraes and others 2007; Diaz-San Segundo and others 2010).

Although these proof-of-concept studies demonstrated that Ad5-pIFNα can rapidly protect swine against FMDV, there are limitations to its utility, including the following: (1) only 1 FMDV serotype has been tested, (2) treatment requires relatively high doses to induce protection in swine, (3) protection against the natural route of FMDV infection has not been examined, and (4) treatment of bovines only results in delay of disease onset and severity (Wu and others 2003). To address some of these limitations, in this study we have tested the efficacy of this approach against other FMDV serotypes, including O1 Manisa and Asia-1; examined its efficacy in a direct contact challenge model, which is the natural route of FMDV infection; and examined alternative routes of administration of the Ad5 vector. Further, we also evaluated the efficacy of an Ad5 vector containing the gene for pIFNβ (Adt-pIFNβ) against ID challenge with A24 Cruzeiro.

Our results indicate that Ad5-pIFNα, at a dose of 10^{11} focus forming units (FFU)/animal, is able to completely protect swine against all 3 serotypes of FMDV, while treatment with a 10-fold lower dose results in complete protection of some animals and delay in disease onset and severity and reduction in virus shedding in the remaining treated animals. Further, Ad5-pIFNα-inoculated animals were also protected when challenged with FMDV A24 Cruzeiro by direct-contact exposure. Pretreatment with a 10^{11} FFU/animal dose of Adt-pIFNβ also completely protected swine against ID challenge with A24 Cruzeiro. Notably, we were able to reduce the protective dose of Ad5-pIFNα 10-fold when swine were inoculated IM at 4 separate sites in the neck. These results demonstrate the utility of this approach in conferring rapid protection in swine after either ID or direct contact challenge with FMDV and suggest that various modifications of this strategy can overcome some of its current practical limitations.

Materials and Methods

Cells and viruses

Baby hamster kidney cells (BHK-21, clone 13) were used to measure FMDV titers in plaque assays, and a swine kidney cell line (IBRS-2) was used to measure antiviral activity in plasma from inoculated animals by a plaque reduction assay (Chinsangaram and others 2001). FMDV serotypes A24 Cruzeiro, O1 Manisa, and Asia-1 were obtained from the vesicular fluid of infected swine, titered in both swine (see below) and in tissue culture, and stored in aliquots at −70°C.

The replication-defective human Ad5 vectors containing the *pIFNα* or *pIFNβ* genes, constructed as described by Gall and others (2007), and the control vectors AdNull and Ad-Luciferase were obtained from GenVec, Inc., through an agreement with the Department of Homeland Security, Office of Science and Technology. The pIFN genes were supplied by our lab to GenVec, Inc., for use in the construction of Ad5 vectors containing type I IFNs (designated Adt-pIFNα and Adt-pIFNβ). All experiments were performed with the same set of vector lots.

Animal studies

All animal experiments were performed under a protocol reviewed and approved by the Institutional Animal Care and Use Committee of the Plum Island Animal Disease Center. Yorkshire pigs weighing about 35–40 lbs each were used in all experiments and acclimated for approximately 4–5 days before the start of the experiments. To determine the challenge dose of each FMDV serotype to use in ID inoculation studies, groups of 4 swine were infected ID in the hind heel bulb using 4 sites of inoculation, 100 μL per site, with low (10^4 tissue culture infectious dose $[TCID]_{50}$/animal), medium (10^5 $TCID_{50}$/animal), or high (10^6 $TCID_{50}$/animal) doses of FMDV A24 Cruzeiro, O1 Manisa and Asia-1 in separate experiments (Supplemental Table S1, available online at www.liebertonline.com). On the basis of these studies we selected a challenge dose of 10^5 $TCID_{50}$ for all serotypes, which is 10-fold higher than the challenge dose recommended by the World Organization of Animal Health (OIE 2004).

In the IFN titration studies, groups of 3 swine were inoculated with 3 different vector doses (10^9 FFU/animal, 10^{10} FFU, and 10^{11} FFU) of Adt-pIFNα or Adt-pIFNβ to evaluate the biological activity of those constructs. Swine inoculated with AdLuciferase or AdNull (10^{11} FFU/animal) were used as controls. Animals were inoculated IM in 1 site in the right hind limb with 2 mL of the respective vector and subsequently monitored for 4 days for possible adverse signs as a result of vector administration and blood assayed for IFN expression and antiviral biological activity.

In the subsequent efficacy studies animals were inoculated IM with 2 mL or 3 mL vector in 1 site in the right hind limb or neck or with 0.50 or 0.75 mL vector per site in 4 sites, 2 in each hind limb or 2 in both sides of the neck. All Adt-pIFNα/β-inoculated animals were housed in double-gated rooms (2 animals per room) so that they had no direct contact, except in the initial A24 Cruzeiro ID challenge experiment, in which all animals in a group were housed in the same room.

A direct contact challenge experiment was performed based on an experimental protocol developed by Pacheco and others (manuscript in preparation). Six donor animals were ID inoculated in the heel bulb with FMDV A24 Cruzeiro. When vesicular lesions were apparent, approximately 2 days postchallenge (dpc), the 6 donor animals were comingled with Adt-pIFNα-treated and control animals in a ratio of 1:2 for 18 h. After exposure, donor animals were euthanized, and the Adt-pIFNα-treated and control animals were relocated to double-gated rooms (2 animals per room).

In all challenge experiments, animals were monitored daily for 10 days for clinical signs, including fever, alertness,

lameness, and development of vesicles on the coronary band of the hooves, on the snout and mouth. Lesion scores of the animals were determined by the number of digits plus snout and mouth with vesicles (maximum score is 17).

Blood and nasal swab sampling

Blood samples were drawn from the anterior vena cava at the times indicated in each experiment. Serum was obtained from blood drawn into nonheparinized tubes and tested for viremia and neutralizing antibodies using a standard plaque reduction assay as described below. Plasma was obtained from the blood drawn into heparinized tubes and tested to determine levels of antiviral biological activity of pIFNα/β as described in the following section and pIFNα protein by ELISA. Nasal swabs were collected starting the day of challenge and for the following 6 days and tested for the presence of FMDV by titration in BHK-21 cells.

Detection of FMDV RNA by real-time reverse transcriptase–polymerase chain reaction

One to 7 dpc frozen serum samples from animals that had no detectable clinical disease were thawed and processed for RNA extraction and real-time reverse transcriptase–polymerase chain reaction (rRT-PCR) as previously described (Pacheco and others 2010). Samples were considered positive when Ct values were <40.

Interferon biological assays

Antiviral activity was evaluated in plasma samples as previously described (Moraes and others 2003; de Avila Botton and others 2006). In brief, samples were obtained at 0–4 days postinoculation (dpi), diluted, and incubated on IBRS-2 cells; after 24 h supernatants were removed, and the cells infected for 1 h with approximately 100 plaque forming units (PFU) of FMDV serotype A12 and overlaid with gum tragacanth. Plaques were observed 24 h later by staining with crystal violet. Antiviral activity (U/mL) was reported as the reciprocal of the highest supernatant dilution that resulted in a 50% reduction in the number of plaques relative to the number of plaques in the mock-treated infected cells.

Interferon-α ELISA

ELISA was performed as previously described (Moraes, and others 2003). Porcine IFNα concentrations were expressed in picograms per milliliter and calculated by linear regression analysis of a standard curve generated with serial 2-fold dilutions of recombinant pIFNα (PBL Biomedical Laboratories). All samples were assayed in duplicate. Levels of pIFNα protein of <200 pg/mL were not considered meaningful.

Plaque reduction neutralization (PRN_{70}) assay

Sera samples were collected at 0, 7, 14 and 21 dpc for each experiment and heated at 56°C for 30 min, and aliquots stored at −70°C. Sera were tested for the presence of neutralizing antibodies against FMDV in a PRN assay (Mason and others 1997). Neutralizing titers were reported as the serum dilution yielding a 70% reduction in the number of plaques (PRN_{70}). A titer of 128 or higher was considered to indicate productive virus replication.

3ABC ELISA assay

Swine sera from 0 and 21 dpc were examined for the presence of antibodies against FMDV nonstructural (NS) protein 3ABC using a PrioCHECK™ FMDV-NS ELISA kit (Prionics AG) following the manufacturer's instructions (Sorensen and others 1998).

Results

Antiviral response in swine inoculated with Adt-pIFNα or Adt-pIFNβ

To determine the doses of Adt-pIFNα and Adt-pIFNβ necessary to produce levels of antiviral activity previously found sufficient to partially or completely protect swine against ID challenge with FMDV A24 Cruzeiro (Chinsangaram and others 2003; Moraes and others 2003), we performed a dose–response potency study. Groups of 3 swine were inoculated IM at 1 site in the right hind limb with low (1×10^9 FFU), medium (1×10^{10} FFU), or high doses (1×10^{11} FFU) of Adt-pIFNα or Adt-IFNβ, and 1×10^{11} FFU of Ad-Luciferase control vector, in 2 separate experiments. Biological activity and levels of pIFNα were assayed in plasma samples at the time of inoculation and for 3 additional days (Table 1). We were unable to determine the levels of pIFNβ protein since the appropriate reagents for this cytokine are not currently available. The average biological activity in plasma samples from animals in the high-dose Adt-pIFNα-inoculated group was 1,333 U/mL at 24 h after inoculation and activity was detectable for 1 additional day (Table 1). The average pIFNα protein at 1 dpi in the high-dose group was 26,977 pg/mL, and this protein was detectable for 2 additional days. In the medium-dose group biological activity was 92 U/mL at 1 dpi and was detectable for an additional day, whereas pIFNα protein (1,184 pg/mL) was only detectable for 1 day. No antiviral activity or pIFNα protein was detected in either the low-dose IFN group or in the control group.

In the Adt-pIFNβ dose–response experiment the average biological activity in plasma samples from animals in the high-dose-inoculated group was 667 U/mL at 1 dpi and was detectable for a second day, whereas biological activity was only detectable for 1 day in the medium-dose group (Table 1). A low level of pIFNα protein was only detectable for 1 day in the high-dose-inoculated group. The animals inoculated with the low-dose pIFNβ or the control vector did not develop either detectable antiviral activity or pIFNα protein. On the basis of these results we selected the medium and high doses of Adt-pIFNα and Adt-pIFNβ to test in efficacy studies.

Clinical response of swine pretreated with Adt-pIFNα and challenged by ID inoculation with FMDV A24 or O1 Manisa

Groups of 3 animals were administered medium (1×10^{10} FFU) or high doses (1×10^{11} FFU) of Adt-pIFNα or a high dose of AdLuciferase or AdNull and challenged 24 h later with 10^5 $TCID_{50}$ of either FMDV A24 or O1 Manisa. In the A24 challenge experiment all the control-inoculated animals developed viremia and clinical disease by 2 dpc and none had detectable antiviral activity or pIFNα protein (Table 2). In the Adt-pIFNα medium-dose group all the animals

Table 1. Dose Response of Swine Inoculated with Adenovirus Type 5 Vector Containing a Porcine Interferon α or β Gene

		Antiviral activity (U/mL)[b]					*pIFNα (pg/mL)*[c]				
Group (dose FFU)[a]	*Animal no.*	*0 dpi*	*1 dpi*	*2 dpi*	*3 dpi*	*4 dpi*	*0 dpi*	*1 dpi*	*2 dpi*	*3 dpi*	*4 dpi*
AdLuciferase (1×10^{11})	06	<25	<25	<25	<25	<25	0	0	0	0	0
	07	<25	<25	<25	<25	<25	0	0	0	0	0
	08	<25	<25	<25	<25	<25	0	0	0	0	0
Adt-pIFNα (1×10^{9})	09	<25	<25	<25	<25	<25	0	0	0	0	0
	10	<25	<25	<25	<25	<25	0	137	0	0	0
	11	<25	<25	<25	<25	<25	0	74	0	0	0
Adt-pIFNα (1×10^{10})	12	<25	25	<25	<25	<25	0	197	0	0	0
	13	<25	50	25	<25	<25	0	820	66	0	0
	14	<25	200	50	<25	<25	0	2,536	380	0	0
Adt-pIFNα (1×10^{11})	15	<25	800	400	25	<25	0	27,688	4,470	239	0
	16	<25	1,600	800	50	<25	0	13,424	6,246	754	30
	17	<25	1,600	400	25	<25	0	39,818	5,495	783	43
AdLuciferase (1×10^{11})	26	<25	<25	<25	<25	<25	0	0	0	0	0
	27	<25	<25	<25	<25	<25	0	0	0	0	0
	28	<25	<25	<25	<25	<25	0	0	0	0	0
Adt-pIFNβ (1×10^{9})	29	<25	<25	<25	<25	<25	0	0	0	0	0
	30	<25	<25	<25	<25	<25	0	0	0	0	0
	31	<25	<25	<25	<25	<25	0	0	4	0	0
Adt-pIFNβ (1×10^{10})	32	<25	<25	<25	<25	<25	0	0	0	0	0
	33	<25	50	25	<25	<25	0	190	39	0	0
	34	<25	<25	<25	<25	<25	0	0	232	0	0
Adt-pIFNβ (1×10^{11})	35	<25	800	400	50	25	0	250	91	0	0
	36	<25	800	100	<25	<25	0	316	100	0	0
	37	<25	400	200	<25	<25	0	139	15	47	0

[a]Dose of inoculum per animal expressed as number of FFU in 2 mL of phosphate buffered saline (PBS).
[b]Highest dilution that reduces foot-and-mouth disease virus A12 plaque number by 50%.
[c]Amount of pIFNα in plasma samples determined by ELISA.
Abbreviations: Adt-pIFNα, adenovirus type 5 vector containing a porcine interferon α gene; dpi, days postinoculation; FFU, focus forming units.

developed low levels of pIFNα protein and antiviral activity on day 1, which lasted for 1 additional day (data not shown). One animal in this group developed very low levels of viremia and clinical disease at 4 dpc (no. 20961), whereas the other 2 animals developed viremia by 6 or 7 dpc and lesions at 7 and 10 dpc, respectively. All 3 animals in the Adt-pIFNα high-dose group had ~14–21,000 pg/mL pIFNα protein and ~1,300–2,300 U/mL antiviral activity 1 day postadministration, and this continued at reduced levels for an additional 2–3 days (data not shown). None of the animals in this group developed clinical disease, viremia, or virus in nasal secretions, and they were all 3ABC and rRT-PCR negative (Tables 2 and 7). However, 2 of the animals, nos. 20962 and 20964, had significant levels of FMDV-specific neutralizing antibodies.

In this initial efficacy study each group of Adt-pIFNα-treated animals was kept in separate rooms and had direct intragroup contact throughout the experiment. Since 1 animal in the medium-dose group, no. 20961, developed lesions at 4 dpc, while the other 2 animals, nos. 20959 and 20960, only developed lesions 3–6 days later, it is possible that the later 2 animals developed FMD because of long-term direct exposure to animal no. 20961 at a time when the protective effects of pIFNα had waned. As a result in all subsequent studies the Adt-pIFNα/β groups were kept 2 animals/room with a double gate separating each animal to prevent direct contact.

In the FMDV O1 Manisa challenge experiment all the control animals developed clinical disease by 1–3 dpc, but only 2 animals in this group had detectable, but low levels of viremia (Table 2). One animal in the group treated with 10^{10} FFU Adt-pIFNα, no. 960, did not develop antiviral activity or meaningful levels of pIFNα and had clinical disease at 3 dpc. Another animal in this group developed lesions by 4 dpc, but disease severity was considerably milder than in the control animals. The other animal, no. 959, was completely protected from clinical disease, had no viremia or virus in nasal swabs, was 3ABC and rRT-PCR negative, and had no detectable FMDV-specific neutralizing antibodies (Tables 2 and 7). All 3 animals in the 10^{11} FFU group had high levels of pIFNα protein and antiviral activity. None of the animals developed clinical disease or viremia, or shed virus, and they were all 3ABC and rRT-PCR negative and had no detectable FMDV-specific neutralizing antibodies (Tables 2 and 7).

Clinical response of swine pretreated with Adt-pIFNα and challenged with FMDV A24 Cruzeiro by contact

Twelve naive animals were inoculated IM with either 1×10^{10} or 1×10^{11} FFU Adt-pIFNα, 1×10^{11} FFU AdNull, or phosphate buffered saline (PBS). Twenty-four hours later they were brought into the same room with donor animals that had been infected 2 days earlier with FMDV and showed clear signs of disease. After 18 h of comingling, the donors were euthanized, whereas the other animals were distributed, 2 animals per room, separated by a double gate and monitored for 10 days. Virus was detected in nasal swab samples from all animals at 24 h postcontact exposure, demonstrating that they were effectively exposed (data not shown).

Table 2. Serological and Clinical Response of Swine Pretreated with Adenovirus Type 5 Vector Containing a Porcine Interferon α Gene and Intradermal Challenged with Foot-and-Mouth Disease Virus A24 Cruzeiro or O1 Manisa

Group (dose FFU)[a]	*Animal no.*	*Foot-and-mouth disease virus*	*Antiviral act./pIFNα*[b]	*Viremia*[c]	*Shedding virus*[d]	*Clinical score*[e]	*PRN_{70}*[f]	*3ABC ELISA*[g]
AdLuciferase[h] (10^{11})	20956	A24	<25/180	$2/1.0\times10^{4}$	$2/1.5\times10^{3}/4$	2/14	1,600	P
	20957		<25/95	$1/8.5\times10^{3}$	$2/3.9\times10^{2}/4$	2/17	3,200	P
	20958		<25/147	$1/2.0\times10^{5}$	$2/2.0\times10^{2}/4$	2/17	12,800	P
Adt-pIFNα[h] (10^{10})	20959	A24	303/3,307	$6/2.1\times10^{4}$	$5/7.0\times10^{0}/2$	10/12	6,400	N
	20960		447/5,615	$7/1.4\times10^{4}$	$5/2.5\times10^{2}/2$	7/12	6,400	P
	20961		226/1,921	$4/3.4\times10^{1}$	$5/2.1\times10^{4}/3$	4/13	6,400	P
Adt-pIFNα[h] (10^{11})	20962	A24	2,011/20,917	0	0	0/0	512	N
	20963		1,305/14,215	0	0	0/0	<8	N
	20964		2,273/20,053	0	0	0/0	512	N
AdNull[i] (10^{11})	955	O1M	<25/183	$1/4.0\times10^{3}/2$	$2/5\times10^{1}/1$	2/17	2,048	P
	956		<25/7	0	0	3/15	256	P
	957		<25/63	$2/5.4\times10^{2}/1$	$3/1.1\times10^{2}/1$	1/17	256	P
Adt-pIFNα[i] (10^{10})	958	O1M	400/626	0	0	4/4	1,024	P
	959		400/1,015	0	0	0/0	8	N
	960		<25/95	0	0	3/17	256	P
Adt-pIFNα[i] (10^{11})	961	O1M	1,600/46,103	0	0	0/0	<8	N
	962		1,600/16,303	0	0	0/0	<8	N
	963		1,600/35,855	0	0	0/0	<8	N

[a]Dose of inoculum per animal expressed as number of FFU in 2 mL of PBS.
[b]Antiviral activity (U/mL) and pIFNα (pg/mL) at 1 day postinoculation.
[c]First day postchallenge (dpc) that viremia was detected, maximum amount of viremia in PFU/mL detected in sera samples, and the duration (days) of viremia.
[d]First dpc that shedding virus was detected, maximum amount of shedding virus in PFU/mL detected in nasal swab samples, and the duration (days) of shedding.
[e]dpc first signs of lesions/highest lesion score.
[f]Neutralizing antibody response reported as serum dilution yielding a 70% reduction in the number of plaques (PRN_{70}) at 21 dpc.
[g]Detection of NS proteins in 21 dpc serum samples by 3ABC ELISA; N, negative; P, positive.
[h]In this experiment all 3 animals in each group were housed in the same room and were in direct contact throughout the experiment.
[i]In this experiment the animals administered IFN were housed 2 per room with a double gate separating them so that they had no direct contact.
Abbreviation: PRN, plaque reduction neutralization; PFU, plaque forming units.

Four of the 6 animals in the control groups developed viremia by 3–4 days postcontact and by 3–5 days all of the viremic animals had clinical disease (Table 3). One control animal developed a lesion at 8 days postcontact, whereas the remaining control animal never developed clinical disease. All 5 control animals that had clinical disease as well as the control animal with no clinical disease developed significant levels of FMDV-specific neutralizing antibodies.

All animals inoculated with 1×10^{10} FFU Adt-pIFNα had detectable levels of pIFNα and antiviral activity 1 day after administration. However, 1 animal in this group, no. 9135, only had antiviral activity and pIFNα for 1 additional day and developed 1 lesion at 6 days postcontact challenge. The other 2 animals had detectable antiviral activity/pIFNα for 2–3 additional days (data not shown); had no clinical disease, viremia, or virus in nasal swabs; were 3ABC and rRT-PCR negative; and had no detectable FMDV-specific neutralizing antibodies (Tables 3 and 7).

All animals inoculated with the high dose of Adt-pIFNα had significant levels of pIFNα and antiviral activity 1 day after administration that persisted for 2–3 additional days. These animals were completely protected from clinical disease, had no detectable virus replication as determined by the absence of viremia or virus in nasal secretions, were 3ABC and rRT-PCR negative, and had no detectable FMDV-specific neutralizing antibodies (Tables 3 and 7).

Clinical response of swine pretreated with Adt-pIFNβ and challenged by ID inoculation with FMDV A24

Groups of 3 swine were inoculated with medium (1×10^{10} FFU) or high doses (1×10^{11} FFU) of Adt-pIFNβ or with 1×10^{11} FFU of AdNull control vector and challenged by ID inoculation with FMDV A24 one day later (Table 4). The control group developed viremia by 2 dpc and clinical disease by 3 dpc. Two of 3 animals in the group inoculated with the medium dose of Adt-pIFNβ developed viremia by 4 or 5 dpc and clinical disease by 4 and 6 dpc, whereas the remaining animal never developed viremia or clinical disease, were 3ABC and rRT-PCR negative, and had a low neutralizing antibody response (Tables 4 and 7). All animals in the Adt-pIFNβ high-dose group were completely protected from clinical disease, had no viremia or virus in nasal swabs, and were 3ABC and rRT-PCR negative (Tables 4 and 7).

Clinical response of swine pretreated with Adt-pIFNα at one or more sites in the hind limb or neck and challenged by ID inoculation with FMDV A24

To possibly enhance the efficacy of pIFNα pretreatment, we examined 2 different anatomic delivery locations (hind limb versus neck) and also compared single versus multiple sites of IM inoculation in both locations (Table 5). In this

Table 3. Efficacy of Adenovirus Type 5 Vector Containing a Porcine Interferon α Gene in a Foot-and-Mouth Disease Virus A24 Cruzeiro Contact Challenge Experiment

Group (dose FFU)[a]	*Animal no.*	*Antiviral act./pIFNα*[b]	*Viremia*[c]	*Shedding virus*[d]	*Clinical score*[e]	PRN_{70}[f]	*3ABC ELISA*[g]
PBS (—)	9127	<25/72	$4/5\times10^3/2$	$5/9\times10^1/2$	5/11	1,600	P
	9128	<25/0	0	0	0	256	P
	9129	<25/0	$3/1\times10^3/2$	$4/6\times10^2/2$	3/17	1,600	P
AdNull (10^{11})	9130	25/11	0	$7/6\times10^1/2$	8/1	3,200	P
	9131	<25/0	$4/5\times10^3/2$	$4/4\times10^1/2$	5/15	3,200	P
	9132	<25/0	$4/9\times10^3/2$	$4/1\times10^3/4$	5/14	3,200	P
Adt-pIFNα (10^{10})	9133	800/4,376	0	0	0	<8	N
	9134	800/11,266	0	0	0	<8	N
	9135	400/2,530	$4/7\times10^3/2$	0	6/1	800	P
Adt-pIFNα (10^{11})	9136	800/13,788	0	0	0	<8	N
	9137	3,200/21,737	0	0	0	<8	N
	9138	3,200/40,305	0	0	0	<8	N

[a]Dose of inoculum per animal expressed as number of FFU in 2 mL of PBS.
[b]Antiviral activity (U/mL) of swine plasma in IBRS-2 cells and pIFNα (pg/mL) detected in swine plasma by ELISA at 1 day postinoculation.
[c]First day postchallenge (dpc) that viremia was detected, maximum amount of viremia in PFU/mL detected in sera samples, and the duration (days) of viremia.
[d]First dpc that shedding virus was detected, maximum amount of shedding virus in PFU/mL detected in nasal swab samples, and the duration (days) of shedding.
[e]dpc first signs of lesions/highest lesion score.
[f]Neutralizing antibody response reported as serum dilution yielding a 70% reduction in the number of plaques (PRN_{70}) at 21 dpc.
[g]Detection of NS proteins in 21 dpc serum samples by 3ABC ELISA; N, negative; P, positive.

study we used a medium dose of 1×10^{10} FFU Adt-pIFNα, since in previous experiments this dose only protected some animals in the group or delayed the onset and severity of clinical disease in the remaining animals. The AdNull control-inoculated animals developed viremia by 1–2 dpc and clinical disease by 2 days (Table 5). All 4 groups administered a total of 1×10^{10} FFU Adt-pIFNα per animal had similar levels of antiviral activity and pIFNα protein detectable for 1–2 days. Two animals, 1 in the group given 4 shots of vector in the neck, no. 817, and the other in the group given 4 shots of vector in the hind limbs, no. 818, were found dead immediately before the start of the experiment or at 1 dpc, respectively. Postmortem histopathology analysis indicated that death was unrelated to the effects of administration of either Adt-pIFNα or FMDV infection (data not shown). The group of animals that received 4 shots in the neck showed the highest level of protection (Table 5). Both remaining animals in this group were completely protected from clinical disease, viremia, and virus in nasal swabs, and were 3ABC and rRT-PCR negative (Tables 5 and 7). In the group given 1 shot in the neck 1 animal was completely protected. The remaining 2 animals in this group both developed

Table 4. Serological and Clinical Response to Pretreatment of Swine with Adenovirus Type 5 Vector Containing a Porcine Interferon β Gene and Intradermal Challenge with Foot-and-Mouth Disease Virus A24 Cruzeiro

Group (dose FFU)[a]	*Animal no.*	*Antiviral activity*[b]	*Viremia*[c]	*Shedding virus*[d]	*Clinical score*[e]	PRN_{70}[f]	*3ABC ELISA*[g]
AdNull (10^{11})	44	<25	$2/7\times10^6/2$	$4/8\times10^0/1$	3/17	6,400	P
	45	<25	$2/5\times10^4/5$	$4/5\times10^2/3$	3/16	3,200	P
	46	<25	$2/2\times10^6/3$	$4/7\times10^2/2$	3/17	6,400	P
Adt-pIFNβ (10^{10})	47	62	$4/2\times10^3/2$	$4/8\times10^1/2$	6/15	6,400	P
	48	87	0	0	0	32	N
	49	43	$5/2\times10^3/1$	$5/4\times10^2/1$	4/15	3,200	P
Adt-pIFNβ (10^{11})	50	404	0	0	0	64	N
	51	429	0	0	0	64	N
	52	218	0	0	0	512	N

[a]Dose of inoculum per animal expressed as number of FFU in 2 mL of PBS.
[b]Antiviral activity (U/mL) of swine plasma in IBRS-2 cells.
[c]First day postchallenge (dpc) that viremia was detected, maximum amount of viremia in PFU/mL detected in sera samples, and the duration (days) of viremia.
[d]First dpc that shedding virus was detected, maximum amount of shedding virus in PFU/mL detected in nasal swab samples, and the duration (days) of shedding.
[e]dpc first signs of lesions/highest lesion score.
[f]Neutralizing antibody response reported as serum dilution yielding a 70% reduction in the number of plaques (PRN_{70}) at 21 dpc.
[g]Detection of NS proteins in 21 dpc serum samples by 3ABC ELISA; N, negative; P, positive.

Table 5. Efficacy of Single-Site Versus Multiple-Site Inoculation of Adenovirus Type 5 Vector Containing a Porcine Interferon α Gene Against Intradermal Challenge with Foot-and-Mouth Disease Virus A24 Cruzeiro

Group[a]	*No. of shots*	*Inoculation site*	*Antiviral Act./ pIFNα*[b]	*Viremia*[c]	*Shedding virus*[d]	*Clinical score*[e]	*PRN_{70}*[f]	*3ABC ELISA*[g]
AdNull								
807	1	Neck	<25/183	$1/3\times10^5/4$	$3/3\times10^3/3$	2/17	8,000	P
808	1	Limb	<25/162	$2/2\times10^5/3$	$3/5\times10^3/3$	2/15	4,000	P
809	4	Neck	<25/168	$1/5\times10^5/4$	$3/4\times10^3/3$	2/17	4,000	P
810	4	Limb	<25/171	$2/1\times10^5/3$	$3/6\times10^3/3$	2/13	4,000	P
Adt-pIFNα								
805	1	Neck	200/3,455	$6/5\times10^1/1$	$1/4\times10^2/1$	8/9	64,000	P
806	1	Neck	100/1,548	0	0	10/4	32,000	P
811	1	Neck	800/4,886	0	0	0	<8	N
Adt-pIFNα								
812	1	Limb	200/6,918	0	0	0	64	N
813	1	Limb	200/4,010	$4/2\times10^3/3$	$2/6\times10^2/2$	6/12	16,000	P
814	1	Limb	25/432	$3/4\times10^2/1$	$2/3\times10^1/2$	4/15	4,000	P
Adt-pIFNα								
815	4	Neck	200/3,225	0	0	0	256	N
816	4	Neck	400/5,178	0	0	0	128	N
817	4	Neck	1600/11,967	NA[h]	NA[h]	NA[h]	NA[h]	NA[h]
Adt-pIFNα								
818	4	Limb	200/3,525	NA[h]	NA[h]	NA[h]	NA[h]	NA[h]
819	4	Limb	800/7,364	0	0	10/5	32,000	P
820	4	Limb	200/2,051	$5/1\times10^4/3$	$2/8\times10^2/2$	5/15	8,000	P

[a]Total dose of inoculum per animal was 1×10^{10} FFU in 2 mL of PBS.
[b]Antiviral activity (U/mL) of swine plasma in IBRS-2 cells and pIFNα (pg/mL) detected in swine plasma by ELISA at 1 day postinoculation.
[c]First day postchallenge (dpc) that viremia was detected, maximum amount of viremia in PFU/mL detected in sera samples, and the duration (days) of viremia.
[d]First dpc that shedding virus was detected, maximum amount of shedding virus in PFU/mL detected in nasal swab samples, and the duration (days) of shedding.
[e]dpc first signs of lesions/highest lesion score.
[f]Neutralizing antibody response reported as serum dilution yielding a 70% reduction in the number of plaques (PRN_{70}) at 21 dpc.
[g]Detection of NS proteins in 21 dpc serum samples by 3ABC ELISA; N, negative; P, positive.
[h]Not applicable (NA). Animals died during the experiment. Cause not related to FMD.

clinical disease, but it was delayed until 8 and 10 dpc and less severe than the controls. In the group given 4 shots in the hind limbs the 2 remaining animals developed delayed clinical disease at 5 and 10 dpc. One animal in the group given 1 shot of Adt-pIFNα in the hind limb never developed clinical disease, viremia, or virus in nasal swabs, and was 3ABC and rRT-PCR negative (Tables 5 and 7). The other 2 animals in this group developed lesions at 4 and 6 dpc, and viremia and virus in nasal swabs was detectable but was 10–1,000-fold lower than the controls.

Clinical response of swine pretreated with Adt-pIFNα and ID challenged with FMDV Asia-1

On the basis of the multiple shot experimental results, swine were inoculated IM with medium (1×10^{10} FFU) or high doses (1×10^{11} FFU) of Adt-pIFNα or AdNull (1×10^{11} FFU) at 4 sites in the neck and challenged with Asia-1 (Table 6). All control AdNull-inoculated animals developed viremia at 1 dpc and lesions at 2 dpc. All animals in the 1×10^{10} FFU Adt-pIFNα-inoculated group had detectable antiviral activity and pIFNα protein for 1–2 days. Two of 3 animals in this group were protected from clinical disease, did not develop viremia, and were 3ABC and rRT-PCR negative (Tables 6 and 7). The third animal in this group developed a low level of viremia (1,000–10,000-fold lower than any of the control animals) for 1 day, shed 10–80-fold less virus than the controls, and developed lesions at 5 dpc. All animals treated with 1×10^{11} FFU Adt-pIFNα had antiviral activity and pIFNα protein for 3–4 days and were completely protected from challenge (Tables 6 and 7).

Discussion

Previously, we demonstrated that swine inoculated IM at 1 site in the hind limb with an Ad5 vector containing the gene for pIFNα were protected from clinical disease and virus replication when challenged by ID inoculation 1 day after with FMDV A24 Cruzeiro (Chinsangaram and others 2003; Moraes and others 2003). In this study we have extended our previous work and examined the efficacy of type I IFN pretreatment of swine challenged with several FMDV serotypes by either ID inoculation or direct contact exposure. We showed that a dose of 10^{11} FFU Adt-pIFNα administered at 1 site in the hind limb could protect all swine challenged, 1 day postadministration, by ID inoculation with FMDV serotypes A24 Cruzeiro or O1 Manisa. Similarly, at this dose, Adt-pIFNβ completely protected swine against challenge with A24 Cruzeiro. In addition, animals pretreated with 10^{11} FFU Adt-pIFNα and challenged by direct contact exposure to A24 Cruzeiro–infected donor animals for 18 h were protected.

Table 6. Serological and Clinical Response of Swine Pretreated with Adenovirus Type 5 Vector Containing a Porcine Interferon α Gene and Intradermal Challenged with Foot-and-Mouth Disease Virus Asia-1

Group (dose FFU)[a]	*Animal no.*	*Antiviral act./pIFNα*[b]	*Viremia (pfu/mL)*[c]	*Shedding virus*[d]	*Clinical score*[e]	*PRN_{70}*[f]	*3ABC ELISA*[g]
AdNull (10^{11})	24094	<25/111	$1/4.7\times10^5/4$	$2/8.8\times10^2/2$	2/17	4,096	P
	24095	<25/192	$1/1.5\times10^5/3$	$3/4.3\times10^2/2$	2/15	1,024	P
	24097	<25/41	$1/1.6\times10^6/4$	$2/1.4\times10^2/2$	2/16	2,048	P
Adt-pIFNα (10^{10})	24092	100/1,163	0/0/0	0/0/0	0/0	32	N
	24093	100/2,024	0/0/0	0/0/0	0/0	16	N
	24096	25/908	$5/3.5\times10^2/1$	$5/1\times10^1/1$	5/9	512	P
Adt-pIFNα (10^{11})	24088	1,600/19,855	0/0/0	0/0/0	0/0	16	N
	24090	1,600/26,876	0/0/0	0/0/0	0/0	<8	N
	24091	1,600/17,505	0/0/0	0/0/0	0/0	<8	N

[a]Total dose of inoculum per animal expressed as number of FFU in 2 mL of PBS.
[b]Antiviral activity (U/mL) and pIFNα (pg/mL) at 1 day postinoculation.
[c]First day postchallenge (dpc) that viremia was detected, maximum amount of viremia in PFU/mL detected in sera samples, and the duration (days) of viremia.
[d]First dpc that shedding virus was detected, maximum amount of shedding virus in PFU/mL detected in nasal swab samples, and the duration (days) of shedding.
[e]dpc first signs of lesions/highest lesion score.
[f]Neutralizing antibody response reported as serum dilution yielding a 70% reduction in the number of plaques (PRN_{70}) at 21 dpc.
[g]Detection of NS proteins in 21 dpc serum samples by 3ABC ELISA; N, negative; P, positive.

We were also able to considerably enhance the potency of Adt-pIFNα by administration of this vector at 4 sites in the neck compared with 1 site in the hind limb so that a 10-fold lower dose could completely protect 4 of 5 animals against ID challenge with either A24 Cruzeiro or Asia-1.

In the current study we used the same Adt-pIFNα and Adt-pIFNβ vector production lots in all of our experiments. Therefore, we initially performed a dose–response experiment with these vectors to determine the optimal doses needed to induce levels of pIFNα and/or antiviral activity that in previous experiments, with vector produced in our laboratory, were required to induce protection against clinical disease. We found that doses of 10^{10} or 10^{11} FFU-induced levels of pIFNα and antiviral activity that we predicted

Table 7. Adenovirus Type 5 Vector Containing a Porcine Interferon α/β Gene Efficacy Studies in Swine: Evaluation of Sterile Protection in Clinically Protected Swine

Study	*Animal no.*	*IFN dose (FFU)*	*Viremia*	*Shedding*	*PRN_{70}*[a]	*3ABC*[b]	*rRT-PCR*[c]
IFNα, A24 challenge, Table 2	20962	10^{11}	0	0	512	N	N
	20963	10^{11}	0	0	<8	N	N
	20964	10^{11}	0	0	512	N	N
IFNα, O1M challenge, Table 2	959	10^{10}	0	0	8	N	N
	961	10^{11}	0	0	<8	N	N
	962	10^{11}	0	0	<8	N	N
	963	10^{11}	0	0	<8	N	N
IFNα, A24 contact challenge, Table 3	9133	10^{10}	0	0	<8	N	N
	9134	10^{10}	0	0	<8	N	N
	9136	10^{11}	0	0	<8	N	N
	9137	10^{11}	0	0	<8	N	N
	9138	10^{11}	0	0	<8	N	N
IFNβ, A24 challenge, Table 4	48	10^{10}	0	0	32	N	N
	50	10^{11}	0	0	64	N	N
	51	10^{11}	0	0	64	N	N
	52	10^{11}	0	0	512	N	N
IFNα, A24 challenge, Table 5	811	10^{10}	0	0	<8	N	N
	812	10^{10}	0	0	64	N	N
	815	10^{10}	0	0	256	N	N
	816	10^{10}	0	0	128	N	N
IFNα, Asia-1 challenge, Table 6	24092	10^{10}	0	0	32	N	N
	24093	10^{10}	0	0	16	N	N
	24088	10^{11}	0	0	16	N	N
	24090	10^{11}	0	0	<8	N	N
	24091	10^{11}	0	0	<8	N	N

[a]Neutralizing antibody response reported as serum dilution yielding a 70% reduction in the number of plaques (PRN_{70}) at 21 days postchallenge (dpc).
[b]Detection of NS proteins in 21 dpc serum samples by 3ABC ELISA; N, negative; P, positive.
[c]rRT-PCR of serum samples at 1–7 dpc. N = Ct ≥40; P = Ct <40.
Abbreviation: rRT-PCR, real-time reverse transcriptase–polymerase chain reaction.

would partially or completely protect swine when challenged 1 day postadministration. Further, we used the same lot of each swine-derived FMDV serotype in all challenge experiments and determined that the dose of each serotype required to reliably induce clinical disease in all control animals by 2–3 days postchallenge was 10^5 $TCID_{50}$. While this dose is 10-fold higher than that recommended by the OIE, we preferred to use a relatively severe challenge to test our model.

The most common mechanism of spread of FMD to swine is by direct contact exposure with infected animals (Alexandersen and others 2003). Therefore, to examine the efficacy of rapid protection against natural infection of swine pretreated with Adt-pIFNα, we utilized an FMD contact transmission model (Pacheco and others, manuscript in preparation). All donor animals developed lesions by 2 dpc and all recipient animals had detectable virus in nasal swab samples 1 day postcontact challenge, indicating a successful contact exposure with the donor animals. Five of the 6 control-inoculated recipient animals (PBS and AdNull) developed clinical disease and all of these animals, including the animal that did not develop lesions, had a high FMDV-specific neutralizing antibody response and were 3ABC ELISA positive, demonstrating that FMDV replication occurred. We found that all animals pretreated with 10^{11} FFU Adt-pIFNα and 2 of 3 animals pretreated with 10^{10} FFU were completely protected from contact challenge. These results confirm that Adt-pIFNα can rapidly protect swine not only against FMDV using an OIE-approved ID challenge model, even at a 10-fold higher challenge dose than recommended, but also against challenge by the natural route of infection. Moreover, since we obtained better protection with less Adt-pIFNα in the contact challenge experiment compared with ID challenge, this suggests that in a natural FMD outbreak the lower dose may be sufficient to limit disease spread beyond the initial farm on which an outbreak occurs.

Although all animals inoculated with 10^{11} FFU Adt-pIFNα/β were protected from FMDV challenge, they developed transient jaundice and generally did not eat well (data not shown; animals inoculated with this dose of the control vectors did not develop jaundice or other adverse effects). Recovery required 2–3 days. To avoid these side effects as well as develop a more potent biotherapeutic, we attempted to lower the protective dose of Adt-pIFNα by comparing single-site versus multiple-site IM inoculation in the hind limb and neck. The data clearly show that inoculation at 4 sites in the neck with 10^{10} FFU Adt-pIFNα was the most efficacious method of administration since both animals in this group were completely protected, and based on the antiviral activity detected in the animal in this group that died 1 dpc, we predict that this animal would also have been protected (Table 5). Further, 2 of the 3 animals administered 10^{10} FFU Adt-pIFNα by this method in the Asia-1 challenge experiment were also completely protected (Tables 6 and 7).

There are limited studies comparing the efficacy of single-site versus multiple-site inoculation, and most of these are vaccination studies. Gardiner and others (2006) showed that multiple-site inoculation of mice at different anatomic locations with a DNA vector containing HIV Gag-specific peptides improved both cellular and humoral immune responses compared with inoculation with the same dose at only 1 site. The authors attributed the enhanced responses to multiple factors, including antigen loading of antigen presenting cells and presentation/recruitment of antigen-specific naïve T-cells at the regional lymph nodes. Similarly, Wansley and others (2008) found that mice vaccinated at multiple sites with a tumor antigen have an enhanced antigen-specific T cell response and resulted in lower tumor volume compared with mice vaccinated at a single site. In the current study the only parameters that we examined in addition to clinical score were the presence of pIFNα protein and antiviral activity in plasma. In both assays the highest level of protein and antiviral activity was detected in animals inoculated at 4 sites in either the hind limb or neck. However, these quantitative differences were not statistically significant when these 2 groups were compared with the other groups. Perhaps based on our previous studies (Diaz-San Segundo and others 2010), examination of ISGs in specific tissues and/or examination of the number and maturation status of DCs and NK cells might show a relationship that would help explain the improved efficacy of the multiple-site inoculation approach.

We examined a number of criteria to assess whether IFN pretreatment completely blocked productive FMDV replication in animals that had no detectable clinical disease, that is, induced sterile immunity (Table 7). On the basis of the absence of (1) viremia, (2) virus shedding, (3) viral RNA in serum by rRT-PCR, (4) antibodies against viral NS protein 3ABC, and (5) the absence or very low levels of FMDV-specific neutralizing antibodies (PRN_{70} less than 100), pretreatment induced sterile immunity in 20 of 25 animals that had no clinical disease. The 5 remaining animals only had a significant FMDV-specific neutralizing antibody responses, that is, nos. 20962, 20964, 52, 815, and 816. The data for these 5 animals suggest that there was very limited virus replication. Nevertheless, IFN pretreatment clearly either dramatically reduced or completely inhibited productive FMDV replication, thereby significantly limiting virus shedding into the environment.

In subsequent studies we plan to examine alternate routes of delivery of the Adt-IFNs. We will also examine if administration of IFNs in combination with other molecules capable of inducing an innate immune response might result in a more robust response and potentially lower the effective Adt-IFN doses needed to rapidly and sterilely protect swine and other susceptible species from FMD.

Acknowledgments

This research was supported in part by the Plum Island Animal Disease Research Participation Program administered by the Oak Ridge Institute for Science and Education through an interagency agreement between the U.S. Department of Energy and the U.S. Department of Agriculture (appointment of Camila C.A. Dias and Fayna Diaz-San Segundo); by CRIS project no. 1940-32000-053-00D, Agricultural Research Service (ARS), U.S. Department of Agriculture (M. J. Grubman, T. de los Santos); and by reimbursable agreement no. 60-1940-7-47 with the Department of Homeland Security (M.J. Grubman).

We thank Juan Pacheco and Luis L. Rodriguez ARS, Plum Island Animal Disease Center (PIADC), for FMDV stocks; George Smoliga and Ethan Hartwig ARS, PIADC, for help with rRT-PCR analysis; and Douglas E. Brough and Damodar Ettyreddy from GenVec, Inc., for supplies of the Adt vectors. We also thank Karen Moran, Ian Olesen, and Samia

Metwally of the Foreign Animal Disease Diagnostic Laboratory (FADDL) at PIADC for performing the 3ABC ELISA assays; Fawzi Mohamed, FADDL, for performing histopathological analysis on the animals that died in the various trials; and the animal care staff at PIADC for their professional support and assistance. We gratefully acknowledge Drs. David Brake and Eva Perez for critical reading of the manuscript.

Author Disclosure Statement

No competing financial interests exist.

References

Ahl R, Rump A. 1976. Assay of bovine interferons in cultures of the porcine cell line IB-RS-2. Infect Immun 14:603–606.

Alexandersen S, Zhang Z, Donaldson AI, Garland AJM. 2003. The pathogenesis and diagnosis of foot-and-mouth disease. J Comp Pathol 129:1–36.

Chinsangaram J, Koster M, Grubman MJ. 2001. Inhibition of L-deleted foot-and-mouth disease virus replication by alpha/beta interferon involves double-stranded RNA-dependent protein kinase. J Virol 75:5498–5503.

Chinsangaram J, Moraes MP, Koster M, Grubman MJ. 2003. A novel viral disease control strategy: Adenovirus expressing interferon alpha rapidly protects swine from foot-and-mouth disease. J Virol 77:1621–1625.

Chinsangaram J, Piccone ME, Grubman MJ. 1999. Ability of foot-and-mouth disease virus to form plaques in cell culture is associated with suppression of alpha/beta interferon. J Virol 73:9891–9898.

de Avila Botton S, Brum MCS, Bautista E, Koster M, Weiblen R, Golde WT, Grubman MJ. 2006. Immunopotentiation of a foot-and-mouth disease virus subunit vaccine by interferon alpha. Vaccine 24:3446–3456.

Der SD, Zhou A, Williams BRG, Silverman RH. 1998. Identification of genes differentially regulated by interferon α, β, or γ using oligonucleotide arrays. Proc Natl Acad Sci USA 95: 15623–15628.

Diaz-San Segundo F, Moraes MP, de los Santos T, Dias CCA, Grubman MJ. 2010. Interferon-induced protection against foot-and-mouth disease virus correlates with enhanced tissue specific innate immune cell infiltration and interferon-stimulated gene expression. J Virol 84:2063–2077.

Domingo E, Escarmís C, Baranowski E, Ruiz-Jarabo CM, Carrillo E, Núñez JI, Sobrino F. 2003. Evolution of foot-and-mouth disease virus. Virus Res 91:47–63.

Fontana JM, Bankamp B, Rota PA. 2008. Inhibition of interferon induction and signalling by paramyxoviruses. Immunological Rev 225:46–67.

Gall JGD, Lizonova A, EttyReddy D, McVey D, Zuber M, Kovesdi I, Aughtman B, King CR, Brough DE. 2007. Rescue and production of vaccine and therapeutic adenovirus vectors expressing inhibitory transgenes. Mol Biotechnol 35:263–273.

Gardiner DF, Huang Y, Basu S, Leung L, Song Y, Chen Z, Ho DD. 2006. Multiple-site DNA vaccination enhances immune responses in mice. Vaccine 24:287–292.

Golde WT, Pacheco JM., Duque H, Doel T, Penfold B, Ferman GS, Gregg DR, Rodriguez LL. 2005. Vaccination against foot-and-mouth disease virus confers complete clinical protection in 7 days and partial protection in 4 days: Use in emergency outbreak response. Vaccine 23:5775–5782.

Grubman MJ. 2003. New approaches to rapidly control foot-and-mouth disease outbreaks. Expert Rev Anti-infect Ther 1:89–96.

Grubman MJ. 2005. Development of novel strategies to control foot-and-mouth disease: Marker vaccines and antivirals. Biologicals 33:227–234.

Grubman MJ, Baxt B. 2004. Foot-and-mouth disease. Clin Microbio Rev 17:465–493.

Mason PW, Piccone ME, McKenna TS-C, Chinsangaram J, Grubman MJ. 1997. Evaluation of a live-attenuated foot-and-mouth virus as a vaccine candidate. Virology 227:96–102.

Moraes MP, Chinsangaram J, Brum MCS, Grubman MJ. 2003. Immediate protection of swine from foot-and-mouth disease: A combination of adenoviruses expressing interferon alpha and a foot-and-mouth disease virus subunit vaccine. Vaccine 22:268–279.

Moraes MP, de los Santos T, Koster M, Turecek T, Wang H, Andreyev VG, Grubman MJ. 2007. Enhanced antiviral activity against foot-and-mouth disease virus by a combination of type I and II porcine interferons. J Virol 81(13):7124–7135.

Moraes MP, Mayr GA, Mason PW, Grubman MJ. 2002. Early protection against homologous challenge after a single dose of replication-defective human adenovirus type 5 expressing capsid proteins of foot-and-mouth disease virus (FMDV) strain A24. Vaccine 20:1631–1639.

OIE. 2004. Section 2.1, List A: Diseases. Chapter 2.1.1: Foot and mouth disease. Manual of diagnostic tests and vaccines for terrestrial animals, 5th edition. Modified May, 2006. pp 111–128.

Pacheco JM, Arzt J, Rodriguez LL. 2010. Early events in the pathogenesis of foot-and-mouth disease in cattle after controlled aerosol exposure. Vet J 183:46–53.

Pacheco JM, Brum MCS, Moraes MP, Golde WT, Grubman MJ. 2005. Rapid protection of cattle from direct challenge with foot-and-mouth disease virus (FMDV) by a single inoculation with an adenovirus vectored FMDV subunit vaccine. Virology 337:205–209.

Sorensen KJ, Madsen KG, Madsen ES, Salt JS, Nquindi J, Mackay DKJ. 1998. Differentiation of infection from vaccination in foot-and-mouth disease by the detection of antibodies to the non-structural proteins 3D, 3AB and 3ABC in ELISA using antigens expressed in baculovirus. Arch Virol 143:1461–1476.

Takaoka A, Yanai H. 2006. Interferon signalling network in innate defence. Cell Microbiol 8:907–922.

Wansley EK, Chakraborty M, Hance KW, Bernstein MB, Boehm AL, Guo Z, Quick D, Franzusoff A, Greiner JW, Schlom J, Hodge JW. 2008. Vaccination with a recombinant *Saccharaomyces cerevisiae* expressing a tumor antigen breaks immune tolerance and elicits therapeutic antitumor responses. Clin Cancer Res 14:4316–4325.

Wu Q, Brum MCS, Caron L, Koster M, Grubman MJ. 2003. Adenovirus-mediated type I interferon expression delays and reduces disease signs in cattle challenged with foot-and-mouth disease virus. J Int Cyt Res 23:371–380.

Address correspondence to:
Dr. Marvin J. Grubman
Plum Island Animal Disease Center
Agricultural Research Service
U.S. Department of Agriculture
North Atlantic Area, P.O. Box 848
Greenport, NY 11944

E-mail: marvin.grubman@ars.usda.gov

Received 27 May 2010/Accepted 20 June 2010

Return to Table of Contents

VIRAL IMMUNOLOGY
Volume 23, Number 1, 2010

Pp. 29–41
DOI: 10.1089/vim.2009.0078

Loss of Plasmacytoid Dendritic Cell Function Coincides with Lymphopenia and Viremia During Foot-and-Mouth Disease Virus Infection

Charles K. Nfon,[1] Felix N. Toka,[1,2] Mary Kenney,[1] Juan M. Pacheco,[1] and William T. Golde[1]

Abstract

Foot-and-mouth disease virus (FMDV) causes an acute, highly contagious disease of livestock. Though FMDV is very sensitive to interferon-α (IFN-α), IFN-β, and IFN-γ, the virus has evolved mechanisms to evade such innate responses. For instance, during acute infection, FMDV suppresses IFN-α production by skin and myeloid dendritic cells (DCs). We have previously reported that FMDV infection induces a transient lymphopenia and interruption of T-lymphocyte responses to mitogenic stimuli. To further understand the immunopathogenesis of FMD, we have now analyzed the serum IFN-α response in relation to lymphopenia, and the number and function of plasmacytoid DCs (pDCs) following infection of pigs with multiple serotypes of FMDV. Serum IFN-α peaked 2–3 d post-infection (PI), regardless of FMDV serotype. Lymphopenia coincided with peak viremia and the serum IFN-α response. Circulating pDC numbers and *in-vitro* pDC IFN-α secretion transiently declined by 48 h following infection. Infection of lymphocytes or pDCs was never detected regardless of the FMDV serotype inoculated or the age of the animal infected. These data indicate that, like other DC subsets, there is suppression of interferon production by pDCs, which abrogates this important innate response. Rapid induction of serum IFN-α, albeit short-lived, may contribute to the rapid resolution of FMDV viremia prior to induction of specific immunity.

Introduction

FOOT-AND-MOUTH DISEASE (FMD) is a highly contagious disease of livestock that continues to be a significant economic problem worldwide. FMDV causes vesicular lesions in the mouth and on coronary bands of the feet of cloven hoofed animals, and is considered one of the most contagious viruses studied (15). An optimum approach to containing outbreaks in FMDV-free countries would be the use of sensitive and rapid-acting antiviral agents and vaccines. To develop these optimal response capabilities, we require a more detailed understanding of the innate and adaptive immune responses of susceptible species to this virus.

FMDV is very sensitive to interferons (IFNs), including IFN-α, IFN-β, and IFN-γ (9,26), and numerous studies suggest that these IFNs may have a role in the resolution of FMDV infection. Type I IFNs were first identified as humoral antiviral agents (21). They constitute a first line of defense against viral infections, inducing the expression of IFN-stimulated genes, which inhibit viral replication in susceptible cells (14,42). Chinsangaram *et al.* have shown that IFN-α-induced RNA-dependent protein kinase (PKR) and 2′-5′-A synthetase/RNase L (OAS) prevent the replication of FMDV in otherwise permissive cells (7). In addition, inoculation of animals with adeno-vectored porcine IFN-α gene leads to protection against FMDV in swine (8), and significantly reduces the severity of the infection in cattle (40). Furthermore, porcine skin DCs are resistant to FMDV because they constitutively express IFN-α and secrete both IFN-α and IFN-β upon exposure to the virus (3).

Other viruses have evolved mechanisms for blocking innate antiviral responses. For example, poxviruses have evolved a number of mechanisms for blocking IFN production and the cellular response to IFN. During infection, toll-like receptor (TLR) stimulators like double-stranded RNA (dsRNA) are sequestered, blocking activation of IFN response molecules like dsRNA-dependent protein kinase. These viruses also encode mimicking cytokines, chemokines, and their receptors, blocking the function of these molecules. There is also interference with secondary signaling molecules, such as blocking degradation of IκB (18,35,36). In addition, bovine herpes virus (27) and pseudorabies virus (1)

[1]Plum Island Animal Disease Center, Agricultural Research Service, U.S. Department of Agriculture, Greenport, New York.
[2]Department of Preclinical Science, Faculty of Veterinary Medicine, Warsaw University of Life Science, Warsaw, Poland.

have been shown to down-modulate expression of MHC class I, making virus-infected cells refractory to NK or CTL killing.

In vitro, infection with FMDV is characterized by the early production of the viral leader protease, which cleaves elongation factor 4G, shutting off cap-dependent translation of cellular mRNA (12). A consequence of this is a blockage of host-cell protein synthesis, which results in inhibition of IFN-α and IFN-β production in infected cells (7,9), permitting viral replication, assembly, and new virus production (15). Furthermore, this results in the lack of the ability of infected cells to translate new MHC molecules containing viral peptides via the endogenous pathway, compromising viral peptide presentation to MHC class I-restricted T cells (34).

During the acute phase of infection in swine, another potential mechanism of immune evasion may be playing a significant role in pathogenesis. We have previously demonstrated that FMDV infection induces a severe lymphopenia and reduced T-cell proliferative response to mitogen. The lymphopenia induced by FMDV is transient, corresponds to the peak of viremia, and there is no infection of lymphocytes *in vivo*. The recovery from the lymphopenia is rapid (2). Furthermore, T-cell proliferative responses to the mitogen, Con A, are lost. Contrarily, analysis of an *in-vitro* propagated C strain of FMDV showed infection of lymphocytes *in vivo* (13). Also, during acute FMDV infection of swine, production of IFN-α from monocyte-derived DCs (MoDCs) and skin-derived DCs (skin DCs) is inhibited. This effect is concurrent with rising viral titer in the blood; however, these cells are not productively infected. Interestingly, there are no changes in the capability of these DCs to take-up particles and process antigens, indicating that the antigen-presenting cell function is normal (28).

In the present studies, we have analyzed FMDV induction of immunosuppression during acute infection of swine to understand the effect of FMDV on porcine plasmocytoid DC numbers and function. Furthermore, we addressed contradictory reports in the literature by comparing lymphopenia and infectivity of lymphocytes by various serotypes of FMDV. Regardless of viral strain, infected pigs showed typical signs of FMDV, including fever, which peaked on days 2–3 post-infection (PI), and was concurrent with viremia and lymphopenia. Lymphocytes isolated during peak viremia were not infected by virus isolation or real-time PCR, and serum IFN-α was detected in all infected pigs 2–3 d PI, again regardless of FMDV serotype. In all animals, circulating pDCs declined sharply in number at 48 h following infection, but returned to pre-infection levels by days 5–6 PI, and pDC function was depressed. These data indicate interruption of IFN-α production by pDCs during the acute phase of infection. However, the early systemic IFN-α response may already initiate an antiviral response in tissues, leading to the rapid resolution of FMDV viremia prior to the induction of specific immunity.

Materials and Methods

Viruses

FMDV A24 Cruzeiro (A24) and O1 Campos (O1C) are natural isolates from Brazil that have been passed in pigs and vesicular fluid diluted in supplemented MEM for inoculation (3). The Plum Island Animal Disease Center (PIADC) Institutional Animal Care and Use Committee approved all procedures performed on these animals. FMDV C-s8C1 is a plaque-purified derivative of the natural isolate of serotype C1 Santa Pau Spain 70. This has been repeatedly passed on BHK-21 and thus is adapted for heparan sulfate binding (20). Pigs at PIADC were infected with the plaque-purified C-s8C1 (FMDV C-s8C1 BHK), and virus collected from vesicular fluid was diluted in supplemented MEM (C-s8C1 PIADC PP1). C-s8C1 PIADC PP1 was again passed in pigs, and virus collected from vesicular fluid was diluted in supplemented MEM as C-s8C1 PIADC PP2. FMDV C3-Resende is a natural isolate (33) that was pig passed prior to use in this experiment. Viral titers were determined on BHK-21 cells by a standard protocol (2).

Animals, virus challenge, and blood sampling

Groups of Yorkshire pigs 2–3 mo old and 6–8 mo old were purchased from Animal Biotech, Inc. (Danboro, PA), and allowed 1 wk to acclimatize before the start of the experiments. Each pig was inoculated with virus intradermally in the heel bulb of both hind feet with 100 μL of 1×10^5 plaque-forming units of either FMDV serotype A24 Cruzeiro, O1 Campos, C3 Resende, plaque-purified C-s8C1, or pig-passed C-s8C1 (C-s8C1 was isolated from vesicles of infected pigs inoculated with plaque-purified virus [C-s8C1 PP1], or C-s8C1 isolated from vesicles of infected pigs inoculated with C-s8C1 PP2 [C-s8C1 PP2]). The animals were examined for clinical signs of infection.

Heparinized and nonheparinized blood collection tubes (Becton Dickinson, Franklin Lakes, NJ) were used for daily blood collection from the anterior vena cava. Serum was obtained from the blood drawn into nonheparinized tubes. Meanwhile, heparinized blood was diluted in an equal volume of PBS and layered over a separation gradient (Lymphoprep™; Life Technologies, Grand Island, NY) for PBMC isolation following the manufacturer's protocol. Whole blood was analyzed on an AcT hematology analyzer (Beckman Coulter, Miami, FL) to determine the percentage of lymphocytes.

Interferon-α ELISA

The IFN-α concentration in serum was determined by an antigen-capture ELISA as previously described (3). Briefly, anti-porcine IFN-α monoclonal antibodies K9 and biotinylated F17 (PBL Biomedical Laboratories, Piscataway, NJ), respectively, were used for capture and detection. The IFN-α concentration in picograms per milliliter was determined by extrapolation from a standard curve.

Virus isolation and detection

Viremia was quantified by a standard assay for isolating virus (31). Briefly, serial 10-fold dilutions of serum samples were added to confluent monolayers of BHK-21 cells in quadruplicate wells in the 96-well format and incubated at 37°C for 24–48 h. The plates were observed for CPE and stained with crystal violet when CPE was detected in the positive control wells. $TCID_{50}$ was calculated from the dilutions. Samples negative for virus isolation were confirmed using real-time PCR detection of viral RNA as previously described (6).

Flow cytometry

CD4a FITC (74-12-4; BD Biosciences, San Jose, CA) and CD172 PE (Southern Biotech, Birmingham, AL) were used in flow cytometry to identify porcine plasmacytoid DCs. Briefly, 1×10^6 PBMCs were washed in chilled FACS buffer prior to being stained for 30 min on ice with optimal dilutions of the above antibodies or their respective isotype controls. Data were acquired by flow cytometry (FACSCalibur; BD Biosciences) and analyzed with Cell Quest Pro (BD Biosciences) for the percentage of $CD4^+CD172low$ pDCs, which was obtained by subtracting the background values.

Phenotype and ELISpot detection of interferon-α-producing cells in PBMCs

Owing to the limited number of pDCs in blood, our experiment was designed to quantify the responses of these cells without the need for separating them from the PBMCs. To attain this goal, we used the unique capability of porcine pDCs to respond to type A CpG (CpG 2216). Guzylack-Piriou *et al.* have previously shown that CD4CD172 double-positive pDCs in the PBMCs of swine are uniquely responsible for IFN-α responses to CpG 2216 (16). However, we started by confirming that the cells secreting IFNα in response to CpG 2216 expressed both CD4 and CD172. Negative selection with Dynal beads (Dynal Corp., Invitrogen, Carlsbad, CA) was used according to the manufacturer's protocol to deplete PBMCs of various cell types, and the remaining cells were tested for IFN-α secretion in response to CpG 2216. Briefly, PBMCs were incubated with mouse antibodies to specific porcine leukocyte markers, followed by the addition of anti-mouse IgG-coated beads. The bead-positive cells were then separated with a magnetic field. T and B lymphocytes were eliminated with antibodies to CD3 and CD21, while using antibodies to CD14 and CD4 eliminated monocytes and pDCs plus $CD4^+$ T cells, respectively. With antibodies to CD172, the PBMCs were depleted of monocytes and DCs. For positive selection to enrich pDCs, the PBMCs were first cultured for 1.5 h to eliminate monocytes by adherence to plastic, then depletion of T and B cells from the non-adherent fraction was performed, followed by incubation with a cocktail of antibodies to porcine CD4 and CD172. The CD4- and CD172-positive cells were then freed of the beads by enzymatic treatment according to the manufacturer's protocol. The efficiency of depletion of cells relative to whole PBMCs was assessed by flow cytometry. The required cell fractions were washed with and suspended in lymphocyte culture medium (LCM; RPMI-1640 with 10% FBS and antibiotics; Life Technologies). For analysis of IFN-α production, whole PBMCs or sorted cells were cultured in 24-well plates at 1.0×10^6 total cells in 1.0 mL LCM, and immediately stimulated with 10 μg/mL CpG 2216. After 24 h of incubation at 37°C, 5% CO_2, and 85% relative humidity, the supernatants were collected and assayed for IFN-α by ELISA as described.

Having established that the cells responding to CpG 2216 were pDCs, these cells were quantified by ELISpot determination of the CpG-induced IFN-α spots. Thus by ELISpot we monitored the effect of FMDV infection in pigs on the number of circulating pDCs responding to CpG 2216. ELISpot was performed according to a previously published protocol (29), with some modifications. Briefly, 96-well MultiScreen™ filtration plates (Millipore Corporation, Bedford, MA) were coated overnight at 4°C with 100 μL of 1.0 μg/mL K9 (PBL) in carbonate/bicarbonate buffer. The plates were washed four times with sterile PBS (pH 7.4), blocked with LCM for 2 h at 37°C, and washed again with sterile PBS. PBMCs stimulated with 10 μg/mL of CpG 2216 in sterile Falcon tubes were dispensed in quadruplicate at 10^5 cells/well in 100 μL, and the plates were incubated overnight at 37°C. The remaining content of the tubes (0.6 mL) was also incubated overnight and the supernatants harvested for IFN-α ELISA as described above. The plates were washed three times with PBS, and once with distilled water to lyse any remaining cells, and rinsed with PBS. The plates were incubated at 37°C for 1 h with 100 μL/well of F17 (PBL) biotinylated at 1 μg/mL in PBS containing 0.5% Tween 20 (PBST). After four washes with PBS, 0.8 μg/mL streptavidin-HRP in PBST (100 μL/well) was added and the plates were incubated at room temperature for 30 min. The plates were washed four times with PBS, and the spots were developed with 100 μL/well of 3,3′-diaminobenzidine (DAB; Sigma, St Louis, MO) containing 0.3% hydrogen peroxide. After 3 min of incubation with DAB, the plates were washed with distilled water, dried overnight, and the spots were counted on an ImmunoSpot reader (CTL Analyzers LLC, Cleveland, OH). The number of spots corresponds to the number of IFN-α-secreting cells (pDCs) responding to CpG 2216.

Statistical analysis

Differences in serum IFN-α response, pDC numbers, and pDC response to CpG 2216 between various days were analyzed by one-way ANOVA and the Newman-Keuls multiple comparison test using GraphPad Prism Software version 5 (GraphPad Software Inc., San Diego, CA).

Results

Infection of swine with FMDV

All challenged animals showed clinical signs of FMD, with development of fever and vesicles on all four feet, snout, and tongue (data not shown). Peak viremia was detected at 2–3 d PI, and it had cleared by 4 d following inoculation (Fig. 1A–G). These results were consistent with our previous report (2), but in conflict with another report showing viremia detected from day 1 to day 10 PI in swine following inoculation of plaque-purified FMDV, strain C-s8C1 (13). Here, using this same strain, we observed viremia on day 1 PI, which rapidly cleared by day 4. All animals had clinically recovered by day 14 PI.

We have previously reported that during infection of young pigs with FMDV strains O1 Taiwan 97 and O1 Campos, a lymphopenia occurs with onset concurrent with the development of viremia (2). We now report identical results with the infection of older (Fig. 2A) and younger (Fig. 2B) animals with O1 Campos. In addition, a lymphopenia was observed when pigs were infected with A24 Cruzeiro and C3 Resende (Fig. 2C and H), indicating that the lymphopenia induced by FMDV is neither serotype-specific nor age-dependent. The results for the plaque-purified virus, C-s8C1, were less clear. First, variability between animals was pronounced, and in addition, the percentage of lymphocytes in some animals declined over the 2-wk study period

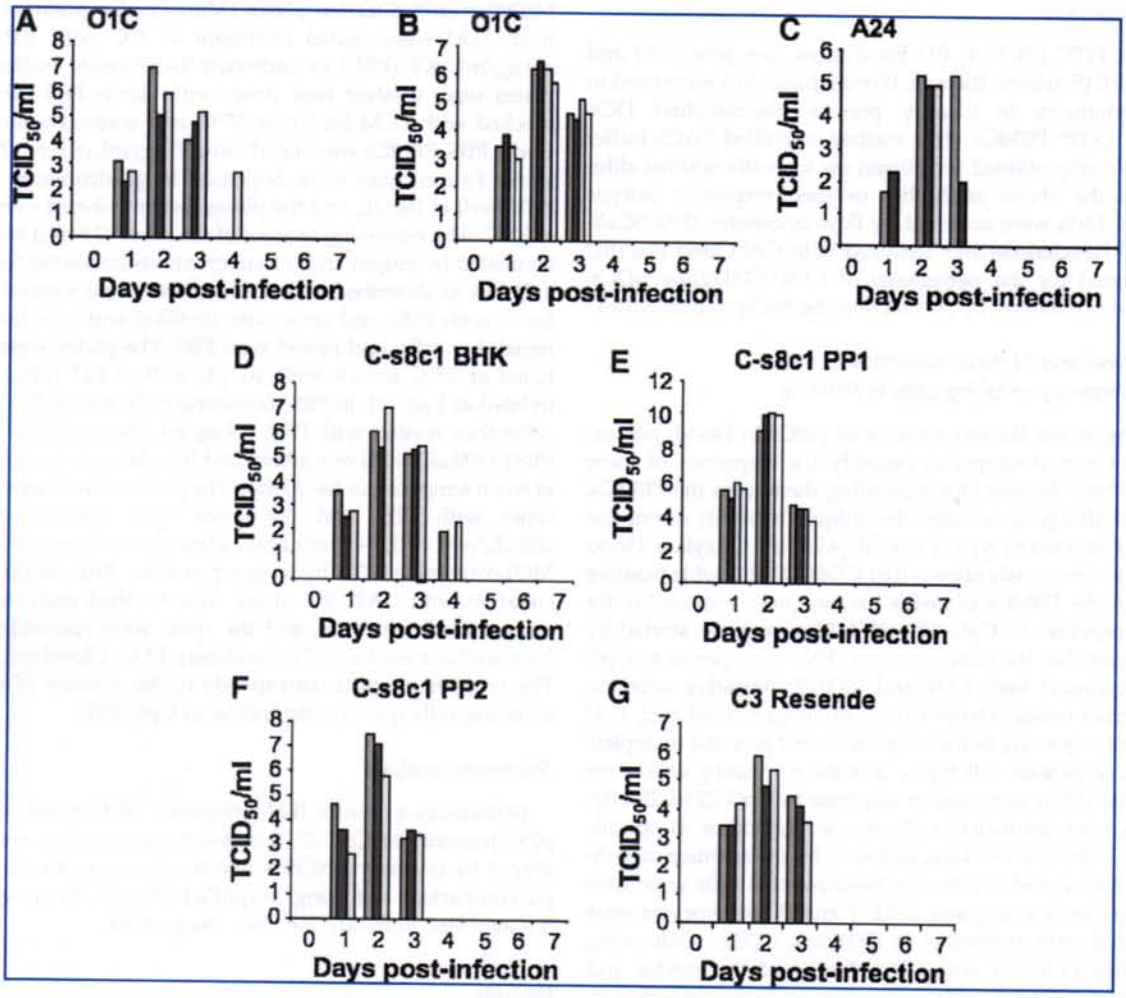

FIG. 1. Viremia in FMDV-infected pigs. Pigs were inoculated with virus intradermally in the heel bulb and serum was collected daily for virus isolation. (**A**) Viremia in 6-mo-old pigs infected with O1 Campos (O1C; n = 3). (**B**) Viremia in 2-mo-old pigs infected with O1C (n = 4). (**C**) Viremia in A24 Cruzeiro-infected pigs (A24; n = 3). (**D**) Viremia in pigs infected with *in-vitro* propagated C-s8C1 (C-s8C1 BHK; n = 3). (**E**) Viremia in pigs infected with C-s8C1 previously passed once in other pigs (C-s8C1 PP1; n = 4). (**F**) Viremia in pigs infected with C-s8C1 previously passed twice in other pigs (C-s8C1 PP2; n = 3). (**G**) Viremia in C3 Resende-infected pigs (C3 Resende; n = 3). The pigs shown in C–G were 2–3 mo old (n = the number of pigs infected with each serotype; virus titers are expressed in $\log_{10}$ $TCID_{50}$ per milliliter).

(Fig. 2D). Testing FMDV strain C-s8C1 harvested from vesicles of these animals (animal-derived virus preparations) in subsequent animal inoculations showed a more familiar pattern, with lymphopenia observed at day 2, and resolving by day 4 (Fig. 2E).

Finally, we confirmed our previous report that porcine PBMCs are not infected by O1 Campos, and further show that PBMCs of swine are neither infected by A24 Cruzeiro nor by C-s8C1 and C3 Resende in both *in-vivo* and *in-vitro* exposure. In all cases, virus isolation was negative (data not shown). We tested lysates of PBMCs by real-time PCR and virus isolation on BHK-21 cells and all were negative (data not shown). We also co-cultured the PBMCs with BHK-21 cells and also detected no virus regardless of the strain of FMDV used to infect the animals. All of this occurred while the plasma contained readily detectable virus (Fig. 1). The data presented here for the strain C-s8C1 contradicts a previous report by Diaz-San Segundo *et al.* (13), in which they used the *in-vitro* propagated, plaque-purified C-s8C1 virus, and showed infection of lymphocytes over an extended period.

Serum IFN-α in pigs infected with FMDV

In vitro, IFN-α has been shown to have strong antiviral effects on FMDV (7,9). In addition, serum IFN-α has been linked to lymphopenia in swine (37) and other animal species (24). Given the rapid clearance of viremia and the transient lymphopenia in porcine FMDV infection, we sought to determine if there was induction of IFN-α secretion early during infection. All pigs had detectable levels of serum IFN-α on day 1 PI, and levels peaked on days 2–3 (Fig. 3). Although peak levels of IFN-α were highly variable, ranging from 200–1500 pg/mL, these reached statistical significance on day 3 compared to day 0 ($p < 0.05$) in all the study groups. The early response pattern was similar in all sero-

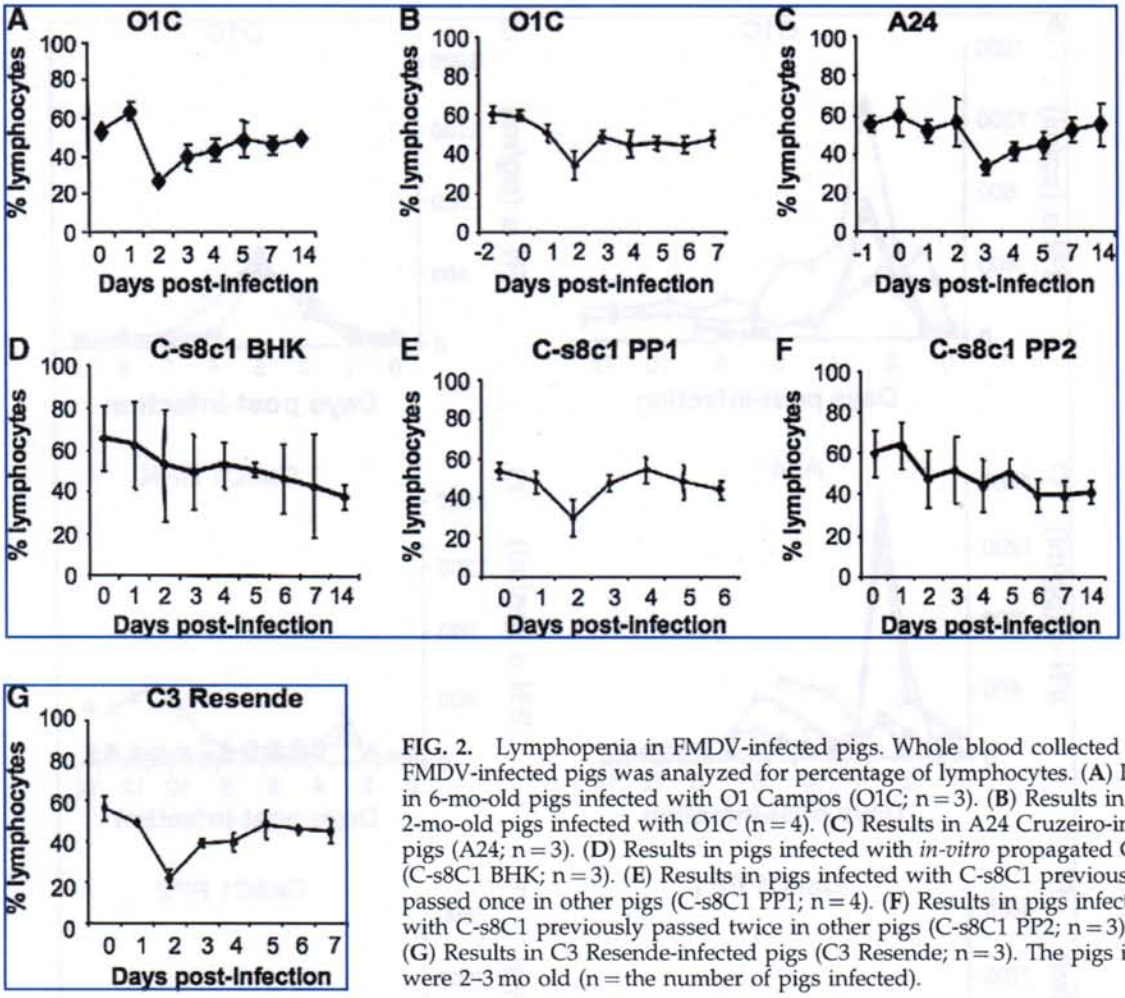

FIG. 2. Lymphopenia in FMDV-infected pigs. Whole blood collected from FMDV-infected pigs was analyzed for percentage of lymphocytes. (**A**) Results in 6-mo-old pigs infected with O1 Campos (O1C; n = 3). (**B**) Results in 2-mo-old pigs infected with O1C (n = 4). (**C**) Results in A24 Cruzeiro-infected pigs (A24; n = 3). (**D**) Results in pigs infected with *in-vitro* propagated C-s8C1 (C-s8C1 BHK; n = 3). (**E**) Results in pigs infected with C-s8C1 previously passed once in other pigs (C-s8C1 PP1; n = 4). (**F**) Results in pigs infected with C-s8C1 previously passed twice in other pigs (C-s8C1 PP2; n = 3). (**G**) Results in C3 Resende-infected pigs (C3 Resende; n = 3). The pigs in C–G were 2–3 mo old (n = the number of pigs infected).

types of FMDV tested. However, a biphasic response of serum IFN-α was detected between days 8 and 12 following infection in a few animals, though none of these were statistically significant compared to pre-infection levels of IFN-α in that animal.

Phenotype of cells in porcine PBMCs responding to CpG 2216

Plasmacytoid DCs usually constitute less than 1% of the PBMCs, and secrete IFN-α in response to viral infection. Porcine pDCs express high levels of CD4 and low levels of CD172, and produce large amounts of IFN-α in response to type A CpG (16). By flow cytometry, we identified this population in porcine PBMCs (Fig. 4A). Cells prepared by negative selection confirmed that pDCs are indeed the cells in porcine PBMCs responding to CpG 2216 by secreting IFN-α (Fig. 4B). This was confirmed by analyzing cells positively selected with anti-CD4 and anti-CD172 (Fig. 4B).

Effect of FMDV infection on number and function of circulating pDCs during acute infection

Since FMDV infection of pigs modulates the immune response via lymphopenia and results in diminished IFN-α secretion by skin DCs and MoDCs (28), we determined the effect of viral infection on pDC numbers, a potential *in-vivo* source of IFN-α. We monitored the proportion of pDCs in PBMCs by flow cytometry following FMDV infection. In the naïve pigs, these cells ranged from 0.5–1.5% of the PBMC population. During infection the numbers progressively declined by days 3–5 PI, as shown in the representative dot plots of a representative animal (Fig. 5). By day 7 these cells had returned to pre-infection levels. This trend was observed in all animals analyzed for pDC numbers in the 7 d following infection.

Furthermore, previously swine pDCs were shown to produce large amounts of IFN-α in response to the TLR 9 agonist type A CpG 2216 (16). This was confirmed here by us (Fig. 4B). Thus, using ELISpot detection of cells secreting IFN-α following CpG 2216 stimulation, we found that the number of pDCs in the blood began to diminish on days 2 through 4, with the lowest percentage detectable on day 4 or 5 (Fig. 6A–H). This effect was seen regardless of virus serotype, and it began concurrently with the onset of viremia. We show individual animals analyzed in these experiments, given the variability in response in these outbred pigs. Nevertheless, this decline in pDCs responding to CpG 2216 was statistically significant ($p < 0.01$) on day 4 relative to day

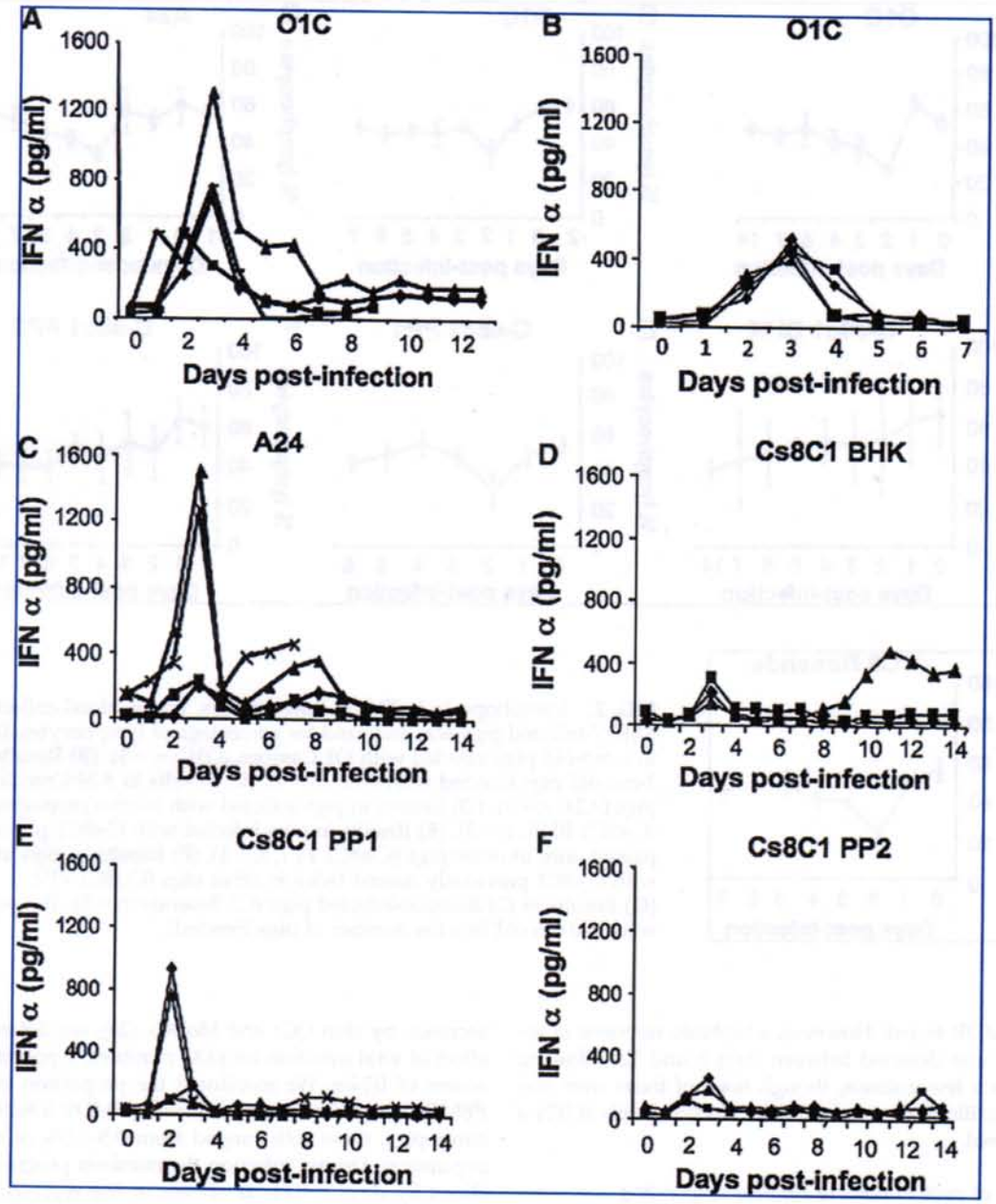

FIG. 3. Porcine serum IFN-α response to FMDV infection. Serum collected from FMDV-infected pigs was assayed for IFN-α by a sandwich ELISA. (**A**) Results from 6-mo-old pigs infected with O1 Campos (O1C; n = 3). (**B**) Results from 2-mo-old pigs infected with O1C (n = 4). (**C**) Results from A24 Cruzeiro-infected pigs (A24; n = 3). A fourth animal infected with A24 was sacrificed on day 7 (x–x). (**D**) Results from pigs infected with *in-vitro* propagated C-s8C1 (C-s8C1 BHK; n = 3). (**E**) Results from pigs infected with C-s8C1 previously passed once in other pigs (C-s8C1 PP1; n = 4). (**F**) Results from pigs infected with C-s8C1 previously passed twice in other pigs (C-s8C1 PP2; n = 3). (**G**) Results from C3 Resende-infected pigs (n = 3). The pigs in C–G were 2–3 mo old (n = the number of pigs infected).

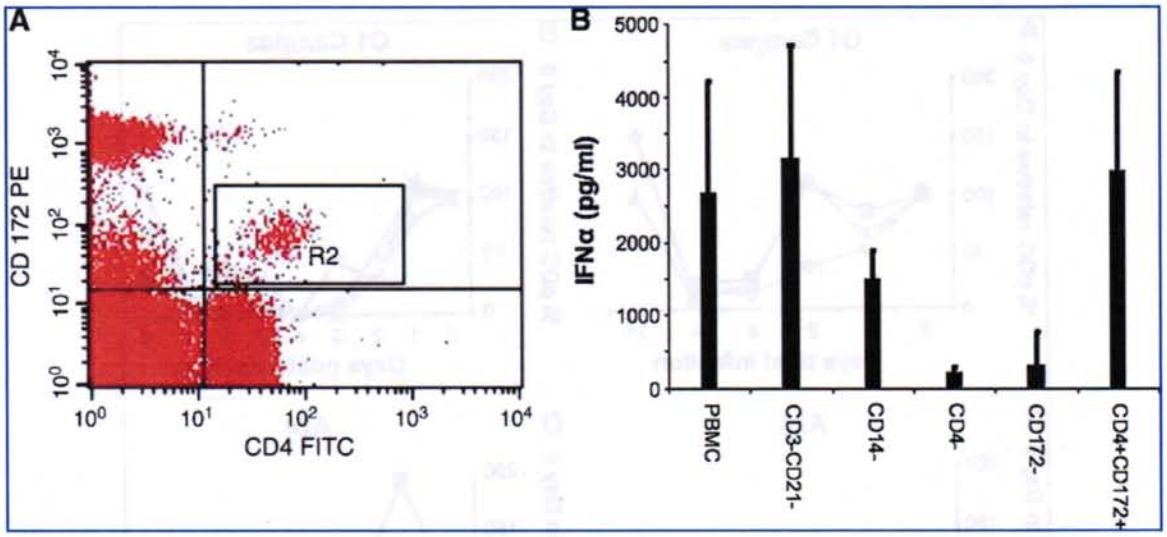

FIG. 4. Phenotype of porcine pDCs and PBMCs responding to CpG 2216. (**A**) PBMCs isolated from uninfected pigs were stained for CD4 and CD172 and analyzed by flow cytometry. Porcine pDCs are identified in gate R2 as $CD4^+CD172$ low. (**B**) Cells responding to CpG 2216 identified as $CD4^+CD172^+$ by negative or positive selection of PBMCs from naïve pigs, followed by stimulation with CpG 2216 and detection of IFN-α in the culture supernatants by ELISA (n = 3). Color image is available online at www.liebertonline.com/vim.

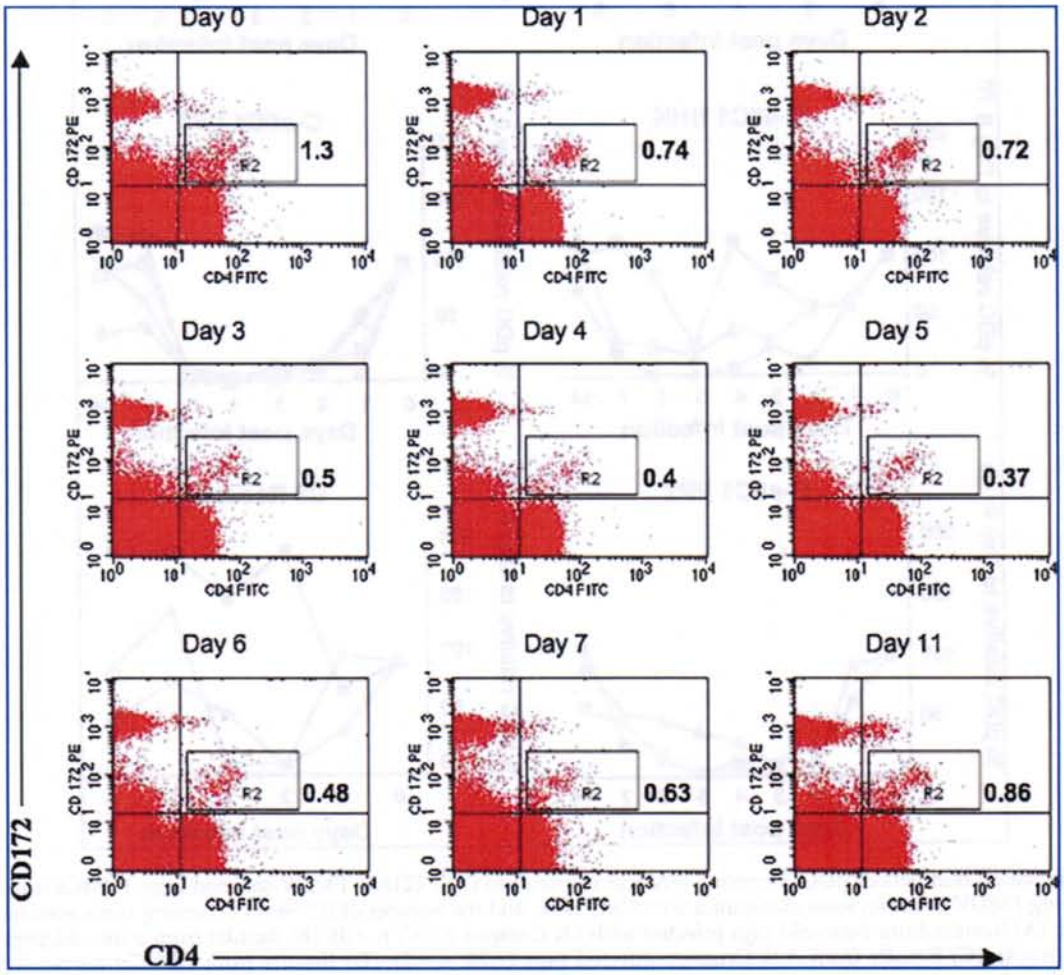

FIG. 5. Decreased numbers of pDCs in FMDV-infected pigs. PBMCs isolated from pigs following FMDV infection were stained for CD4 and CD172 and analyzed by flow cytometry. The effect of infection on porcine pDC numbers identified in gate R2 as $CD4^+CD172$low were monitored. Plots are representative of eight different experiments. Color image is available online at www.liebertonline.com/vim.

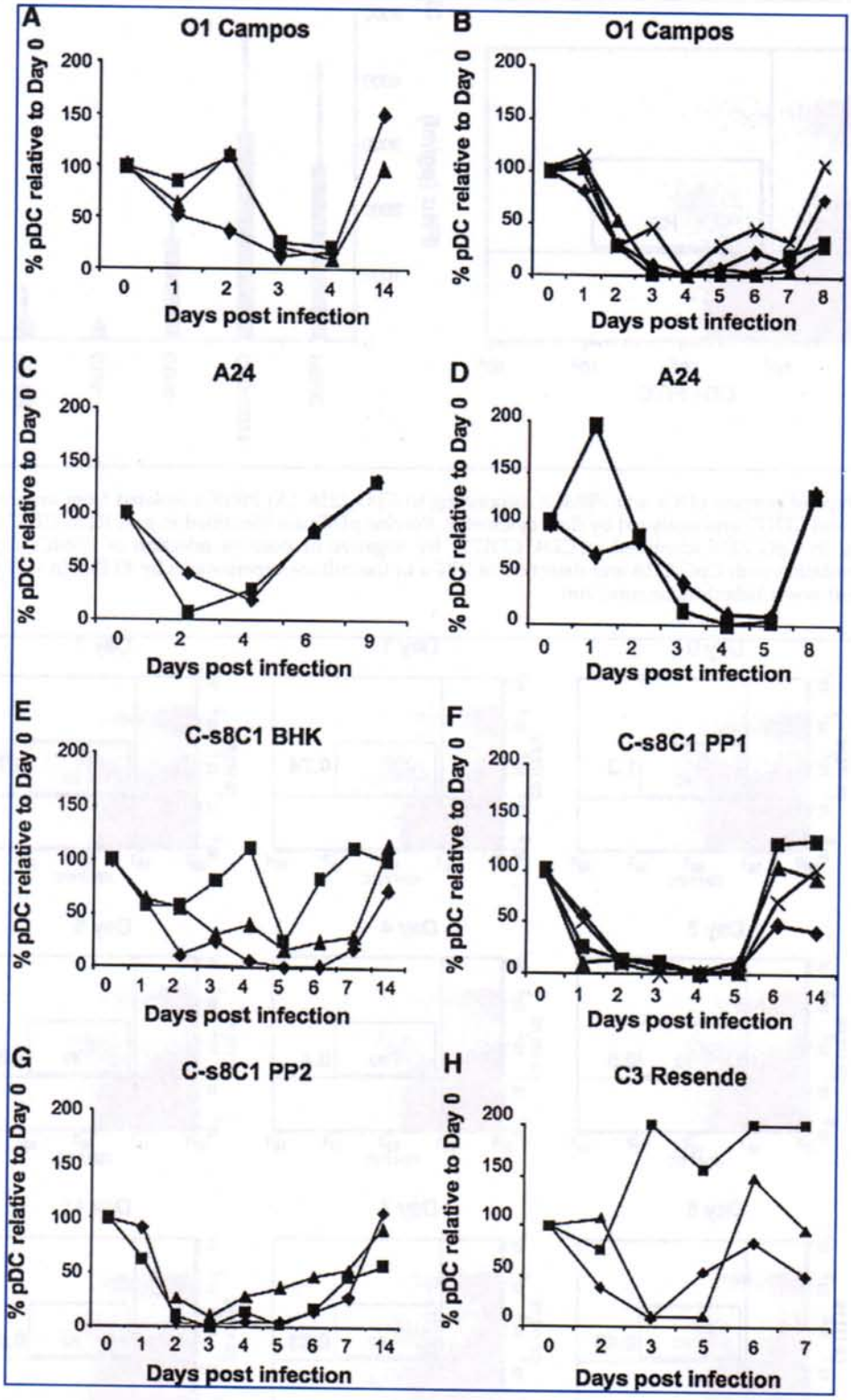

FIG. 6. Decreased numbers of pDCs secreting IFN-α in response to CpG 2216 in FMDV-infected pigs. PBMCs isolated from pigs following FMDV infection were stimulated with CpG 2216, and the number of IFN-α spot-forming units was determined by ELISpot. (**A**) Results from 6-mo-old pigs infected with O1 Campos (O1C; n = 3). (**B**) Results from 2-mo-old pigs infected with O1C (n = 4). (**C**) Results from A24 Cruzeiro-infected pigs (A24; n = 2). (**D**) Results from A24 Cruzeiro-infected pigs (n = 2). (**E**) Results from pigs infected with *in-vitro* propagated C-s8C1 (C-s8C1 BHK; n = 3). (**F**) Results from pigs infected with C-s8C1 previously passed once in other pigs (C-s8C1 PP1; n = 4). (**G**) Results from pigs infected with C-s8C1 previously passed twice in other pigs (C-s8C1 PP2; n = 3). (**H**) Results from C3 Resende-infected pigs (n = 3). The pigs in E–H were 2–3 mo old (n = the number of pigs infected.

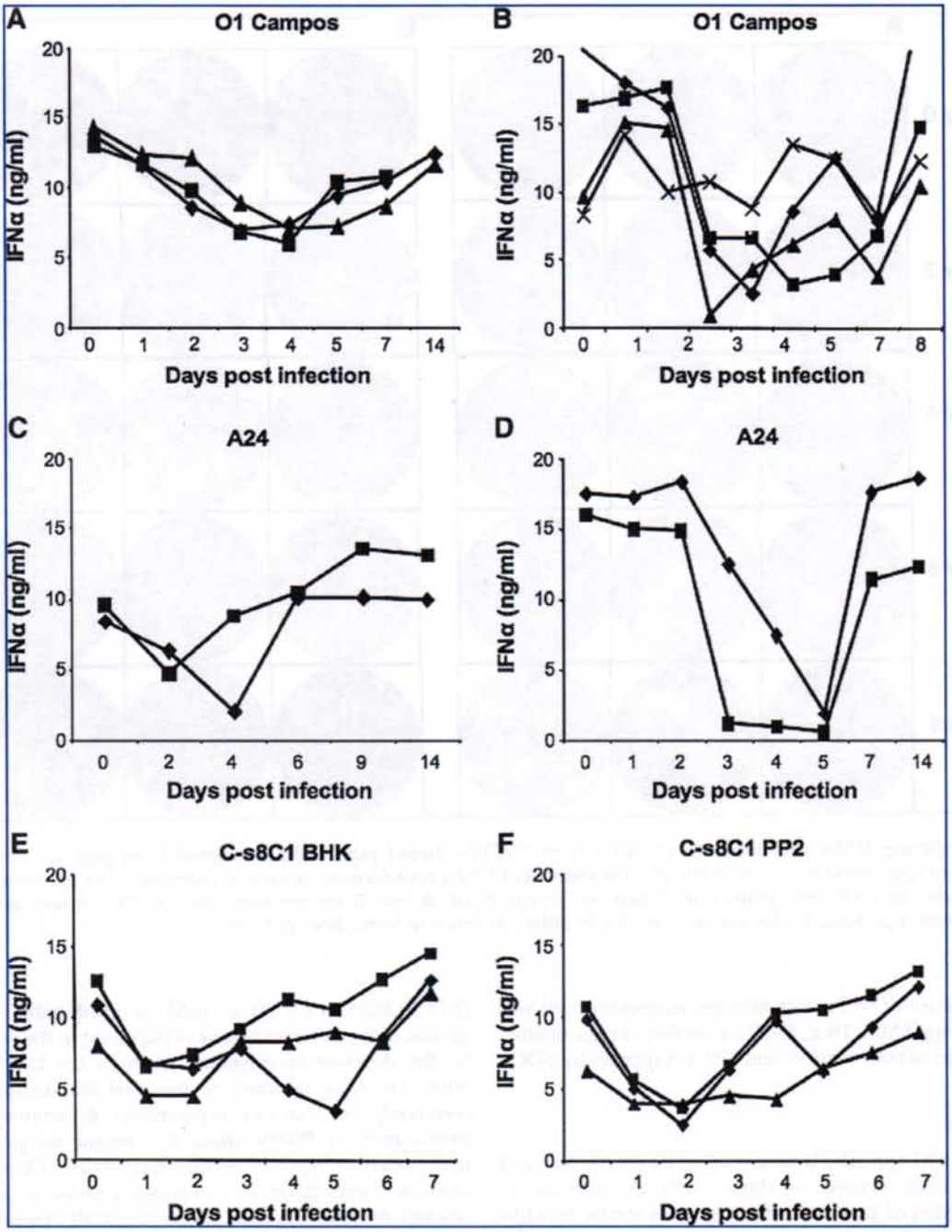

FIG. 7. PBMCs from FMDV-infected pigs secrete less IFN-α in response to CpG 2216. PBMCs isolated from pigs following FMDV infection were stimulated with CpG 2216 and the supernatants were assayed for IFN-α by ELISA. (**A**) Results from 6-mo-old pigs infected with O1 Campos (O1C; n = 3). (**B**) Results from 2-mo-old pigs infected with O1C (n = 4). (**C**) Results from A24 Cruzeiro-infected pigs (A24; n = 2). (**D**) Results from A24 Cruzeiro-infected pigs (n = 2). (**E**) Results from pigs infected with *in-vitro* propagated C-s8C1 (C-s8C1 BHK; n = 3). (**F**) Results from pigs infected with C-s8C1 previously passed twice in other pigs (C-s8C1 PP2; n = 3; n = the number of pigs infected).

0 for the virus strains O1C, A24, C-s8C1 PP1, and C-s8C1 PP2.

We then measured IFN-α protein in supernatants of cultures of PBMCs stimulated with CpG 2216. These supernatants contained declining amounts of IFN-α, beginning by 1–3 days PI (Fig. 7 A–F), and nearly all animals showed a lack of IFN-α by days 3–5. The exceptions were the animals infected with strain C-s8C1, in which this effect occurred on day 2 in all animals tested. Recovery of IFN-α production varied, with some animals recovering rapidly and others showing a low response for 1–3 d. This observation could be due to the low numbers of pDCs in the PBMCs during acute FMDV infection. However, as shown in Fig. 8, the immunospot intensity was also low on days 2–4 PI, indicating

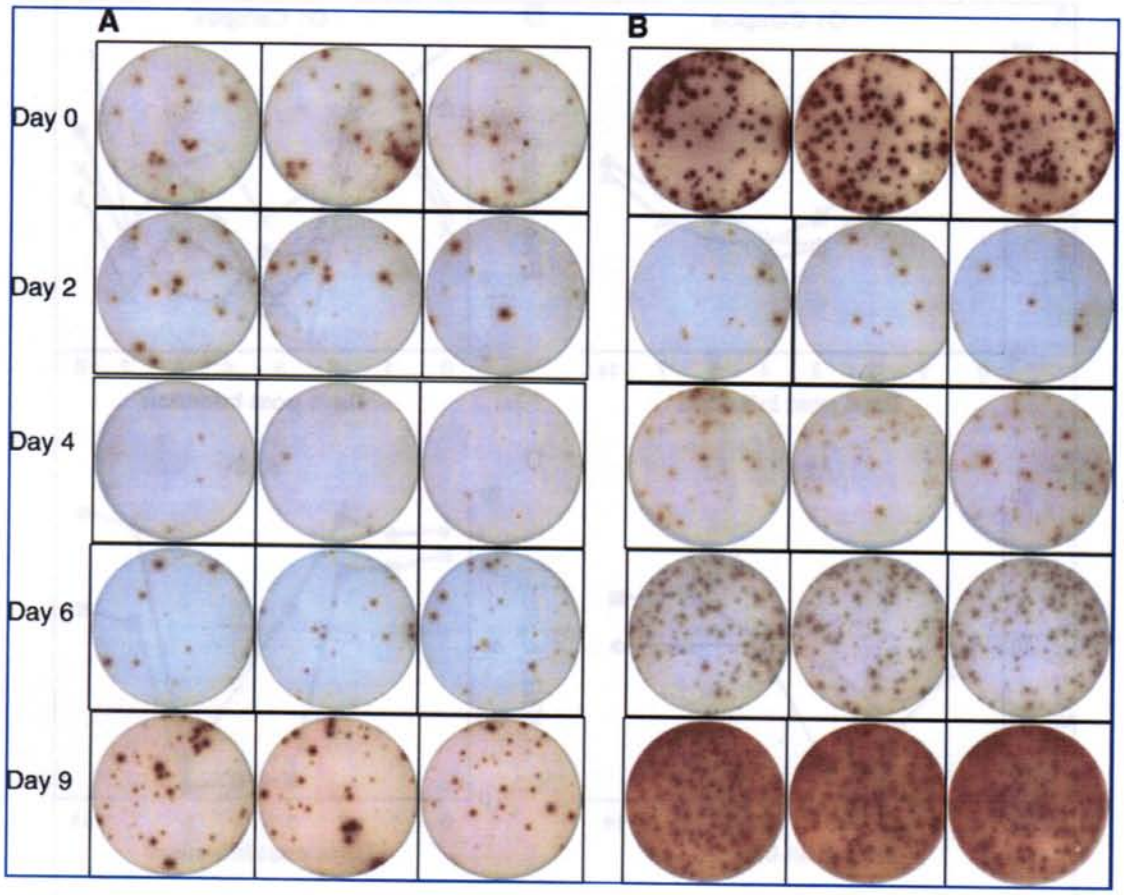

FIG. 8. Declining IFN-α spot intensity of pDCs from FMDV-infected pigs. PBMCs isolated from pigs following FMDV infection were stimulated with CpG 2216, and the number of IFN-α spot-forming units was determined by ELISpot. Photos of triplicate wells for each time point were taken on ImmunoSpot. **A** and **B** are representative of 23 different animals that showed a similar pattern. (Color image is available online at www.liebertonline.com/vim.)

that the amount of IFN-α secretion per responding cell was reduced during FMD. Thus, FMDV infection of pigs resulted in a reduction of both number and IFN-α responses by pDCs.

Discussion

Fever, loss of appetite, lameness, vesicles on the feet and snout, and early viremia on days 1–4 PI are common in FMDV infection of pigs, regardless of virus strain. In addition, lymphopenia has been identified as a hallmark of porcine (2,11,13), and to a lesser extent bovine (25), FMDV infection. However, the mechanism of the lymphopenia remains largely unknown. Apoptosis has been ruled out as being responsible for lymphocyte destruction (2,13), and in this and our previous reports (2,28) we could not isolate virus from lymphocytes, even at peak viremia. However, Diaz-San Segundo *et al.* reported isolation of virus from lymphocytes recovered from FMDV strain C-s8C1-infected pigs beginning on day 2 and extending until day 10 PI (13). Animals infected with this *in-vitro*-derived virus isolate were also reported to have viremia lasting more than 10 d, an uncommon finding among reports of porcine FMDV infection.

Most reports of swine infection show that upon needle inoculation of FMDV, viremia is cleared on day 4–5 PI (2,11,19,26,28,30,40). This could be attributable to the response of the different breeds of pigs used in the experiments by the different investigators, such as the Landrace-large white cross, as opposed to the Yorkshire-Landrace cross commonly used in our experiments. In addition, *in-vitro* propagation of FMDV alters its receptor recognition, and may widen its types of cellular targets (20). Of note is that Diaz-San Segundo *et al.* monitored viremia in euthanized animals only, as opposed to longitudinally monitoring the same animals over the 10-d period. All of these differences could account for their unique results.

The presence of IFN-α in serum has been linked to lymphopenia. In pigs infected with classical swine fever virus (CSFV), lymphopenia and a decline in pDC numbers correlates with the levels of IFN-α in the serum (37). Similarly, mice injected with poly I:C exhibit a lymphopenia linked to their serum IFN-α levels (22,24). In this article, the lowest lymphocyte and pDC numbers in the blood occurred when the serum IFN-α response was at its peak. Thus, the serum IFN-α response could partly account for the observed lymphopenia and reduction in number of pDCs, as is the case in CSFV infection (37). The IFN-α-induced lymphopenia is completely reversible and may be due to enhanced lymphocyte adhesion to endothelium of blood vessels during acute infection (24).

Viremia is rapidly cleared in FMDV-infected pigs, and there is no evidence of persistent infections (2). In this article, peak serum IFN-α occurred on days 2–3 PI, and preceded the rapid clearance of viremia by day 4. However, IgM, which is the first antibody isotype secreted in a primary response, was only detected in serum on day 7 (data not shown), after the viremia had resolved. In similar studies, neutralizing antibodies detected by plaque reduction assays were first detected on day 7 after inoculation (15). Therefore, other mechanisms in addition to neutralizing antibodies likely contribute to the early elimination of FMDV from the blood. Considering the high sensitivity of FMDV to IFN-α, the presence in serum of this cytokine reported here likely contributes to the early clearance of FMDV, by inducing an antiviral state *in vivo*. Such high serum levels of IFN-α have been shown to be protective against FMDV challenge (8). Therefore, the early IFN-α response renders virus-susceptible cells refractory to infection, thereby preventing further replication and spread of the virus within the host, and resulting in a rapid reduction of viremia.

Zhang *et al.* observed high levels of type I and II IFN mRNA in nasal-associated lymphoid tissues of cattle during the acute phase of FMD, and postulated that the inhibitory effects of these cytokines account in part for the mechanism by which FMDV is controlled *in vivo* (41). Similarly, an attenuated FMDV strain lacking the leader protease (LLA12) does not spread beyond the site of infection, due to a rapid local IFN-α response (5). It has been demonstrated that IFN-α activates expression of IFN-stimulated genes such as PKR and OAS, which results in the blocking of FMDV replication (7). Furthermore, it has been shown that this cytokine activates NK cells, which not only kill virus-infected cells, but also secrete cytokines such as IFN-γ that activate T and B cells (4,38). Furthermore, FMDV is sensitive to the antiviral activity of IFN-γ (26).

We have previously shown that upon exposure to FMDV *in vitro*, skin DCs secrete IFN-α and IFN-β (3). Similarly, porcine MoDCs propagated from PBMCs secrete IFN-α in response to FMDV (28). These data indicate that these DC populations may constitute the cellular sources of the serum IFN-α response to FMDV. Plasmacytoid DCs (pDCs) require FMDV complexed with immune serum for uptake and response to the virus *in vitro* (17). This would suggest that pDCs are an unlikely source of IFN-α in the early phase of infection in naïve animals (days 1–4). However, these cells might behave differently *in vivo*. Additional sources of IFN-α include macrophages and fibroblasts. A role for fibroblasts in the innate response to FMDV is suggested by the fact that various porcine kidney fibroblast cell lines (SK6, PK15, and IBRS2) secrete IFN-α when challenged with the virus (7,9).

However, the rapid progression of FMDV infection in pigs within the first 2 d of infection suggests the possibility of a window of opportunity for the virus to replicate. Either the virus downregulates the secretion of cytokines early after infection, delaying the attainment of sufficient levels of IFN-α in the serum, or high titers of virus are required to induce IFN-α secretion by the responding cells. The possibility of the former is suggested by the fact that skin DCs and MoDCs isolated from pigs 48 h post-FMDV infection show severely reduced secretion of IFN-α upon *in-vitro* stimulation (28).

This report provides more evidence for early modulation of the innate responses via the reduced number pDCs and the low IFN-α secretion of pDCs isolated from acutely infected pigs. Similar observations have been made upon analysis of infection with other porcine and human viruses. In addition to CSFV and FMDV infection, *in-vitro* infection of porcine pDCs with porcine circovirus type 2 results in inhibition of their response to stimulation with TLR 7 and 9 agonists. This is also observed in infection with pseudorabies virus and transmissible gastroenteritis virus. All of these effects are independent of viral replication (39). In humans, a blunted response of blood pDCs and reduced cell numbers are evident in dengue virus infection, although these cells are not productively infected with dengue virus and still remain sensitive to stimulation with CpG 2216 (32). Furthermore, severe infection with herpes simplex virus type 2 leads to a rapid loss of pDC and NK cells (10). Similarly, primary infections with human immunodeficiency virus are characterized by impaired type I IFN production and low counts of pDCs (23). To date we have not demonstrated what causes the low numbers of pDCs during FMDV infection, but one attractive hypothesis is the possibility that these cells migrate from the bloodstream into sites of inflammation.

Conclusion

In summary, the data presented here are consistent with the contribution of IFN-α to the early resolution of viremia in FMDV-infected pigs, before the detection of antibodies to the virus. However, this response is modulated by the virus, creating a narrow but sufficient window of opportunity for replication and shedding. This article lends support to ongoing research to develop systems that induce interferons to augment the host response as an intervention strategy during outbreaks of FMD.

Acknowledgments

This work was supported by Current Research Information System (CRIS) #1940-32000-052-00D (W.T.G.) from the Agricultural Research Service, U.S. Department of Agriculture (USDA), and an interagency agreement (no. 60-1940-8-037) between the Department of Homeland Security, Science and Technology Directorate, and the USDA (W.T.G.). C. Nfon was the recipient of a PIADC Research Participation Program fellowship, administered by the Oak Ridge Institute for Science and Education through an interagency agreement between the U.S. Department of Energy and the USDA. We would like to thank Drs. Noami Sevilla and Fayna Diaz-San Segundo (Instituto Nacional de Investigacion y Technologia Agraria (INIA), Madrid, Spain) for providing the FMDV strain C-s8C1 for this analysis. We would also like to thank Mr. Geoffrey Ferman and Ms. Mital Pandya for their technical assistance, and the animal care staff at the Plum Island Animal Disease Center for their professional support and assistance.

References

1. Ambagala AP, Hinkley S, and Srikumaran S: An early pseudorabies virus protein down-regulates porcine MHC class I expression by inhibition of transporter associated with antigen processing (TAP). J Immunol 2000;164:93–99.
2. Bautista EM, Ferman GS, and Golde WT: Induction of lymphopenia and inhibition of T cell function during acute infection of swine with foot and mouth disease virus (FMDV). Vet Immunol Immunopathol 2003;92:61–73.

3. Bautista EM, Ferman GS, Gregg D, Brum MC, Grubman MJ, and Golde WT: Constitutive expression of alpha interferon by skin dendritic cells confers resistance to infection by foot-and-mouth disease virus. J Virol 2005;79: 4838–4847.
4. Biron CA, Nguyen KB, Pien GC, Cousens LP, and Salazar-Mather TP: Natural killer cells in antiviral defense: function and regulation by innate cytokines. Annu Rev Immunol 1999;17:189–220.
5. Brown CC, Chinsangaram J, and Grubman MJ: Type I interferon production in cattle infected with 2 strains of foot-and-mouth disease virus, as determined by in situ hybridization. Can J Vet Res 2000;64:130–133.
6. Callahan JD, Brown F, Osorio FA, *et al.*: Use of a portable real-time reverse transcriptase-polymerase chain reaction assay for rapid detection of foot-and-mouth disease virus. J Am Vet Med Assoc 2002;220:1636–1642.
7. Chinsangaram J, Koster M, and Grubman MJ: Inhibition of L-deleted foot-and-mouth disease virus replication by alpha/beta interferon involves double-stranded RNA-dependent protein kinase. J Virol 2001;75:5498–5503.
8. Chinsangaram J, Moraes MP, Koster M, and Grubman MJ: Novel viral disease control strategy: adenovirus expressing alpha interferon rapidly protects swine from foot-and-mouth disease. J Virol 2003;77:1621–1625.
9. Chinsangaram J, Piccone ME, and Grubman MJ: Ability of foot-and-mouth disease virus to form plaques in cell culture is associated with suppression of alpha/beta interferon. J Virol 1999;73:9891–9898.
10. Dalloul A, Oksenhendler E, Chosidow O, *et al.*: Severe herpes virus (HSV-2) infection in two patients with myelodysplasia and undetectable NK cells and plasmacytoid dendritic cells in the blood. J Clin Virol 2004;30:329–336.
11. de Avila Botton S, Brum MC, Bautista E, Koster M, Weiblen R, Golde WT, and Grubman MJ: Immunopotentiation of a foot-and-mouth disease virus subunit vaccine by interferon alpha. Vaccine 2006;24:3446–3456.
12. Devaney MA, Vakharia VN, Lloyd RE, Ehrenfeld E, and Grubman MJ: Leader protein of foot-and-mouth disease virus is required for cleavage of the p220 component of the cap-binding protein complex. J Virol 1988;62:4407–4409.
13. Diaz-San Segundo F, Salguero FJ, de Avila A, de Marco MM, Sanchez-Martin MA, and Sevilla N: Selective lymphocyte depletion during the early stage of the immune response to foot-and-mouth disease virus infection in swine. J Virol 2006;80:2369–2379.
14. Goodbourn S, Didcock L, and Randall RE: Interferons: cell signalling, immune modulation, antiviral response and virus countermeasures. J Gen Virol 2000;81:2341–2364.
15. Grubman MJ, and Baxt B: Foot-and-mouth disease. Clin Microbiol Rev 2004;17:465–493.
16. Guzylack-Piriou L, Balmelli C, McCullough KC, and Summerfield A: Type-A CpG oligonucleotides activate exclusively porcine natural interferon-producing cells to secrete interferon-alpha, tumour necrosis factor-alpha and interleukin-12. Immunology 2004;112:28–37.
17. Guzylack-Piriou L, Bergamin F, Gerber M, McCullough KC, and Summerfield A: Plasmacytoid dendritic cell activation by foot-and-mouth disease virus requires immune complexes. Eur J Immunol 2006;36:1674–1683.
18. Haga IR, and Bowie AG: Evasion of innate immunity by vaccinia virus. Parasitology 2005;130(Suppl):S11–S25.
19. Harmsen MM, Fijten HP, Dekker A, and Eble PL: Passive immunization of pigs with bispecific llama single-domain antibody fragments against foot-and-mouth disease and porcine immunoglobulin. Vet Microbiol 2008;132:56–64.
20. Harwood LJ, Gerber H, Sobrino F, Summerfield A, and McCullough KC: Dendritic cell internalization of foot-and-mouth disease virus: influence of heparan sulfate binding on virus uptake and induction of the immune response. J Virol 2008;82:6379–6394.
21. Honda K, Yanai H, Negishi H, *et al.*: IRF-7 is the master regulator of type-I interferon-dependent immune responses. Nature 2005;434:772–777.
22. Jiang J, Gross D, Nogusa S, Elbaum P, and Murasko DM: Depletion of T cells by type I interferon: differences between young and aged mice. J Immunol 2005;175:1820–1826.
23. Kamga I, Kahi S, Develioglu L, *et al.*: Type I interferon production is profoundly and transiently impaired in primary HIV-1 infection. J Infect Dis 2005;192:303–310.
24. Kamphuis E, Junt T, Waibler Z, Forster R, and Kalinke U: Type I interferons directly regulate lymphocyte recirculation and cause transient blood lymphopenia. Blood 2006;108: 3253–3261.
25. Mohan MS, Gajendragad MR, Gopalakrishna S, and Singh N: Comparative study of experimental foot-and-mouth disease in cattle (*Bos indicus*) and buffaloes (*Bubalis bubalus*). Vet Res Commun 2008;32:481–489.
26. Moraes MP, de Los Santos T, Koster M, Turecek T, Wang H, Andreyev VG, and Grubman MJ: Enhanced antiviral activity against foot-and-mouth disease virus by a combination of type I and II porcine interferons. J Virol 2007; 81:7124–7135.
27. Nataraj C, Eidmann S, Hariharan MJ, Sur JH, Perry GA, and Srikumaran S: Bovine herpesvirus 1 downregulates the expression of bovine MHC class I molecules. Viral Immunol 1997;10:21–34.
28. Nfon CK, Ferman GS, Toka FN, Gregg DA, and Golde WT: Interferon-alpha production by swine dendritic cells is inhibited during acute infection with foot-and-mouth disease virus. Viral Immunol 2008;21:68–77.
29. Nowacki W, Cederblad B, Renard C, La Bonnardiere C, and Charley B: Age-related increase of porcine natural interferon alpha producing cell frequency and of interferon yield per cell. Vet Immunol Immunopathol 1993;37:113–122.
30. Oem JK, Yeh MT, McKenna TS, *et al.*: Pathogenic characteristics of the Korean 2002 isolate of foot-and-mouth disease virus serotype O in pigs and cattle. J Comp Pathol 2008;138: 204–214.
31. Pacheco JM, Henry TM, O'Donnell VK, Gregory JB, and Mason PW: Role of nonstructural proteins 3A and 3B in host range and pathogenicity of foot-and-mouth disease virus. J Virol 2003;77:13017–13027.
32. Pichyangkul S, Endy TP, Kalayanarooj S, *et al.*: A blunted blood plasmacytoid dendritic cell response to an acute systemic viral infection is associated with increased disease severity. J Immunol 2003;171:5571–5578.
33. Sagedahl A, Giraudo AT, De Mello PA, Bergmann IE, La Torre JL, and Scodeller EA: Biochemical characterization of an aphthovirus type C3 strain Resende attenuated for cattle by serial passages in chicken embryos. Virology 1987;157: 366–374.
34. Sanz-Parra A, Sobrino F, and Ley V: Infection with foot-and-mouth disease virus results in a rapid reduction of MHC class I surface expression. J Gen Virol 1998;79(Pt 3): 433–436.
35. Seet BT, Johnston JB, Brunetti CR, *et al.*: Poxviruses and immune evasion. Annu Rev Immunol 2003;21:377–423.

36. Smith GL, Symons JA, Khanna A, Vanderplasschen A, and Alcami A: Vaccinia virus immune evasion. Immunol Rev 1997;159:137–154.
37. Summerfield A, Alves M, Ruggli N, de Bruin MG, and McCullough KC: High IFN-alpha responses associated with depletion of lymphocytes and natural IFN-producing cells during classical swine fever. J Interferon Cytokine Res 2006;26:248–255.
38. Toka FN, Nfon CK, Dawson H, Mark Estes D, and Golde WT: Activation of porcine natural killer (NK) cells and lysis of foot-and-mouth disease virus (FMDV) infected cells. J Interferon Cytokine Res 2009;29.
39. Vincent IE, Balmelli C, Meehan B, Allan G, Summerfield A, and McCullough KC: Silencing of natural interferon producing cell activation by porcine circovirus type 2 DNA. Immunology 2007;120:47–56.
40. Wu Q, Brum MC, Caron L, Koster M, and Grubman MJ: Adenovirus-mediated type I interferon expression delays and reduces disease signs in cattle challenged with foot-and-mouth disease virus. J Interferon Cytokine Res 2003;23:359–368.
41. Zhang Z, Bashiruddin JB, Doel C, Horsington J, Durand S, and Alexandersen S: Cytokine and toll-like receptor mRNAs in the nasal-associated lymphoid tissues of cattle during foot-and-mouth disease virus infection. J Comp Pathol 2006;134:56–62.
42. Zhou A, Paranjape JM, Der SD, Williams BR, and Silverman RH: Interferon action in triply deficient mice reveals the existence of alternative antiviral pathways. Virology 1999; 258:435–440.

Address correspondence to:
Dr. William T. Golde
Plum Island Animal Disease Center
Agricultural Research Service
U.S. Department of Agriculture
P.O. Box 848
Greenport, NY 11944-0848

E-mail: william.golde@ars.usda.gov

Received September 11, 2009; accepted November 9, 2009.

Return to Table of Contents

The Veterinary Journal 183 (2010) 46–53

Contents lists available at ScienceDirect

The Veterinary Journal

journal homepage: www.elsevier.com/locate/tvjl

Early events in the pathogenesis of foot-and-mouth disease in cattle after controlled aerosol exposure

Juan M. Pacheco, Jonathan Arzt, Luis L. Rodriguez *

Plum Island Animal Disease Center, Foot-and-Mouth Disease Unit PIADC, ARS, USDA, P.O. Box 848, Greenport, NY 11944, USA

ARTICLE INFO

Article history:
Accepted 30 August 2008

Keywords:
Foot-and-mouth disease virus (FMDV)
Cattle
Aerosol infection
Pathogenesis

ABSTRACT

The goal of this study was to identify the primary sites of replication of foot-and-mouth disease virus (FMDV) in cattle subsequent to aerogenous inoculation. A novel aerosol inoculation method was developed to simulate natural, airborne transmission and thereby allow the identification of early replication sites. Virus distribution after aerosol inoculation was compared at 24 h post inoculation with simple nasal instillation. Aerosol inoculation of FMDV consistently resulted in virus detection by real-time reverse transcriptase-polymerase chain reaction and viral isolation in the soft palate, pharynx, and lungs. Viral antigen was also detected in each of these tissues by immunohistochemistry. Aerosol exposure resulted in typical clinical signs of FMD when animals were kept alive long enough to develop disease. This aerosol infection method is highly reproducible regarding inoculum dose and volume, and allowed the detailed study of early events in FMDV-infected cattle. Extensive postmortem sampling and trimodal virus detection system allows a more precise determination of FMDV localization than previously reported.

Published by Elsevier Ltd.

Introduction

Foot-and-mouth disease (FMD) is a highly contagious picornaviral disease affecting domestic and wild cloven-hoofed animals. Inhalation of aerosolized foot-and-mouth disease virus (FMDV) is generally considered to be the most important route of transmission within and between herds of cattle so that under appropriate environmental conditions virus-laden droplets may travel vast distances whilst maintaining infectivity (Alexandersen et al., 2003; Grubman and Baxt, 2004).

Over the course of more than 100 years of investigation of FMD, numerous animal models have been developed to investigate the pathogenesis of the disease. The goals of these models were to closely simulate naturally occurring disease and to be reproducible across experimental subjects. In cattle, FMD has been experimentally reproduced by exposing animals to virus via direct or indirect contact with infected animals, via injection by various routes, by intra-tracheal aerosol infection, by intra-pulmonary implantation, or via respired aerosol (Alexandersen et al., 2003; Sellers and Gloster, 2008). Injection infection models, though highly consistent, bypass the respiratory tract (Alexandersen et al., 2003), and thus, preclude the possibility of investigating early events in pathogenesis. Contact exposure closely simulates natural infection, but has the intrinsic limitations of inability to quantitate viral dose or precisely standardize exposure conditions across infected animals. Direct introduction of virus to the bovine respiratory tract offers the advantages of standardization of viral dose and simulation of the natural route of transmission, while preserving the capacity to examine early events in pathogenesis. As such, this infection method has been widely used (Sellers and Gloster, 2008).

Early bovine FMD models utilizing respiratory exposure achieved infection by depositing virus in the nasal cavity of cattle with a latex tube mounted to a syringe (intra-nasal instillation) (McVicar et al., 1970; McVicar and Sutmoller, 1976). Later models utilized improvised containment chambers enclosing the heads of cattle while introducing virus suspensions aerosolized with deVilbiss nebulizers (Brown et al., 1992, 1996; McVicar and Eisner, 1983). Using such a technique, 76% of mean aerosolized particles within the exposure chamber were <3 μm and 7% were >6 μm immediately after shutting off the nebulizer (McVicar and Eisner, 1983). Consideration of nebulized particle size is important since this influences the anatomical distribution of the aerosol. Particles <3 μm are more likely to progress to the lungs, whereas particles >6 μm are likely to lodge in the upper respiratory tract. During natural aerosol infection of cattle it is likely that particles <3 μm predominate (McVicar and Eisner, 1983) whereas those <6 μm are most likely to be responsible for long-distance transmission (Gloster et al., 1981).

Variable exposure conditions, virus strains, detection methods, and tissues examined confound comparison of results across published FMD pathogenesis studies. Despite abundant effort to elucidate the early events of infection, a clear consensus still does not exist regarding the natural portal of FMDV infection.

* Corresponding author. Tel.: +1 631 323 3364; fax: +1 631 323 3006.
E-mail address: luis.rodriguez@ars.usda.gov (L.L. Rodriguez).

1090-0233/$ - see front matter Published by Elsevier Ltd.
doi:10.1016/j.tvjl.2008.08.023

The purpose of this work was to investigate the early, pre-viremic events of FMD in cattle using a highly reproducible infection model that closely simulated natural exposure.

Materials and methods

Experimental animals, virus, and inoculation systems

Eleven 9–12 month-old Holstein steers weighing 300–400 kg were obtained from an experimental-livestock provider (Thomas-Morris Inc.). Animals were housed in individual rooms in a BSL-3 animal facility from inoculation until time of necropsy. Seven steers were inoculated with FMDV either by aerosol (animals 66, 670, 671, 760) or by intranasal instillation (animals 67, 672, 673) of FMDV. Prior to inoculation, steers were sedated with xylazine given IM (0.22 mg/kg) so as to maintain sternal recumbency for the duration of the procedure. Upon completion of the inoculation procedure, sedation was reversed by giving Tolazine (Lloyd Inc.) slowly IV (2–4 mg/kg). One steer inoculated by aerosol (animal 760) was euthanased 10 days post inoculation (dpi) in order to characterize the course of clinical disease and viremia. The other six animals were euthanased and necropsied 24 h post inoculation (hpi) for tissue collection.

The challenge virus consisted of clarified macerated tongue epithelium harvested from two steers experimentally infected with the FMDV strain O1 Manisa as previously described (Golde et al., 2005). The macerate was pooled, aliquoted and stored at −70 °C. Challenge virus was titrated in the tongue of a steer to determine 50% bovine tongue infectious doses ($BTID_{50}$). All animals were inoculated with 10^7 $BTID_{50}$ either in 1 mL of minimum essential medium (MEM) for the first steer infected in each group or in 2 mL for the remaining steers.

The inoculum titer is expressed in $BTID_{50}$ as we have determined this method is the most sensitive for quantifying this bovine-adapted strain. We tested LFBK cells, a previously described cell line of bovine origin (Swaney, 1988), and found that an inoculum containing 10^7 $BTID_{50}$/mL (Ct = 13 by rRT-PCR) (Callahan et al., 2002) yielded a titer of 10^6 in LFBK cells, as compared to 10^1 in BHK-alphaVbeta6 cells (Duque et al., 2004) and 10^0 in BHK or primary lamb kidney cells (Supplementary Figs. 1 and 2).

Aerosol inoculation was performed with a jet nebulizer (Whisper Jet, Marquest Medical Products) attached to a commercially available aerosol delivery system (Equine Aeromask, Medium Size, Trudell Medical). The delivery mask, although originally designed for horses, fitted the muzzles of the cattle sufficiently well to ensure complete delivery of the inoculum. This nebulizer generates particles with an average size of 5 μm that distribute throughout the upper and lower respiratory tract (Hess et al., 1996). Compressed air, at 25 psi, is used to jet-nebulize the inoculum directly into the holding chamber. Upon inspiration, the nebulized inoculum is inhaled through a one-way valve into the delivery mask which covers the distal portion of the muzzle including the nares.

Intranasal instillation was performed with Accuspray,[1] an intranasal delivery system designed for use in humans. This device's droplet size distribution, as reported by the manufacturer, is 85% of particles 10–150 μm in diameter and 4% of particles <10 μm. This ensures that the instillation is delivered predominantly to the upper respiratory tract and not the lungs. For each inoculation, the device was inserted into both nostrils and the syringe plunger compressed with a single brisk motion. Inoculation volume for instillation was 0.5 mL (animal 67) or 1.0 mL (animals 672 and 673) per nostril. In both cases the infectious dose was 10^7 $BTID_{50}$.

A preliminary infection was carried out to confirm that the course of clinical FMD after aerosol exposure was comparable with that seen after direct inoculation or contact exposure. In brief, two steers (animals 624 and 625) were placed in a single room and inoculated via intra-dermolingual injection with 10^4 BTID of the same FMDV O1 Manisa inoculum administered to the aerosol and instilled steers. After 24 h, two naïve steers (animals 626 and 627) were introduced into the same room and the four animals remained in direct contact until 10 dpi.

Sample collection

For the aerosol treated and instilled cattle, oral and nasal swabs and serum samples were collected at 0, 6 and 24 hpi. At 24 hpi animals 66, 67, 670, 671, 672, and 673 were euthanased by IV injection of Fatal Plus (Vortech Pharmaceuticals Ltd.), and 35 anatomically distinct tissue samples were collected from the oral cavity, nasal cavity, soft palate, pharynx, larynx, trachea, and lungs (Table 1). Sample collection was based upon previously published reports of the relevance of particular tissues in the pathogenesis of FMD. Gross and microscopic anatomical characteristics were used to identify and subdivide the samples.

All tissues (excluding lung and tonsils) were collected as specimens with a full-thickness epithelium with 1–3 mm of associated subjacent stroma. Palatine and pharyngeal tonsil samples were collected as wedge specimens including the luminal aspect of these structures. Lung samples were all from the right lung. For each lung lobe, samples were designated: 'proximal' (included bronchial epithelium only); 'mid' (included bronchial epithelium and adjacent pulmonary parenchyma); and 'distal' (included pulmonary parenchyma only). Primary bronchial samples were mucosal specimens collected at the level of the tracheal bifurcation. For all specimens with 'cranial' and 'caudal' designations, the tissue was bisected at the midpoint of the cranio-caudal axis and the sample collected from the middle segment of the bisected specimen. For each anatomically defined specimen, two 30 mg tissue samples were aliquoted into separate screw-cap 1.5 mL tubes and frozen immediately in liquid nitrogen for transfer, within 2 h to a −70 °C freezer until time of processing.

An adjacent tissue specimen from each tissue was placed in a cryomold, embedded in optimal cutting temperature compound (OCT) (Sakura Finetek), frozen on liquid nitrogen, and stored at −70 °C for immunohistochemistry (IHC). In the case of animal 760, swabs were collected at 24 h intervals for the duration of the experiment and serum was sampled at 1 h intervals for the first 6 hpi, 6 h intervals from 6–78 hpi, and 24 h intervals from 78–240 hpi (10 dpi) when euthanasia and tissue sampling was performed. Serum was collected at 24 h intervals from animals 624, 625, 626 and 627. All animals allowed to survive beyond 24 hpi (624, 625, 626, 627, and 760) were sedated daily for clinical evaluation.

Foot-and-mouth disease virus RNA detection

Two sample containers of each tissue listed in Table 1 per animal were thawed and immediately macerated by adding two 5 mm stainless steel beads (Qiagen, Catalogue No. 69989) and 0.9 mL of MEM-25 mM Hepes, and shaken in a TissueLyser bead beater (Qiagen) for 2 min at a frequency of 22/s. After maceration, 50 μL of sample were transferred to 96-well plates (King Fisher No. 97002540) containing 150 μL lysis/binding solution. RNA was then extracted using Ambion's MagMax-96 Viral RNA Isolation Kit (Ambion, Catalogue No. 1836) on a King Fisher-96 Magnetic Particle Processor (Thermo Electron Corp.). Briefly, after the initial 5 min lysis/binding step, the RNA sample underwent a series of four washing steps, a drying step, and a final elution step. RNA was eluted in a final volume of 25 μL. At each of the above steps, RNA was magnetically bound to the beads contained in the lysis/binding solution and was transferred to the different extraction solutions. Once extracted, the RNA was analyzed by rRT-PCR using 2.5 μL of RNA on the ABI 7000 as previously described (Callahan et al., 2002). Samples were considered positive when Ct values were <40.

The remaining macerated tissue was clarified (1000 *g* for 2 min at 4 °C) and the supernatant was cleared of bacterial contamination using centrifuge tube filters (Spin-X, Costar). Clarified and cleared samples were stored at −70 °C until virus isolation (VI) was performed.

Virus isolation

After 48 h, flasks seeded with 1×10^6 LFBK cell monolayers (Swaney, 1988) were rinsed with serum-free media and inoculated with 100 μL of sera, swabs or clarified and filtered samples obtained from the tissues. After 1 h of adsorption, 5 mL of media with 1% serum were added to the flasks. Due to the potential toxicity of the swab samples, the inoculum was removed and 5 mL of media containing 1% serum were added. To avoid a high concentration of sera in flasks that received serum samples, the inoculum was removed and replaced with 5 mL of media with 1% serum.

Inoculated flasks were incubated for 3–5 days at 37 °C on a rocking platform. Upon detection of a cytopathic effect (CPE), samples were confirmed as FMDV-positive by rRT-PCR. Samples in which no CPE was observed were amplified through three complete blind passages and the supernatants tested by rRT-PCR before they were deemed negative.

Immunohistochemistry

Samples for IHC were OCT-embedded, cryosectioned at 4 μm onto electrostatically charged glass slides (Superfrost Plus, Fisher Scientific), fixed for 10 min in acetone at −20 °C, and air-dried at 20 °C. These sections were blocked for 2 h at 20 °C with 0.01 M phosphate buffered saline with 0.05% Tween 20, pH 7.4, containing 6% mixed serum and 2% powdered non-fat milk.

A mouse monoclonal primary antibody designated 12AF4.2.3 (Stave et al., 1986) targeting the FMDV 12S fraction (VP 1, 2, 3) was diluted in blocking buffer and applied to tissue sections for 18 h at 4 °C. Specific anti-FMDV immunoreactivity was detected with a commercial kit (Vectastain ABC-AP, Vector Laboratories). The manufacturer's protocol was modified in that secondary antibody was applied diluted with 20% mixed serum to decrease background staining. An alkaline phosphatase substrate (Vector Red, Vector Laboratories) was applied and allowed to develop for 15 min. Slides were counterstained with Gill's hematoxylin and coverslipped using routine methods.

For each test section, a duplicate, negative-control serial section treated with a mouse monoclonal anti-VSV-Indiana antibody of similar concentration was prepared. Additional negative control tissue sections from a steer that received a virus-free aerosol inoculum and was killed at 24 hpi were included. Most tissues were additionally screened by IHC using a primary monoclonal antibody against the FMDV RNA polymerase 3D (Yang et al., 2007).

[1] See: DB brochure, http://www.bd.com/pharmaceuticals/pdfs/accuspray-brochure.pdf.

Table 1
The distribution of foot-and-mouth disease virus strain O1 Manisa as determined by rRT-PCR and virus isolation (VI) in tissues collected post mortem from cattle inoculated by aerosol or nasal instillation

Anatomical region	Tissue sub-division	Aerosol animals 66, 670, and 671		Nasal instillation animals 67, 672, and 673	
		rRT-PCR	VI	rRT-PCR	VI
Oral cavity	Lower lip (mucosa)	– + –	+ – –	– – –	– – –
	Dental pad	– – –	– – –	– – –	– – –
	Cranial tongue	– + –	– – –	– – –	– – –
	Mid tongue	– – –	– – –	– – –	– – –
	Lingual torus	– – –	– – –	– – –	– – –
	Lingual tonsil	– – –	– – –	– – –	– – –
	Cranial hard Palate	– – –	– – –	– – –	– – –
	Caudal hard palate	– – –	– – –	– – –	– – –
	Palatine tonsil	– – –	– – –	+ – –	– – –
Nasal cavity/exterior	Nasal planum	– – –	– – –	– – –	– – –
	Alar fold	+ – –	– – –	– – –	– – –
	Cranial turbinates	– – –	– – –	– – –	– – –
	Caudal turbinates	– – –	+ – –	– – –	– – +
Soft palate	Cranial ventral soft palate	+ + –	+ – –	+ – –	– – –
	Caudal ventral soft palate	+ + –	+ – –	– – –	– – –
	Cranial dorsal soft palate	+ – +	+ – +	– – –	– – –
	Caudal dorsal soft palate	+ + +	+ + +	– – +	– – +
Pharynx	Cranial dorsal nasopharynx	+ – +	+ + +	– – +	– – +
	Caudal dorsal nasopharynx	+ + +	+ + +	– – –	+ – –
	Pharyngeal tonsil	+ – –	– – –	– – –	+ – –
Larynx	Cranioventral epiglottis	+ + –	– – +	+ – –	+ – –
	Ventral larynx	+ + +	+ + –	– – –	– – +
Trachea	Trachea 10*	– – –	– – –	– – –	– – –
	Trachea 20	– – –	– – –	– – –	– – –
	Trachea 30	– – –	– – –	– – –	– – –
Lungs	Primary bronchus	– + +	– – –	– – +	– – –
	Cranial lobe, proximal	+ + –	– – –	– – +	– – +
	Cranial lobe, mid	+ – –	+ – –	– – +	– – –
	Cranial lobe, distal	+ – –	+ – –	– – –	– – –
	Middle lobe, proximal	+ + –	+ – –	– – –	– – –
	Middle lobe, mid	+ – –	+ – –	– – +	– – –
	Middle lobe, distal	+ + –	+ – –	– – +	– – –
	Caudal lobe, proximal	+ + –	– – –	– – –	– – –
	Caudal lobe, mid	– + –	– – –	– – –	– – –
	Caudal lobe, distal	+ + –	– – –	– – –	– – –

* Trachea 10, 20 and 30 correspond to samples of trachea taken 10, 20 and 30 cm caudal to the larynx, respectively.

Immunohistochemical labeling was considered positive when there was an intense cell-associated signal within the tissue with the absence of such staining in the negative controls.

Results

Clinical profiles of FMDV-infected cattle

Clinical signs of FMD (vesiculation, lameness, increased salivation, loss of appetite or fever) were not detected in the six animals euthanased at 24 hpi subsequent to either aerosol administration or intranasal instillation with FMDV. Virus isolation and rRT-PCR data from sera and swab samples are presented in Table 2. All serum samples (0, 6, and 24 hpi) from these animals were negative for FMDV by both VI and rRT-PCR indicating all six were non-viremic up to time of necropsy regardless of route of virus exposure. Given the importance of this data, the rRT-PCR detection procedure was repeated on $\geqslant$10 replicates per sample and VI was run in triplicate to confirm the negative results.

Virus was not isolated at any time from nasal or oral (saliva) swabs in three aerosol exposed animals with only viral RNA detectable at 6 and 24 hpi in oral and nasal swabs. Virus was isolated only from two nasal swab specimens from instilled steers at 24 hpi, but several saliva and nasal samples were positive for viral RNA at 6 and 24 hpi.

In order to confirm that aerosol exposure would produce typical FMD, one steer (animal 760) was aerosol-inoculated and allowed to survive for 10 days by which time clinical signs and viremia have ceased (Fig. 1). In this animal, disease progression was characterized by fever from 3 to 4 dpi, virus in sera at 2 and 3 dpi as determined by VI, and from 1 to 5 dpi as determined by rRT-PCR, and vesicles on all four feet and on the tongue first detected 2 dpi and of maximum severity at 5 dpi. These clinical signs are similar to those in steers infected by the intradermal-lingual route and by contact exposure with this FMDV strain (Fig. 1).

Tissue-specific localization of FMDV by VI and rRT-PCR

Thirty-five tissues were collected and processed by VI and rRT-PCR from each of the six steers euthanased at 24 hpi. Using both techniques, virus was most frequently detected in the soft palate, pharynx, larynx, and lungs and few positive samples were found from the oral or nasal cavity or from the trachea (Table 1). Of the 105 specimens from aerosol-exposed cattle, 39 (37.1%) had detectable FMDV RNA and 23 (21.9%) contained viable FMDV. Among comparable tissues from instilled steers, 10 (9.5%) had detectable FMDV RNA and 8 (7.6%) contained viable FMDV. Thus, both detection techniques indicated a greater dissemination of FMDV in aerosol-exposed animals. Throughout the experiment BHK and BHK-alphaVbeta6 cells (Duque et al., 2004) were much less effective in isolating the bovine-derived FMDV O1Manisa strain used in this experiment than were LFBK cells.

Table 2
The distribution of foot-and-mouth disease virus strain O1 Manisa as determined by rRT-PCR and virus isolation (VI) in samples collected ante-mortem from cattle inoculated by aerosol or nasal instillation

Sample	Time post-inoculation (h)	Aerosol animals 66, 670, and 671		Nasal instillation animals 67, 672, and 673	
		rRT-PCR	VI	rRT-PCR	VI
Serum	0	– – –	– – –	– – –	– – –
	6	– – –	– – –	– – –	– – –
	24	– – –	– – –	– – –	– – –
Saliva	0	– – –	– – –	– – –	– – –
	6	+ – –	– – –	+ + –	– – –
	24	– – +	– – –	+ – –	– – –
Nasal swab	0	– – –	– – –	– – –	– – –
	6	+ – +	– – –	+ – –	– – –
	24	– – +	– – –	+ + +	+ – +

Oral and nasal cavities

Most samples from the oral cavity of both aerosol-exposed and instilled steers were negative (50/54, 92.6%) for virus and viral RNA (Table 1). In aerosol treated steers FMDV was detected in the oral cavity in just three samples: from the lower lip of two steers (one by rRT-PCR and one by VI), and one from the cranial tongue of one steer (by rRT-PCR only). A sample from the palatine tonsil was the only positive sample from the instilled steers and this was for viral RNA. Similar results were obtained from nasal tissue samples, of which most were negative (21/24, 87.5%). Only one aerosol-exposed steer was positive for viral RNA and by VI in the caudal turbinate and only one instilled steer was VI positive at this site.

Soft palate

For aerosol-exposed steers the ventral soft palate (cranial and caudal), was positive by VI and/or rRT-PCR in 2/3 animals. The cranial dorsal soft palate was positive by both rRT-PCR and VI in 2/3 steers, whereas the caudal dorsal soft palate was positive by both rRT-PCR and VI in all three animals. For instilled steers only three positive results were obtained. This included a caudal dorsal soft palate sample positive by both rRT-PCR and VI in one steer. The cranial segment of ventral soft palate was positive by rRT-PCR in another animal but was negative by VI (Table 1).

Pharynx

For aerosol-exposed steers all specimens of cranial and caudal dorsal nasopharynx were VI-positive and all but one specimen (cranial dorsal pharynx of animal 670) were positive for viral RNA. For instilled steers, only the cranial dorsal nasopharynx of one steer was positive by both rRT-PCR and VI and caudal dorsal nasopharynx and pharyngeal tonsil from another animal was positive for RNA only (Table 1).

Larynx

For aerosol-exposed steers, the epiglottis and ventral larynx were positive by rRT-PCR and/or VI in the three steers. For the instilled steers, only the epiglottis of one steer was positive by both rRT-PCR and VI, and ventral larynx of another by VI (Table 1).

Lungs and trachea

For aerosol-exposed steers, 53.3% (16/30) of lung specimens were positive for viral RNA, but virus was isolated from only five specimens from animal 66. All lung specimens from animal 671 were negative by both detection techniques with the exception of the primary bronchus where viral RNA was detected. Only one instilled steer had five positive lung samples by rRT-PCR of which only one was VI-positive. Tracheal specimens from three distinct levels were uniformly negative for virus and viral RNA from all steers (Table 1).

Immunohistochemical localization of FMDV antigens

Tissues positive by VI and rRT-PCR were further examined by IHC using monoclonal antibodies directed against structural and non-structural viral proteins. In general there was good correlation with IHC indicating tissue viral replication was occurring. All rRT-PCR and VI-negative tissues were also negative using IHC. In lung samples, cells with strong cytoplasmic anti-FMDV immunoreactivity were infrequently identified individually or in small clusters within the pulmonary parenchyma (Fig. 2A). Within the alveoli, immunoreactive cells were morphologically consistent with alveolar macrophages. Within alveolar walls, similar immunoreactivity was observed in cells suspected to be pneumocytes or intra-vascular macrophages.

In tissues from the dorsal soft palate, nasopharynx, and larynx, anti-FMDV immunoreactivity was infrequently identified in the pseudostratified columnar, stratified squamous, and attenuated epithelial regions and in the lymphofollicular, interfollicular, and stromal regions of the submucosa. In some instances, immunoreactive intra-epithelial cells appeared morphologically similar to adjacent epithelial cells. Specific anti-FMDV immunoreactivity was rarely identified in attenuated epithelial cells overlying lymphoid follicles (Fig. 2C), cells interpreted as possible M-cells. Sloughed lingual vesicular epithelium from animal 760 at 4 dpi contained abundant immunoreactive keratinocytes within the necrotic stratum spinosum (Fig. 2E) confirming that clinically visible vesicles occurred in association with the presence of virus.

Discussion

Donaldson et al. (1987) highlighted the respiratory tract as the most susceptible natural portal of FMD virus entry for cattle and that the only infection route that approached this in terms of infectivity was intradermal (IDL) inoculation of the tongue. Though IDL inoculation has great utility in terms of repeatability of infecting dose and location of inoculum delivery, it is a minor route of infection in cattle (Donaldson, 1987) that probably by-passes many of the early phases of natural infection.

In order to study early events in FMDV pathogenesis, we compared the distribution of virus in tissues of animals inoculated using the Accuspray device, a direct nasal instillation device and using the Aeromask pulmonary nebulization system. Given their size, the delivery of particles produced by the Accuspray device would be limited to the upper respiratory tract whereas particles

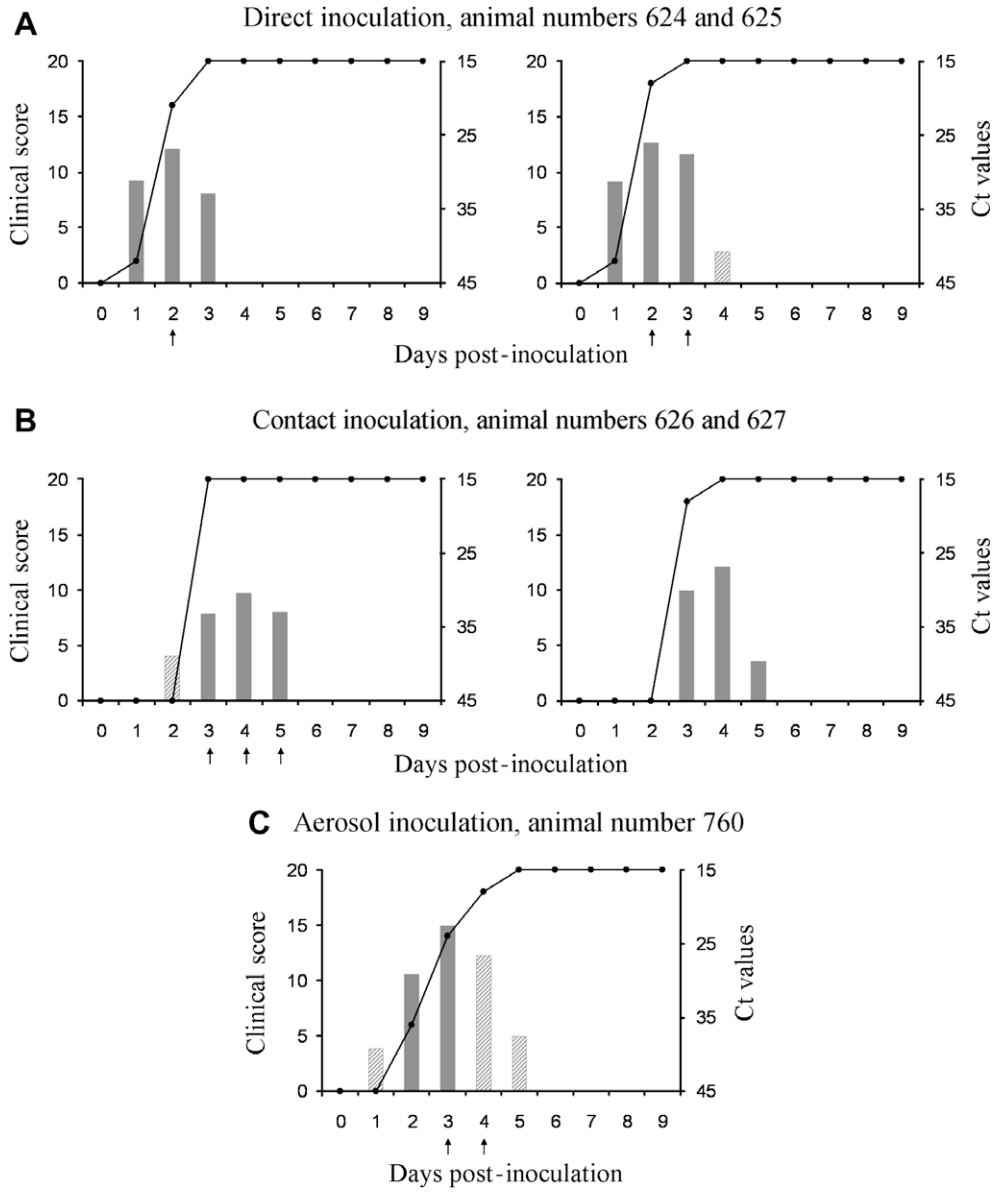

Fig. 1. Graphs illustrating the time course of infection in cattle: directly inoculated (intradermolingually) with foot-and-mouth virus strain O1 Manisa (A); in contact with directly inoculated cattle (B); or inoculated by aerosol exposure (C). Time on the *X*-axes is in days post-inoculation/contact. The left *Y*-axes represent the clinical scores (●) based on the number and size of vesicles in the oral cavity and/or on the feet. Bars indicate Ct values of viral RNA detection in serum (Ct scale on right *Y*-axes). Solid grey and hatched bars represent samples positive and negative on virus isolation, respectively. Arrows denote that the animals were pyrexic ($\geqslant$40 °C).

produced by the nebulizer system, designed for intra-pulmonary drug deposition, would be expected to deposit in the lungs and in the upper respiratory tract. Standardizing the size of infectious particles is critical to an early pathogenesis model as it dictates the transmission distances and anatomical distribution of the infectious aerosol thus influencing the relevance of the model system. Aerosolized particles <6 μm in diameter are minimally affected by gravity and can therefore transmit virus over long distances (Gloster et al., 1981). Additionally, only particles in this size range can reach the lower respiratory tract (Gloster et al., 1981). Those >6 μm in diameter are only likely to transmit FMDV over short distances and to deposit in the upper or middle regions of the respiratory tract (Gloster et al., 1981; McVicar and Eisner, 1983; Alexandersen et al., 2003).

In the current study, cattle exposed to FMDV via intranasal instillation had substantially fewer positive tissues relative to aerosol-exposed animals. Considering that both groups received the same quantity of virus and that the delivery of inoculum by nasal instillation should be limited to the upper respiratory tract, animals infected by this method were anticipated to have more FMDV infection of the pharynx, larynx and soft palate than were aerosol treated animals. However, in contrast, aerosol-exposed animals had more FMDV-positive tissues in all regions except the palatine tonsil. Our extensive post mortem sampling protocol determined more precisely the localization of FMDV than did previous studies. The detection of FMDV and viral RNA in palatine, pharyngeal, laryngeal, and pulmonary samples from animals inoculated with the nebulizer system suggests that all levels of the respiratory tract were exposed to viral inoculum, a situation similar to that occurring in naturally occurring aerosol transmission. Thus the evidence suggests nebulization to be a superior infection model system and the remainder of this discussion focuses on the data generated from animals inoculated using this method.

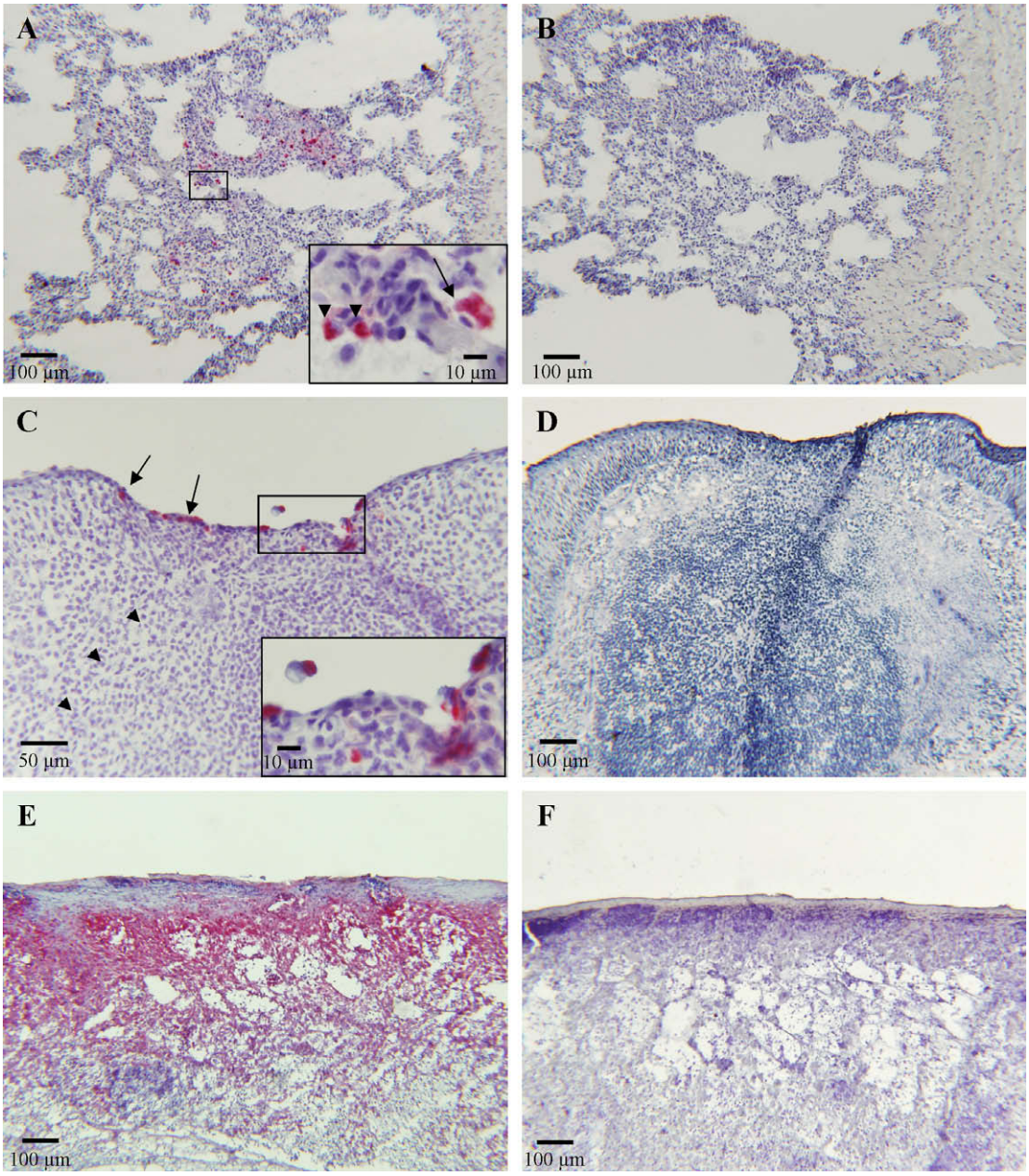

Fig. 2. Photomicrographs illustrating foot-and-mouth disease virus (FMDV) antigen (red staining) in immunohistochemical cryosections from animals 24 (A–D) and 96 (E–F) h post aerosol infection with strain O1 Manisa. Antibodies against FMDV VP-1, 2, 3 (A, C, and E) and VSV-Indiana (B, D, and F) were used: (A) proximal cranial lung tissue from animal 670 illustrating alveolar macrophages (arrow) cells in the alveolar wall (arrowheads) with cytoplasmic immunoreactivity (×6, inset ×40); (B) negative control for (A) (×6); (C) caudal dorsal nasopharynx from animal 66 exhibiting several attenuated surface epithelial (M-like) cells (arrows) and a few paracortical cells with cytoplasmic immunoreactivity. There is a subjacent lymphoid follicle (arrowheads) (×16, inset ×40); (D) negative control for (C) (×6); (E) sloughed lingual vesicular epithelium from animal 760 illustrating numerous immunoreactive keratinocytes within the stratum spinosum (×6); (F) negative control for (E) (×6). Immunohistochemical stain for FMDV antigen with hematoxylin counterstain.

The rRT-PCR, VI and IHC results strongly suggest that FMDV is replicating primarily in the upper respiratory tract of the aerosol-exposed steers at 24 hpi. Furthermore, the fact that most oral and nasal swab samples remained negative suggests that the inoculum is rapidly removed from oral and nasal secretions.

The tissue distribution data of FMDV O1 Manisa in aerosol-inoculated cattle provides novel insights into the pathogenesis of bovine FMD. Although many of the tissues sampled in this work have been examined previously, the further anatomical subdivision of the sampled sites provides more detail and precision in characterizing virus distribution and disease pathogenesis. The data generated from animals at 24 hpi are largely in agreement with previous FMD early pathogenesis studies in that the dorsal soft palate and nasopharynx, and to a lesser extent the lungs, are strongly implicated sites of early infection. The finding that laryngeal tissues are frequently FMDV-positive is novel, but most likely reflects the fact that these tissues have not previously been specifically examined. The finding that almost all exterior and oral cavity samples were negative on VI is consistent with previous evidence that intact keratinized epithelia are resistant to primary FMDV infection (Cottral et al., 1965). The few rRT-PCR-positive, VI-negative findings in these regions most likely represent viral RNA deposited on the epithelial surfaces from other locations.

The use of IHC to localize FMDV within tissues during early bovine FMD has not been previously reported. The localization of FMDV antigens within alveolar macrophages and within alveolar walls is consistent with previous studies that reported similar findings using in situ hybridization (ISH) in an aerosol-inoculation model (Brown et al., 1992, 1996). However, the previous ISH-based work did not localize FMDV to the soft palate or respiratory-associated lymph nodes until 72 hpi in contrast to our findings of viral RNA, infectious virus and FMDV immunoreactivity within pharyngeal tissues at 24 hpi. This difference may be due to differences in aerosol technique, the sensitivity of detection, the tissues sampled and/or the strain-specific viral tissue tropism. Foot-and-mouth disease virus has been detected in bovine pharyngeal and palatine tissues at later stages of infection using ISH (Prato Murphy et al., 1999; Zhang and Kitching, 2001). The current findings are in agreement with these studies in suggesting that pharyngeal and palatine tissues are involved in FMD pathogenesis. However, the time of onset of FMDV replication in these tissues, and thus their role as primary versus secondary sites of replication remains unresolved. Our preliminary IHC data suggests that early in FMDV infection of cattle, replication occurs in the upper respiratory tract within respiratory-associated lymphoid tissue. However, it remains unclear if infection at these sites proceeds directly to systemic disease.

Our tissue-specific data demonstrate good correlation between the detection of viable FMDV by VI and of FMDV RNA by rRT-PCR with agreement between the two techniques of 77.1% (81/105) between specimens from the aerosol-exposed cattle. The finding of viral RNA but no infectious virus in a number of samples (20/105) was expected since virus could be inactivated yet the RNA could still be detectable. The fact that 15 such samples were from lung may indicate that pulmonary tissue is poorly permissive to FMDV replication. The few instances (4/105) when infectious virus but no viral RNA was detected suggests the presence of minute quantities of virus that required multiple passages in culture and/or that rRT-PCR inhibitors were present. The greater quantity of tissue macerate used to inoculate cells for VI compared to that used to extract RNA for rRT-PCR may also have contributed to this finding. Alternatively, the patchy distribution of FMDV infection (Monaghan et al., 2005) might explain why adjacent tissue did not contain similar quantities of infected cells. The almost 100% correlation in finding viral RNA and infectious virus in only the caudal dorsal soft palate, caudal dorsal nasopharynx and ventral larynx suggests these are primary viral replication sites.

We confirmed that aerosol exposure simulated clinical FMD, by infecting, examining and sampling one animal. Work at our laboratory with the FMDV O1 Manisa and A24 Cruzeiro strains using this and other infection systems has resulted in the development of a similar clinical picture (Rodriguez, personal communication) so that cattle euthanased at 24 hpi can be considered pre-viremic and pre-clinical and would have gone on to develop clinical FMD.

Conclusions

The results of this study identify specific regions of the respiratory tract as primary sites of FDMV replication in aerosol-exposed cattle. The aerosol infection method used, the detailed tissue sampling protocol, and the trimodal virus detection methodology employed have allowed us to pinpoint the tissue distribution of FMDV in greater detail than previously. This well defined, repeatable model will facilitate the future investigation of FMD pathogenesis and, in contrast to earlier models, the equipment required is commercially available. This experimental system has the potential to better define how localized primary infection progresses to systemic disease and to be used in the assessment of FMDV vaccines and other control measures to minimize the impact of this disease.

Conflict of interest statement

None of the authors of this paper has a financial or personal relationship with other people or organizations that could inappropriately influence or bias the content of the paper.

Acknowledgements

We want to thank the research animal resource unit personnel at PIADC for their patience and help in caring and collecting samples from animals. We also acknowledge Dr. Douglas Gregg for help in some of the necropsies. Diana Alejo, Elizabeth Bishop, Ethan Hartwig and George Smoliga played a key role in collecting and processing samples. We thank Dr. A. Clavijo for supplying monoclonal antibodies to FMDV 3D polymerase. This research was funded by ARS-CRIS Project 1940-32000-052-00D.

Appendix A. Supplementary data

Supplementary data associated with this article can be found in the online version at doi:10.1016/j.tvjl.2008.08.023.

References

Alexandersen, S., Zhang, Z., Donaldson, A.I., Garland, A.J., 2003. The pathogenesis and diagnosis of foot-and-mouth disease. Journal of Comparative Pathology 129, 1–36.

Brown, C.C., Meyer, R.F., Olander, H.J., House, C., Mebus, C.A., 1992. A pathogenesis study of foot-and-mouth disease in cattle, using in situ hybridization. Canadian Journal of Veterinary Research 56, 189–193.

Brown, C.C., Piccone, M.E., Mason, P.W., McKenna, T.S., Grubman, M.J., 1996. Pathogenesis of wild-type and leaderless foot-and-mouth disease virus in cattle. Journal of Virology 70, 5638–5641.

Callahan, J.D., Brown, F., Osorio, F.A., Sur, J.H., Kramer, E., Long, G.W., Lubroth, J., Ellis, S.J., Shoulars, K.S., Gaffney, K.L., Rock, D.L., Nelson, W.M., 2002. Use of a portable real-time reverse transcriptase-polymerase chain reaction assay for rapid detection of foot-and-mouth disease virus. Journal of the American Veterinary Medical Association 220, 1636–1642.

Cottral, G.E., Patty, R.E., Gailiunas, P., Scott, F.W., 1965. Sensitivity of cell cultures, cattle, mice, and guinea-pigs for detection of nineteen foot-and-mouth disease viruses. Bulletin of Office international des Epizooties 63, 1607–1625.

Donaldson, A.I., 1987. Foot-and-mouth disease: the principal features. Irish Veterinary Journal 41, 325–327.

Donaldson, A.I., Gibson, C.F., Oliver, R., Hamblin, C., Kitching, R.P., 1987. Infection of cattle by airborne foot-and-mouth disease virus: minimal doses with O1 and SAT 2 strains. Research in Veterinary Science 43, 339–346.

Duque, H., LaRocco, M., Golde, W.T., Baxt, B., 2004. Interactions of foot-and-mouth disease virus with soluble bovine alphaVbeta3 and alphaVbeta6 integrins. Journal of Virology 78, 9773–9781.

Gloster, J., Blackall, R.M., Sellers, R.F., Donaldson, A.I., 1981. Forecasting the airborne spread of foot-and-mouth disease. Veterinary Record 108, 370–374.

Golde, W.T., Pacheco, J.M., Duque, H., Doel, T., Penfold, B., Ferman, G.S., Gregg, D.R., Rodriguez, L.L., 2005. Vaccination against foot-and-mouth disease virus confers complete clinical protection in 7 days and partial protection in 4 days: use in emergency outbreak response. Vaccine 23, 5775–5782.

Grubman, M.J., Baxt, B., 2004. Foot-and-mouth disease. Clinical Microbiology Reviews 17, 465–493.

Hess, D., Fisher, D., Williams, P., Pooler, S., Kacmarek, R.M., 1996. Medication nebulizer performance. Effects of diluent volume, nebulizer flow, and nebulizer brand. Chest 110, 498–505.

McVicar, J.W., Eisner, R.J., 1983. Aerosol exposure of cattle to foot-and-mouth disease virus. Journal of Hygiene (London) 91, 319–328.

McVicar, J.W., Sutmoller, P., 1976. Growth of foot-and-mouth disease virus in the upper respiratory tract of non-immunized, vaccinated, and recovered cattle after intranasal inoculation. Journal of Hygiene (London) 76, 467–481.

McVicar, J.W., Graves, J.H., Sutmoller, P., 1970. Growth of foot-and-mouth disease virus in the bovine pharynx. In: Proceedings of the 74th Annual Meeting of the United States Animal Health Association, pp. 230–234.

Monaghan, P., Simpson, J., Murphy, C., Durand, S., Quan, M., Alexandersen, S., 2005. Use of confocal immunofluorescence microscopy to localize viral nonstructural proteins and potential sites of replication in pigs experimentally infected with foot-and-mouth disease virus. Journal of Virology 79, 6410–6418.

Prato Murphy, M.L., Forsyth, M.A., Belsham, G.J., Salt, J.S., 1999. Localization of foot-and-mouth disease virus RNA by in situ hybridization within bovine tissues. Virus Research 62, 67–76.

Sellers, R., Gloster, J., 2008. Foot-and-mouth disease: a review of intranasal infection of cattle, sheep and pigs. The Veterinary Journal 177, 159–168.

Stave, J.W., Card, J.L., Morgan, D.O., 1986. Analysis of foot-and-mouth disease virus type O1 Brugge neutralization epitopes using monoclonal antibodies. Journal of General Virology 67, 2083–2092.

Swaney, L.M., 1988. A continuous bovine kidney cell line for routine assays of foot-and-mouth disease virus. Veterinary Microbiology 18, 1–14.

Yang, M., Clavijo, A., Li, M., Hole, K., Holland, H., Wang, H., Deng, M.Y., 2007. Identification of a major antibody binding epitope in the non-structural protein 3D of foot-and-mouth disease virus in cattle and the development of a monoclonal antibody with diagnostic applications. Journal of Immunological Methods 321, 174–181.

Zhang, Z.D., Kitching, R.P., 2001. The localization of persistent foot and mouth disease virus in the epithelial cells of the soft palate and pharynx. Journal of Comparative Pathology 124, 89–94.

Return to Table of Contents

Virology 404 (2010) 32–40

Contents lists available at ScienceDirect

Virology

journal homepage: www.elsevier.com/locate/yviro

Differential gene expression in bovine cells infected with wild type and leaderless foot-and-mouth disease virus

James Zhu [a], Marcelo Weiss [a,b], Marvin J. Grubman [a], Teresa de los Santos [a,*]

[a] Plum Island Animal Disease Center, North Atlantic Area, Agricultural Research Service, U.S. Department of Agriculture, Greenport, New York 11944, USA
[b] Oak Ridge Institute for Science and Education, PIADC Research Participation Program, Oak Ridge, TN 37831, USA

ARTICLE INFO

Article history:
Received 29 December 2009
Returned to author for revision
18 January 2010
Accepted 22 April 2010
Available online 23 May 2010

Keywords:
Picornaviruses
FMDV
Microarray
NF-κB

ABSTRACT

The leader proteinase (L^{pro}) of foot-and-mouth disease virus (FMDV) plays a critical role in viral pathogenesis. Molecular studies have demonstrated that L^{pro} inhibits translation of host capped mRNAs and transcription of some genes involved in the innate immune response. We have used microarray technology to study the gene expression profile of bovine cells infected with wild type (WT) or leaderless FMDV. Thirty nine out of approximately 22,000 bovine genes were selectively up-regulated by 2 fold or more in leaderless versus WT virus infected cells. Most of the up-regulated genes corresponded to IFN-inducible genes, chemokines or transcription factors. Comparison of promoter sequences suggested that host factors NF-κB, ISGF3G and IRF1 specifically contributed to the differential expression, being NF-κB primarily responsible for the observed changes. Our results suggest that L^{pro} plays a central role in the FMDV evasion of the innate immune response by inhibiting NF-κB dependent gene expression.

Published by Elsevier Inc.

Introduction

Foot-and-mouth disease (FMD) is a highly contagious vesicular viral disease that affects wild and domestic cloven-hoofed animals and is considered a major threat to animal health worldwide (Grubman and Baxt, 2004). The etiologic agent, FMD virus (FMDV) belongs to the *aphthovirus* genus of the Picornaviridae family and contains a single-stranded positive-sense RNA genome of about 8500 bases surrounded by a non-enveloped icosahedral protein capsid. Upon infection, the viral genome is translated into a long polyprotein precursor which is subsequently processed by three viral encoded products, the proteinases L^{pro} and $3C^{pro}$, and the 18 amino-acid peptide 2A, resulting in four structural proteins (VP4-1A, VP2-1B, VP3-1C and VP1-1D) and ten non-structural viral proteins (L, 2A, 2B, 2C, 3A, $3B_{1,2,3}$ 3C and 3D) (Mason et al., 2003; Ryan et al., 1991). L^{pro}, positioned at the N-terminus of the polyprotein, is a papain-like proteinase that in addition to processing itself from the viral protein precursor (Strebel and Beck, 1986), is involved in cleaving the host translation initiation factor eIF4G (Devaney et al., 1988, Kirchweger et al., 1994). This process results in the shut-off of host cap-dependent protein synthesis without affecting viral cap-independent protein translation, thus diverting the cellular machinery to virus production. We have previously shown that L^{pro} plays an important role in FMDV pathogenesis. A genetically engineered FMDV strain lacking the L^{pro} coding region (leaderless virus) is viable in tissue culture (Piccone et al., 1995) but remarkably, it does not cause clinical disease when inoculated into cattle or swine (Mason et al., 1997; Chinsangaram et al., 1998) and it does not spread from the original site of infection when aerosolized in cattle (Brown et al., 1996). Further studies have demonstrated that supernatants of primary cell cultures infected with leaderless virus contain higher levels of antiviral activity than supernatants of cells infected with wild type (WT) virus (Chinsangaram et al., 1999). Using cells derived from knockout mice for type I interferon (IFN)-receptor, double-stranded RNA-dependent protein kinase (PKR) or RNase L, it was demonstrated that the antiviral activity elicited by leaderless virus was type I IFN-specific (Chinsangaram et al., 2001). Furthermore, viral replication was inhibited by pre-treatment of cells with IFN-α, suggesting that FMDV cannot overcome the antiviral effects of IFN stimulated genes (ISGs) once they have been established (Chinsangaram et al., 2001). More recently, we have found that in addition to blocking IFN protein synthesis, FMDV L^{pro} also inhibits the induction of transcription of IFN-β and at least three ISGs including PKR, 2′, 5′ oligoadenylate synthetase (OAS1) and Mx1 (de los Santos et al., 2006). Moreover, we have observed that FMDV inhibition of cellular transcription correlates with degradation of the p65 subunit of the transcription factor, nuclear factor-κB (NF-κB) (de los Santos et al., 2007). The intrinsic proteinase activity of L^{pro} and its proper nuclear localization and retention are required for this function (de los Santos et al., 2007, 2009).

NF-κB belongs to a conserved family of proteins that form multiple homo- and heterodimers with transcriptional activity (Hayden et al., 2006). In resting cells, NF-κB dimers are retained in the cytoplasm by their interaction with specific protein inhibitors known as IκBs. A

* Corresponding author. Plum Island Animal Disease Center, USDA, ARS, NAA, P.O. Box 848, Greenport, New York 11944, USA. Fax: +1 631 323 3006.
E-mail address: teresa.delossantos@ars.usda.gov (T. de los Santos).

0042-6822/$ – see front matter. Published by Elsevier Inc.
doi:10.1016/j.virol.2010.04.021

variety of inducing stimuli such as viral infection, cellular stress, etc., triggers a cascade of signal transduction events leading to phosphorylation of IκBs, which are subsequently ubiquitinated and degraded by the proteasome. These events result in the release of NF-κB from IκB, followed by translocation into the nucleus. Once in the nucleus, NF-κB binds specific sequences in the promoter/enhancer regions of numerous genes including cytokines, chemokines and other products involved in the regulation of cellular differentiation, survival and proliferation, thereby controlling various aspects of the innate and adaptive immune response (Hayden and Ghosh, 2008). Transcription of hundreds of genes is regulated by the signaling events activated by IFNs and by NF-κB. More than 300 ISGs have been reported as induced by human type I IFNs (Der et al., 1998, de Veer et al., 2001) and more than 500 genes may be affected by NF-κB (Gilmore, 2008).

In this study we have taken a functional genomics approach using microarray technology to systematically study the differences in gene expression induced by WT and leaderless FMDV infection of primary bovine cells. We have examined the pattern of expression of 43,803 bovine gene probes, corresponding to approximately 22,000 genes, using a custom designed bovine microarray. Consistent with our previous data, we found that in cells infected with leaderless FMDV there is a significant increase in the levels of expression of several genes, most of them involved in the innate immune response. Our analysis suggests that L^{pro} modulates multiple pathways of the cellular response to viral infection by primarily interfering with NF-κB dependent gene expression.

Results

Differentially expressed genes between WT and leaderless FMDV infected cells

In the current study we analyzed gene expression upon FMDV infection of bovine cells (embryonic bovine kidney cells [EBK]). Cells were infected at a multiplicity of infection (MOI) of 10 and RNA samples collected at 2, 4 and 6 h post infection (hpi). Since the RNA extracted from WT infected cells at 6 hpi showed signs of partial degradation, microarray analyses were performed with samples collected at 2 and 4 hpi. RNA extracted from mock infected cells served as a normalizer for indirect comparison between WT and leaderless virus and gene transcriptional differences were reported as the relative expression in leaderless with respect to WT virus infection. We found that no genes were differentially expressed by 2-fold or more (leaderless vs WT virus) in samples taken at 2 hpi, and no cytopathic effect (CPE) was observed in the cultures (data not shown). However, by 4 hpi the gene expression profile for both viruses was significantly different and approximately 20% and 5% CPE was observed in the WT and leaderless virus infected cells, respectively. Three biological replications were performed with samples taken at 4 hpi. Based on the significant threshold of false discovery rate of 0.2 or lower and differential expression equal to or greater than 2-fold, 39 genes were determined as differentially expressed in EBK cells infected with leaderless vs WT FMDV (Table 1). The expression of all 39 genes was up-regulated in leaderless as compared to WT virus infected cells, suggesting that L^{pro} had an inhibitory effect on gene expression. Analysis of the available literature indicated that the majority of the differentially expressed genes (DEGs) were IFN-stimulated and included: 1) genes with antiviral activity (IFIT2, RSDA2, ISG15, OAS1, Mx1 and ZC3HAV1); 2) cytokines/chemokines (IL28B, CXCL3, CCL2 and CX3CL1); 3) transcription factors (ISGF3G, IRF8); 4) genes involved in regulation of apoptosis (pro-apoptotic: PMAIP1, SAT1, NF-κB1A and UBE1L; anti-apoptotic: IER3 and IFI6); 5) Genes involved in cell proliferation (GBP1); and 6) genes involved in regulation of IFN signaling (LGP2 and USP18). All of the above DEGs were related to the innate immune response.

A number of additional genes not known to be IFN-stimulated, including transcription factors DSCR1, BATF2, GTF2B, SERTA D1 and TCFL1 were also up-regulated, in leaderless vs WT infected cells, as well as genes involved in RNA metabolism such as DTX3L and ZFP36. We also observed induction of eIF4E a factor required for translation, PARP14 and TREX1, genes also involved in apoptosis, SLC25A28, a mitochondrial ion transporter, MARCKSL1, a gene predicted to be involved in the protein kinase C-calmodulin signal transduction pathway and FAM46A and C6orf150, genes of unknown functions.

To corroborate the results obtained with the microarray analysis, we performed quantitative (real time) reverse transcription-polymerase chain reaction (qRT-PCR) on a selected group of genes for which we had a standardized method available in the lab. Similar to the microarray analysis, we observed up-regulation of CCL2, IL28B, ISG15, Mx1 and OAS1 (Table 2). Although the differential gene expression detected with microarray analysis was always smaller than that measured by qRT-PCR, the fold induction values followed the same pattern in both assays. In addition, IFN-β was increased by approximately 50-fold and PKR by 2.3 fold for leaderless as compared to WT virus infection. In summary, there was consistency between the results of microarray and qRT-PCR analyses showing both, a higher level of expression of genes that participate in the stress/antiviral cellular immune response in leaderless virus infected as compared to WT virus infected cells.

Inferred transcription factors involved in the differential expression

Transcription is a process tightly regulated by the binding of transcription factors to promoter and regulatory sequences. Using the Neural Network Promoter Prediction (NNPP) program and expression sequences, we were able to predict the promoter sequences of 35 out of the 39 DEGs that were further analyzed with the Over-represented Transcription Factor Binding Site Prediction Tool (OTFBS). When comparing to random sequences, we detected six transcription factor-binding matrices over-represented (33 to 137 hits) in the selected regions of the regulatory sequences with P-values $\leq 5.92E-05$ (Table 3). The transcription factors that bind the over-represented matrices included ISGF3G, IRF1, IRF2, NF-κB (two reported matrices M00194, NFKB_Q6, and M00054, NF-kappaB) and C-rel. For comparison, 33 corresponding human promoter sequences described in the human promoter database were used in the same analysis (Table 4). We found that binding sites for NF-κB (NF-kappaB -M00194) and ISGF3G (interferon-stimulated response element -ISRE-M00258) were also significantly over-represented in the regulatory sequences of the up-regulated gene probes as compared to the promoter sequences of all genes included in the microarray. Therefore, both human and bovine promoter sequences of the DEGs, showed over-representation for the binding sites of NF-κB and ISGF3G transcription factors.

Additionally, the number of these transcription factor binding sites in the upstream regulatory sequences of the bovine DEGs was used to perform correlation analysis with respect to signal intensity, fold change or impact factor for the identified matrices in the 35 DEGs (Supplementary Table 1). We observed significant correlation between the number of binding sites for ISGF3G and IRF1 and signal intensity with coefficients of 0.43 and 0.41 and between the number of binding sites and fold change with coefficients of 0.62 and 0.58, respectively. With this analysis, however, we did not see significant correlation for the number of NF-κB (NFKAPPAB_01, NFKB_Q6 or NFKB total) or c-Rel binding sites, although almost all DEGs have these recognition sequences in their promoters or regulatory elements.

We also analyzed the transcriptional regulatory networks affecting the differential expression using CARRIE software (Table 5). This program is a computational method that analyzes microarray data including signal intensity, fold changes, and promoter sequence data to infer a transcriptional regulatory network from the response to a

Table 1
List of genes that displayed significant differential expression at 4 hpi in primary EBK cells infected with leaderless or WT FMDV.

Gene	*P*-value	*Q*-value	Fold	Gene description	Function	Reference
IFIT2	8.54E−06	0.05	11.5	Interferon-induced protein with tetratricopeptide repeats 2 (ISG54)	ISG. Involved in blocking translation by binding eIF3	Terenzi et al. (2006).
RSAD2	8.54E−06	0.05	8.1	Radical S-adenosyl methionine domain containing 2 (viperin)	ISG. Antiviral	Chin and Cresswell (2001).
PMAIP1	1.15E−04	0.09	7.1	Phorbol-12-myristate-13-acetate-induced protein 1	Inducer of apoptosis	Oda et al. (2000).
BATF2	1.24E−04	0.09	6.9	Basic leucine zipper transcription factor, ATF-like 2	Predicted as general transcription factor activated by MAP kinases in response to stress	Strausberg et al. (2002).
ISG15	6.83E−05	0.08	6.9	ISG15 ubiquitin-like modifier	ISG. ISG15 is conjugated to proteins involved in innate immunity	Loeb and Haas (1992).
CXCL3	4.27E−05	0.08	4.7	Chemokine (C-X-C motif) ligand 3	ISG. Chemokine. Attracts monocytes.	Geiser et al. (1993).
SAT1	1.45E−04	0.09	4.5	Spermidine/spermine N1-acetyltransferase 1	NF-κB regulated. Stops proliferation and induces apoptosis	Babbar et al. (2006).
IL28B	4.70E−04	0.12	3.8	Interleukin 28B (interferon, lambda 3)	ISG. Type III IFN	Kotenko et al. (2003). Sheppard et al. (2003).
OAS1	2.13E−04	0.09	3.8	2′,5′-oligoadenylate synthetase 1	ISG; synthesizes 2′,5′ oligoadenylates that activate RNase L to degrade viral RNA	Ghosh et al. (1991).
GTF2B	5.98E−05	0.08	3.4	General transcription factor IIB	Transcription factor involved in recognition of promoter sequences during RNA pol II dependent transcription	Reines et al. (1996).
USP18	1.07E−04	0.09	3.4	Ubiquitin specific peptidase 18	ISG; removes ISG15 from conjugated proteins	Malakhov et al. (2002).
CCL2	2.48E−04	0.10	3.4	Chemokine (C-C motif) ligand 2	ISG; chemokine that recruits immune cells to site of infection/injury	Carr et al. (1994).
SOCS1	8.54E−05	0.09	3.3	Suppressor of cytokine signaling 1	Inhibits JAK/STAT pathways. Targets proteins for degradation	Prêle et al. (2008).
ZFP36	5.98E−05	0.08	3.3	Zinc finger protein 36	Involved in nucleating proteins involved in silencing AU rich RNA. Binds TNFa and GMCSF mRNAs promoting instability.	Lai et al. (2002).
CX3CL1	7.22E−04	0.15	3.2	Chemokine (C-X3-C motif) ligand 1	ISG; involved in leukocyte adhesion and migration at the endothelium.	Bazan et al. (1997).
PARP14	2.99E−05	0.07	3.1	Poly (ADP-ribose) polymerase family, member 14	Enzyme that modifies histones and other nuclear proteins by adding poly(ADP-ribosyl) groups leading to cell death.	Amé et al. (2004).
C6orf150	3.42E−05	0.07	3.0	Chromosome 6 open reading frame 150	Unknown	
NFKBIA	9.14E−04	0.16	2.9	Nuclear factor of κ light polypeptide gene enhancer in B-cells inhibitor, α (IκB α)	Inhibits NF-κB activity by retaining it in the cytoplasm	Haskill et al. (1991).
IFI6	1.79E−04	0.09	2.9	Interferon, alpha-inducible protein 6	ISG; suppresses apoptosis	Tahara et al. (2005).
DTX3L	9.82E−05	0.09	2.7	Deltex 3-like (Drosophila)	Ubiquitin ligase activity. Binds promoter regions	Takeyama et al. (2003).
FBXO33	3.03E−04	0.10	2.6	F-box protein 33	May work as protein ubiquitin-ligase	Jin et al. (2004).
Mx1	1.32E−04	0.09	2.6	Myxovirus (influenza virus) resistance 1	ISG; antiviral; GTPase that targets viral RNP structures	Haller et al. (2007).
GBP1	1.96E−04	0.09	2.6	Guanylate binding protein 1	ISG; GTP binding protein; inhibits endothelial cell proliferation	Guenzi et al. (2001).
UBE1L	6.49E−04	0.14	2.5	Ubiquitin-activating enzyme E1-like	E1-ubiquitin activating enzyme. Induces apoptosis.	Kitareewan et al. (2002).
ZNFX1	1.71E−04	0.09	2.5	Zinc finger, NFX1-type containing 1	DNA exonuclease with putative function during DNA repair	Perrino et al. (1994).
LGP2	2.18E−04	0.09	2.5	Laboratory of genetics and physiology 2	ISG. Inhibits IFN signaling by competing with RIGI and MDA5	Yoneyama et al. (2005)
TREX1	1.62E−04	0.09	2.5	Three prime repair exonuclease 1	3′ 5′ DNA exonuclease activity. Contributes to granzyme A induced cell death	Chowdhury et al. (2006).
SERTAD1	2.39E−04	0.10	2.5	SERTA domain containing 1	Acts at E2F responsive promoters stimulating transcription factors and cyclin dependent kinase 4	Sugimoto et al. (1999).
TCF7L1	5.85E−04	0.13	2.5	Transcription factor 7-like 1	HMG box transcription factor involved in induction of apoptosis	Franchini et al. (2006).
ATF3	1.37E−04	0.09	2.2	Cyclic AMP-dependent transcription factor 3	Transcription factor member of CREB family. Represses transcription. Induced by stress. Promotes cell survival	Lu et al. (2007).
ISGF3G	3.54E−04	0.11	2.1	Interferon-stimulated transcription factor 3, gamma (IRF9)	ISG. Transcription factor that mediates IFN signaling inducing ISGs	Veals et al. (1992).
IER3	5.12E−04	0.12	2.1	Immediate early response 3	Prevents FAS or TNF induced apoptosis.	Wu, (2003).
IRF8	1.26E−03	0.17	2.1	Interferon regulatory factor 8	ISG. Transcription factor that binds ISRE seq. Required for expression of IFNs	Sharf et al. (1995)
DSCR1	9.39E−04	0.16	2.1	Down syndrome critical region gene 1	Transcription factor that inhibits calcineurin-dependent signaling pathways.	Yamashita et al. (2000).
SLC25A28	4.95E−04	0.12	2.0	Solute carrier family 25, member 28	Mithocondrial iron transporter that mediates iron uptake	Li et al. (2001).
EIF4E	9.65E−04	0.16	2.0	Eukaryotic translation initiation factor 4E	Protein that binds 5′mRNA cap, part of the translation initiation complex that links the RNA to the ribosomes.	Rychlik et al. (1987).
ZC3HAV1	7.77E−04	0.15	2.0	Zinc finger CCCH-type, antiviral 1	ISG. Inhibits retroviral gene expression and induce an innate immunity response	Gao et al. (2002).
FAM46A	4.95E−04	0.12	2.0	Family with sequence similarity 46, member A	Unknown function	
MARCKSL1	1.32E−03	0.17	2.0	MARCKS-like 1	Might be involved in coupling protein kinase C and calmodulin signal transduction pathways	Verghese et al. (1994).

Table 2
Confirmation of array results by real time RT-PCR. GAPDH was used as internal control for data normalization.

Gene	Fold induction: leaderless/WT	
	RT-PCR	Array
CCL2	3.81 ± 1.39	3.40
IFN-β	52.57 ± 12.66	NI[a]
IL28B	15.51 ± 7.80	3.80
ISG15	12.56 ± 8.15	6.90
La35	0.98 ± 0.07	1.00
Mx1	5.02 ± 2.52	2.60
OAS1	4.87 ± 2.32	3.80
PKR	2.26 ± 0.70	1.80
GAPDH	1.00 ± 0.00	1.00
FMDV	0.15 ± 0.00	0.13

[a] NI: not included. This gene was not represented in the microarray.

specific stimulus (Haverty et al., 2004). From this analysis we concluded that NF-κB binding sites are the most over-represented in the DEGs, considering all known promoter recognition sequences. Six out of the top eight most significantly over-represented sequences are NF-κB binding sites with *P*-values ≤ 8.83E−21. The NF-kappaB (p50) binding site from the M00051 sequence matrix was the most frequent (*P*-value = 3.46E−35). Although not in the top eight, the representation of the binding site for c-Rel, another member of the NF-κB family, was also highly significant (*P*-value = 4.18E−11). Binding sites for IRFs and for ISGF3G (listed in the table as ISRE) were also significantly over-represented using this analysis, with *P*-values of 4.34 E−05 and 6.01E−05 respectively. In addition, the NF-κB (p50) binding site was over-represented in 22 out of 35 DEG regulatory sequences with *P*-values between 9.1E−03 and 5.4E−15 (Supplementary Table 2). Interestingly, binding sites for transcription factors ISGF3G and IRF8 were over-represented in 2 of the 22 genes containing NF-κB binding sites, and moreover, the promoter sequence of IL28B that can lead to activation of ISGF3G also contains over-represented NF-kappaB binding sites. These results suggest that NF-κB dependent transcription is primarily responsible for the differential gene expression observed in leaderless vs WT FMDV infected cells.

Biological processes affected by differential expression

To identify the cellular processes that could be associated with the differential gene expression, we used the GenMapp program. This program tested if DEGs are significantly over-represented within a list of genes involved in a known particular biological process or pathway. We observed that the detected DEGs were significantly over-represented in the gene list of apoptosis, protein ubiquitination and response to "pest, pathogen, and parasite", as defined by the software, with permutated *P*-values of 0.017, <0.001, and <0.001, respectively. In the detailed analysis of response to pest, pathogen and parasite, the response to virus, inflammatory response, and detection of pest, pathogen and parasite, were significant (*P*-values<0.001, 0.004, and <0.001 respectively). These results suggested that the differential gene expression between leaderless and WT FMDV infection reflects mechanisms that are known to relate to evasion of the cellular innate immune response to virus infection.

Table 3
Significantly over-represented transcription factor binding sites in DEGs. Promoter sequences were analyzed using OTFBS software.

Bovine promoter sequences					
Matrix[a]	Transcription factor binding site	Transcription factor	Threshold	Hits	*P*-value
M00253	V$CAP_01	Cap signal for transcription initiation	0.98	74	2.04E−06
M00258	V$ISRE_01	ISGF3G	0.85	33	3.66E−18
M00062	V$IRF1_01	IRF-1	0.83	34	1.72E−09
M00063	V$IRF2_01	IRF-2	0.77	79	2.10E−09
M00194	V$NFKB_Q6	NF-kappaB	0.77	137	1.04E−08
M00054	V$NFKAPPAB_01	NF-kappaB	0.87	37	1.25E−06
M00053	V$CREL_01	c-Rel	0.82	124	5.92E−05
Human promoter sequences					
Matrix[a]	Transcription factor binding site	Transcription factor	Threshold	Hits	P-value
M00194	V$NFKB_Q6	NF-kappaB	0.77	110	3.74E−07
M00258	V$ISRE_01	ISGF3G	0.91	11	5.38E−09

[a] Matrix: different combinations of nucleotide sequences that can be recognized by specific transcription factors.

Differential gene expression in EBK cells infected with leaderless or SAP mutant FMDV in relation to WT FMDV

We have previously shown that leaderless virus grows more slowly than WT virus in secondary bovine cells (Chinsangaram et al., 1999). Indeed, inclusion of FMDV probes in the microarray allowed us to determine that by 4 hpi there was an average of 8 fold more viral RNA in WT as compared to leaderless virus infected EBK cells. Furthermore, relative quantitation of the viral RNA by qRT-PCR yielded a 6.7 fold higher level for WT as compared to leaderless virus infected cells confirming the microarray result (Table 2). To verify that the differential gene expression between WT and leaderless virus was not simply due to the significant differences in the amount of viral RNA present during the infection, we used a recently identified mutant of FMDV, SAP, that has point mutations in the L^{pro} coding region; the SAP mutant is defective in inducing NF-κB degradation but not in cleaving eIF4G and can grow better than leaderless virus in cell culture (de los Santos et al., 2009). The differential gene expression for the SAP mutant with respect to WT virus was determined and a control with leaderless vs WT was run at the same time (Table 6). The relative average fold induction of the 39 DEGs for the SAP mutant with respect to WT was 3.05 as compared to 2.56 for leaderless with respect to WT. Statistical analysis showed high correlation between the two data sets with a correlation coefficient value of 0.92 (*P*<0.0001) indicating that there were no significant differences between the samples (SAP vs WT compared to leaderless vs WT). Comparison of the viral RNA levels in this microarray indicated that there was only 1.56 fold more RNA in WT as compared to SAP mutant virus infected cells, while there was 5.36 fold more RNA in WT as compared to leaderless virus infected cells. Analysis of viral RNA by qRT-PCR indicated relative values of 2.44 and 6.81 respectively. In sum, cells infected with the SAP mutant had similar gene expression profiles as cells infected with leaderless virus despite the presence of about 3 times more FMDV RNA by 4 hpi.

Discussion

Previously, we have observed that the induction of transcription of IFN-β and some ISGs was significantly higher in porcine cells infected with leaderless as compared to WT FMDV (de los Santos et al., 2006). In this study, using microarray technology, we have analyzed 43,803 gene probes representing approximately 22,000 genes, to determine the differences in host gene expression in bovine cells infected with leaderless or WT FMDV. We took samples at 4 hpi because we wanted to examine early responses that could provide information about primary effects on host transcription. Within the limitations of our system, e.g. 5% of the bovine genome was not covered by the microarray and an arbitrary cut off set at 2 fold, we found that 39 genes were significantly and differentially up-regulated in leaderless as compared to WT FMDV infected cells and no significant differential gene down-regulation was observed. Confirmation of some of these results by qRT-PCR showed higher sensitivity, suggesting that more

Table 4
Number of transcription factor binding sites in the regulatory regions of DEGs, average microarray signal intensity and relative fold changes.

Genes	ISRE[a,b]	IRF1[a,c]	IRF2[a,d]	c-Rel[a,e]	NFKAPPAB [a,f]	NFKB[a,g]	Intensity	Fold change
IFIT2	4	4	6	5	2	3	334	11.5
RSAD2	2	2	3	1	0	2	404	8.1
PMAIP1	2	1	2	6	0	2	138	7.1
ISG15	6	6	4	4	1	1	2504	6.9
CXCL3	0	1	1	5	2	3	112	4.7
SAT1	0	0	1	2	1	5	153	4.5
IL28B	2	3	3	4	1	2	110	3.8
OAS1	2	3	4	4	1	1	1013	3.8
GTF2B	1	0	1	4	2	2	435	3.4
USP18	0	2	3	3	1	1	476	3.4
CCL2	0	0	4	1	0	3	1313	3.4
SOCS1	1	2	2	4	1	1	93	3.3
PARP14	0	0	0	2	1	3	188	3.1
C6orf150	0	1	3	2	0	1	79	3.0
NFKBIA	0	0	2	8	4	7	585	2.9
IFI6	4	3	6	3	2	2	78	2.9
DTX3L	2	2	2	4	1	5	710	2.7
FBXO33	0	0	2	3	0	2	377	2.6
MX1	2	1	2	3	2	5	465	2.6
GBP1	1	0	0	0	0	0	535	2.6
UBE1L	0	0	2	1	1	2	476	2.5
ZNFX1	1	1	3	6	3	6	304	2.5
LGP2	0	1	0	2	1	4	108	2.5
TREX1	0	0	0	2	2	2	94	2.5
SERTAD1	0	0	2	0	0	1	192	2.5
ATF3	0	0	0	2	0	5	845	2.2
ISGF3G	0	0	3	1	0	4	1030	2.1
IER3	0	0	0	2	1	3	195	2.1
IRF8	0	0	0	2	1	3	155	2.1
DSCR1	0	1	2	3	1	2	858	2.1
SLC25A28	1	1	1	0	0	0	95	2.0
EIF4E	1	1	1	0	0	0	189	2.0
ZC3HAV1	1	0	1	3	1	2	225	2.0
FAM46A	0	0	1	3	0	4	227	2.0
MARCKSL1	0	2	4	0	0	2	153	2.0

[a] Transcription binding sites are spelled as in the database according to the matrices numbers.
[b] M00258.
[c] M00062.
[d] M00063.
[e] M00053.
[f] M00054.
[g] M00194.

genes could be up-regulated by 2 fold or more, nevertheless we considered that our sample was large enough for further analysis to determine if a global control mechanism was involved. Most of the up-regulated genes in leaderless virus infected cells are implicated in the innate immune response to pathogen infection. More importantly, the data suggests that the presence of L^{pro} correlates with a block in

Table 5
Over-represented transcription factor binding sites in the promoter regions of DEGs calculated with CARRIE.

Pattern[a]	*P*-value	Name	Pattern	*P*-value	Name
M00051	3.46E−35	NF-kappaB (p50)	M00514	2.14E−06	Activating transcription factor 4
M00803	4.66E−29	E2F	M00695	2.94E−06	ETF
M00054	1.53E−27	NF-kappaB	M00106	4.53E−06	Cut-like homeodomain protein
M00208	1.32E−23	NF-kappaB binding site	M00322	4.53E−06	c-Myc/Max binding sites
M00194	1.34E−23	NF-kappaB	M00699	5.56E−06	ICSBP
M00052	2.67E−22	NF-kappaB (p65)	M00114	1.04E−05	Tax/CREB complex
M00716	3.91E−21	ZF5	M00199	1.31E−05	AP-1 binding site
M00774	8.83E−21	NF-kappaB	M00037	1.32E−05	NF-E2 p45
M00189	1.15E−13	Activator protein 2	M00232	2.54E−05	Myogenic MADS factor MEF-2
M00196	5.44E−13	Stimulating protein 1	M00720	2.90E−05	CAC-binding protein
M00469	7.55E−13	AP-2α	M00684	3.06E−05	XPF-1
M00800	2.73E−12	AP-2	M00332	3.21E−05	Winged-helix factor nude
M00324	1.52E−11	Muscle initiator sequence-20	M00650	3.74E−05	MTF-1
M00652	2.27E−11	Nrf-1	M00480	4.32E−05	LUN-1
M00053	4.18E−11	c-Rel	M00772	4.34E−05	IRF
M00256	6.58E−10	Neuron-restrictive silencer factor	M00619	5.31E−05	Alx-4
M00470	8.27E−10	AP-2γ	M00083	5.81E−05	MZF1
M00321	2.17E−09	Muscle initiator	M00258	6.01E−05	ISRE
M00257	3.52E−07	Ras-responsive element binding protein 1	M00104	7.99E−05	Cut-like homeodomain protein
M00255	6.36E−07	GC box elements	M00025	8.71E−05	Elk-1
M00323	8.87E−07	Muscle initiator sequences-19	M00797	8.71E−05	Hypoxia induced factor
M00721	1.01E−06	CACCC-binding factor			

[a] Equivalent to matrix numbers: different combinations of nucleotide sequences that can be recognized by specific transcription factors.

Table 6
Gene expression profiles in EBK cells infected with SAP or leaderless relative to WT FMDV.

Gene[a]	SAP[b]	LLV[c]	Gene	SAP	LLV	Gene	SAP	LLV
IFIT2	9.8	8.9	NFKBIA	3.0	3.5	ZNFX1	2.0	1.5
RSAD2	8.9	5.8	ZC3HAV1	3.0	2.4	UBE1L	2.0	1.7
BATF2	5.4	4.1	OAS1	2.9	1.9	ZFP36	1.9	2.3
ISG15	5.0	4.3	DTX3L	2.7	1.8	PARP14	1.9	1.4
IL28B	4.8	7.3	CXCL3	2.5	2.3	MARCKSL1	1.9	1.7
SAT1	4.7	5.1	GBP1	2.4	1.6	ATF3	1.8	2.2
PMAIP1	4.3	4.2	MX1	2.3	1.8	FBXO33	1.8	1.4
FAM46A	4.1	2.9	IFI6	2.3	1.9	SERTAD1	1.7	1.7
CCL2	3.7	3.4	C6orf150	2.2	1.7	DSCR1	1.6	1.5
USP18	3.6	2.3	TREX1	2.2	1.8	IRF8	1.5	1.2
SOCS1	3.5	3.6	ISGF3G	2.2	1.9	IER3	1.4	1.4
TCF7L1	3.3	2.3	GTF2B	2.1	1.9	EIF4E	1.4	1.2
CX3CL1	3.2	1.8	LGP2	2.1	1.6	SLC25A28	1.4	1.2

[a] Gene name abbreviation.
[b] Relative gene expression in SAP vs WT FMDV (Cy3 labeled SAP vs Cy5 labeled WT).
[c] Relative gene expression in leaderless (LLV) vs WT FMDV (Cy3 labeled LLV vs Cy5 labeled WT).

the induction of host transcription, primarily dependent on the ubiquitous transcription factor NF-κB and possibly the IFN induced transcription factor ISGF3G, also known as IRF9.

Among the DEGs in leaderless vs WT FMDV infection, the highest difference, 11.5 fold, was observed for IFIT2 (ISG54). The product of IFIT2 is a protein that binds eIF3 and blocks translation (Terenzi et al., 2006). Interestingly, one of the best characterized functions of FMDV L^{pro} is its ability to cleave the translation initiation factor eIF4G resulting in the shut off of host cap-dependent translation without affecting the viral IRES dependent translation (Devaney et al., 1988). Since eIF3 is required for both, cellular and viral translation, it is possible that WT FMDV may benefit from decreasing the levels of IFIT2 therefore reducing its inhibitory effect on eIF3. We also found that eIF4E, a translation factor required for binding the 7 methyl-guanosine cap of cellular RNAs (Rychlik et al., 1987), was expressed at two-fold higher levels in leaderless infected cells as compared to WT infected cells; likewise, a decreased amount of eIF4E may contribute to the reduction of host cap-dependent translation observed during FMDV infection.

Another group of genes up-regulated in leaderless vs WT virus infected cells, included those involved in post-translational protein modification and among them, ISG15, an ubiquitin-like modifier whose expression rapidly increases after IFN treatment or viral infection (Haas et al., 1987). Recent studies have shown that, in vivo, ISG15 functions as a critical antiviral molecule against influenza, herpes and Sindbis viruses (Lenschow et al., 2007) although the mechanism of action still remains unclear. Moreover, ISG15 has been reported as an important factor for dendritic cell (DC) maturation (Padovan et al., 2002).

We also identified some cytokines/chemokines with higher levels of expression in leaderless vs WT virus infected cells. Because the IFN-β gene probe was not present in the microarray, we tested its expression by qRT-PCR. Similar to our earlier studies, infection of primary EBK cells showed that leaderless virus was a more potent inducer of IFN-β transcription as compared to WT virus (de los Santos et al., 2006, 2007) indicating that, L^{pro} blocks expression of IFN-β. Interestingly, expression of a bovine gene homologous to a recently discovered cytokine, IL28B (Kotenko et al., 2003; Sheppard et al., 2003), reached higher levels upon infection with leaderless as compared to WT virus. This cytokine has been classified as a new member of the IFN gene family, type III IFN, and has antiviral activity against a selected group of viruses (Ank et al., 2006). Higher levels of mRNA for the chemokines CCL2, CXCL3 and CX3CL1 were also detected in leaderless virus infected cells. Our group has observed that treatment of swine with type I and type II IFNs induces expression of CCL2, which may be involved in conferring cell-mediated protection against FMDV (Diaz-San Segundo et al., 2010).

L^{pro} also inhibited the expression of other genes with known antiviral properties including OAS1 and Mx1. Since selective up-regulation of PKR was not detected by the microarray, we measured it by qRT-PCR and observed a modest selective up-regulation in the expression (2.3 fold). Both PKR and OAS/RNase L have been shown to inhibit FMDV replication (Chinsangaram et al., 2001, de los Santos et al., 2006).

Increased expression of a group of genes that are inducers of apoptosis, PMAIP1, SAT1, NF-κB1A, UBE1L, PARP14, TCF7L1, IER3 and IFI6, in leaderless infected cells suggests that WT FMDV might have an anti-apoptotic effect. However, the role of apoptosis during FMDV infection is controversial; although some investigators have found that FMDV induces apoptosis (Jin et al., 2007; Peng et al., 2004), others have shown no effect either in vitro or in infected animals (Díaz-San Segundo et al., 2006; de los Santos et al., 2007).

Our analysis of the promoter regions in genes differentially expressed between WT and leaderless FMDV infected cells shows a significant over-representation of binding sites for several transcription factors including NF-κB, ISGF3G, IRF1 and IRF2 that are involved in the innate immune response, suggesting that these transcription factors are responsible for the differential expression. We have previously demonstrated that NF-κB dependent gene induction is lower in WT than in leaderless virus infected cells (de los Santos et al., 2007, 2009). Our results on promoter sequence analysis show that the binding motif sequences for NF-κB are the most over-represented in the promoter sequence of the detected DEGs and the binding sites of NF-κB were also found in the promoter sequences of ISGF3G and IRFs. Moreover, relative quantitation of IFN-β by qRT-PCR whose transcription depends on the transcription factors NF-κB, IRFs and AP1 (Thanos and Maniatis, 1995; Honda et al., 2006), detected 50 fold more RNA in leaderless vs WT infected cells, consistent with our previous observations. Based on these results we propose that NF-κB is the primary effector of the differential gene expression observed by infection with leaderless vs WT FMDV.

It is possible that this response is mainly triggered by higher amounts of IFN protein in the culture media of leaderless as compared to WT virus infected cells. However, we have been unable to detect any difference in the amount of IFN protein in the supernatants of cells infected with WT or leaderless virus by 4 hpi although differences are detectable at later times, e.g. 16–24 hpi (Chinsangaram et al., 1999; de los Santos et al., 2006, 2009). Type I and type III IFN proteins induce transcription of ISGs through the binding of the STATs/ISGF3G protein complexes to ISRE elements contained within regulatory elements of promoter regions (Stark et al., 1998). In fact, we detected ISRE elements over-represented in the promoter analyses but not at a frequency as high as NF-κB sites (Table 4). Furthermore, up-regulation of several genes which do not contain ISREs in their promoters or whose transcription depends directly on viral infection, suggests that this effect might be secondary to the effect of NF-κB or other IRFs (e.g. IRF3) that do not require IFN protein for activation (Thanos and Maniatis, 1995; Onoguchi et al., 2007; Osterlund et al., 2007).

It is important to consider the differences of growth kinetics of leaderless virus as compared to WT virus at the time of sampling. The array data for FMDV probes showed that by 4 hpi, there was approximately an 8 fold higher level of viral RNA in WT as compared to leaderless virus infected cells, even when the same number of cells is infected based on an infectious center assay (Chinsangaram et al., 1999). To address this issue we utilized a virus that contains mutations in L^{pro} (SAP mutant virus). The SAP mutant does not induce degradation of NF-κB and grows to higher titers than leaderless virus, inducing transcription of IFN-β to similar or sometimes higher levels than the leaderless virus (de los Santos et al., 2009). Microarray analysis showed that infection with SAP mutant virus resulted in

essentially the same pattern of differential gene expression as leaderless virus with respect to WT virus with a correlation coefficient of 0.92, even though the level of FMDV RNA in SAP virus infected cells was about 3 fold higher than the level of RNA in leaderless virus infected cells. These results suggest that the differential pattern of gene expression in leaderless vs WT virus infected cells may reflect the inability of leaderless virus to cause NF-κB degradation instead of the reduced expression of other viral proteins. Moreover, the actual difference in protein expression of DEGs is probably greater than gene expression in leaderless as compared to WT virus infection considering the inhibition of cellular translation by L^{pro}.

In summary, our microarray data analysis suggests that the majority of the genes differentially expressed in cells infected with FMDV WT vs leaderless or SAP mutants, are involved in the innate immune response. Above all, NF-κB is the primary factor responsible for the differential transcription. These results support our earlier experimental work which demonstrated that L^{pro} dependent degradation of NF-κB contributes to FMDV evasion of the immune response.

Materials and methods

Cells and viruses

Primary EBK cells were provided by the Animal, Plant, and Health Inspection Service, National Veterinary Service Laboratory, Ames, Iowa. These cells were maintained in minimal essential medium (MEM, GIBCO BRL, Invitrogen, Carlsbad, CA) containing 10% fetal bovine serum and supplemented with 1% antibiotics and non-essential amino acids. BHK-21 cells (baby hamster kidney cells strain 21, clone 13, ATCC CL10), obtained from the American Type Culture Collection (ATCC, Rockville, MD) were maintained in MEM containing 10% calf serum and 10% tryptose phosphate broth supplemented with 1% antibiotics and non-essential amino acids and used to propagate virus stocks and measure virus titers. Cell cultures were incubated at 37 °C in 5% CO_2. FMDV A12-WT virus was generated from the full-length serotype A12 infectious clone, pRMC35 (Rieder et al., 1993), FMDV A12-LLV2 (leaderless virus) was derived from the infectious clone lacking the Lb coding region, pRM-LLV2 (Piccone et al., 1995) and FMDV A12#49 (SAP mutant) was derived from the infectious clone containing I55A and L58A mutations in the Lb coding region (de los Santos et al., 2009).

FMDV infections

Primary EBK cell cultures were infected with FMDV at an MOI of 10 for 30 min at 4 °C followed by 30 min at 37 °C. After adsorption, cells were rinsed twice and incubated with MEM at 37 °C for 2, 4 and 6 h. At the end of the incubation period, cells were rinsed with PBS and lysed in RLT buffer (Qiagen, Valencia, CA) for RNA extraction. Mock-infected control cells were treated identically. Four independent experiments using different lots of EBK cells were performed.

RNA isolation

Total RNA was isolated using an RNeasy isolation kit (Qiagen) following the manufacturer's directions. RNA yield and quality was determined in a NanoDrop 1000 spectrophotometer (Thermo Fisher, Walthman, MA) and in a 2000 Bioanalyzer (Agilent Technologies, Santa Clara, CA).

DNA microarray design

All bovine expressed sequence tags (ESTs) and RNA sequences were downloaded from the National Center for Biotechnology Information (NCBI) database and assembled into unique sequences using CAP3 software (Huang and Madan, 1999). The assembled sequences were aligned with the bovine genome sequences and displayed on the University of California Santa Clara (UCSC) genome browser (Karolchik et al., 2003). Non-redundant bovine expressed sequences including predicted gene sequences with homology to genes of other species but without EST or RNA information were selected for probe design. RepeatMasker software (http://www.repeatmasker.org) was used to avoid repetitive DNA sequences in the probe design. The probe sequences were designed with bias towards the 3′-end of RNA sequences to increase signal intensity obtained with labeling chemistry using poly-T priming. A custom bovine whole genome expression microarray with 43,803 60-oligonucleotide sense probes was designed with Array Designer 4.0 software (Applied Biosystems, Foster City, CA). The annotation of the bovine microarray was based on the results of BLAST (NCBI) against human reference proteins/RNAs and non-reference RNAs and manual curation was based on the probe sequence locations in the bovine genome sequence and genetic information displayed on the UCSC genome browser. The custom designed bovine microarrays were manufactured by Agilent Technologies (Santa Clara, CA).

Microarray analysis

For the microarray analysis of leaderless vs WT, total RNA prepared from virus- or mock-infected samples was labeled using Agilent low-input RNA labeling kit following the manufacturer's directions (Agilent Technologies). RNA extracted from infected cells was labeled with Cy5, and RNA extracted from mock-infected samples was labeled with Cy3. Cy3-labeled RNA from mock-infected control was co-hybridized with a Cy5-labeled RNA sample derived from WT or leaderless virus infected samples per array. For the microarray analysis of SAP vs WT, total RNA isolated from infected cells was labeled with Cy3 for the SAP mutant (or leaderless virus run in a parallel control experiment) and with Cy5 for the WT, as indicated earlier. Cy3-labeled RNA from SAP (or leaderless) infected cells was co-hybridized with Cy5-labeled RNA from WT infected cells. The entire procedure of microarray analysis was conducted according to protocols provided by Agilent Technologies. Array slides were scanned using a GenePix 4000B scanner and GenePix Pro 6 program (Molecular Devices Sunnyvale, CA) at 10 μm resolution with a spot diameter of approximately 100 μm.

Data analysis

The expression data were extracted and filtered based on feature quality and signal intensity with criteria recommended in GenPix Pro 6.0 program (Molecular Devices). Data were imported into a SQL database created with Microsoft SQL Server 2000 (Microsoft, Redmond, WA) and normalized with the LOWESS program implemented in Acuity® 4.0 Enterprise Microarray Informatics software (Molecular Devices). After normalization, only the features that passed quality check in all four samples (WT, leaderless, SAP and mock-infected) were included in the following analysis: Log ratios, Log2 (infected/mock-infected), were calculated for *t*-test statistical analysis and *P*-value correction for multiple statistical tests was conducted using false discovery rate (*Q*-value) calculated with EDGE program (Leek et al., 2006). Significant differential gene expression between leaderless and WT virus infected cultures was determined at the false discovery rate of 0.20 with |Log ratio| equal to or greater than 1 (equivalent to a 2 fold difference).

The transcription regulatory sequences (600 base pairs upstream of the promoters) of differentially expressed genes were extracted from the bovine genome sequence based on both, NNPP software (Reese, 2001) and the 5′-end of expressed sequences if available. Over-represented cis-elements or transcription factor binding sites in the regulatory sequences were identified and analyzed with the

OTFBS program (Zheng et al., 2003) to infer the transcription factors involved in the differential expression. This program compares selected regulatory DNA sequences to default random sequences based on statistical analysis for over-representation. For comparison, human promoter sequences of genes with differential expression were downloaded from PromoSer database (Halees et al., 2003) and analyzed with the same software. For inferential statistics, correlation between the number of transcription factor binding sites and signal intensity, fold change, and impact factor (product of signal intensity and fold change) were determined and analyzed with the SAS program (SAS Institute Inc., Cary, NC). Significant correlations were declared for P-values ≤ 0.05.

Analysis of transcription regulatory network involved in differential expression was performed with CARRIE software (Haverty et al., 2004). Because a bovine promoter database is not available, the entire set of human promoter sequences was downloaded from PromoSer database and used for the analysis except that human promoter sequences of the differentially expressed genes detected in this experiment were substituted with corresponding bovine promoter sequences identified as stated earlier. This program is a computational method that analyzes microarray data including signal intensity, fold changes, and promoter sequence data to infer a transcriptional regulatory network from the response to a specific stimulus. The promoter sequences of genes with least differences between the treatments were selected by the program based on the microarray data as the control sequences for the statistical analysis of over-representation of transcription binding sites. P-values were adjusted with the option provided in the program to account for multiple statistical tests in one experimental project. To identify biological processes affected by the differential expression, GenMAPP 2 software (Salomonis et al., 2007) was applied for statistical analysis.

Analysis of mRNA by polymerase chain reaction (PCR)

A quantitative (real-time) reverse transcription PCR (qRT-PCR) assay was used to confirm results obtained with the microarray. Standard procedures were followed (de los Santos et al., 2007). Eight genes with different fold change were selected for the test, including IFN-β which was not included in the microarray and PKR which was only induced 1.8 fold, both previously reported to be affected by FMDV infection (de los Santos et al., 2006). La35 with unchanged expression in the microarray was included as a control. The sequences of primers and probes are listed in Supplementary Table 4.

Acknowledgments

This research was supported in part by the Plum Island Animal Disease Research Participation Program administered by the Oak Ridge Institute for Science and Education through an interagency agreement between the U.S. Department of Energy and the U.S. Department of Agriculture (appointment of Marcelo Weiss), by CRIS project number 1940-32000-052-00D, ARS, USDA (J. Zhu, M. J. Grubman and T. de los Santos) and by reimbursable agreement #60-1940-7-47 with the Department of Homeland Security. We thank Dr. Fayna Diaz-San Segundo for critical reading of the manuscript.

Appendix A. Supplementary data

Supplementary data associated with this article can be found, in the online version, at doi:10.1016/j.virol.2010.04.021.

References

Amé, J.-C., Spenlehauer, C., de Murcia, G., 2004. The PARP superfamily. Bioassays 8, 882–893.

Ank, N., West, H., Bartholdy, C., Eriksson, K., Thomsen, A.R., Paludan, S.R., 2006. Lambda interferon (IFN-λ), a type III IFN, is induced by viruses and IFNs and displays potent antiviral activity against select virus infections in vivo. J. Virol. 80, 4501–4509.

Babbar, N., Hacker, A., Huang, Y., Casero Jr., R.A., 2006. Tumor necrosis factor alpha induces spermidine/spermine N1-acetyltransferase through nuclear factor kappa B in non-small cell lung cancer cells. J. Biol. Chem. 281, 24182–24192.

Bazan, J.F., Bacon, K.B., Hardiman, G., Wang, W., Soo, K., Rossi, D., Greaves, D.R., Zlotnik, A., Schall, T.J., 1997. A new class of membrane-bound chemokine with a CX3C motif. Nature 385, 640–644.

Brown, C.C., Piccone, M.E., Mason, P.W., McKenna, T.S., Grubman, M.J., 1996. Pathogenesis of wild-type and leaderless foot-and-mouth disease virus in cattle. J. Virol. 70, 5638–5641.

Carr, M.W., Roth, S.J., Luther, E., Rose, S.S., Springer, T.A., 1994. Monocyte chemoattractant protein 1 acts as a T-lymphocyte chemoattractant. Proc. Natl Acad. Sci. USA 91, 3652–3656.

Chin, K.C., Cresswell, P., 2001. Viperin (cig5), an IFN-inducible antiviral protein directly induced by human cytomegalovirus. Proc. Natl Acad. Sci. USA 98, 15125–15130.

Chinsangaram, J., Mason, P.W., Grubman, M.J., 1998. Protection of swine by live and inactivated vaccines prepared from a leader proteinase-deficient serotype A12 foot-and-mouth disease virus. Vaccine 16, 1516–1522.

Chinsangaram, J., Koster, M., Grubman, M.J., 2001. Inhibition of L-deleted foot- and-mouth disease virus replication by alpha/beta interferon involves double-stranded RNA-dependent protein kinase. J. Virol. 75, 5498–5503.

Chinsangaram, J., Piccone, M.E., Grubman, M.J., 1999. Ability of foot-and-mouth disease virus to form plaques in cell culture is associated with suppression of alpha/beta interferon. J. Virol. 73, 9891–9898.

Chowdhury, D., Beresford, P.J., Zhu, P., Zhang, D., Sung, J.S., Demple, B., Perrino, F.W., Lieberman, J., 2006. The exonuclease TREX1 is in the SET complex and acts in concert with NM23-H1 to degrade DNA during granzyme A-mediated cell death. Mol. Cell. 23, 133–142.

de los Santos, T., de Avila Botton, S., Weiblen, R., Grubman, M.J., 2006. The leader proteinase of foot-and-mouth disease virus inhibits the induction of beta interferon mRNA and blocks the host innate immune response. J. Virol. 80, 1906–1914.

de los Santos, T., Diaz-San Segundo, F., Grubman, M.J., 2007. Degradation of nuclear factor kappa B during foot-and-mouth disease virus infection. J. Virol. 81.

de los Santos, T., Diaz-San Segundo, F., Zhu, J., Koster, M., Dias, C.C., Grubman, M.J., 2009. conserved domain in the leader proteinase of foot-and-mouth disease virus is required for proper subcellular localization and function. J. Virol. 83, 1800–1810.

Der, S.D., Zhou, A., Williams, B.R.G., Silverman, R.H., 1998. Identification of genesdifferentially regulated by interferon α, β or γ using oligonucleotide arrays. Proc. Natl Acad. Sci. USA 95, 15623–15628.

Devaney, M.A., Vakharia, V.N., Lloyd, R.E., Ehrenfeld, E., Grubman, M.J., 1988. Leader protein of foot-and-mouth disease virus is required for cleavage of the p220 component of the cap-binding protein complex. J. Virol. 62, 4407–4409.

de Veer, M.J., Holko, M., Frevel, M., Walker, E., Der, S., Paranjape, J.M., Silverman, R.H., Williams, B.R.G., 2001. Functional classification of interferon-stimulated genes identified using microarrays. J. Leukoc. Biol. 69, 912–920.

Diaz-San Segundo, F., Moraes, M.P., de los Santos, T., Dias, C.C.A., Grubman, M.J., 2010. Interferon-induced protection against foot-and-mouth disease virus correlates with enhanced tissue specific innate immune cell infiltration and interferon stimulated gene expression. J. Virol. 84, 2063–2077.

Díaz-San Segundo, F., Salguero, F.J., de Avila, A., de Marco, M.M., Sánchez-Martín, M.A., Sevilla, N., 2006. Selective lymphocyte depletion during the early stage of the immune response to foot-and-mouth disease virus infection in swine. J. Virol. 80, 2369–2379.

Franchini, C., Fontana, F., Minuzzo, M., Babbio, F., Privitera, E., 2006. Apoptosis promoted by up-regulation of TFPT (TCF3 fusion partner) appears p53 independent, cell type restricted and cell density influenced. Apoptosis 12, 2217–2224.

Gao, G., Guo, X., Goff, S.P., 2002. CCCH-type zinc finger protein inhibition. Science 297, 1703–1716.

Geiser, T., Dewald, B., Ehrengruber, M.U., Clark-Lewis, I., Baggiolini, M., 1993. The interleukin-8-related chemotactic cytokines GROa, GROB, and GROT activate human neutrophil and basophil leukocytes. J. Biol. Chem. 268 15419-15424 Gilmore T.D. 2008. www.NF-kB.org.

Ghosh, S.K., Kusari, J., Bandyopadhyay, S.K., Samanta, H., Kumar, R., Sen, G.C., 1991. Cloning, sequencing, and expression of two murine 2′-5′-oligoadenylate synthetases: structure-function relationships. J. Biol. Chem. 266, 15293–15299.

Grubman, M.J., Baxt, B., 2004. Foot-and-mouth disease. Clin. Microbiol. Rev. 17, 465–493.

Guenzi, E., Töpolt, K., Cornali, E., Lubeseder-Martellato, C., Jörg, A., Matzen, K., Zietz, C., Kremmer, E., Nappi, F., Schwemmle, M., Hohenadl, C., Barillari, G., Tschachler, E., Monini, P., Ensoli, B., Stürzl, M., 2001. The helical domain of GBP-1 mediates the inhibition of endothelial cell proliferation by inflammatory cytokines. EMBO J. 20, 5568–5577.

Haas, A.L., Ahrens, P., Bright, P.M., Ankel, H., 1987. Interferon induces a 15-kilodalton protein exhibiting marked homology to ubiquitin. J. Biol. Chem. 262, 11315–11323.

Halees, A.S., Leyfer, D., Weng, Z., 2003. PromoSer: A large-scale mammalian promoter and transcription start site identification service. Nucleic Acids Res. 31, 3554–3559.

Haller, O., Staeheli, P., Kochs, G., 2007. Interferon-induced Mx proteins in antiviral host defense. Biochimie 89, 812–818.

Haskill, S., Beg, A.A., Tompkins, S.M., Morris, J.S., Yurochko, A.D., Sampson Johannes, A., Mondal, K., Ralph, P., Baldwin Jr., A.S., 1991. Characterization of an immediate-early gene induced in adherent monocytes that encodes IκB-like activity. Cell 65, 1281–1299.

Haverty, P.M., Frith, M.C., Weng, Z., 2004. CARRIE web service: automated transcriptional regulatory network inference and interactive analysis. Nucleic Acids Res. 32 Web Server issue), W213-6.

Hayden, M.S., West, A.P., Ghosh, S., 2006. NF-κB and the immune response. Oncogene 25, 6758–676780.
Hayden, M.S., Ghosh, S., 2008. Shared principles in NF-κB signaling. Cell 132, 344–362.
Huang, X., Madan, A., 1999. CAP3: A DNA sequence assembly program. Genome Res. 9, 868–877.
Honda, K., Yanai, H., Takaoka, A., Taniguchi, T., 2006. Regulation of the type I IFN induction: a current view. Int. Immunol. 17, 1367–1378.
Jin, J., Cardozo, T., Lovering, R.C., Elledge, S.J., Pagano, M., Harper, J.W., 2004. Systematic analysis and nomenclature of mammalian F-box proteins. Genes Dev. 18, 2573–2580.
Jin, H., Xiao, C., Zhao, G., Du, X., Yu, Y., Kang, Y., Wang, B., 2007. Induction of immature dendritic cell apoptosis by foot and mouth disease virus is an integrin receptor mediated event before viral infection. J. Cell. Biochem. 102, 980–991.
Karolchik, D., Baertsch, R., Diekhans, M., Furey, T.S., Hinrichs, A., Lu, Y.T., Roskin, K.M., Schwartz, M., Sugnet, C.W., Thomas, D.J., Weber, R.J., Haussler, D., Kent, W.J., 2003. The UCSC genome browser database. Nucleic Acids Res. 31, 51–54.
Kirchweger, R., Ziegler, E., Lamphear, B.J., Waters, D., Liebig, H.D., Sommergruber, W., Sobrino, F., Hohenadl, C., Blaas, D., Rhoads, R.E., Skern, T., 1994. Foot-and-mouth disease virus leader proteinase: purification of the Lb form and determination of its cleavage site on eIF-4 gamma. J. Virol. 68, 5677–5684.
Kitareewan, S., Pitha-Rowe, I., Sekula, D., Lowrey, C.H., Nemeth, M.J., Golub, T.R., Freemantle, S.J., Dmitrovsky, E., 2002. UBE1L is a retinoid target that triggers PML/RARα degradation and apoptosis in acute promyelocytic leukemia. Proc. Natl Acad. Sci. USA 99, 3806–3811.
Kotenko, S.V., Gallagher, G., Baurin, V.V., Lewis-Antes, A., Shen, M., Shah, N.K., Langer, J.A., Sheikh, F., Dickensheets, H., Donnelly, R.P., 2003. IFN-λs mediate antiviral protection through a distinct class II cytokine receptor complex. Nat. Immunol. 4, 69–76.
Lai, W.S., Kennington, E.A., Blackshear, P.J., 2002. Interactions of CCCH-zinc finger proteins with mRNA. J. Biol. Chem. 27, 9606–9613.
Leek, J.T., Monsen, E., Dabney, A.R., Storey, J.D., 2006. EDGE: extraction and analysis of differential gene expression. Bioinformatics 22, 507–508.
Lenschow, D.J., Lai, C., Frias-Staheli, N., Giannakopoulos, N.V., Lutz, A., Wolff, T., Osiak, A., Levine, B., Schmidt, R.E., García-Sastre, A., Leib, D.A., Pekosz, A., Knobeloch, K.P., Horak, I., Virgin 4th, H.W., 2007. IFN-stimulated gene 15 functions as a critical antiviral molecule against influenza, herpes and Sindbis viruses. Proc. Natl Acad. Sci. USA 104, 1371–1376.
Li, F.Y., Nikali, K., Gregan, J., Leibiger, I., Leibiger, B., Schweyen, R., Larsson, C., Suomalainen, A., 2001. Characterization of a novel human putative mitochondrial transporter homologous to the yeast mitochondrial RNA splicing proteins 3 and 4. FEBS Lett. 494, 79–84.
Loeb, K.R., Haas, A.L., 1992. The interferon-inducible 15-kDa ubiquitin homolog conjugates to intracellular proteins. J. Biol. Chem. 267, 7806–7813.
Lu, D., Chen, J., Hai, T., 2007. he regulation of ATF3 gene expression by mitogen activated protein kinases. Biochem. J. 401, 559–567.
Malakhov, M.P., Malakhova, O.A., Kim, K.I., Ritchie, K.J., Zhang, D.-E., 2002. UBP43 (USP18) specifically removes ISG15 from conjugated proteins. J. Biol. Chem. 277, 9976–9981.
Mason, P.W., Piccone, M.E., McKenna, T.S., Chinsangaram, J., Grubman, M.J., 1997. Evaluation of a live-attenuated foot-and-mouth disease virus as a vaccine candidate. Virology 227, 96–102.
Mason, P.W., Grubman, M.J., Baxt, B., 2003. Molecular basis of pathogenesis of FMDV. Virus Res. 91, 9–32.
Oda, E., Ohki, R., Murasawa, H., Nemoto, J., Shibue, T., Yamashita, T., Tokino, T., Taniguchi, T., Tanaka, N., 2000. Noxa, a BH3-only member of the Bcl-2 family and candidate mediator of p53-induced apoptosis. Science 288, 1053–1058.
Onoguchi, K., Yoneyama, M., Takemura, A., Akira, S., Taniguchi, T., Namiki, H., Fujita, T., 2007. Viral infections activate Types I and III Interferon genes through a common mechanism. J. Biol. Chem. 282, 7576–7581.
Osterlund, P.I., Pietila, T.E., Veckman, V., Kotenko, S.V., Julkunen, I., 2007. IFN regulatory factor family members differentially regulate the expression of type III IFN (IFNlambda) genes. J. Immunol. 179, 3434–3442.
Padovan, E., Terracciano, L., Certa, U., Jacobs, B., Reschner, A., Bolli, M., Spagnoli, G.C., Borden, E.C., Heberer, M., 2002. Interferon stimulated gene 15 constitutively produced by melanoma cells induces e-cadherin expression on human dendritic cells. Cancer Res. 62, 3453–3458.
Peng, J.M., Liang, S.M., C.M., Liang, 2004. VP1 of foot-and-mouth disease virus induces apoptosis via the Akt signaling pathway. J. Biol. Chem. 279, 52168–52174.
Perrino, F.W., Miller, H., Ealey, K.A., 1994. Identification of a 3′→5′-exonuclease that removes cytosine arabinoside monophosphate from 3′ termini of DNA. J. Biol. Chem. 269, 16357–16363.
Piccone, M.E., Rieder, E., Mason, P.W., Grubman, M.J., 1995. The foot-and-mouth disease virus leader proteinase gene is not required for viral replication. J. Virol. 69, 5376–5382.
Prêle, C.M., Woodward, E.A., Bisley, J., Keith-Magee, A., Nicholson, S.E., Hart, P.H., 2008. SOCS1 regulates the IFN but not NFB pathway in TLR-stimulated human monocytes and macrophages. J. Immunol. 181, 8018–8026.
Reese, M.G., 2001. Application of a time-delay neural network to promoter annotation in the Drosophila melanogaster genome. Comput. Chem. 26, 51–56 HYPERLINK http://www.fruitfly.org/~martinr/index.html.
Reines, D., Conaway, J.W., Conaway, R.C., 1996. The RNA polymerase II general elongation factors. Trends Biochem. Sci. 21, 351–355.
Rieder, E., Bunch, T., Brown, F., Mason, P.W., 1993. Genetically engineered foot-and mouth disease viruses with poly(C) tracts of two nucleotides are virulent in mice. J. Virol. 67, 5139–5145.
Ryan, M.D., King, A.M., Thomas, G.P., 1991. Cleavage of foot-and mouth disease virus polyprotein is mediated by residues located within a 19 amino acid sequence. J. Gen. Virol. 72, 2727–2732.
Rychlik, W., Domier, L.L., Gardner, P.R., Hellmann, G.M., Rhoads, R.E., 1987. Amino acid sequence of the mRNA cap-binding protein from human tissues. Proc. Natl Acad. Sci. USA 84, 945–949.
Salomonis, N., Hanspers, K., Zambon, A.C., Vranizan, K., Lawlor, S.C., Dahlquist, K.D., Doniger, S.W., Stuart, J., Conklin, B.R., Pico, A.R., 2007. GenMAPP 2: new features and resources for pathway analysis. BMC Bioinform. 8, 217–229.
Sharf, R., Azriel, A., Lejbkowicz, F., Winograd, S.S., Ehrlich, R., Levi, B.Z., 1995. Functional domain analysis of interferon consensus sequence binding protein (ICSBP) and its association with interferon regulatory factors. J. Biol. Chem. 270, 13063–13069.
Sheppard, P., Kindsvogel, W., Xu, W., Henderson, K., Schlutsmeyer, S., Whitmore, T.E., Kuestner, R., Garrigues, U., Birks, C., Roraback, J., Ostrander, C., Dong, D., Shin, J., Presnell, S., Fox, B., Haldeman, B., Cooper, E., Taft, D., Gilbert, T., Grant, F.J., Tackett, M., Krivan, W., McKnight, G., Clegg, C., Foster, D., Klucher, K.M., 2003. IL-28, IL-29 and their class II cytokine receptor IL-28R. Nat. Immunol. 4, 63–68.
Stark, G.R., Kerr, I.M., Williams, B.R., Silverman, R.H., Schreiber, R.D., 1998. How cells respond to interferons. Annu. Rev. Biochem. 67, 227–264.
Strausberg, R.L., et al., 2002. Mammalian Gene Collection (MGC) Program Team. Generation and initial analysis of more than 15,000 full-length human and mouse cDNA sequencesProc. Natl Acad. Sci. USA 99, 16899–16903.
Strebel, K., Beck, E., 1986. A second protease of foot-and-mouth disease virus. J. Virol. 58, 893–899.
Sugimoto, M., Nakamura, T., Ohtani, N., Hampson, L., Hampson, I.N., Shimamoto, A., Furuichi, Y., Okumura, K., Niwa, S., Taya, Y., Hara, E., 1999. Regulation of CDK4 activity by a novel CDK4-binding protein, p34 (SEI-1). Genes Dev. 13, 3027–3033.
Tahara Jr, E., Tahara, H., Kanno, M., Naka, K., Takeda, Y., Matsuzaki, T., Yamazaki, R., Ishihara, H., Yasui, W., Barrett, J.C., Ide, T., Tahara, E., 2005. G1P3, an interferon inducible gene 6-16, is expressed in gastric cancers and inhibits mitochondrial-mediated apoptosis in gastric cancer cell line TMK-1 cell. Cancer Immunol. Immunother. 54, 729–740.
Takeyama, K., Aguiar, R.C., Gu, L., He, C., Freeman, G.J., Kutok, J.L., Aster, J.C., Shipp, M.A., 2003. The BAL-binding protein BBAP and related Deltex family members exhibit ubiquitin-protein isopeptide ligase activity. J. Biol. Chem. 278, 21930–21937.
Terenzi, F., Hui, D.J., Merrick, W.C., Sen, G.C., 2006. Distinct induction patterns and functions of two closely related interferon-inducible human genes, ISG54 and ISG56. J. Biol. Chem. 281, 34064–34071.
Thanos, D., Maniatis, T., 1995. Virus induction of human IFN-β gene expression requires the assembly of an enhanceosome. Cell 83, 1091–1100.
Veals, S.A., Schindler, C., Leonard, D., Fu, X.Y., Aebersold, R., Darnell Jr, J.E., Levy, D.E., 1992. Subunit of an alpha-interferon-responsive transcription factor is related to interferon regulatory factor and Myb families of DNA-binding proteins. Mol. Cell. Biol. 12, 3315–3324.
Verghese, G.M., Johnson, J.D., Vasulka, C., Haupt, D.M., Stumpo, D.J., Blackshear, P.J., 1994. Protein kinase C-mediated phosphorylation and calmodulin binding of recombinant myristoylated alanine-rich C kinase substrate (MARCKS) and MARCKS-related protein. J. Biol. Chem. 269, 9361–9367.
Wu, M.X., 2003. Roles of the stress-induced gene IEX-1 in regulation of cell death and oncogenesis. Apoptosis 8, 11–18.
Yamashita, M., Katsumata, M., Iwashima, M., Kimura, M., Shimizu, C., Kamata, T., Shin, T., Seki, N., Suzuki, S., Taniguchi, M., Nakayama, T., 2000. T cell receptor-induced calcineurin activation regulates T helper type 2 cell development by modifying the interleukin 4 receptor signaling complex. J. Exp. Med. 191, 1869–1879.
Yoneyama, M., Kikuchi, M., Matsumoto, K., Imaizumi, T., Miyagishi, M., Taira, K., Foy, E., Loo, Y.-M., Gale Jr, M., Akira, S., Yonehara, S., Kato, A., Fujita, T., 2005. Shared and unique functions of the DExD/H-box helicases RIG-I, MDA5, and LGP2 in antiviral innate immunity. J. Immunol. 175, 2851–2858.
Zheng, J., Wu, J., Sun, Z., 2003. An approach to identify over-represented cis-elements in related sequences. Nucleic Acids Res. 31, 1995–2005.

Return to Table of Contents

Preventive Veterinary Medicine 93 (2010) 258–264

Contents lists available at ScienceDirect

Preventive Veterinary Medicine

journal homepage: www.elsevier.com/locate/prevetmed

Spatial and phylogenetic analysis of vesicular stomatitis virus over-wintering in the United States

Andres M. Perez [a,b,*], Steven J. Pauszek [c], Daniel Jimenez [a], William N. Kelley [d], Zachary Whedbee [a], Luis L. Rodriguez [c]

[a] Center for Animal Diseases Modeling and Surveillance (CADMS), Department of Medicine and Epidemiology, School of Veterinary Medicine, University of California, Davis, CA 95616, USA
[b] CONICET and Fac. Ciencias Veterinarias UNR, Argentina
[c] United States Department of Agriculture (USDA), Agricultural Research Service (ARS), Foreign Animal Disease Research Unit, Plum Island Animal Disease Center, Orient, NY, USA
[d] United States Department of Agriculture (USDA), Animal and Plant Health Inspection Service (APHIS), Centers for Epidemiology and Animal Health (CEAH), Fort Collins, CO, USA

ARTICLE INFO

Keywords:
Vesicular stomatitis virus
Epidemiology
Over-wintering
Spatial clustering
Phylogeny

ABSTRACT

From 2004 through 2006, 751 vesicular stomatitis (VS) outbreaks caused by vesicular stomatitis virus serotype New Jersey (VSNJV) were reported in nine states of the southwestern United States. The normal model of the spatial scan statistic and phylogenetic techniques were used to assess whether the spatial and genetic relations among VSNJV outbreaks were consistent with the hypothesis that VSNJV over-wintered in specific regions of the southwestern United States infected in 2004 and 2005, respectively. Use of the spatial scan statistic led to the identification of two clusters of outbreaks for which the Euclidean distance to the nearest outbreak reported in the previous or following year, whichever was shorter, was significantly ($P < 0.01$) shorter than the epidemic's (2004–2006) mean. Clusters were centered at Colorado and Wyoming and included 375 and 21 outbreaks, respectively. Results were supported by the phylogenetic analysis of 49 VSV samples collected from 2004 through 2006 in the United States and 10 VSV samples originated from Mexico. These findings, which were displayed using a publicly accessible web-based system referred to as the FMD BioPortal, were consistent with over-wintering of specific sub-lineages of VSNJV in a limited geographical region of the United States affected by a VS epidemic in 2005 and 2006.

1. Introduction

Vesicular stomatitis (VS) is a zoonotic disease of horses, cattle, swine, and certain wild life species caused by a rhabdovirus referred to as vesicular stomatitis virus (VSV). Two VSV serotypes, New Jersey (VSNJV) and Indiana, are responsible for the endemic presentation of the disease from northern South America through to southern Mexico (Rodriguez and Nichol, 1999).

VS is typically associated with low mortality and morbidity levels, but in susceptible populations the infection can spread rapidly over wide geographical areas (Rodriguez, 2002). VSV infection in humans is rare and results in mild influenza-like symptoms. In susceptible domestic animals, clinical manifestation of VSV infection is characterized by the presence of blister lesions that are primarily located in nostrils, lips, oral mucosa, and tongue. Blister lesions can also occur in teats and in the coronary band of the hooves. The pain caused by the rupture of

* Corresponding author at: Center for Animal Diseases Modeling and Surveillance (CADMS), Department of Medicine and Epidemiology, School of Veterinary Medicine, University of California, Davis, CA 95616, USA. Tel.: +1 530 297 4621; fax: +1 530 297 4618.
E-mail address: amperez@ucdavis.edu (A.M. Perez).

0167-5877/$ – see front matter © 2009 Elsevier B.V. All rights reserved.
doi:10.1016/j.prevetmed.2009.11.003

vesicles often leads to the refusal of animals to eat, drink, and walk. Those signs may consequently cause weight loss and, in dairy cows, a severe drop in milk production. In addition to the potential zoonotic nature and direct economic impact of the disease, VS is important because its clinical signs in ruminants and pigs resemble those caused by foot-and-mouth disease (FMD) virus infection (Letchworth et al., 1999). Because FMD was eradicated from the United States more than 80 years ago, there is a reasonable concern that early signs of a potential FMD epidemic in the country may be erroneously confused with VS, leading to delays in diagnosis.

The southwestern United States has been incidentally affected by VSV epidemics during the last 100 years, with the last episodes being reported in 2004–2006 (Rainwater-Lovett et al., 2007). Previous studies suggest that VS epidemics in the southwestern United States are caused by genetically distinct VSV strains introduced from endemic areas of southern Mexico (Rodriguez, 2002; Rodriguez et al., 2000). VS epidemics typically follow a seasonal pattern in the southwestern United States and it is believed that the ability of the virus to over-winter explains the re-emergence of the disease frequently observed during the years that follow an initial introduction of the virus (Rodriguez, 2002). Mechanisms of VSV transmission are, however, not fully understood. Direct contact of susceptible animals with infected individuals or with fomites such as contaminated water, feed bunks, or milking machines seems to play a role in disease transmission. However, transmission between premises and over large geographical areas is believed to be mediated by certain species of insects, as suggested by the reduced risk for the disease observed in stabled animals and on farms that implement insect control programs (Hurd et al., 1999). Three insect species have been experimentally demonstrated to be biological vectors of VSNJV; *Simulium vittatum* (*Diptera: Simuliidae*) (Mead et al., 2004), *Lutzomyia trapidoi* (*Diptera: Psicodidae*) (Tesh et al., 1971) and *Culicoides sonorensis* (*Diptera: Ceratopogonidae*) (Perez de Leon and Tabachnick, 2006). In addition, VSNJV has been isolated from a variety of field-collected arthropods such as eye gnats (*Chloropidae spp.*), root-maggot flies (*Anthomyiidae spp.*), house flies (*Musca spp.*), biting midges (*Culicoides spp.*), black flies (*Simuliidae spp.*), sand flies (*Lutzomyia spp.*), and mosquitoes (*Aedes spp.*) (USAHA, 2008).

Insect-borne transmission may explain the seasonal pattern observed for VS epidemics in the southwestern United States. Trans-ovarian transmission, which has been suggested to occur in black flies (Mead et al., 2004) and sand flies (Tesh et al., 1972) could play a role in VS maintenance and spread in the region, specifically by potentially allowing over-wintering.

Spatial clustering and phylogenetic techniques were used in a web-based GIS framework to obtain evidence that the 2005 and 2006 VS outbreaks may have been associated with VSNJV over-wintering in certain regions of the United States affected by the disease in the previous year. Gaining knowledge on epidemiological aspects of VSV infection in the United States is important in order to develop effective prevention and control strategies for the disease. Moreover, such knowledge will also help to establish differences with the expected behavior of a potential FMD epidemic in the country.

2. Methods

2.1. Study population

From 2004 through 2006, 751 outbreaks caused by the VSNJV were reported in the United States' southwestern states of Arizona, Colorado, Idaho, Montana, Nebraska, New Mexico, Texas, Utah, and Wyoming (Table 1). All 751 outbreaks were confirmed by analysis of samples submitted to the national veterinary services laboratories (NVSL) at either Ames, IA, or Plum Island, NY.

Information on the geographic location (latitude, longitude) and susceptible species (bovine, equine, other) of the 751 VSNJV-infected premises was provided by the United States Department of Agriculture's Animal & Plant Health Inspection Service (APHIS). Infected premises were geo-located considering either the location of the front gate or the point where the private drive way intersects a public road. The system used to geo-locate the data was recorded for 460 (61.2%) outbreaks, from which 392 (85.2%), 42 (9.1%), and 26 (5.7%) were geo-located using global positioning system (GPS) receivers, by geo-coding the address, and by mapping or aerial photography interpolation, respectively. We have no reason to believe that missing information on the type of system used to geo-locate the outbreaks, or use of one system or another, was associated with any particular source of systematic error that may have introduced any kind of bias to the study. Moreover, most of the outbreaks (>85%) were geo-located using one single geo-location system, i.e., GPS receivers.

2.2. Identification of spatial clusters

The Euclidean distance (measured in km) to the nearest VSNJV outbreak reported in the previous or following year (d), whichever was shorter, was recorded for each of the 751 confirmed outbreaks. A variation of the spatial scan statistic, referred to as the normal model of the spatial scan statistic, was used to identify clusters

Table 1
Number of vesicular stomatitis outbreaks reported in the United States from 2004 through 2006, stratified by State and year of reporting.

State	Year			Total
	2004	2005	2006	
Arizona	0 [0]	27 [1]	0 [0]	27 [1]
Colorado	196 [18]	102 [2]	0 [0]	298 [20]
Idaho	0 [0]	2 [0]	0 [0]	2 [0]
Montana	0 [0]	46 [1]	0 [0]	46 [1]
Nebraska	0 [0]	3 [2]	0 [0]	3 [2]
New Mexico	80 [8]	23 [2]	0 [0]	103 [10]
Texas	16 [3]	0 [0]	0 [0]	16 [3]
Utah	0 [0]	105 [2]	0 [0]	105 [2]
Wyoming	0 [0]	138 [4]	13 [6]	151 [10]
Total	292 [29]	446 [14]	13 [6]	751 [49]

Numbers in brackets indicate the number of samples sequenced.

of outbreaks for which the value of d was shorter than the background value of d estimated for the whole region affected by the epidemic. The difference between the normal model of the spatial scan statistic and more traditional applications of the technique, such as the Bernoulli or Poisson models, is that the former is used to identify significant clusters of a continuous variable, rather than clusters of counts or rates. Because the parameter assessed here was measured as a continuous variable (d), use of the normal model of the spatial scan statistic was appropriate. A detailed description of this particular variation of the spatial scan statistic is available elsewhere (Kulldorff et al., 2009). As in any other application of the spatial scan statistic, circular windows of candidate clusters were sequentially placed over each infected premises with the size of window varying up to a maximum of 50% of the outbreaks (Kulldorff and Nagarwalla, 1995; Kulldorff et al., 1998). The mean value of d was computed for premises located within each candidate cluster c (d_c). The value of d_c was compared with the mean value of d estimated throughout the study region (d_m), so that the value of d_c is included for the computation of d_m; thus, d_m represents the null hypothesis of uniform distribution of d. Because this technique bases the detection of clusters on the computation of mean values for the variable of interest, results are sensitive to the presence of outliers in the dataset. No outliers were found in the dataset used here (Grubb's test, $P > 0.05$). A maximum cluster size of 50% of the outbreaks was selected because a larger cluster of outbreaks with a significant small value of d_c would likely be the reflection of significant high values of d outside the cluster rather than a true cluster of small values of d_c within the cluster (Kulldorff et al., 1998). The values of d observed at each location i (d_i) and their corresponding geo-locations were randomly permuted to create 999 data sets that represent random distributions of the values. For each candidate cluster, a log likelihood ratio was computed for the set of observed values of d (L_d) and for each of the 999 simulations (L_s). The value of L_d was compared with the 999 values of L_s to estimate the number of times (N) in which the condition $L_d > L_s$ was observed. The P-value of each candidate cluster c was subsequently computed as $N_c/(999 + 1)$. Clusters with a value of d_c significantly ($P < 0.05$) shorter than d_m were interpreted to represent geographical locations in which the probability of finding VSNJV outbreaks in consecutive years was significantly higher than expected under the null hypothesis of a homogenous probability distribution. Therefore, such clusters were considered geographical regions where VSNJV over-wintering was likely to occur. In the normal model of the spatial scan statistic it is possible to weight the values of the continuous variable to adjust for the uncertainty in true value of the parameter associated with each particular location. Because the variable of interest here (d) was computed from the data as a point estimate, no weighting factor was used in the analysis. The spatial scan statistic was run using SaTScan v. 8.0 (http://www.satscan.org) and the Grubb's test was computed using GraphPad Quickcalcs (http://www.graphpad.com/quickcalcs/index.cfm).

2.3. Genetic analysis

Fifty-nine VSNJV isolates were included in the phylogenetic analysis (Table 1). Although samples were collected from different States and at different periods of time, no formal random design was used for the sampling scheme. Ten of these isolates were isolated from Mexican outbreaks from 2000 through 2004, whereas the remaining 49 isolates were obtained from the southwestern United States (29 in 2004; 14 in 2005; 6 in 2006). Isolates collected from 2000 through 2005 ($n = 53$) have been described elsewhere (Rainwater-Lovett et al., 2007). The six VSNJV isolates collected in 2006 originated from Wyoming, the only state with confirmed infection in 2006, and were processed using previously described methods (Rainwater-Lovett et al., 2007). Briefly, viral RNA was extracted using the RNeasy Mini kit (Qiagen) and reverse transcribed with random hexamers and SuperScript II RNAse H reverse transcriptase (Invitrogen) as per the manufacturers' instructions. The hypervariable region of the phosphoprotein used in the phylogenetic analysis was amplified with Pfu DNA polymerase and the previously described primers NJP-102F and NJP-831R (Rodriguez et al., 1993). Single band products were confirmed visually on an agarose gel and purified using QIAquick PCR purification kits (Qiagen). PCR products were sequenced using a BigDye Terminator Sequencing kit on a 3730A automated sequencer (Applied Biosystems). Sequencher v4.1 software (GeneCodes) was used to analyze chromatograms and Clustal_X (Thompson et al., 1997) was used to create sequence alignments and a 450 nt region of the VSNJV phosphoprotein, commonly referred to as the hypervariable region, was used for phylogenetic analysis.

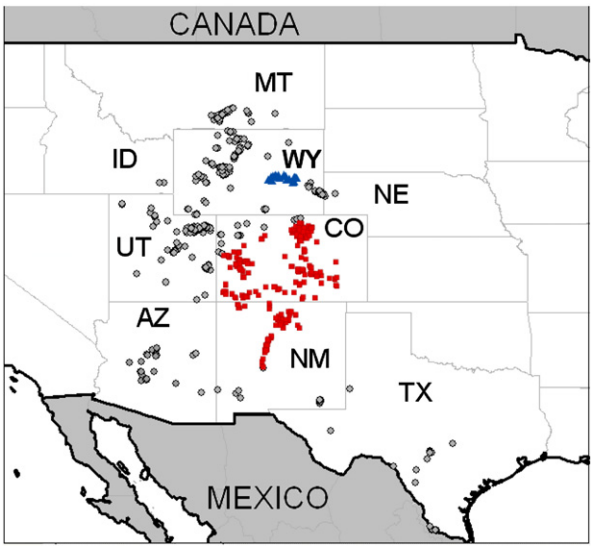

Fig. 1. Location of vesicular stomatitis virus outbreaks reported in the United States in 2004–2006. Triangles and squares indicate two clusters for which the distance to the nearest outbreak reported in the previous or following year, whichever was shorter, was significantly ($P < 0.01$) smaller than the epidemic's mean. Acronyms indicate the names of the States affected by the epidemic (AZ, Arizona; CO, Colorado; ID, Idaho; MT, Montana; NE, Nebraska; NM, New Mexico; TX, Texas; UT, Utah; WY, Wyoming).

Phylogenetic analysis was performed using the maximum-likelihood optimality criterion as implemented in PAUP* version β10 (Swofford, 1998). Parameters of nucleotide substitution were estimated using Modeltest, version 3.7 (Posada and Crandall, 1998). Sequences of the six isolates that were reported here for the first time were submitted to GenBank (Accession numbers: FJ595501–FJ595506). The associations between the spatial and phylogenetic clusters detected were assessed using Chi squared tests.

2.4. Visualization tools

A publicly accessible web-based system, referred to as the FMD BioPortal (https://fmdbioportal.ucdavis.edu/) was used to display the results of the spatial clustering and phylogenetic analyses. A description of the technical attributes and capabilities of the FMD BioPortal along with an illustration of its functionality has been presented elsewhere (Perez et al., 2009).

3. Results

Two clusters of VS outbreaks were identified with values of d_c significantly ($P < 0.01$) smaller than the country's mean value ($d_m = 136$ km) (Fig. 1). The average value of d_c was 2.47 times smaller than d_m in a cluster of 375 outbreaks reported in Colorado and New Mexico ($d_c = 54.8$ km; $SD_{dc} = 50.6$; $n = 375$). A cluster centered in Wyoming included 21 outbreaks for which the value of d_c

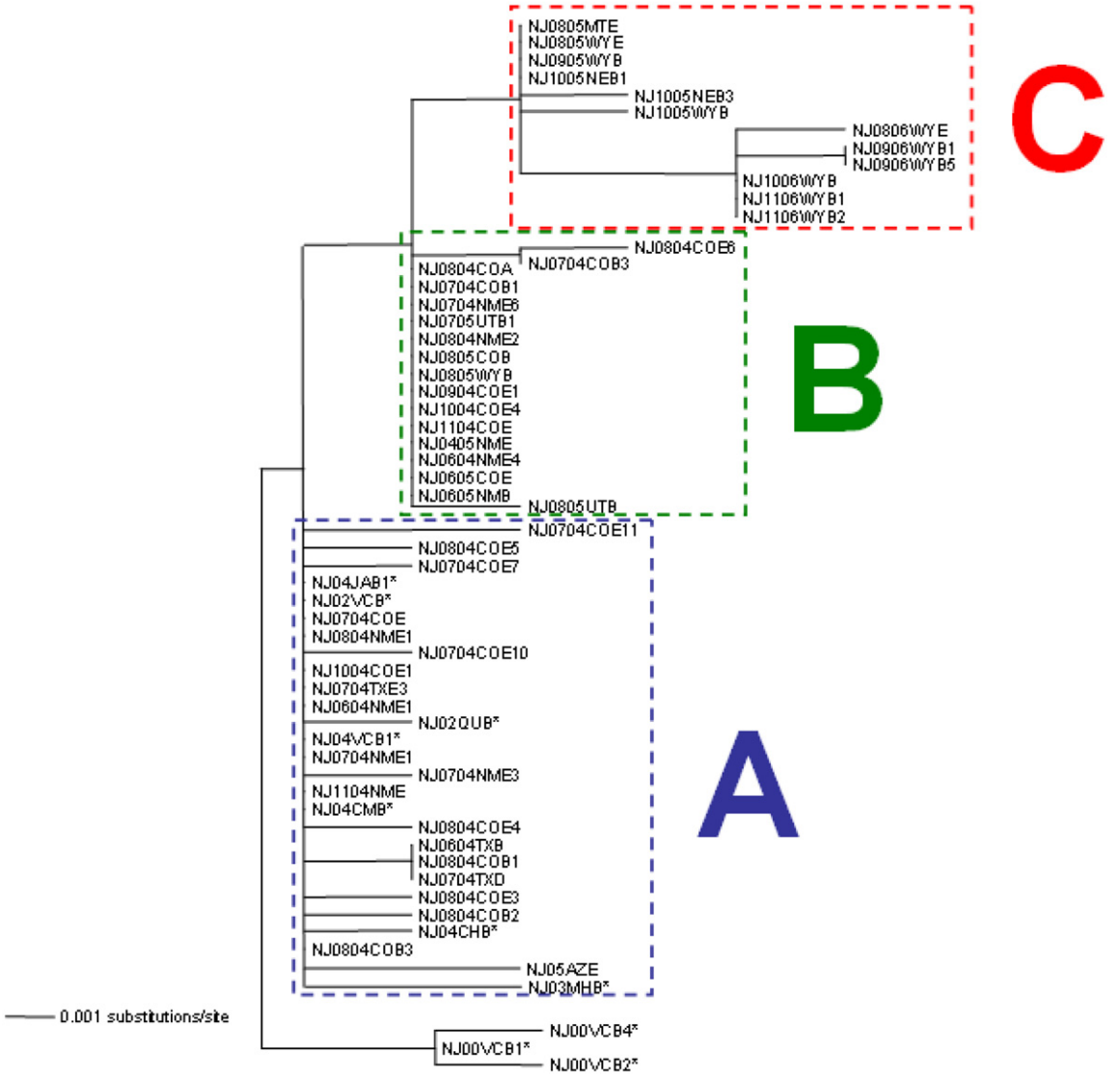

Fig. 2. Maximum-likelihood analysis of vesicular stomatitis viruses associated with outbreaks reported in the southwestern United States (2004–2006) and in Mexico (2000–2004). Sequence names indicate the serotype (NJ), the month (when available) and year of isolation, the United States (see Fig. 1 for reference) or Mexican (CH, Chihuahua; CM, Colima; JA, Jalisco; MH, Michoacan; QU, Queretaro; VC, Veracruz) state of origin, and the species affected (A, alpaca; B, bovine; D, donkey; E, equine). Mexican isolates are indicated by an (*). Groups indicate isolates from Mexico and from the United States in 2004 (A), and from the United States in 2004–2005 (B), and 2005–2006 (C).

was 11.3 times smaller than the value of d_m (d_c = 12.5 km; SD_{dc} = 7.8; n = 21).

Sequencing and phylogenetic analysis of 49 VSNJV United States isolates and 10 VSNJV Mexican isolates suggests the presence of at least three different groups of viruses. The first group comprised of 27 viruses, which included 19 and one United States viruses isolated in 2004 and 2005, respectively, and seven closely related viruses from Mexico isolated from 2002 through 2004. The sequences of four of the seven Mexican viruses were identical to those of isolates collected in Texas, Colorado, and New Mexico in 2004 (Fig. 2A). The second group included 10 isolates from 2004 and seven isolates from 2005 (Fig. 2B); 14 of those 17 isolates (82.4%) were part of the spatial cluster centered in Colorado and New Mexico (Fig. 1). The third group encompassed six isolates from 2005 and the six isolates from 2006 (Fig. 2C), from which nine (69.2%) were obtained from outbreaks located within the spatial cluster centered in Wyoming (Fig. 1). The second and third groups did not include viruses from Mexico. Associations between the cluster centered in Colorado and New Mexico and isolates from the first or second phylogenetic groups, and between the cluster centered in Wyoming and isolates from the second or third phylogenetic groups were significant (Fisher exact test, $P < 0.01$).

A video demonstration of these findings using the FMD BioPortal and including the simultaneous visualization of the geographical, temporal, and genetic relation of isolates is publicly accessible at (http://fmdbioportal.ucdavis.edu/vsv/demo.avi).

4. Discussion

Over-wintering has been proposed as a possible biological mechanism associated with the re-emergence of VSV during consecutive spring and summer seasons in the southwestern United States following initial introduction of the virus from endemic areas (Rainwater-Lovett et al., 2007). The study here presents results of the combined application of phylogenetic analysis and techniques for identification of spatial clustering. The results are consistent with the hypothesis that VSV-over-wintering was likely to occur in 2005 and in 2006 in two discrete geographical regions of the southwestern United States affected by the epidemic.

Two spatial clusters of outbreaks could be identified within which the average distance to previous or following year's outbreaks was significantly smaller than outside these clusters ($P < 0.01$) (Fig. 1). Spatial clusters of outbreaks that took place in consecutive years suggest the presence of ecological, epidemiological, or demographic factors or forces in the region that facilitate or promote disease infection or spread. One would expect that if over-wintering occurs, premises close to the place where the virus over-winters will be more likely to be infected during consecutive years than far-away located herds. Thus, the spatial clusters detected here may represent geographical locations where over-wintering is likely to occur. Note, however, that the estimates of spatial clustering detected here alone do not provide sufficient evidence that over-wintering has occurred in the region. Spatial clustering may also have resulted from a number of factors promoting the re-introduction of the virus into the region from endemic or infected zones, including, for example, the consistent movement of animals or introduction of contaminated products during consecutive years.

Phylogenetic analysis of the isolates, however, provides additional support for the hypothesis of over-wintering. Two of the three genetic lineages or groups of VSV identified during the epidemic (Fig. 2B and C) mostly overlap with the geographical location of the two spatial clusters identified. Isolates from the spatial cluster of herds located in Colorado and New Mexico correspond to a specific group of genetically related VSV identified in 2004 and 2005 (Fig. 2B). This group seems to be phylogenetically closely related to the group of VSV detected early in 2004, which was similar and in some cases identical to viruses originating in Mexico. Viruses from the spatial cluster of herds located in Wyoming were isolated in 2005 and 2006 and corresponded to a lineage phylogenetically distant from the Mexican and early 2004 United States isolates. Previously, it was shown that two distinct genotypes existed in spatially separated areas of Wyoming in 2005 (Rainwater-Lovett et al., 2007) with an isolate from western Wyoming belonging to Group B (Fig. 2) and those isolated in eastern Wyoming belonging to Group C. It is likely that viruses from the Group C genotype, found in eastern but not in western Wyoming, gave rise to the 2006 viruses that were isolated only in eastern Wyoming, and not in any other part of the southwestern United States.

There are a number of factors that may have biased the results of the spatial and phylogenetic clustering analyses. Spatial heterogeneity of the susceptible population may have resulted in significantly smaller values of d in densely populated regions, which may have biased the results of the spatial analyses towards the detection of clusters in most densely populated areas. On the other hand, the phylogenetic analysis may have been affected by a selection bias associated with the absence of a formal random design to select samples for sequencing. Incomplete or absence of information on the distribution of the susceptible population and absence of a random sampling design are common drawbacks in the investigation of outbreaks and epidemics. For those reasons, arguable, the use of either a phylogenetic or spatial approach, as typically occurs in most scientific contributions dealing with analogous problems, would not have resulted in sufficient evidence to test the hypothesis of over-wintering. Here, we conducted both phylogenetic and spatial analytical approaches and, because sources of potential bias are likely independent for each of the methods, consistency in the results was interpreted as evidence that conclusions were unlikely influenced by potential sources of bias. Consequently, combined interpretation of the phylogenetic and spatial clustering analyses provided more evidence than if either of the methods would have been conducted alone and suggest that VSV may have over-wintered in 2004–2005 in certain regions of New Mexico and Colorado and in 2005–2006 in a limited area of eastern Wyoming. Moreover, virus over-wintering likely resulted in a distinct genetic lineage that evolved from that

Table 2
Association between phylogenetic groups of vesicular stomatitis virus (VSV) and spatial clusters of VSV outbreaks for which the distance to the nearest outbreak reported in the previous or following year, whichever was shorter, was significantly ($P < 0.01$) smaller than the epidemic's mean estimated for VSV outbreaks reported in the United States in 2004–2006.

Cluster	Phylogenetic groups		*P*-value*
Colorado and New Mexico	A + B	C	<0.001
Inside	30	0	
Outside	7	12	
Wyoming	A	B + C	0.003
Inside	0	10	
Outside	20	19	

* Fisher's exact test.

detected in the previous year within each of the specific clusters, as suggested by the associations estimated between lineages A and B and the cluster centered in Colorado and New Mexico, and between lineages B and C and the cluster centered in Wyoming (Table 2). Thus, when results of the phylogenetic and spatial analyses are interpreted together, they suggest that certain regions of Colorado, Wyoming, and New Mexico may offer ecological, epidemiological, or demographic conditions that facilitate over-wintering, adaptation and evolution of the VSNJV.

Unfortunately, no VSV isolates collected after 2004 from Mexico were available to us for comparison with the strains collected in the United States in 2005 and 2006. However, the phylogenetic analysis presented here shows that 2005 and 2006 outbreaks in the United States were caused by monophyletic viral lineages whose closest ancestors are viruses isolated in the previous year and in the same geographical region. The geographical region affected by the epidemic in 2006 was also affected in 2005, it is far-away located from the Mexican border, and no VSV outbreak was detected in any other region of the southern United States in 2006. For those reasons, interpretation of the results of the phylogenetic and spatial analyses conducted here indicates that it is most likely that the new lineages of VSV identified in the United States in 2005 and 2006 were the result of local evolution of the virus following a period of over-wintering, rather than the consequence of new virus introductions from Mexico.

Specific factors associated with conditions that favor over-wintering are still to be assessed. One may hypothesize, however, that if insect-borne transmission plays a role in the spread of the disease, then persistence, latency or maintenance of the virus in biotic or abiotic substrates may occur during winter, followed by reactivation of the mechanisms of infection in the next warm season. Thus, a possible explanation for the geographical and genetic association detected here could be the selective presence of such factors or forces in the geographical regions where spatial clusters were detected. Noteworthy is the observation that genetically similar VSV were identified from outbreaks that affected Colorado and New Mexico in 1995 and 1997 (Rodriguez et al., 2000), supporting the hypothesis that this particular region may offer conditions that favor over-wintering of the VSV.

VSV epidemics cause alarm and concern in the United States because the disease is clinically indistinguishable from FMD and because of the impact that VS has on producers operations and trade. The results presented here may have impact on the development and establishment of prevention and control strategies for the disease. Control of VSV epidemics is based on the quarantine of infected premises and the recommendation to apply measures aimed at reducing the exposure of susceptible animals to biting insects. Identification of areas where over-wintering may be more likely to occur will help to establish early control and prevention measures in order to prevent the occurrence of new outbreaks in following years. For example, herds in areas at high risk of over-wintering may be tested at the beginning of the summer in order to early detect and prevent the possible re-emergence and spread of the virus and as part of a risk-based surveillance program. Although nine southwestern states of the United States have suffered VSV outbreaks between 2004 and 2006, the evidence for VSV over-wintering offered here affected only the states of Colorado, New Mexico, and Wyoming. This finding suggests that there may be factors in most of the regions affected by the epidemic that limit the spread of the disease to one single season, whereas some specific regions potentially allow over-wintering of the virus. Assessment of the factors or conditions associated with disease over-wintering will help to design and apply measures aimed at preventing or controlling the presence or frequency of such factors in those regions where over-wintering is more likely to occur.

5. Conclusion

This study presents evidence that is consistent with the hypothesis that VSV over-wintering may have occurred in certain regions of the Southwestern United States affected by the VSV epidemic in 2004–2006. These results will inform the development and application of disease prevention strategies in the event of future VS epidemics. The joint application of techniques for the identification of spatial clusters of disease and phylogenetic analysis in a web-based framework such as the one presented here may be easily applied to modeling and surveillance of other animal diseases and regions of the world.

Conflict of interest

None declared.

Acknowledgments

This paper was funded in part by the United States National Center for Medical Intelligence, by the United States Department of Agriculture (USDA) Agricultural Research Service (ARS), and by the United States Department of Energy Oak Ridge Institute for Science and Education (ORISE).

References

Hurd, H.S., McCluskey, B.J., Mumford, E.L., 1999. Management factors affecting the risk for vesicular stomatitis in livestock operations in the western United States. J. Am. Vet. Med. Assoc. 215, 1263–1268.

Kulldorff, M., Athas, W.F., Feurer, E.J., Miller, B.A., Key, C.R., 1998. Evaluating cluster alarms: a space-time scan statistic and brain cancer in Los Alamos, New Mexico. Am. J. Public Health 88, 1377–1380.

Kulldorff, M., Nagarwalla, N., 1995. Spatial disease clusters: detection and inference. Stat. Med. 14, 799–810.

Kulldorff, M., Huang, L., Konty, K., 2009. A scan statistic for continuous data based on the normal probability model. Int. J. Health Geogr. 8, 58.

Letchworth, G.J., Rodriguez, L.L., Del cbarrera, J., 1999. Vesicular stomatitis. Vet. J. 157, 239–260.

Mead, D.G., Gray, E.W., Noblet, R., Murphy, M.D., Howerth, E.W., Stallknecht, D.E., 2004. Biological transmission of vesicular stomatitis virus (New Jersey serotype) by *Simulium vittatum* (*Diptera: Simuliidae*) to domestic swine (*Sus scrofa*). J. Med. Entomol. 41, 78–82.

Perez, A.M., Zeng, D., Tseng, C.J., Chen, H., Whedbee, Z., Paton, D., Thurmond, M.C., 2009. A Web-based system for near real-time surveillance and time-space cluster analysis of animal diseases. Prev. Vet. Med. 91 (1), 39–45.

Perez de Leon, A.A., Tabachnick, W.J., 2006. Transmission of vesicular stomatitis New Jersey virus to cattle by the biting midge *Culicoides sonorensis* (*Diptera: Ceratopogonidae*). J. Med. Entomol. 43, 323–329.

Posada, D., Crandall, K.A., 1998. MODELTEST: testing the model of DNA substitution. Bioinformatics, vol. 14. Oxford, England, pp. 817–818.

Rainwater-Lovett, K., Pauszek, S.J., Kelley, W.N., Rodriguez, L.L., 2007. Molecular epidemiology of vesicular stomatitis New Jersey virus from the 2004–2005 US outbreak indicates a common origin with Mexican strains. J. Gen. Virol. 88, 2042–2051.

Rodriguez, L.L., 2002. Emergence and re-emergence of vesicular stomatitis in the United States. Virus Res. 85, 211–219.

Rodriguez, L.L., Nichol, S.T., 1999. Vesicular stomatitis viruses. In: Webster, R.G., Granoff, A. (Eds.), Encyclopedia of Virology. 2nd ed. Academic Press, London, pp. 1910–1919.

Rodriguez, L.L., Bunch, T.A., Fraire, M., Llewellyn, Z.N., 2000. Re-emergence of vesicular stomatitis in the Western United States is associated with distinct viral genetic lineages. Virology 271, 171–181.

Rodriguez, L.L., Letchworth, G.J., Spiropoulou, C.F., Nichol, S.T., 1993. Rapid detection of vesicular stomatitis virus New Jersey serotype in clinical samples by using polymerase chain reaction. J. Clin. Microbiol. 31, 2016–2020.

Swofford, D.L. (Ed.), 1998. PAUP*. Phylogenetic Analysis Using Parsimony. Version 4. Sinauer Associates, Sunderland.

Tesh, R.B., Chaniotis, B.N., Johnson, K.M., 1971. Vesicular stomatitis virus, Indiana serotype: multiplication in and transmission by experimentally infected phlebotomine sandflies (*Lutzomyia trapidoi*). Am. J. Epidemiol. 93, 491–495.

Tesh, R.B., Chaniotis, B.N., Johnson, K.M., 1972. Vesicular stomatitis virus (Indiana serotype): transovarial transmission by phlebotomine sandlies. Science 175, 1477–1479.

Thompson, J.D., Gibson, T.J., Plewniak, F., Jeanmougin, F., Higgins, D.G., 1997. The CLUSTAL_X windows interface: flexible strategies for multiple sequence alignment aided by quality analysis tools. Nucleic Acids Res. 25, 4876–4882.

USAHA, 2008. Vesicular stomatitis. In: Brown, C., Torres, A. (Eds.), Foreign Animal Diseases, Committee on Foreign and Emerging Diseases of the United States Animal Health Association. Boca Publication Group, Boca Raton, pp. 423–428.

Return to Table of Contents

Virology 396 (2010) 152–159

Contents lists available at ScienceDirect

Virology

journal homepage: www.elsevier.com/locate/yviro

The region between the two polyprotein initiation codons of foot-and-mouth disease virus is critical for virulence in cattle

Maria E. Piccone [a,b], Juan M. Pacheco [a], Steven J. Pauszek [a], Ed Kramer [a], Elizabeth Rieder [a], Manuel V. Borca [a], Luis L. Rodriguez [a,*]

[a] Foreign Animal Disease Research Unit, Agricultural Research Service, U.S. Department of Agriculture, Plum Island Animal Disease Center, P.O. Box 848, Greenport, NY 11944-0848, USA
[b] Department of Pathobiology and Veterinary Sciences, Univ. of Connecticut, Storrs, CT, USA

ARTICLE INFO

Article history:
Received 2 September 2009
Returned to author for revision
16 September 2009
Accepted 13 October 2009
Available online 7 November 2009

Keywords:
Foot-and-mouth disease
Virus
Pathogenesis
Virulence
Cattle

ABSTRACT

To explore the role in viral pathogenesis of the region located between the two functional AUG (inter-AUG) in foot-and-mouth disease virus (FMDV), we derived viruses containing transposon (tn) inserts from a mutagenized cDNA infectious clone of FMDV (pA24-WT). Mutant viruses containing an in-frame 57-nt transposon insertion grew at a slower rate and had a smaller plaque size phenotype than the parental virus (A24-WT). A mutant virus containing a 51-nt deletion in inter-AUG had a similar phenotype in cell culture to that of A24-WT. When tested by aerosol inoculation in cattle (3 animals per virus), the deletion mutant was fully virulent as was A24-WT. Mutant viruses containing insertions in inter-AUG did not cause clinical disease or viremia. However, viruses that partially or totally removed the tn insertion during animal infection reverted to virulence in 2 inoculated steers. Therefore, this study identified inter-AUG as an FMDV viral virulence determinant in cattle infected by aerosol route.

Published by Elsevier Inc.

Introduction

Foot-and-mouth disease virus (FMDV) causes a highly contagious, debilitating disease in cloven-hoofed animals with devastating economic consequences (Grubman and Baxt, 2004). FMDV belongs to the genus Aphthovirus within the family *Picornaviridae* and has a single-stranded positive-sense RNA genome approximately 8500 nt in length. The 1300-nt 5′ untranslated region (5′UTR) is followed by a single long open reading frame (ORF), the 3′ untranslated region (3′ UTR), and poly(A) tail. The FMDV polyprotein processing begins by cleavage of the leader (L) from the nascent protein chain followed by processing of P1-2A, P2, and P3 regions. Cleavage of P1-2A yields the structural proteins (VP1, VP2, VP3, and VP4), while processing of P2 and P3 produces the viral non-structural proteins (Grubman et al., 1984). Translation of the viral polyprotein in picornaviruses initiates by a cap-independent mechanism at an internal AUG located downstream from an internal ribosome entry site (IRES) in the 5′ untranslated region (UTR). In the case of foot-and-mouth disease virus (FMDV), there are two functional AUGs separated by 75–84 nucleotides (inter-AUG) (Beck et al., 1983; Carrillo et al., 2005; Sangar et al., 1987). Polyprotein synthesis initiates at one of the two start codons resulting in two forms of the L protein, named Lab and Lb, that differ only at their N-termini but have identical proteolytic activities (Cao et al., 1995; Medina et al., 1993). Leader is a cysteine proteinase that cleaves itself (both in *trans* and *cis*) from the polyprotein and degrades the eukaryotic initiation factor eIF4G resulting in impairment of cap-mediated mRNA translation (Devaney et al., 1988; Strebel and Beck, 1986). It also translocates to the nucleus and interferes with the host innate response (de Los Santos et al., 2006, 2007). In infected cells, initiation at the second AUG is strongly favored by a selection mechanism that remains uncertain (Belsham, 1992; Cao et al., 1995; Clarke et al., 1985; Lopez de Quinto and Martinez-Salas, 1998; Piccone et al., 1995b). The role of the inter-AUG region is not clearly defined, and of the few studies that have been published, none have evaluated the role of this region on pathogenesis in a natural animal host (Andreev et al., 2007; Belsham, 1992; Lopez de Quinto and Martinez-Salas, 1998, 1999; Piccone et al., 1995a; Thomas et al., 1996). In fact, few viral regions containing virulence determinants for natural hosts have been identified in FMDV including L protease, VP1, and 3A (Brown et al., 1996; Mason et al., 2003; Pacheco et al., 2003; Sa-Carvalho et al., 1997).

Here, we generated and characterized FMD viruses containing insertions or deletions in the inter-AUG region. The presence of insertions in this region resulted in changes in AUG usage for initiation of translation, delayed protein synthesis, and delayed growth in cultured cells. Importantly, these viruses showed a severe attenuation in cattle inoculated by a natural aerosol route. Mutant viruses that lost the insertion regained full virulence in cattle. These results suggest that the region located between the two functional AUGs contains viral determinants for FMDV virulence in cattle.

* Corresponding author. Fax: +1 631 323 3006.
E-mail address: Luis.Rodriguez@ars.usda.gov (L.L. Rodriguez).

0042-6822/$ – see front matter. Published by Elsevier Inc.
doi:10.1016/j.virol.2009.10.020

Results

Generation of FMDV mutants

Four A24-FMDV plasmids containing tn insertions in the region located between the two AUG initiation codons were selected from the plasmid library described in Materials and methods and sequenced to confirm the tn insertion site. Plasmids were named according to the position of the insertion as follows: pA24-L1115, pA24-L1123a, pA24-L1123b, and pA24-L1159. RNA derived from mutant plasmids and from the parental infectious clone plasmid (pA24) were electroporated into BHK-21 cells and the supernatants from transfected cells were passed in BHK-$\alpha_V\beta_6$ cells until a cytopathic effect (CPE) appeared. After four or five passages in these cells, virus stocks were aliquoted and used in all subsequent experiments.

Full-length genomic sequencing (inclusive of the termini) of the four resulting viruses revealed that viruses derived from pA24-L1115 and pA24-L1123a maintained the tn insertion and were named A24-L1115 and A24-L1123, respectively. Virus derived from pA24-L1159 removed the tn insertion and reverted to wild type (WT) and was not further characterized. Virus derived from pA24-L1123b had also removed the tn insertion along with additional 17 codons in the inter-AUG region starting at position 1094 and was named A24-L1094del (Fig. 1). In addition to the insertions or deletions described above, mutant viruses contained a total of four point mutations compared with the A24-WT virus. These were at nt positions 552 (A-G) and 1470 (T-C) in mutant A24-L1115; position 915 (T-C) in A24-L1123; and nt position 4686 (A-G) in A24-L1094del. Mutations in the ORF (nt positions 1470 and 4686) were both synonymous.

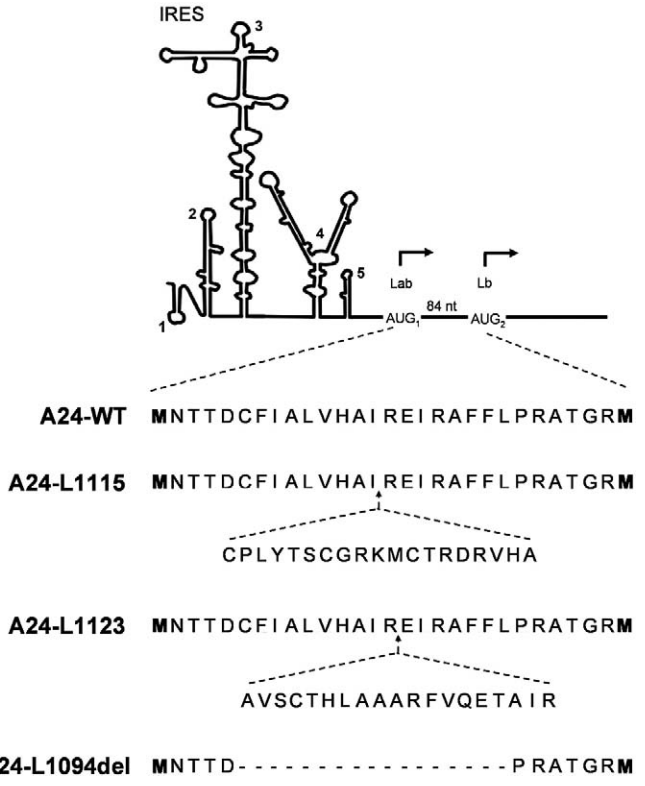

Fig. 1. Diagram of the FMDV mutants generated by tn insertion mutagenesis. The 27-amino acid region between the two functional initiation codons for L protein (Lb and Lab) is shown. In-frame insertions/deletion are shown below the A24-WT sequence. Mutants are named by the location of the insertion/deletion in pA24Cru. IRES: internal ribosomal entry site. Domain numbering is based on a model previously proposed (Pilipenko et al., 1989).

Effect of tn insertions on in vitro translation and leader proteinase functions

To evaluate the effect of tn insertions on viral translation, full-length RNA transcripts derived from pA24-WT and mutant plasmids pA24-L1115, pA24-L1123a, and pA24-L1123b were *in vitro* translated in rabbit reticulocyte lysates. The translation products derived from all mutant transcripts were indistinguishable from those produced by pA24-WT transcripts, except that the Lb band was absent in all three mutants. Instead, all A24-L mutants yielded a product that migrated slower than Lb, suggesting that protein synthesis occurred at the first functional AUG and L contained the 19 amino acids encoded by the tn insertion (Fig. 2A). The identity of the protein product, presumably Lab plus 19 amino acids (Lab^{+19}), was confirmed by immunoprecipitation using anti-L serum (Fig. 2B). These results suggest that insertions in the region located between the two AUG initiation codons had no effect on the self-cleavage of L from the viral polyprotein tested by *in vitro* transcription and translation (Fig. 2A). In addition to self-cleavage, L is also responsible for cleavage of the eukaryotic initiation factor 4G (eIF4G). In order to test their ability to cleave eIF4G, we incubated *in vitro* translation products of pA24-WT and each of the mutant plasmids with HeLa cell extracts, as a source of eIF4G. Western blot analysis revealed that translation products from mutant plasmids degraded intact eIF4G as well as those from pA24-WT despite their having 19 additional amino acids in L (Fig. 2C).

Replication of A24-L mutant viruses in cell culture

A24-L mutant viruses were evaluated for their ability to form plaques on three cell lines: BHK-21, IBRS-2, and LF-BK of hamster, swine, and bovine origins, respectively, and secondary lamb kidney cells (LK). Virus mutant A24-L1123 had the smallest plaque size phenotype in all three cell lines followed by A24-L1115, whereas A24-L1094del had A24-WT-like plaque phenotype. Interestingly, A24-L1123 and A24-L1115 viruses failed to produce visible plaques on secondary LK cell line at a low dilution, where the A24-WT and A24-L1094del viruses completely destroyed the monolayer (Fig. 3A).

The growth kinetics of the A24-L mutant viruses in each of the four cell types described above were compared to that of the A24-WT at a low (0.01) and high (10) MOI. Viruses A24-L1123 and A24-L1115 grew slower and to a slightly lower titer than A24-WT. Differences observed among viruses at MOI 10 were less noticeable (Fig. 3B) than those observed at MOI 0.01. The delay was most visible at 4 hpi at the lower MOI especially in bovine and porcine cell lines as well as in secondary lamb cells. Consistent with the plaque phenotype results, A24-L1094del grew similarly to A24-WT virus at both MOI tested. Similar results were obtained at MOI 0.1 (data not shown).

Effect of inter-AUG mutations on the synthesis of viral proteins in infected cells

To analyze viral protein synthesis, LF-BK cells were infected with A24-L mutants or A24-WT in the presence of [^{35}S] methionine and at various times post-infection, equal amounts of radiolabeled proteins were immunoprecipitated using a bovine FMDV convalescent serum and the products examined by SDS–PAGE (Fig. 4A). Virus A24-WT reached maximum protein expression levels by 6 hpi. Mutant virus A24-L1115 showed a delay in protein synthesis noticeable at 5 and 6 hpi, but by 8 hpi, it showed similar protein levels as the A24-WT. Mutant A24-L1123 showed severe delay in protein synthesis, and even by 8 hpi, this virus had not reached the 5 hpi protein synthesis levels of A24-WT. In contrast, mutant A24-L1094del demonstrated protein synthesis levels similar to the A24-WT virus at 5 hpi and thereafter (Fig. 4A).

To investigate the nature of the L protein synthesized in infected cells, lysates from A24-WT and A24-L mutant-infected LF-BK cells

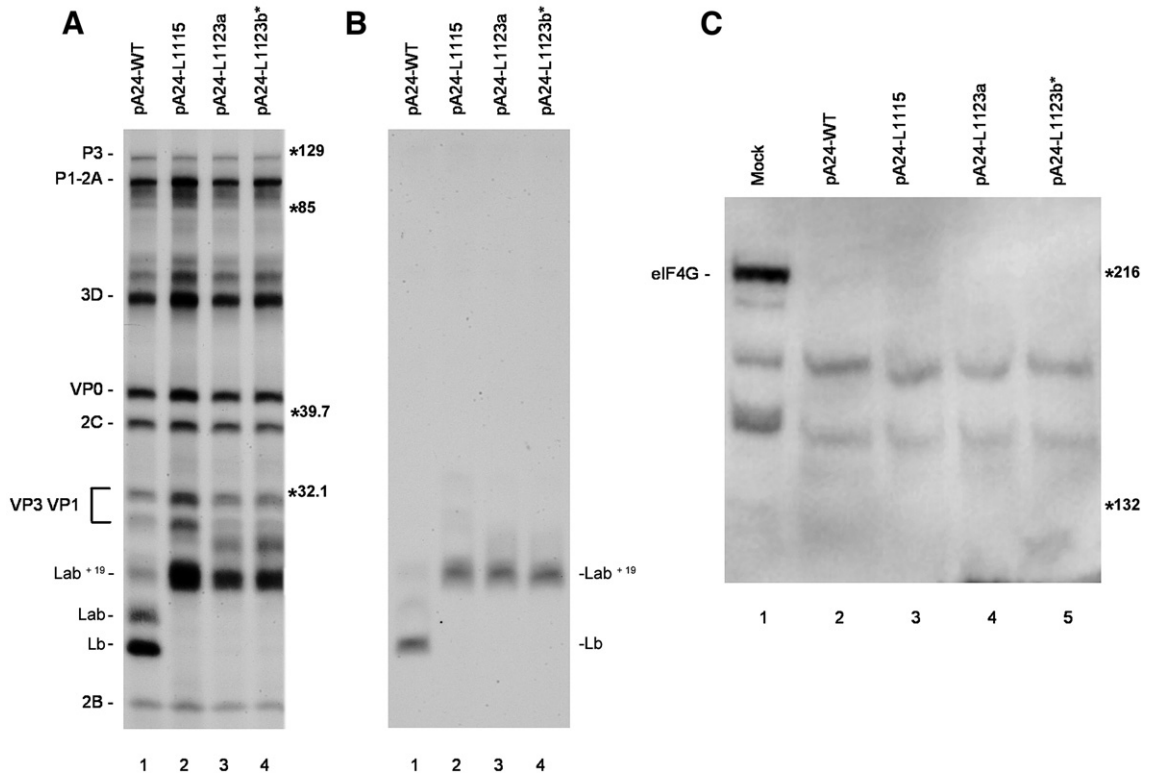

Fig. 2. Effect of the tn insertions on the autocatalytic cleavage of L from the viral polyprotein (A and B) and the cleavage of the eukaryotic initiation factor eIF4G (C). (A) *In vitro* translation reactions programmed with RNA transcripts derived from pA24Cru and pA24-L mutants were carried out in rabbit reticulocyte lysates at 30 °C in the presence of [^{35}S] methionine. Aliquots were removed at 2 hours and analyzed by SDS–PAGE on a 12% gel. Viral-specific proteins are indicated on the left side of the panel. (B) Immunoprecipitation of translation products from panel A using a rabbit polyclonal anti-L serum. (C) HeLa S10 was incubated overnight alone (lane 1) or with equal volumes of the indicated *in vitro* translation mixes (lanes 2 to 5). Samples were analyzed by SDS–7.5% PAGE and Western blotting done with rabbit antiserum specific for eIF4G. The position of eIF4G is indicated. (*) Plasmid pA24-L1123b contains a tn insertion but mutant virus A24-L1094del recovered upon RNA transfection deleted the tn and 17 amino acids from the inter-AUG region.

were analyzed by Western blot utilizing a rabbit polyclonal anti-leader antibody (Fig. 4B). The A24-WT virus showed a strong band corresponding to Lb and a fainter, slower band (presumably Lab). A similar pattern was observed for mutant A24-L1123 except that the fainter band had slower mobility than the putative Lab protein (presumably Lab + 19 amino acids). In the case of mutant A24-L1115, a single band was observed that localized between Lb and Lab suggesting translation initiation from an additional AUG present in the tn insertion upstream of the second AUG. Finally deletion mutant A24-1094del showed a single strong band consistent with Lb.

Virulence in cattle

Virulence of the parental and L mutant FMD viruses was assessed utilizing an aerosolization inoculation method that resembles natural infection (Pacheco et al., 2008). Viral virulence was determined by examination of clinical signs and virus growth and distribution in relevant tissues. Aerosol inoculation of three animals with A24-WT virus resulted in shedding of virus in saliva, viremia (in two animals), and fever by 2 dpi with clinical signs appearing by 2–4 dpi and reaching a high clinical score by 5–7 dpi when neutralizing antibodies were first detectable (Fig. 5A). An animal inoculated with A24-L1094del showed clinical disease and viral shedding undistinguishable from A24-WT (not shown). In contrast, three animals inoculated with mutant A24-L1123 did not show fever, viremia, or any clinical signs (Fig. 5A). Animals showed delayed low-titer shedding of virus in saliva at days 6–8 and delayed appearance of low titers of neutralizing antibodies beginning at 7–8 dpi and 14 dpi sera from these animals recognized viral proteins in a RIP assay (data not shown). Similarly, one of the three animals (animal no. 763) inoculated with A24-L1115 did not show fever, virus shedding, viremia, or clinical signs and low titers of neutralizing antibodies were detected for the first time at 9 dpi. The remaining two animals (animals nos. 7197 and 7203) inoculated with A24-L1115 showed viral shedding and viremia similar to A24-WT and delayed clinical signs starting at 5 dpi with full-blown FMD by 5–6 dpi (Fig. 5A). Viruses recovered from the sick animals (nos. 7197 and 7203) showed partial or total removal of the tn insertion (Fig. 5B). Due to the lack of virus recovery from sera or secretions of cows nos. 763, 764, 7139, and 7140, insert retention could not be assessed for these viruses.

Tissue distribution of mutant FMDV

To assess the invasiveness of FMDV mutants, we euthanized one animal inoculated with each virus at 24 hpi. Previous studies in our laboratory showed that after infection using an aerosol exposure method, FMDV replicates in the nasal-pharyngeal region (soft palate and pharynx) and lungs before invading the blood stream and causing secondary lesions in the mouth and feet of susceptible cattle (Pacheco et al., 2008). Both A24-WT and A24-L1094del infected the nasopharynx as well as the lung by 24 hpi. Although mutants A24-L1115 and A24-L1123 reached the same tissues, the number of positive samples in soft palate and pharynx was smaller and had lower viral titers than those of A24-WT and A24-L1094del (Table 1).

Discussion

The purpose of this study was to explore the effect of disruption of the sequence in the region located between the two AUG initiation codons of FMDV in viral virulence both *in vitro* and *in vivo* in cattle. The presence of two functional initiation codons is conserved among all serotypes and subtypes of FMDV sequenced to date, although the

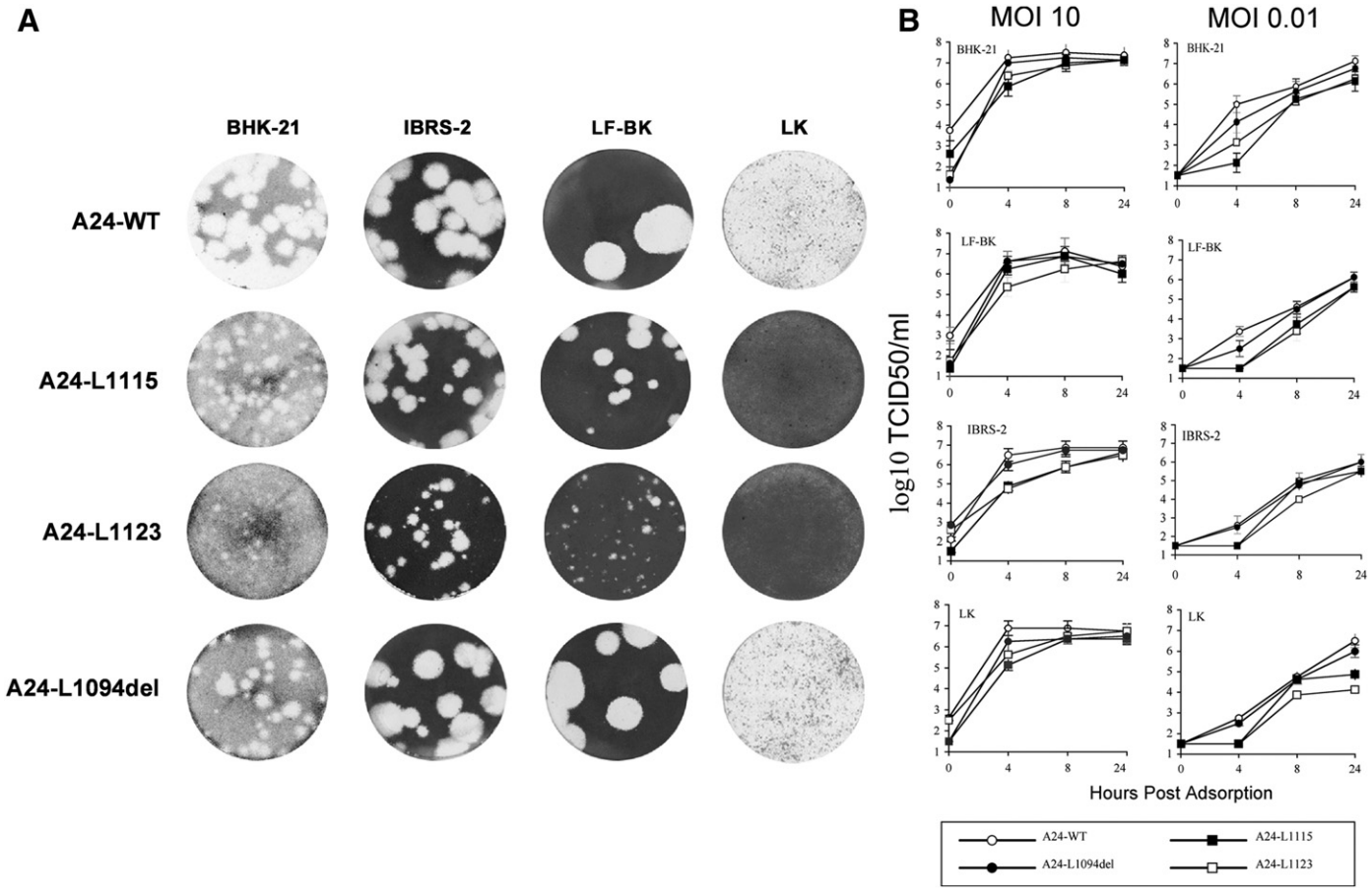

Fig. 3. Plaque morphology of A24-WT and A24-L mutant viruses on BHK-21, IBRS-2, LF-BK, and LK cells. (A) Cells were infected with the different viruses and after 1 hour of adsorption, 0.6% gum tragacanth overlay was added and 48 hours later stained for plaques with crystal violet. Growth curve of A24-WT and A24-L mutant viruses in different cell lines. (B) BHK-21, IBRS-2, LF-BK or LK cells were infected at an MOI 10 or 0.01 as described in Materials and methods. At the times indicated, cells and supernatants were frozen and virus titers were determined on the supernatant by $TCID_{50}$ assay on BHK-21 cells. Results shown are from four independent experiments; bars indicate the standard deviations.

length and sequence of the region between the two initiation AUG is somewhat variable (Carrillo et al., 2005). Little is known about the role of this region in FMDV pathogenesis in natural hosts. Previous studies carried out *in vitro* indicate that the inter-AUG region influences codon preference with the second AUG always being preferred (Lopez de Quinto and Martinez-Salas, 1999). In this study, *in vitro* transcripts derived from A24-FMDV plasmids each containing a 57-nt tn insertion resulted in a shift in initiation of translation from the second AUG to the first AUG. A previous study showed that stabilization of a stem–loop in the inter-AUG region resulted in decreased initiation at the second AUG (Andreev et al., 2007). Translation of all the insertion mutant transcripts showed a larger form of the L protein, indicating that initiation at the second AUG was either abrogated or greatly diminished. This contrasts previous reports where changes in the inter-AUG region decreased but never abrogated initiation from the second AUG (Andreev et al., 2007; Lopez de Quinto and Martinez-Salas, 1999).

The insertions did not interrupt the viral ORF but introduced 19 additional codons at the L protein amino terminus. These L proteins containing 19 amino acids of variable sequence were all functional, as evidenced by their ability to cleave themselves from the FMDV polyprotein and also the eIF4G ribosomal subunit, a well-described mechanism of FMDV pathogenesis (Chinsangaram et al., 2001, 1999). Our data showed that an additional 19-amino acid insertion in Lab does not interfere with the proteolytic functions of *in vitro* produced leader protease.

Previous studies and our data described above were done *in vitro* in the absence of infectious virus. The fact that our insertion mutagenesis study was done using a full-length FMDV infectious cDNA allowed us the recovery of infectious virus. Analysis of viral protein synthesis in infected cells showed that the presence of insertions in A24-L1115 and A24-L1123 resulted in delayed protein synthesis. This delay was most severe in A24-L1123 which even by 8 hpi had not reached the 5 hpi level of protein synthesis of the WT virus. This delay in viral protein synthesis is consistent with delays observed in the one-step growth curves. On the other hand deletion mutant A24-L1094del showed levels of protein synthesis and growth similar to the WT virus. This finding is hard to explain as few reports that characterize *in vitro* growth of FMDV-containing mutations in the inter-AUG region exist. But a previous report described a tissue culture-generated FMDV mutant with a deletion in the inter-AUG-region that was associated to fitness gain (Escarmis et al., 1999).

Analysis of the L proteins produced by the mutant viruses, as determined by reactivity of infected cell lysates with L specific antibodies in Western blot, showed that A24-L1115 had a single L protein with slower mobility than the WT Lb. This slower-moving L is likely the product of initiation at an AUG introduced by the tn insertion upstream from AUG2. This suggests that the presence of the additional 57 nt in this virus resulted in decreased initiation of translation from the second functional AUG. This change in initiation codon preference is consistent with a previous report showing that introduction of a new AUG upstream resulted in decreased translation

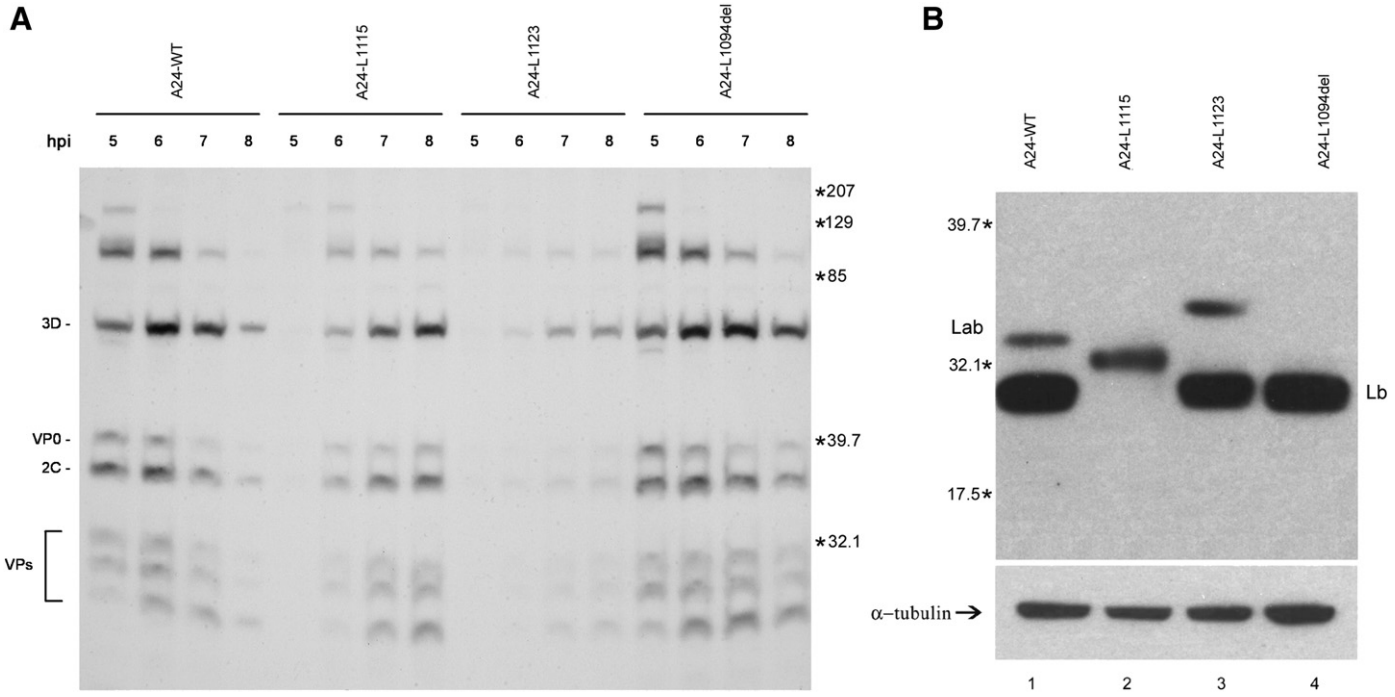

Fig. 4. Effect of tn insertions on the synthesis of viral proteins in infected cells. (A) LF-BK, cells were infected with A24-WT or A24-L mutant viruses at MOI 10 and radiolabeled with [^{35}S] methionine for 1 hour at 5, 6, 7, and 8 hours post-inoculation (hpi). Equal amounts of radiolabeled protein were immunoprecipitated with bovine convalescent serum. The position of specific viral proteins is indicated. (B) For Western blotting, LF-BK cells were infected with A24-WT or A24-L mutant viruses and cytoplasmic extract were prepared after 24 hpi. Equal volumes of cell extracts were resolved by 12% SDS–PAGE, transferred to nitrocellulose membranes and revealed using rabbit polyclonal anti-L serum (top) or mouse monoclonal anti-tubulin antibody as loading control (bottom).

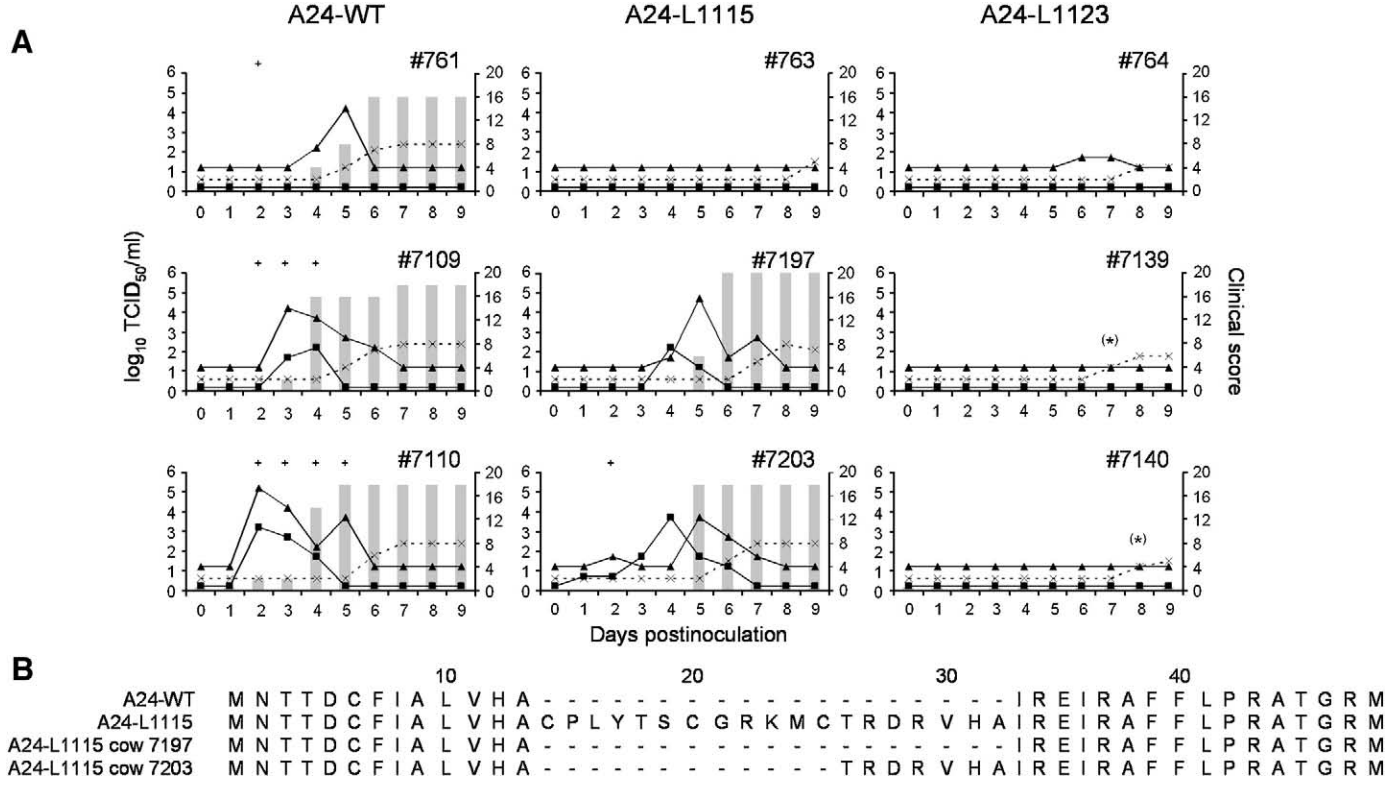

Fig. 5. Virulence of A24-WT and A24-L mutant viruses in cattle. (A) Three animals were inoculated with an aerosol containing 10^7 $TCID_{50}$ and monitored for 9 days post-infection. Saliva and serum samples were collected daily and tested for the presence of virus and/or neutralizing antibodies against FMDV. Viremia (■), virus in saliva (▲), and serum-neutralizing antibodies titers (X) are expressed in the left axes; the clinical score (bars) based on the presence of vesicle(s) in the four feet and mouth/tongue are expressed in the right axes. (+) denotes fever (>40 °C) detected that day. (*) denotes virus isolated from saliva on that day only after blind passages. Mutant A24-L1094del virus showed a disease pattern similar to that of the A24-WT virus (data not shown). (B) Amino acid sequences of viruses recovered from animals inoculated with mutant A24-L1115.

Table 1
Distribution of foot-and-mouth disease virus in tissues obtained from cattle 24 hours post-infection.

Tissue sample[a]	A24-WT		A24-L1094del		A24-L1115		A24-L1123	
	vRNA[b]	Virus infectivity[c]	vRNA	Virus infectivity	vRNA	Virus infectivity	vRNA	Virus infectivity
Pharynx								
Anterior dorsal soft palate	4.84	Pos	5.11	1.75	Neg	Neg	Neg	Pos
Posterior dorsal soft palate	3.85	2.5	6.49	4	6.45	2	3.93	2.5
Anterior dorsal nasopharynx	6.14	Pos	6.89	Neg	5.61	Neg	6.62	Neg
Posterior dorsal nasopharynx	5.12	2.5	4.63	3.25	Neg	1.75	Neg	2.5
Lung								
Primary bronchus	5.77	1.75	5.51	Pos	4.49	Neg	Neg	Neg
Anterior lobe, distal	7.81	3.5	6.56	3.5	4.78	2	4.65	2.25
Medial lobe, distal	6.11	2.5	8.39	4	6.14	2.25	5.06	2
Posterior lobe, distal	7.48	1.75	4.69	Pos	5.63	2	5.66	Pos

[a] One animal was infected with each virus, and after euthanasia, tissues were collected for virus isolation and viral RNA detection.
[b] Viral RNA (vRNA) was quantitated by real-time RT–PCR as previously described. Values were expressed as RNA copies per milliliter of tissue macerate (Pacheco et al., 2008).
[c] Virus infectivity was determined in BHK-21 cells with a sensitivity of 1.75 $\log_{10}$ $TCID_{50}$/ml.

from the second functional AUG (Escarmis et al., 1999). In the cases of mutant A24-L1123 and the WT virus, there were two L protein bands, one corresponding to Lb and a slower band likely the product of initiation of translation from the first AUG (Lab). The mobility of this band in the mutant virus is consistent with a Lab protein containing an additional 19 amino acids. It is remarkable that this mutant despite having an additional 57 nt in the inter-AUG region initiated translation at both functional AUGs. Although not the focus of this article, our results are consistent with previous *in vitro* studies (Andreev et al., 2007; Belsham, 1992) indicating that the structure of the inter-AUG region is critical for initiation of translation for FMDV.

Clinical results showed that the presence of the insertion in the inter-AUG region had a strong attenuating effect on the viruses that retained the tn insertion (A24-1115 and A24-1123). Animals inoculated with these viruses not only did not show fever or any other clinical signs of FMD but also had nondetectable levels of infectious virus in their blood and little to nondetectable viral shedding in saliva for 1–2 days. This is in contrast with A24-WT inoculated animals that showed full-blown FMD clinical signs including fever, viremia, and large amounts (4–5 $\log_{10}$ $TCID_{50}$ per ml) of viral shedding in saliva. Previous studies showed that FMDV lacking the leader protein was attenuated in cattle and that the possible mechanism of attenuation was based on the inability of leaderless virus to shut down the host cap-mediated translation and inhibit the host innate response (Brown et al., 1996; de Los Santos et al., 2006). In our L insertion mutants, this might not be the case as the full-length leader protein was present in the attenuated viruses.

Two animals inoculated with A24-1115 showed full-blown FMD although delayed by 1 day compared to the WT virus. Virus recovered from lesions in these animals had in one case completely removed the insertion and reverted to WT and in another case removed all but seven amino acids of the tn insertion. In both cases, these spontaneous revertants regained their virulence and presented clinical signs, viremia, and viral shedding undistinguishable from the WT virus suggesting that the presence of the insert was an attenuating factor. Interestingly, one animal inoculated with mutant A24-1094del showed clinical disease undistinguishable from A24-WT despite having only 30 nt in the inter-AUG region, demonstrating that these 30 nt are sufficient to carry out the functions of the inter-AUG region for pathogenesis *in vivo*.

Tissue distribution 24 hours after aerosol inoculation of WT and mutant viruses showed that the attenuated viruses reached the same primary replication sites in pharynx and lung as the WT virus. However, the level of infection in these tissues was lower for the insertion-containing mutants (A24-L1115 and A24-L1123). This result suggests that rather than differences in tropism between the WT and attenuated viruses, virus–host interactions at primary replication sites determined the clinical outcome of the viral infection. The mechanism of attenuation of viruses with insertions in the inter-AUG region is currently under investigation but it is possible that the presence of an additional 57 nt in this region resulted in delays in viral replication and allowed the host to control the infection before generalization occurred. Other potential mechanisms of attenuation include lower efficiency to recognize the initiation codons or inefficient recruitment of ribosomal subunits to initiate translation due to changes in the stem–loop structure in the inter-AUG region. This is plausible and would be consistent with our observed lower efficiency in translation both *in vitro* and in cells infected with tn-containing mutants.

In conclusion, we have shown the inter-AUG region of FMDV contains viral virulence determinants in cattle. Further studies are in progress to better define the molecular mechanisms involved in viral attenuation. Mutant viruses generated in this study could be useful tools in understanding early interactions of FMDV with its relevant hosts.

Materials and methods

Cells and viruses

Wild-type FMDV and viral mutants containing single in-frame insertions or deletions in the region located between the two functional initiation codons were derived from a plasmid encoding the complete FMDV A24 Cruzeiro genome (pA24-WT) (Rieder et al., 2005). In order to maintain adequate bovine receptor usage, virus stocks were grown in a derivative of baby hamster kidney (BHK-21 ATCC catalogue no. CCL-10) cells expressing the bovine $\alpha_V\beta_6$ integrin (BHK-$\alpha_V\beta_6$) (Duque et al., 2004) and titrated on BHK-21 cells by calculating the 50% tissue culture infectious dose per ml ($TCID_{50}$/ml). *In vitro* phenotype was characterized by plaque assays in BHK-21 cells, a bovine kidney cell line (LF-BK) (Swaney, 1988), a porcine kidney cell line (IBRS-2), and secondary lamb kidney cells (LK) (House and House, 1989). Plaques were evidenced by staining monolayers at 48 hours using crystal violet as previously described (Chinsangaram et al., 1999; Piccone et al., 1995a).

Construction of transposon-containing FMDV mutants

To identify virulence determinants within the FMDV genome, we constructed a library of infectious FMDV full-length genome plasmids of (pA24-WT) containing single random insertions (1 per genome), using the EZ-Tn5™ In-Frame Linker Insertion kit (Epicentre Biotechnologies, Madison, WI). Briefly, pA24-WT was subjected to a one-step *in vitro* reaction to introduce a single EZ-Tn transposon, containing a kanamycin resistance marker flanked by *Not*I restriction sites. The product of the transposition reaction was transformed into

competent DH5 *Escherichia coli* cells (Invitrogen, Carlsbad, CA) and plated on kanamycin selection plates. Approximately 1050 colonies were picked, and the exact location of each tn was determined by sequencing using a pair of tn-specific primers to yield the sequence from each tn and its flanking regions. Once clones were chosen, the kanamycin resistance gene was excised from the tn by *Not*I digestion. Each *Not*I-digested clone was then ligated and transformed into DH5 *E. coli*. The resulting clones each contained a single, random 19-codon in-frame insertion.

Plasmids derived from pA24-WT containing an insertion between the first (residues 1078–1080) and the second AUG (residue 1162–1164) initiation codons were selected for further study. These plasmids each contained an insertion at residue 1115, 1123 (2), and 1159 and were named pA24-L1115, pA24-L1123a, pA24-L1123b, and pA24-L1159, respectively. All nucleotide designations are based on the sequence of A24-WT (Rieder et al., 2005).

T7 RNA transcripts of *Swa*I-linearized pA24-L1115, pA24-L1123a, pA24-L1123b, pA24-L1159, and pA24-WT were produced using a MegaScript kit (Ambion, Austin, TX) and transfected into BHK-21 cells by electroporation as described previously (Piccone et al., 1995a; Rieder et al., 1993). Mutant viruses obtained from these transfections were named according to the site of insertion (or deletion), namely pA24-L1115 yielded virus A24-L1115 and pA24-L1123a yielded A24-L1123. However, pA24-L1123b yielded a virus containing a 51-nucleotide deletion starting at nucleotide 1094 and was named A24-L1094del. Both the parental plasmid and pA24-L1159 yielded WT virus named A24-WT. Virus stocks were prepared and the complete viral genome sequence was determined.

Genome sequencing

Extracted viral RNA was reverse-transcribed with equimolar amounts of random hexamers (Invitrogen) and a 3′RACE adapter primer (Invitrogen, Carlsbad, CA) using M-MLV reverse transcriptase (Invitrogen, Carlsbad, CA) according to manufacturer's instructions. The 5′ terminus was determined using the 5′ RACE System for Rapid Amplification of cDNA Ends, Version 2.0 (Invitrogen, Carlsbad, CA) as per the manufacturer's instructions. The viral genome was PCR-amplified in eight overlapping fragments using A24-WT specific primers (primer sequences available from the authors upon request). PCR fragments were visualized, purified, and sequenced as previously described (Rainwater-Lovett et al., 2007). SEQUENCHER software v4.1 (Gene-Codes, Ann Arbor, Michigan, USA) was used to analyze the chromatograms.

Virus growth and metabolic labeling

To characterize *in vitro* growth, BHK-21, IBRS-2, LF-BK and LK cells were infected for 1 hour at multiplicities of infection (MOI) of 10 and 0.01 as indicated in the figure legends, washed with PBS morpholineethanesulfonic acid (MES) buffer (pH 6) to inactivate unadsorbed virus, and incubated at 37 °C. At indicated times post-infection, cells were harvested, and virus was released from the cells by one freeze/thaw cycle, and the titer of the clarified supernatant was determined by $TCID_{50}$ as described above.

For metabolic labeling, infected cells, grown in six-well plates, were labeled from 5 to 8 hours post-infection (hpi) with [^{35}S] methionine (New England Nuclear, Waltham, MA) as previously described (Piccone et al., 1995a). Cells were lysed by adding 1% sarcosyl and clarified by centrifugation, and samples were analyzed by radioimmunoprecipitation (RIP) analysis as described below.

In vitro translation and RIP analysis

In vitro translation reactions were performed with the rabbit reticulocyte lysate (Ambion) in the presence of [^{35}S] methionine essentially as described by the manufacturer. Equal numbers of trichloroacetic acid-precipitable counts from *in vitro* translation reactions or infected cells were immunoprecipitated with bovine convalescent sera using fixed *Staphylococcus aureus* bacteria, analyzed by SDS–PAGE using a 12% polyacrylamide gel and visualized by autoradiography.

Western blot analysis

The ability of the WT or mutants L proteins to cleave the eukaryotic initiation factor 4G (eIF4G) was tested as previously described (Piccone et al., 1995b). Briefly, an S10 extract of HeLa cells was incubated at 30 °C overnight with *in vitro* translation products from WT or mutants pA24-FMDV. Samples were resolved in a SDS–7.5% PAGE and transferred to a PVDF membrane. Cellular eIF4G was detected using eIF4G1 antibody (1:1000 dilution) (GeneTex Inc, San Antonio, TX) and peroxidase-labeled anti-rabbit antibodies (Invitrogen, Carlsbad, CA).

For the detection of leader protein, LF-BK cells were infected at low MOI and at 24 hpi, cell lysates were prepared and fractionated on a 12% SDS–PAGE, blotted, and probed with a rabbit polyclonal anti-leader antibody (kindly provided by Marvin Grubman, ARS). An antitubulin monoclonal antibody (MAb) was purchased from Lab Vision. Western blots were visualized using the WesternBreeze Chemoluminescent Immunodetection System (Invitrogen).

Virulence studies in cattle

Cattle experiments were performed under biosafety level 3 in the animal facilities at PIADC following a protocol approved by the Institutional Animal Use and Care Committee. Steers (300–400 kg) were infected using an aerosolization method that resembles natural infection (Pacheco et al., 2008). Briefly, animals were sedated and inoculated with 10^7 $TCID_{50}$ in 2 ml of MEM delivered by aerosol with a jet nebulizer (Whisper Jet, Marquest Medical Products, CO) attached to an aerosol delivery system (Equine Aeromask, Medium Size, Trudell Medical, London, Ontario, Canada). Three steers were inoculated and held in individual animal rooms for each virus (A24-WT, A24-L1115, and A24-L1123). Animals were clinically examined daily and rectal temperature monitored for 9 days post-inoculation (dpi). Serum and oral swabs were collected and cows were sedated daily for clinical evaluation. Clinical scores were determined by scoring 1–4 points for the mouth and each foot depending on the number and size of vesicles observed for a maximum clinical score of 20. Animals that developed FMD were humanely euthanized at 9 dpi and animals not showing clinical signs were observed for 13–15 days before euthanasia. One additional animal for each virus mentioned above and for A24-L1094del was similarly inoculated and euthanized at 24 hpi. Oral and nasal swabs and serum samples were collected at 0, 6, and 24 hpi for each animal. After postmortem examination, tissues were collected to evaluate virus distribution by virus isolation and real-time reverse transcription PCR (RT–PCR) as previously described (Pacheco et al., 2008). Eight tissue samples were collected including soft palate, nasopharynx, and lung. Approximately 30 mg was collected from each anatomical region and frozen immediately in liquid nitrogen. Samples were stored at −70 °C until processed. The presence or absence of each mutation was confirmed by RT–PCR sequencing on viruses isolated from animals.

Virus, viral RNA, and antibody detection

Virus isolation and viral RNA detection from tissues were performed in BHK-21 cells as previously described (Pacheco et al., 2008). Viral titration in swabs and sera was done as described above and expressed in $TCID_{50}$/ml. Neutralizing antibody titers were determined as previously described (Golde et al., 2005). Sera were also tested for the presence of antibodies against viral proteins by a RIP assay as previously described (Piccone et al., 1995a).

Acknowledgments

We acknowledge the valuable contributions and technical support from Elizabeth Bishop, George Smoliga, Ethan Hartwig, and Jolene Carlson; Kathy Apicelli for help with graphic work and Dr. Teresa Delos Santos for help with Western blot analysis. We thank Dr. Marvin Grubman for his valuable advice and critical reading of the manuscript. We also thank the Plum Island Animal Resource Unit personnel for their help during animal experiments and the USDA-APHIS Foreign Animal Disease Diagnostic Laboratory for providing the LK cells.

References

Andreev, D.E., Fernandez-Miragall, O., Ramajo, J., Dmitriev, S.E., Terenin, I.M., Martinez-Salas, E., Shatsky, I.N., 2007. Differential factor requirement to assemble translation initiation complexes at the alternative start codons of foot-and-mouth disease virus RNA. RNA 13 (8), 1366–1374.

Beck, E., Forss, S., Strebel, K., Cattaneo, R., Feil, G., 1983. Structure of the FMDV translation initiation site and of the structural proteins. Nucleic Acids Res. 11 (22), 7873–7885.

Belsham, G.J., 1992. Dual initiation sites of protein synthesis on foot-and-mouth disease virus RNA are selected following internal entry and scanning of ribosomes *in vivo*. EMBO J. 11 (3), 1105–1110.

Brown, C.C., Piccone, M.E., Mason, P.W., McKenna, T.S., Grubman, M.J., 1996. Pathogenesis of wild-type and leaderless foot-and-mouth disease virus in cattle. J. Virol. 70 (8), 5638–5641.

Cao, X., Bergmann, I.E., Fullkrug, R., Beck, E., 1995. Functional analysis of the two alternative translation initiation sites of foot-and-mouth disease virus. J. Virol. 69 (1), 560–563.

Carrillo, C., Tulman, E.R., Delhon, G., Lu, Z., Carreno, A., Vagnozzi, A., Kutish, G.F., Rock, D.L., 2005. Comparative genomics of foot-and-mouth disease virus. J. Virol. 79 (10), 6487–6504.

Chinsangaram, J., Piccone, M.E., Grubman, M.J., 1999. Ability of foot-and-mouth disease virus to form plaques in cell culture is associated with suppression of alpha/beta interferon. J. Virol. 73 (12), 9891–9898.

Chinsangaram, J., Koster, M., Grubman, M.J., 2001. Inhibition of L-deleted foot-and-mouth disease virus replication by alpha/beta interferon involves double-stranded RNA-dependent protein kinase. J. Virol. 75 (12), 5498–5503.

Clarke, B.E., Sangar, D.V., Burroughs, J.N., Newton, S.E., Carroll, A.R., Rowlands, D.J., 1985. Two initiation sites for foot-and-mouth disease virus polyprotein *in vivo*. J. Gen. Virol. 66 (Pt 12), 2615–2626.

de Los Santos, T., de Avila Botton, S., Weiblen, R., Grubman, M.J., 2006. The leader proteinase of foot-and-mouth disease virus inhibits the induction of beta interferon mRNA and blocks the host innate immune response. J. Virol. 80 (4), 1906–1914.

de Los Santos, T., Diaz-San Segundo, F., Grubman, M.J., 2007. Degradation of nuclear factor kappa B during foot-and-mouth disease virus infection. J. Virol. 81 (23), 12803–12815.

Devaney, M.A., Vakharia, V.N., Lloyd, R.E., Ehrenfeld, E., Grubman, M.J., 1988. Leader protein of foot-and-mouth disease virus is required for cleavage of the p220 component of the cap-binding protein complex. J. Virol. 62 (11), 4407–4409.

Duque, H., LaRocco, M., Golde, W.T., Baxt, B., 2004. Interactions of foot-and-mouth disease virus with soluble bovine alphaVbeta3 and alphaVbeta6 integrins. J. Virol. 78 (18), 9773–9781.

Escarmis, C., Davila, M., Domingo, E., 1999. Multiple molecular pathways for fitness recovery of an RNA virus debilitated by operation of Muller's ratchet. J. Mol. Biol. 285 (2), 495–505.

Golde, W.T., Pacheco, J.M., Duque, H., Doel, T., Penfold, B., Ferman, G.S., Gregg, D.R., Rodriguez, L.L., 2005. Vaccination against foot-and-mouth disease virus confers complete clinical protection in 7 days and partial protection in 4 days: use in emergency outbreak response. Vaccine 23 (50), 5775–5782.

Grubman, M.J., Baxt, B., 2004. Foot-and-mouth disease. Clin. Microbiol. Rev. 17 (2), 465–493.

Grubman, M.J., Robertson, B.H., Morgan, D.O., Moore, D.M., Dowbenko, D., 1984. Biochemical map of polypeptides specified by foot-and-mouth disease virus. J. Virol. 50 (2), 579–586.

House, C., House, J.A., 1989. Evaluation of techniques to demonstrate foot-and-mouth disease virus in bovine tongue epithelium: comparison of the sensitivity of cattle, mice, primary cell cultures, cryopreserved cell cultures and established cell lines. Vet. Microbiol. 20 (2), 99–109.

Lopez de Quinto, S., Martinez-Salas, E., 1998. Parameters influencing translational efficiency in aphthovirus IRES-based bicistronic expression vectors. Gene 217 (1-2), 51–56.

Lopez de Quinto, S., Martinez-Salas, E., 1999. Involvement of the aphthovirus RNA region located between the two functional AUGs in start codon selection. Virology 255 (2), 324–336.

Mason, P.W., Grubman, M.J., Baxt, B., 2003. Molecular basis of pathogenesis of FMDV. Virus Res. 91 (1), 9–32.

Medina, M., Domingo, E., Brangwyn, J.K., Belsham, G.J., 1993. The two species of the foot-and-mouth disease virus leader protein, expressed individually, exhibit the same activities. Virology 194 (1), 355–359.

Pacheco, J.M., Henry, T.M., O'Donnell, V.K., Gregory, J.B., Mason, P.W., 2003. Role of nonstructural proteins 3A and 3B in host range and pathogenicity of foot-and-mouth disease virus. J. Virol. 77 (24), 13017–13027.

Pacheco, J.M., Arzt, J., Rodriguez, L.L., 2008. Early events in the pathogenesis of foot-and-mouth disease in cattle after controlled aerosol exposure. Vet. J. doi:10.1016/j.tvjl.2008.08.023.

Piccone, M.E., Rieder, E., Mason, P.W., Grubman, M.J., 1995a. The foot-and-mouth disease virus leader proteinase gene is not required for viral replication. J. Virol. 69 (9), 5376–5382.

Piccone, M.E., Zellner, M., Kumosinski, T.F., Mason, P.W., Grubman, M.J., 1995b. Identification of the active-site residues of the L proteinase of foot-and-mouth disease virus. J. Virol. 69 (8), 4950–4956.

Pilipenko, E.V., Blinov, V.M., Chernov, B.K., Dmitrieva, T.M., Agol, V.I., 1989. Conservation of the secondary structure elements of the 5′-untranslated region of cardio- and aphthovirus RNAs. Nucleic Acids Res. 17 (14), 5701–5711.

Rainwater-Lovett, K., Pauszek, S.J., Kelley, W.N., Rodriguez, L.L., 2007. Molecular epidemiology of vesicular stomatitis New Jersey virus from the 2004–2005 US outbreak indicates a common origin with Mexican strains. J. Gen. Virol. 88 (Pt. 7), 2042–2051.

Rieder, E., Bunch, T., Brown, F., Mason, P.W., 1993. Genetically engineered foot-and-mouth disease viruses with poly(C) tracts of two nucleotides are virulent in mice. J. Virol. 67 (9), 5139–5145.

Rieder, E., Henry, T., Duque, H., Baxt, B., 2005. Analysis of a foot-and-mouth disease virus type A24 isolate containing an SGD receptor recognition site *in vitro* and its pathogenesis in cattle. J. Virol. 79 (20), 12989–12998.

Sa-Carvalho, D., Rieder, E., Baxt, B., Rodarte, R., Tanuri, A., Mason, P.W., 1997. Tissue culture adaptation of foot-and-mouth disease virus selects viruses that bind to heparin and are attenuated in cattle. J. Virol. 71 (7), 5115–5123.

Sangar, D.V., Newton, S.E., Rowlands, D.J., Clarke, B.E., 1987. All foot and mouth disease virus serotypes initiate protein synthesis at two separate AUGs. Nucleic Acids Res. 15 (8), 3305–3315.

Strebel, K., Beck, E., 1986. A second protease of foot-and-mouth disease virus. J. Virol. 58 (3), 893–899.

Swaney, L.M., 1988. A continuous bovine kidney cell line for routine assays of foot-and-mouth disease virus. Vet. Microbiol. 18 (1), 1–14.

Thomas, A.A., Rijnbrand, R., Voorma, H.O., 1996. Recognition of the initiation codon for protein synthesis in foot-and-mouth disease virus RNA. J. Gen. Virol. 77 (Pt 2), 265–272.

Return to Table of Contents

Virology 407 (2010) 129–136

Contents lists available at ScienceDirect

Virology

journal homepage: www.elsevier.com/locate/yviro

Effects of the interactions of classical swine fever virus Core protein with proteins of the SUMOylation pathway on virulence in swine

D.P. Gladue [a], L.G. Holinka [a], I.J. Fernandez-Sainz [a], M.V. Prarat [a], V. O'Donell [a,b], N. Vepkhvadze [a], Z. Lu [c], K. Rogers [b], G.R. Risatti [b], M.V. Borca [a,*]

[a] Plum Island Animal Disease Center, ARS, USDA, Greenport, NY 11944, USA
[b] Department of Pathobiology and Veterinary Science, University of Connecticut, Storrs, CT 06269, USA
[c] Plum Island Animal Disease Center, DHS, Greenport, NY 11944, USA

ARTICLE INFO

Article history:
Received 29 May 2010
Returned to author for revision 21 July 2010
Accepted 26 July 2010

Keywords:
Virulence
Pathogenesis
Attenuation
Core protein
Classical swine fever virus
SUMOylation
Vaccines

ABSTRACT

Here we have identified host cell proteins involved with the cellular SUMOylation pathway, SUMO-1 (small ubiquitin-like modifier) and UBC9, a SUMO-1 conjugating enzyme that interact with classical swine fever virus (CSFV) Core protein. Five highly conserved lysine residues (K179, K180, K220, K221, and K246) within the CSFV Core were identified as putative SUMOylation sites. Analysis of these interactions showed that K179A, K180A, and K221A substitutions disrupt Core-SUMO-1 binding, while K220A substitution precludes Core-UBC9 binding. In vivo, Core mutant viruses (K179A, K180A, K220A, K221A) and (K220A, K221A) harboring those substitutions were attenuated in swine. These data shows a clear correlation between the disruption of Core protein binding to SUMO-1 and UBC9 and CSFV attenuation. Overall, these data suggest that the interaction of Core with the cellular SUMOylation pathway plays a significant role in the CSFV growth cycle *in vivo*.

Published by Elsevier Inc.

Introduction

Classical swine fever (CSF) is a highly contagious disease of swine. The etiological agent, classical swine fever virus (CSFV), is a small, enveloped virus with a positive, single-stranded RNA genome and, along with bovine viral diarrhea virus (BVDV) and border disease virus (BDV), is classified as a member of the genus Pestivirus within the family *Flaviviridae* (Fauquet et al., 2005). The approximately 12.3-kb CSFV genome contains a single open reading frame that encodes a 3898-amino-acid polyprotein and ultimately yields 11 to 12 final cleavage products (NH_2-Npro-C-E^{rns}-E1-E2-p7-NS2-NS3-NS4A-NS4B-NS5A-NS5B-COOH) through co- and posttranslational processing of the polyprotein by cellular and viral proteases (Rice, 1996). Structural components of the CSFV virion include the Core protein and glycoproteins E^{rns}, E1, and E2. The function of glycoproteins, as major virulence determinants in swine, has been studied in detail (Meyers et al., 1999; Risatti et al., 2005a,b, 2006, 2007; Tews et al., 2009; Van Gennip et al., 2004). Limited knowledge exists to explain the function of the Core protein in Pestiviruses. CSFV Core protein, as in other Pestiviruses, is a small, highly basic polypeptide (Meyers et al., 1989). In BVDV, Core protein has been described as lacking significant secondary structure and, being a highly basic protein, capable of binding to RNA, although with low affinity and specificity (Murray et al., 2008). In CSFV, Core, expressed as recombinant protein, has been associated with the regulation of cellular transcriptional activation (Liu et al., 1998). A broader knowledge of the biological properties of hepatitis C virus (HCV) Core protein, a close relative of Pestiviruses, is available. HCV Core has been shown to interact with itself for self-assembling in nucleocapsid-like particles in the presence of nucleic acids (Kunkel et al., 2001); with HCV proteins NS5A and E1 (Goh et al., 2001; Lo et al., 1996; Masaki et al., 2008), with HCV RNA (Fan et al., 1999; Shimoike et al., 1999; Tanaka et al., 2000), and with host cellular proteins (Jin et al., 2000; Mamiya and Worman, 1999; Otsuka et al., 2000; Yoshida et al., 2002; You et al., 1999). Interaction of Core protein with cellular proteins leads to modulation of signaling pathways, cell transformation and proliferation, regulation of cellular and viral gene expression, apoptosis, and alteration of lipid metabolism that affects HCV pathogenesis (Giannini and Brechot., 2003; Lai and Ware, 2000; Levrero, 2006; McLauchlan, 2000; Ray and Ray, 2001; Tellinghuisen and Rice, 2002). Interaction of HCV Core protein with cell molecules impairs the host's immune response by mechanisms that result in suppression of IL-12 synthesis in human

* Corresponding author. Plum Island Animal Disease Center, USDA/ARS/NAA, PO Box 848, Greenport, NY 11944-0848, USA. Fax: +1 631 323 3006.
E-mail addresses: douglas.gladue@ars.usda.gov (D.P. Gladue), lauren.holinka@ars.usda.gov (L.G. Holinka), ignacio.fernandezsainz@ars.usda.gov (I.J. Fernandez-Sainz), melanie.prarat@ars.usda.gov (M.V. Prarat), zlu@dhs.gov (Z. Lu), kara.rogers@uconn.edu (K. Rogers), guillermo.risatti@uconn.edu (G.R. Risatti), manuel.borca@ars.usda.gov (M.V. Borca).

0042-6822/$ – see front matter. Published by Elsevier Inc.
doi:10.1016/j.virol.2010.07.040

macrophages (Eisen-Vandervelde et al., 2004), T cell dysfunction (Yao et al., 2007), and inhibition of T-lymphocyte activation and proliferation (Chen et al., 1994; Kittlesen et al., 2000; Yao et al., 2001). Discovery of host proteins that interact with CSFV proteins may unravel the biological properties of CSFV Core protein, including the unknown roles in virus virulence and pathogenesis.

To increase understanding of the functions of CSFV Core protein, we identified swine proteins that directly interact with Core of CSFV strain Brescia by means of the yeast two-hybrid system using a swine primary macrophage cDNA expression library. Screening revealed that swine proteins specifically bind to Core protein. Of particular interest, two proteins SUMO-1 and UBC9 involved in the cellular SUMOylation pathway (Niedenthal, 2007), specifically bind to Core protein. SUMOylation is a process that involves covalent attachment of small ubiquitin-like modifier (SUMO) proteins to specific lysine residues in target proteins (Kerscher, 2007; Sarge and Park-Sarge., 2009). Three SUMO isoforms, SUMO-1, SUMO-2 and SUMO-3, are expressed in cells; in addition, a pseudogene encoding SUMO-4 has also been described (Bohren et al., 2007). UBC9 is the SUMO-conjugating enzyme (Niedenthal, 2007). Like ubiquitin, attachment of SUMO to proteins involves several enzymatic steps, including cleavage of SUMO by the specific activity of sentrin-specific protease (SENP), to yield a mature-SUMO protein that is attached covalently to the SUMO-activating enzyme dimer (SAE1-SAE2), an E1 protein (Okuma et al., 1999). The SUMO protein is then transferred from SAE1–SAE2 to SUMO-conjugating enzyme (UBC9), an E2 protein, which attach SUMO to lysine in the target protein. Typically, SUMOylation occurs in the consensus sequence ψKxD/E/P/G (ψ represents a hydrophobic amino acid) (Desterro et al., 1997; Johnson and Blobel., 1997; Rodriguez et al., 2001; Sampson et al., 2001). SUMO E3 proteins are able to increase the efficiency of these reactions by associating with UBC9 and target proteins but are not always required for proteins to be SUMOylated (Geiss-Friedlander and Melchior, 2007; Mukhopadhyay and Dasso, 2007). Conjugation of SUMO can induce protein activation, affect protein stability, and cause changes in protein intracellular locations (Kerscher, 2007). SUMOylation also plays a role in the replication of the cell genome and regulation of gene expression (Seeler and Dejean., 2003). Several viruses, including human cytomegalovirus, Epstein–Barr virus, dengue virus, Moloney murine leukemia virus, and vaccinia virus, induce modifications to the host SUMOylation pathway as a mechanism to evade the host immune response (Chiu et al., 2007; Huh et al., 2008; Palacios et al., 2005; Sadanari et al., 2005; Shirai and Mizuta., 2008; Yueh et al., 2006).

Mapping of the Core–SUMO binding interface was performed by constructing a panel of Core protein mutants where lysine (K) residues were substituted to alanine (A) residues at the predicted SUMO-1 binding motifs and then tested for interactions by means of the yeast two-hybrid system. Similar mutations were introduced into full-length cDNA clones of highly virulent CSFV strain Brescia. Rescued mutant viruses were used to investigate whether the removal of these sites could affect viral infectivity and virulence in swine. Interestingly, K-to-A substitutions in Core that affect binding to SUMO-1 and UBC9 also showed an effect on induction of attenuation of CSFV in swine.

Results

CSFV structural Core protein binds swine SUMO-1 and UBC9 host proteins

A yeast two-hybrid system was used to identify interactions between swine macrophage cellular proteins and CSFV Core protein. An N-terminal fusion of the GAL4 protein DNA binding domain (BD) with CSFV Core protein was utilized as "bait" to screen a swine primary macrophage cDNA library expressed as N-terminal fusion of the GAL4 activation domain (AD). More than 1×10^7 independent yeast colonies were screened from a library representing ~3×10^6 independent clones. Protein interactions were selected after cotransfecting yeast strain AH109 with BD–Core fusion and cDNA library constructs and selecting colonies for growth in defined media lacking amino acids leucine, tryptophan, histidine, and nucleobase adenine. Plasmids recovered from selected yeast colonies were sequenced, and in-frame ORFs were retested for assessing the specificity of the observed protein interaction with CSFV Core protein. To address the issue of false positive interactions, human lamin C protein expressed as fusion with BD (BD–Lam) was used as "bait" in AH109 yeast cotransfected with the swine macrophage cDNA expression library. Nonspecific interactors were discarded (data not shown). Several specific protein interactions with CSFV Core protein were observed. Two of these proteins, SUMO-1 and UBC9, were selected for further study as both proteins are involved in the cellular SUMOylation pathway. AD–SUMO-1 and AD–UBC9 fusion proteins specifically interacted with CSFV BD–Core fusion protein, but no protein interactions were observed with BD protein alone (Fig. 1). Also, no interactions were observed between AD–SUMO-1 and BD–Lam proteins. As expected, AD–UBC9 protein interacted with BD–Lam protein, as previously reported (Zhong et al., 2005).

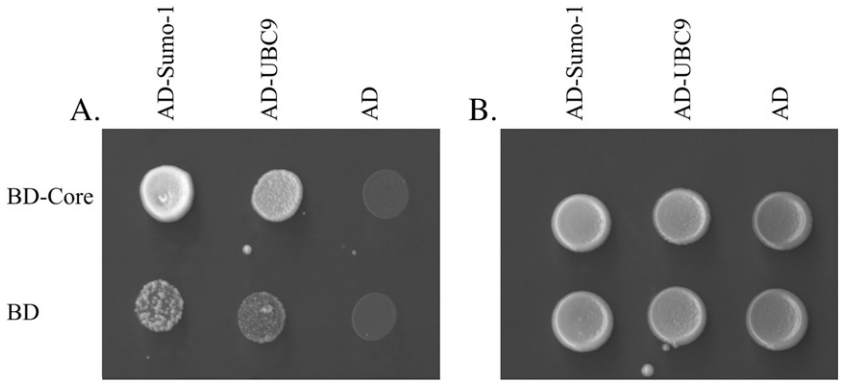

Fig. 1. Protein–protein interaction of CSFV Core with swine SUMO-1 and UBC9 proteins in the yeast two-hybrid system. Yeast strain AH109 was transformed with either GAL4-binding domain (BD) or CSFV Core fused to GAL4 binding domain (CORE–BD). These strains were then transformed with GAL4 activation domain (AD), Sumo-1 fused to GAL4 activation domain (Sumo-1–AD), or UBC9 fused to GAL4 activation domain (UBC9–AD) as indicated above. Spots of strains, 10 μl, expressing the indicated constructs containing 2×10^6 yeast cells were spotted on (A) selective media for protein–protein interaction in the yeast two-hybrid system, SD–Ade/His/Leu/Trp plates, and (B) nonselective SD–Leu/Trp for plasmid maintenance only.

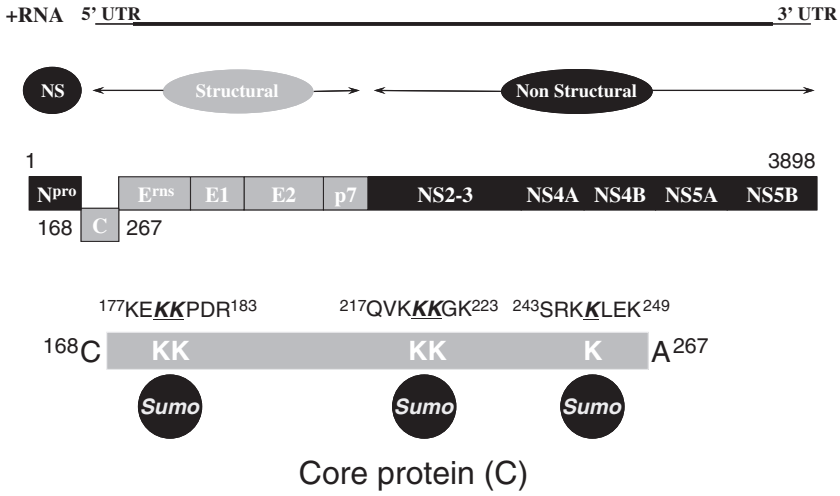

Fig. 2. Schematic representation of putative SUMO binding motifs found in CSFV Core protein. Sites were predicted using SUMOplot Analysis Program (www.abgent.com/tools/sumoplot) with CSFV strain Brescia Core protein amino acid sequence (BICv, GenBank accession number AY578687). Shown here is the CSFV polyprotein with numbers indicating amino acid positions relative to the CSFV Brescia polypeptide.

Mapping areas of CSFV Core protein critical for SUMO-1 recognition

SUMOylation generally occurs at specific lysine (K) residues within target proteins harboring the consensus motif ψKxD/E/P/G (where ψ is a bulky hydrophobic residue). The SUMOplot Analysis Program (www.abgent.com/tools/SUMOplot) predicted putative SUMOylation sites harboring the consensus ΨKxD/E/P/G sequence within CSFV strain Brescia Core protein (Fig. 2). Five residues within CSFV Core, K179, K180, K220, K221, and K246 (relative to the CSFV polyprotein) were identified as putative SUMOylation sites. Multiple alignment of CSFV Core protein derived from isolates of diverse geographical and temporal origins revealed a high degree of conservancy for those K residues (Fig. 3). To assess the effects of these residues on Core protein interactions with SUMO-1 and UBC9 proteins, K-to-A substitutions were introduced into CSFV Core gene to yield mutant proteins CoreΔS179, CoreΔS180, CoreΔS220, CoreΔS221, CoreΔS246, CoreΔS179/180, CoreΔS220/221, and CoreΔS179/180/220/221 (Table 1) fused to the BD–GAL4. Protein–protein interactions using the yeast two-hybrid system showed that K220A substitution (CoreΔS220) alone interferes with the ability of Core to interact with UBC9 (Fig. 4). However, none of the K-to-A substitutions affected the ability of Core to interact with SUMO-1 (data not shown). Moreover, double substitutions K179A/K180A and K220A/K221A within Core did not affect Core–SUMO-1 protein interactions (Fig. 4). Thus, to determine if there is a cooperative effect mediating Core–SUMO binding, truncated forms of the protein were assayed in the yeast two-hybrid system for interactions with SUMO-1. Both amino and carboxyl termini halves of Core retained their SUMO-1 binding capabilities (Fig. 4). However, double substitutions K179A/K180A within the Core truncated carboxyl construct and single substitution K221A within the Core-truncated amino construct lack the ability to interact with SUMO-1 (Fig. 4). Altogether, mapping data indicate that Core residues K179, K180, and K221 mediate the interaction with SUMO-1, while the interaction between Core and UBC9 seems to be mediated by K220.

Development of CSFV SUMO-1 (CoreΔSv) mutant viruses

K-to-A substitutions of the predicted SUMOylation sites in Core (Table 1) were introduced into the genetic background of an

```
BICv AY578687          CSDDGASASKEKKPDRINKGKLKIAPKEHEKDSRTKPPDATIVVEGVKYQVKKKGKVKGKNTQDGLYHNKNKPPESRKKLEKALLAWAVIAIMLYQPVAA

Alfort 187 X87939      .......G.....................................................................................E.
LOM EU789580           .......G.....................................................................................E.
cF114 AF333000         .......G.....................................................................................E.
Alfort A19 U90951      .......G.....................................................................................E.
GPE- D49533            .......G.....................................................................................E.
Shimen AY775178        .......G.....................................................................................E.
JL1(06)EU497410        .......G.....................................................................................E.
SWH DQ127910           .......G.....................................................................................E.
Thiverval EU490425     .......G.....................................R.....................T.....................E.
Eystrup NC002657       .......G.....................................................S.....................E.
ALD D49532             .......G.....................................................S.....................E.
CAP X96550             .......G.....................................R.....................V.....E.
Glentorf U45478        .......G.....................................R.....................V.....E.
HCLV AF531433          .......G.....................R.....................................................E.
Strain C AY805221      .......G.....................R.....................................................E.
Riems AY259122         .......G.....................R.....................................................E.
CS AY578688            .......G.............T.....................................................................
GXWZ02 AY367767        ......GG..D.....M.............K.....................................................VT.V.......
virus 39 AF407339      .......G..D.....M.............K..S..................R.....................V..V.......
Spain01 FJ265020       .......GN.D.....M.............K.....................I.....................V.......
96TD AY554397          ....S.GG..D.....MS............K.....................N.V.....................T.V.......
0406 Taiwan AY568569   ......GG..D.....M.............K.....................................K.....V.....V.
Paderborn AY072924     ......GG.E......M.............K.....................................T.V.......
```

Fig. 3. Multiple alignments of CSFV Core proteins revealed the presence of highly conserved putative SUMOylation sites (underlined). Shown here is a Core protein amino acid sequence comparison between CSFV isolates geographically and temporally separated. Sumoylation sites were predicted with SUMOplot Analysis Program (www.abgent.com/tools/sumoplot).

Table 1
Set of CSFV CoreΔS mutants constructed in this study.

CSFV polypeptide position	Wild-type sequence[a]	Mutant sequence	Mutant ID
179	KE**KK**PDR	KE**A**KPDR	CoreΔS179v
180	KEK**K**PDR	KEK**A**PDR	CoreΔS180v
179/180	KE**KK**PDR	KE**AA**PDR	CoreΔS179/180v
220	QVQ**K**KGK	QVQ**A**KGK	CoreΔS220v
221	QVQK**K**GK	QVQK**A**GK	CoreΔS221v
220/221	QVQ**KK**GK	QVQ**AA**GK	CoreΔS220/221v
246	SRK**K**LEK	SRK**A**LEK	CoreΔS246v
179, 180, 220, 221	KE**KK**PDR, QVQ**KK**GK,	KE**AA**PDR, QVQ**AA**GK,	CoreΔS179/180/220/221v

[a] Bold case letters indicate the K-to-A substitutions.

infectious full-length cDNA clone (pBIC) (Risatti et al., 2005a) of the highly virulent CSFV strain Brescia. Rescued mutant viruses, named CoreΔS179/180/220/221v, CoreΔS179/180v, CoreΔS220/221v, CoreΔS179v, CoreΔS180v, CoreΔS220v, CoreΔS221v, and CoreΔS246v, bear a set of single or combined K-to-A substitutions in Core at residues K179, K180, K220, K221, and K246 (Table 1 and Fig. 2). Nucleotide sequences of mutant virus genomes were identical to their parental DNA plasmids, confirming the presence of the introduced substitutions and lacking undesirable mutations.

Replication of CoreΔSv mutants in vitro

In vitro growth characteristics of mutant viruses CoreΔS179/180/220/221v, CoreΔS179/180v, CoreΔS220/221v, CoreΔS179v, CoreΔS180v, CoreΔS220v, CoreΔS221v, and CoreΔS246v were evaluated relative to parental pBIC-derived virus BICv, in a multistep growth curve (Fig. 5). Primary swine macrophage cell cultures were infected at a multiplicity of infection (MOI) of 0.01 $TCID_{50}$ per cell. Virus was adsorbed for 1 hour (time zero), and samples were collected at 2, 24, 48, and 72 hours postinfection (hpi). All mutant viruses exhibited titers similar to parental BICv except CoreΔS179/180/220/221v, with a virus yield approximately 2.5-3 $\log_{10}$ $TCID_{50}$/ml lower than BICv (Fig. 5). This indicates that although none of the introduced mutations individually affected the virus titer, combined mutations significantly affected virus yield.

Evaluation of the role of CSFV Core SUMOylation sites in CSFV virulence in swine

To examine the effects of deletion of Core SUMOylation sites on CSFV virulence, CoreΔSv mutant viruses CoreΔS179/180v, CoreΔS220/221v, CoreΔS220v, CoreΔS221v, CoreΔS246v and CoreΔS179/180/220/221v were intranasally (IN) inoculated into naïve swine, at doses of 10^5 $TCID_{50}$, and monitored for clinical disease relative to swine inoculated with virulent parental virus. BICv exhibited a characteristic virulent phenotype (Table 2): none of the control pigs ($n=6$) survived the infection, dying, or being euthanized around 8 dpi. Interestingly, quadruple mutant CoreΔS179/180/220/221v was completely attenuated in swine. Animals ($n=4$) survived the infection and remained clinically normal throughout the entire observation period (21 days). This virus harbors K-to-A substitutions at residues K179, K180, K220, and K221 indentified as mediators of Core–SUMO-1 (K179, K180, and K221) and Core-UBC9 (K220) interactions. In contrast, all animals ($n=5$) inoculated with double mutant CoreΔS179/180 (K179A/K180A) displayed severe signs of CSF with three out of five animals succumbing to the disease, while swine inoculated with double mutant CoreΔS220/221v ($n=7$) (K220A, K221A) did not show clinical signs during the observation period (21 days) with the exception of one animal showing a transient rise of body temperature by 8 and 12 dpi. Animals ($n=8$) inoculated with single mutant CoreΔS221v (K221A) presented a variable behavior: half of the inoculated animas ($n=4$) die with CSF-associated symptoms but a significant delay when compared with those animals infected with parental BICv (16.2 dpi, SD = 1.9, VS 8 dpi, SD = 0.9, respectively). The other four animals inoculated with CoreΔS221v survived the disease presenting either a mild CSF disease (two animals) or were asymptomatic showing only a transitory rise in body temperature around 4 dpi. However, animals ($n=6$) inoculated with CoreΔS220v (K220A), a substitution that abolishes the Core–UBC9 protein interaction, displayed a milder and delayed onset of the disease relative to animals inoculated with virulent BICv, succumbing to CSF around 17 dpi (SD = 6.4). Meanwhile, pigs ($n=4$) inoculated with single mutant CoreΔS246v (K246A), harboring a mutation that does not affect Core-SUMO-1 or Core–UBC9 protein interactions, displayed a progression of disease indistinguishable from parental BICv infection (Table 2 and Fig. 6). Overall, these animal experiments suggest that there appears to be a close correlation between disrupting the protein interaction between Core–SUMO-1 and Core–UBC9 as detected in the yeast two-hybrid system with the induction of CSFV attenuation.

The effects of mutations introduced in Core on CSFV *in vivo* spreading were analyzed in inoculated animals. Virus shedding (as per quantification of virus in tonsil scrapings and nasal swabs) and viremia were quantified at times post-inoculation (Fig. 6). Virus was not detected in samples obtained from animals inoculated with attenuated mutant virus CoreΔS179/180/220/221v (sensitivity of detection ≥1.8 $TCID_{50}$/ml). Virus shedding was also limited in animals inoculated with CoreΔS220/221v, where three of five animals showed transient and low virus titers in blood, tonsil scrapings, and nasal swabs samples around 14 dpi. Shedding of virus was clearly observed in samples obtained from animals inoculated with CoreΔS220v, although observed titers were lower (1.5 to 2.5 $\log_{10}$ depending of the time point considered) than those measured in samples obtained from animals inoculated with parental BICv (Fig. 6). A similar pattern of virus shedding was observed in samples coming from animals inoculated with mutant CoreΔS179/180v (Fig. 6). Virus titers from clinical samples from animals inoculated with CoreΔS221v presented heterogeneous values, with the higher values being associated with the presence of CSF-related symptoms. Therefore, animals appearing as clinically normal do not show detectable virus titers. Conversely, animals dying of the disease or surviving but presenting CSF-associated symptoms present virus titers in all clinical samples although with values substantially lower than those of the

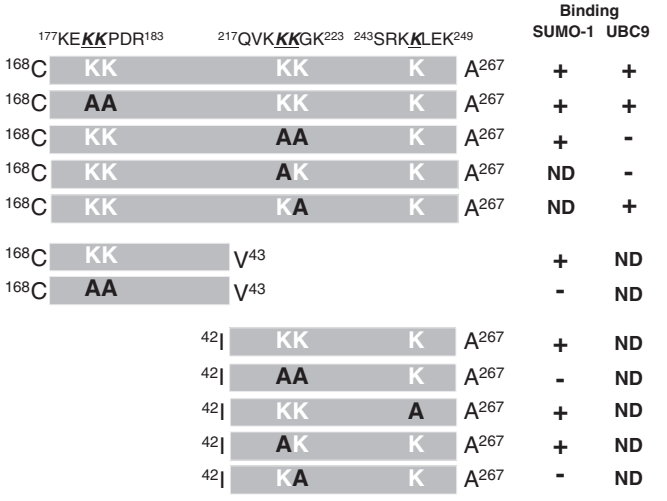

Fig. 4. Schematic representation showing the observed binding patterns between wild type and CSFV Core protein mutants with SUMO-1 and UBC9 proteins. Depicted are putative SUMO-1 and UBC9 binding sites and K-to-A substitutions in CSFV Core proteins. Numbers indicate amino acid position relative to CSFV strain Brescia polypeptide.

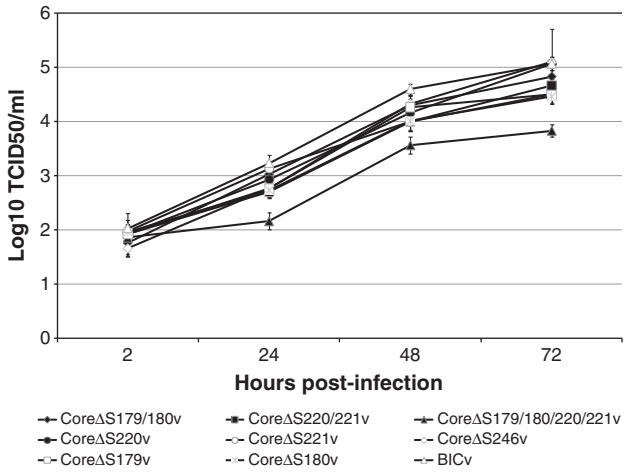

Fig. 5. *In vitro* growth characteristics of CoreΔS mutants and parental BICv. Primary swine macrophage cell cultures were infected (MOI = 0.01) with each of the Core mutants or BICv and virus progeny yield titrated at different times after infection in SK6 cells. Data represent means and standard deviations from two independent experiments. Sensitivity of virus detection: $\geq \log_{10} 1.8$ $TCID_{50}$/ml.

BICv-infected animals. Virulent mutant CoreΔS246v showed a pattern of virus shedding indistinguishable from parental BICv (Fig. 6). As with virus attenuation, shedding of CSFV as well as generalization of infection is affected by mutations in the Core protein that have an effect on Core protein interaction with SUMO-1 or UBC9.

Animals that survive inoculation with CoreΔS179/180/220/221v and CoreΔS220/221v were challenged with virulent BICv by 28 dpi were not protected, succumbing to the infection as naïve pigs (data not shown). CSFV-specific antibodies were not detected in sera of animals infected with either CoreΔS179/180/220/221v or CoreΔS220/221v at the time of challenge.

Discussion

Here, we have observed that the structural Core protein of CSFV specifically interacts with SUMOylation pathway proteins SUMO-1 and UBC9. SUMO-1 binds to target proteins as part of posttranslational modifications while UBC9, a protein with a strong sequence similarity to ubiquitin carrier proteins (E2s), catalyzes conjugation of SUMO-1 to a variety of target proteins (Desterro et al., 1997; Gong et al., 1997; Johnson and Blobel., 1997). SUMO proteins attach covalently to and detach from target proteins to modify their functions (Kerscher, 2007). Several studies indicate that viral infections affect the cellular SUMOylation pathway (Chang et al., 2009; Chiocca, 2007). In this work, the specific residues within CSFV Core protein mediating the interaction with SUMO-1 and UBC9 proteins were identified. Disruption of CSFV Core protein interaction yielded recombinant viruses with attenuated phenotypes and limited spreading within infected swine. These data suggest a novel role for Core protein in CSFV pathogenesis and virulence that is associated with the ability of Core protein to interact with host proteins in the cellular SUMOylation pathway.

Modifications of SUMO-1 and UBC9 binding sites in Core yielded a virus (CoreΔS179/180/220/221v) with substantially altered growth characteristics in primary swine macrophage cultures (Fig. 5). These quadruple K-to-A substitutions might affect virus growth by compromising other uncharacterized functions of CSFV Core, such as roles in virus replication or virion assembly. As might be expected, CoreΔS179/180/220/221v growth defects correlated with attenuation in infected pigs. Although the attenuated CoreΔS viruses did not show a severe growth defect *in vitro*, they had severe replication impairments during infection in animals. Thus, attenuation and spread of these viruses *in vivo* might be a function of altered growth in cells, other than macrophages, that normally support growth of wild-type CSFV. Other viral infections have been shown to affect the cellular SUMOylation pathway. Ebola virus Zaire VP35, adenovirus CELO Gam1, dengue virus envelope protein, human herpesvirus 6 IE2, and human cytomegalovirus IE2 have been shown to interact with proteins in the SUMOylation pathway either by preventing or inducing SUMO conjugation of target proteins (Ahn et al., 2001; Chang et al., 2009; Chiocca, 2007; Tomoiu et al., 2006), resulting on viral interference with key cellular pathways. As observed with CSFV protein Core, UBC9 also has been shown to interact with the capsid (CA) protein of the Moloney murine leukemia virus (MMLV) (Yueh et al., 2006). Binding K residues, mapped by alanine-scanning mutagenesis, were within a consensus motif for SUMOylation, and mutations of those residues reduced or abolished MMLV CA SUMOylation. Different from what we have observed, MMLV CA SUMOylation mutants displayed inhibited virus replication, being unable to produce circular viral DNAs or integration into the nucleus. Conversely, CSFV Core mutants were able to establish productive infections both *in vitro* and *in vivo*. Therefore, it is possible that CSFV Core protein interactions with the host SUMOylation pathway contributes to curtailing viral clearance, a function that has been removed from Core mutants.

Although the K220A substitution in Core disrupts binding to conjugating enzyme UBC9 in the yeast two-hybrid system, we cannot rule out the possibility that SUMOylation of Core still occurs in the absence of binding to the SUMO-1 conjugating enzyme. That might be reflected by the fact that in swine, mutant CoreΔS220v harboring the K220A substitution that disrupts interaction with UBC9 retained its virulence, albeit animals died later relative to animals inoculated with wild-type virus. Similarly, mutant CoreΔS221v was only partially attenuated in swine. Individual K179A or K180A substitutions in BICv do not affect virus virulence (data not shown); only the double mutant CoreΔS179/180v was partially attenuated in swine. Interestingly, simultaneous mutation of K220A and K221A in CΔS220/221v, losing the binding to both SUMO-1 and UBC9, leads to a strong attenuation of

Table 2
Swine survival and fever response following infection with CSFV CoreΔS mutants and parental BICv.

Virus	No. survivors/total no.	Mean time to death (days ± SD)	Fever		
			No. days to onset (days ± SD)	Duration no. days (days ± SD)	Max daily temperature (± SD)
CoreΔS179/180/220/221v	4/4	No	No	No	103.3 (0.4)
CoreΔS179/180v	2/5[a]	15.3 (0.6)	4.4 (1.5)	11.8 (3.4)	106.1 (1)
CoreΔS220/221v	7/7	No	8[b]	4	103.1 (0.4)
CoreΔS220v	0/6	17.5 (6.4)	4.2 (0.8)	11 (2.9)	106.4 (0.4)
CoreΔS221v	4/8[c]	16.2 (1.9)	5.8 (2.7)	8.8 (4)	105.6 (0.4)
CoreΔS246v	0/4	9 (0)	4.6 (0.7)	4.7 (0.8)	105.8 (0.4)
BICv	0/6	8 (0.9)	3.1 (0.7)	5.6 (1.2)	106.4 (0.9)

[a] The surviving animals showed severe signs of CSF at the end of the experimental period (21 days).
[b] Only one animal showed rise in body temperature.
[c] Data analysis is based in values obtained from animals showing disease.

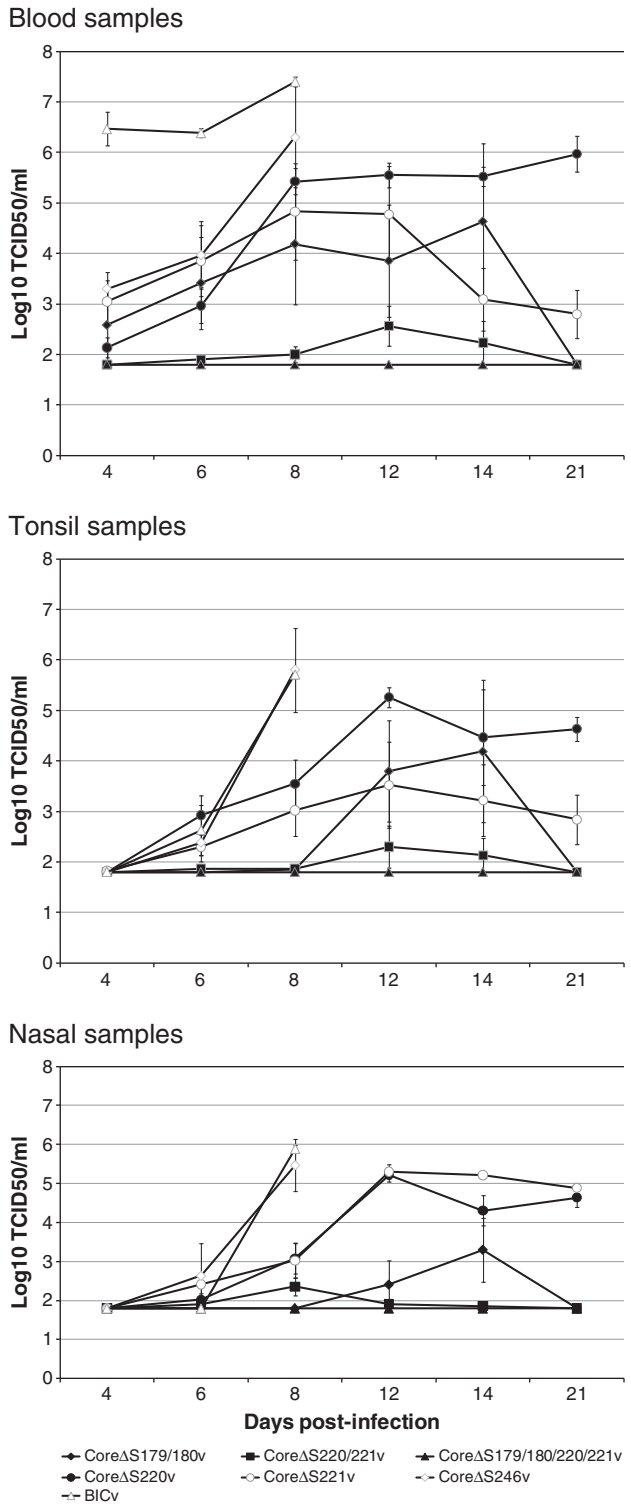

Fig. 6. Virus titers in clinical samples (blood, tonsil scrapings, and nasal swabs) from pigs infected with CoreΔS mutants and parental BICv. Each point represents the mean $\log_{10}$ $TCID_{50}$/ml and standard deviations from at least two animals. Sensitivity of virus detection: $\geq \log_{10}$ 1.8 $TCID_{50}$/ml.

the virulence in swine. It is possible that *in vivo*, Core–SUMO-1/UBC9 binding requires all four Lys residues (K179. K180, K220, and K221), since complete attenuation of wild-type virus was observed only when all four K-to-A substitutions were introduced into Core protein.

In general, SUMO-targeted proteins exhibit SUMOylation-dependent subcellular localization (Sarge and Park-Sarge, 2009). However, substitution of SUMOylation site lysines in ataxin-1 did not affect ataxin-1, a cellular protein, nuclear localization or its ability to form inclusions. Analysis of CSFV Core protein localization in swine cells using GFP–Core fusion proteins showed that substitutions of all putative SUMOylation sites do not affect cellular localization with core appearing in the nucleus, and in small structures within the cell (data not shown).

In summary, we identified the first swine host protein-binding partners for the CSFV Core protein: SUMO-1 and UBC9. Both of these proteins are involved in the SUMOylation pathway, and the putative binding/SUMOylation residues were mapped to two distinct regions in the Core protein. Furthermore, it is shown that disruption of specific residues within these distinct regions of Core protein completely abrogate virus virulence, demonstrating that acquisition of attenuation correlates with loss of binding to components of the SUMOylation pathway, SUMO-1 and UBC9. Although the role of SUMOylation within CSFV Core function is not clear, data indicates that the mechanism may support virus proliferation. It is of paramount importance to gain insights into host–viral protein interactions to understand the mechanisms of viral virulence and immune system evasion. Understanding the pathways and the protein players involved is necessary for developing and understanding better countermeasures to control virus infection in swine.

Materials and methods

Viruses and cells

Swine kidney cells (SK6) (Terpstra et al., 1990), free of BVDV, were cultured in Dulbecco's minimal essential media (DMEM) (Gibco, Grand Island, NY) with 10% fetal calf serum (FCS) (Atlas Biologicals, Fort Collins, CO). CSFV strain Brescia was propagated in SK6 cells and used for the construction of an infectious cDNA clone (IC) (Risatti et al., 2005a). Growth kinetics was assessed on primary swine macrophage cell cultures prepared as described (Zsak et al., 1996). Titration of CSFV from clinical samples was performed using SK6 cells in 96-well plates (Costar, Cambridge, MA). Viral infectivity was detected, after 4 days in culture, by an immunoperoxidase assay using the CSFV monoclonal antibody WH303 (Edwards et al., 1991) and the Vectastain ABC kit (Vector Laboratories, Burlingame, CA). Titers were calculated using the method of Reed and Muench, 1938 and expressed as $TCID_{50}$/ml. As performed, test sensitivity was ≥ 1.8 $TCID_{50}$/ml.

Construction of CSFV CoreΔS (CΔS) mutants

A full-length IC of the virulent CSFV Brescia strain (pBIC) (Risatti et al., 2005a) was used as a template in which putative SUMO binding sites in the Core protein were mutated. SUMO binding sites were predicted using the SUMOplot Analysis Program (www.abgent.com/tools/SUMOplot) with the consensus sequence ΨKxD/E/P/G (where Ψ is a bulky hydrophobic residue) within CSFV strain Brescia Core protein [GenBank accession number AY578687, (Risatti et al., 2005a)] (Figs. 2 and 3). Lysine (K)-to-alanine (A) amino acid substitutions were introduced by site-directed mutagenesis using the QuickChange XL Site-Directed Mutagenesis kit (Stratagene, Cedar Creek, TX; Table 1) performed per manufacturer's instructions and using the following primers (only forward primer sequences are shown): CoreΔS179: 5′-ggtgcaagtgcaagtaaagaggcgaaaccagataggatcaacaa-3′; CoreΔS180: 5′-gcaagtgcaagtaaagaga aggcaccagataggatcaacaaggg-3′; CoreΔS220: 5′-ggaaggagtaaaataccaggtcaaagcgaaaggtaaagttaagggaaag aat-3′; CoreΔS221: 5′-aggagtaaaataccaggtcaaaaaggcaggtaaagttaagggaaagaa tacc-3′; CoreΔS246: 5′-aataa accaccagaatctaggaaggcattagaaaaagccc tattggcatg-3′; CoreΔS179/180: 5′-ttgtagtggaaggagtaaaataccaggtc a aagcggcaggtaaagttaagggaaagaatacc-3′ CoreΔS220/221: 5′-gatggtg caagtgcaagtaaagaggcggcaccagataggat caacaagggtaa-3′; and CoreΔS179/180/220/221: 5′-ttgtagtggaaggagtaaaataccaggtcaaagcggcaggtaaa gttaagggaaagaatacc-3′ and 5′-gatggtgcaagtgcaagtaaagaggcggcaccaga taggatcaacaagggtaa-3′ .

In vitro rescue of CSFV Brescia and CΔS mutants

Full-length genomic clones were linearized with *SrfI* and *in vitro* transcribed using the T7 MEGAscript system (Ambion, Austin, TX). RNA was precipitated with LiCl and transfected into SK6 cells by electroporation at 500 V, 720 Ω, 100 W with a BTX 630 electroporator (BTX, San Diego, CA). Cells were seeded in 12-well plates and incubated for 4 days at 37 °C and 5% CO_2. Virus was detected by immunoperoxidase staining as described above, and stocks of rescued viruses were stored at −70 °C.

DNA sequencing and analysis

Full-length clones and *in vitro*-rescued viruses were completely sequenced with CSFV-specific primers by the dideoxynucleotide chain-termination method (Sanger et al., 1977). Viruses recovered from infected animals were sequenced in the mutated region. Sequencing reactions were prepared with the Dye Terminator Cycle Sequencing Kit (Applied Biosystems, Foster City, CA). Reaction products were sequenced on an ABI PRISM 3730xl automated DNA sequencer (Applied Biosystems, Foster City, CA). Sequence data were assembled with the Phrap software program (http://www.phrap.org), with confirmatory assemblies performed using CAP3 (Huang and Madan., 1999). The final DNA consensus sequence represented an average five-fold redundancy at each base position. Sequence comparisons were conducted using BioEdit software (http://www.mbio.ncsu.edu/BioEdit/bioedit.html).

Development of the cDNA library

A porcine macrophage cDNA expression library was constructed (Clontech, Mountain View, CA) using monocytes/macrophages obtained from healthy noninfected 40-lb swine. Macrophage cultures were prepared from defibrinated swine blood. Cells were cultured in plastic Primaria tissue culture flasks (BD Falcon, Franklin Lakes, NJ) in Roswell Park Memorial Institute-1640 medium (RPMI 1640; Invitrogen, Carlsbad, CA) containing 30% vol./vol. L929 cell supernatant, 20% fetal bovine serum (Invitrogen), and antibiotics–antimycotics (Invitrogen), for 48 hours (37 °C in 5% CO_2). Adherent cells were detached from the plastic by using 10 mM EDTA in phosphate-buffered saline and then reseeded into Primaria 6-well dishes at a density of 5×10^6 cells per well and incubated for an additional 24 hours at 37 °C in 5% CO_2. Cells were detached using 10 mM EDTA in phosphate-buffered saline, spun at 500×*g* for 10 minutes, with subsequent total RNA extraction using an RNeasy Mini kit (Qiagen, Valencia, CA). Contaminant genomic DNA was removed by DNase treatment using TURBO DNA-*free* (Ambion, Austin, TX). After DNase treatment, genomic DNA contamination of RNA stocks was assessed by real-time PCR amplification targeting the porcine β-actin gene. RNA quality was assessed by using RNA Nano chip on an Agilent Bioanalyzer 2100 (Agilent, Santa Clara, CA). Cellular proteins were expressed as GAL4 activation domain (AD) fusion proteins while CSFV proteins were expressed as GAL4-binding domain (BD) fusion proteins.

Library screening

The GAL4-based yeast two-hybrid system provides a transcriptional assay for detection of protein–protein interactions (Chien et al., 1991; Fields and Song, 1989). The "bait" protein, CSFV strain Brescia Core protein, was expressed with an N-terminus fusion to the GAL4 binding domain (BD). Full-length Core protein (amino acid residues 168–268 of the CSFV polyprotein) was used for screening and for full-length mutant protein construction. The Core fragments used for mapping were made using amino acids 168–212 for the amino half and amino acids 211–268 for the carboxyl half. As "prey," the previously described swine macrophage cDNA library containing proteins were fused to the GAL4 activation domain (AD) was used. Histidine and adenine reporter genes were used for growth selection in addition to two-color selection genes, X-gal ($blue^+/white^-$) and X-α-gal ($blue^+/white^-$). The swine macrophage library used here contains 3×10^6 independent cDNA clones. To screen, yeast strain AH109 (Clontech) carrying Core protein was transformed with library plasmid DNA with subsequent selection on plates lacking tryptophan, leucine, histidine, and adenine. Tryptophan and leucine are used for plasmid selection, while histidine and adenine are used for identification of positive interacting library fusions. Once identified, the positive library plasmids were recovered in *Escherichia coli* and sequenced to identify the cellular interacting protein. Sequence analysis also determined if the library proteins (cellular) were in-frame with the activation domain. To eliminate false positive interactions all library–activation domain fusion proteins were retransformed into strains carrying the viral protein-binding domain fusion proteins, as well as into strains carrying a Lam-binding domain fusion, with vectors that only contain the binding domain as negative controls. Lam is human Lamin C, commonly used as a negative control in the yeast two-hybrid system, as Lamin C does not form complexes or interact with most other proteins; however, some studies have shown Lamin C to interact with UBC9, thus binding domain-only vector was used for this purpose. The SUMO-1 recovered from the library contained amino acids (29–101) of porcine SUMO-1 (NCBI Reference Sequence: NP_001106146.1) amino terminal fused to the GAL4 activation domain. The UBC9 protein recovered was similar to *Homo sapiens* UBC9 (93% identity) and contained amino acids 2–172 of *H. sapiens* UBC9 (BAD92225) amino terminal fused to the GAL4 activation domain.

Animal infections

Each of the Core mutants or CoreΔSv was initially screened for its virulence phenotype in swine relative to the virulent strain Brescia. Swine used in all animal studies were 10 to 12 weeks old, 40-lb commercial breed pigs inoculated intranasally with 10^5 $TCID_{50}$ of either mutant or wild-type parental virus (BICv). For screening, pigs were randomly allocated into groups of at least two animals each, and pigs in each group were inoculated with one of the CoreΔSv (Table 1) or BICv. Clinical signs (anorexia, depression, purple skin discoloration, staggering gait, diarrhea, and cough) and changes in body temperature were recorded daily throughout the 21-day experiment. Total and differential white blood cell and platelet counts were obtained using a Beckman Coulter ACT (Beckman, Coulter, CA). Blood, serum, nasal swabs and tonsil scrapings were collected at times after challenge. Samples were processed for virus detection as described before (Risatti et al., 2005a).

For protection studies, pigs were inoculated with 10^5 $TCID_{50}$ of the corresponding CoreΔSv. At 28 days postinoculation (DPI) animals were intranasally challenged with 10^5 $TCID_{50}$ of BICv. Clinical signs and body temperature were recorded daily throughout the experiment as described above. CSFV antibodies were detected in sera using a commercially available ELISA (IDEXX HerdCheck CSFV Antibody Test Kit, Westbrook, ME).

Acknowledgments

We thank the Plum Island Animal Disease Center animal care unit staff for excellent technical assistance. This work was partially supported by National Pork Board grant no. 09-111 and USDA Agricultural and Food Research Initiative (AFRI) grant no. 2009-01614.

References

Ahn, J.H., Xu, Y., Jang, W.J., Matunis, M.J., Hayward, G.S., 2001. Evaluation of interactions of human cytomegalovirus immediate-early IE2 regulatory protein with small ubiquitin-like modifiers and their conjugation enzyme Ubc9. J. Virol. 75, 3859–3872.

Bohren, K.M., Gabbay, K.H., Owerbach, D., 2007. Affinity chromatography of native SUMO proteins using His-tagged recombinant UBC9 bound to Co^{2+}-charged talon resin. Protein Expr. Purif. 54, 289–294.
Chang, T.H., Kubota, T., Matsuoka, M., Jones, S., Bradfute, S.B., Bray, M., Ozato, K., 2009. Ebola Zaire virus blocks type I interferon production by exploiting the host SUMO modification machinery. PLoS Pathog. 5, e1000493.
Chen, C.H., Sheu, J.C., Wang, J.T., Huang, G.T., Yang, P.M., Lee, H.S., Lee, C.Z., Chen, D.S., 1994. Genotypes of hepatitis C virus in chronic liver disease in Taiwan. J. Med. Virol. 44, 234–236.
Chien, C.T., Bartel, P.L., Sternglanz, R., Fields, S., 1991. The two-hybrid system: a method to identify and clone genes for proteins that interact with a protein of interest. Proc. Natl. Acad. Sci. U. S. A. 88, 9578–9582.
Chiocca, S., 2007. Viral control of the SUMO pathway: Gam1, a model system. Biochem. Soc. Trans. 35, 1419–1421.
Chiu, M.W., Shih, H.M., Yang, T.H., Yang, Y.L., 2007. The type 2 dengue virus envelope protein interacts with small ubiquitin-like modifier-1 (SUMO-1) conjugating enzyme 9 (Ubc9). J. Biomed. Sci. 14, 429–444.
Desterro, J.M., Thomson, J., Hay, R.T., 1997. Ubch9 conjugates SUMO but not ubiquitin. FEBS Lett. 417, 297–300.
Edwards, S., Moennig, V., Wensvoort, G., 1991. The development of an international reference panel of monoclonal antibodies for the differentiation of hog cholera virus from other pestiviruses. Vet. Microbiol. 29, 101–108.
Eisen-Vandervelde, A.L., Waggoner, S.N., Yao, Z.Q., Cale, E.M., Hahn, C.S., Hahn, Y.S., 2004. Hepatitis C virus core selectively suppresses interleukin-12 synthesis in human macrophages by interfering with AP-1 activation. J. Biol. Chem. 279, 43479–43486.
Fan, Z., Yang, Q.R., Twu, J.S., Sherker, A.H., 1999. Specific in vitro association between the hepatitis C viral genome and core protein. J. Med. Virol. 59, 131–134.
Fauquet, C.M., Mayo, M.A., Maniloff, J., Desselberger, U., Ball, L.A. (Eds.), 2005. VIRUS TAXONOMY: VIIIth Report of the International Committee on Taxonomy of Viruses. ICTV.
Fields, S., Song, O., 1989. A novel genetic system to detect protein–protein interactions. Nature 340, 245–246.
Geiss-Friedlander, R., Melchior, F., 2007. Concepts in sumoylation: a decade on. Nat. Rev. Mol. Cell Biol. 8, 947–956.
Giannini, C., Brechot, C., 2003. Hepatitis C virus biology. Cell Death Differ. 10 (Suppl 1), S27–S38.
Goh, P.Y., Tan, Y.J., Lim, S.P., Lim, S.G., Tan, Y.H., Hong, W.J., 2001. The hepatitis C virus core protein interacts with NS5A and activates its caspase-mediated proteolytic cleavage. Virology 290, 224–236.
Gong, L., Kamitani, T., Fujise, K., Caskey, L.S., Yeh, E.T., 1997. Preferential interaction of sentrin with a ubiquitin-conjugating enzyme, Ubc9. J. Biol. Chem. 272, 28198–28201.
Huang, X., Madan, A., 1999. CAP3: a DNA sequence assembly program. Genome Res. 9, 868–877.
Huh, Y.H., Kim, Y.E., Kim, E.T., Park, J.J., Song, M.J., Zhu, H., Hayward, G.S., Ahn, J.H., 2008. Binding STAT2 by the acidic domain of human cytomegalovirus IE1 promotes viral growth and is negatively regulated by SUMO. J. Virol. 82, 10444–10454.
Jin, D.Y., Wang, H.L., Zhou, Y., Chun, A.C., Kibler, K.V., Hou, Y.D., Kung, H., Jeang, K.T., 2000. Hepatitis C virus core protein-induced loss of LZIP function correlates with cellular transformation. EMBO J. 19, 729–740.
Johnson, E.S., Blobel, G., 1997. Ubc9p is the conjugating enzyme for the ubiquitin-like protein Smt3p. J. Biol. Chem. 272, 26799–26802.
Kerscher, O., 2007. SUMO junction—what's your function? New insights through SUMO-interacting motifs. EMBO Rep. 8, 550–555.
Kittlesen, D.J., Chianese-Bullock, K.A., Yao, Z.Q., Braciale, T.J., Hahn, Y.S., 2000. Interaction between complement receptor gC1qR and hepatitis C virus core protein inhibits T-lymphocyte proliferation. J. Clin. Invest. 106, 1239–1249.
Kunkel, M., Lorinczi, M., Rijnbrand, R., Lemon, S.M., Watowich, S.J., 2001. Self-assembly of nucleocapsid-like particles from recombinant hepatitis C virus core protein. J. Virol. 75, 2119–2129.
Lai, M.M., Ware, C.F., 2000. Hepatitis C virus core protein: possible roles in viral pathogenesis. Curr. Top. Microbiol. Immunol. 242, 117–134.
Levrero, M., 2006. Viral hepatitis and liver cancer: the case of hepatitis C. Oncogene 25, 3834–3847.
Liu, J.J., Wong, M.L., Chang, T.J., 1998. The recombinant nucleocapsid protein of classical swine fever virus can act as a transcriptional regulator. Virus Res. 53, 75–80.
Lo, S.Y., Selby, M.J., Ou, J.H., 1996. Interaction between hepatitis C virus core protein and E1 envelope protein. J. Virol. 70, 5177–5182.
Mamiya, N., Worman, H.J., 1999. Hepatitis C virus core protein binds to a DEAD box RNA helicase. J. Biol. Chem. 274, 15751–15756.
Masaki, T., Suzuki, R., Murakami, K., Aizaki, H., Ishii, K., Murayama, A., Date, T., Matsuura, Y., Miyamura, T., Wakita, T., Suzuki, T., 2008. Interaction of hepatitis C virus nonstructural protein 5A with core protein is critical for the production of infectious virus particles. J. Virol. 82, 7964–7976.
McLauchlan, J., 2000. Properties of the hepatitis C virus core protein: a structural protein that modulates cellular processes. J. Viral Hepat. 7, 2–14.
Meyers, G., Rumenapf, T., Thiel, H.J., 1989. Molecular cloning and nucleotide sequence of the genome of hog cholera virus. Virology 171, 555–567.
Meyers, G., Saalmuller, A., Buttner, M., 1999. Mutations abrogating the RNase activity in glycoprotein E(rns) of the pestivirus classical swine fever virus lead to virus attenuation. J. Virol. 73, 10224–10235.
Mukhopadhyay, D., Dasso, M., 2007. Modification in reverse: the SUMO proteases. Trends Biochem. Sci. 32, 286–295.
Murray, C.L., Marcotrigiano, J., Rice, C.M., 2008. Bovine viral diarrhea virus core is an intrinsically disordered protein that binds RNA. J. Virol. 82, 1294–1304.
Niedenthal, R., 2007. Ubc9 fusion-directed SUMOylation (UFDS). Biochem. Soc. Trans. 35, 1430–1432.
Okuma, T., Honda, R., Ichikawa, G., Tsumagari, N., Yasuda, H., 1999. In vitro SUMO-1 modification requires two enzymatic steps, E1 and E2. Biochem. Biophys. Res. Commun. 254, 693–698.
Otsuka, M., Kato, N., Lan, K., Yoshida, H., Kato, J., Goto, T., Shiratori, Y., Omata, M., 2000. Hepatitis C virus core protein enhances p53 function through augmentation of DNA binding affinity and transcriptional ability. J. Biol. Chem. 275, 34122–34130.
Palacios, S., Perez, L.H., Welsch, S., Schleich, S., Chmielarska, K., Melchior, F., Locker, J.K., 2005. Quantitative SUMO-1 modification of a vaccinia virus protein is required for its specific localization and prevents its self-association. Mol. Biol. Cell 16, 2822–2835.
Ray, R.B., Ray, R., 2001. Hepatitis C virus core protein: intriguing properties and functional relevance. FEMS Microbiol. Lett. 202, 149–156.
Reed, L.J., Muench, H.A., 1938. A simple method of estimating fifty per cent endpoints. Am. J. Hyg. 27, 493–497.
Rice, C.M., 1996. *Flaviviridae*: the viruses and their replication, In: Knipe, B.N.F.D.M., Howley, P. (Eds.), Fundamental Virology, Third ed. Lippincott Raven, Philadelphia, pp. 931–959.
Risatti, G.R., Borca, M.V., Kutish, G.F., Lu, Z., Holinka, L.G., French, R.A., Tulman, E.R., Rock, D.L., 2005a. The E2 glycoprotein of classical swine fever virus is a virulence determinant in swine. J. Virol. 79, 3787–3796.
Risatti, G.R., Holinka, L.G., Lu, Z., Kutish, G.F., Tulman, E.R., French, R.A., Sur, J.H., Rock, D. L., Borca, M.V., 2005b. Mutation of E1 glycoprotein of classical swine fever virus affects viral virulence in swine. Virology 343, 116–127.
Risatti, G.R., Holinka, L.G., Carrillo, C., Kutish, G.F., Lu, Z., Tulman, E.R., Sainz, I.F., Borca, M.V., 2006. Identification of a novel virulence determinant within the E2 structural glycoprotein of classical swine fever virus. Virology 355, 94–101.
Risatti, G.R., Holinka, L.G., Fernandez Sainz, I., Carrillo, C., Lu, Z., Borca, M.V., 2007. N-linked glycosylation status of classical swine fever virus strain Brescia E2 glycoprotein influences virulence in swine. J. Virol. 81, 924–933.
Rodriguez, M.S., Dargemont, C., Hay, R.T., 2001. SUMO-1 conjugation *in vivo* requires both a consensus modification motif and nuclear targeting. J. Biol. Chem. 276, 12654–12659.
Sadanari, H., Yamada, R., Ohnishi, K., Matsubara, K., Tanaka, J., 2005. SUMO-1 modification of the major immediate-early (IE) 1 and 2 proteins of human cytomegalovirus is regulated by different mechanisms and modulates the intracellular localization of the IE1, but not IE2, protein. Arch. Virol. 150, 1763–1782.
Sampson, D.A., Wang, M., Matunis, M.J., 2001. The small ubiquitin-like modifier-1 (SUMO-1) consensus sequence mediates Ubc9 binding and is essential for SUMO-1 modification. J. Biol. Chem. 276, 21664–21669.
Sanger, F., Nicklen, S., Coulson, A.R., 1977. DNA sequencing with chain-terminating inhibitors. Proc. Natl. Acad. Sci. U. S. A. 74, 5463–5467.
Sarge, K.D., Park-Sarge, O.K., 2009. Sumoylation and human disease pathogenesis. Trends Biochem. Sci. 34, 200–205.
Seeler, J.S., Dejean, A., 2003. Nuclear and unclear functions of SUMO. Nat. Rev. Mol. Cell Biol. 4, 690–699.
Shimoike, T., Mimori, S., Tani, H., Matsuura, Y., Miyamura, T., 1999. Interaction of hepatitis C virus core protein with viral sense RNA and suppression of its translation. J. Virol. 73, 9718–9725.
Shirai, C., Mizuta, K., 2008. SUMO mediates interaction of Ebp2p, the yeast homolog of Epstein–Barr virus nuclear antigen 1-binding protein 2, with a RING finger protein Ris1p. Biosci. Biotechnol. Biochem. 72, 1881–1886.
Tanaka, Y., Shimoike, T., Ishii, K., Suzuki, R., Suzuki, T., Ushijima, H., Matsuura, Y., Miyamura, T., 2000. Selective binding of hepatitis C virus core protein to synthetic oligonucleotides corresponding to the 5′ untranslated region of the viral genome. Virology 270, 229–236.
Tellinghuisen, T.L., Rice, C.M., 2002. Interaction between hepatitis C virus proteins and host cell factors. Curr. Opin. Microbiol. 5, 419–427.
Terpstra, C., Woortmeyer, R., Barteling, S.J., 1990. Development and properties of a cell culture produced vaccine for hog cholera based on the Chinese strain. Dtsch. Tierarztl. Wochenschr. 97, 77–79.
Tews, B.A., Schurmann, E.M., Meyers, G., 2009. Mutation of cysteine 171 of pestivirus E^{rns} RNase prevents homodimer formation and leads to attenuation of classical swine fever virus. J. Virol. 83, 4823–4834.
Tomoiu, A., Gravel, A., Tanguay, R.M., Flamand, L., 2006. Functional interaction between human herpesvirus 6 immediate-early 2 protein and ubiquitin-conjugating enzyme 9 in the absence of sumoylation. J. Virol. 80, 10218–10228.
Van Gennip, H.G., Vlot, A.C., Hulst, M.M., De Smit, A.J., Moormann, R.J., 2004. Determinants of virulence of classical swine fever virus strain Brescia. J. Virol. 78, 8812–8823.
Yao, Z.Q., Nguyen, D.T., Hiotellis, A.I., Hahn, Y.S., 2001. Hepatitis C virus core protein inhibits human T lymphocyte responses by a complement-dependent regulatory pathway. J. Immunol. 167, 5264–5272.
Yao, Z.Q., King, E., Prayther, D., Yin, D., Moorman, J., 2007. T cell dysfunction by hepatitis C virus core protein involves PD-1/PDL-1 signaling. Viral Immunol. 20, 276–287.
Yoshida, T., Hanada, T., Tokuhisa, T., Kosai, K., Sata, M., Kohara, M., Yoshimura, A., 2002. Activation of STAT3 by the hepatitis C virus core protein leads to cellular transformation. J. Exp. Med. 196, 641–653.
You, L.R., Chen, C.M., Yeh, T.S., Tsai, T.Y., Mai, R.T., Lin, C.H., Lee, Y.H., 1999. Hepatitis C virus core protein interacts with cellular putative RNA helicase. J. Virol. 73, 2841–2853.
Yueh, A., Leung, J., Bhattacharyya, S., Perrone, L.A., de los Santos, K., Pu, S.Y., Goff, S.P., 2006. Interaction of Moloney murine leukemia virus capsid with Ubc9 and PIASy mediates SUMO-1 addition required early in infection. J. Virol. 80, 342–352.
Zhong, N., Radu, G., Ju, W., Brown, W.T., 2005. Novel progerin-interactive partner proteins hnRNP E1, EGF, Mel 18, and UBC9 interact with lamin A/C. Biochem. Biophys. Res. Commun. 338, 855–861.
Zsak, L., Lu, Z., Kutish, G.F., Neilan, J.G., Rock, D.L., 1996. An African swine fever virus virulence-associated gene NL-S with similarity to the herpes simplex virus ICP34.5 gene. J. Virol. 70, 8865–8871.

Return to Table of Contents

Virus Research 151 (2010) 10–18

Contents lists available at ScienceDirect

Virus Research

journal homepage: www.elsevier.com/locate/virusres

Patterns of gene expression in swine macrophages infected with classical swine fever virus detected by microarray

Douglas P. Gladue, James Zhu, Lauren G. Holinka, Ignacio Fernandez-Sainz, Consuelo Carrillo, Melanie V. Prarat, Vivian O'Donnell, Manuel V. Borca *

Plum Island Animal Disease Center, Agricultural Research Service, US Department of Agriculture, Greenport, NY 11944, United States

ARTICLE INFO

Article history:
Received 11 January 2010
Received in revised form 11 March 2010
Accepted 12 March 2010
Available online 17 March 2010

Keywords:
Classical swine fever virus
Virulence
Pathogenesis
Microarray
CSFV
Immune response

ABSTRACT

Infection of domestic swine with highly virulent, classical swine fever virus (CSFV) strain Brescia, causes lethal disease in all infected animals. However, the molecular mechanisms involved in modulating the host cellular processes and evasion of the immune response have not been clearly established. To gain insight into, the early host response to CSFV, we analyzed the pattern of gene expression in infected swine macrophages, using custom designed swine microarrays. Macrophages, the target cell for CSFV infection, were isolated from primary cultures of peripheral blood mononuclear cells, allowing us to utilize identical uninfected macrophages at the same time points as CSFV-infected macrophages, allowing only genes induced by CSFV to be identified. First, microarray probes were optimized by screening 244,000 probes for hybridization with RNA from infected and uninfected macrophages. Probes that hybridized and passed quality control standards were used to design a 44,000 probe microarray for this study. Changes in expression levels of 79 genes (48 up- and 31 down-regulated) during the first 48 h post-infection were observed. As expected many of the genes with an altered pattern of expression are involved in the development of an innate immune response. Several of these genes had differential expression in an attenuated strain NS4B.VGIv, suggesting that some of these differences are responsible for virulence. The observed gene expression profile might help to explain the immunological and pathological changes associated with infection of pigs with CSFV Brescia.

Published by Elsevier B.V.

1. Introduction

Classical swine fever (CSF) is a highly contagious disease of swine that is characterized by fever, hemorrhage, leukopenia, abortion, and high mortality. The etiological agent, CSF virus (CSFV), is classified as a *Pestivirus*, along with Bovine Viral Diarrhea Virus (BVDV) and Border Disease Virus (BDV), within the family *Flaviviridae* (Becher et al., 2003). Like other members of the family, including the genera *Flavivirus* and *Hepacivirus*, pestiviruses are small, enveloped viruses with a positive, single-stranded RNA genome. The 12.5 kb CSFV genome consists of one large open reading frame (ORF) that encodes an approximately 4000-amino-acid polyprotein which is co- and post-translationally processed into 11–12 final cleavage products (NH_2-Npro-C-E^{rns}-E1-E2-p7-NS2-NS3-NS4A-NS4B-NS5A-NS5B-COOH) using cellular and viral proteases (Rice, 1996). The ORF is flanked by untranslated regions (UTRs) that are highly conserved among virus isolates (Risatti et al., 2003).

Acute and chronic forms of CSF can be distinguished based on virulence and host range phenotype. Infection with highly virulent CSFV strains leads to morality rates approaching 100%, whereas isolates of moderate to low virulence induce a prolonged chronic disease (van Oirschot, 1999). In addition, BVDV and BDV, etiologic agents of disease in bovine and ovine species, respectively, can also infect swine without inducing clinical disease (van Oirschot, 1999). Despite the availability of various CSFV genomic sequences representing varying virulence phenotypes, the genetic basis of CSFV virulence in the natural host remains poorly understood (van Oirschot, 1999). However, several viral determinants of virulence have been identified: in Npro (Mayer et al., 2004; Meyers et al., 1999; Moser et al., 2001; Risatti et al., 2005a,b, 2006, 2007a,b; Ruggli et al., 2005, 2003; Tratschin et al., 1998; van Gennip et al., 2002, 2004, 2005; van Rijn et al., 1994).

The Brescia strain of CSFV has a highly virulent pathotype; infected animals die within 8–14 days after exposure. Brescia rep-

* Corresponding author at: Plum Island Animal Disease Center, USDA/ARS/NAA, P.O. Box 848, Greenport, NY 11944-0848, United States. Tel.: +1 631 323 3019; fax: +1 631 323 3006.
E-mail addresses: Douglas.Gladue@ars.usda.gov (D.P. Gladue), James.Zhu@ars.usda.gov (J. Zhu), Lauren.Holinka@ars.usda.gov (L.G. Holinka), Ignacio.Fernandez-Sainz@ars.usda.gov (I. Fernandez-Sainz), Melanie.Prarat@ars.usda.gov (M.V. Prarat), Vivian.Odonnell@ars.usda.gov (V. O'Donnell), manuel.borca@ars.usda.gov (M.V. Borca).

0168-1702/$ – see front matter Published by Elsevier B.V.
doi:10.1016/j.virusres.2010.03.007

Table 1
Gene expression (changes ≥2-fold) at 24 h and 48 hpi.

		WT	WT	VGI	VGI	*p*-Value
		24 h	48 h	24 h	48 h	
Immune response						
IL-8	Interleukin-8	9.09	6.44	**32.46**	**10.24**	<1.00E−07
CXCL5	Chemokine (C–X–C motif) ligand 5	7.47	6.11	**28.05**	**13.67**	<1.00E−07
CXCR4	Chemokine (C–X–C motif) receptor 4 isoform b	3.93	5.21	**6.10**	5.21	<1.00E−07
IL-1β	Interleukin-1 beta	3.78	3.89	**10.43**	4.02	2.86E−06
CXCL2	Chemokine (C–X–C motif) ligand 2	2.89	2.61	**7.70**	3.41	1.45E−05
IL1R2	Interleukin 1 receptor, type II	2.69	3.85	**9.70**	**8.86**	<1.00E−07
Transcription factors						
EPAS1	Endothelial PAS domain protein 1	2.68	2.83	**6.31**	**5.97**	1.00E−06
ETS2	Similar to v-ets erythroblastosis virus E26 oncogene homolog 2	2.46	2.21	**4.61**	3.31	1.00E−06
Nitric oxide inhibitors						
ARG1	Arginase, type I	4.43	6.30	**8.05**	**9.06**	<1.00E−07
PPARG	Peroxisome proliferative activated receptor gamma isoform 2	2.27	2.03	**5.45**	5.89	3.05E−05
Amino acid transporter						
SLC7A11	Solute carrier family 7, member 11	3.09	2.71	**5.12**	3.87	1.50E−06
Unknown protein function						
TM7SF4	Transmembrane member 7 superfamily 4	2.53	2.75	**5.46**	**6.79**	3.56E−03

Bold values represent a <2 fold change of VGI compared to WT.

resents the genotype 1 group (Lowings et al., 1994) of CSFV isolates that consists of virulent strains isolated before 1964 (including Eystrup, Weybridge, ALD, Alfort/187) that presumably no longer are in global circulation among swine populations. Highly virulent CSFV strains, like Brescia, produce a consistent clinical outcome in swine, providing a reliable method for studying viral mechanisms underlying virulence, pathogenesis, and virus–host interactions. Here we have used the Brescia strain to study the response of swine macrophages, a CSFV primary target cell *in vivo*, upon infection. Cultured primary swine macrophages were infected with CSFV Brescia derived from an infectious cDNA clone, pBIC (Risatti et al., 2005a). Microarray analysis was implemented in order to characterize the *in vitro* macrophage response to infection by virulent CSFV Brescia by assessing changes in patterns of gene expression in peripheral blood-derived swine macrophages. Our results describe changes in levels of expression of 148 genes during the first 48 h following the infection. The observed gene expression profile might help to explain the immunological and pathological changes characteristically associated with infection of pigs with CSFV Brescia.

2. Results and discussion

Microarray analysis was used to characterize the early host macrophage response to infection by virulent CSFV Brescia by assessing changes in patterns of gene expression in peripheral blood-derived swine macrophages infected *in vitro* with highly virulent CSFV Brescia strain. Macrophages have been described as the primary target cell of CSFV infection *in vivo* and appear to play a central role in the pathogenesis of the infection (Gomez-Villamandos et al., 2001; Sanchez-Cordon et al., 2002, 2003; Summerfield et al., 1998). Primary swine macrophages were used so that we could differentiate gene expression changes directly caused by CSFV, by utilizing a negative control of uninfected macrophages from the same animal at identical time points. We used *in vitro* conditions where the majority of cultured cells were characterized by direct immunofluorescence as macrophages since 88.5% are CD14+ (SD = 3.7), 14.9% CD3+ (SD = 2.1), 13.4% SLA-DR+ (SD = 3.1) and 4.69% CD27+ (SD = 2.76) (data not shown). At time of harvesting most of the cells were infected (84.1% with a SD of 6.4), being positive for the expression of the CSFV structural glycoprotein E2 (data not shown).

Changes in primary swine macrophage gene expression profiles during CSFV infection as determined by microarray analysis, showed a significant up-regulation of 12 genes (more than a 2-fold increase with a *p*-value of <0.05) at both sample time points (Table 1). These genes can be functionally divided into several groups: immune response processes, transcription factors, inhibitors of nitric oxide, amino acid transportation, and some of unknown protein function. Eleven genes were up-regulated more than 2-fold ($p \leq 0.05$) only at 24 hpi: genes involved in regulating the immune response, protein phosphorylation, nucleic acid salvage, glucose transporter and other with unclassified function (Table 2). Finally, at 48 hpi, 28 genes were up-regulated and 31 genes were down-regulated (more than 2-fold) (Tables 3–6). These genes are involved in immune response pathways, DNA replication,

Table 2
Genes with expression increased (≥2-fold) at 24 hpi.

Immune response	Gene name	WT	VGI	*p*-Value
CCL7	Chemokine (C–C motif) ligand 7	3.68	**8.33**	2.10E−05
CCL8	Chemokine (C–C motif) ligand 8	3.64	**7.66**	1.70E−05
CMPK2	Cytidine monophosphate (UMP-CMP) kinase 2, mitochondrial	4.21	2.27	7.52E−03
EPSTI1	Epithelial stromal interaction 1 isoform 1	3.68	2.47	8.80E−03
IFIH1	Interferon induced with helicase C domain 1	3.18	2.24	1.51E−03
ISG15	ISG15 ubiquitin-like modifier	3.54	2.72	<1.00E−07
MTMR7	myotubularin related protein 7	2.56	**7.94**	6.42E−04
MX1	myxovirus resistance protein 1	4.00	2.63	3.16E−03
OAS1	2′,5′-Oligoadenylate synthetase 1 isoform 2	3.85	2.28	1.72E−03
SLC2A3	Solute carrier family 2 (facilitated glucose transporter), member 3	2.64	**6.04**	2.00E−06
SLC46A2	Solute carrier family 46, member 2	2.22	**5.05**	0.003555

Bold values represent a <2 fold change of VGI compared to WT.

Table 3
Increased expression in immune response genes (≥2-fold) at 48 hpi.

Gene name		WT	VGI	*p*-Value
Up-regulated				
AoAH	Acyloxyacyl hydrolase (neutrophil)	3.07	3.00	1.80E−05
SAA3	Serum amyloid A3	5.57	6.12	4.10E−04
SAA4	Serum amyloid A4	4.34	4.68	3.14E−04
SAA1	Serum amyloid A1	4.34	4.54	2.12E−04
SAA2	Serum amyloid A2	3.92	4.10	1.82E−04
BTG1	B-cell translocation protein 1	2.28	1.55	7.34E−04
Down-regulated				
BANK1	B-cell scaffold protein with ankyrin repeats 1 isoform 2	−3.93	−4.85	1.00E−06
SLA-1	MHC class I antigen 1	−4.58	−1.85	3.39E−02
ITGA4	Integrin alpha 4	−3.43	−2.64	<1.00E−07
C4BPA	Complement component 4 binding protein, alpha	−3.14	−6.43	4.66E−05
HLA-DMB	Major histocompatibility complex, class II, DM beta	−2.41	−1.38	<1.00E−07

Table 4
DNA replication gene expression down-regulated (≥2-fold) at 48 hpi.

Symbol	Gene name	WT	VGI	*p*-Value
CDC45L	CDC45-like	−2.26	−1.13	2.46E−02
HIST1H2AG	Histone cluster 1, H2ag	−2.81	−1.36	3.52E−03
MAD2L1	MAD2-like 1	−2.51	−1.45	2.81E−02
MCM4	Minichromosome maintenance complex component 4	−2.86	−1.40	1.03E−02
MSH6	MutS homolog 6	−2.23	−1.40	2.12E−03
RECQL4	RecQ protein like 4	−2.79	−1.42	1.32E−02
SMC2	Structural maintenance of chromosomes 2 like 1	−2.51	−1.42	1.35E−03
SPC24	Spindle pole body component 24	−3.49	−1.52	1.49E−02

Table 5
Up-regulated gene expression (≥2-fold) at 48 hpi.

Symbol	Gene name	WT	VGI	*p*-Value
CTSL1	Cathepsin L1 preproprotein	2.07	2.68	8.59E−04
DUSP1	Dual specificity phosphatase 1	2.77	1.34	9.59E−04
FAM14A	Family with sequence similarity 14, member A	2.62	1.40	1.59E−02
FJX1	Four jointed box 1	2.39	1.64	1.96E−03
GYG2	Glycogenin 2 isoform a	2.78	3.12	1.95E−03
HIP1R	Huntingtin interacting protein 1	2.60	2.63	1.00E−06
MALAT1	Metastasis associated lung adenocarcinoma transcript 1	2.67	2.73	4.71E−06
NRP1	Neuropilin 1	2.41	2.10	8.11E−03
OTUD3	OTU domain containing 3	2.47	2.24	<1.00E−07
PAQR5	Progestin and adipoQ receptor family member V	2.13	3.34	8.00E−06
RFTN1	Raft-linking protein	2.07	2.11	3.10E−05
RPL37A	Ribosomal protein L37a	2.24	2.37	1.05E−04
SDC1	Syndecan 1	2.21	2.28	1.00E−04
SDS	Serine dehydratase	2.00	1.86	1.52E−04
SNORD12B	Small nucleolar RNA, C/D box 12B	2.38	2.74	1.70E−05
ZNF503	Zinc finger protein 503	2.34	2.00	1.40E−05

Table 6
Down-regulated gene expression (≥2-fold) at 48 hpi.

Symbol	Gene name	WT	VGI	*p*-Value
ACP5	Acid phosphatase 5, tartrate resistant	−2.43	**−5.72**	7.37E−05
CD36	CD36 antigen	−2.20	**−5.82**	2.20E−05
CST3	Cystatin C	−2.41	−3.17	1.41E−04
DUT	Deoxyuridine triphosphatase isoform 1	−2.27	−1.37	7.70E−03
E2F2	E2F transcription factor 2	−3.72	−2.15	1.75E−04
FAM149A	Family with sequence similarity 149, member A	−2.68	−2.62	<1.00E−07
GGCT	Gamma-glutamyl cyclotransferase	−2.28	−1.83	<1.00E−07
MRC2	Mannose receptor, C type 2	−3.00	−3.91	1.00E−06
MTSS1	Metastasis suppressor 1	−2.33	−2.07	5.20E−05
PLBD1	Phospholipase B domain containing 1	−2.62	−4.08	1.10E−05
PTRF	Polymerase I and transcript release factor	−3.07	−3.06	3.06E−03
SEPP1	Selenoprotein P, plasma, 1	−2.27	**−5.56**	2.47E−05
SNN	Stannin	−2.03	−2.07	3.39E−03
TCF19	Transcription factor 19	−5.63	**−2.12**	2.90E−02
TUBB6	Tubulin, beta 6	−4.51	−3.56	7.00E−06
UF	Uteroferrin	−2.28	**−6.05**	5.06E−04

Bold values represent a <2 fold change of VGI compared to WT.

post-translational protein modification, cell movement, cysteine proteases, amino acid metabolism, protein transcription, apoptosis, iron binding, caveolae formation, as well as various other functions.

2.1. Cytokines and chemokines related genes

CSFV, as well as other viruses, successfully evade the immune system and insures their own survival by modulating the host immune response (Bensaude et al., 2004; Doceul et al., 2008; Ruggli et al., 2003; Schweizer et al., 2006; Seago et al., 2007). Previous studies have focused on genes regulating adhesion and trafficking of different types of leukocytes to further understand the mechanisms of CSFV pathogenesis (Bautista et al., 2002; Borca et al., 2008; Carrasco et al., 2004). Results presented here identified increased gene expression of several proinflammatory cytokines/chemokines at 24 and/or 48 hpi in *in vitro* CSFV-infected macrophages. Interleukin-1 beta (IL-1β) was up-regulated 3.78- and 3.89-fold at 24 and 48 hpi, respectively. IL-1β is produced by activated macrophages, in response to infection, and both are critical mediators of the inflammatory response. The interleukin 1 receptor type II (IL1R2) was up-regulated 2.69- and 3.85-fold at 24 and 48 hpi, respectively. IL1R2 is a decoy receptor which binds and deactivates IL-1α, IL-1β and IL1R1, possibly to help keep the IL-1 from stimulating cells which secrete IL-1. These results are in accordance with our previous reports showing increased accumulation IL-1β (Borca et al., 2008; Zaffuto et al., 2007) mRNA in swine macrophages following CSFV Brescia infection.

Proinflammatory cytokines, cell adhesion molecules and blood coagulation factors induced in endothelial cells likely contribute to the appearance of vascular lesions characteristic of CSF (Bautista et al., 2002; Knoetig et al., 1999; Gomez-Villamandos et al., 2000; Sanchez-Cordon et al., 2002, 2003). IL-1 is a potent inducer of vascular permeability and mediates pathologic changes that favor development of high fever, coagulation defects, and bleeding observed in infections with some single-stranded RNA viruses (Bray and Geisbert, 2005). Macrophages are an important source of signaling mediators, such as IL-1 that affects the vascular dysfunctions observed in swine during CSFV Brescia infection. Another function of IL-1 involves activation of endothelial cells leading to the expression of adhesion molecules, and recruitment of leukocytes to inflammatory sites (Gabay, 2006). IL-1 stimulates the production and release of potent chemokines such as interleukin-8 (IL-8), chemokine (C–X–C motif) ligand 5 (CXCL5), chemokine (C–C motif) ligand 7 (CCL7), and chemokine (C–C motif) ligand 8 (CCL8) (Bersinger et al., 2008; Gouwy et al., 2008; Van Coillie et al., 1999). Our results show up-regulation of these chemokines: CXCL5 (7.47- and 6.11-fold at 24 and 48 hpi, respectively), IL-8 (9.09- and 6.44-fold at 24 and 48 hpi, respectively), CCL7 (3.68-fold at 24 hpi), and CCL8 (3.64-fold at 24 hpi). Additionally, chemokine CXCL2 was up-regulated (2.89- and 2.61-fold at 24 and 48 hpi, respectively), and chemokine (C–X–C motif) receptor 4 isoform b (CXCR4) (3.93- and 5.21-fold at 24 and 48 hpi, respectively). These observations, together with mast cell degranulation and activation of the complement system in infected swine (Gomez-Villamandos et al., 2000), may account for the vascular dysfunctions observed during *in vivo* CSFV infection. The increased gene expression of particular cytokines/chemokines in CSFV infection may be responsible for monocyte/macrophage activation and the recruitment of different types of leukocytes to sites of inflammation; together these cytokines may contribute to leukocyte infiltration and to the production of an antiviral state during infection. Although the up-regulation of most of these genes constitutes a novel report, the elevated transcription levels of IL-8 gene and CCL8 (also named MCP-2) have already been reported by us (Borca et al., 2008) and others (Bensaude et al., 2004).

Endothelial pas domain protein 1 (EPAS1) is a hypoxia induced transcription factor that is up-regulated 2.68- and 2.83-fold at 24 and 48 hpi, respectively. This transcription factor is involved in mediating the inflammatory response caused by IL-1β (Tanaka et al., 2002). Another transcription factor, V-ets erythroblastosis virus E26 oncogene homolog 2 (ETS2), up-regulated 2.46- and 2.21-fold at 24 and 48 hpi, respectively, is involved in the regulation of cytokine expression (Gallant and Gilkeson, 2006). It is not surprising that CSFV infection causes up-regulation of transcription factors especially those involved in the regulation of cytokine expression, or the inflammatory response.

Interferon stimulated protein 15 kDa (ISG15) is an ubiquitin-like modifier that is up-regulated 3.54-fold at 24 hpi (Table 2). ISG15 becomes conjugated to many cellular proteins in response to INF-α and INF-β. ISG15 inhibits NF-κB activation and has critical roles in the innate immune response, especially in the regulation of INF signaling (Zhao et al., 2005). ISG15 is the critical component in IFN-mediated inhibition of HIV-1 release, which may also be true for CSFV infection (Okumura et al., 2006).

The 2′,5′-oligoadenylate synthetase 1 (OAS1) gene is up-regulated 3.85-fold at 24 hpi. OAS1 is essential in the development of the innate immune response to viral infection. Induced by INF, OAS1 activates RNAase L which degrades viral RNA and prevents viral replication (Austin et al., 2005; Scherbik et al., 2006).

Interferon induced with helicase C domain 1 (IFIH1) is a dead box gene found to be up-regulated 3.18-fold at 24 hpi. IFIH1 is induced with either IFN-α or IFN-β. DEAD box proteins have a conserved Asp-Glu-Ala-Asp motif, and are putative RNA helicases that are implicated in a number of cellular processes including alteration of RNA secondary structure. Many viruses utilize DEAD box proteins for altering their own RNA secondary structure (Ariumi et al., 2007; Kalverda et al., 2009; Owsianka and Patel, 1999; Wang et al., 2009), thus suggesting the possibility that IFIH1 could be involved in altering CSFV RNA secondary structure to modulate replication and translation of CSFV.

2.2. Other immunologically relevant genes

There is a rather functionally heterogeneous group of immunologically relevant genes that have decreased levels of gene expression at 48 hpi (Table 3). Down-regulation of these genes, could in several scenarios, facilitate the spread of virus during infection. For example, MHC class I antigen 1 (SLA-1) is down-regulated −4.58-fold. Down-regulation of SLA-1 prevents lysis of infected cells by cytotoxic T-cells (Crotzer and Blum, 2009). Thus, this down-regulation would help to decrease the immune response against viral antigens. B-cell scaffold protein with ankyrin repeats 1 (BANK1) demonstrated significantly lower levels of expression (−3.93-fold) at 48 hpi. BANK1 is a B-cell-specific scaffold protein that appears to be a novel scaffold protein that regulates, B-cell antigen receptor induced calcium mobilization, by connecting protein tyrosine kinases to inositol 1,4,5-trisphosphate receptors (Yokoyama et al., 2002). Integrin alpha 4 (ITGA4) is down-regulated −3.43-fold. Integrin down-regulation has been shown with a number of viruses as a way to neutralize the host immune response (Dransfield et al., 1990; Takada et al., 2000). Down-regulation of complement component 4 binding protein (C4BPA) (−3.14-fold), an inhibitor of complement activation (Borsos, 1989).

In contrast to the down-regulation of genes just described, a group of genes (Table 3) are up-regulated at 48 hpi, perhaps as a result of the emergent immune response triggered by the initial steps of virus replication. B-cell translocation gene 1 (BTG1), up-regulated 2.28-fold, is an anti-proliferative gene that interacts with several nuclear receptors, regulating cell growth and differentiation. Serum amyloid proteins (SAA1, SAA2, SAA3, and SAA4) were

up-regulated 4.34-, 3.92-, 5.57-, and 4.34-fold, respectively. SAA proteins are up-regulated in response to IL-1, and are known to play important roles in the acute phase of the inflammatory reaction and in the functionality of the innate immune response (Vallon et al., 2001). Acyloxyacyl hydrolase (AoAH) gene was up-regulated 3.07-fold. AoAH plays a role in the inflammatory response predominately to bacterial endotoxins.

Activated macrophages, stimulated by gamma interferon (Noel et al., 2004), eradicate invading microorganisms through direct generation of cytotoxic products such as nitric oxide a product obtained from L-arginine by the nitric oxide synthase (Noel et al., 2004; Rauh et al., 2005). Macrophages having altered nitric oxide synthase function, cannot limit the growth of intracellular pathogens efficiently (Noel et al., 2004). Two genes involved in the inhibition of nitric oxide synthase were up-regulated in swine macrophages infected by CSFV. Peroxisome proliferative activated receptor gamma isoform 2 (PPARG) was up-regulated 2.27- and 2.03-fold at 24 and 48 hpi, respectively, while arginase-1 (Arg1) was up-regulated 4.43- and 6.3-fold at 24 and 48 hpi, respectively. Both PPARG and ARG1 are inhibitors of nitric oxide in activated macrophages. PPARG has been shown to inhibit inducible nitric oxide synthase (Ricote et al., 1998). The inhibition of nitric oxide may be induced by CSFV to prevent the effects of IL-1β, and promote virus survival in macrophages. Similar results for Arg1 up-regulation were seen in our previous studies (Zaffuto et al., 2007).

Myxovirus resistance 1 (MX1) is up-regulated 4-fold at 24 hpi. Mx1 belongs to the class of dynamin-like large GTPases, known to be involved in intracellular vesicle trafficking, organelle homeostasis. Mx1 has been shown to block several virus in their replication, such as influenza viruses, members of the bunyavirus family and African swine fever virus (Netherton et al., 2009; Stertz et al., 2007). Although up-regulation of OAS1 or MX1 may be unfavorable for CSFV, it is a host response to CSFV infection, and its possible that CSFV blocks a downstream component of the OAS1 and MX1 pathways.

Additionally, manipulation of protein phosphorylation was up-regulated. Dual specificity phosphatase 1 (DUSP1) was up-regulated 2.77-fold at 48 hpi. DUSP1 has sequence similarity to Vaccina virus late gene H1, which prevents the phosphorylation of Stat1 and Stat2 when stimulated with INF-α or INF-β (Mann et al., 2008). The up-regulation of DUSP1, and down-regulation of kinases, suggest that this is a mechanism used by CSFV to evade the host immune system.

2.3. Genes involved in DNA replication

Eight genes that are involved in DNA replication had increased gene expression levels at 48 hpi (Table 4), and two genes had increased gene expression levels at 28 hpi (Table 4). Decreased expression of DNA replication genes during CSFV infection is likely due to the virus trying to increase its own nucleic acid replication at the expense of the host DNA replication machinery. Minichromosome maintenance complex components 4 (MCM4) is down-regulated −2.86-fold. MCM4 is part of the minichromosome maintenance complex, essential for the initiation of DNA replication. MCM4 has DNA helicase activity and functions by unwinding the DNA, and possibly initiates the replication fork (Kanter et al., 2008). CDC45-like protein (CDC45L), shown to interact with the minichromosome maintenance complex, is also down-regulated −2.26-fold RecQ protein like 4 (RECQL4) is down-regulated −2.79-fold and is involved in DNA replication and is thought to modulate the replication fork. During DNA replication, chromatin assembly constitutes a critical step. Several genes that we found down-regulated in macrophages 48 hpi with CSFV are involved in chromatin assembly. Histone cluster 1 family 2AG (HIST1H2AG), was down-regulated −2.81 fold, and is a component of the histone octomer, in which DNA is wrapped around to form condensed chromosomes (Kaufman et al., 1995). Structural maintenance of chromosomes 2 (SMC2) was down-regulated −2.51-fold and is one of the core components of condensin complexes, and is responsible for chromosome assembly (Losada and Hirano, 2005).

Several DNA integrity proteins were also found to be down-regulated at 48 hpi in CSFV-infected swine macrophages. DNA integrity proteins are involved in the process of ensuring that DNA remains intact and without errors. RECQ protein like 4 (RECQL4), down-regulated −2.79-fold, is involved in the response to DNA damage and repair of DNA double-stranded breaks in homologous recombination (Fan and Luo, 2008). MutS Homolog 6 (MSH6), down-regulated −2.23-fold, is involved in recognizing mismatched nucleotides so they can be repaired (Yang et al., 2004).

Chromatin separation is essential for cell division. Once chromosomes are replicated they have to separate so that cell division can occur. In this process, formation of the centromere is a critical step. We found two cell transcripts involved in this process, that were down-regulated in swine macrophages 48 hpi (Table 4). Spindle pole body component 24 (SPC24), down-regulated −3.49-fold is a protein involved in the active kinetochore complex (Ma et al., 2007). MAD2-like protein 1 (MAD2L1) down-regulated −2.51-fold, prevents anaphase until the chromosomes are properly aligned (Ho et al., 2008).

2.4. Evaluating custom swine macrophage microarray for determining changes of transcription profiles in attenuated strains of CSFV

To gain a better understanding of attenuated strains of CSFV, it is important to have as a tool, a way to determine changes in transcription profiles in a broad microarray based approach. Therefore, the transcriptional activity of swine macrophages infected with an attenuated strain of CSFV was analyzed. This CSFV strain contains a triple mutation in the CSFV polyprotein (V2566A, G2567A, I2568A) in the non-structural protein NS4B. These mutations were introduced in order to delete a protein motif that resembles a Toll/Interleukin-1 receptor (TIR)-like domain. *In vivo*, NS4B.VGIv was completely attenuated in swine, displaying a reduced replication in the oronasal cavity and limited spread from the inoculation site to secondary target organs (Sainz et al., 2009).

In vitro growth characteristics of the mutant virus NS4B.VGIv relative to parental BICv was evaluated in a multistep growth curve during the first 24 h post-infection. Primary swine macrophage cell cultures were infected at a MOI of 0.01 $TCID_{50}$. Virus was adsorbed for 1 h (time zero), and samples were collected at times post-infection through 24 h. NS4B.VGIv exhibited a slight disadvantage in growth characteristics when compared to BICv (Fig. 1A). Growth abilities analyzed between 24 and 72 h confirm this result although at 72 hpi titers of both viruses are undistinguishable (Fernadez Sainz et al., 2010). In addition, the kinetics of RNA synthesis in macrophages infected with either with BICv or NS4B.VGIv was evaluated by real time RT-PCR during the first 24 hpi. RNA isolation and detection was performed as described by Risatti et al. (2003). Consequent with the results obtained in the growth curve, RNA is produced earlier in BICv infected cultures than in those infected with NS4B.VGIv (Fig. 1B).

Comparison of the transcriptional activity of swine macrophages infected with NS4B.VGIv showed a increased activity of immunoregulatory genes particularly at 24 hpi: IL-8, CXCL5, CXCR4, IL-1β, CXCL2, IL1R2, CCL7, CCL8, MTMR7, SLC2A3, and SLC46A2 (with an increase of 3.57, 3.76, 1.55, 2.76, 2.66, 3.61, 2.26, 2.1, 3.1, 296, and 2.74 times over the BICv value, respectively) (Tables 1 and 2). As discussed earlier, IL-1β is a critical mediator of the inflammatory response, causing activation of endothelial cells leading to the expression of adhesion molecules, and recruit-

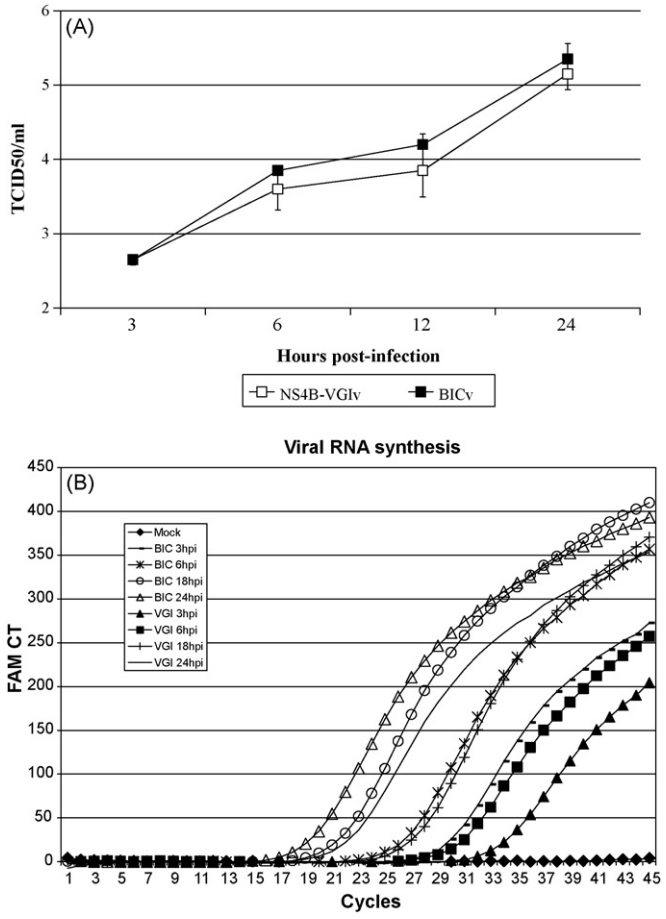

Fig. 1. (A) *In vitro* growth characteristics of CSFV NS4B.VGIv and parental BICv during the first 24 hpi. Primary swine macrophage cell cultures were infected (MOI = 0.01) with each of the mutants or BICv and virus yield titrated at times post-infection in SK6 cells. Data represent means and standard deviations from two independent experiments. Sensitivity of virus detection: $\geq \log_{10}$ 1.8 $TCID_{50}$/ml and (B) virus RNA synthesis in primary swine macrophage cell cultures as described in Risatti et al. (2003).

ment of leukocytes to inflammatory sites (Gabay, 2006). Higher expression of genes IL-8, CXCL5, CXCR4, CXCL2, CCL7 and CCL8 would favor the difference of immunoresponsive cells to the foci of infection, presumably restricting the spreading of infection.

Other genes with increased transcription in NS4B.VGIv at both 24 and 48 hpi are EPAS1 (2.35 and 2.22 times, respectively), PPARG (2.4 and 2.9 times, respectively), and TM7FS4 (2.15 and 2.46 times, respectively) (Table 1). Genes with decreased transcription 48 hpi are C4BPA, ACP5, CD36, SEPP1, and UF (2.05, 2.35, 2.65, 2.45, and 2.65 times below the BICv value, respectively) (Tables 5 and 6).

Previously we have analyzed the gene activation profile of swine macrophages infected either with NS4B.VGIv (Fernandez Sainz et al., 2010) or BICv by means of real time RT-PCR (Borca et al., 2008). This approach identified 8 genes differentially expressed in primary porcine macrophages infected with NS4B.VGIv or BICv: IL-8, AMCF-2, INF-α, IL-1α, IL-1β, IL-6, CCL8 and NCP-1. AMCF-1, AMCF-2, INF-α, IL-1α, and NCP-1 were slightly augmented at 24 hpi. IL-1β was significantly increased at 24 hpi, and increased levels of MCP-2 were detected at 48 hpi. Levels of IL-6 were significantly increased both at 24 and 48 hpi in cultures infected with NS4B.VGIv (Fernandez Sainz et al., 2010). Increases of IL-8, IL-1β, and CCL8 were presented here were also identified using a more targeted RT-PCR technique.

Our custom swine macrophage microarrays are useful in determining gene profile differences with attenuated strains of CSFV. However these arrays have there limitations, for one, several gene changes of unknown proteins were identified, and little can be extrapolated from this data: Genbank accession # AK232462, AK232504.1, AK23093.1, AK230767 and trophoblast derived non-coding RNA (−7.71, −3.38, 3.02, 3.89, 2.05, respectively at 48 hpi) in BICv. One of these AK230767 was shown to have a significant difference with NS4B.VGIv up-regulated 2.42-fold over BICv at 48 hpi. In addition genes such as IL-6 found to be significantly up-regulated in RT-PCR (Fernandez Sainz et al., 2010) were not found on our microarray, it is possible that our probes on the microarray are not adequate for detecting changes in IL-6. Some of the differences between the patterns of gene activation in macrophages infected either with BICv or NS4B.VGIv could be at least partially explained by the dissimilar amount of intracellular virus RNA which may differentially trigger the host cell responses. Nonetheless, our custom swine macrophage microarrays may be useful in a global approach to determine the genes involved in novel attenuated strains of CSFV.

Gene profiles during CSFV infection determined by microarray have been recently shown differently (Shi et al., 2009). In their study, monocytes were purified from pigs 7 days post-infection. We decided to look at early virus events, 24 and 48 hpi to determine the early infection gene profiles. Our analysis was performed in primary porcine macrophages so we could subtract uninfected similarly treated macrophages from the same pig at the same time points. We noticed a significant change in untreated macrophages over time, and differences between untreated macrophages between pigs, and found it necessary to subtract these background gene changes to have a workable number of genes directly influenced by CSFV infection. However, we see many general similarities with Shi's lab (Shi et al., 2009), in terms of changes in gene activation belonging to the same general groupings: kinase activity, immune response, apoptosis, receptor activity, signal transduction, cytokine and chemokine expression, cell cycle (DNA replication) and transcription proteins.

These results are a significant extension of our previous reports (Zaffuto et al., 2007; Borca et al., 2008). The same system (primary cell cultured blood-derived swine macrophages infected with CSFV strain Brescia) for determining changes in gene expression during CSFV infection was used. In fact, as expected, several genes having altered patterns of gene expression in previous studies are also described here (IL-1β, CCL8, IL-8, Arg1), corroborating results presented in our previous reports.

In summary, we presented here the altered transcriptional profile of 79 genes during the infection of swine macrophages with highly virulent CSFV strain Brescia. Most of the genes are involved in immunoregulatory/effector mechanisms of innate immune response. The observed gene expression profile might help to explain the immunological and pathological changes associated with infection of pigs with Brescia strain, a highly virulent CSFV. In addition our microarrays will be valuable for future studies to determine altered gene expression profiles *in vitro* for attenuated strains of CSFV. The complex patterns of gene expression observed here and by others, and the potential relationships inferred from those observations warrant further assessment of the role of those genes during infection in swine.

3. Materials and methods

3.1. RNA preparation

Primary swine macrophage cell cultures were derived from pig peripheral blood and were prepared as described (Zsak et al., 1996). CSFV Brescia (BICv) was derived from pBIC, an infectious cDNA clone (Risatti et al., 2005a). Macrophages were seeded in 6-well plates (Primaria Falcon, Becton Dickinson, Franklin Lakes, NY) and infected at MOI = 1. Macrophage infection experiments were performed in parallel using three different animals as a source of

macrophages. Total cellular RNA was extracted from primary swine macrophage cell cultures infected with indicated virus, or mock infected at 24 and 48 h post-infection (hpi) (representing the logarithmic phase of infectious virus assembly and release by infected cells and the peak of viral progeny yield, respectively) (Borca et al., 2008). Cells were harvested and lysed with Qiashredder columns (Qiagen, Valencia, CA) and RNA was isolated using an RNeasy mini kit (Qiagen) according to the manufacturer's instructions. The RNA quality was then determined using an Agilent 2100 bioanalyzer (Santa Clara, CA) using a RNA nanochip according to the procedures outlined by Agilent Technologies (Santa Clara, CA). RNA was quantified using a Nanodrop 1000 (Thermo Scientific, Waltham, MA).

3.2. DNA microarray design

All porcine EST and RNA sequences were downloaded from the NCBI database and assembled into unique sequences using the CAP3 software program (Huang and Madan, 1999). The resulting non-redundant sequences were used to design 60mer oligonucleotide microarray probes with a low probability of cross-reacting with other genes, with bias to the 3′-end of RNA sequences with ArrayDesigner 4.0 (Applied Biosystems, Foster City, CA). The probes were synthesized in a 244 K microarray by Agilent Technologies. This microarray was used to screen for probes that pass quality filtering using criteria recommended in the GenPix Pro 6.0 software program (Molecular Devices, Sunnyvalle, CA) after hybridization with microarray targets prepared from a pooled RNA sample of non-infected and CSFV-infected pig macrophages. The selected probes were synthesized on a smaller 44 K Agilent microarray for this study. The annotation of the porcine microarray was based on the results of BLAST searches human reference proteins, reference RNA, and all RNA and/or manual curation based on the porcine expressed sequences aligned in the bovine or porcine genome sequence on the UCSC genome browser and NCBI nucleotide database if possible.

3.3. Microarray analysis

Custom designed porcine microarrays were manufactured by Agilent Technologies and used for this study. A RNA sample pooled from all total RNA samples was labeled with Cy5 as a universal control, whereas the individual RNA samples were labeled with Cy3 using an Agilent low-input RNA labeling kit (Agilent Technologies). The Cy5-labeled control was co-hybridized with each Cy3-labeled sample in one array. The entire procedure of microarray analysis was conducted according to protocols provided by Agilent Technologies. Array slides were scanned using a GenePix 4000B scanner with the GenePix Pro 6.0 software at 5 μM resolution.

3.4. Data analysis

The expression data were extracted and filtered based on feature quality and signal intensity with criteria recommended in the GenPix Pro 6.0 program (Molecular Device). The data were then imported into a SQL database created with Microsoft SQL Server 2000 and normalized with the LOWESS program implemented in Acuity 4.0 Enterprise Microarray Informatics software (Molecular Device). After normalization, only the features that were ranked as good were included in the following analysis. Infected macrophage values were first normalized to uninfected macrophages of the given time point using the Acuity® 4.0 Enterprise Microarray Informatics software. Then, log ratios, log 2 (infected/not infected), were calculated for *t*-test statistical analysis and *p*-value correction was calculated with the Acuity® 4.0 Enterprise Microarray Informatics software implementing the two-way ANOVA significance test. Significant differential gene expression between infected and uninfected macrophages was determined at the false discover rate of 0.050 with |log ratio| equal to or greater than 1 (2-fold difference). Three sets of macrophages from separate pigs were used in this study. In order to eliminate variation between different animals, only genes which show significant changes in gene expression in the three sets of macrophages were considered in this study. For tables in this study the mean value was calculated for individual genes, and then log ratios were then converted to fold change.

3.5. Fluorescence microscopy

Primary swine macrophage cells grown on 12 mm glass coverslips in 24-well tissue culture dishes were fixed 48 h later with 4% paraformaldehyde (EMS, Hatfield, PA) and processed for immunofluorescence. Briefly, after fixation, paraformaldehyde was removed, and the cells permeabilized with 0.5% Triton X-100 for 5 min at room temperature (RT) and incubated in blocking buffer (phosphate-buffered saline [PBS], 5% normal goat serum, 2% bovine serum albumin, 10 mM glycine) for 1 h at RT. Primary monoclonal antibodies, WH303 (1/50), anti-porcine CD3 (1/50, VMRD), anti-pig SLA-DR (1/100, Becton Dickinson), anti-porcine CD14 (1/50, clone MIL12, Antigenix America, Huntington Station, NY) and anti-CD21-FITC labeled (1/100, Abcam, Cambridge, MA), were diluted in blocking buffer and incubated with cells overnight at 4 °C. After being washed with PBS, the cells were incubated with the secondary antibody, goat anti-mouse IgG (1/400; Alexa Fluor 488 or Alexa Fluor 594 Molecular Probes, Carlsbad, CA), for 1 h at RT. Following this incubation, the cells were washed with PBS, counterstained with the nuclear stain TOPRO-iodide 642/661 (Molecular Probes) for 5 min at RT, washed, mounted, and examined using an Olympus Microscope Model BX-40.

References

Ariumi, Y., Kuroki, M., Abe, K., Dansako, H., Ikeda, M., Wakita, T., Kato, N., 2007. DDX3 DEAD-box RNA helicase is required for hepatitis C virus RNA replication. J. Virol. 81 (24), 13922–13926.

Austin, B.A., James, C., Silverman, R.H., Carr, D.J., 2005. Critical role for the oligoadenylate synthetase/RNase L pathway in response to IFN-beta during acute ocular herpes simplex virus type 1 infection. J. Immunol. 175 (2), 1100–1106.

Bautista, M.J., Ruiz-Villamor, E., Salguero, F.J., Sanchez-Cordon, P.J., Carrasco, L., Gomez-Villamandos, J.C., 2002. Early platelet aggregation as a cause of thrombocytopenia in classical swine fever. Vet. Pathol. 39 (1), 84–91.

Becher, P., Avalos Ramirez, R., Orlich, M., Cedillo Rosales, S., Konig, M., Schweizer, M., Stalder, H., Schirrmeier, H., Thiel, H.J., 2003. Genetic and antigenic characterization of novel pestivirus genotypes: implications for classification. Virology 311 (1), 96–104.

Bensaude, E., Turner, J.L., Wakeley, P.R., Sweetman, D.A., Pardieu, C., Drew, T.W., Wileman, T., Powell, P.P., 2004. Classical swine fever virus induces proinflammatory cytokines and tissue factor expression and inhibits apoptosis and interferon synthesis during the establishment of long-term infection of porcine vascular endothelial cells. J. Gen. Virol. 85 (4), 1029–1037.

Bersinger, N.A., Frischknecht, F., Taylor, R.N., Mueller, M.D., 2008. Basal and cytokine-stimulated production of epithelial neutrophil activating peptide-78 (ENA-78) and interleukin-8 (IL-8) by cultured human endometrial epithelial and stromal cells. Fertil. Steril. 89 (5), 1530–1536.

Borca, M.V., Gudmundsdottir, I., Fernandez-Sainz, I.J., Holinka, L.G., Risatti, G.R., 2008. Patterns of cellular gene expression in swine macrophages infected with highly virulent classical swine fever virus strain Brescia. Virus Res. 138 (1–2), 89–96.

Borsos, T., 1989. Immune complex mediated activation of the classical complement pathway. Behring Inst. Mitt. 84, 93–101.

Bray, M., Geisbert, T.W., 2005. Ebola virus: the role of macrophages and dendritic cells in the pathogenesis of Ebola hemorrhagic fever. Int. J. Biochem. Cell Biol. 37 (8), 1560–1566.

Carrasco, C.P., Rigden, R.C., Vincent, I.E., Balmelli, C., Ceppi, M., Bauhofer, O., Tache, V., Hjertner, B., McNeilly, F., van Gennip, H.G., McCullough, K.C., Summerfield, A., 2004. Interaction of classical swine fever virus with dendritic cells. J. Gen. Virol. 85 (Pt. 6), 1633–1641.

Crotzer, V.L., Blum, J.S., 2009. Autophagy and its role in MHC-mediated antigen presentation. J. Immunol. 182 (6), 3335–3341.

Doceul, V., Charleston, B., Crooke, H., Reid, E., Powell, P.P., Seago, J., 2008. The Npro product of classical swine fever virus interacts with IkappaBalpha, the NF-kappaB inhibitor. J. Gen. Virol. 89 (8), 1881–1889.

Dransfield, I., Buckle, A.M., Hogg, N., 1990. Early events of the immune response mediated by leukocyte integrins. Immunol. Rev. 114, 29–44.
Fan, W., Luo, J., 2008. RecQ4 facilitates UV light-induced DNA damage repair through interaction with nucleotide excision repair factor xeroderma pigmentosum group A (XPA). J. Biol. Chem. 283 (43), 29037–29044.
Gabay, C., 2006. Interleukin-6 and chronic inflammation. Arthritis Res. Ther. 2 (8), S3.
Gallant, S., Gilkeson, G., 2006. ETS transcription factors and regulation of immunity. Arch. Immunol. Ther. Exp. (Warsz) 54 (3), 149–163.
Gomez-Villamandos, J.C., Ruiz-Villamor, E., Bautista, M.J., Quezada, M., Sanchez, C.P., Salguero, F.J., Sierra, M.A., 2000. Pathogenesis of classical swine fever: renal haemorrhages and erythrodiapedesis. J. Comp. Pathol. 123 (1), 47–54.
Gomez-Villamandos, J.C., Ruiz-Villamor, E., Bautista, M.J., Sanchez, C.P., Sanchez-Cordon, P.J., Salguero, F.J., Jover, A., 2001. Morphological and immunohistochemical changes in splenic macrophages of pigs infected with classical swine fever. J. Comp. Pathol. 125 (2–3), 98–109.
Gouwy, M., Struyf, S., Noppen, S., Schutyser, E., Springael, J.Y., Parmentier, M., Proost, P., Van Damme, J., 2008. Synergy between coproduced CC and CXC chemokines in monocyte chemotaxis through receptor-mediated events. Mol. Pharmacol. 74 (2), 485–495.
Ho, C.Y., Wong, C.H., Li, H.Y., 2008. Perturbation of the chromosomal binding of RCC1 Mad2 and survivin causes spindle assembly defects and mitotic catastrophe. J. Cell. Biochem. 105 (3), 835–846.
Huang, X., Madan, A., 1999. CAP3: a DNA sequence assembly program. Genome Res. 9 (9), 868–877.
Kalverda, A.P., Thompson, G.S., Vogel, A., Schroder, M., Bowie, A.G., Khan, A.R., Homans, S.W., 2009. Poxvirus K7 protein adopts a Bcl-2 fold: biochemical mapping of its interactions with human DEAD box RNA helicase DDX3. J. Mol. Biol. 385 (3), 843–853.
Kanter, D.M., Bruck, I., Kaplan, D.L., 2008. Mcm subunits can assemble into two different active unwinding complexes. J. Biol. Chem. 283 (45), 31172–31182.
Kaufman, P.D., Kobayashi, R., Kessler, N., Stillman, B., 1995. The p150 and p60 subunits of chromatin assembly factor I: a molecular link between newly synthesized histones and DNA replication. Cell 81 (7), 1105–1114.
Knoetig, S.M., Summerfield, A., Spagnuolo-Weaver, M., McCullough, K.C., 1999. Immunopathogenesis of classical swine fever: role of monocytic cells. Immunology 97 (2), 359–366.
Losada, A., Hirano, T., 2005. Dynamic molecular linkers of the genome: the first decade of SMC proteins. Genes Dev. 19 (11), 1269–1287.
Lowings, J.P., Paton, D.J., Sands, J.J., De Mia, G.M., Rutili, D., 1994. Classical swine fever: genetic detection and analysis of differences between virus isolates. J. Gen. Virol. 75 (Pt. 12), 3461–3468.
Ma, L., McQueen, J., Cuschieri, L., Vogel, J., Measday, V., 2007. Spc24 and Stu2 promote spindle integrity when DNA replication is stalled. Mol. Biol. Cell 18 (8), 2805–2816.
Mann, B.A., Huang, J.H., Li, P., Chang, H.C., Slee, R.B., O'Sullivan, A., Anita, M., Yeh, N., Klemsz, M.J., Brutkiewicz, R.R., Blum, J.S., Kaplan, M.H., 2008. Vaccinia virus blocks Stat1-dependent and Stat1-independent gene expression induced by type I and type II interferons. J. Interferon Cytokine Res. 28 (6), 367–380.
Mayer, D., Hofmann, M.A., Tratschin, J.D., 2004. Attenuation of classical swine fever virus by deletion of the viral N(pro) gene. Vaccine 22 (3–4), 317–328.
Meyers, G., Saalmuller, A., Buttner, M., 1999. Mutations abrogating the RNase activity in glycoprotein E(rns) of the pestivirus classical swine fever virus lead to virus attenuation. J. Virol. 73 (12), 10224–10235.
Moser, C., Bosshart, A., Tratschin, J.D., Hofmann, M.A., 2001. A recombinant classical swine fever virus with a marker insertion in the internal ribosome entry site. Virus Genes 23 (1), 63–68.
Netherton, C.L., Simpson, J., Haller, O., Wileman, T.E., Takamatsu, H.H., Monaghan, P., Taylor, G., 2009. Inhibition of a large double-stranded DNA virus by MxA protein. J. Virol. 83 (5), 2310–2320.
Noel, W., Raes, G., Hassanzadeh Ghassabeh, G., De Baetselier, P., Beschin, A., 2004. Alternatively activated macrophages during parasite infections. Trends Parasitol. 20 (3), 126–133.
Okumura, A., Lu, G., Pitha-Rowe, I., Pitha, P.M., 2006. Innate antiviral response targets HIV-1 release by the induction of ubiquitin-like protein ISG15. Proc. Natl. Acad. Sci. U.S.A. 103 (5), 1440–1445.
Owsianka, A.M., Patel, A.H., 1999. Hepatitis C virus core protein interacts with a human DEAD box protein DDX3. Virology 257 (2), 330–340.
Rauh, M.J., Ho, V., Pereira, C., Sham, A., Sly, L.M., Lam, V., Huxham, L., Minchinton, A.I., Mui, A., Krystal, G., 2005. SHIP represses the generation of alternatively activated macrophages. Immunity 23 (4), 361–374.
Rice, C.M., 1996. Flaviviridae: the viruses and their replication. In: Fields, B.N., Knipe, D.M., Howley, P.M. (Eds.), Fundamental Virology, Third ed. Lippincott Raven, Philadelphia, pp. 931–959.
Ricote, M., Li, A.C., Willson, T.M., Kelly, C.J., Glass, C.K., 1998. The peroxisome proliferator-activated receptor-gamma is a negative regulator of macrophage activation. Nature 391 (6662), 79–82.
Risatti, G.R., Borca, M.V., Kutish, G.F., Lu, Z., Holinka, L.G., French, R.A., Tulman, E.R., Rock, D.L., 2005a. The E2 glycoprotein of classical swine fever virus is a virulence determinant in swine. J. Virol. 79 (6), 3787–3796.
Risatti, G.R., Callahan, J.D., Nelson, W.M., Borca, M.V., 2003. Rapid detection of classical swine fever virus by a portable real-time reverse transcriptase PCR assay. J. Clin. Microbiol. 41 (1), 500–505.
Risatti, G.R., Holinka, L.G., Carrillo, C., Kutish, G.F., Lu, Z., Tulman, E.R., Sainz, I.F., Borca, M.V., 2006. Identification of a novel virulence determinant within the E2 structural glycoprotein of classical swine fever virus. Virology 355 (1), 94–101.
Risatti, G.R., Holinka, L.G., Fernandez Sainz, I., Carrillo, C., Kutish, G.F., Lu, Z., Zhu, J., Rock, D.L., Borca, M.V., 2007a. Mutations in the carboxyl terminal region of E2 glycoprotein of classical swine fever virus are responsible for viral attenuation in swine. Virology 364 (2), 371–382.
Risatti, G.R., Holinka, L.G., Fernandez Sainz, I., Carrillo, C., Lu, Z., Borca, M.V., 2007b. N-linked glycosylation status of classical swine fever virus strain Brescia E2 glycoprotein influences virulence in swine. J. Virol. 81 (2), 924–933.
Risatti, G.R., Holinka, L.G., Lu, Z., Kutish, G.F., Tulman, E.R., French, R.A., Sur, J.H., Rock, D.L., Borca, M.V., 2005b. Mutation of E1 glycoprotein of classical swine fever virus affects viral virulence in swine. Virology 343 (1), 116–127.
Ruggli, N., Bird, B.H., Liu, L., Bauhofer, O., Tratschin, J.D., Hofmann, M.A., 2005. N(pro) of classical swine fever virus is an antagonist of double-stranded RNA-mediated apoptosis and IFN-alpha/beta induction. Virology 340 (2), 265–276.
Ruggli, N., Tratschin, J.D., Schweizer, M., McCullough, K.C., Hofmann, M.A., Summerfield, A., 2003. Classical swine fever virus interferes with cellular antiviral defense: evidence for a novel function of N(pro). J. Virol. 77 (13), 7645–7654.
Sainz, I.F., Gladue, D.P., Holinka, L.G., O'Donnell, V., Gudmundsdottir, I., Prarat, M.V., Patch, J.R., Golde, W.T., Lu, Z., Zhu, J., Carrillo, C., Risatti, G.R., Borca, M.V., 2009. Mutations in NS4B of classical swine fever virus affect virulence in swine. J. Virol., PMID:19923180.
Sanchez-Cordon, P.J., Romanini, S., Salguero, F.J., Nunez, A., Bautista, M.J., Jover, A., Gomez-Villamos, J.C., 2002. Apoptosis of thymocytes related to cytokine expression in experimental classical swine fever. J. Comp. Pathol. 127 (4), 239–248.
Sanchez-Cordon, P.J., Romanini, S., Salguero, F.J., Ruiz-Villamor, E., Carrasco, L., Gomez-Villamandos, J.C., 2003. A histopathologic, immunohistochemical, and ultrastructural study of the intestine in pigs inoculated with classical swine fever virus. Vet. Pathol. 40 (3), 254–262.
Scherbik, S.V., Paranjape, J.M., Stockman, B.M., Silverman, R.H., Brinton, M.A., 2006. RNase L plays a role in the antiviral response to West Nile virus. J. Virol. 80 (6), 2987–2999.
Schweizer, M., Matzener, P., Pfaffen, G., Stalder, H., Peterhans, E., 2006. "Self" and "nonself" manipulation of interferon defense during persistent infection: bovine viral diarrhea virus resists alpha/beta interferon without blocking antiviral activity against unrelated viruses replicating in its host cells. J. Virol. 80 (14), 6926–6935.
Seago, J., Hilton, L., Reid, E., Doceul, V., Jeyatheesan, J., Moganeradj, K., McCauley, J., Charleston, B., Goodbourn, S., 2007. The Npro product of classical swine fever virus and bovine viral diarrhea virus uses a conserved mechanism to target interferon regulatory factor-3. J. Gen. Virol. 88 (Pt. 11), 3002–3006.
Shi, Z., Sun, J., Guo, H., Tu, C., 2009. Genomic expression profiling of peripheral blood leukocytes of pigs infected with highly virulent classical swine fever virus strain Shimen. J. Gen. Virol..
Stertz, S., Dittmann, J., Blanco, J.C., Pletneva, L.M., Haller, O., Kochs, G., 2007. The antiviral potential of interferon-induced cotton rat Mx proteins against orthomyxovirus (influenza), rhabdovirus, and bunyavirus. J. Interferon Cytokine Res. 27 (10), 847–855.
Summerfield, A., Hofmann, M.A., McCullough, K.C., 1998. Low density blood granulocytic cells induced during classical swine fever are targets for virus infection. Vet. Immunol. Immunopathol. 63 (3), 289–301.
Takada, A., Watanabe, S., Ito, H., Okazaki, K., Kida, H., Kawaoka, Y., 2000. Downregulation of beta1 integrins by Ebola virus glycoprotein: implication for virus entry. Virology 278 (1), 20–26.
Tanaka, T., Akiyama, H., Kanai, H., Sato, M., Takeda, S., Sekiguchi, K., Yokoyama, T., Kurabayashi, M., 2002. Endothelial PAS domain protein 1 (EPAS1) induces adrenomedullin gene expression in cardiac myocytes: role of EPAS1 in an inflammatory response in cardiac myocytes. J. Mol. Cell. Cardiol. 34 (7), 739–748.
Tratschin, J.D., Moser, C., Ruggli, N., Hofmann, M.A., 1998. Classical swine fever virus leader proteinase Npro is not required for viral replication in cell culture. J. Virol. 72 (9), 7681–7684.
Vallon, R., Freuler, F., Desta-Tsedu, N., Robeva, A., Dawson, J., Wenner, P., Engelhardt, P., Boes, L., Schnyder, J., Tschopp, C., Urfer, R., Baumann, G., 2001. Serum amyloid A (apoSAA) expression is up-regulated in rheumatoid arthritis and induces transcription of matrix metalloproteinases. J. Immunol. 166 (4), 2801–2807.
Van Coillie, E., Van Aelst, I., Fiten, P., Billiau, A., Van Damme, J., Opdenakker, G., 1999. Transcriptional control of the human MCP-2 gene promoter by IFN-gamma and IL-1beta in connective tissue cells. J. Leukoc. Biol. 66 (3), 502–511.
van Gennip, H.G., Bouma, A., van Rijn, P.A., Widjojoatmodjo, M.N., Moormann, R.J., 2002. Experimental non-transmissible marker vaccines for classical swine fever (CSF) by trans-complementation of E(rns) or E2 of CSFV. Vaccine 20 (11–12), 1544–1556.
van Gennip, H.G., Hesselink, A.T., Moormann, R.J., Hulst, M.M., 2005. Dimerization of glycoprotein E(rns) of classical swine fever virus is not essential for viral replication and infection. Arch. Virol. 150 (11), 2271–2286.
van Gennip, H.G., Vlot, A.C., Hulst, M.M., De Smit, A.J., Moormann, R.J., 2004. Determinants of virulence of classical swine fever virus strain Brescia. J. Virol. 78 (16), 8812–8823.
van Oirschot, J.T., 1999. Classical swine fever (Hog Cholera). In: Barbara, D.A., Straw, E., Mengeling, W.M., Taylor, K. (Eds.), Disease of Swine. Wiley-Blackwell, Ames, pp. 159–172.
van Rijn, P.A., Miedema, G.K., Wensvoort, G., van Gennip, H.G., Moormann, R.J., 1994. Antigenic structure of envelope glycoprotein E1 of hog cholera virus. J. Virol. 68 (6), 3934–3942.
Wang, H., Kim, S., Ryu, W.S., 2009. DDX3 DEAD-box RNA helicase inhibits hepatitis B viral reverse transcription by incorporation into nucleocapsids. J. Virol..

Yang, Q., Zhang, R., Wang, X.W., Linke, S.P., Sengupta, S., Hickson, I.D., Pedrazzi, G., Perrera, C., Stagljar, I., Littman, S.J., Modrich, P., Harris, C.C., 2004. The mismatch DNA repair heterodimer, hMSH2/6, regulates BLM helicase. Oncogene 23 (21), 3749–3756.

Yokoyama, K., Su Ih, I.H., Tezuka, T., Yasuda, T., Mikoshiba, K., Tarakhovsky, A., Yamamoto, T., 2002. BANK regulates BCR-induced calcium mobilization by promoting tyrosine phosphorylation of IP(3) receptor. EMBO J. 21 (1–2), 83–92.

Zaffuto, K.M., Piccone, M.E., Burrage, T.G., Balinsky, C.A., Risatti, G.R., Borca, M.V., Holinka, L.G., Rock, D.L., Afonso, C.L., 2007. Classical swine fever virus inhibits nitric oxide production in infected macrophages. J. Gen. Virol. 88 (Pt. 11), 3007–3012.

Zhao, C., Denison, C., Huibregtse, J.M., Gygi, S., Krug, R.M., 2005. Human ISG15 conjugation targets both IFN-induced and constitutively expressed proteins functioning in diverse cellular pathways. Proc. Natl. Acad. Sci. U.S.A. 102 (29), 10200–10205.

Zsak, L., Lu, Z., Kutish, G.F., Neilan, J.G., Rock, D.L., 1996. An African swine fever virus virulence-associated gene NL-S with similarity to the herpes simplex virus ICP34.5 gene. J. Virol. 70 (12), 8865–8871.

Return to Table of Contents

Virus Research 153 (2010) 82–91

Contents lists available at ScienceDirect

Virus Research

journal homepage: www.elsevier.com/locate/virusres

Mapping of amino acid residues responsible for adhesion of cell culture-adapted foot-and-mouth disease SAT type viruses

Francois F. Maree[a,*], Belinda Blignaut[a,b], Tjaart A.P. de Beer[c,1], Nico Visser[d], Elizabeth A. Rieder[e]

[a] Transboundary Animal Diseases Programme, Onderstepoort Veterinary Institute, Agricultural Research Council, Onderstepoort 0110, South Africa
[b] Department of Microbiology and Plant Pathology, Faculty of Agricultural and Natural Sciences, University of Pretoria, Pretoria 0002, South Africa
[c] Bioinformatics and Computational Biology Unit, University of Pretoria, Pretoria 0002, South Africa
[d] Intervet/Schering-Plough, Boxmeer 5830AA31, The Netherlands
[e] Foreign Animal Disease Research Unit, United States Department of Agriculture, Agricultural Research Service, Plum Island Animal Disease Center, Greenport, NY 11944, USA

ARTICLE INFO

Article history:
Received 29 March 2010
Received in revised form 6 July 2010
Accepted 8 July 2010
Available online 15 July 2010

Keywords:
Chimera
Foot-and-mouth disease virus
Glycosaminoglycan
Heparan sulfate proteoglycan
Cell receptor

ABSTRACT

Foot-and-mouth disease virus (FMDV) infects host cells by adhering to the α_V subgroup of the integrin family of cellular receptors in a Arg–Gly–Asp (RGD) dependent manner. FMD viruses, propagated in non-host cell cultures are reported to acquire the ability to enter cells via alternative cell surface molecules. Sequencing analysis of SAT1 and SAT2 cell culture-adapted variants showed acquisition of positively charged amino acid residues within surface-exposed loops of the outer capsid structural proteins. The fixation of positively charged residues at position 110–112 in the βF–βG loop of VP1 of SAT1 isolates is thought to correlate with the acquisition of the ability to utilise alternative glycosaminoglycan (GAG) molecules for cell entry. Similarly, two SAT2 viruses that adapted readily to BHK-21 cells accumulated positively charged residues at positions 83 and 85 of the βD–βE loop of VP1. Both regions surround the fivefold axis of the virion. Recombinant viruses containing positively charged residues at position 110 and 112 of VP1 were able to infect CHO-K1 cells (that expresses GAG) and demonstrated increased infectivity in BHK-21 cells. Therefore, recombinant SAT viruses engineered to express substitutions that induce GAG-binding could be exploited in the rational design of vaccine seed stocks with improved growth properties in cell cultures.

1. Introduction

Foot-and-mouth disease (FMD) is a highly contagious vesicular disease of cloven-hoofed animals causing significant distress and suffering in animals. Although mortality is usually low (<5%) (Thomson, 1995), morbidity can reach 100% and the impact can be catastrophical when an outbreak occurs in a FMD-free region with immunologically naïve population of livestock. Consequently FMD is classified by the OIE as one of the most important infectious diseases of livestock (Office International des Épizooties Terrestrial Manual, 2009). The economically critical effects to livestock farming due to the high cost of disease control and international trade restrictions (Sellers and Daggupaty, 1990) was evidenced during the 2000–2001 outbreaks in Europe and the virus escape that occurred more recently, in 2007 in the United Kingdom (Samuel and Knowles, 2001; Cottam et al., 2008). In endemic regions, FMD is controlled by restricting animal movement, the implementation of vaccination programmes and biosecurity measures. In disease-free countries where vaccination is normally not applied, ring-vaccination is only used in an emerging outbreak with subsequent slaughtering of vaccinated animals (Müller et al., 2001; Tomassen et al., 2002).

In South Africa, other regions of the African continent, as well as in some Asian and South American countries, regular immunisation is essential for disease control, and in maintaining FMD-free status. Current FMD vaccines are chemically inactivated preparations of concentrated, virus-infected cell culture supernatants (Office International des Épizooties Terrestrial Manual, 2009). Therefore, large-scale vaccine production utilize a suitable cell line, like BHK-21 cells, and requires that the vaccine strain is adapted and propagated in cell culture (Amadori et al., 1994, 1997). However, these cell lines have limited (monolayers) or no (in suspension) expression of the required primary receptor for infection by FMDV

Abbreviations: FMD, foot-and-mouth disease; FMDV, FMD virus; GAG, glycosaminoglycan; HSPG, heparan sulfate proteoglycan; SAT, South African Territories.

* Corresponding author at: Transboundary Animal Diseases Programme, Onderstepoort Veterinary Institute, Private Bag X05, Onderstepoort 0110, South Africa. Tel.: +27 12 529 9560/85; fax: +27 12 529 9505.
E-mail address: Mareef@arc.agric.za (F.F. Maree).
[1] Currently at: European Bioinformatics Institute, Wellcome Trust Campus, Hinxton, Cambridge, CB10 1SD, United Kingdom.

0168-1702/$ – see front matter © 2010 Elsevier B.V. All rights reserved.
doi:10.1016/j.virusres.2010.07.010

(Amadori et al., 1994). In the early 1980s it was noted that viruses of the three SAT serotypes, endemic in Africa, are notorious for their difficulty to adapt to BHK-21 cells (Pay et al., 1978; Preston et al., 1982). It is thought that the cell surface molecules, which may act as virus receptors, exert an important selective pressure on viral RNA quasi-species, thereby enabling adaptation. Studies have shown that repeated passaging of FMDV in cultured cells rapidly gave rise to mutant viruses within the population (Rieder et al., 1994; Herrera et al., 2007). Adaptation of wild-type SAT viruses in cell culture to produce high yields of stable antigen is an intricate and time-consuming process that is often associated with a low success rate.

FMD virus (FMDV), the type species of the *Aphtovirus* genus in the family *Picornaviridae* (Racaniello, 2006), infects epithelial cells by adhering to any of four members of the α_V subgroup of the integrin family of cellular receptors, *i.e.* $\alpha_V\beta1$, $\alpha_V\beta3$, $\alpha_V\beta6$ and $\alpha_V\beta8$ (Berinstein et al., 1995; Neff et al., 1998, 2000; Jackson et al., 1997, 2000, 2002, 2004; Duque and Baxt, 2003). Attachment to the receptors is mediated via a highly conserved Arg–Gly–Asp (RGD) motif (Fox et al., 1989; Baxt and Becker, 1990; Mason et al., 1994; Leippert et al., 1997) located within the structurally disordered βG–βH loop of VP1 (Acharya et al., 1989; Lea et al., 1995; Curry et al., 1997). Following FMDV–receptor interactions, the virus is internalised and the viral genome is released in the cytosol. Adaptation of FMD field isolates to enable efficient replication in cultured cells is accompanied by changes in viral properties, including the acquisition of the ability to bind to alternative cellular receptors such as cell surface glycosaminoglycans (GAGs) (Jackson et al., 1996, 2001; Sa-Carvalho et al., 1997; Zhao et al., 2003). The interactions of a diverse group of ligands, such as growth factors, chemokines, herpes simplex virus (HSV), human immunodeficiency virus, respiratory syncytial virus, alphaviruses, dengue virus, adeno-associated virus and FMDV, to the highly sulfated GAGs (also known as heparan sulfate proteoglycans, HSPG) is typically via a positively charged domain on these proteins (Patel et al., 1993; Gromm et al., 1995; Jackson et al., 1996; Chen et al., 1997; Krusat and Streckert, 1997; Sa-Carvalho et al., 1997; Byrnes and Griffin, 1998; Klimstra et al., 1998; Summerford and Samulski, 1998; Fry et al., 1999, 2005; Zhao et al., 2003). The ability of a type O virus to enter cells following adhesion to HSPG is thought to be dependent on the presence of the positively charged Arg residue at position 56 of VP3 which results in a net gain of positive charge on the virion surface (Sa-Carvalho et al., 1997; Fry et al., 1999).

Replacement of the external capsid-coding sequence of an infectious cDNA clone with the corresponding region of an outbreak virus results in the transfer of surface-exposed epitopes from the aetiological agent to the recombinant virus (Zibert et al., 1990; Rieder et al., 1993; Almeida et al., 1998; Van Rensburg and Mason, 2002; Van Rensburg et al., 2004). The chimeric viruses, produced in this manner, induce a protective immune response in animals similar to that of the outbreak virus. However, co-transferral of undesirable traits, such as capsid instability and poor cell culture adaptation of the field virus may also occur. Therefore, application of reverse genetics technology in FMD vaccinology includes the identification of amino acid sequences associated with the acquisition of HSPG-binding during cell culture adaptation of SAT viruses and the introduction of these changes into chimeric constructs.

In this report we identify novel amino acid residues within the capsid proteins of SAT1 and SAT2 viruses that affect the virus' ability to grow in different cell lines. We demonstrated that cell culture adaptation to BHK-21 cells is acquired following repeated passaging of the field viruses in these cells. Furthermore, we illustrated that this phenotype can be transferred to an infectious cDNA clone of a FMD field virus from which viable cell culture-adapted viruses were recovered.

2. Materials and methods

2.1. Cells, viruses and plasmids

Baby hamster kidney (BHK) cells, strain 21, clone 13 (ATCC CCL-10) were maintained as described by Rieder et al. (1993). Chinese hamster ovary (CHO) cells strain K1 (ATCC CCL-61) were maintained in Ham's F-12 medium (Invitrogen), supplemented with 10% foetal calf serum (Delta Bioproducts). Primary pig kidney (PK) and Instituto Biologico renal suino (IB-RS-2) cells Plaque assays were performed using a tragacanth overlay method and 1% methylene blue staining (Rieder et al., 1993).

Viruses used in this study included four SAT1 viruses, *i.e.* KNP/196/91, SAR/9/81, NAM/307/98 and ZAM/2/93; and four SAT2 isolates, *i.e.* ZIM/14/90, ZIM/5/83, ZAM/7/96, and KNP/19/89. The host species the viruses were isolated from is summarized in Table 1. The SAT2/ZIM/7/83 vaccine strain is a derivative of ZIM/5/83 and is used in inactivated vaccines to assist with control of FMD along the borders of South Africa. The viruses were isolated in primary pig kidney cells (PK) and grown on IB-RS-2 cells (parental viruses) prior to adaptation to BHK-21 cells (vaccine strains). To distinguish the low passage, parental viruses from their BHK-21 culture-adapted derivatives, we will refer to the field isolate by its accession code followed by P (parental) or Vac/BHK (vaccine or BHK-21 cell-adapted strain) superscript. The passage histories of the viruses are summarised in Table 1.

The construction of plasmids pSAT2, pNAM/SAT and pSAU/SAT is described elsewhere (Böhmer, 2004; Van Rensburg et al., 2004; Storey et al., 2007). In short, the pNAM/SAT and pSAU/SAT were constructed by replacing the outer capsid-coding region of pSAT2 with the corresponding region of SAT1/NAM/307/98 and SAT2/SAU/6/00 using the unique restriction sites SspI and XmaI in VP2 and 2A-coding regions, respectively (Böhmer, 2004; Storey et al., 2007).

2.2. RNA extraction, cDNA synthesis, PCR amplification and nucleotide sequencing

RNA was extracted from infected cell lysates using either a guanidium-based nucleic acid extraction method (Bastos, 1998) or TRIzol® reagent (Life Technologies) according to the manufacturer's specifications and used as template for cDNA synthesis. Viral cDNA was synthesised with SuperScript III™ (Life Technologies) and oligonucleotide 2B208R (Bastos et al., 2001). cDNA copies of the *ca.* 3.0 kb Leader/capsid-coding regions of the viral isolates were obtained by PCR amplification using AdvanTaq™ DNA polymerase (Clontech) with specific oligonucleotides (NCR2: 5′-GCTTCTATGCCTGAATAGG and WDA: 5′-GAAGGGCCCAGGGTTGGACTC) following the manufacturer's recommendations. Sequencing of the amplicons was performed using the ABI PRISM™ BigDye Terminator Cycle Sequencing Ready Reaction Kit v3.0 (PerkinElmer Applied Biosystems). The GeneBank accession numbers of the wild-type (low passage history) virus P1 sequences are as follows: DQ009715 (SAR/9/81); DQ009716 (KNP/196/91); DQ009717 (NAM/307/98); DQ009719 (ZAM/2/93); DQ009726 (ZIM/7/83); DQ009728 (ZIM/14/90); DQ009741 (ZAM/7/96); DQ009735 (KNP/19/89). The differences in deduced amino acid sequences between the wild-type and cell culture-adapted strains are summarised in Table 2.

2.3. Site-directed mutagenesis of cDNA clones

Site-directed mutagenesis of plasmids pNAM/SAT and pSAU/SAT was accomplished by using amplicon overlap site-directed mutagenesis. The forward mutagenesis primer for

Table 1
Summary of SAT1 and SAT2 viruses and their derivatives used in production, field isolate and their derivatives, passage histories, titres prior to and after adaptation and properties in cell culture.

Serotype	Viruses[a]	Host species	Passage history[b]	Vaccine stock[c]	Titre (pfu/ml) in BHK cells	CHO-K1 infectivity[d]
SAT1	KNP/196/91^{P}	Buffalo	PK_1	–	5.2×10^7	1.08×10^{-4}
	KNP/196/91^{Vac}	–	$PK_1RS_4B_1BHK_5$	MSV	1.3×10^8	2.80×10^6
	SAR/9/81^{Epi}	Impala	epithelium	–	9.6×10^7	6.40×10^{-3}
	SAR/9/81^{Vac}	–	$PK_1RS_4BHK_5$	MSV	7.2×10^9	1.10×10^6
	NAM/307/98^{P}	Buffalo	PK_1RS_1	–	–	–
	NAM/307/98^{BHK}	–	$PK_1RS_1BHK_5$	–	1.1×10^7	–
	ZAM/2/93^{P}	Buffalo	BTY_1RS_2	–	8.6×10^6	2.82×10^{-4}
	ZAM/2/93^{BHK}	–	$BTY_1RS_2BHK_5$	–	2.2×10^8	1.06×10^7
SAT2	KNP/19/89^{P}	Buffalo	$PK_1RS_1B_1$	–	2.2×10^5	1.19×10^{-5}
	KNP/19/89^{Vac}	–	$B_1PK_1RS_1BHK_4$	MSV	1.1×10^7	5.06×10^6
	ZIM/5/83^{P}	Bovine	BTY_4RS_1	–	1.8×10^5	5.91×10^{-5}
	ZIM/5/83^{BHK}	–	$BTY_4RS_2BHK_8$	–	3.4×10^7	–
	ZIM/7/83^{Vac}	Bovine	$B_1BHK_4B_1BHK_5$	MSV	1.8×10^7	6.58×10^6
	ZIM/14/90^{P}	Buffalo	BTY_1RS_3	–	1.0×10^5	–
	ZIM/14/90^{BHK}	–	$BTY_1RS_3BHK_8$	–	2.0×10^6	–
	ZAM/7/96^{P}	Buffalo	BTY_1RS_2	–	8.0×10^6	–
	ZAM/7/96^{BHK}	–	$BTY_2RS_2BHK_8$	–	5.6×10^7	–

[a] The viruses used in this study were notated by the superscript P = most primary isolate for that strain defined as the lowest passage history; Vac = vaccine strain adapted on BHK-21 for production purpose; Epi = isolate from the epithelium tissue of the host species; BHK = propagated in BHK-21 monolayers.
[b] The passage history of the primary isolates and their derivates are indicated by cell type followed by the number of passages: B = bovine; PK = primary pig kidney cells; BTY = bovine thyroid cells; RS = IB-RS-2 cells; BHK = baby hamster kidney cells (strain 21, clone 13).
[c] MSV = master seed virus.
[d] The infectivity in CHO-K1 cells is expressed as a titre difference between a 1 and 24 h post-infection of CHO-K1 cells. A negative value is indicative of inability to infect and replicate in CHO-K1 cells, whereas a positive value indicate infection and replication in the same cell line. "–" has not been done.

pNAM/SAT was CAGTCGTCTTCTCCaaacGAcGCACCACTCGCTTCGC (NAMmut4; lower cased letters represent altered bases), replacing the wild-type KGG sequence at position 110–112 of VP1 with KRR. Similarly the mutagenesis primers for pSAU/SAT were GTGGGCGACCACCggcgcGCCTTTTGGCAGCCTAAC (SAUmut1) and GTACGCTGACAGCAaGCACaaactcCCGTCAACCTTC (SAUmut2). The latter primers introduced the E85R and E161K substitutions respectively. Briefly, the first PCR reactions were performed using NAMmut4, SAUmut1 and SAUmut2 as the sense mutagenic and cDNA-2A (CGCCCCGGGGTTGGACTCAACGTCTCC; XmaI site underlined) as the antisense oligonucleotides. The second PCR reactions were performed with the reverse complements of NAMmut4, SAUmut1 and SAUmut2 as antisense mutagenic in combination with 5′-specific sense oligonucleotides, cDNA-NAM (CGGAATATTGACCACCAGCCATGGTACCACCAC; SspI site underlined) or cDNA-SAU (CGGAATATTGACCACACGTCACGGAACCACGAC; SspI site underlined). Cycling conditions for both PCRs were as follows: 95 °C for 20 s, 60 °C for 20 s, and 72 °C for 1 min (20 cycles). The amplicons of the first two reactions were combined in equimolar amounts, denatured at 95 °C for 20 s, extended and enriched by another 25 cycles of amplification with cDNA-NAM or cDNA-SAU and cDNA-2A using TaKaRa Ex Taq™ (Takara). The resulting *ca.* 2.2 kb DNA fragment (containing either pNAM/SAT or pSAU/SAT mutations) was digested with SspI and XmaI and cloned into the corresponding region of pSAT2. The mutations were verified by nucleotide sequencing of the complete P1-coding region using selected oligonucleotides and no unintended site mutations were found.

2.4. In vitro RNA synthesis, transfection and virus recovery

Plasmids containing genome-length cDNAs, chimeric cDNA or site-directed mutated cDNA clones were linearised at the SwaI site downstream of the poly-A tract and used as templates for RNA synthesis utilising the MEGAscript™ T7 kit (Ambion). Transcript RNAs were examined in agarose gels for their integrity and quantitated by spectrometry. BHK-21 cell monolayers in 35 mm cell culture plates (Nunc™) were transfected with 2–3 μg of the *in vitro* synthesised RNA using Lipofectamine2000™ (InVitrogen). Transfected monolayers were incubated at 37 °C with a 5% CO_2 influx for 48 h in Eagle's basal medium (BME) containing 1% foetal calf serum (v/v) and 25 mM HEPES. The virus-containing supernatants were used to infect fresh BHK-21 monolayers (35 mm cell culture plates) using 1/10th of clarified infected supernatants and incubated for 48 h at 37 °C. Viruses were subsequently harvested from infected cells by a freeze–thaw cycle and passaged four times on BHK-21 cells, using 10% of the supernatant of the previous passage. Following the recovery of viable viruses, the presence of the mutations was verified once again with automated sequencing.

2.5. Evaluation of the ability of SAT types of FMDV to infect and replicate in CHO-K1 cells

Twenty-four hours growth kinetics was performed in CHO-K1 cells which express GAG receptors (Jackson et al., 1996; Sa-Carvalho et al., 1997). Monolayers of CHO-K1 cells in 35 mm cell culture plates were infected with a MOI of 5–10 of the parental and vaccine strains (Table 1) for 1 h or 24 h at 37 °C. Infected monolayers were then frozen at −70 °C and thawed. Viruses from the lysed monolayers were titrated on BHK-21 monolayers and viral growth was calculated by subtracting the 24 h titre results from the 1 h titre results. Positive titers were an indication that the viruses are able to infect and replicate in CHO-K1 cells, suggesting the ability to utilise GAG receptors for cell entry. The nucleotide sequences of the isolates that were able to infect and replicate in CHO-K1 cells within 24 h were determined and compared to those of the parental viruses.

2.6. Sequence alignments and structural modelling

Homology models of the capsid proteins (VP1-4) for a representative virus of each of the SAT1 and two serotypes (SAT1/SAR/9/81, SAT2/ZIM/7/83) were built using Modeller 9v3 (Sali and Blundell, 1993) with 1FOD (Logan et al., 1993) as the template. SAR/9/81 and ZIM/7/83 capsid proteins were aligned with that of O1BFS

Table 2
Comparison of the capsid amino acid sequences of the SAT1 and SAT2 primary isolates and their cell culture-adapted derivatives.

Protein	β–β Structure	SAT1 isolate[a]			
		SAR/9/81	KNP/196/91	NAM/307/98	ZAM/2/93
VP2	βB-βC	–	Q2074R[b]	–	–
		–	Q2170H	–	–
		–	S2196N	–	–
VP3		–	D3009V	–	–
	βE–βF	–	–	**E3135K**[b]	–
	βG–βH	–	–	**E3175K**[b]	–
		–	–	–	A3180V
		D3192Y	–	–	–
		–	–	S3203T	–
		S3217I	–	–	–
		–	–	S3219L	–
VP1		–	Y1018H	–	–
		–	–	T1025A	–
		–	–	A1033T	–
		–	R1049K	–	–
		A1069G	–	–	–
		–	–	–	K1086Q
	βF–βG	**N1110K**[b]	**K1110K**[b]	–	–
	βF–βG	–	–	–	**N1111K**[b]
		G1112R[b]	**G1112R**[b]	G1112D	**G1112R**[b]
		–	–	K1157A	–
		–	–	E1177Q	–
		–	V1179E	–	–
		–	K1206R	–	–
		–	K1210R	–	–

Protein	β–β Structure	SAT2 isolate[a]			
		KNP/19/89	ZIM/5/83 vs. ZIM/7/83	ZAM/7/96	ZIM/14/90
VP2		I2032V	–	–	–
		–	M2077T	–	–
		–	–	–	E2096Q
	βG–βH	–	–	–	**Q2170R**[b]
VP3		H3036	–	–	–
		T3043S	–	–	–
		Q3049E	–	–	–
	βE–βF	–	–	–	**T3129K**[b]
		–	–	–	D3132N
		–	–	E3148K	–
		P3192T	–	–	–
VP1		–	M1028V	–	–
		–	A1064G	–	–
	βD–βE	–	–	**E1083K**[b]	–
	βD–βE	**Q1085R**[b]	–	–	–
		R1098T	–	–	–
	βG–βH	–	**E1161K**[b]	–	–
		–	Y1169H	–	–
		T1171A	–	–	–
		F1194L	–	–	–
		V1207A	–	–	–

[a] The amino acid residues have been numbered independently for each protein. For each residue, the first digit indicates the protein (VP1, VP2 or VP3) and the last three digits the amino acid position in either a SAT1 or SAT2 alignment. The P1 polypeptide of SAT1 viruses is 744 amino acids and that of SAT2 viruses 741 amino acids.
[b] Amino acid changes to a positive charge in surface-exposed loops are shown in bold.

using ClustalX and the sequence similarities for both were above 80%. The homology structure was calculated by the satisfaction of spatial restraints as described by empirical databases. Structural checks of the model were done using WHAT CHECK (Hooft et al., 1996).

The complete P1 sequences of 56 low passage SAT viruses (26 SAT1 and 30 SAT2) from 17 different countries in Africa, available on GenBank, were translated in BioEdit and aligned using ClustalX. The viruses used in the alignment were isolated from clinical material on PK cells and grown 1–4 passages in IBRS-2 cells (Bastos et al., 2001, 2003) and were referred to as wild-type viruses. The P1 sequences of the wild-type viruses were compared to the BHK-21 adapted viruses.

3. Results

3.1. Adaptation of SAT viruses in cell culture selects variants that gain a net positive charge on the virion surface

SAT viruses used for vaccine production are typically adapted to cultured cells following limited passages in BHK-21 cells. In this study, we have investigated the phenotypic and genetic changes associated with the transition of SAT viruses from wild-type to the cell culture-adapted phenotype. The morphology of virus plaques produced on BHK-21 cell monolayers following infection with SAT1 and SAT2 vaccine strains differed from the plaques produced by the parental strains which have not been adapted to BHK-21 cell

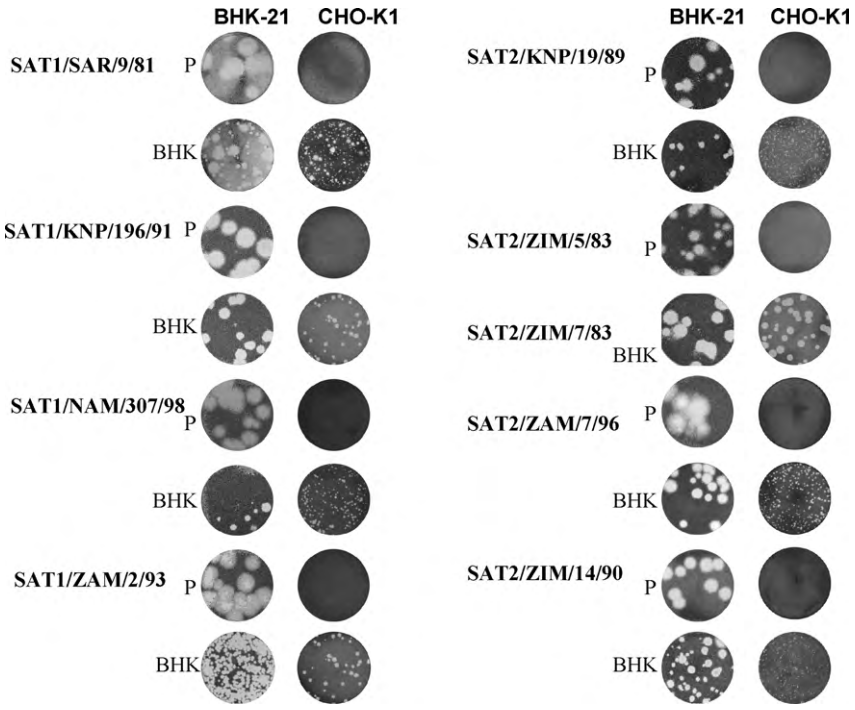

Fig. 1. Plaque morphologies of the parental (P) and cell culture (BHK) derived viruses obtained using monolayers of BHK-21 and CHO-K1 cells. Cells infected with the indicated viral strains were incubated with tragacanth overlay for 40 h prior to staining with 1% methylene blue. Plaques for SAT1 and SAT2 wild-type viruses are generally large with opaque edges and adaptation is accompanied by smaller to medium plaques and clear edges.

culture (Fig. 1). In particular, SAT1/KNP196/91^{P} (isolated on primary pig kidney cells) and SAT1/SAR/9/81^{P} (epithelium of infected impala) viruses displayed large plaques (7–8 mm) with opaque edges. In contrast, plaques produced by the corresponding vaccine derivatives, KNP/196/91^{Vac} and SAR/9/81^{Vac} viruses (high passage), exhibited a mixture of small (1–2 mm), medium (3–4 mm) to large plaques with clearly defined edges. Whereas the parental strains failed to infect CHO-K1 cells, both vaccine strains produced small and clear plaques on CHO-K1 cells (Fig. 1) and reached titers of 2.8×10^6 and 1.1×10^6 pfu/ml after 24 h growth on CHO-K1 cells, respectively (Table 1). Table 2 summarizes the amino acid differences of the low and high passage viruses. Comparison of the amino acid sequence in the outer capsid proteins of the KNP196/91^{P} and KNP/196/91^{Vac}, in particular, revealed 11 amino acid substitutions in the adapted strain, *i.e.* three substitutions in VP2, one in VP3 and seven in VP1.

The structural location of these 11 residues in the capsid proteins was mapped to a SAT1 capsid protomer. Fig. 2 illustrates two substitutions, the first in VP1 (Gly112 → Arg) and the second in VP2 (Gln74 → Arg), of neutral amino acids with positively charged residues which are located within surface-exposed loops that connect β-sheet structures. The Gln74 → Arg substitution in VP2 is located in the βB–βC loop which is characteristically hypervariable (see Table 3 for details). The proximity of this substitution to three other positively charged residues, Lys206 → Arg, Arg208 and Lys210 → Arg, located in the C-terminus of VP1 (Table 2 and Fig. 2) is noteworthy since these residues were reported to form part of the walls of a heparin-binding depression of serotype A viruses (Fry et al., 2005). Positively charged residues were found to be conserved at these positions in a complete alignment of SAT1 isolates (data not shown). The Gly112 → Arg substitution in VP1 forms part of a novel sequence in the βF–βG loop comprising three residues (KGG for KNP/196/91^{P}) where positively charged residues (KGR) accumulated during cell culture adaptation of SAT1 viruses (Table 2). The altered amino acid sequence correlates with the Asn110 → Lys and Gly112 → Arg substitutions in the VP1 protein of SAT1/SAR/9/81^{Vac}. The 3D structural model of a protomeric unit revealed that the positively charged SAT1 substitutions, at positions 110 and 112 in each of the interacting VP1 subunits, surround the pore located at the fivefold axis of the virion (Fig. 2). An interesting observation was that adjacent to this positively charged sequence of the VP1 βF–βG loop a Val was selected for in the place of an Asp at position 9 of VP3 in KNP/196/91^{Vac} (Table 2; Fig. 2) which may increase the local positive charge on the virion surface even more and increase the virus' ability to adhere to negatively charged sulfated polysaccharides.

Similar to KNP/196/91 and SAR/9/81, two other SAT1 field viruses (NAM/307/98 and ZAM/2/93) adapted and acquired the ability to infect CHO-K1 cells upon repeated passages in BHK-21 cells. The parental NAM/307/98 virus, isolated from buffalo (*Syncerus caffer*) in the West Caprivi Game Reserve in Namibia in 1998 (Bastos et al., 2001; Storey et al., 2007) underwent slow adaptation to cell culture, only attaining titers of 10^5 pfu/ml after eight passages in BHK-21 cells, and progeny viruses failed to infect CHO-K1 cells (Fig. 1). Only following repeated passaging in BHK-21 cells, this isolate finally adapted to BHK-21 cells (NAM/307/98^{BHK}) as measured by its ability to infect CHO-K1 cells and by producing titers in excess of 10^7 pfu/ml in BHK-21 cells (Table 1). NAM/307/98^{BHK} yielded clear plaques of small (1–2 mm) and medium (3–5 mm) sizes and acquired the ability to infect CHO-K1 cells (Fig. 1). Sequence analysis revealed nine amino acid substitutions in the capsid proteins of the adapted strain (Table 2). Only two of these were positively charged and located within surface-exposed loops of VP3, *i.e.* residues Glu135 → Lys and Glu175 → Lys. The residues are located around the threefold axis of the pentamer unit (Fig. 2). Another SAT1 field isolate, ZAM/2/93 (Fig. 1), adapted rapidly in BHK-21 cells, only requiring two rounds of passaging, and the progeny viruses acquired two positively charged amino acids at position 111–112 of VP1 (Asn111 → Lys and Gly112 → Arg) (Table 2). This result is in agreement with the substitutions observed for the SAT1 vaccine strains KNP/196/91 and SAR/9/81. Therefore, we have identified a sequence "hotspot"

Table 3
A summary of the amino acid variation in the putative HSPG-binding sites identified for SAT1 and SAT2 BHK-21 adapted strains. The residue variation was obtained from complete P1 alignments of 24 SAT1 and 24 SAT2 field viruses.

	Amino acid variation					
	VP2	VP3		VP1		
	2074[a]	3135	3175	1083–1085	1110–1112	1161
SAT1	Q/R/A/K/E/N/S	E/N/A/D/V/S/T	E		N/K/H/R/A/T-G/N/D-G/N/D	
SAT2				E/D/I/T/K-H-E/R/K/T/S/Q/A		T/A/E/S/Q

/ denotes differences at the same aa position and "-" indicates the next aa.
[a] The first digit indicates the protein (VP1, VP2 or VP3) and the last three digits the amino acid position in either a SAT1 or SAT2 alignment.

(amino acids 110–112 of VP1) for the accumulation of positive charges during cell culture adaptation of SAT1 viruses.

We subsequently investigated whether SAT2 viruses that have acquired BHK-21 cell adaptation, do so by selecting positive charge substitutions in "hotspots" on the external capsid proteins. The SAT2 vaccine strain KNP/19/89^{Vac} (Table 1) was originally isolated from buffalo in the Kruger National Park (KNP/19/89^{P}). Whereas the viral plaques produced by the KNP/19/89^{Vac} strain on BHK-21 monolayers were medium (3–5 mm) in size and clearly defined, those produced on CHO-K1 cells were needle point (<1 mm) to small (1–2 mm) in size (Fig. 1). The KNP/19/89^{Vac} attained a titer of 5×10^6 pfu/ml at 24 h post-infection of CHO-K1 cells (Table 1). Another SAT2 vaccine strain, ZIM/7/83, passaged five times in BHK-21 cells, infected and replicated effectively in CHO-K1 cells, reaching a titer of 6.5×10^6 pfu/ml 24 h post-infection of CHO-K1 cells (Table 1), and produced medium-sized plaques in this cell line. The parental virus ZIM/5/83 failed to grow in CHO-K1 cells. For the two SAT2 vaccine strains (KNP/19/89^{Vac} and ZIM/7/83), only substitutions in VP1, *i.e.* Gln85 → Arg for KNP/19/89 and Glu161 → Lys for ZIM/7/83 (Table 2), effected in significant charge difference on the virion surface (Fig. 2). The latter substitution in VP1 is preceded by two positively charged residues, *i.e.* Lys159–His160, at the C-terminal base of the βG–βH loop. The Gln85 → Arg found in KNP/19/89^{Vac}, is structurally neighbouring the fivefold axis of the virion and forms part of a three positively charged amino acid sequence in the βD–βE loop of VP1. However, since VP1 residue 85 was conserved as Glu in ZIM/7/83, the amino acids at position 159–161 (Lys–His–Glu) of VP1 that changed to Lys–His–Lys in the vaccine strain may be necessary for BHK-21 cell adaptation in this strain.

The role of the three residues at position 83–85 in VP1 in the cell culture adaptation of SAT2 viruses was supported following the adaptation and characterisation of the field virus ZAM/7/96 (Table 1), isolated from buffalo (Bastos et al., 2003). Whereas this parental isolate produced large (6–7 mm) plaques on BHK-21 monolayers, the cell culture-adapted variant produced a mixture of medium (3–5 mm) and large plaques and was able to infect CHO-K1 cells, unlike its parental counterpart (Fig. 1). A Glu → Lys substitution was observed at position 83 of VP1, as well as residue 148 of VP3 (Table 2). Whether the two substitutions contributed synergistically or independently to the cell culture-adapted phenotype is not known. The ability of high passage ZIM/14/90 to infect and replicate in CHO-K1 cells (Fig. 1) was associated with Gln170 → Arg and Thr129 → Lys substitutions in VP2 and VP3,

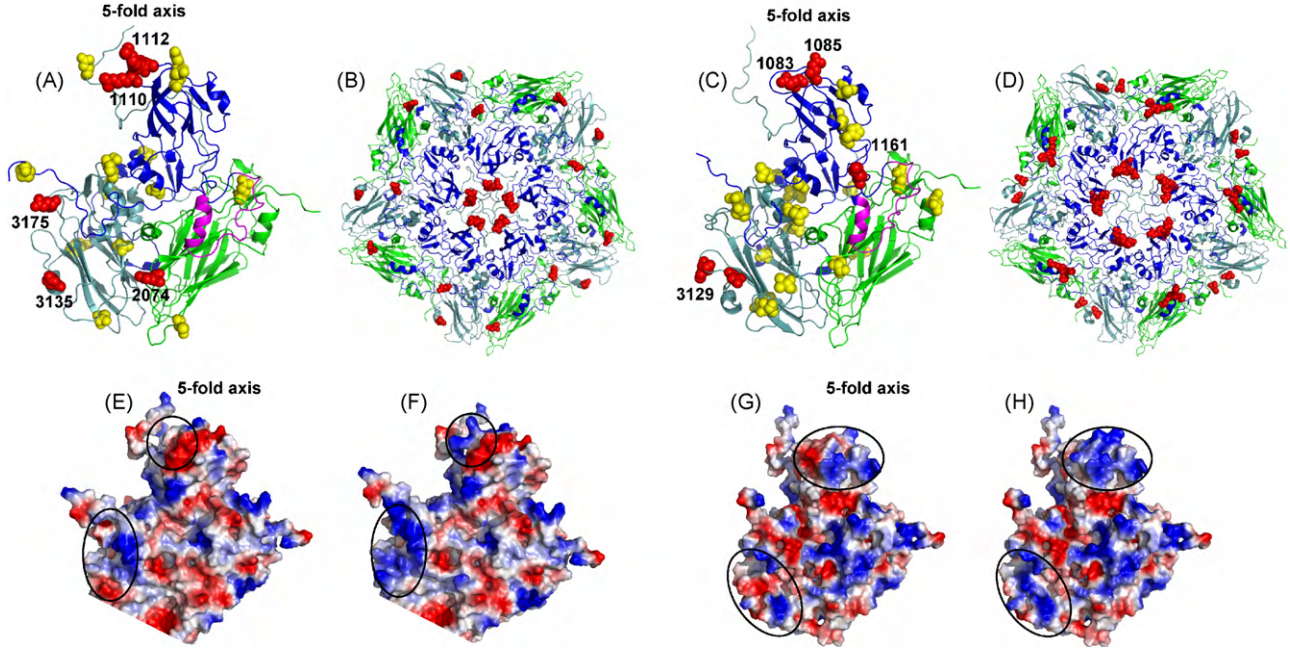

Fig. 2. 3D structure of a SAT1 and SAT2 protomeric subunit (A and C) and pentamer (B and D), modelled using the O1BFS co-ordinates (1FOD) as template. (A and B) The position of surface-exposed positive charge amino acid changes observed in cell culture-adapted SAT1 viruses is indicated in red. KRR, KGR and HRK positively charged residues were observed for SAR/9/81, KNP/196/91 and ZAM/2/93 at residue positions 110–112 of VP1. Lysines were present at residues 135 and 175 of VP3 in NAM/307/98 and an arginine at position 74 of VP2 in KNP/196/91. (C and D) For SAT2 viruses the positively charged residues at VP1 positions 83 and 85 (red) is surrounding the pore at the fivefold axis. The protein subunits and structural features for both models are colour coded: VP1 (blue), VP2 (green) and VP3 (light-teal), the G–H loop of VP1 containing the RGD motif (magenta). Other residue changes observed in SAT1 and SAT2 viruses are shown in yellow (see Table 2 for detail). (E–H) The electrostatic, accessible surface view of the SAT1 and SAT2 modelled biological protomers are shown. The electrostatic potential was coloured with positive charge as blue and negative in red and the scale of colouring was kept constant. The position of the charge change during adaptation is outline in black and is shown from E to F for SAT1 and G to H for SAT2 viruses.

respectively (Table 2). As indicated in Fig. 2, the selection of positively charged residues during adaptation occurred against a background of existing positive charges on the virion surface.

3.2. Genetic characterisation of residues involved in binding to CHO-K1 cells

Examination of the outer capsid protein sequences of 26 SAT1 and 30 SAT2 viruses from our database revealed a high level of variability at the residue positions associated with change during cell culture adaptation of the viruses (Table 3). For instance, residue 74 of VP2 is characterised by high entropy (Hx > 1.5) and forms part of a variable loop extending from residue 60–85, as is evident from a complete alignment of the capsid proteins of SAT1 viruses. At least 30% of the SAT1 viruses ($n = 8$) in the complete capsid protein alignment contained a Lys or Arg residue at position 74. However, the SAT1 isolates ($n = 26$) did not display the ability to infect and replicate in CHO-K1 cells (results not shown). In contrast, residue position 135 of VP3, also characterised by high entropy (Hx > 1.8), does not contain positively charged residues in any of the SAT1 field isolates, while position 175 of VP3 contains a conserved Glu residue in all 26 isolates. The VP1 residues 110–112, located in the short, variable βF–βG loop, display entropy of Hx > 0.7 and the absence of positively charged amino acids at positions 111 and 112. Where a Lys or Arg residue did occur at position 110, it was, however, followed by a negatively charged Asp residue at positions 111 or 112 in 50% of the cases.

A complete amino acid alignment of 30 SAT2 field isolates depicted the βD–βE loop of VP1 as a hypervariable region with residues 83 and 85 displaying high entropy (Hx > 1.3), while the His at position 84 was conserved. Only one isolate, KEN/3/57, an archive vaccine strain, contained a Lys–His–Lys sequence at this position, similar to that observed in a vaccine strain, KNP/19/89^{Vac}, and an adapted strain, ZAM/7/96^{BHK}. An Arg residue was repeatedly observed at position 85 of VP1 during adaptation of KNP/19/89 to BHK-21 cells. Residue 161 of VP1 was found to be variable in SAT2 viruses and a Lys residue was present at this position only in the cell culture-adapted strain ZIM/7/83^{Vac}. Notably, this residue follows two other positively charged residues, Lys159–His160, in VP1 of this virus.

The genetic changes observed in the case of cell culture-adapted SAT2/ZIM/14/90 were more complex and their implication for cell adaptation was less apparent (Table 2). From a structural perspective, the acquired positively charged residues at position 170 of VP2 and 129 of VP3 were neither surface exposed, nor were they located in the small heparin-binding depression (Fry et al., 2005) on the virion surface (Fig. 2). These changes were selected against a background of existing positively charged residues surrounding the threefold axis of the virus. This resulted in an increase in the positive polarity at local regions of the virion. In support of this observation was the finding that selection occurred against a negatively charged Asp residue at position 132 of VP3, which mutated to an Asn. Residues 129 and 132 of VP3 are located within a highly variable region, as observed from the P1 alignment of 30 SAT2 viruses, and the possibility that this area may function as an epitope cannot be excluded.

3.3. Generation and characterisation of recombinant viruses with altered surface charges

To study the effect of individual mutations in a defined genetic background, we constructed recombinant virus mutants in FMDV SAT2 infectious cDNA. Of the 26 SAT1 and 21 SAT2 amino acid changes introduced during cell culture adaptation of the parental virus isolates, we selected the following residue positions in VP1 for the generation of site-directed mutant recombinant viruses (Fig. 3A): (1) RGD to KRR at position 110–112 in a SAT1/SAT2 chimeric construct, *i.e.* pNAM/SAT (Storey et al., 2007); (2) Gln85 → Arg which increased the net positive charge of VP1 surrounding the fivefold axis of SAT2 virions and (3) Glu161 → Lys which was unique in that SAT2/ZIM/7/83 accumulated three positively charged residues at the base of the βG–βH loop. The latter two mutations were constructed in a SAT2/SAT2 chimeric infectious clone, pSAU/SAT, containing the outer capsid-coding region of the SAT2/SAU/6/00 virus in the pSAT2 genetic background (Böhmer, 2004). The SAU/6/00 isolate caused a severe outbreak in dairy herds in Saudi Arabia in 2000. However, production of a SAU/6/00 vaccine is hindered by low 146S antigen yields, a consequence of SAU/6/00 being notoriously difficult to adapt to BHK-21 cells.

The effect of these mutations on surface charge distributions is shown in Fig. 2(E, F and G, H). The SAT1 mutations at position 110–112 (Fig. 2E and F) and the SAT2 mutations at position 83–85 of VP1 (Fig. 2G and H) had a strong effect on the local surface electrostatic potential. A distinct local surface area, neighbouring the fivefold axes, lost its negative charge and gained a predominantly positive charge in both SAT1 and SAT2 viruses, although the amino acid positions were dissimilar. However, the positively charged region spanning residues 159–161 of the SAT2 vaccine strain (ZIM/7/83), was located at the base of the βG–βH loop and did not conform to the region surrounding the fivefold axis or the depression at the VP2/VP3/VP1 border (Fry et al., 2005).

Viable recombinant mutant viruses, designated vNAM(KRR)/SAT, vSAU(E85R)/SAT and vSAU(E161K)/SAT, were recovered from all three mutant clones and passaged in BHK-21 cells until CPE was observed (3–5 passages). Sequencing of the capsid-coding region of the progeny viruses revealed that the introduced KRR mutation was fixed in the population as a KGR sequence, but no other unintentional mutations were introduced in the mutant viruses.

3.4. Plaque phenotypes and relative infectivity titers

We subsequently investigated the ability of the recombinant mutant viruses to infect CHO-K1 cells, and the effect these mutations had on infectivity titers in BHK-21 cells. Confirmation of the role of positively charged residues, located at position 110–112 in VP1 of SAT1 vaccine strains, in the adaptation to BHK-21 cells was obtained by introducing a KRR sequence into the vNAM/SAT interserotype chimeric virus. The vNAM/SAT virus contain the outer capsid-coding region of a Namibian buffalo isolate, *i.e.* NAM/307/98 (Bastos et al., 2001), and displays poor growth and adaptation to BHK-21 cells. Furthermore, vNAM/SAT lacked BHK-21 cell culture adaptation as measured by the inability to infect CHO-K1 cells and poor titers on BHK-21 cells. The plaques in Fig. 3B illustrate the transition of the large, opaque wild-type plaques produced by the vNAM/SAT (wild-type outer capsid) to small, well-defined plaques on BHK-21 cell monolayers of the mutated progeny virus, vNAM(KRR)/SAT. The vNAM(KRR)/SAT also attained titers of 10^6 pfu/ml within 5 passages in BHK-21 cells, while viruses harbouring the corresponding wild-type outer capsid-coding region only produced titers of 10^5 pfu/ml after eight passages. In summary, the mutations in the VP1 βF–βG loop neighbouring the fivefold axis of the SAT1 viruses, a site prone to variation, conferred the ability to adapt rapidly to BHK-21 cells and grow in CHO-K1 cells. This ability of the virus is probably due to utilisation of alternative HSPG receptors for cell binding and entry in cultured cells.

The effect of an Arg at VP1 position 83 or a Lys at 161 of vSAU/SAT is shown in Fig. 3B. No significant differences were observed in the plaque morphologies of the progeny virus populations obtained from the non-mutated vSAU/SAT and vSAU(E85R)/SAT and vSAU(E161K)/SAT mutated viruses (Fig. 3B). On BHK-21 mono-

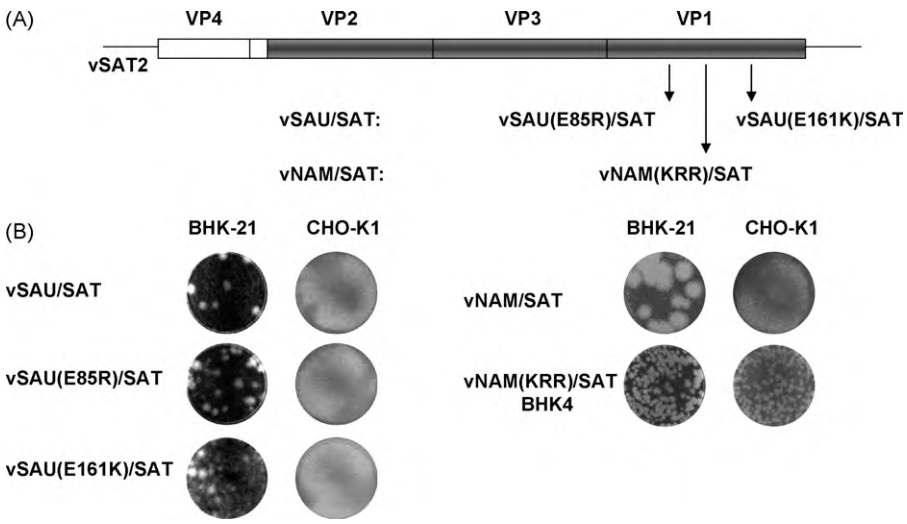

Fig. 3. (A) Schematic representation of the chimeric FMDV constructs and the introduction of mutations described in this study. (B) Plaque morphologies of chimeric viruses containing the wild-type outer capsid proteins of SAT1/NAM/307/98 and SAT2/SAU/6//00 cloned into the genetic background of pSAT2. The change in plaque phenotype on BHK-21 cells and the susceptibility of CHO-K1 cells for infection by the mutant vNAM(KRR)/SAT is shown. The mutant vSAU(E85R)/SAT and vSAU(E161K)/SAT displayed the same plaque morphology than the wild-type chimera and did not grow in CHO-K1 cells.

layers, the virus plaques were opaque, a phenotype commonly associated with viruses which have not been adapted to BHK-21 cells. Furthermore, CHO-K1 cells were not able to sustain infection by the vSAU/SAT or mutated virus populations. The infectivity titers on BHK-21 cells were also comparable for the three virus populations. Neither vSAU/SAT, nor the two mutants, vSAU(E85R)/SAT and vSAU(E161K)/SAT, were able to utilise HSPG for cell entry.

An in-depth analysis of the amino acid sequences neighbouring the introduced mutations in vSAU/SAT revealed that the introduced Lys85 was preceded by an acidic Glu residue at position 83, while the Lys161 was preceded by a DSTH sequence at VP1 residue positions 157–160. In both instances the added positive charge was compromised by acidic residues in its immediate environment, which may explain the absence of interaction with the negatively charged HSPG molecules.

4. Discussion

Despite the success of conventional vaccines in the control of FMD in the developed world, inactivated vaccines are unable to cover the vast antigenic variability within the SAT types in southern Africa (Hunter, 1996). Recombinant inactivated SAT type vaccines, structurally designed to be effective for specific geographic regions, may overcome the limitation of antigenic variation (Van Rensburg et al., 2004). However, the transfer of antigenic determinants during the replacement of the outer capsid proteins is simultaneously accompanied by the transfer of the receptor preferences of the field isolate. This could impact adversely on the use of recombinant viruses as vaccine seed stock due to the lack of cell culture adaptation and the consequent low yields in 146S particles. In addition, adaptation to the BHK-21 production cell line is often a cumbersome, time consuming and expensive process (Rieder et al., 1993; Van Rensburg et al., 2004).

To address the limitation of acquiring this adaptation phenotype by selection, we investigated the accumulated genetic changes of SAT1 and SAT2 viruses which have been adapted to BHK-21 cells, including efficacious vaccine strains. Our study supports the evidence from diverse virus families that cell culture adaptation of viruses (Patel et al., 1993; Chen et al., 1997; Krusat and Streckert, 1997; Byrnes and Griffin, 1998; Klimstra et al., 1998; Summerford and Samulski, 1998), and more specifically, FMDV (Jackson et al., 1996; Sa-Carvalho et al., 1997; Fry et al., 1999), selects from the quasi-species population variants with affinity for HSPG as observed by the ability to infect and replicate in CHO-K1 cells. Comparison of the outer capsid proteins of SAT1 and SAT2 viruses, with and without this phenotype, revealed a pattern of mutations with the common property of increasing the net positive charges on the virion surface, particularly surrounding the fivefold axis of the virion. Adaptation of the viruses in BHK-21 monolayer cells select for positively charged, surface-exposed residues which are most probably involved in the facilitation of cell entry via HSPG molecules.

Binding of viruses to HSPG or other GAGs occurs mainly through electrostatic interactions between positively charged Lys and Arg groups on the virus surface and the negatively charged N and O sulfated groups of the GAG molecules (Gromm et al., 1995; Byrnes and Griffin, 1998, 2000). Similarly to FMDV, repeated passaging of alphaviruses in BHK-21 cells also leads to reduced plaque size and an increased HSPG-binding ability (Marshall et al., 1962; Heydrick et al., 1966; Byrnes and Griffin, 1998). The accumulated positively charged residues and increased affinity to HSPG probably leads to direct interaction between the Arg or Lys and the polysaccharide backbone. In numerous other HSPG-binding proteins the strength of binding to the substrate was affected by the degree of sulfation of the polysaccharide backbone (Byrnes and Griffin, 1998). The selection of positively charged residues during cell-culture adaptation was previously reported for type O viruses (Sa-Carvalho et al., 1997; Jackson et al., 1996, 2001). Adaptation of the O1 Campos virus to cell culture selected viruses with an H → R change at position 56 of VP3 (Jackson et al., 1996; Sa-Carvalho et al., 1997). The 3D structure of the virion revealed that the positively charged residue 56 of VP3 is located within the recessed heparin-binding site, a depression on the virion surface situated at the junction of VP1, VP2 and VP3 (Fry et al., 1999).

Although we did not observe any of these changes in the VP3 proteins of the SAT1 or SAT2 viruses, residue changes at positions 135 and 175 in the VP3 were present in SAT1/NAM/307/98. Both these changes may contribute singly or accumulatively to the adaptation phenotype. The effect of each of these changes individually and accumulatively on cell culture adaptation and possible HSPG-binding is, therefore, not known and needs investigation to fully understand the mechanisms of cell culture adaptation. Furthermore, this is the first report on the fixation of positively charged residues 110–112 in the βF–βG loop of VP1 of SAT1 isolates and

its possible correlation with the ability of SAT1 viruses to replicate in CHO-K1 cells. The importance of this amino acid sequence in adaptation of SAT1 isolates to cultured BHK-21 cells and its possible function as a HSPG-binding site is evident from: (1) the KNP/196/91^{Vac} and SAR/9/81^{Vac} vaccine strains (Fig. 1) with the ability to infect and replicate in CHO-K1 cells; (2) the field isolate ZAM/2/93 adapted rapidly to cell culture as observed by the appearance of small plaques on BHK-21 cells and growth in CHO-K1 cells; (3) variation at the residue positions 110 and 112 of the VP1 capsid protein in an alignment of 26 SAT1 wild-type viruses with the inability to grow on CHO-K1 cells (Table 3); and (4) the introduction of the positively charged residues 110–112 in the vNAM/SAT chimeric virus was consistent with the small plaque phenotype and growth in CHO-K1 cells of the KNP/196/91 and SAR/9/81 vaccine strains. With the exception of SAT1/KNP/196/91, none of the other SAT1 viruses showed genetic changes in VP2 between the primary isolates and cell culture-adapted derivatives. The Gln74 → Arg substitution in VP2 is structurally associated with the shallow depression observed at the junction of the three major capsid proteins described by Fry et al. (2005).

The only mutations in VP3 observed during adaptation of SAT2 viruses were the Glu148 → Lys change of ZAM/7/96 and the Thr129 → Lys substitution of ZIM/14/90, although both residues were not fully exposed on the virion surface and did not correlate with the shallow HSPG-binding depression (Fry et al., 2005). These mutations, however, did not occur in isolation in these viruses and were possibly selected against a background of existing positively charged residues (Fig. 2). In the case of Thr129 → Lys mutation, it was accompanied by an Asp132 → Asn mutation, with the removal of a surface-exposed negative charge. Whether the two substitutions contributed synergistically or independently to the cell culture adaptation phenotype is not known. The ability of ZIM/14/90 to infect and replicate in CHO-K1 cells (Fig. 1) was associated with Gln170 → Arg change in VP2 together with the Thr129 → Lys substitution in VP3, an indication that the accumulative contribution may play a role. Noteworthy is the observation of existing positively charged residues in close approximation of these changes, suggesting that the selection of positively charged residues during adaptation transpired against a background of existing positive charges on the virion surface. The residue changes at position 83–85 of VP1 were observed for both the SAT2 viruses, KNP/19/89 and ZAM/7/96. The role of these residues, protruding from the fivefold axis, in BHK-21 adaptation and possible binding of HSPG is in agreement with observation for SAT1 viruses.

Phenotypic characterisation of the recombinant mutants revealed that the variants that were able to infect CHO-K1 cells shared a small plaque phenotype in BHK-21 cells. The small plaque phenotype produced by the vNAM(KRR)/SAT mutant in BHK-21 cells was consistent with the small plaques observed for the SAT1 vaccine strains SAR/9/81^{Vac} and KNP/196/91^{Vac}. Introduction of the cell culture adaptation phenotype during the construction of a chimeric virus may thus be advantagous for improved infectivity in cultured BHK-21 cells used in the production of FMD vaccines. On the contrary, neither vSAU(E85R)/SAT nor vSAU(E161K)/SAT produced plaques with altered morphology on BHK-21 cells compared to vSAU/SAT with the wild-type outer capsid. A systematic analysis of the sequences adjacent to both mutations revealed the presence of negatively charged residues which may act as a repelling force to the negatively charged sulfated groups of GAG's. Therefore, the role of the VP1 amino acid sequences of SAT2 isolates in cell culture adaptation requires further investigation.

The development of new vaccine strains to protect against emerging SAT viruses relies strongly on the virus yield of the new strain in the production cell line, the yield of 146S particles, stability of the virus and antigen, and a close antigenic relationship to field isolates causing current FMD outbreaks. BHK-21 cells are the cell line of choice for production of inactivated FMD vaccines and SAT viruses are notorious for their difficulty to adapt to BHK-21 cells (as outlined in Section 1). Our results demonstrated that for the purpose of SAT type vaccine production, viruses previously impossible to adapt to cell culture, can be designed with improved growth properties in cell cultures. Introductions of the cell culture adaptation phenotype to chimeric FMDV may be beneficial to the productivity in BHK-21 cells and the production 146S antigen.

Acknowledgments

This work was supported by funding from Intervet–Schering-Plough and the U.S. Department of Agriculture, Agricultural Research Service. The cell culture-adapted SAT1 and SAT2 viruses were received from the vaccine unit at Transboundary Animal Diseases of the ARC-OVI. We thank Juanita van Heerden for her contributions with sequencing part of SAT2/KNP/19/89. We would also like to thank Dr. Otto Koekemoer, Ms. Sonja Maree and Erika Kirkbride for critical reading of the manuscript.

References

Acharya, R., Fry, E., Stuart, D., Fox, G., Rowlands, D., Brown, F., 1989. The three-dimensional structure of foot-and-mouth disease virus at 2.9 Å resolution. Nature 337, 709–716.

Almeida, M.R., Rieder, E., Chinsangaram, J., Ward, G., Beard, C., Grubman, M.J., Mason, P.W., 1998. Construction and evaluation of an attenuated vaccine for foot-and-mouth disease, difficulty adapting the leader proteinase-deleted strategy to the serotype O1 virus. Virus Res. 55, 49–60.

Amadori, M., Berneri, C., Archetti, I.L., 1994. Immunogenicity of foot-and-mouth disease virus grown in BHK-21 suspension cells. Correlation with cell ploidy alterations and abnormal expression of the alpha 5 beta 1 integrin. Vaccine 12, 159–166.

Amadori, M., Volpe, G., Defilippi, P., Berneri, C., 1997. Phenotypic features of BHK-21 cells used for production of foot-and- mouth disease vaccine. Biologicals 25, 65–73.

Bastos, A.D.S., 1998. Detection and characterization of foot-and-mouth disease virus in sub-Saharan Africa. Onderstepoort J. Vet. Res. 65, 37–47.

Bastos, A.D.S., Haydon, D.T., Forsberg, R., Knowles, N.J., Anderson, E.C., Nel, L.H., Thomson, G.R., Bengis, R.G., 2001. Genetic heterogeneity of SAT-1 type foot-an-d-mouth disease viruses in southern Africa. Arch. Virol. 146, 1537–1551.

Bastos, A.D.S., Haydon, D.T., Sangare, O., Boshoff, C.I., Edrich, J.L., Thomson, G.R., 2003. The implications of virus diversity within the SAT 2 serotype for control of foot-and-mouth disease in sub-Saharan Africa. J. Gen. Virol. 84, 1595–1606.

Baxt, B., Becker, Y., 1990. The effect of peptides containing the arginine–glycine–aspartic acid sequence on the adsorption of foot-and-mouth disease virus to tissue culture cells. Virus Genes 4, 73–83.

Berinstein, A., Roivainen, M., Hovi, T., Mason, P.W., Baxt, B., 1995. Antibodies to the victronectin receptor (Integrin $\alpha_v\beta3$) inhibit binding and infection of foot-and-mouth disease virus to cultured cells. J. Virol. 69, 2664–2666.

Böhmer, B., 2004. Engineering of a chimeric SAT2 foot-and-mouth disease virus for vaccine production. M.Sc. thesis, University of Pretoria, South Africa.

Byrnes, A.P., Griffin, D.E., 1998. Binding of Sindbis virus to cell surface heparan sulfate. J. Virol. 72 (9), 7349–7356.

Byrnes, A.P., Griffin, D.E., 2000. Large-plaque mutants of Sindbis virus show reduced binding to heparan sulfate, heightened viremia, and slower clearance from the circulation. J. Virol. 74, 644–651.

Chen, Y., Maguire, T., Hileman, R.E., Fromm, J.R., Esko, J.D., Linhardt, R.J., Marks, R.M., 1997. Dengue virus infectivity depends on envelope protein binding to target cell heparan sulfate. Nat. Med. 3, 866–871.

Cottam, E.M., Thébaud, G., Wadsworth, J., Gloster, J., Mansley, L., Paton, D.J., King, D.P., Haydon, D.T., 2008. Integrating genetic and epidemiological data to determine transmission pathways of foot and mouth disease virus. Proc. Biol. Sci. 275 (1637), 887–895.

Curry, S., Fry, E., Blakemore, W., Abu-Ghazaleh, R., Jackson, T., King, A., Lea, S., Newman, J., Stuart, D., 1997. Dissecting the roles of VP0 cleavage and RNA packaging in picornavirus capsid stabilization, the structure of empty capsids of foot-and-mouth disease virus. J. Virol. 71, 9743–9752.

Duque, H., Baxt, B., 2003. FMDV receptors: comparison of bovine av integrin utilization by type A and O viruses. J. Virol. 77, 2500–2511.

Fox, G., Parry, N.R., Barnett, P.V., McGinn, B., Rowlands, D.J., Brown, F., 1989. The cell attachment site on foot-and-mouth disease virus includes the amino acid sequence RGD (arginine–glycine–aspartic acid). J. Gen. Virol. 70 (Pt 3), 625–637.

Fry, E.E., Lea, S.M., Jackson, T., Newman, J.W.I., Ellard, F.M., Blakemore, W.E., Abu-Ghazaleh, R., Samuel, A., King, A.M.Q., Stuart, D.I., 1999. The structure and function of a foot-and-mouth disease virus-oligosaccharide receptor complex. EMBO J. 18 (3), 543–554.

Fry, E.E., Newman, J.W.I., Curry, S., Najjam, S., Jackson, T., Blakemore, W., Lea, S.M., Miller, L., Burman, A., King, A.M.Q., Stuart, D.I., 2005. Structure of FMDV serotype

$A1O_{61}$ alone and complexed with oligosaccharide receptor, receptor conservation in the face of antigenic variation. J. Gen. Virol. 86, 1909–1920.
Gromm, J.R., Hilemann, R.E., Caldwell, E.E.O., Weiler, J.M., Linhardt, R.J., 1995. Differences in the interaction of heparin with arginine and lysine and the importance of these basic amino acids in the binding of heparin to acidic fibroblast growth factor. Arch. Biochem. Biophys. 323, 279–287.
Herrera, M., García-Arriaza, J., Pariente, N., Escarmís, C., Domingo, E., 2007. Molecular basis for a lack of correlation between viral fitness and cell killing capacity. PLoS Pathog. 3 (4), e53.
Heydrick, F.P., Wachter, R.F., Hearn, H.J., 1966. Host influence on the characteristics of Venezuelan equine encephalomyelitis virus. J. Bacteriol. 91, 2343–2348.
Hooft, R.W.W., Vriend, G., Sander, C., Abola, E.E., 1996. Errors in protein structures. Nature 381, 272–1272.
Hunter, P., 1996. The performance of southern African territories serotypes of foot and mouth disease antigen in oil-adjuvanted vaccines. Rev. Sci. Tech. 15, 913–922.
Jackson, T., Ellard, F.M., Abu-Ghazaleh, R., Brookes, S.M., Blakemore, W.E., Corteyn, A.H., Stuart, D.I., Newman, J.W.I., King, A.M.Q., 1996. Efficient infection of cells in culture by type O foot-and-mouth disease virus requires binding to cell surface heparan sulfate. J. Virol. 70, 5282–5287.
Jackson, T., Sharma, A., Ghazaleh, R.A., Blakemore, W.E., Ellard, F.M., Simmons, D.L., Newman, J.W.I., Stuart, D., King, A.M.Q., 1997. Arginine-glycine-aspartic acid-specific binding by foot-and-mouth disease viruses to the purified integrin αvß3 *in vitro*. J. Virol. 71 (11), 8357–8361.
Jackson, T., Sheppard, D., Denyer, M., Blakemore, W., King, A.M.Q., 2000. The epithelial integrin alpha-v-beta-6 iis a receptor for foot-and-mouth disease virus. J. Virol. 74 (11), 4949–4956.
Jackson, T., Ellard, F.M., Ghazaleh, R.A., Brookes, S., Blakemore, W., Corteyn, A., Stuart, D., Newman, J.W.I., King, A.M.Q., 2001. Efficient infection of cells in culture by type O FMDV requires binding to cell surface heparan sulfate. J. Virol. 70, 5282–5287.
Jackson, T., Mould, A.P., Sheppard, D., King, A.M.Q., 2002. Integrin αvβ1 is a receptor for foot-and-mouth disease virus. J. Virol. 76, 935–941.
Jackson, T., Clarck, S.J., Berryman, S., Burman, A., Cambier, S., Mu, D., Nishimura, S., King, A.M.Q., 2004. Integrin αvβ8 functions as a receptor for Foot-and-mouth disease virus, role of the α-chain cytodomain in integrin-mediated infection. J. Virol. 78, 4533–4540.
Klimstra, W.B., Ryman, K.D., Johnston, R.B., 1998. Adaptation of Sindbis Virus to BHK cells selects for use of heparan sulfate as an attachment receptor. J. Virol. 72, 7357–7366.
Krusat, T., Streckert, H.-J., 1997. Heparin-dependent attachment of respiratory syncytial virus (RSV) to host cells. Arch. Virol. 142, 1247–1254.
Lea, S., Abu-Ghazaleh, R., Blakemore, W., Curry, S., Fry, E., Jackson, T., King, A., Logan, D., Newman, J., Stuart, D., 1995. Structural comparison of two strains of foot-and-mouth disease virus subtype O_1 and a laboratory antigenic variant G67. Structure 3, 571–580.
Leippert, M., Beck, E., Weiland, F., Pfaff, E., 1997. Point mutations within the betaG-betaH loop of foot-and-mouth disease virus O1K affect virus attachment to target cells. J. Virol. 71, 1046–1051.
Logan, D., Abu-Ghazaleh, R., Blakemore, W., Curry, S., Jackson, T., King, A., Lea, S., Lewis, R., Newman, J., Parry, N., 1993. Structure of a major immunogenic site on foot-and-mouth disease virus. Nature 362 (6420), 566–568.
Marshall, I.D., Scrivani, R.P., Reeves, W.C., 1962. Variation in the size of plaques produced in tissue culture by strains of western equine encephalitis virus. Am. J. Hyg. 76, 216–224.
Mason, P.W., Rieder, E., Baxt, B., 1994. RGD sequence of foot-and-mouth disease virus is essential for infecting cells via the natural receptor but can be bypassed by an antibody-dependent enhancement pathway. Proc. Natl. Acad. Sci. U.S.A. 91, 1932–1936.
Müller, H., Johne, R., Raue, R., Haas, B., Bätza, H.J., 2001. Persistence of FDMV and its effects on disease control strategies. Dtsch. Tierarztl. Wochenschr. 108 (12), 513–518.
Neff, S., Sa-Carvalho, D., Rieder, E., Mason, P.W., Blystone, S.D., Brown, E.J., Baxt, B., 1998. Foot-and-mouth disease virus virulent for cattle utilizes the integrin alpha(v)beta3 as its receptor. J. Virol. 72, 3587–3594.
Neff, S., Mason, P.W., Baxt, B., 2000. High-efficiency utilization of the bovine integrin $\alpha_v\beta3$ as a receptor for foot-and-mouth disease virus is dependent on the bovine $\alpha_v\beta$ subunit. J. Virol. 74, 7298–7306.
Office International des Epizooties, 2009. Manual of Diagnostic Tests and Vaccines for Terrestrial Animals 2009. Office International des Epizooties, Paris, France, Chapter 2.1.5, pp. 1–25.
Patel, M., Yanagishita, M., Roderiquez, G., Bou-Habib, D.C., Oravecz, T., Hascall, B.C., Norcross, M.A., 1993. Cell-surface heparan sulfate proteoglycan mediates HIV-1 infection of T-cell lines. AIDS Res. Hum. Retroviruses 9, 167–174.
Pay, T.W.F., Rweyemamu, M.M., O'Reilly, K.J., 1978. Experiences with Type SAT 2 foot-and-mouth disease vaccines in Southern Africa. In: XVth Conference of the Office International Des Epizzoties Permanent Commission on foot-and-mouth disease, pp. 1–25.
Preston, K.J., Owens, H., Mowat, G.N., 1982. Sources of variations encountered during the selection and production of three strains of FMD virus for the development of vaccine for use in Nigeria. J. Biol. Stand. 10, 35–45.
Racaniello, V.R., 2006. One hundred years of poliovirus pathogenesis. Virology 344 (1), 9–16.
Rieder, E., Bunch, T., Brown, F., Mason, P.W., 1993. Genetically engineered foot-and-mouth disease viruses with poly(C) tracts of two nucleotides are virulent in mice. J. Virol. 67, 5139–5145.
Rieder, E., Baxt, B., Mason, P.W., 1994. Animal-derived antigenic variants of foot-and-mouth disease virus type A_{12} have low affinity for cells in culture. J. Virol. 68 (8), 5296–5299.
Sa-Carvalho, D., Rieder, E., Baxt, B., Rodarte, R., Tanuri, A., Mason, P.W., 1997. Tissue culture adaptation of foot-and-mouth disease virus selects viruses that bind to heparin and are attenuated in cattle. J. Virol. 71, 5115–5123.
Sali, A., Blundell, T.L., 1993. Comparative protein modelling by satisfaction of spatial restraints. J. Mol. Biol. 234, 779–815.
Samuel, A.R., Knowles, N.J., 2001. Foot-and-mouth disease virus, cause of the recent crisis for the UK livestock industry. Trends Genet. 17 (8), 421–424.
Sellers, R.F., Daggupaty, S.M., 1990. The epidemic of foot-and-mouth disease in Saskatchewan, Canada, 1951–1952. Can. J. Vet. Res. 54 (4), 457–464.
Storey, P., Theron, J., Maree, F.F., O'Neill, H.G., 2007. A second RGD motif in the 1D capsid protein of a SAT1 type foot-and-mouth disease virus field isolate is not essential for attachment to target cells. Virus Res. 124, 184–192.
Summerford, C., Samulski, R.J., 1998. Membrane-associated heparin sulfate proteoglycan is a receptor for adeno-associated virus type 2 virions. J. Virol. 72, 1438–1445.
Thomson, G.R., 1995. Overview of foot and mouth disease in southern Africa. Rev. Sci. Tech. Off. Int. Epiz. 14 (3), 503–520.
Tomassen, F.H., de Koeijer, A., Mourits, M.C., Dekker, A., Bouma, A., Huirne, R.B., 2002. A decision-tree to optimise control measures during the early stage of a foot-and-mouth disease epidemic. Prev. Vet. Med. 54 (4), 301–324.
Van Rensburg, H.G., Mason, P., 2002. Construction and evaluation of a recombinant foot-and-mouth disease virus. Implications for inactivated vaccine production. Ann. N. Y. Acad. Sci. 969, 83–87.
Van Rensburg, H.G., Henry, T., Mason, P.W., 2004. Studies of genetically defined chimeras of a European type A virus and a South African Territories type 2 virus reveal growth determinants for foot-and-mouth disease virus. J. Gen. Virol. 85, 61–68.
Zhao, Q., Pacheco, J.M., Mason, P.W., 2003. Evaluation of genetically engineered derivatives of a Chinese strain of foot-and-mouth disease virus reveals a novel cell-binding site which functions in cell culture and in animals. J. Virol. 77, 3269–3280.
Zibert, A., Maas, G., Strebel, K., Falk, M.M., Beck, E., 1990. Infectious foot-and-mouth disease virus derived from a cloned full-length cDNA. J. Virol. 64, 2467–2473.

Return to Table of Contents

Virology 405 (2010) 149–156

Contents lists available at ScienceDirect

Virology

journal homepage: www.elsevier.com/locate/yviro

Domain disruptions of individual 3B proteins of foot-and-mouth disease virus do not alter growth in cell culture or virulence in cattle

Juan M. Pacheco [a], Maria E. Piccone [a,b], Elizabeth Rieder [a], Steven J. Pauszek [a], Manuel V. Borca [a], Luis L. Rodriguez [a,*]

[a] Agricultural Research Service, U.S. Department of Agriculture, Plum Island Animal Disease Center, Greenport, New York, USA
[b] Department of Pathobiology and Veterinary Sciences, University of Connecticut, Storrs, CT, USA

ARTICLE INFO

Article history:
Received 15 January 2010
Returned to author for revision
23 February 2010
Accepted 27 May 2010
Available online 30 June 2010

Keywords:
Foot-and-mouth disease
Protein 3B
Mutagenesis
Cattle

ABSTRACT

Picornavirus RNA replication is initiated by a small viral protein primer, 3B (also known as VPg), that is covalently linked to the 5' terminus of the viral genome. In contrast to other picornaviruses that encode a single copy of 3B, foot-and-mouth disease virus (FMDV) encodes three copies of 3B. Viruses containing disrupted native sequence or deletion of one of their three 3B proteins were derived from a FMDV A24 Cruzeiro full-length cDNA infectious clone. Mutant viruses had growth characteristics similar to the parental virus in cells. RNA synthesis and protein cleavage processes were not significantly affected in these mutant viruses. Cattle infected by aerosol exposure with mutant viruses developed clinical disease similar to that caused by the parental A24 Cruzeiro. Therefore, severe domain disruption or deletion of individual 3B proteins in FMDV do not affect the virus' ability to replicate *in vitro* and cause clinical disease in cattle.

Published by Elsevier Inc.

Introduction

Foot-and-mouth disease (FMD) is a highly contagious viral disease of cattle, pigs, sheep, goats, and wild cloven-hoofed animals. The disease is characterized by fever and vesicular lesions of the epithelium of the mouth, tongue, feet, and teats (Alexandersen et al., 2003). The causal agent, FMD virus (FMDV), is a positive-stranded RNA virus that is the type species of the Aphthovirus genus of the *Picornaviridae* family.

The 8-kb FMDV genome is involved in translation and in replication. During replication, the genome is expressed as a single open reading frame (ORF) that is processed into mature polypeptide products. Translation of the ORF begins with a proteinase (Lpro), which is followed by the structural proteins of the P1 region (1A, 1B, 1C, and 1D) and the remaining nonstructural proteins of the P2 (2A, 2B and 2C) and P3 regions (3A, 3B, 3Cpro, and 3Dpol) (Grubman and Baxt, 2004). The 3C protease is responsible for most of the cleavages during the FMDV polyprotein processing (Vakharia et al., 1987), and 3Dpol is the viral RNA-dependent RNA polymerase (Grubman and Baxt, 2004). Protein 3B is covalently bound to the 5′ end of the genome and antigenome, and functions in priming picornavirus RNA synthesis (Wimmer, 1982). In addition to the four terminal P3 cleavage products (3A, 3B, 3C, and 3D proteins) and the uncleaved P3 polyprotein, several "intermediates" are observed in infected cells (3AB, 3CD, and 3BCD proteins) (Oh et al., 2009). As reviewed by Oh et al. (2009), it has been shown for poliovirus that these intermediate cleavage products of the P3 region can have different functions from their terminal cleavage products (3A, 3B, 3C and 3D).

In FMDV, 3B is present in three similar but nonidentical copies ($3B_1$, $3B_2$ and $3B_3$) (Forss and Schaller, 1982) that are 23 or 24 amino acids in length (King et al., 1980). Although not all three copies of FMDV 3B are needed to maintain infectivity (Falk et al., 1992; Pacheco et al., 2003), there are no reports of naturally occurring FMDV strains with fewer than three copies of 3B, suggesting that there is a strong selective pressure toward maintaining this redundancy (Carrillo et al., 2007; MacKenzie et al., 1975). This is an unusual finding, since FMDV is known to readily undergo homologous recombination to remove redundant genetic material (King et al., 1982). However, it has been reported that deletion of the $3B_3$ coding sequence within the context of the full-length infectious cDNA resulted in the production of a noninfectious RNA transcript (Falk et al., 1992). Additionally, $3B_3$ seems to be the most efficient substrate for the FDMV 3Dpol activity when each of the FMDV 3Bs is uridylylated *in vitro* (Nayak et al., 2005). It has been described that the loss of $3B_3$ sequence may also have a deleterious effect on FMDV RNA replication (Nayak et al., 2005). Laboratory-generated viruses lacking the first two 3B peptides were impaired in their ability to replicate in porcine cells in culture and caused attenuated disease in pigs showing that the presence of three 3Bs appear to control the virus' pathogenic potential and host range (Pacheco et al., 2003).

In this work we analyzed the *in vitro* and *in vivo* characteristics and pathogenic potential of viruses derived from a FMDV A24 Cruzeiro full-length cDNA infectious clone (A24-WT) containing modified forms or deletion of individual 3B peptides. Three viruses were created carrying an in-frame 57-nucleotide (19 amino acid) insertion randomly located into

* Corresponding author.
E-mail address: luis.rodriguez@ars.usda.gov (L.L. Rodriguez).

0042-6822/$ – see front matter. Published by Elsevier Inc.
doi:10.1016/j.virol.2010.05.036

one of the three different 3Bs resulting in severe disruption of the native amino acid sequence of the target proteins. Two additional viruses were also obtained which eliminated not only the 57 nucleotide transposon insertion after transfection but also had a partial deletion of the 3B region (3′ end of $3B_1$ and 5′ end of $3B_2$, in both cases). Interestingly, our results demonstrated that all 5 mutant viruses grew similarly, showed similar RNA replication kinetics and had similar plaque size in cell culture to those of the parental virus. Additionally, cattle infected by aerosol exposure with each of the five viruses developed infection and clinical disease similar to that caused by the parental FMDV A24-WT. Therefore, we provide evidence that the introduction of significant individual domain alterations on each of the 3B proteins do not have a significant effect on virus growth *in vitro* nor in virus virulence *in vivo*.

Results

Generation of FMDV 3B mutants

Using a full-length FMDV A24-WT cDNA clone (Rieder et al., 2005), nine plasmids containing 19mer inserts in the 3B region were generated by random transposon mediated insertion mutagenesis. Mutated plasmids were completely sequenced to confirm the exact insertion site. RNA derived from each of nine plasmids containing individual insertions in each of the 3B proteins were use for electroporation of BHK-21 cells giving origin to five viruses showing either insertions or deletions in 3B and additional changes elsewhere in the genome after amplification in BHK-21 cells (Table 1). Viruses derived from plasmids pA24-VPg_1-5873, pA24-VPg_2-5934 and pA24-VPg_3-6007 harbored individual inserts in one of their 3B proteins and were named A24-VPg_1-5873, A24-VPg_2-5934 and A24-VPg_3-6007 respectively (Fig. 1A). Two plasmids with inserts in $3B_1$ (pA24-VPg_1-5853 and pA24-VPg_1-5869) yielded viruses that lost the original insert along with one full 3B, including the 3′ end of $3B_1$ and the 5′ end of $3B_2$ resulting in mutant viruses A24-ΔVPg-5853 and A24-ΔVPg-5869, respectively (Fig. 1B). The full-length genome of the five mutant viruses was sequenced and showed very few differences throughout the genome besides their 3B insertions or deletions (Table 1).

Cell growth characteristics of FMDV 3B mutants

The growth kinetics of the five mutant viruses was compared with the parental virus A24-WT in EBK cells (primary embryonic bovine kidney cells). Cell cultures were infected with each of the viruses at high and low multiplicity of infection (MOIs) (5, 0.1 and 0.01). At different time points post-infection samples were taken and titrated on BHK-21 cells. At all MOIs mutant viruses demonstrated growth kinetics similar to that of the parental virus (Fig. 2). All viruses obtained at 24 h time point from the growth curve generated with an MOI of 0.01 were full-length sequenced to confirm that the original insertions and deletions were still present in a mostly homogeneous viral population. No changes were detected in any of the viruses analyzed (results not shown).

Plaque morphology of the FMDV 3B mutant viruses was evaluated on five FMDV susceptible cell lines: BHK-21 (hamster kidney-derived cells), BHK- $\alpha_V\beta_6$ (BHK-21 cells constitutively expressing bovine integrins (Duque et al., 2004)), IBRS2 (swine-derived cell line), LFBK (bovine-derived cell line (Swaney, 1988)) and EBK. No significant differences in the titer (Fig. 3A) or plaque sizes were found, with the exception of A24-VPg_3-6007 that showed a 40–50% smaller plaque size in BHK-21, BHK-$\alpha_V\beta_6$ and EBK cells, but not in LFBK or IBRS2 cells (Fig. 3B).

Kinetics of viral RNA synthesis in FMDV with altered 3B proteins

The effect of modifications in 3B proteins on viral RNA synthesis during infection of BHK-21 and EBK cell was analyzed. Cultures were infected with each of the mutant or parental A24-WT viruses at an MOI of 5 and 0.05. Total intracellular FMDV RNA concentrations were determined by quantitative rRT-PCR (Callahan et al., 2002) at different sampling points during the first 4 h post-adsorption. Mutant viruses showed similar pattern of RNA synthesis to A24-WT at both low and high MOI in both cell types. Only a small delay in RNA synthesis at 1–2 h post-adsorption in BHK-21 cells was observed in mutant A24-Vpg_3-6007 (Fig. 4).

Processing of 3A and 3B proteins in FMDV 3B mutants

Since 3B is too small to be readily resolved by standard polyacrylamide gel electrophoresis, its presence is usually visualized in partially processed intermediates (Falk et al., 1992; Pacheco et al., 2003). Top (I) and center (II) portions of Fig. 5 show a Western blot developed using a rabbit polyclonal serum that recognizes the conserved N-terminal portion of 3A (O'Donnell et al., 2001). The bottom portion (III) of Fig. 5 shows reactivity with a pool of monoclonal antibodies against 3B to confirm the assignment of products made on the top and center portions of the figure. A typical A24-WT electrophoretic pattern shows five 3A-3B proteins and the mobility observed for these proteins was slightly slower than predicted, as previously reported (Garcia-Briones et al., 2006; O'Donnell et al., 2001; Pacheco et al., 2003; Strebel et al., 1986). The fastest migrating band (band 1) represents degraded-3A (Pacheco

Table 1
Nucleotide and amino acid sequence of mutant viruses obtained after transfection or from clinical samples.

Plasmid	Virus obtained in cell culture	Nucleotide and amino acid changes related to FMDV A24-WT[c]							Partial sequence (3B region) of viruses obtained from infected animals[f]
		5'UTR[d]		VP1	3D				
		542[e]	924	3730	6752	6952	7041	7294	
pA24-WT	FMDV A24-WT	A	T	C (Ala)	C (Leu)	T (Val)	A (Glu)	T (Pro)	
pA24-VPg_1-5853	A24-ΔVPg-5853[a]	A	T	T (Ala)	T (Leu)	C (Val)	A (Glu)	T (Pro)	No change in sequence
pA24-VPg_1-5869	A24-ΔVPg-5869[b]	A	T	C (Ala)	T (Leu)	T (Val)	A (Glu)	C (Pro)	No change in sequence
pA24-VPg_1-5873	A24-VPg_1-5873	A	-	C (Ala)	T (Leu)	T (Val)	C (Ala)	T (Pro)	No change in sequence or deletion at nucleotides 5842–5878 and 5936–5967[g]
pA24-VPg_2-5934	A24-VPg_2-5934	C	T	C (Ala)	T (Leu)	T (Val)	A (Glu)	T (Pro)	No change in sequence
pA24-VPg_3-6007	A24-VPg_3-6007	A	T	C (Ala)	T (Leu)	T (Val)	A (Glu)	T (Pro)	No change in sequence

[a] Virus with deletion at nt 5829–5897.
[b] Virus with deletion at nt 5856–5924.
[c] Full-length genome sequencing of 6 high titer stock viruses was performed.
[d] Virus region.
[e] Nucleotide position.
[f] Partial sequence including only the 3B region of viruses obtained from cows during the acute stage of the disease (days 4–6 post-inoculation) to confirm non-reversion to wild-type.
[g] Viruses from clinical samples collected from this cow were partially sequenced and they either retained the insert in 3B or contained deletions of the 3′ end of $3B_1$ and 5′ end of $3B_2$, resulting in a virus similar to the A24-ΔVPg viruses.

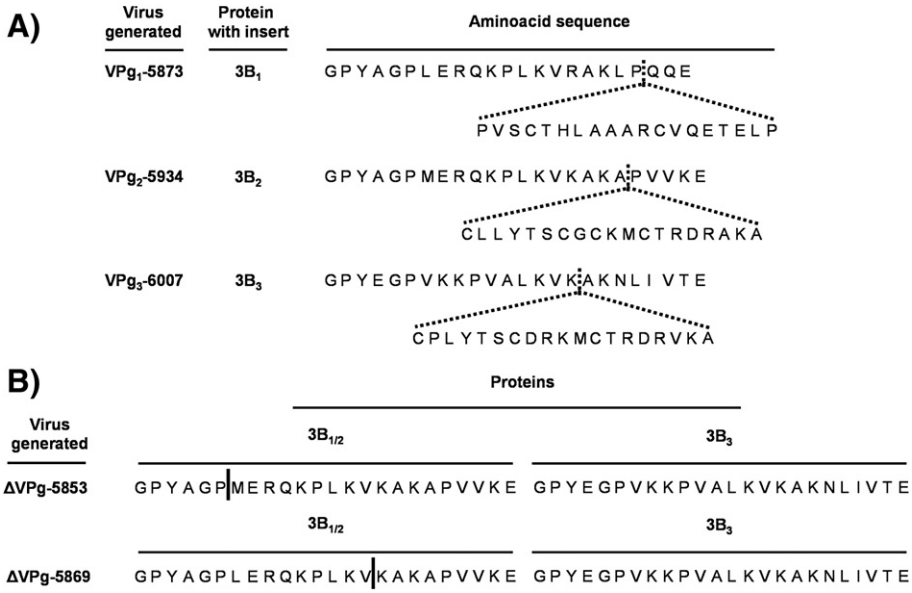

Fig. 1. Diagram of FMDV A24-3B mutants named based on the location of the mutation in pA24-WT. (A) Transposon-containing mutants with altered 3B protein shown for each virus. Remaining 3B amino acid sequences are the same as the parental virus (A24-WT). The amino acid at which the insertion occurred is marked with the dotted line. (B) Deletion-containing mutants. Solid line indicates where deletion took place and separates original regions of $3B_1$ (to the left) and $3B_2$ (to the right) in the resulting viruses.

et al., 2003) and the remaining four bands correspond to 3A (band 2), $3AB_1$ (band 3), $3AB_1B_2$ (band 4) and $3AB_1B_2B_3$ (band 5). In order to better visualize several weak bands a longer exposure of the same gel is shown in top portion of Fig. 5. Doublets observed (e.g. bands 3 and 4) could result from incomplete reduction of these proteins (Garcia-Briones et al. (2006)) or from uridylation of the 3B portion of the proteins or unspecific protease activity as previously described by Strebel et al. (1986). All 3B containing bands (3, 4 and 5) were also visualized with anti-3B antibodies (Fig. 5, panel III). The two mutants with one 3B deleted (A24-ΔVPg) showed the same bands 1 and 2 as A24-WT, and two bands very similar in size to bands 3 and 4 corresponding to $3AB_{1/2}$ (band 6) and $3AB_{1/2}B_3$ (band 7) respectively. As expected, a band corresponding to the form with three 3Bs (band 5) was absent in these viruses as confirmed in longer film exposures (top portion). In these two mutants only one 3B band was detected by anti-3B antibodies, suggesting that the $3AB_{1/2}B_3$ (band 7) is not recognized

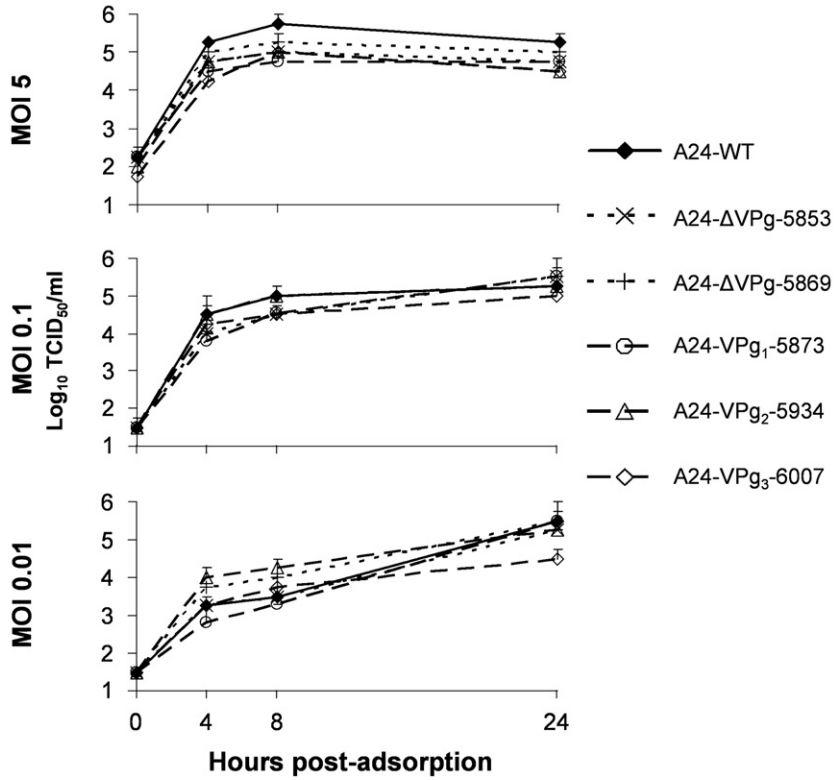

Fig. 2. Multi-step growth curve of either A24-mutants or A24-WT viruses. EBK cell cultures were infected at an MOI 5 (top panel), 0.1 (center panel) or 0.01 (bottom panel). Virus titers were performed on BHK-21 cells and expressed as $TCID_{50}$/ml on BHK-21 cells. Values are averages and standard deviations representative of two independent experiments.

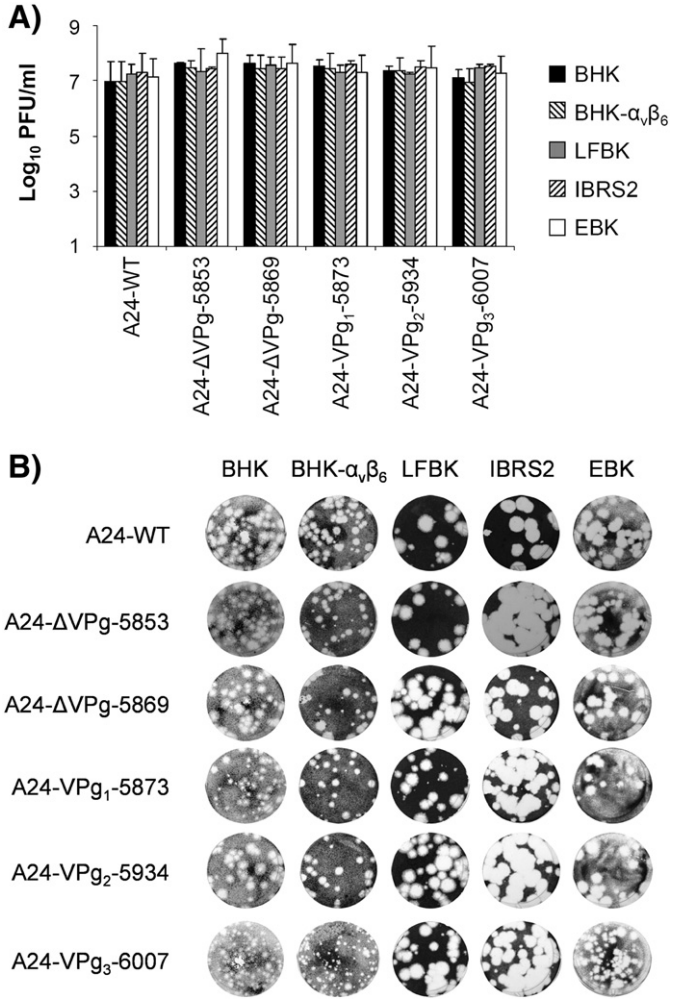

Fig. 3. (A) Ability of the FMDV A24 3B mutant viruses to form plaques in cell cultures derived from different animal species. PFU/ml values were determined starting with viruses at dilutions containing 10^7 PFU/ml, as previously determined in BHK-21 cells. Values are averages and standard deviations representative of two independent experiments. (B) Plaque size assessment of either A24-mutants or A24-WT viruses on BHK-21, BHK- $\alpha_V\beta_6$, LFBK, IBRS2 and EBK cells. Cells were infected and after 1 h adsorption, 0.6% gum tragacanth overlay was added, followed 48 h later with crystal violet staining.

by these antibodies (Fig. 5, panel III). Virus A24-VPg$_1$-5873, containing an insert in 3B$_1$, showed bands 1 and 2 without modifications and a single band (identified as band 8) co-migrating with band 3 (3AB$_1$) of A24-WT. We expected band 8 to be a product of larger size than band 3 due to the presence of the transposon insert, but a putative 3C cleavage site (www.expasy.org/tools/peptidecutter) present within the 3′ end of the insert itself may have resulted in a 3AB product similar in size to wild-type 3AB$_1$. Additionally for this virus, differences were found with respect to A24-WT in the processing of the 3′ end of P3 after the transposon (bands 9 and 10). However, all 3B containing putative bands (8, 9 10) were detected by anti-3B antibodies (Fig. 5, panel III). Virus A24-VPg$_2$-5934 showed bands 1–3 as A24-WT and band 11 co-migrating with band 4. Again, we expected a larger 3AB$_1$B$_2$ due to the presence of the transposon insert in 3B$_2$, but putative 3C cleavage sites within the transposon might explain the smaller than expected 3AB$_1$B$_2$ (band 11). Similar to what is described for A24-VPg$_1$-5873, the 3′ end of P3 showed a different pattern than A24-WT (bands 12 and 13) but all putative 3B containing bands reacted with anti-3B (Fig. 5, panel III). Virus A24-VPg$_3$-6007 showed bands 1–4 same as A24-WT, band 14 likely formed by cleavage within the transposon and 3AB$_1$B$_2$B$_3$-19mer and an unknown processing pattern for the 3′ end of P3 (band 15), all reactive with anti-3B antibodies (Fig. 5, panel III). Mock inoculated cells confirmed the specificity of the antibodies used in the Western blot. When analyzed with a pool of monoclonal antibodies against 3C no bands were detected, indicating that cleavage at site 3B$_3$/3C is not affected by the presence of the insert or deletions (results not shown). Taken together, these results indicate that with the presence of deletions or insertions in 3B, mutant FMD viruses yield different 3AB protein products in infected BHK-21 cells.

Assessment of FMDV 3B mutant virulence in cattle

Virulence of mutants and parental A24-WT was assessed utilizing a well established aerosolization inoculation method that resembles natural infection (Pacheco et al., 2008). Cows were inoculated with 10^7 TCID$_{50}$ of mutant or parental A24-WT and viral infection and clinical signs were monitored daily (Pacheco et al., 2008). Results demonstrated that all five animals, each inoculated with one of the mutant viruses developed clinical FMD as did the A24-WT infected animal and all reached a maximum or close to the maximum clinical score by the end of the study (9 days post-infection (dpi). However, fever was sporadic and the appearance of clinical signs was delayed in animals inoculated with 3B mutants compared to the animal inoculated with A24-WT. Interestingly, while viremia lasted three days in the cow inoculated with FMDV A24-WT, as well as in cows inoculated with mutants A24-ΔVPg-5869 and A24-VPg$_1$-5873, cows inoculated with the three remaining mutant viruses (A24-ΔVPg-5853, A24-VPg$_2$-5934 and A24-VPg$_3$-6007), presented a viremia that lasted one or two days. Virus shedding (from saliva) was detected in all animals from 2 to 8 dpi, with the exception of the animal inoculated with A24-VPg$_2$-5934, where virus was detected in very low amounts only at 2 and 6 dpi. Serum neutralizing antibodies were detected in all animals starting at 5 or 6 dpi (Fig. 6). Table 1 shows partial genomic sequence of multiple viruses recovered from lesions in animals inoculated with 3B mutant viruses confirming that the disease was caused by mutant viruses and not by reversions to wild-type virus. The only exception was a virus from one of five samples obtained from the animal inoculated with A24-VPg$_1$-5873. This virus had not only lost the insert but also removed an entire 3B, a similar mutation previously seen with the two 3B deletion mutants described above (A24-ΔVPg-5853 and A24-ΔVPg-5869).

Discussion

Among the picornaviruses, FMDV has a unique genomic feature: the presence of redundant copies of the 3B protein. This redundancy was analyzed in the past. Falk et al. reported that although not all three copies of 3B are needed to maintain infectivity, 3B copy number influences RNA synthesis and production of infectious FMDV particles in cell culture. Their 3B deleted mutants had reduced viral RNA synthesis levels after infection and the levels of viral RNA synthesis and infective particle formation were found to correlate with the number of functional 3Bs left in the mutant viruses. These authors suggested a direct correlation of 3B gene dosage and viral RNA synthesis, with a secondary effect on infective particle formation (Falk et al., 1992). In poliovirus, it was shown that the 3B uridylylation reaction may employ a 3B-containing precursor (3AB or 3BC (D)) rather than the processed 3B (Liu et al., 2007; Oh et al., 2009; Pathak et al., 2008). Based on these reports, it could be hypothesized that the presence of three 3Bs could benefit FMDV replication due to the additive presence of multiple 3B or 3B-precursors proteins.

To address the importance of 3B in viral virulence, particularly in cattle, one of the main natural FMDV hosts, we created viruses with insertions in each of the 3B proteins as well as viruses with only two 3Bs in the genetic backbone of FMDV A24-WT, a virus that is fully virulent in cattle. It is important to note that each 3B protein was disrupted by the insertion of an amino acid sequence (19mer) similar in size to a single 3B protein itself. Therefore it is expected that this insertion severely altered the structure and affected the function of the individual 3B.

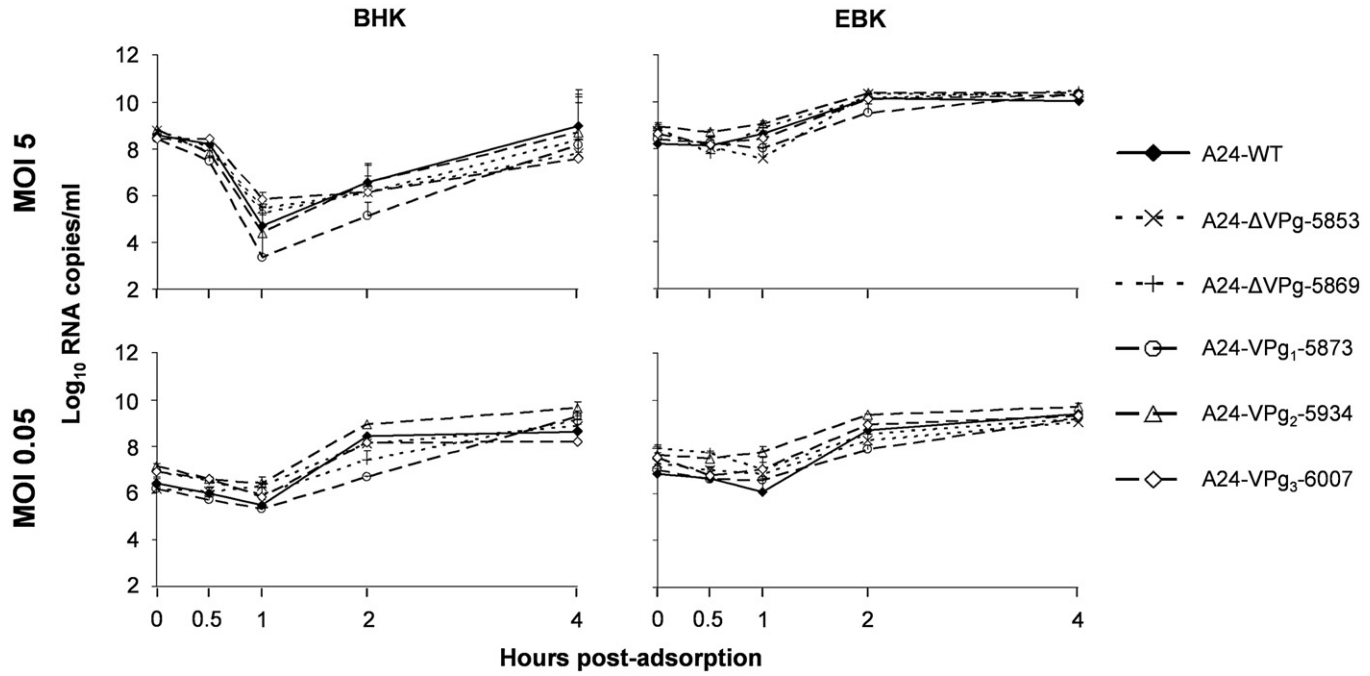

Fig. 4. Synthesis of viral intracellular RNA in cell cultures infected with either FMDV A24-3B mutants or parental virus. Values are expressed as amounts of RNA copy numbers recovered from BHK-21 and EBK cell cultures infected at an MOI of 5 or 0.05, and quantified by rRT-PCR. Data represents values and error bars from data obtained in an independent experiment. Experiments were reproduced at least three times.

In previous work it was shown that modifications in viral proteins 3A and 3B could decrease RNA synthesis and virus yield in different cell lines, particularly in bovine-derived cells (O'Donnell et al., 2001; Pacheco et al., 2003). It has also been described that expression of 3AB proteins resulted in an increase of FMDV replication *in vitro*, suggesting that the redundancy of 3B may be related with simultaneous presence of 3AB and 3B that would improve FMDV replication and translation (Rosas et al., 2008). Nevertheless, here we could not find significant differences in the level of RNA synthesis among all mutants when compared with the parental virus. Similar results were obtained when the growth abilities of the mutant viruses were analyzed in single or multistep growth curves. Thus, in our hands, severe domain disruptions in individual 3B proteins did not significantly affect the ability of FMDV to synthesize viral RNA nor to replicate and grow in susceptible cell lines.

Each of the three distinct FMDV 3B peptides is an efficient substrate in the FMDV VPgpU(pU) uridylation reaction, but $3B_3$ has been shown to have the highest activity (Nayak et al., 2005). Although it has been reported that modifications of the $3B_3$ coding sequence result in production of a noninfectious RNA transcript (Falk et al., 1992), we were able to derive a viral mutant containing a severe disruption of $3B_3$ (A24-Vpg$_3$-6007), albeit this virus showed a slight delay in viral growth.

It has been shown that Tyr-3 of 3B is critical in the process of poliovirus replication (Kuhn et al., 1988a,b; Liu et al., 2007; Paul et al., 2003; Reuer et al., 1990). Consistent with these previous results, our plasmid constructs containing inserts near the Tyr-3 residue of $3B_2$ or $3B_3$ (pA24-VPg$_2$-5887, pA24-VPg$_2$-5889, pA24-VPg$_2$-5949 and pA24-VPg$_3$-5974), yielded viruses that had reverted to wild-type genotype or did not yield viable progeny, despite the fact that the other two 3Bs were not affected (not shown).

To determine whether insertions or deletions in the individual 3Bs altered the processing of the P3 region, we analyzed the proteolytic cleavage products of the five mutant viruses *in vitro*. All 3B mutants maintained processing of P3 region (3A, 3B and 3C (not shown)) although an altered pattern of 3B protein processing was observed in some mutant viruses. Our proposed interpretation of the band patterns observed in Fig. 5 was based on the size and reactivity of these bands with specific anti-3A and anti-3B antibodies and previous studies documenting this processing (Pacheco et al., 2003).

In previous work it was reported that FMDV containing only one of the 3B proteins was partially attenuated when inoculated in swine (Pacheco et al., 2003). It has been suggested that there is an association between 3B copy number and virulence *in vivo* and this may explain why three copies of 3B are present in all FMDV strains characterized to date (Carrillo et al., 2007; MacKenzie et al., 1975). In contrast, when viruses were analyzed *in vivo* in this study, virulence was not drastically decreased in the 3B mutants compared to the parental wild-type FMDV except for some minor delays in the appearance of viremia and clinical signs and extent of shedding. Therefore, in our hands FMDV appears to have considerable flexibility in accepting insertions and deletions of the 3B region. Our results indicate that as long as two functional 3Bs (viruses A24-ΔVPg-5853 and A24-ΔVPg-5869) were maintained, the virus was able to replicate *in vitro* and cause disease in cattle. Although our data might suggest that two copies of 3B are sufficient for FMDV virulence, the minor delays in establishing infection and decreased shedding may be detrimental during the natural transmission cycle preventing these mutations to be maintained. Interestingly the mutants with 3B deletions (A24-ΔVPg-5853 and A24-ΔVPg-5869) combined parts of $3B_1$ and $3B_2$ while always conserving $3B_3$ intact. This was also true in the deletion mutant virus recovered from a cow inoculated with virus A24-VPg$_1$-5873. This could be due to the similarity of the first two 3Bs or to the critical need for $3B_3$ for adequate FMDV replication, as has been previously suggested (Nayak et al., 2005).

In summary we present data showing that severe domain disruptions of individual 3B proteins do not drastically affect FMDV RNA synthesis, virus replication or virulence in cattle. It is remarkable that the introduction of a 19 amino acid insert in a 23–24 amino acid protein does not appear to interfere with the basic viral activity during *in vitro* replication or even causing disease in cattle. The independence of FMDV virulence from the presence of three intact 3B proteins is difficult to reconcile with the conserved presence of these three proteins across hundreds of FMDV strains in all seven serotypes sequenced to date, suggesting that the redundancy of these genomic elements is required for viral processes not measured in this study.

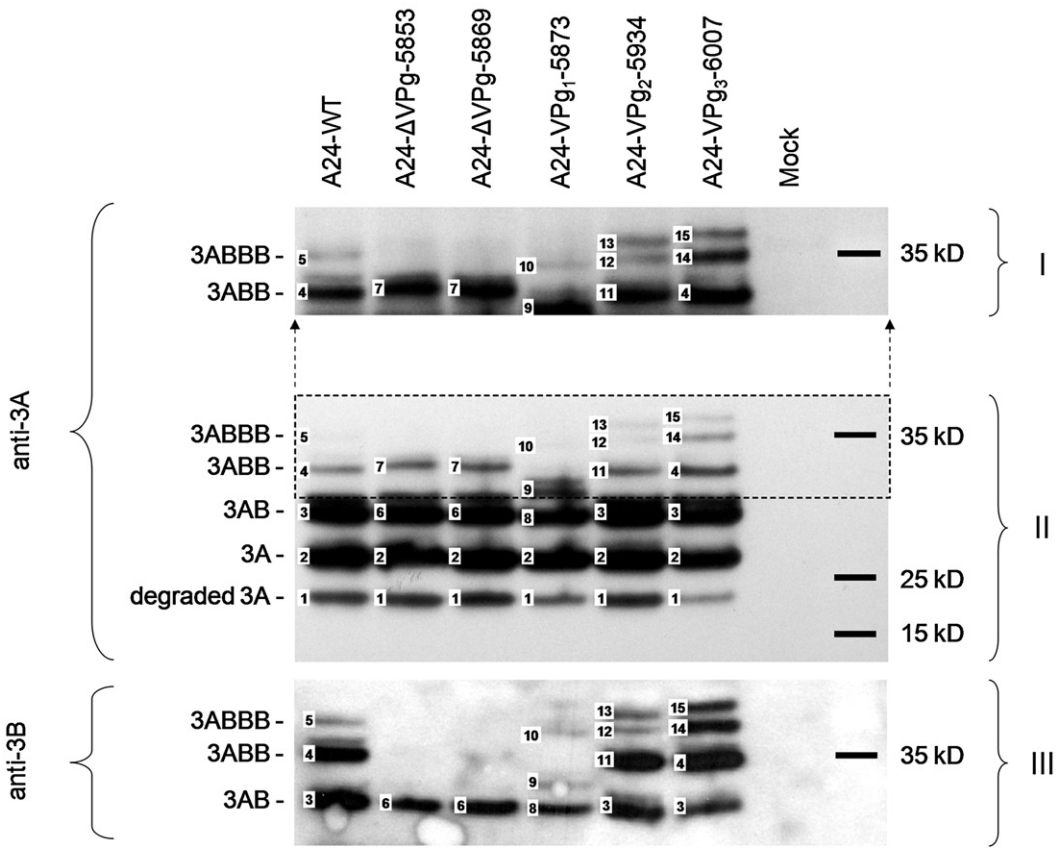

Fig. 5. Western blot to detect 3A and 3B proteins. Lysates of BHK-21 cells infected with either A24-3B mutants or parental virus were separated on SDS-PAGE. Western blotting was performed using a specific rabbit polyclonal serum against the N-terminal portion of 3A of FMDV-A12 (panels I and II) or monoclonal antibodies against FMDV 3B (panel III).

Materials and methods

Construction of transposon-containing FMDV mutants

To identify virulence determinants within the FMDV genome, we constructed a library of infectious FMDV full-length genome plasmids of pA24Cru (Rieder et al., 2005) containing single random insertions (1 per genome), using the EZ-Tn5™ Insertion Kit (Piccone et al., 2009; Piccone et al., 2010). Plasmids containing a 57 nt insertion in the 3B encoding region were selected for further study. Each of these plasmids contained an insertion at residues 5853, 5869, 5873, 5887, 5889, 5934, 5949, 5974 or 6007 and were named according to the mutation location in 3B, as pA24-VPg$_1$-5853, pA24-VPg$_1$-5869, pA24-VPg$_1$-5873, pA24-VPg$_2$-5887, pA24-VPg$_2$-5889, pA24-VPg$_2$-5934, pA24-VPg$_2$-5949, pA24-VPg$_3$-5974 and pA24-VPg3-6007, respectively. All nucleotide designations are based on the nucleotide sequence of A24 Cruzerio. T7 RNA transcripts of *SwaI*-linearized plasmids, including pA24Cru, were produced using a MegaScript T7 Kit (Ambion, Austin, Texas) followed by subsequent transfection into BHK-21 cells by electroporation as described previously (Piccone et al., 1995; Rieder et al., 1993). Mutant viruses obtained from these transfections were named according to the site of insertion (see below).

Cells and viruses

Viruses containing single in-frame insertions or deletions in the 3B region were derived from the mutant plasmids and the A24-WT described above. In order to maintain adequate bovine receptor usage, virus stocks were grown in a derivative of baby hamster kidney (BHK-21) (baby hamster kidney cell line, ATCC, catalogue number CCL-10) cells expressing the bovine $\alpha_V\beta_6$ integrin (BHK-$\alpha_V\beta_6$) (Duque et al., 2004) and titrated on BHK-21 cells by calculating the 50% tissue culture infectious dose per ml ($TCID_{50}$/ml). Two of the plasmids yielded viruses containing one insert in 3B namely A24-VPg$_2$-5934 and A24-VPg$_3$-6007. Two other plasmids gave origin to viruses that lost the insert and a full 3B and these viruses were named A24-ΔVPg-5853, A24-ΔVPg-5869, respectively. After several attempts, the remaining five plasmids (pA24-VPg$_1$-5873, pA24-VPg$_2$-5887, pA24-VPg$_2$-5889, pA24-VPg$_2$-5949 and pA24-VPg$_3$-5974) gave no progeny or yielded viruses that had reverted to wild-type genotype when grown in BHK-$\alpha_V\beta_6$ cells with subsequent culturing in BHK-21 cells. The only virus with an insert obtained in a second round of transfections was A24-VPg$_1$-5873. Virus stocks were prepared with A24-WT, A24-ΔVPg-5853, A24-ΔVPg-5869, A24-VPg$_1$-5873, A24-VPg$_2$-5934 and A24-VPg$_3$-6007 and the complete viral sequence was determined using FMDV-specific primers designed to cover the entire genome. High titer stocks were determined in BHK-21 cells. *In vitro* phenotype was characterized by plaque assays in BHK-21 cells, BHK-$\alpha_V\beta_6$ cells, a bovine kidney cell line (LFBK) (Swaney, 1988), a porcine kidney cell line (IBRS2) (de Castro, 1964) and primary embryonic bovine kidney cells (EBK, kindly provided by Dr S. Wessman, USDA, APHIS, AMES, Iowa).

Comparative ability to grow and to form plaques

In order to characterize *in vitro* growth, plaque assays were performed in the 5 different cell types described above (BHK-21, BHK-$\alpha_V\beta_6$, IBRS2, LFBK and EBK cells) with the 6 selected viruses described above (FMDV A24-WT, A24-ΔVPg-5853, A24-ΔVPg-5869, A24-VPg$_1$-5873, A24-VPg$_2$-5934 and A24-VPg$_3$-6007) to compare plaque size and ability to replicate in the different cell types. The ability of these viruses to replicate in different cell types was determined by testing serial 10-fold dilutions of virus (starting with 10^7 PFU/ml [as measured previously on BHK-21 cells]) to form plaques on these different cells.

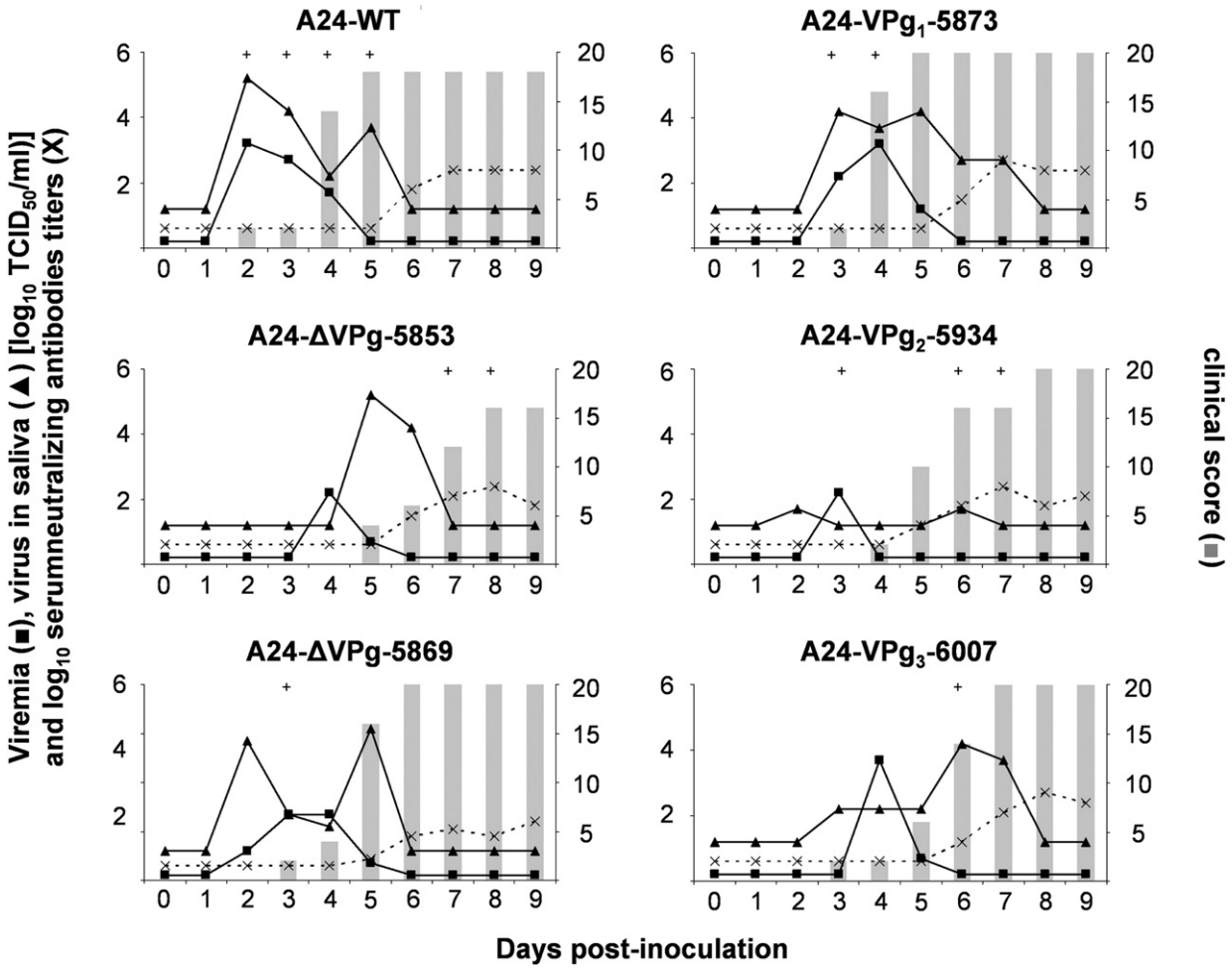

Fig. 6. Comparison of disease induced in cattle by either A24-3B mutants or A24-WT viruses. Animals were inoculated with aerosol containing 10^7 $TCID_{50}$. Viremia (■), virus in saliva (▲) and serum-neutralizing antibody titers (X) are expressed in the left axes; the clinical score (bars) are expressed in the right axes. + denotes fever (>40 °C).

Briefly, preformed 95% confluent monolayers were inoculated with dilutions of each virus. Tragacanth gum overlay (0.6%) was added after 1 h adsorption and after 48 h the plates were fixed and stained with crystal violet. Analyses were performed side-by-side with BHK-21 cells, and the resulting data was used to calculate the PFU/ml. All samples were run simultaneously to avoid inter-assay variability.

Virus growth curve in primary tissue culture

Growth curves were performed in EBK cells. Preformed monolayers were prepared in 24-well plates and infected with the six viruses described above (A24-WT, A24-ΔVPg-5853, A24-ΔVPg-5869, A24-VPg_1-5873, A24-VPg_2-5934 and A24-VPg_3-6007) at MOIs of 5, 0.1 and 0.01 (based on $TCID_{50}$ previously determined in BHK-21 cells). After 1 h of adsorption at 37 °C the inoculum was removed and the cells were rinsed two times with ice-cold 145 mM NaCl, 25 mM MES (pH 5.5) to remove residual virus particles. The monolayers were then rinsed with media containing 1% fetal calf serum and 25 mM Hepes (pH 7.4) and incubated for 0, 4, 8 and 24 h at 37 °C. At appropriate times post-infection, the cells were frozen at −70 °C and the thawed lysates were used to determine titers by $TCID_{50}$/ml on BHK-21 cells.

Determination of intracellular viral RNA concentration

BHK-21 and EBK cells were seeded in 24-well plates, infected at MOIs of 0.5 and 5 with all 6 viruses (A24-WT, A24-ΔVPg-5853, A24-ΔVPg-5869, A24-VPg_1-5873, A24-VPg_2-5934 and A24-VPg_3-6007), adsorbed and acid washed as described above. After 0, 0.5, 1, 2 and 4 h incubations at 37 °C, cell supernatants were discarded and total cellular RNA was extracted from monolayers with Lysis/Binding Solution (Ambion, Austin, TX), then frozen until further use. Quantitation of FMDV RNA was performed by rRT-PCR as previously described (Pacheco et al., 2008). Three separate experiments were performed and CT values converted to the number of RNA copies/ml based on FMDV RNA specific calibration curves developed with *in vitro*- synthesized RNA.

Western blot analyses of 3A and 3B polypeptides in infected cells

BHK-21 cells were infected with every mutant and parental A24 viruses at an MOI of 5 and when 60–70% of the cells displayed CPE (approximately 6 hpi) the supernatant was discarded and the cell monolayers were lysed with TNET buffer (10 mM Tris [pH 7.5], 150 mM NaCl, 1 mM EDTA, 1% [wt/vol] Triton X-100) for 20 min on ice; after clarification, the cell lysates were stored at −70 °C. Samples were resolved by 12% sodium dodecyl sulfate-polyacrylamide gel electrophoresis gels (NuPAGE® Novex® Bis-Tris Mini Gels; Invitrogen) and electroblotted onto polyvinylidene difluoride membranes (Millipore) by standard methods. FMDV-specific proteins were detected with a chemiluminescent Western Blot immunodetection kit (WesternBreeze®, Invitrogen). For detection of the different forms of 3AB, a polyclonal rabbit serum generated by using an Escherichia coli-expressed N-terminal fragment of 3A of FMDV-A12 (O'Donnell et al., 2001) diluted 1/500 was used as the primary antibody. For detection of 3B a pool of monoclonal antibodies was used as the primary antibody diluted 1:500 (monoclonals 1G7 and 1A10,

kindly provided by Dr. E. Brocchi). For detection of 3C a pool of monoclonal antibodies was used as the primary antibody diluted 1:500 (monoclonals 2B7 and 1H6, kindly provided by Dr. E. Brocchi).

Viral virulence in cattle, serology and virus isolation

Cattle experiments were performed under Biosafety level 3 conditions in the animal facilities at PIADC following a protocol approved by the Institutional Animal Use and Care Committee. Steers (300–400 kg) were infected using an aerosolization method that resembles natural infection (Pacheco et al., 2008). Briefly, animals were sedated and inoculated with 10^7 $TCID_{50}$ in 2 ml of MEM delivered by aerosol with a jet nebulizer (Whisper Jet, Marquest Medical Products, CO) attached to an aerosol delivery system (Equine Aeromask, Medium Size, Trudell Medical, London, ON, Canada). One steer per virus (FMDV A24-WT, A24-ΔVPg-5853, A24-ΔVPg-5869, A24-VPg_1-5873, A24-VPg_2-5934 and A24-VPg_3-6007) was inoculated and held in individual animal rooms. Steers were clinically examined, including rectal temperature recordings, for 9 days after inoculation, and then humanely euthanized. Serum and oral swabs were collected and cows were sedated daily for clinical evaluation. After collection, samples were aliquoted and frozen at −70 °C. Neutralizing antibody titers in serum were determined as described elsewhere (Golde et al., 2005). Briefly, serial dilutions of serum were incubated with a virus dose of 100 $TCID_{50}$ of FMDV A24 for 1 h at 37 °C and then BHK-21 cells were added on top and incubated at 37 °C for 48–72 h. End-point titers were calculated as the reciprocal of the last serum dilution to neutralize 100 $TCID_{50}$ of virus in 50% of the wells. One serum and one swab aliquot were used to perform viral titration on BHK-21 cells by calculating the 50% tissue culture infectious dose per ml ($TCID_{50}$/ml) as described elsewhere (Pacheco et al., 2003). Clinical scoring, with a maximum of 20, was performed based on severity of lesions on the four feet, the snout, and the mouth as described elsewhere (Pacheco et al., 2008).

Acknowledgments

We thank Elizabeth Bishop, Ethan Hartwig and George Smoliga for technical assistance. We would particularly wish to thank Melanie Prarat for editing the manuscript. We also thank the PIADC animal care staff for excellent technical assistance. This research was funded by ARS-CRIS Project 1940-32000-052-00D.

References

Alexandersen, S., Zhang, Z., Donaldson, A.I., Garland, A.J., 2003. The pathogenesis and diagnosis of foot-and-mouth disease. J. Comp. Pathol. 129 (1), 1–36.
Callahan, J.D., Brown, F., Osorio, F.A., Sur, J.H., Kramer, E., Long, G.W., Lubroth, J., Ellis, S.J., Shoulars, K.S., Gaffney, K.L., Rock, D.L., Nelson, W.M., 2002. Use of a portable real-time reverse transcriptase-polymerase chain reaction assay for rapid detection of foot-and-mouth disease virus. J. Am. Vet. Med. Assoc. 220 (11), 1636–1642.
Carrillo, C., Lu, Z., Borca, M.V., Vagnozzi, A., Kutish, G.F., Rock, D.L., 2007. Genetic and phenotypic variation of foot-and-mouth disease virus during serial passages in a natural host. J. Virol. 81 (20), 11341–11351.
de Castro, M.P., 1964. Comportamiento do virus aftoso em cultura de celulas: susceptibilidade da linhagem de celulas suinas IB-RS-2. Arq Inst Biol (Sao Paulo) 31 (3), 63–78.
Duque, H., LaRocco, M., Golde, W.T., Baxt, B., 2004. Interactions of foot-and-mouth disease virus with soluble bovine alphaVbeta3 and alphaVbeta6 integrins. J. Virol. 78 (18), 9773–9781.
Falk, M.M., Sobrino, F., Beck, E., 1992. VPg gene amplification correlates with infective particle formation in foot-and-mouth disease virus. J. Virol. 66 (4), 2251–2260.
Forss, S., Schaller, H., 1982. A tandem repeat gene in a picornavirus. Nucleic Acids Res. 10 (20), 6441–6450.
Garcia-Briones, M., Rosas, M.F., Gonzalez-Magaldi, M., Martin-Acebes, M.A., Sobrino, F., Armas-Portela, R., 2006. Differential distribution of non-structural proteins of foot-and-mouth disease virus in BHK-21 cells. Virology 349 (2), 409–421.
Golde, W.T., Pacheco, J.M., Duque, H., Doel, T., Penfold, B., Ferman, G.S., Gregg, D.R., Rodriguez, L.L., 2005. Vaccination against foot-and-mouth disease virus confers complete clinical protection in 7 days and partial protection in 4 days: use in emergency outbreak response. Vaccine 23 (50), 5775–5782.
Grubman, M.J., Baxt, B., 2004. Foot-and-mouth disease. Clin. Microbiol. Rev. 17 (2), 465–493.
King, A.M., McCahon, D., Slade, W.R., Newman, J.W., 1982. Recombination in RNA. Cell 29 (3), 921–928.
King, A.M., Sangar, D.V., Harris, T.J., Brown, F., 1980. Heterogeneity of the genome-linked protein of foot-and-mouth disease virus. J. Virol. 34 (3), 627–634.
Kuhn, R.J., Tada, H., Ypma-Wong, M.F., Dunn, J.J., Semler, B.L., Wimmer, E., 1988a. Construction of a "mutagenesis cartridge" for poliovirus genome-linked viral protein: isolation and characterization of viable and nonviable mutants. Proc. Natl. Acad. Sci. U. S. A. 85 (2), 519–523.
Kuhn, R.J., Tada, H., Ypma-Wong, M.F., Semler, B.L., Wimmer, E., 1988b. Mutational analysis of the genome-linked protein VPg of poliovirus. J. Virol. 62 (11), 4207–4215.
Liu, Y., Franco, D., Paul, A.V., Wimmer, E., 2007. Tyrosine 3 of poliovirus terminal peptide VPg(3B) has an essential function in RNA replication in the context of its precursor protein, 3AB. J. Virol. 81 (11), 5669–5684.
MacKenzie, J.S., Slade, W.R., Lake, J., Priston, R.A., Bisby, J., Laing, S., Newman, J., 1975. Temperature-sensitive mutants of foot-and-mouth disease virus: the isolation of mutants and observations on their properties and genetic recombination. J. Gen. Virol. 27 (1), 61–70.
Nayak, A., Goodfellow, I.G., Belsham, G.J., 2005. Factors required for the Uridylylation of the foot-and-mouth disease virus 3B1, 3B2, and 3B3 peptides by the RNA-dependent RNA polymerase (3Dpol) in vitro. J. Virol. 79 (12), 7698–7706.
O'Donnell, V.K., Pacheco, J.M., Henry, T.M., Mason, P.W., 2001. Subcellular distribution of the foot-and-mouth disease virus 3A protein in cells infected with viruses encoding wild-type and bovine-attenuated forms of 3A. Virology 287 (1), 151–162.
Oh, H.S., Pathak, H.B., Goodfellow, I.G., Arnold, J.J., Cameron, C.E., 2009. Insight into poliovirus genome replication and encapsidation obtained from studies of 3B-3C cleavage site mutants. J. Virol. 83 (18), 9370–9387.
Pacheco, J.M., Henry, T.M., O'Donnell, V.K., Gregory, J.B., Mason, P.W., 2003. Role of nonstructural proteins 3A and 3B in host range and pathogenicity of foot-and-mouth disease virus. J. Virol. 77 (24), 13017–13027.
Pacheco, J.M., Arzt, J., Rodriguez, L.L., 2010. Early events in the pathogenesis of foot-and-mouth disease in cattle after controlled aerosol exposure. Vet. J. 183, 46–53.
Pathak, H.B., Oh, H.S., Goodfellow, I.G., Arnold, J.J., Cameron, C.E., 2008. Picornavirus genome replication: roles of precursor proteins and rate-limiting steps in oril-dependent VPg uridylylation. J. Biol. Chem. 283 (45), 30677–30688.
Paul, A.V., Peters, J., Mugavero, J., Yin, J., van Boom, J.H., Wimmer, E., 2003. Biochemical and genetic studies of the VPg uridylylation reaction catalyzed by the RNA polymerase of poliovirus. J. Virol. 77 (2), 891–904.
Piccone, M.E., Pacheco, J.M., Pauszek, S.J., Kramer, E., Rieder, E., Borca, M.V., Rodriguez, L.L., 2010. The region between the two polyprotein initiation codons of foot-and-mouth disease virus is critical for virulence in cattle. Virology 396 (1), 152–159.
Piccone, M.E., Pauszek, S., Pacheco, J., Rieder, E., Kramer, E., Rodriguez, L.L., 2009. Molecular characterization of a foot-and-mouth disease virus containing a 57-nucleotide insertion in the 3'untranslated region. Arch. Virol. 154 (4), 671–676.
Piccone, M.E., Rieder, E., Mason, P.W., Grubman, M.J., 1995. The foot-and-mouth disease virus leader proteinase gene is not required for viral replication. J. Virol. 69 (9), 5376–5382.
Reuer, Q., Kuhn, R.J., Wimmer, E., 1990. Characterization of poliovirus clones containing lethal and nonlethal mutations in the genome-linked protein VPg. J. Virol. 64 (6), 2967–2975.
Rieder, E., Bunch, T., Brown, F., Mason, P.W., 1993. Genetically engineered foot-and-mouth disease viruses with poly(C) tracts of two nucleotides are virulent in mice. J. Virol. 67 (9), 5139–5145.
Rieder, E., Henry, T., Duque, H., Baxt, B., 2005. Analysis of a foot-and-mouth disease virus type A24 isolate containing an SGD receptor recognition site in vitro and its pathogenesis in cattle. J. Virol. 79 (20), 12989–12998.
Rosas, M.F., Vieira, Y.A., Postigo, R., Martin-Acebes, M.A., Armas-Portela, R., Martinez-Salas, E., Sobrino, F., 2008. Susceptibility to viral infection is enhanced by stable expression of 3A or 3AB proteins from foot-and-mouth disease virus. Virology 380 (1), 34–45.
Strebel, K., Beck, E., Strohmaier, K., Schaller, H., 1986. Characterization of foot-and-mouth disease virus gene products with antisera against bacterially synthesized fusion proteins. J. Virol. 57 (3), 983–991.
Swaney, L.M., 1988. A continuous bovine kidney cell line for routine assays of foot-and-mouth disease virus. Vet. Microbiol. 18 (1), 1–14.
Vakharia, V.N., Devaney, M.A., Moore, D.M., Dunn, J.J., Grubman, M.J., 1987. Proteolytic processing of foot-and-mouth disease virus polyproteins expressed in a cell-free system from clone-derived transcripts. J. Virol. 61 (10), 3199–3207.
Wimmer, E., 1982. Genome-linked proteins of viruses. Cell 28 (2), 199–201.

Return to Table of Contents

JCM Accepts, published online ahead of print on 15 September 2010
J. Clin. Microbiol. doi:10.1128/JCM.01081-10

Specific Detection of Rinderpest Virus by Real-Time RT-PCR in Preclinical and Clinical Samples of Experimentally Infected Cattle

Running title: Rinderpest virus real-time PCR

C. Carrillo[1,2]*, M. Prarat[2], A. Vagnozzi[2], J.D. Calahan[3^], G. Smoliga[2], W.M. Nelson[3] and L.L. Rodriguez [2]

[1] Foreign Animal Disease Diagnostic Laboratory-National Veterinary Services Laboratories, Animal Plant Health Inspection Service and ,[2]Foreign Animal Disease Research Unit, Agricultural Research Service, US Department of Agriculture, Plum Island Animal Disease Center, Orient Pt. NY 11957; [3]Tetracore Inc. 9901 Belward Campus Drive Rockville, MD 20850.

^current address: Midwest Research Institute, Rockville, MD, USA

*Mailing Address: PIADC-APHIS-FADDL
P.O. Box 848
Greenport, NY 11944-0848
Phone: 631-323 3352/3243
Fax: 631-323 3360
e-mail: consuelo.carrillo@APHIS.USDA.GOV

Keywords: real-time RT-PCR, Rinderpest, RPV, PPRV, Morbillivirus

SUMMARY

A highly sensitive detection test for Rinderpest virus (RPV), based on a real time RT-PCR system, was developed. Five different RPV genomic targets were examined and one was selected and optimized to detect viral RNA in infected tissue culture fluid with a level of detection ranging from 0.59 to 87.5 $TCID_{50}$ per reaction depending on the viral isolate. The strain sensitivity of the test was validated on 16 RPV strains belonging to all three phylogenetic branches described for RPV. No cross-reactivity was detected with closely related peste des petit ruminants or with symptomatically similar viruses including all seven serotypes of foot-and-mouth disease virus, two serotypes of vesicular stomatitis virus, blue tongue virus and bovine herpes virus type 2. In samples from experimentally infected cattle our real time RT-PCR test was significantly more sensitive than the gold standard test of virus isolation allowing detection of the disease 2-4 days prior to the appearance of clinical signs. Comparison of clinical samples with putative diagnostic value from live animals showed that conjunctival swabs and blood buffy coat were the samples of choice for epidemiological surveillance, while lymph nodes performed the best as *post-mortem* specimens. This portable and rapid rRT-PCR has the capability of pre-clinical detection of RPV and provides differential diagnosis with look a-like diseases of cattle. As RPV is declared globally eradicated, this test provides an important rapid virus detection tool that does not require use of infectious virus and allows processing of a large number of samples.

INTRODUCTION

Rinderpest virus (RPV), a member of the *Morbillivirus* genus of the *Paramyxoviridae* family, causes an acute, highly contagious and often fatal disease in cattle, buffaloes and yaks (1, 18). The disease affects the gastrointestinal and respiratory tracts of infected animals and is characterized by fever, nasal and ocular discharges, diarrhea, oral erosions and lymphoid tissue necrosis (2). Like all morbilliviruses, RPV is an enveloped, single-stranded, non-segmented, negative-sense RNA virus, antigenically and genetically related to other member of the genus such as measles virus (MV), peste des petits ruminants virus (PPRV) and canine distemper Virus (CDV) (3, 15). The 15.8 kb viral genome contains six genes in the following order, 3'-N-P-M-F-H-L-5' (each with their own start and polyA signals), an intergenic region between M and F genes and two flanking untranslated regions (UTRs) at both ends of the genome (8). Although the disease is expected to be declared eradicated in 2010 (http: //www.fao.org/ docs/eims/upload/ 258696/ak064e00.pdf), records indicate that field isolates during the last outbreaks were of low virulence and transmissibility and low mortality, opening the possibility that outbreaks might go undetected (5). The molecular bases for the differences in RPV pathogenicity are unknown, but the mild disease presentation seen lately (described as sub-acute infections), constitutes a problem for the early detection of RPV, as outbreaks involving large numbers of animals occur after failure to recognize the index case in a population. RP also affects sheep, goats, certain breeds of pigs and a wide range of wildlife species, but infection in these animals is usually sub-clinical (2) and sometimes indistinguishable from PPRV. Sub-acute infection in cattle is most often observed in countries where the disease remained enzootic (5). Therefore, early pre-clinical detection

of infected animals using a rapid diagnostic test capability for differentiation between RPV and PPRV would be very useful in surveillance of suspected cases after eradication. In case of suspected RPV activity having a rapid and precise viral detection test in place will be critical for disease containment. Current diagnosis of RPV relies on a number of serologic methods such as indirect ELISA, competitive ELISA and sero-neutralization (VN) tests, which are not ideal for outbreak detection and in the case of SN, require the use of live virus. RPV antibodies start to develop between two and five days after the onset of clinical disease in virulent infections and six to ten days (up to 17 days) after infection with attenuated strains (5, 13, 16), that is between 2 to 4 weeks after infection. Therefore, serological approaches for diagnostic, although sensitive and specific, would allow wide spread of the disease before alert and implementation of the appropriate control measures. Antigen detection has been historically carried out by VI in monolayers of primary calf kidney (B95), a marmoset lymphoblastoid on African green monkey kidney (Vero) cells and agar gel immunodifusion (AGID). Although these are reliable methods, they are only available in well established laboratories and are not readily available for field use, for import/export purposes, and/or animal movement regulation. These techniques do not perform well during outbreaks or acute investigations and lack the necessary speed and sensitivity required for outbreak control situations. Moreover, none of these tests or clinical observation can differentiate between RPV and PPRV requiring further differential diagnostic and further delay. Differential immunocapture ELISA is fast and specific, but not sensitive enough for clinical samples. Finally, immunofluorescence, histopathology and immunohistochemistry are very useful techniques for *post-mortem* but not for *in vivo* diagnostics.

Conventional reverse transcription polymerase chain reaction (RT-PCR) with viral RNA purified from post-mortem samples (spleen, lymph node and tonsil) or *in vivo* from peripheral blood lymphocytes (PBLs) or swabs from eye or mouth lesions, have been previously used (10, 11). Conventional RT-PCR allows for fast turnaround times, but is not portable and requires qualified instrumentation available only in centralized laboratory facilities. Real time RT-PCR (rRT-PCR) has demonstrated superior sensitivity and specificity when compared to the currently used antigen detection methods of virus isolation and conventional RT-PCR for other diseases of the livestock, and has also proved reliable in generating fast results in a portable format. Besides, it has the capability of pre-clinical diagnosis in the event of a potential disease outbreak (7, 22, 27). Here we present the design and optimization of an rRT-PCR and its use for early detection of RPV in samples from experimentally infected cattle.

MATERIALS AND METHODS

Virus isolates: The viral isolates used in this study were obtained from FADDL-APHIS-USDA (Foreign Animal Diseases Diagnostic Laboratory of the Animal and Plant Health Inspection Service of the USDA) repository collection (Table 1). These isolates are representative of several geographic areas and include all RPV genetic lineages described to date (Fig. 1) (26).

Virus Isolation: Tissue and swab samples from experimentally infected cattle were tested for VI in Vero cell cultures, following Office International des Epizooties (OIE) protocols (17). Briefly, approximately 0.2 g of tissue was macerated in 1 ml DMEM, clarified by centrifugation and 50 µl of supernatant were used to infect Vero cell

monolayers in 96 well plates in quadruplicate, using 3 ten fold dilutions (undiluted, 1:10 and 1:100). Presence of cytopathic effect (CPE) in the infected cell was monitored daily up to 7 days post-infection (dpi). Plates were frozen and thawed and used to infect fresh Vero cells. VI was determined by microscopic observation and crystal violet staining. Additionally, all wells corresponding to the same sample were pooled, the total RNA was extracted and tested by conventional RT-PCR, as previously described (11) to confirm VI results.

Virus titrations: Serial dilutions of viral suspension were inoculated in Vero cell monolayers with four replicates for each sample and observed for CPE, as described above. Titers were calculated according to Reed and Muench (21) and expressed as log10 $TCID_{50}$/ml.

RNA extraction: RNA was extracted from 140 µl of cell culture supernatant, culture media containing clinical swabs or buffy coat samples. The RNeasy extraction kit (Qiagen, Stanford, California) was used for RNA extraction from cell cultures and viral suspensions, according to the manufacturer's specifications. Tissue samples obtained post-mortem, were homogenized and treated with QIAshredder (Qiagen, Stanford, California) prior to RNA extraction. RNA was eluted in 40 µl of RNase-free water, and stored at -70^0C until the PCR test was performed.

Real time RT-PCR (rRT-PCR): the assay was performed using ABI TaqMan RT-PCR Core Reagents (Applied Biosystems, product #N8080232) with 5 mM Mn(OAc2), 0.1 units rTth DNA polymerase and 0.2 mM dNTPs mix (supplied as 10 mM dilution each and mixed 1:1:1:1 by volume) in a final 25 µl reaction. Primer/probes sequences and their position in the RPV genome are summarized in Table 2. Molarities for primers and

probes were optimized individually and detailed in the Results section. Real time RT-PCR was done using a SmartCycler® machine (Cepheid, Sunnyvale, CA), Reverse transcription was allowed to take place for 30 minutes at 60^0C, followed by a 2 minutes denaturing step at 95^0C and 45 amplification cycles of 95^0C for 10 seconds and 55^0C for 60 seconds.

Animal infections: Six steers, weighing approximately 230 kilograms were inoculated with 10^4 $TCID_{50}$ of the Kabete O strain of RPV by intramuscular injection. Body temperature and clinical samples were taken daily from the infected animals. Clinical signs of infection included fever, conjunctivitis, emaciation, salivation, nasal discharge, respiratory distress, and recumbence, mucopurulent discharge through eyes and nose and complete prostration during the final stages of disease. Clinical samples were collected with dacron swabs into tubes containing 500µl of DMEM (Invitrogen, San Diego, California) including nasal, oral, conjunctival, vaginal/preputial and anal swabs (Table 7). Blood samples were collected into BD Vacutainer Cell Preparation Tubes with Sodium Heparin (BD Franklin Lakes, NJ). Buffy coats were separated by centrifugation in a swinging rotor at 1,380 rpm (700 g) on Ficoll-Hypaque cushion, collected and washed 3 times in phosphate-buffered saline (PBS) and resuspended in 1 ml DMEM. Approximately 7 days post-inoculation all animals were euthanized when found moribund. Tissue samples from tonsils, Peyer's patches, lymph nodes, spleen, abomasum and others (Table 7) were collected at necropsy and immediately frozen at -70^0C until used.

RESULTS

Primers/probe design and assay optimization. Genes N, F, H and L, which were previously identified as the most conserved regions on the RPV genome (Carrillo et al. manuscript in preparation) were selected for the design of five primer/probe sets. Partial RPV sequences available in the GenBank were added to the complete array of sequences we had generated in our lab (Table 1) and input into Primer Express software (Applied Biosystems, Foster City, Calif.) for primer/probe design. All the putative primer/probe sets obtained were blasted against the NBCI nucleotide database and selected based on maximum RPV specificity and minimum number of mismatches with the RPV sequences. Finally, the primers shown in Table 2 were selected.

Primer/probe sets were initially tested for their ability to detect RPV Kabete "O" RNA as template at probe and primer concentrations ranging from 50 nM to 200 nM, and 100 nM to 500 nM respectively. Optimal primer/probe combinations (defined as those resulting in the lowest ct value and highest specific fluorescence) were 200/400 nM for H, N and L9; and 100/500 nM for F and L10 (Table 3). Using these optimized conditions primer/probe sets were tested for detection of sixteen RPV isolates representing the main genetic lineages described for RPV (Table 4). Only N and L-10 primer/probe sets were able to detect all sixteen RPV isolates.

Therefore, further optimization continued for these two primer/probe sets only. Annealing temperature optimization using 50^0C, 55^0C and 60^0C did not show significant differences in the efficiency for amplification of the RPV RNA (data not shown). A close RPV relative, PPRV, was used as genetic near neighbor RNA target to control for specificity of the test at each temperature setting. Probe L10 specifically detected RPV at all annealing temperatures and did not detect PPRV at any annealing temperature (Table

183 5). The N system adequately recognized RPV at the three temperatures tested but showed
184 non-specific amplification of PPRV at all annealing temperatures (Table 5). Therefore no
185 further testing was done with the N gene primer/probe set.
186 To determine the effect of annealing temperature in the sensitivity and/or specificity for
187 detecting different RPV strains with the L10 rRT-PCR assay, conditions previously
188 optimized for the Kabete "O" were tested with all seven RPV strains representatives of
189 all known genetic lineages. The two highest annealing temperatures (55^0C and 60^0C)
190 with the two best primer/probe concentrations of (500/100 nM and 400/200 nM) were
191 tested. No significant differences were observed in relation to the annealing temperatures
192 (data not shown); however, the 400/200 nM primer/probe concentration performed better
193 and more consistently in detecting all seven reference isolates (Figure 2).
194 To assess the robustness of the selected conditions for L10 rRT-PCR assay, 21 repetitions
195 of the same RNA sample (Kabete "O") were performed by 3 separate operators and on 4
196 different thermo cycler units. No significant differences were observed between runs,
197 indicating that the L10 rRT-PCR was highly reliable to detect RPV RNA within a range
198 of +/- 2.0 FAM Ct in 21 independent repetitions (data not shown). L10 rRT-PCR assay
199 reproducibility was also analyzed running tenfold dilutions of RPV RNA from different
200 RPV isolates: Kabete O (8 replicates), Pakistan (3 replicates), Yemen (3 replicates), India
201 (2 replicates), Sokoto (5 replicates). Results indicated low degree of variability between
202 runs and viral isolates (Fig. 3).
203 **Specificity of amplification of L10 rRT-PCR.** The analytical specificity of the L10
204 rRT-PCR assay was tested against a collection of viruses that either show close genetic
205 relationship with RPV (near neighbors) or cause a disease that can be difficult to

differentiate clinically from RP (look alike). Near neighbors included 17 strains of PPRV from various geographical and temporal origins. Look-alike disease agents tested included Bluetongue Virus (BTV), Bovine Viral Diarrhea Virus (BVDV), Bovine Herpes Virus 2 (BHV-2), seven serotypes of Foot-and-Mouth Disease Virus (FMDV), and Vesicular Stomatitis Viruses (VSV) serotypes Indiana and New Jersey. The L10 rRT-PCR assay showed no reactivity with any of the 25 non-RPV agents tested (data shown in supplemental table 1).

Analytical sensitivity and Amplification Efficiency of L10 rRT-PCR. The analytical sensitivity was determined based on the ability of the assay to detect RNA extracted from different titrated RPV isolates. The viral suspension was serially diluted in log10 steps in DMEM in duplicate, RNA was extracted from each sample and tested by rRT-PCR to determine the level of detection (LOD), defined as the smallest detectable amount of analyte. The assay was repeated for five RPV isolates (Kabete O, Pakistan, Yemen, Indiana and Sokoto) that encompassed all genotypic variants (Figure 1). For each isolate, a titration curve was generated with at least 3 independent RNA extractions from each virus supernatant. After adjustment for extraction (140 µl) and sample volume per reaction (2.5 µl), the LOD values of the five representative RPV isolates ranged from 0.59 to 87.5 $TCID_{50}$ per reaction (Table 6). The amplification efficiency (AE), an indicator of the linearity and efficiency of the amplification reaction ($10^{(-1/slope)}$), that optimally should be around 2 indicating the doubling of the product in each cycle, ranged from 1.95 - 2.29 (average 2.13) with an R^2 from 0.992-0.999 (average 0.913) and little variability observed among the isolates tested (Table 6, Figure 3).

Clinical sensitivity: The ability of the L10 rRT-PCR assay to detect RPV RNA was evaluated in clinical samples collected from six steers inoculated intramuscularly with 10^4 $TCID_{50}$ of the Kabete "O" strain of RPV. All animals developed the expected clinical signs of RP disease, including fever, beginning at 4 dpi, followed by excessive salivation, dental pad lesions and ocular and nasal discharges, starting at 5 dpi. This was followed by diarrhea, depression, emaciation and dehydration, muco-purulent nasal and conjunctival discharges and prostration by 6 to 8 dpi. All animals were euthanized when found moribund by 6 to 8 dpi. At necropsy, no significant differences in severity of the lesions were found between animals. Clinical samples were collected from 0-8 dpi and in post-mortem examination at 8 dpi (Table 7).

In general, theL10 rRT-PCR demonstrated pre-clinical diagnostic value in several samples and better sensitivity than VI. The L10 rRT-PCR was able to detect RPV antigen in conjunctival and nasal swabs as early as 3 dpi (in 2 and 1 of 4 infected animals, respectively) and by 5 and 4 dpi in all 4 cattle, respectively (Table 7). This is as early as 3 days before clinical signs were observed. These samples remained positive until the day of euthanasia (8 dpi). Preputial swabs were also positive by 3 dpi, suggesting this as a good potential *in vivo* sample. Oral swabs and anal swabs were late positives indicating they are not the sample of choice. Buffy coat from heparin-blood seemed to be as sensitive as conjunctival and nasal swabs, with positive results by rRT-PCR at 3 dpi, which makes it an excellent *in vivo* sample of choice for detecting RPV before clinical signs are observed. Blood samples are also obtained as part of surveillance programs for other diseases providing a possible surveillance tool for RPV. Post mortem samples from

250 infected animals such as lymph nodes, spleen, Peyer's patches, tonsils and others were
251 consistently positive by rRT-PCR.
252 The L10 rRT-PCR test was compared with the gold standard method of virus isolation
253 (VI). The results showed that rRT-PCR was able to identify the RPV at least 1 or 2 days
254 before VI positive results, with the advantage that rRT-PCR results are obtained on the
255 same day rather than a week later for VI (Table 7). In some cases, CPE was difficult to
256 identify, probably due to the presence of inhibitors or toxic substances in the tissue
257 homogenates for the cell cultures, giving inconclusive VI results that required
258 confirmation using a conventional RPV RT-PCR test (not shown). In none of the cases
259 was VI more sensitive than L10 rRT-PCR (Table 7).
260 **Determination of the cycle cut-off values:** The optimum cut-off value for L10 RPV
261 rRT-PCR was determined using samples from experimentally infected and non-infected
262 cattle or from tissue culture. A total number of 60 known positive and 85 known negative
263 viral samples, were tested by both L10 rRT-PCR and VI followed by conventional RT-
264 PCR confirmatory test, as described above. The mean Ct value of the tissue culture
265 samples known to be positive was 24.58±3.87, while the mean Ct value of clinical
266 specimens that were known positives was 31.96±2.67 ($\alpha \leq 0.05$, *t test*), indicating that
267 even the weak positive samples were crossing the fluorescence threshold before 35
268 cycles. No values >0.00 Ct were detected among the 85 known negative samples after 55
269 cycles (data not shown) indicating the absence of false positives in that range of cycles
270 and threshold. The *describe* program of the WINPEPI statistical package
271 (www.brixtonhealth.com) was also used to calculate the best cut-off point depending on
272 weights given to false positives (FPs) and false negatives (FNs). The resulting optimum

cut-off value was 30.89 cycles for equal weights and up to 37 cycles resulted in a sensitivity of 100% without compromising the specificity for FNs. Therefore, based in our results of known positives and known negatives, we chose 40 cycles as cut-off to ensure maximum sensitivity.

DISCUSSION

RP has long been recognized as one of the most devastating diseases of livestock. The Global Rinderpest Eradication Program (GREP) from the Food and Agriculture Organization of the United Nations (FAO) based on intensive vaccination of susceptible animals, has been ongoing over the last decades. As a result, there has been a significant decrease of reported outbreaks and there is the potential declaration of total eradication of RPV by 2011 (12, 23). What remains to be done now is not only to ensure that the virus is not circulating in animal populations, but also that it does not escape (either deliberately or accidentally) from storage virus repositories. RPV has recently been active in many developing countries, disaster zones and war zones that would need some monitoring for a few more years. Hence, there is a new big scientific challenge following eradication of RP, which is to maintain large scale surveillance to avoid re-emergence of the disease within a naïve non-vaccinated susceptible population. Several factors point out that RP can still pose a major risk: (i) the proven capability of the virus to reappear after long periods of absence as it happened in 1994, 1996 and 2001 with RPV lineage 2 in wildlife after a period of 30 years of silence (5, 9, 12, 14, 23, 25); (ii) the fact that the most recently circulating RPV field isolates had evolved to such mild pathology that they could escape veterinary attention in remote areas (5, 9); and (iii) the difficulties to

296 distinguish between infected and vaccinated animals by using serological tests, seriously
297 compromising the efforts and achievements of the successful eradication program
298 (www.fao.org). All these premises lead to a real need for a highly sensitive and specific
299 diagnostic based on clinical observation and *in vivo* samples instead of necropsy findings
300 that can detect the presence of the virus in the absence of clinical signs.
301 Here we described a highly sensitive one-step rRT-PCR able to detect RPV with high
302 specificity and to provide a differential diagnosis with other look-alike diseases, PPRV
303 and other closely related viruses. The availability of this rRT-PCR test could aid in the
304 timely and prompt diagnosis both in the laboratory and also potentially in the field. The
305 rRT-PCR has been proven to be a technique that is easily adaptable for high-throughput
306 monitoring of animals and can also be use in conjunction with a whole diagnostic panel
307 for other diseases. It is accepted to be at least as sensitive and specific than VI, if not
308 more, and rRT-PCR assays have been widely demonstrated capable of early diagnosis in
309 many other animal viral diseases (1, 20, 24, 25). In addition test results can be obtained in
310 2-4 hours after arrival of the samples to the lab and can also be adapted to the field. We
311 compared the performance on the rRT-PCR on a variety of clinical samples from
312 experimentally infected natural hosts and showed the suitability of this test for early
313 detection of the RPV RNA in conjunctival or nasal swab, blood specimens before of the
314 appearance of clinical symptoms. Blood samples and buffy coat are ideal samples either
315 for surveillance or during an investigation case, and allow for 2-3 days pre-clinical
316 detection of the antigen. In case where bleeding of animals were not feasible, nasal, and
317 oral and/or conjunctival swabs would be samples of choice for epidemiological
318 surveillance and investigation, allowing RPV detection 1-2 days earlier than VI. Finally,

319 we confirmed previous evidence indicating the usefulness of lymph nodes as post-
320 mortem diagnostic samples for diagnostic.
321 Detection of infected animals 1-3 days before clinical signs are apparent will help in
322 culling infected animals prior to the peak of viral shedding (6). Virus isolation is widely
323 used as the gold standard for diagnosing RPV infection but can take over 2 weeks to
324 generate results, allowing ample time for spread of RPV within a herd (5, 15, 16, 18, 19,
325 20). VI reading is sometimes affected by the presence of inhibitors or toxicity of the
326 tissue homogenates, the bad preservation of the samples and contaminants with other
327 viral, bacterial or fungal microorganisms.
328 Out of five different combinations of primer sets tested in this study, only two detected
329 all the isolates and just one was specific enough to distinguish RPV from genetically
330 close relative PPRV. We believe that this difference is not related to the ratio of
331 concentrations of the primer pairs or some other reaction conditions, since those were
332 independently optimized for each primer/probe set. As other members of the
333 mononegavirales, RPV mRNA transcription is regulated by the order of the genes in the
334 viral genome (3'-N-P/C/V-M-F-H-L-5'). Transcription proceeds in a stepwise pattern
335 from a single promoter at the 3' end of the genome. Therefore, there is a decrease in
336 abundance of mRNAs as the polymerase complex moves away from the single promoter
337 at the 3' end resulting in L being the least abundant transcript (3). Despite this
338 differential expression the L primer set demonstrated better sensitivity suggesting that
339 sequence conservation in the L sequence played a more important role in detection than
340 differential mRNA expression.

The L10 rRT-PCR assay did not display cross-reactions with other viruses such as PPRV, BT, BTV, BVDV, FMDV and VSV indicating a high degree of specificity for RPV. Although the L10 test was based on a conserved genomic area, it is possible that new variants not detectable by the assay might emerge if RPV makes a comeback. In that case further field validation will be needed in order to assure the validity of this test as a diagnostic tool. In summary, the one step L10 rRT-PCR assay described in this report is a simple, sensitive, specific and rapid method for detection of RPV in field samples from live or dead animals.

Acknowledgements. The authors want to acknowledge the assistance of the Animal Care Unit of PIADC and the APHIS-FADDL school staff during the animal inoculations and sampling. We also thank Kaitlin Rainwater-Lovett for her help with the manuscript. And Dr. Dan L. Rock for facilitating the RPV sequences used in the design of the test.

REFERENCES:

1. **Agüero, M., E. San Miguel, A. Sánchez, C. Gómez-Tejedor, and M.A. Jiménez-Clavero.** 2007. A fully automated procedure for the high-throughput detection of avian infuenza virus by real-time reverse transcription-polymerase chain reaction. Avian Dis. **51**:35-41.
2. **Anderson, E.** 1995. Morbillivirus infections in wildlife (in relation to their population biology and disease control in domestic animals). Vet. Microbiol. **44:** 319.

3. **Baron, M.D. and T. Barrett.** 1995. The sequence of the N and L genes of rinderpest virus, and the 5' and 3' extragenic sequences: the completion of the genome sequence of the virus. Vet. Microbiol. 44:175–185.
4. **Barrett, T., S. Subbarao, G. Belsham, and B. Mahy.** 1991. The Molecular Biology of the Morbillivirus. The Paramyxoviruses. Kingsbury David. Plenum Press, New York Chapter 3. pp 83-102.
5. **Barrett, T. and P. Rossiter.** 1999. Rinderpest: The disease and its impact on humans and animals. Advances in Virus Research. **53**: 89.
6. **Blood, D., O. Radostits, J. Henderson, J. Arundel, and C. Gay.** 1988. Rinderpest. Med. Vet. 5ª edicion en Español, ed. Interamericana, pp. 817-821.
7. **Callahan, J., F. Brown, F. Osorio, J. Sur, E. Kramer, G. Long, J. Lubroth, S. Ellis, K. Shoulars, K. Gaffney, D. Rock, and W. Nelson.** 2002. Use of a portable real-time reverse transcriptase-polymerase chain reaction assay for rapid detection of foot-and-mouth disease virus. J Am Vet Med Assoc. **220**: 1636.
8. **Cattaneo, R., K. Kaelin, K. Baczko, and M. A. Billiter.** 1989. Measles virus editing provides an additional cysteine-rich protein. Cell **56**:759-764.
9. **Daszak, P., A. Cunningham, and A. Hyatt.** 2000. Emerging infectious diseases of wildlife-threats to biodiversity and human health. Science. **287:** 443.
10. **Forsyth, M., and T. Barrett.** 1995. Evaluation of Polymerase Chain Reaction for the detection and characterization of Rinderpest and Peste des Petits Ruminants Viruses for epidemiological studies. Virus Res. **39:** 151-163.

11. **Forsyth, M., S. Parida, S. Alexandersen, G. Belsham, and T. Barret.** 2003. Rinderpest virus lineage differentiation using RT-PCR and SNAP-ELISA. J Virol Methods. **107**: 29.

12. **Kock, R. A., H.M. Wamwayi, P.B. Rossiter, G. Libeau, E. Wambwa, J. Okori, F.S. Shiferaw, and T.D. Mlengeya.** 2006. Re-infection of wildlife populations with rinderpest virus on the periphery of the Somali ecosystem in East Africa. Prev. Vet Med. **75**:63-80.

13. **Lund, B., A. Tiwari, S. Galbraith, M. Baron, I. Morrison, and T. Barret.** 2000. Vaccination of cattle with attenuated Rinderpest Virus stimulates CD4+ T Cell responses with broad viral Aantigen specificity. J. Gen. Virol. **81:** 2137.

14. **Mariner, J.C, and P.L. Roeder.** 2003. Use of participatory epidemiology in studies of the persistence of lineage 2 rinderpest virus in East Africa. Vet. Rec. **152**:641-647.

15. **Norby, E., H. Sheshberdaran, K. Mc Cullough, W. Carpeter, and C. Orvell.** 1985. Is Rinderpest Virus the archevirus of the Morbillivirus Genus? Intervirology. **23:** 228.

16. **Norby, E.** 1991. Immunobiology of Paramyxoviruses. The Paramyxoviruses. Kingsbury David. Plenum Press, New York Chapter 18. pp 481-507.

17. **OIE/GREP.** 2007. Manual on the diagnosis of Rinderpest. PART III. Confirmatory and Differential diagnosis. Chapter 9.

18. **Plowright, W.** 1962. Rinderpest Virus. Ann. N.Y. Acad. Sci. **101:** 548.

19. **Plowright, W., and R. Ferris.** 1962. Studies with Rinderpest Virus in tissue culture. A technique for the detection and titration of virulent virus in cattle tissues. Res. Vet. Sci. **3:** 94.

20. **Plowright, W., and R. Ferris.** 1957. Cytopathogenicity of Rinderpest Virus in tissue culture. Nature. **179:** 316.

21. **Reed, L. and H. Muench.** 1938. Simple method of estimating fifty per cent endpoints. *Am J Hyg* **27**: 493.

22. **Risatti, G., J. Callahan, W. Nelson, and M. Borca.** 2003. Rapid detection of Classical Swine Fever Virus by a portable real time reverse transcriptase PCR assay. J. Clinical Microbiology. **41:** 500-505.

23. **Roeder, P.L., J. Lubroth and P. Taylor.** 2004. Experience with eradicating Rinderpest by vaccination. Dev. Biol. **119:**73-91.

24. **Shaw, A.E., S.M. Reid, K. Ebert, G. H. Hutchings, N.P. Ferris, D.P. King.** 2007. Implementation of a one-step real-time RT-PCR protocol for diagnosis of foot-and-mouth disease. J. Virol. Methods. **143:**81-85.

25. **Taylor, W.P., P. L. Roeder, M.M. Rweyemamu, J. N. Melewas, P. Majuva, R. T. Kimaro, J. N. Mollel, B. J. Mtei, P. Wambura, J. Anderson, P. B. Rossiter, R. Kock, T. Melengeya, and R. Van den Ende.** 2002. The control of rinderpest in Tanzania between 1997 and 1998. Trop. Anim. Health Prod. **34**:471-487.

26. **Wanwayi, H. M., M. Fleming, and T. Barret.** 1995. Characterisation of African isolates of Rinderpest virus. Vet. Microb. **44:** 112-119.

27. **Zsak, L., M. Borca, G. Risatti, A. Zsak, R. French, Z. Lu, G. Kutish, J. Neilan, J. Callahan, W. Nelson, and D. Rock.** 2005. Preclinical diagnosis of

428 African Swine Fever in contact-exposed swine by a Real-Time PCR assay. J.
429 Clinical Microb. **43:**112-119.
430
431

TABLE 1. RPV isolates used for nucleotide alignment to design the primers-probe sets

Isolates	Genbank Acc. No.	Genomic Data
[1]Kabete O	To be determined	Complete genome
[1]RBok	To be determined	Complete genome
[1]Pak Chong	To be determined	Complete genome
[1]Pendik	To be determined	Complete genome
[1]RBT	To be determined	Complete genome
[1]Saudi	To be determined	Complete genome
[1]Kuwait 21	To be determined	Complete genome
[1]Nigeria Buffalo	To be determined	Complete genome
[1]Yemen	To be determined	Complete genome
[1]India	To be determined	Complete genome
[1]Nigeria Sokoto	To be determined	Complete genome
[1]Kuwait	To be determined	Complete genome
[1]Sokoto	To be determined	Complete genome
[1]Pakistan	To be determined	Complete genome
[1]Nigeria vero	To be determined	Complete genome
[1]Egypt	To be determined	Complete genome
RBOK	Z30697	N, P, C, M, F, H, and L
Kabete 'O'	NC 006296	FL
LATC	AF515676	N
RBOK	X68311, S54798	N, P, V, and C
Kuwait 82/1	Z34262	N
Kabete 'O'	U02679	N
Kabete 'O'	AY035887	F
Kabete 'O' Lapinized	M20870	F
Kabete 'O'	M21514	F
Egypt/84	Z31655	F
RBOK	Z30700	F
RBT1	Z31656	F
Kabete 'O'	M21513	H
LA	D82982	H
Kabete 'O'	AF132934	H
Kabete 'O' Lapinized	M17434	H
RBOK	Z30699	H
Kabete 'O'	Y18816	H
Kabete 'O'	Z33634	L
Kuwait 82/1	Z33636	L
Kabete 'O'	X98291	N, P, M, F, H, and L
RBOK	Z30698	L

[1] These RPV isolates were previously full length sequenced (Carrillo et al unpublished results).

435 **TABLE 2.** Sequences and genomic position of the primer-probe sets.
436

Viral gene	Genome Position*	Oligonucleotide Sense/Function	5'-3' Sense Nucleotide Sequence
H	7315	Forward Primer	GAA CAC TCG GGT GGT TCT TAA TAA A
	7426	Reverse Primer	TGC GAT AGC TAA TAG CCC GAC
		Probe	ACG GTG TTG TTT GTC ATG T
F	6956	Forward Primer	TGA TTG CAG TAG TGG GTA TCC TCA
	7092	Reverse Primer	TGA CCG TAC GTA GGA TTT GGA TG
		Probe	ACC TGT TGC TGT AGG AAG
N	1020	Forward Primer	TGG GTG AAC TGG CTC C
	1120	Reverse Primer	CCC ATA GCA TAG CTC CA
		Probe	TTC AGT GCA GGA GCA
L9	9157	Forward Primer	GCAACATACAAACGGCTACCAA
	9303	Reverse Primer	TGGCAACCAGCTTGTTAGTCA
		Probe	CTG TAT TTC ACC ATG GAC TC
L10	10376	Forward Primer	RAT GAA AGG WCA TGC CAT ATT
	10450	Reverse Primer	GGT GGC CAG CTC C
		Probe	ATC ATC AAC GGG TAT CG

437
438 (*) Numbers indicate the 5' nucleotide position of the primer/probe, counting from the 5'
439 end of the full length genome sequence of RPV, according to O Kabete sequence
440 NC006296.

TABLE 3. Ct and FAM values obtained during the Primer/Probe concentration optimization for every set using 55^0C of annealing temperature and 55 cycles and Kabete 'O' viral RNA template.

Probe Concentration		Primer Concentration (25 µl reaction) 100nM Ct	100nM Δ Fluor	200nM Ct	200nM Δ Fluor	300nM Ct	300nM Δ Fluor	400nM Ct	400nM Δ Fluor	500nM Ct	500nM Δ Fluor
H	50nM	0.00	0	17.58	74	16.99	73	16.73	81	16.57	78
	100nM	20.69	132	16.44	190	15.93	195	15.88	204	15.51	238
	200nM	17.92	546	14.88	590	14.74	476	**14.40**	552	14.31	547
N	50nM	20.89	244	18.89	217	18.92	235	17.75	232	17.75	219
	100nM	26.23	312	21.71	419	21.75	417	21.47	423	21.20	454
	200nM	18.64	842	16.82	881	15.90	843	**15.99**	997	15.42	908
F	50nM	16.00	0	16.00	68	16.00	87	16.00	87	16.00	108
	100nM	17.77	87	15.91	162	15.58	231	15.64	263	**15.39**	293
	200nM	15.87	147	14.42	243	15.62	142	14.51	327	15.13	286
L9	50nM	0.00	0	19.92	74	18.94	97	18.82	99	19.38	81
	100nM	20.94	73	17.80	175	17.63	209	17.64	199	17.55	236
	200nM	18.21	204	17.16	342	17.44	279	**16.79**	434	17.32	318
L10	50nM	27.46	131	21.20	127	19.80	122	19.45	110	19.43	108
	100nM	24.23	275	20.30	340	19.48	303	19.11	302	**15.34**	646
	200nM	18.75	465	17.80	189	15.55	425	**15.47**	589	18.40	362

TABLE 4. RPV strains detected by rRT-PCR assay at 55°C annealing temperature and 55 cycles, with pre-optimized concentrations of primer-probe for each set.

RPV Isolate	Primer/Probe set				
	H[a]	N[b]	F[c]	L9[d]	L10[e]
K15	0	33.42	0	0	28.52
Kabete 'O'	35.07	32.09	31.72	28.18	24.85
Pakchong	42.05	22.67	0	0	13.52
NAK 3	44.58	30.25	0	0	23.31
RBOK	31.09	28.4	27.51	21.58	18.77
RB Nigeria	37.8	19.74	0	0	26.81
Pakistan	0	23.49	0	0	19.89
Yemen	0	25.47	0	0	19.22
Pendik	0	25.4	0	0	19.72
Nig. Buffalo	46.2	22.7	0	0	21.09
Kuwait	0	25.75	0	0	18.89
Saudi Arabia	0	18.26	0	0	13.93
RBT	0	20.87	0	0	15.74
India	29.36	27.66	27.05	21.37	18.65
Sokoto	0	32.13	0	0	24.26
Egypt	37.8	24.31	0	0	22.99

Real Time PCR was run under standard conditions of:

[a] Primer Probe set H (200 nM probe-400nM primers)
[b] Primer Probe set F(100nM probe-500nM primers)
[c] Primer Probe set N (200 nM probe-400nM primers)
[d] Primer Probe set L9 (200nM probe-400nM primers)
[e] Primer Probe set L10 (200 nM probe-400 nM primers)

TABLE 5. PPRV cross-detection with primer/probe sets L10 and N.

Primer/ Probe	Viral Isolate	Annealing Temperature	
L10	RPV[(1)]	50	19.09 +/- 0.27
		55	18.79 +/- 0.04
		60	21.26 +/- 1.06
	PPR[(2)]	50	0.00 +/- 0.00
		55	0.00 +/- 0.00
		60	0.00 +/- 0.00
N	RPV[(1)]	50	18.66 +/- 0.34
		55	18.33 +/- 0.12
		60	18.54 +/- 1.34
	PPR[(2)]	50	35.69 +/- 2.45
		55	51.48 +/- 1.73
		60	36.88 +/- 1.87

Results are expressed as average FAM Ct value from two different isolates. [(1)] RPV isolate was either Kabete O or India in two different experiments.[(2)] PPRV isolate was either Burkina or Cote d'Ivoire, in two different experiments.

TABLE 6. Analytical Sensitivity and Amplification Efficiency of L10 primer-probe rRT-PCR.

Isolate	$TCID_{50}$/100uL (log10)	FAM C_t Value	LOD ($TCID_{50}$/2.5uL Reaction)[1]	Amplification Efficiency[2]	Amplification Efficiency R^2 Value
Kabete 'O'	7.63	19.39			
	6.63	23.13			
	5.63	25.89			
	4.63	29.04			
	3.63	32.40			
	2.63	35.46	37.3	2.06	0.999
Pakistan	4.83	21.93			
	3.83	24.81			
	2.83	27.27			
	1.83	30.37			
	0.83*	33.69	0.59	2.29	0.998
Yemen	6.0	20.75			
	5.0	23.86			
	4.0	27.24			
	3.0	30.35			
	2.0	33.59			
	1.0	35.84	0.88	2.11	0.997
Sokoto	5.0	21.49			
	4.0	25.08			
	3.0	28.56			
	2.0	32.77			
	1.0	34.84	0.88	1.95	0.992
India	6.0	25.26			
	5.0	27.17			
	4.0	30.03			
	3.0	33.91	87.5	2.22	0.977
			Average:	2.13	0.993

[1] Level of detection (LOD) calculation assumes 100% viral RNA extraction recovery. RNA was extracted from undiluted, titrated tissue culture supernatant, 10-fold serial dilutions were made of the extracted RNA. Positive Ct cut-off was subsequently set at ≤ 35.0.

[2] The amplification efficiency (the measure of an assay's ability to double product after each cycle) was measured as described in the materials and methods section.

* For RPV Pakistan, the $10^{0.83}$LOD is theoretical, using Ct <40 as a cut-off.

TABLE 7. L10 rRT-PCR sensitivity on clinical samples from O Kabete RPV experimentally infected cattle

In vivo	Sample	Days P.I.	VI	rt RT-PCR
	Nasal swab	3	0/4	1/4
		4	0/4	4/4
		5	4/4	4/4
	Conj. Swab	3	0/4	2/4
		4	3/4	3/4
		5	4/4	4/4
	Oral swab	3	0/4	0/4
		4	0/4	2/4
		5	1/4	4/4
	Rectal swab	3	0/4	1/4
		4	1/4	2/4
		5	2/4	3/4
	Preputial swab	3	1/2	2/2
		4	2/2	2/2
		5	2/2	2/2
	Plasma	3	0/2	0/2
		4	0/2	0/2
		5	0/2	0/2
	WBC	3	0/2	2/2
		4	0/2	2/2
		5	1/2	2/2
	Whole blood	3	0/2	1/2
		4	0/2	2/2
		5	0/2	2/2
Post Mortem	**Sample**	**Days P.I.**	**VI**	**rt RT-PCR**
	Spleen	6	6/6	6/6
	LN	6	16/17	17/17
	Abomasum	6	4/4	4/4
	Lingual Tonsil	6	2/2	2/2
	Palatine Tonsil	6	2/2	2/2
	Third eyelid	6	2/2	2/2
	Peyer's patches	6	3/3	3/3
	Gall bladder	6	1/1	1/1

Results are expressed as number of RPV rRT-PCR positive animals over the total number of infected animals tested. P.I.: post infection. VI: virus isolation confirmed by conventional RT-PCR.

526 **Fig. 1:** Phylogenetic representation of the complete sequenced RPV isolates used for the
527 design and optimization of rRT-PCR.
528
529

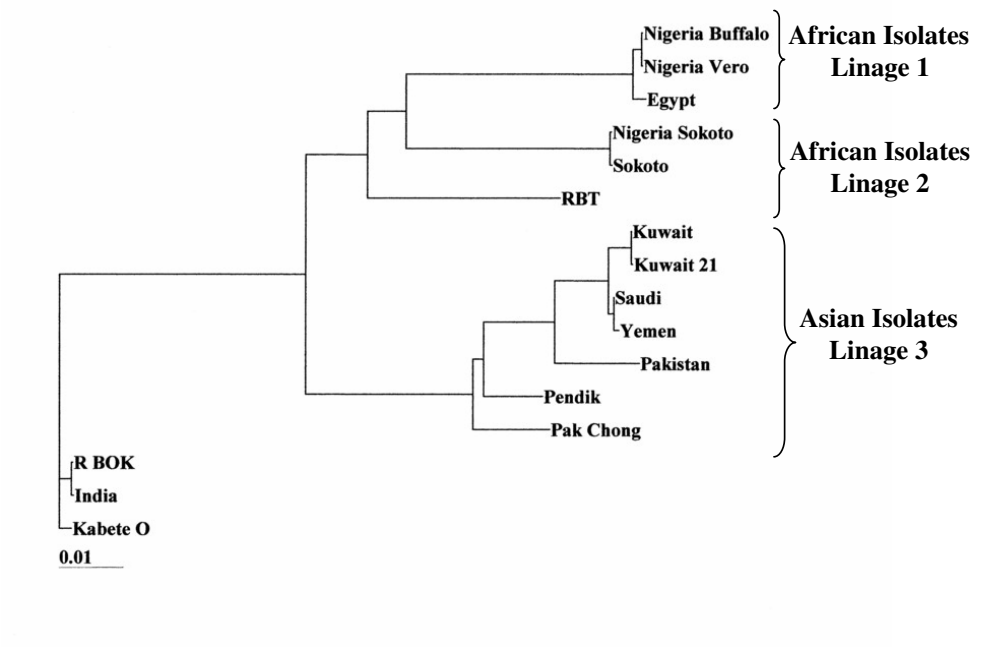

530

Fig. 2: Optimal concentration of L10 primer-probe set for 45 cycles. Two combinations of L10 primer-probe set (200 nM probe-400 nM primers and 100nM probe-500 nM primer) were tested against different RPV isolates (Yemen, Sokoto, Pakistan, India, Saudi A., Kuwait and RBOK).

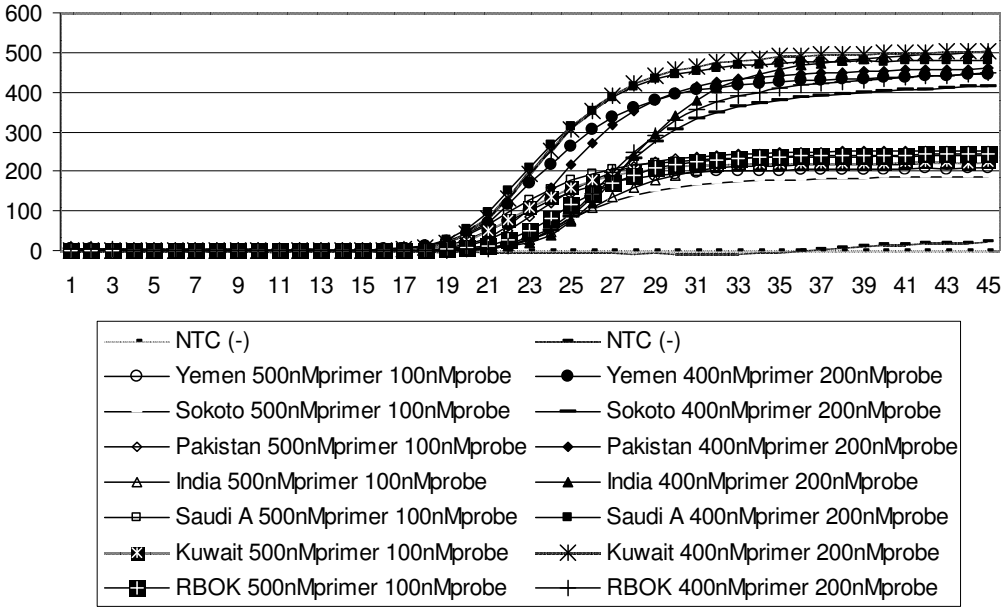

Fig.3: L10 primer-probe real time RT-PCR Assay Reproducibility. Graphic representation of average and Standard Deviation of the FAM Ct values obtained for ten fold dilutions of RPV RNA from different isolates: Kabete O (8 replicates), Pakistan (3 replicates), Yemen (3 replicates), India (2 replicates), Sokoto (5 replicates).

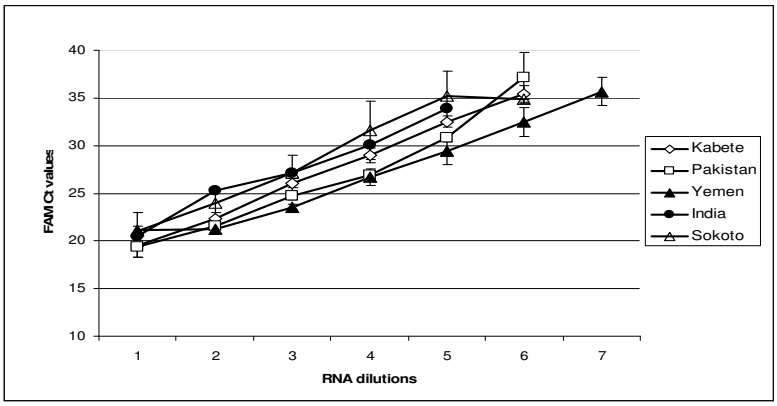

Return to Table of Contents

J. Vet. Sci. (2010), **11**(2), 133−142
DOI: 10.4142/jvs.2010.11.2.133

JOURNAL OF
Veterinary
Science

Evaluation of infectivity and transmission of different Asian foot-and-mouth disease viruses in swine

Juan M. Pacheco[1,*], P. W. Mason[2]

[1]*Plum Island Animal Disease Center, North Atlantic Area, Agricultural Research Service, United States Department of Agriculture, PO Box 848, Greenport, NY 11944-0848, USA*
[2]*Microbial Molecular Biology, Novartis Vaccines and Diagnostics, 350 Massachusetts Avenue, Cambridge, MA 02139, USA*

Most isolates of foot-and-mouth disease virus (FMDV) display a broad host range. Since the late 1990s, the genetic lineage of PanAsia topotype FMDV serotype O has caused epidemics in the Far East, Africa, the United Kingdom, France, the Netherlands, and numerous other countries throughout Europe and Asia. In contrast, there are several FMDV isolates that exhibit a more restricted host range. A Cathay topotype isolate of FMDV serotype O from the 1997 epizootic in Taiwan (O/TAW/97) demonstrated restricted host specificity, only infecting swine. Methods used to evaluate infectivity and pathogenicity of FMDV isolates in cattle are well-documented, but there has been less progress studying transmission and pathogenicity of FMDV isolates in pigs. In previous studies designed to examine pathogenicity, various chimeric viruses derived from O/TAW/97 were intradermally inoculated in the heel bulb of pigs. Subsequent quantitative scoring of disease and evaluation of virus released into nasal secretions and blood was assessed. Here we prove the usefulness of this method in direct and contact inoculated pigs to evaluate infectivity, pathogenicity and transmission of different Asian FMDV isolates. Virus strains within the Cathay topotype were highly virulent in swine producing a synchronous disease in inoculated animals and were efficiently spread to in-contact naïve pigs, while virus strains from the PanAsia topotype displayed more heterogeneous properties.

Keywords: Cathay topotype, FMDV, infectivity, PanAsia topotype, pathogenicity, pigs

Introduction

Foot-and-mouth disease (FMD) is one of the most dreaded ailments of livestock due to its broad host range and high rate of contagious spread. Efforts to control FMD outbreaks have resulted in regional and international quarantine laws and regulations. Recent outbreaks in historically FMD-free countries (e.g., reintroductions into Argentina, Brazil, Uruguay [25,27] and Western Europe in the 2000s, in Japan in 2000 after 90 years [36], and in Korea in 2000 and 2002 after 66 years [30,31]) suggest a need for more information about how FMD spreads. Among the seven serotypes of FMD virus (FMDV), serotype O has the broadest distribution, occurring worldwide [22]. FMDV can infect all even-toed ungulates, although some FMDV isolates exhibit a restricted host range. One of these, the virus responsible for the devastating epizootic in Taiwan in 1997 (O/TAW/97), affects swine but does not cause disease in cattle [10]. We have previously reported that O/TAW/97 has a shortened form of the non-structural viral protein 3A, which is associated with the inability of this virus to replicate or grow in bovine cells in culture [5,21,29]. We have also reported that this deletion is associated with attenuation in cattle but not in pigs [5,33]. This shortened form of 3A is characteristic of one topotype of Asian viruses [21], designated the Cathay topotype [37]. Interestingly, the earliest available member of the Cathay topotype examined, a 1970 virus recovered from a pig in Hong Kong (O/HKN/21/70), grows well in bovine cells, despite expressing a truncated form of 3A [21]. Other members of this topotype were recently isolated in Hong Kong in the years 2001 and 2002, named O/HKN/2001 and O/HKN/2002, respectively [7,11,28]. Following the multibillion-dollar outbreak in Taiwan caused by O/TAW/97 [39] a second FMDV strain was isolated in 1999 in the Kinmen Island prefecture of Taiwan, several kilometers from the coast of mainland China. The Kinmen Island virus is a member of the PanAsia topotype of FMDV [22,24] and contains a full-length 3A-coding region [21]. Interestingly, the 1999 Kinmen Island isolate (represented in this study by O/TAW/2/99) did not cause disease in cattle (the presence of virus was only detected serologically and in probang

*Corresponding author
Tel: +1-631-323-3223; Fax: +1-631-323-3006
E-mail: juan.pacheco@ars.usda.gov

samples collected from disease-free animals [21]). FMDV was subsequently discovered on the main part of Taiwan, where it caused clinically apparent disease in cattle and goats, but not pigs (although some isolates could induce disease in experimentally infected pigs) [20]. In 2000, PanAsia topotype FMD viruses closely related to O/TAW/2/99 were detected in Japan, South Korea, Far Eastern Russia, and Mongolia, where they affected various species of even-toed ungulates [12,23]. PanAsia topotype viruses eventually spread out of Asia, and were responsible for an outbreak in the South African Republic in 2000 and the catastrophic European epidemic in 2001 [23]. In 2002, a PanAsian virus was isolated again in South Korea, designated as O/SKR/02 [30]. More recently, outbreaks in Turkey caused by this topotype were associated with myocarditis in lambs [15].

The efficiency and speed of dissemination of FMD depends on the FMDV strain involved, the quantities of virus shed, the rate of contact and the susceptibility of the recipient animals. As mentioned by Alexandersen *et al*. [3], there is an urgent need for additional quantitative information on excretion and transmission of FMDV and on disease parameters. This information will help to improve models used to predict the spread of the disease, especially if such predictions are to be used in FMD control (i.e., vaccination or treatment with biotherapeuthics). This report illustrates findings of FMDV excretion and transmission in pigs infected by direct or contact inoculation with isolates representative of the two topotypes described above (Cathay and PanAsia). When studied in cattle, FMDV infectivity can be readily accomplished by inoculating graded dilutions of virus intradermally into sites in the tongue, with scoring of lesions forming 24 to 72 h later [16,17]. However, the epidermis of the porcine tongue is thinner and more fragile than the bovine tongue, preventing application of this method to pigs [6]. Here we describe the adaptation of an intradermal heel-bulb inoculation method described by Burrows in 1966 [6] for the determination of porcine infectious dose of several FMDV isolates. This method was previously successfully applied for the comparison of swine infectivity with different chimeric viruses derived from O/TAW/97 [33]. Because the primary route of infection in pigs is by direct contact [1,2], we decided to evaluate transmission from directly inoculated pigs to pigs in direct contact for a limited period of 4 h. Preliminary application of these methods to the same strains evaluated *in vitro* demonstrates their utility in comparison of virulence, and suggests that the PanAsian viruses are more heterogeneous than the Cathay topotype viruses in terms of their ability to cause disease in pigs.

Materials and Methods

Virus strains and cell cultures

Table 1 describes the sources of viruses as well as the precise passage history of the viruses at the time of receipt and further passages made in our lab. Viruses prepared as described in this table were stored frozen at −70°C until needed. Baby hamster kidney cell monolayers (BHK, strain 21, clone 13, ATCC CL10, passage 62 to 66) were used to determine virus titers in terms of plaque forming units (PFU) [18]. The ability of these viruses to replicate in BHK, primary fetal bovine kidney cells (FBK) and primary fetal porcine kidney cells (FPK) [13,14] was determined as described previously [33]. All samples were run simultaneously to avoid inter-assay variability.

Evaluation of the disease after pig inoculation, and determination of porcine infectivity and pathogenicity

All animal manipulations were performed following

Table 1. Origin and passage history of foot-and-mouth disease virus (FMDV) strains used in this study

Virus*	Topotype	Species of origin†	Source/previous passage history‡	Plum Island passage history§
O/TAW/97	Cathay	Porcine	FADDL/APHIS PIGp1	PIGp2‖
O/HKN/21/70	Cathay	Porcine	WRL/BTYp4, RSp1	BHKp2
O/TAW/2/99	PanAsia	Bovine¶	WRL/BHKp3, BTYp1	BHKp2
O/SKR/00	PanAsia	Bovine	FADDL/field	BHKp1
O/SAR/19/00	PanAsia	Bovine	OVI/ PK2, RS1	BHKp2
O/UKG/35/2001	PanAsia	Porcine	FADDL/field	PIGp2**

*Nomenclature for all viruses is as follows: serotype/three-letter location code for country or place of origin/accession number (if applicable)/year of isolation. TAW: Taiwan, HKN: Hong Kong, SKR: South Korean Republic, SAR: South African Republic, UKG: United Kingdom. †Livestock species of origin. ‡Institute of origin (FADDL: Foreign Animal Disease Diagnostic Laboratory, APHIS, VS, Plum Island, NY, USA; WRL: World Reference Laboratory for FMD, Pirbright, Woking, Surrey, UK; OVI: Onderstepoort Veterinary Institute, Onderstepoort, SAR). Passages (p) were performed in pigs (PIG), bovine thyroid cells (BTY), IBRS2 porcine kidney cell line (RS), baby hamster kidney cell line 21 clone 13 (BHK), or porcine kidney cells (PK) prior to receipt. §Amplifications made in our lab for inoculation studies. ‖The sample received was vesicular fluid that was inoculated in a pig and vesicular fluid from this pig was harvested and aliquoted for inoculations *in vivo* and *in vitro*. ¶The virus was isolated from an esophageal/pharyngeal sample obtained from an animal exhibiting a subclinical infection. **Original sample from the outbreak was directly inoculated in one pig, and vesicular fluid was harvested from another pig placed in direct contact with the inoculated one. Aliquots from this vesicular fluid were used for all inoculations *in vivo* and *in vitro*.

protocols approved by the Plum Island Animal Disease Center (PIADC) Animal Care and Use Committee. Determination of virus infectious dose in pigs was performed as previously described [33]. Briefly, four co-housed 20～40 kg out-bred white pigs were sedated and inoculated intradermally in the heel bulb of each major digit of each foot with 10^2, 10^3, 10^4 or 10^5 PFU of virus/5 μL (estimated volume retained in the inoculation site as described by Burrows [6]) achieved by inserting a 23G needle 1 cm along the superficial layer of the epidermis (Fig. 1A). Immediately following injection, the titer of the virus stock was confirmed by plaque assay in BHK cells. Formation of vesicles at the inoculation sites was scored 24 h after inoculation (Figs. 1B and C), and data from all four animals was used to determine the number of PFUs of virus capable of producing a 50% pig heel infectious dose ($PHID_{50}$) [34]. To demonstrate ability of transmission by direct contact between pigs, two days after inoculation the four directly inoculated pigs were combined with four similar-sized naïve pigs in a fenced 4 m^2 area within an animal isolation room, with water but without food during the exposure time. Four h later, the exposed pigs were placed into four rooms with separate HEPA-filtered ventilation systems containing hermetically sealed doors facing clean hallways. Heparinized blood and nasal swabs were collected and processed for virus isolation or IgM detection as previously described [33]. Records of the sites containing vesicles were prepared each day as previously described [33]. A maximum lesion score of 12 was possible in directly inoculated pigs (the eight injected digits were not counted in the former determinations) and a score of 20 was possible for direct contact pigs. The same team of investigators visited the 8 pigs for the indicated number of days, showering and changing clothing between each animal room. In all cases directly inoculated animals were examined after the direct contact animals. Pigs were humanely euthanized 5～7 days after they produced lesions or, in absence of lesions, when virus-specific IgM could be detected by ELISA or on day 20 after exposure. In some cases, once secondary vesicles appeared, animals were sedated and euthanized to collect samples that were used for other experiments (animals # 48, 97, 103, 292, 293 and 296). No animals died as a result of FMDV infection.

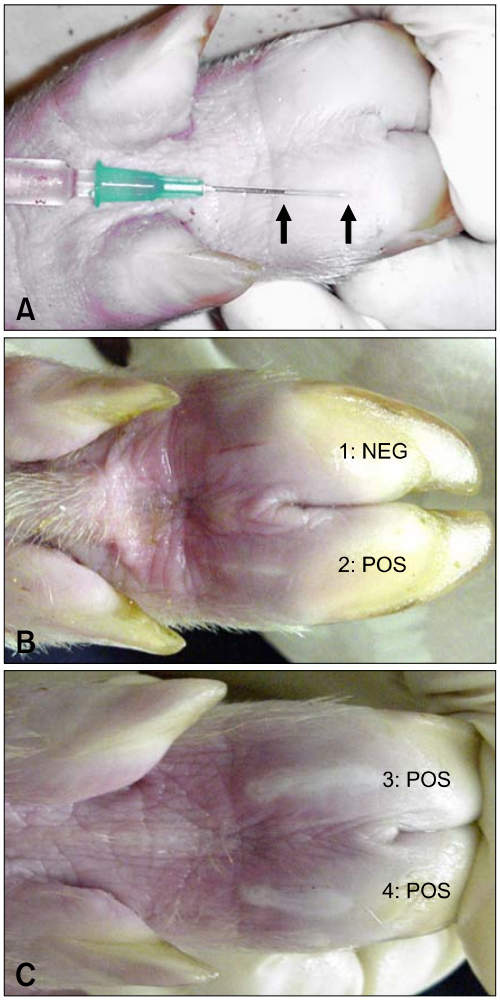

Fig. 1. (A) Intradermal inoculation in the heel bulb. The space between the two arrows marks the portion of the needle that lays within the dermis, approximately 1.2 cm. Inoculums were released while slowly removing the needle. (B and C) Replication of O/UKG/35/01 at the inoculation site 24 h after intradermal inoculation with 700 PFU/5 μL (1 and 2) and 70,000 PFU/5 μL (3 and 4). The presence of a vesicle (POS) indicates a positive result. The absence of a vesicle (NEG) indicates a negative result.

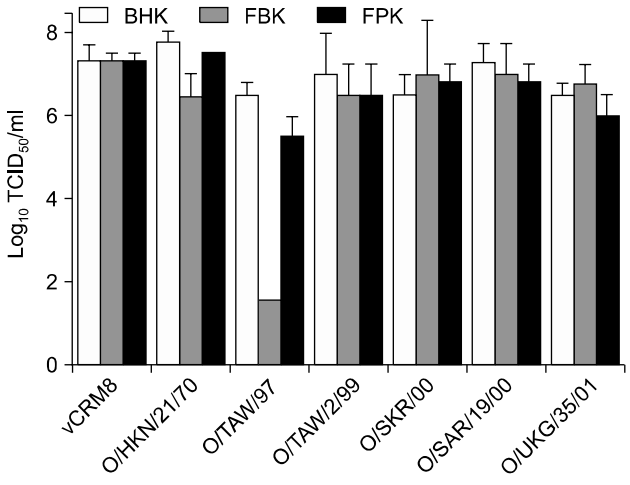

Fig. 2. Species specificity in primary bovine and porcine kidney cells (FBK and FPK, respectively) compared with BHK cells. $TCID_{50}$/mL was estimated for each virus starting with 10^7 PFU/mL, as previously determined in BHK cells. The vertical bar and the extended bar illustrate the results from two independent experiments. The name of each virus and species of origin are described in Table 1. vCRM8 (a chimeric virus experimentally shown to be infectious in cattle and swine) was added as an internal positive control.

Results

Different topotypes show different species specificity when analyzed *in vitro*

To determine species specificity *in vitro*, an assay was developed to measure the minimum infectious dose of virus able to propagate an infection on various cell types (Fig. 2). For these experiments, multi-well plates with BHK, FBK, and FPK cells were infected with 10-fold dilutions of virus [starting with 10^7 PFU/mL (as measured previously on BHK cells)] and examined to determine the lowest dose of virus able to cause complete cytopathic effect (CPE) at 48 h. These results were expressed as $TCID_{50}$/mL. All six strains and a positive control virus (vCRM8, a genetically engineered virus which is highly virulent in bovine and swine [4,35]) showed similar ability to cause CPE in hamster- and swine-derived cells (values close to 10^7 $TCID_{50}$/mL). In bovine-derived cells, all viral isolates except O/TAW/97 were able to replicate at similar titers.

Different topotypes demonstrate different infectivity when inoculated in swine

To study differences of infectivity (PFU/$PHID_{50}$), each one of the six strains were inoculated intradermally in the heel bulb of four pigs as described above. At 24 h post-inoculation the inoculation sites were scored as negative or positive (Fig. 1) to determine the $PHID_{50}$/mL present in the inoculums. Table 2 shows an example with the results obtained for O/SKR/00. Table 3 shows the $PHID_{50}$/mL and the infectivity obtained for each strain. Although we started the experiment with all viruses at similar PFU/mL values (ranging from 9.5×10^6 to 2.8×10^7), the $PHID_{50}$/mL values were broadly different. With O/TAW/97 we obtained a value of 10^5 $PHID_{50}$/mL; with O/HKN/21/70, O/SKR/00 and O/UKG/35/01 we obtained values of 10^3; and with O/TAW/2/99 and O/SAR/19/00 we obtained values less than 10^2. The five strains also showed different relative infectivities when compared to O/TAW/97. Twenty to 62 times more virus would be needed to produce a vesicle at the inoculation site with O/HKN/21/70, O/SKR/00 and O/UKG/35/01 while greater than 5,000 times more virus would be needed for the remaining two strains, O/TAW/2/99 and O/SAR/19/00.

Table 2. Results obtained after direct inoculation with FMDV O/SKR/00 in porcine heel bulb for determination of concentration of the inoculum as 50% pig heel infectious doses per mL ($PHID_{50}$/mL)

No.*	47,500 PFU†	4,750 PFU	475 PFU	47 PFU
783	+ +‡	+ +	− −	− −
781	+ +	+ +	− −	− −
794	+ +	+ −	− −	− −
799	+ +	+ −	− −	− −

*Animal number. †Amount of virus in each inoculation site. ‡Each sign represents one main digit. "+" indicates a macroscopic lesion was formed at the site of inoculation. "−" indicates that no lesion was visible.

Cathay topotype FMDVs are highly infectious and produce severe disease in pigs

When we studied the various parameters of infection of O/TAW/97 (Fig. 3), the direct inoculation of 10^5 PFU (10^3 $PHID_{50}$, Table 3) produced an acute and synchronous disease in the inoculated animals. In the O/TAW/97- inoculated animals, virus in blood was detected as early as 1 day post-inoculation (dpi) and virus was isolated from nasal swabs at 1 to 3 dpi. At 2 dpi, all the animals expressed peak amounts of virus in blood, nasal swabs and vesicles at secondary sites of replication. The highest value of lesion

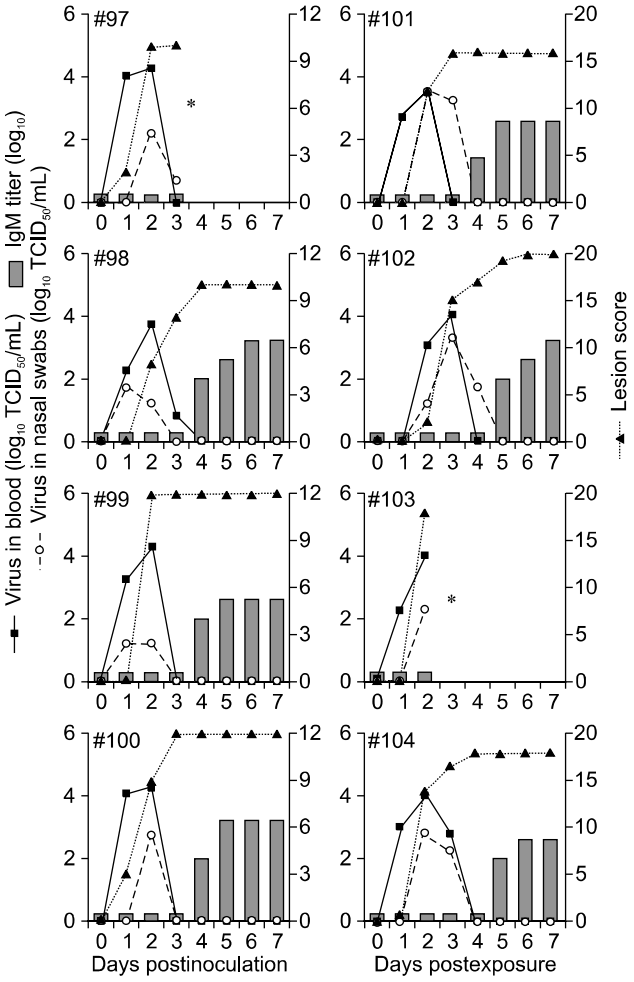

Fig. 3. Viremia, virus in nasal secretions, vesicular lesions and IgM titers in pigs directly inoculated with O/TAW/97 (left panels) or exposed to O/TAW/97 (right panels). *Indicates the day animals were euthanized to obtain samples for other studies.

Table 3. Infectivity results obtained with different Asian FMDV strains in comparison with O/TAW/97

Virus	PFU /mL*	$PHID_{50}$ /mL†	PFU /$PHID_{50}$‡	PFU /animal§	$PHID_{50}$ /animal‖	Relative infectivity¶
O/TAW/97	9.75×10^6	1.0×10^5	9.4×10^1	1.0×10^5	1.150	1
O/HKN/21/70	2.0×10^7	3.4×10^3	5.8×10^3	2.2×10^5	38	62
O/TAW/2/99	2.0×10^7	≤ 45	$\geq 4.4 \times 10^5$	2.2×10^5	≤ 0.5	≥ 4.680
O/SKR/00	9.5×10^6	4.3×10^3	2.2×10^3	1.0×10^5	47	23
O/SAR/19/00	2.8×10^7	≤ 25	$\geq 1.1 \times 10^6$	3.1×10^5	≤ 0.27	≥ 11.702
O/UKG/35/01	1.4×10^7	7.3×10^3	1.9×10^3	1.5×10^5	82	20

*Viral concentration of inoculums expressed as plaque forming units per mL (PFU/mL) obtained in BHK cells. †Determination of 50% pig heel infectious doses ($PHID_{50}$/mL) in inoculums after intradermal inoculation in the heel bulb. ‡PFU of virus calculated to be one $PHID_{50}$. §Each pig received values of 10^5 PFU of virus, projected by multiplying the value of PFU/mL by 11.11 µL the estimated volume of inoculums (5 µL × 2 of first dilution plus three more dilutions of a volume of 1/10 of the immediate previous dilution). ‖Determination of $PHID_{50}$ that each animal received, based on volume estimated above. ¶Relative infectivity of each virus compared with porcine infectivity of O/TAW/97. This number indicates how many more viral particles than O/TAW/97 are needed to obtain 1 $PHID_{50}$.

score was equal to or higher than 10 (out of a maximum of 12) and was reached at 2 to 4 dpi. In all O/TAW/97-infected pigs, blood IgM was detected following clearance of detectable virus (a similar result was obtained in all six experiments in all pigs showing detectable viremia regardless of the strain they were inoculated with, Figs. 3-8). After direct contact at 2 dpi with O/TAW/97 direct inoculated pigs for a limited period of 4 h, FMDV readily spread to direct contact animals that also showed a rapid, acute and synchronous disease indistinguishable from directly inoculated animals.

When we studied the various parameters of infection with O/HKN/21/70 (Fig. 4), the direct inoculation of 10^5 PFU (38 $PHID_{50}$, Table 3) produced an acute and synchronous disease in the inoculated animals, similar to O/TAW/97-inoculated pigs. FMDV readily spread to direct contact animals that also displayed a rapid, acute and synchronous disease indistinguishable from directly inoculated animals. In conclusion, independent of previous history of amplification in cells or differences in infectivity, the disease in these 16 animals inoculated with strains from the Cathay topotype was synchronous, acute and severe.

Some PanAsia topotype viruses are as virulent as the Cathay topotype, whereas others are less virulent in pigs

When we studied the various parameters of infection of O/SKR/00 (Fig. 5) or O/UKG/35/01 (Fig. 6), the direct inoculation of 10^5 PFU (47 to 82 $PHID_{50}$, Table 3) produced an acute and synchronous disease in the inoculated animals, indistinguishable from the results obtained in pigs directly inoculated with the Cathay topotypes. However, differences between the Cathay topotype and these two PanAsian strains were found after limited direct contact. Specifically, for both strains, O/SKR/00 or O/UKG/35/01 (Figs. 5 and 6, respectively) one out of four direct contact animals never

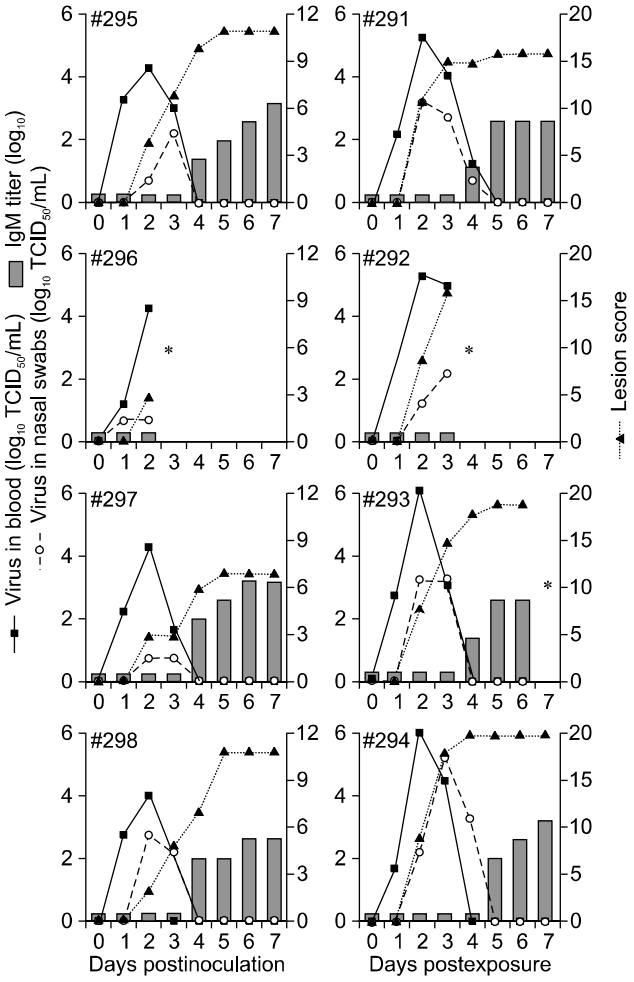

Fig. 4. Viremia, virus in nasal secretions, vesicular lesions and IgM titers in pigs directly inoculated with O/HKN/21/70 (left panels) or exposed to O/HKN/21/70 (right panels). *Indicates the day animals were euthanized to obtain samples for other studies.

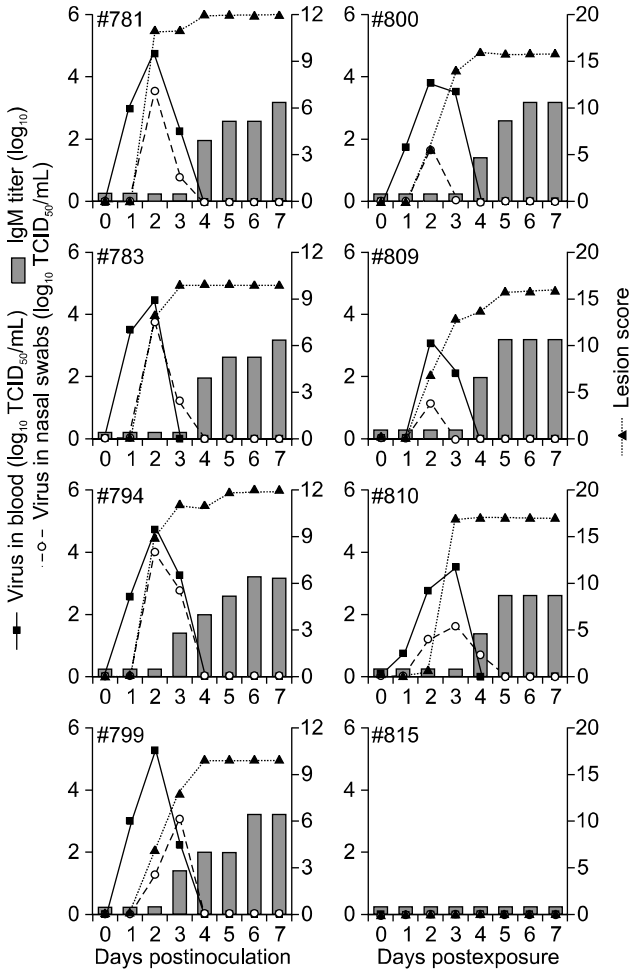

Fig. 5. Viremia, virus in nasal secretions, vesicular lesions and IgM titers in pigs directly inoculated with O/SKR/00 (left panels) or exposed to O/SKR/00 (right panels).

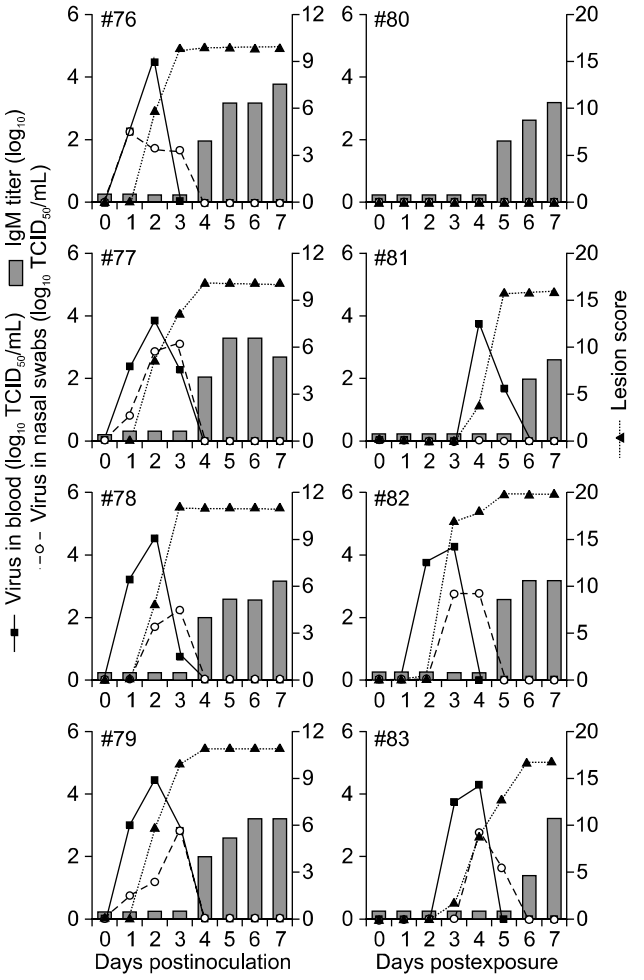

Fig. 6. Viremia, virus in nasal secretions, vesicular lesions and IgM titers in pigs directly inoculated with O/UKG/35/01 (left panels) or exposed to O/UKG/35/01 (right panels).

displayed clinical disease; only subclinical disease was detected by means of detection of IgM antibodies at 5 dpi for pig #80 (Fig. 6) and 13 dpi for pig #815 (results not shown). Additionally, in O/UKG/35/01 direct contact animals, 2 pigs produced a delayed disease (pigs # 81 and 83, Fig. 6).

For the two remaining strains, O/TAW/2/99 and O/SAR/19/00 (Figs. 7 and 8), the various parameters of disease differed drastically from the Cathay topotype. Even though the pigs received a direct inoculation of 10^5 PFU, the $PHID_{50}$ was below 1 for both strains (Table 3). Accordingly, these two strains produced a less acute and less synchronized disease in the inoculated animals when compared to the Cathay topotype. After direct contact FMDV did not readily spread to direct contact animals, probably due to the low shedding of FMDV by the donor animals. In conclusion, disease in animals inoculated with the PanAsia topotype strains was much more heterogeneous than the disease in animals inoculated with the Cathay topotype.

Discussion

Experimental infection of livestock with FMDV can be achieved by a variety of methods. These include contact with infected animals, contact with aerosols produced by infected animals, contact with men who have been in contact with infected animals, and parenteral administration by intradermal, intravenous, intramuscular, and subcutaneous inoculation. Using these methods, virulence can be quantified by evaluating the dose of virus capable of causing disease, severity and kinetics of development of disease, amount of virus present in blood, amount of virus shed by infected animals, and ability of virus to spread to other animals [38]. Taken together, these properties can be used to predict the pathogenic potential of different FMDV isolates.

To learn more about the Cathay topotype of FMDV, we attempted to develop a model for evaluation of transmission by aerosol. These initial experiments showed that O/TAW/97 as well as a South American virus, O1 Campos, were

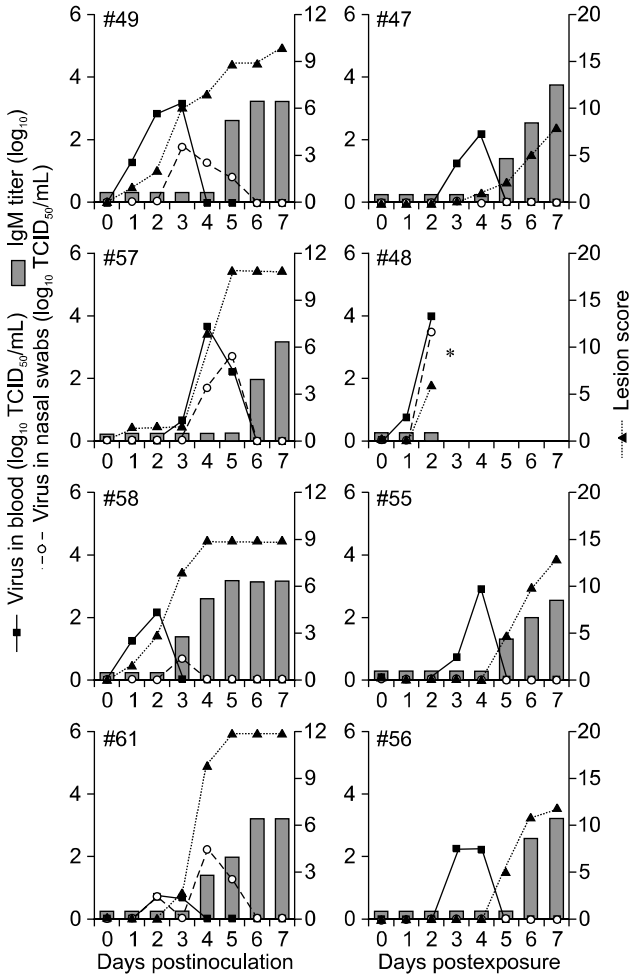

Fig. 7. Viremia, virus in nasal secretions, vesicular lesions and IgM titers in pigs directly inoculated with O/TAW/2/99 (left panels) or exposed to O/TAW/2/99 (right panels). *Indicates the day this animal was euthanized to obtain samples for other studies.

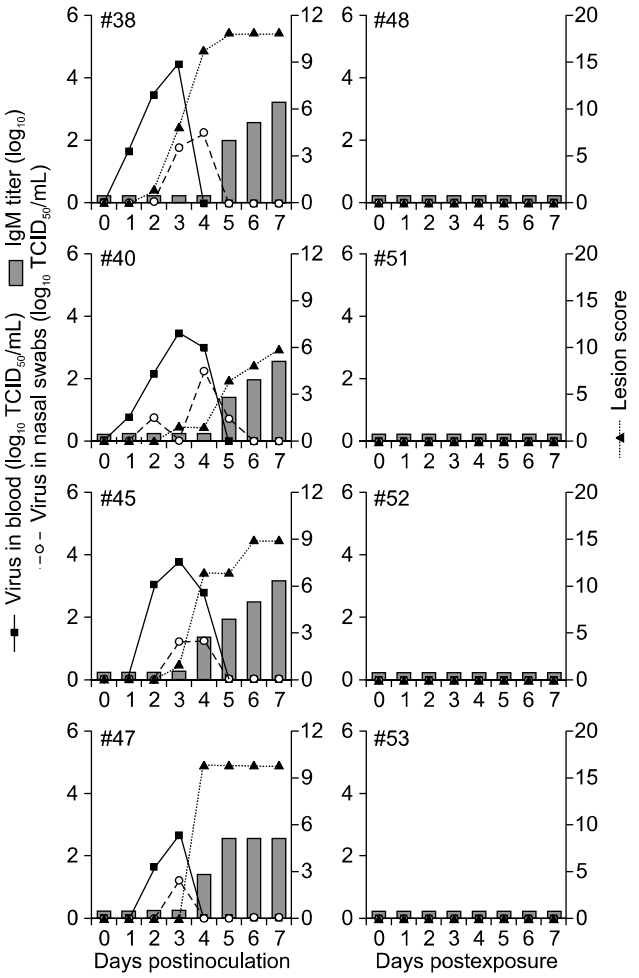

Fig. 8. Viremia, virus in nasal secretions, vesicular lesions and IgM titers in pigs directly inoculated with O/SAR/19/00 (left panels) or exposed to O/SAR/19/00 (right panels).

highly virulent in directly inoculated pigs and were readily transmitted by contact, but clinical disease could not be transmitted to naïve pigs across a 1.3 m gap between open fencing in an animal isolation room. Preliminary experiments demonstrated that 3 of 19 exposed animals displayed a subclinical infection as measured by specific IgM responses to FMDV detected 10 or more days following exposure (results not shown). These results are consistent with the relatively low susceptibility of pigs to infection by the aerosol route, as reviewed by Alexandersen *et al*. [1,2].

Based on these findings, we selected a different experimental design to evaluate virulence and spread of six different FMDV isolates in pigs. First, we started determining the infectivity (PFU/$PHID_{50}$) of each strain by means of inoculating intradermally in the heel bulb [6] with graded dilutions of virus and scored for the appearance of lesions at the inoculation sites 24 h later, to determine the concentration of virus expressed as $PHID_{50}$/ mL of each of the individual isolates. An example of the reproducible nature of the heel-bulb inoculation method in pigs and its usefulness to calculate a $PHID_{50}$/mL value are shown in this study. Second, a quantitative evaluation of disease in all direct-inoculated animals was accomplished using a variety of criteria. These included a quantitative lesion score (based on a daily thorough examination of each animal, which included a close examination of the mouth, nose, feet and all four digits) as well as evaluation of virus titers in the blood, nasal swab samples, and titer of IgM in blood. Third, a direct contact transmission was accomplished for the six strains involved. For this, we selected day 2 post direct inoculation to place four naïve animals for 4 h in close contact with the four injected animals. This time point was chosen based on previous experience with different strains of FMDV serotype O in our lab (results not shown). Quantitative evaluation of disease in contact inoculated animals was accomplished as described for direct inoculated

animals.

The most substantial differences among the strains we have evaluated, namely the ratio of tissue culture infectious doses to animal infectious dose, could be interpreted as resulting from adaptation of some of the strains to grow well in BHK cells, rather than inherent differences in their infectivity in pigs. Although there is some evidence to indicate that that cell lines may not be as sensitive as primary cell systems for assaying animal-derived FMDV [19], we have found that carefully maintained low-passage cultures of BHK cells are just as sensitive as other methods utilized for evaluation of pig-derived strains. Specifically, in our hands, BHK cells (passage 62 ~ 66), IBRS2 cells (passage 117 ~ 122) [8], and FPK cells gave nearly identical titers *in vitro* with all six strains used, including the isolates that had never been in cell culture like O/TAW/97 (results not shown). Another widely used primary cell culture system, BTY cells, has been reported to be more sensitive than other systems [32]. However, this cell type does not support the growth of O/TAW/97 [10], thus, we did not employ BTY cells in our studies. It is also described that BTY and BHK cells were equally sensitive in titrations of PanAsia isolates derived from pig and cow [9]. These small differences, readily explainable in terms of batch-to-batch variation in virus production, emphasize that BHK cells display similar sensitivity to infection by all six strains used in our studies, irrespective of the fact that several of these strains were propagated in cell culture. Thus, based on all of these analyses, it appears certain that the differences we have reported in $PFU/PHID_{50}$ in Table 3 are due to differences in porcine infectivity, and not to differences in tissue culture infectivity of these six FDMV strains.

Using our virulence evaluation systems, we found that the Cathay topotype virus from the 1997 outbreak in Taiwan, which has never been amplified in cells, was highly virulent in swine, producing a synchronous disease in inoculated pigs and efficient spread to direct contact animals. These results are consistent with reports of rapid spread of disease in the 1997 porcine outbreak in Taiwan [39]. Interestingly, the second Cathay virus we examined, O/HKN/21/70, showed similar infectivity, pathogenicity and spread, despite a substantially different passage history (including multiple passages in cell culture at WRL prior to our acquisition.). Additionally, we found that O/HKN/21/70 was not able to replicate at the intradermal lingual inoculation site in a single cow (results not shown) even though it grew well in bovine-derived cells, as described here and previously [21]. Thus, these results suggest that O/TAW/97 does not display any significant new properties *in vivo*; rather, it appears to be similar to a virus isolated almost 30 years earlier. Furthermore, in our hands, animals directly inoculated with other FMDV serotype O strains (O1 Campos and O1 Manisa) in an identical method of inoculation have shown the same pattern of disease as those animals inoculated with the Cathay topotype (results not shown).

The results obtained from the PanAsia topotype viruses showed much more heterogeneity. Two strains in this topotype, O/SKR/00 and O/UKG/35/01, produced a porcine disease pattern similar to the two Cathay topotype viruses in direct inoculated animals and their $PFU/PHID_{50}$ values were similar to O/HKN/21/70. Interestingly, this similar infectivity among the three isolates (O/HKN/21/70, O/SKR/00 and O/UKG/35/01) is independent of the fact that these three viruses have undergone different numbers of cell amplification cycles. However, pigs exposed to O/SKR/00- or O/UKG/35/01-inoculated pigs showed a pattern of disease different from that obtained with the Cathay topotype viruses. Specifically, these PanAsian virus-exposed animals had lower virus titers in blood and nasal secretions, and a delayed appearance of clinical signs. In addition, one pig in each of these two contact exposure groups only displayed evidence of a subclinical infection, without any detectable virus recovered from blood or nasal secretions. The two remaining PanAsia topotype viruses (O/TAW/2/99 and O/SAR/19/00) produced milder disease in directly inoculated animals, consistent with a much lower infectious dose inoculated into these animals (in terms of $PHID_{50}$). In addition, these two strains transmitted very poorly, especially O/SAR/19/00, which failed to produce a clinical disease in any contact exposed pig (one pig, #52 displayed a subclinical disease based on the detection of IgM at 8 dpi, results not shown). This poor transmission is consistent with the fact that on the day of exposure (day 2) we were unable to detect virus in any nasal swab samples obtained from the four SAR/19/00-inoculated animals, and only from one-of-four O/TAW/2/99-inoculated animals. Thus, transmission of these strains cannot be readily compared to the other four strains we tested. Since these last two strains had been amplified extensively in tissue culture under conditions that we cannot readily confirm, we cannot be sure that their dramatically reduced virulence in animals is not due to some type of selection in cell culture, or related to the fact that the virus was isolated from a probang sample, in the case of O/TAW/2/99. A complete sequence analysis of the four PanAsian strains identified here reveals only a small number of differences [26], which are not readily reconcilable with the observed differences in pathogenicity in livestock. The disease patterns induced by PanAsia topotype viruses were much more heterogeneous than those produced by O/TAW/97 and O/HKN/21/70, even though PanAsian viruses are much more closely related to each other [23] than this pair of Cathay topotype viruses [21].

In conclusion, we have described a method to evaluate the pathogenicity and transmission of different FMDV strains that allow us to demonstrate diverse FMD pathogenesis outcomes after direct inoculation of swine. Additionally, differences in FMD pathogenesis were also found after

limited direct contact of naïve pigs with severely sick donor animals. Future projects include development of similar experiments in swine with FMDV strains A24 Cruzeiro and O1 Manisa to be used for FMD challenge and pathogenesis studies, as well as in vaccine efficacy and preventive biotherapeutic trials.

Acknowledgments

We thank Dr. Juan Lubroth, FADDL, PIADC, Greenport, NY, USA for supplying O/TAW/97, O/SKR/00, O/UKG/35/01; Dr. Wilna Vosloo, OVI, Onderstepoort, SAR, for supplying O/SAR/19/00, and Dr. Nick Knowles, WRL, Pirbright, UK for supplying O/HKN/21/70 and O/TAW/2/99. We thank the PIADC Animal Caretakers for assistance with animal experiments. This work was partially supported by the Agricultural Research Service of the USDA (CRIS Project #1940-32000-035-00D) and by a grant from the National Research Initiative Competitive Grants program of USDA/CSREES (Grant #99-35204-7949). We also thank Ms. Melanie Prarat for editing the manuscript.

References

1. **Alexandersen S, Brotherhood I, Donaldson AI.** Natural aerosol transmission of foot-and-mouth disease virus to pigs: minimal infectious dose for strain O1 Lausanne. Epidemiol Infect 2002, **128**, 301-312.
2. **Alexandersen S, Donaldson AI.** Further studies to quantify the dose of natural aerosols of foot-and-mouth disease virus for pigs. Epidemiol Infect 2002, **128**, 313-323.
3. **Alexandersen S, Zhang Z, Donaldson AI, Garland AJ.** The pathogenesis and diagnosis of foot-and-mouth disease. J Comp Pathol 2003, **129**, 1-36.
4. **Almeida MR, Rieder E, Chinsangaram J, Ward G, Beard C, Grubman MJ, Mason PW.** Construction and evaluation of an attenuated vaccine for foot-and-mouth disease: difficulty adapting the leader proteinase-deleted strategy to the serotype O1 virus. Virus Res 1998, **55**, 49-60.
5. **Beard CW, Mason PW.** Genetic determinants of altered virulence of Taiwanese foot-and-mouth disease virus. J Virol 2000, **74**, 987-991.
6. **Burrows R.** The infectivity assay of foot-and-mouth disease virus in pigs. J Hyg (Lond) 1966, **64**, 419-429.
7. **Chen X, Feng Q, Wu Z, Liu Y, Huang K, Shi R, Chen S, Lu W, Ding M, Collins RA, Fung YW, Lau LT, Yu AC, Chen J.** RNA-dependent RNA polymerase gene sequence from foot-and-mouth disease virus in Hong Kong. Biochem Biophys Res Commun 2003, **308**, 899-905.
8. **de Castro MP.** Behaviour of the foot-and-mouth disease virus in cell cultures: Susceptibility of the IB-RS-2 cell line. Arq Inst Biol (Sao Paulo) 1964, **31**, 63-78.
9. **Donaldson AI, Sellers RF.** Transmission of FMD by people. Vet Rec 2003, **153**, 279-280.
10. **Dunn CS, Donaldson AI.** Natural adaption to pigs of a Taiwanese isolate of foot-and-mouth disease virus. Vet Rec 1997, **141**, 174-175.
11. **Feng Q, Chen X, Ma O, Liu Y, Ding M, Collins RA, Ko LS, Xing J, Lau LT, Yu AC, Chen J.** Serotype and VP1 gene sequence of a foot-and-mouth disease virus from Hong Kong (2002). Biochem Biophys Res Commun 2003, **302**, 715-721.
12. **Ferguson NM, Donnelly CA, Anderson RM.** Transmission intensity and impact of control policies on the foot and mouth epidemic in Great Britain. Nature 2001, **413**, 542-548.
13. **Freshney RI.** Culture of Animal Cells: A Manual of Basic Technique. p. 144, Liss, New York, 1987.
14. **George VG, Hierholzer JC, Ades EW.** Cell culture. In: Mahy BWJ, Kangro HO (eds.). Virology Methods Manual. pp. 3-23, Academic Press, London, 1996.
15. **Gulbahar MY, Davis WC, Guvenc T, Yarim M, Parlak U, Kabak YB.** Myocarditis associated with foot-and-mouth disease virus type O in lambs. Vet Pathol 2007, **44**, 589-599.
16. **Henderson WM.** The Quantitative Study of Foot-and-Mouth Disease Virus. Report Series of Agricultural Research Council. No. 8. pp. 1-50, Her Majesty's Stationery Office, London, 1949.
17. **Henderson WM.** A comparison of different routes of inoculation of cattle for detection of the virus of foot-and-mouth disease. J Hyg (Lond) 1952, **50**, 182-194.
18. **Hierholzer JC, Killington RA.** Virus isolation and quantitation. In: Mahy BW, Kangro HO (eds.). Virology Methods Manual. pp. 25-46, Academic Press, London, 1996.
19. **House C, House JA.** Evaluation of techniques to demonstrate foot-and-mouth disease virus in bovine tongue epithelium: comparison of the sensitivity of cattle, mice, primary cell cultures, cryopreserved cell cultures and established cell lines. Vet Microbiol 1989, **20**, 99-109.
20. **Huang CC, Lin YL, Huang TS, Tu WJ, Lee SH, Jong MH, Lin SY.** Molecular characterization of foot-and-mouth disease virus isolated from ruminants in Taiwan in 1999-2000. Vet Microbiol 2001, **81**, 193-205.
21. **Knowles NJ, Davies PR, Henry T, O'Donnell V, Pacheco JM, Mason PW.** Emergence in Asia of foot-and-mouth disease viruses with altered host range: characterization of alterations in the 3A protein. J Virol 2001, **75**, 1551-1556.
22. **Knowles NJ, Samuel AR.** Molecular epidemiology of foot-and-mouth disease virus. Virus Res 2003, **91**, 65-80.
23. **Knowles NJ, Samuel AR, Davies PR, Kitching RP, Donaldson AI.** Outbreak of foot-and-mouth disease virus serotype O in the UK caused by a pandemic strain. Vet Rec 2001, **148**, 258-259.
24. **Knowles NJ, Samuel AR, Davies PR, Midgley RJ, Valarcher JF.** Pandemic strain of foot-and-mouth disease virus serotype O. Emerg Infect Dis 2005, **11**, 1887-1893.
25. **Malirat V, de Barros JJ, Bergmann IE, Campos Rde M, Neitzert E, da Costa EV, da Silva EE, Falczuk AJ, Pinheiro DS, de Vergara N, Cirvera JL, Maradei E, Di Landro R.** Phylogenetic analysis of foot-and-mouth disease virus type O re-emerging in free areas of South America. Virus Res 2007, **124**, 22-28.
26. **Mason PW, Pacheco JM, Zhao QZ, Knowles NJ.** Comparisons of the complete genomes of Asian, African and European isolates of a recent foot-and-mouth disease virus type O pandemic strain (PanAsia). J Gen Virol 2003, **84**, 1583-1593.
27. **Mattion N, König G, Seki C, Smitsaart E, Maradei E, Robiolo B, Duffy S, León E, Piccone M, Sadir A, Bottini**

R, Cosentino B, Falczuk A, Maresca R, Periolo O, Bellinzoni R, Espinoza A, Torre JL, Palma EL. Reintroduction of foot-and-mouth disease in Argentina: characterisation of the isolates and development of tools for the control and eradication of the disease. Vaccine 2004, **22**, 4149-4162.

28. **Mingqiu Z, Qingli S, Jinding C, Lijun C, Yanfang X.** Sequence analysis of the protein-coding regions of foot-and-mouth disease virus O/HK/2001. Vet Microbiol 2008, **130**, 238-246.
29. **O'Donnell VK, Pacheco JM, Henry TM, Mason PW.** Subcellular distribution of the foot-and-mouth disease virus 3A protein in cells infected with viruses encoding wild-type and bovine-attenuated forms of 3A. Virology 2001, **287**, 151-162.
30. **Oem JK, Lee KN, Cho IS, Kye SJ, Park JH, Joo YS.** Comparison and analysis of the complete nucleotide sequence of foot-and-mouth disease viruses from animals in Korea and other PanAsia strains. Virus Genes 2004, **29**, 63-71.
31. **Oem JK, Lee KN, Cho IS, Kye SJ, Park JY, Park JH, Kim YJ, Joo YS, Song HJ.** Identification and antigenic site analysis of foot-and-mouth disease virus from pigs and cattle in Korea. J Vet Sci 2005, **6**, 117-124.
32. **OIE.** Manual of Standards for Diagnostic Tests and Vaccines. Chapter 2.1.1. Foot and Mouth Disease. pp. 77-92, OIE, Paris, 2000.
33. **Pacheco JM, Henry TM, O'Donnell VK, Gregory JB, Mason PW.** Role of nonstructural proteins 3A and 3B in host range and pathogenicity of foot-and-mouth disease virus. J Virol 2003, **77**, 13017-13027.
34. **Reed LJ, Muench H.** A simple method of estimating fifty percent endpoints. Am J Hyg 1938, **27**, 493-497.
35. **Sa-Carvalho D, Rieder E, Baxt B, Rodarte R, Tanuri A, Mason PW.** Tissue culture adaptation of foot-and-mouth disease virus selects viruses that bind to heparin and are attenuated in cattle. J Virol 1997, **71**, 5115-5123.
36. **Sakamoto K, Kanno T, Yamakawa M, Yoshida K, Yamazoe R, Murakami Y.** Isolation of foot-and-mouth disease virus from Japanese black cattle in Miyazaki Prefecture, Japan, 2000. J Vet Med Sci 2002, **64**, 91-94.
37. **Samuel AR, Knowles NJ.** Foot-and-mouth disease type O viruses exhibit genetically and geographically distinct evolutionary lineages (topotypes). J Gen Virol 2001, **82**, 609-621.
38. **Sellers RF.** Quantitative aspects of the spread of foot and mouth disease. Vet Bull 1971, **41**, 431-439.
39. **Yang PC, Chu RM, Chung WB, Sung HT.** Epidemiological characteristics and financial costs of the 1997 foot-and-mouth disease epidemic in Taiwan. Vet Rec 1999, **145**, 731-734.

Return to Table of Contents

Virus Research xxx (2010) xxx–xxx

Contents lists available at ScienceDirect

Virus Research

journal homepage: www.elsevier.com/locate/virusres

Introduction of tag epitopes in the inter-AUG region of foot and mouth disease virus: Effect on the L protein

Maria E. Piccone[a,b,*], Fayna Diaz-San Segundo[a,c], Edward Kramer[a], Luis L. Rodriguez[a], Teresa de los Santos[a]

[a] Plum Island Animal Disease Center, ARS, USDA, Greenport, NY, United States
[b] Department of Pathobiology and Veterinary Science, University of Connecticut, Storrs, CT, United States
[c] Oak Ridge Institute for Science and Education, PIADC Research Program, Oak Ridge, TN, United States

ARTICLE INFO

Article history:
Received 7 July 2010
Received in revised form 1 September 2010
Accepted 7 September 2010
Available online xxx

Keywords:
Foot-and-mouth disease
Viral translation
Leader protein

ABSTRACT

Foot-and-mouth disease virus (FMDV) initiates translation from two in-frame AUG codons producing two forms of the leader (L) proteinase, Lab (starting at the first AUG) and Lb (starting at second AUG). In a previous study, we have demonstrated that a cDNA-derived mutant FMDV (A24-L1123) containing a 57-nucleotide transposon (tn) insertion between the two AUG initiation codons (inter-AUG region) was completely attenuated in cattle, suggesting that this region is involved in viral pathogenesis. To investigate the potential role of the Lab protein in attenuation, we have introduced two epitope tags (Flag: DYKDDDK and HA: YPYDVPDYA) or a small tetracysteine motif (tc: CCGPCC) into the pA24-L1123 infectious DNA clone. Mutant viruses with a small plaque phenotype similar to the parental A24-L1123 were recovered after transfection of constructs encoding the Flag tag and the tc motif. However, expression of the Flag- or tc-tagged Lab protein was abolished or greatly diminished in these viruses. Interestingly, the A24-L1123/Flag virus acquired an extra base in the inter-AUG region that resulted in new AUG codons in-frame with the second AUG, and produced a larger Lb protein. This N terminal extension of the Lb protein in mutant A24-L1123/Flag did not affect virus viability or L functions in cell culture.

1. Introduction

Foot-and-mouth disease virus (FMDV) belongs to the genus *Aphthovirus* of the family *Picornaviridae* and exists as seven distinct serotypes throughout the world. The FMDV genome is a single-stranded RNA molecule of approximately 8500 nucleotides (nt) and translates as a large polyprotein which is processed to yield three viral precursors, P1-2A, P2 and P3, by autoproteolytic cleavage (Grubman and Baxt, 2004). At the amino terminus of the viral polyprotein is the leader (L) protein of 199–202 amino acids, depending on the viral serotype (Carrillo et al., 2005; van Rensburg et al., 2002). L is a papain-like proteinase that removes itself from the viral polyprotein (Kleina and Grubman, 1992; Piccone et al., 1995b; Roberts and Belsham, 1995) and also cleaves the eukaryotic translation initiation factor 4G (eIF4G), resulting in the shutoff of the cap-dependent host protein synthesis, without affecting cap-independent viral protein synthesis (Devaney et al., 1988; Kirchweger et al., 1994). In addition, L plays a role in FMDV virulence by regulating the host innate immune responses (Chinsangaram et al., 1999; de los Santos et al., 2006, 2007, 2009).

The leader protein is produced in two forms, Lab and Lb, through the initiation of translation at two in-frame AUG codons located 84 nt apart (inter-AUG region). These two AUG codons have been shown to be present in viruses of all seven serotypes (Carrillo et al., 2005; Sangar et al., 1987). The smaller protein (Lb) is initiated from the second functional AUG and is synthesized in excess with respect to Lab despite its downstream location, both in *in vitro* translation reactions and in infected cells (Clarke et al., 1985; Sangar et al., 1987). Previous investigations have shown that the relative use of each initiation site is dependent on its surrounding nucleotide sequence and the RNA structure upstream and downstream of the initiation AUG (Belsham, 1992; Lopez de Quinto and Martinez-Salas, 1998; Ohlmann and Jackson, 1999). In addition, it has been demonstrated that the presence of the second AUG initiation codon, but not the first one, is essential for virus replication (Cao et al., 1995). Both forms of the L protein possess similar proteolytic activities (Medina et al., 1993; Strebel et al., 1986), and therefore it is not known why the two forms of L are synthesized during the FMDV infection. Notably, the L protein exhibits

Abbreviations: FMDV, foot-and-mouth disease virus; L, leader protein; HA, influenza-hemagglutinin; tc, tetracysteine motif; NCR, non coding region; SAT, South African territories.

* Corresponding author at: Plum Island Animal Disease Center, P.O. Box 848, Greenport, NY 11944-0848, United States. Tel.: +1 631 323 3102, fax: +1 631 323 3006.
E-mail address: maria.piccone@ars.usda.gov (M.E. Piccone).

0168-1702/$ – see front matter © 2010 Elsevier B.V. All rights reserved.
doi:10.1016/j.virusres.2010.09.004

variability comparable to that of the structural proteins, the most variable being the inter-AUG region (Tosh et al., 2004; van Rensburg et al., 2002).

We have recently shown that the inter-AUG region can tolerate insertions of heterologous sequences. Importantly, mutant viruses carrying a 57 nt transposon (tn) insertion within that region replicated more slowly than the wild type (WT) virus, and were highly attenuated in bovines (Piccone et al., 2010). The tn insertion did not interrupt the polyprotein reading-frame of these viruses, but the amino acid composition of the N terminus of the L protein was profoundly altered. It is possible that these changes accounted for the attenuation phenotype.

To date, no studies have been reported addressing the individual role of each form of L in virus replication and pathogenesis. With the aim of differentiating the individual forms of L, we have introduced two "epitope tags" (HA and Flag) and a small tetracysteine (tc) motif in the inter-AUG region of a tn-containing virus. The HA and Flag tags are particularly useful for immunoreactive experiments. On the other hand, the tc motif has been very valuable in visualizing many dynamic processes in living cells (Arhel and Charneau, 2009; Das et al., 2009; Perlman and Resh, 2006; Rudner et al., 2005), and could allow visualization of Lab within infected cells by fluorescence microscopy. Here, we report the characterization of the recovered L-mutant viruses and the effect of the tags on L functions. We discuss these results with respect to the mechanism of attenuation of the previously reported tn containing mutant viruses.

2. Materials and methods

2.1. Cells, plasmid constructs and mutant viruses

BHK-21 αVβ6 cells (Duque et al., 2004) were used to propagate virus and BHK-21, bovine kidney cell line (LF-BK) (Swaney, 1988) and secondary lamb kidney (LK) cells (House and House, 1989) were used for titration, *in vitro* growth and plaque assays. Flag (DYKDDDK), influenza-hemagglutinin (HA) (YPYDVPDYA), or a small tetracysteine motif (tc) (CCPCC) tags were introduced at the unique NotI restriction site of previously constructed mutant plasmid pA24-L1123. This plasmid derives from the infectious clone pA24-WT and contains a 57 nt transposon (tn) insertion in the inter-AUG region (Piccone et al., 2010). Briefly, pA24-L1123 was used as template in a PCR amplification using synthetic oligos: (sense) 5′-CACTTTATTGCGGCCGCA**GACTAT AAGGACGATGATGACAAG**AGATGTGTACAAGAGACAGCTATC-3′ (Flag, bold case); 5′-CACTTTATTGCGGCCGCA**TACCCATACGATGTTCCAGATTACGCT**AGATGTGTACAAGAGACAGCTATC-3′ (HA, bold case) or 5′-CACTTTATTGCGGCCGCA**TGTTGTGGCCCTTGTTGT**AGATGTGTACAAGAGAC-3′ (tc, bold case) and antisense oligo nt 2924—5′-CTTTGAATCAGTGGAACCTG-3′ on the unique SpeI site of the pA24-WT plasmid. The PCR products were digested with NotI and SpeI and cloned between the NotI and SpeI sites of pA24-L1123. All the tagged mutant plasmids were sequenced to confirm the presence of the tag using an Applied Biosystems 3730 xl automated DNA sequencer (Applied Biosystems, Foster City, CA).

RNA derived from pA24-WT and pA24-L tag mutants were transfected into BHK-21 cells by electroporation as described previously (Mason et al., 1994). Viruses recovered from these transfections were passed three times in BHK-21 αVβ6 and virus stocks were prepared and sequenced.

2.2. In vitro transcription and translations assays

To generate RNA for translation assays, L mutant plasmids and parental pA24-WT were linearized with SpeI, and plasmid pL (encoding the L gene containing both AUGs) with BamHI. Transcription was performed using the MegaScript T7 kit (Ambion, Austin, TX) as recommended by the manufacturer. For the transcription of the pL control, the reactions were performed in the presence of the cap analog [m7G(5′)ppp(5′)G].

In vitro translation assays were carried out using rabbit reticulocyte lysate (Promega, Fitchburg, WI) as described by Piccone et al. (2010). Translation products were separated by gradient 10–20% SDS-PAGE and detected by autoradiography.

2.3. Analysis of growth of L tagged FMD mutant viruses

Mutant viruses were characterized by plaque assays in BHK-21, LK (House and House, 1989) and LF-BK cells (Swaney, 1988). Plaques were visualized under a gum tragacanth overlay stained at 48 h post-infection (hpi). One-step growth curves were performed in LF-BK cells. Briefly, cells were infected at a multiplicity of infection (MOI) of 10 at 37 °C. After 1 h adsorption, cells were rinsed with 150 mM NaCl 20 mM morpholineethanesulfonic acid (MES) pH 6 to inactivate unadsorbed virus and incubated at 37 °C. At 4, 8 and 24 hpi, cells were harvested and virus titrated on BHK-21 cells as described previously (Piccone et al., 1995a).

2.4. Western blot analysis

Cell lysates from infected LF-BK cells were prepared and fractioned on a 12% SDS-PAGE. Proteins were transferred to PVDF membranes and probed with rabbit polyclonal anti-leader and anti-p220 antibodies (kindly provided by Dr. Grubman), anti-NF-κB-p65/RelA (Ab-1 RB-1638, NeoMarkers, Lab Vision, Freemont, CA), anti-VP1 (6HC4 (Baxt et al., 1984)), and anti-tubulin-α (Ab-2 MS-581 Clone DM1A, NeoMarkers, Lab Vision). For detection, an Immun-Star™ HRP chemiluminescent kit (Biorad, Hercules, CA) was used following the manufacturer's directions.

2.5. Immunofluorescence microscopy

Viral proteins were detected in infected cell cultures by indirect immunofluorescence microscopy as described previously by de los Santos et al. (2007). Briefly, LF-BK cells grown on glass coverslips were infected with A24-WT or L tagged mutant viruses at MOI 10. At different hpi, cells were fixed in 4% paraformaldehyde, permeabilized with 0.5% Triton X-100® (Sigma) in PBS, blocked with blocking buffer (PBS, 2% bovine serum albumin [BSA], 5% normal goat serum, 10 mM glycine) and immunostained using antibodies against leader (rabbit polyclonal) or structural protein VP1 (6HC4 (Baxt et al., 1984)). Alexa Fluor 488 and Alexa Fluor 594 (Molecular Probes, Invitrogen, Carlsbad, CA) conjugated secondary antibodies were used for detection. Nuclei were visualized by DAPI staining included in ProLong Gold Antifade mounting media (Invitrogen). Cells were examined in an Olympus BX40 fluorescence microscope and pictures were taken with DP-70 digital camera/DP-BSW v2.2 software (Olympus America, Central Valley, PA).

3. Results

3.1. Generation and characterization of L tagged FMD mutant viruses

In the absence of reagents that allow differentiating between the Lab and Lb proteins, we introduced a tag sequence in the inter-AUG region of a previously constructed mutant plasmid pA24-L1123 (Piccone et al., 2010). As shown in Fig. 1A, three different tag sequences (Flag, HA and tc) were inserted into the unique NotI site contained in the tn insertion of pA24-L1123.

Please cite this article in press as: Piccone, M.E., et al., Introduction of tag epitopes in the inter-AUG region of foot and mouth disease virus: Effect on the L protein. Virus Res. (2010), doi:10.1016/j.virusres.2010.09.004

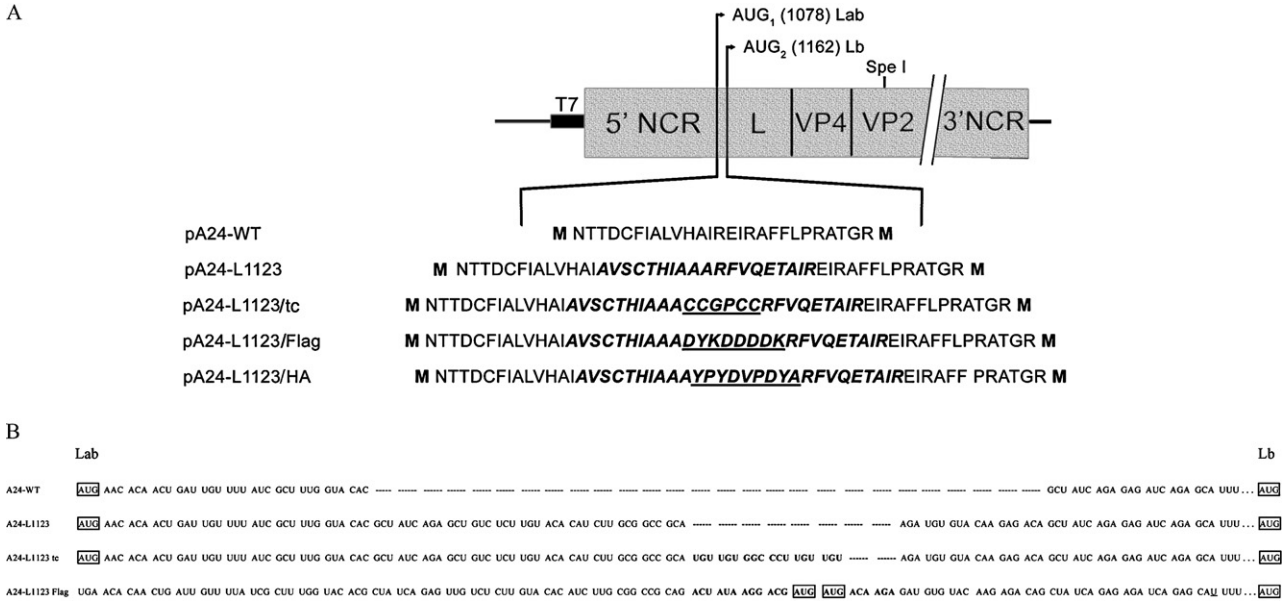

Fig. 1. (A) Schematic diagram of the FMDV genome and plasmids used in this study. The FMDV full-length genome cDNAs in these plasmids derived from the infectious cDNA clone, pA24-WT, were preceded by a synthetic T7 RNA polymerase promoter. The AUG codons at positions 1078 and 1162, corresponding to the two initiation sites of FMDV type A24 (accession number AY593768) are shown. Mutant plasmid pA24-L1123 was produced by transposon (tn) insertion mutagenesis of pA24-WT and contains an insertion of 19 amino acids indicated in italic and bold at position 1123. Leader-tag proteins were constructed by inserting various tag sequences in the NotI restriction site present in the tn insertion of pA24-L1123. Amino acid sequences of the tag are underlined. Unique SpeI restriction site is indicated. NCR: non-coding region. (B) Nucleotide sequence analysis of the L-tagged virus recovered. Alignment of partial sequences of the region located between the first and the second AUG initiation codons of A24-WT and L mutant viruses. AUG initiation codons corresponding to Lab, Lb as well as potential initiation sites in the A24-L1123/Flag mutant are boxed. The nucleotide sequence of each tag is indicated in bold. The position of the extra U is underlined. (–) indicates an absent sequence.

Viable viruses were obtained from cells transfected with RNA derived from the constructs containing the Flag and the tc tag after BHK-21 αVβ6 cell passages. Mutant virus A24-L1123/Flag showed a cytophatic effect (CPE) after three passages, whereas mutant A24-L1123/tc showed an extensive CPE at 24 hpi in passage 2. In contrast, we were not able to recover viruses from the HA tagged constructs even after several attempts, probably indicating that the nucleotide sequence (or derived amino acid sequence) of the HA tag was not compatible with the generation of viable virus. Sequence analysis of the rescued viruses revealed the presence of the expected tag sequence for the A24-L1123/tc mutant, while the A24-L1123/Flag mutant contained an extra base in the Flag insertion. Due to this insertion, the second AUG was out-of-frame with respect to the first AUG codon, but two new adjacent AUG codons in-frame with the second AUG codon appeared at positions −78 and −75 (Fig. 1B).

We then examined the mutant viruses by their plaque sizes and growth characteristic in cell cultures. Side-by-side comparison of plaques in BHK-21, LF-BK and LK cells showed that both A24 L tag mutant viruses formed plaques smaller than those formed by WT virus, but similar to those of attenuated mutant virus A24-L1123 (Piccone et al., 2010) (Fig. 2A). A single-step growth kinetics in LF-BK cells revealed no significant differences between the viruses, although the overall yields of the L mutant viruses were lower than for A24-WT (Fig. 2B).

3.2. Effect of the tags in self-processing of L

To test the ability of the tagged L proteins to self remove from its precursors, pA24-WT and pA24-L mutant plasmids were digested with SpeI, which cleaves within the structural protein VP2 (position 2512) and removes the downstream portion of the viral genome from the plasmids allowing a clearer interpretation of the viral protein pattern in the SDS-PAGE. T7 RNA transcripts of SpeI-digested pA24-WT, pA24-L1123 and pA24-L tag mutants, as well as transcript of control plasmid pL, were translated *in vitro* in rabbit reticulocyte lysates. Fig. 3 shows that all synthesized L mutant proteins were able to cleave themselves from the precursor L-Vp4-Vp2′ and that the Lb band was absent in all L mutant translation reactions. We were surprised to find several bands present in the mutant translation products, since no other viral proteins of similar size were expected. Moreover, all these products were immunoprecipitated by an anti-L antiserum (data not shown). It should be noted that proteins synthesized in a rabbit reticulocyte lysate do not necessarily reflect the viral proteins produced during an infection in cell culture or *in vivo*.

With the exception of pA24-L1123/Flag, all mutant translation mixes showed a profile similar to that of the parental pA24-L1123, including a band that was also present in the WT translation mix. A unique larger L product was observed in the Flag-tagged L plasmid, consistent with initiation of translation at the first AUG and containing the Flag tag (lane 4). However, this protein was not immunoprecipitated by an anti-Flag antiserum (data not shown), suggesting that initiation occurred at an alternative initiation codon contained within the insertion and disrupting the proper Flag amino acid composition. Similarly, translation products derived from pA24-L1123/HA showed a faint higher molecular weight band.

These results indicate that the presence of the tn insertion in these mutant L plasmids forces translation initiation *in vitro* from other than the second AUG codon since no Lb was detected.

3.3. Expression of functional tagged L proteins in infected cells

The WT and mutant L proteins expressed in LF-BK cells were detected by western blotting analysis using a rabbit polyclonal anti-leader antibody (Fig. 4). Because the L mutant viruses showed different growth rates as compared to the WT virus in these cells (see Fig. 2B), we used higher multiplicities of infection in order to have comparable amounts of protein.

Please cite this article in press as: Piccone, M.E., et al., Introduction of tag epitopes in the inter-AUG region of foot and mouth disease virus: Effect on the L protein. Virus Res. (2010), doi:10.1016/j.virusres.2010.09.004

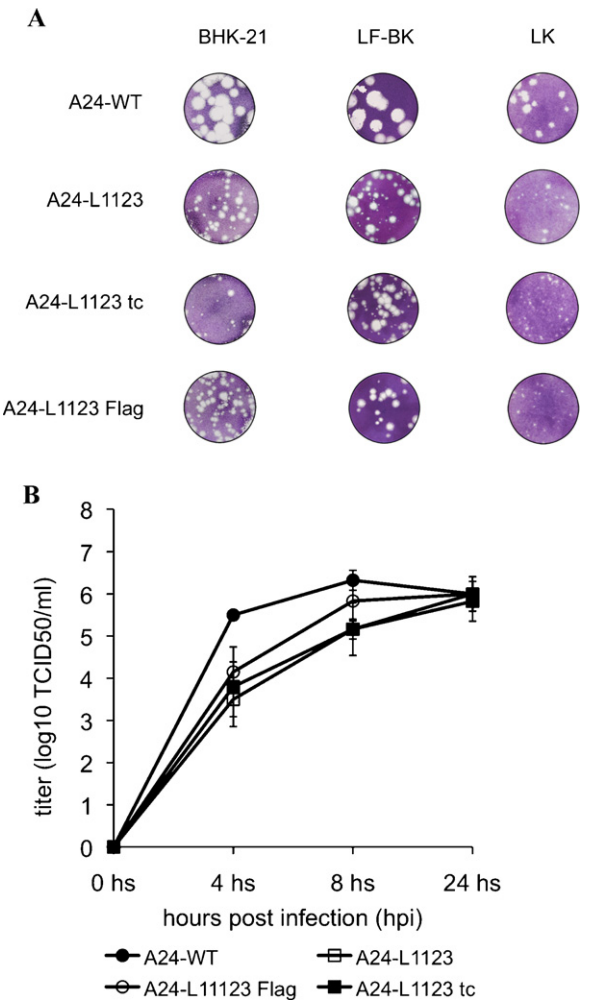

Fig. 2. (A) Plaque morphology of A24-WT and A24-L mutant viruses in different cells. Viruses were plaque-assayed under tragacanth gum on BHK-21, LF-BK and LK cells and cells were stained at 48 h post-infection (hpi). Plaques from appropriate dilutions are shown. (B) Growth of FMDV L-mutants in cell culture. LF-BK cells were infected with WT or L-mutant viruses at a multiplicity of infection (MOI) of 10. At 0, 4, 8 and 24 hpi, cells and supernatants were harvested and the viral titers were determined by TCID50/ml on BHK-21 cells. The error bars indicate the standard deviation. The values of the viral titer represent the average obtained from triplicate experiments.

Results revealed that mutant viruses A24-L1123 and A24-L1123/tc produced mainly Lb protein (lanes 2 and 3 respectively), indicating that the insertions did not interfere with initiation from the second AUG codon. For A24-WT, a band of higher molecular weight was detected, suggesting translation initiation from the first AUG (Lab). Minor bands of slower mobility were also observed for the L mutant viruses, suggesting that L proteins were translated from the first AUG and contained the amino acid sequences encoded by the tn and the tc motif. However, the nature and the origin of the product of intermediate size in the A24-L1123/tc lane was unclear, since – based on their apparent size – there were no AUG codons between the tc tag and the second AUG codon. Interestingly, A24-L1123/Flag virus (lane 4) showed an L protein slightly bigger than Lb, consistent with initiation of translation from a new AUG acquired in the inter-AUG region during viral growth, as shown in Fig. 1B.

We have previously demonstrated that Lb translocates to the nucleus of infected cells and regulates the activity of transcription nuclear factor NFκB (de los Santos et al., 2007). To investigate if viruses expressing the extended L protein are able of processing cellular proteins in a manner similar to that of the WT virus, we examined the pattern of NFκB protein in infected cell extracts. Western blot analysis showed that the p65 subunit of NFκB disappeared during the infection by either WT or L mutant viruses (Fig. 5).

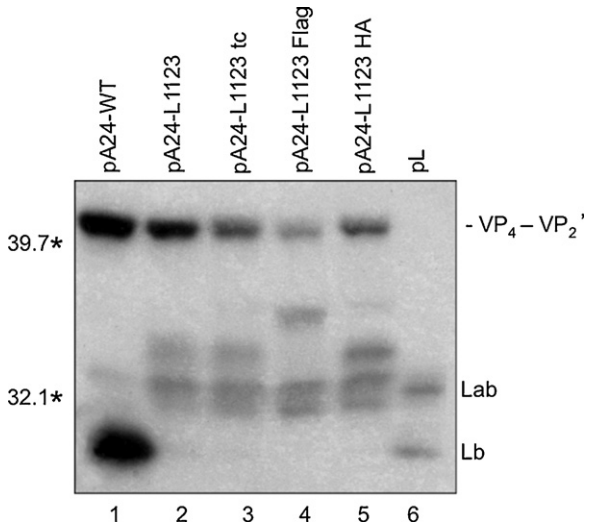

Fig. 3. *In vitro* translation products of WT and L-mutant plasmid RNA transcripts. Transcripts derived from plasmids pA24-WT (lane 1) and pA24-L mutants (lanes 2–5) linearized by restriction enzyme SpeI were used to program protein synthesis in rabbit reticulocyte lysates. The (^{35}S) methionine-labeled proteins were analyzed by SDS-PAGE (10–20% acrylamide gradient) and autoradiography. Lane 6 shows translation products of transcripts derived from a plasmid (pL) encoding for the L gene and containing both AUG initiation codons under the control of a T7 RNA polymerase promoter. Molecular weight markers and cleavage products are indicated on the left and right of the panel respectively.

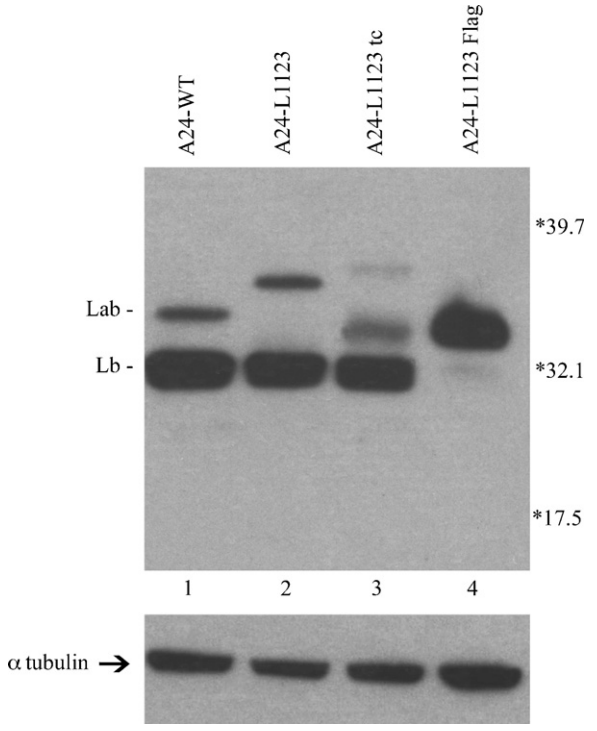

Fig. 4. Expression of the leader protein in LF-BK cells infected with L-mutant viruses. LF-BK cells were infected with wild-type virus A24-WT (lane 1) and the L-mutant viruses (lanes 2–4) at low MOI (0.0001 and 0.01 respectively) and cytoplasmic cell extracts were prepared after 24 hpi. Equal amounts of cell extracts were separated by 12% SDS-PAGE, blotted, and probed with a rabbit polyclonal anti-leader antibody (top) or mouse monoclonal anti-tubulin antibody as a loading control (bottom). Protein size markers (kDa) are indicated on the right.

Please cite this article in press as: Piccone, M.E., et al., Introduction of tag epitopes in the inter-AUG region of foot and mouth disease virus: Effect on the L protein. Virus Res. (2010), doi:10.1016/j.virusres.2010.09.004

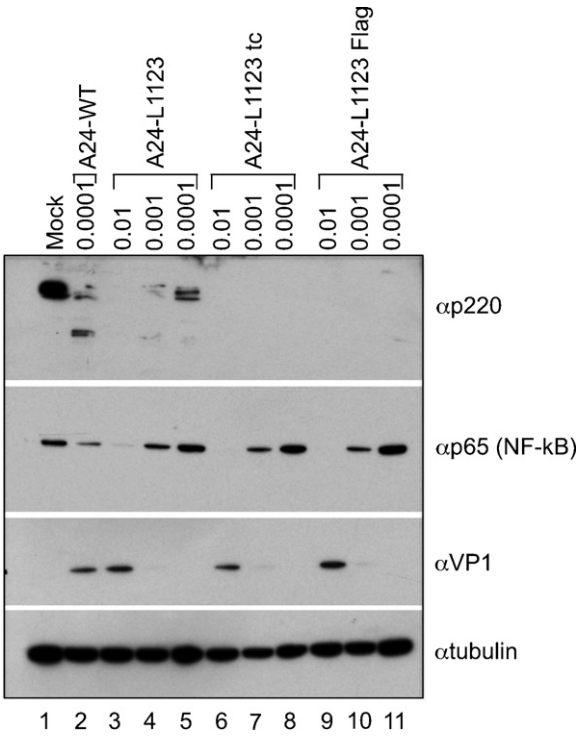

Fig. 5. Processing of cellular proteins during infection with WT and L-mutant viruses. LF-BK cells were infected with A24-WT (lane 2) and L-mutant viruses at the indicated MOIs (lanes 3–11). At 24 hpi, cytoplasmic cell extracts were prepared and analyzed by western blotting using anti-p220, anti-NFκB, anti-VP1 and anti-tubulin antibodies.

Similarly, cleavage of the translation factor eIF-4G (p220) was basically complete when comparable amounts of structural protein VP1 were present in the cell lysates (Fig. 5). These results are in agreement with those reported by Strebel et al. (1986) indicating that the proteolytic function of L is not affected by an N extension of the protein.

Finally, we explored the sub-cellular localization of L mutant viruses by immunofluorescence analysis in LF-BK infected cells (Fig. 6). Very early during infection (2 hpi), there was an L positive signal in WT virus infected cells when no VP1 signal could still be detected. By 3 hpi, the L signal was mainly localized to the nuclei of infected cells, while VP1 was detected in the cytoplasm; thereafter the L signal was detected throughout the whole cell, as previously described for FMDV type A12 (de los Santos et al., 2007, 2009). The pattern of L sub-cellular localization of the L mutant viruses was similar to the WT virus, except for a delay in the cytoplasmic L protein signal. These results demonstrated that the extended Lb protein in mutant A24-L1123/Flag did not affect the functions or cellular localization of L in cell culture.

4. Discussion

The FMDV leader proteinase exists in two forms, termed Lab and Lb, which exhibit similar proteolytic activities (Cao et al., 1995; Medina et al., 1993; Strebel et al., 1986). This conclusion is based on *in vitro* studies that used plasmids expressing each individual form of L. However, it remains unknown whether each form of L plays a distinctive role in viral replication and pathogenesis. Because Lab and Lb only differ at their amino terminus, a polyclonal anti-L antiserum cannot differentiate between them. Moreover, the hydrophobic character of this region makes difficult to generate a specific antiserum against it. Therefore in this study, we introduced a tag (HA, Flag or tc) in a mutant virus (A24-L1123) that already contains a tn insertion of 57 nt extras in the inter-AUG region and analyzed the functions of the resulting tagged Lab protein on viral translation and replication.

In vitro translation assays showed that the processing of L was unaffected by the presence of the N-terminal tags, however we only recovered infectious A24-L1123/Flag and A24-L1123/tc mutant viruses. These mutant viruses showed small plaque phenotype compared to the WT virus in cell cultures similarly to the parental mutant virus A24-L1123. However, we could not detect the expression of the flag or tc tags in the recovered mutant viruses. Interestingly, mutant virus A24-L1123/Flag acquired an extra base in the inter-AUG region that resulted in new AUG codons in-frame with the second AUG codon. This mutation restored the 75 nt distance between initiation codons that occurs naturally in FMDV serotypes SAT 1–3. Western blot analysis of A24-L1123/Flag infected cell extracts revealed a unique L protein slightly bigger than Lb, consistent with translation initiation from these AUGs. Remarkably, this extended Lb protein performed as well as the WT Lb for all known functions of L in cell culture. This result is consistent with the fact that the N-terminus of the Lab protein is highly variable among all FMDV serotypes (George et al., 2001; Tosh et al., 2004). In the case of mutant virus A24-L1123/tc, western blot analysis showed a prominent band for Lb and a fainter slower band, presumably tc tagged L protein. Unfortunately, we could not visualize the presence of the tc tag in this species, probably because there was not enough protein to be detected with the available fluorescent reagents (data not shown).

These results are consistent with previous studies by Cao et al. (1995) where utilizing another approach that consisted in generating mutant viruses that encoded only one form of the L protein; could not produce mutant virus encoding for the Lab protein. Although we failed to visualize the Lab protein, in this study we derived several mutant FMD viruses that allowed us to explore the role of the inter-AUG region in viral translation.

Most studies concerning the involvement of inter-AUG region in translation use *in vitro* systems with bicistronic expression plasmid constructs (Belsham, 1992; Lopez de Quinto and Martinez-Salas, 1999; Ohlmann and Jackson, 1999; Poyry et al., 2001). In a previous study in cell culture, we demonstrated that the inter-AUG region is essential for virus replication since viable L-deleted virus could only be obtained when this region was maintained and translation of the viral polyprotein started from the second AUG codon (Piccone et al., 1995a).

Initiation of translation can occur at more than one AUG codon in some picornavirus (Hinton et al., 2000; Hollister et al., 2008; Kaminski et al., 1994; Kong and Roos, 1991; Tesar et al., 1992) by a poorly understood mechanism of selection. The selection of the correct initiation codon is critical, since incorrect AUG selection could lead to miscoded or truncated proteins. In the case of FMDV, it has been proposed that initiation occurs at the second AUG by a mechanism similar to the ribosome scanning model of Kozak (1989). The recognition of the correct initiation codon during this process has been shown to be inhibited by RNA structures and by the presence of additional AUG codons (Belsham, 1992; Jackson and Kaminski, 1995). Alternatively, Andreev et al. (2007) have hypothesized that selection of the second AUG occurs independently of the recognition of the first AUG codon. Interestingly, the tn insertion in our mutant viruses creates a stem-loop structure with a ΔG of −43.5 kcal/mol according to the mfold program (Zuker, 2003). Therefore, according to the scanning model, the introduction of the tn should have inhibited the initiation from the second AUG. However, under the experimental conditions assayed in Fig. 4, the tn did not have any effect on the initiation from the Lb site in mutant viruses A24-L1123 or A24-L1123/tc. Nevertheless, it is possible that the presence of the tn slowed down the scanning of the 40S ribosomal complex, thereby allowing internal initiation from the second

Please cite this article in press as: Piccone, M.E., et al., Introduction of tag epitopes in the inter-AUG region of foot and mouth disease virus: Effect on the L protein. Virus Res. (2010), doi:10.1016/j.virusres.2010.09.004

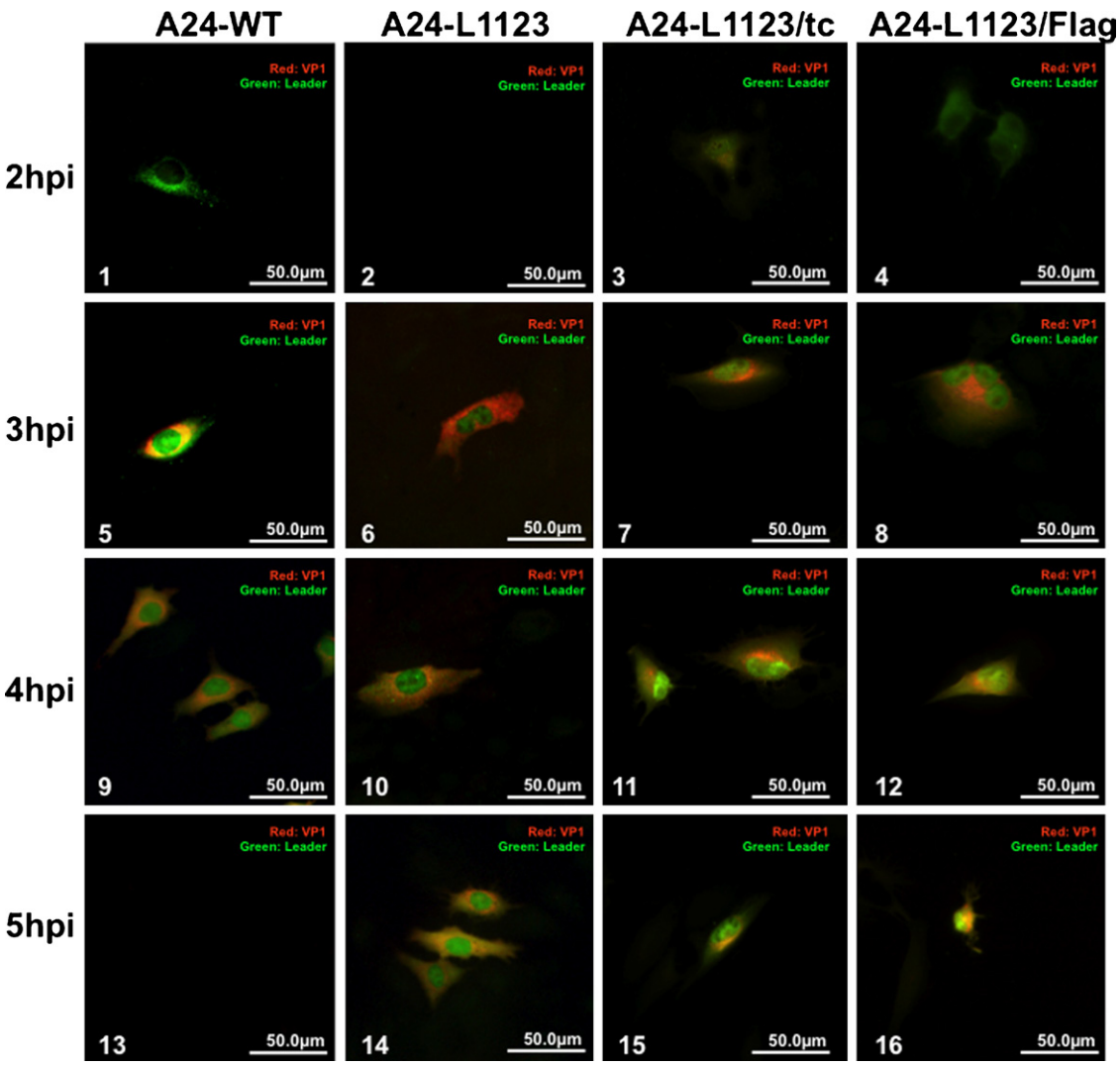

Fig. 6. Localization of leader in WT and L-mutant viruses in infected cells. LF-BK cells were infected with A24-WT (panels 1, 5, 9 and 13), A24-L1123 (panels 2, 6, 10 and 14), A24-L1123/tc (panels 3, 7, 11 and 15) or A24-L1123/Flag (panels 4, 8, 12 and 16) at MOI 10. At given times post-infection, cells were fixed with 4% paraformaldehyde and stained with anti-leader and anti-VP1 antibodies. Leader was detected with Alexa fluor 488 (green) and VP1 with Alexa fluor 594 (red) conjugated secondary antibodies.

AUG codon. Slowed viral translation could explain the attenuated phenotype observed by the tn-L mutant viruses, as shown in Fig. 5 by the delayed virus growth in cell culture. Decrease virus load could give the host enough time to develop an antiviral response and control infection. In addition to the proposed structure, the insertion of the tn increased the distance between both AUGs to 141–168 nt. However, such an increase in the length of the inter-AUG region had minimum effect on the initiation of translation from the second AUG. Similar results were reported by Lopez de Quinto and Martinez-Salas (1998).

Overall, the data shown here suggest that attenuation of the tn-L mutant viruses does not to correlate with the amino acid sequence of the N-terminus of the L protein, but probably with the structure of the inter-AUG region. It is, however, possible that the tn insertion interferes with binding of cellular factors required for efficient translation. Further mutational analysis will determine the biological role of the inter-AUG region of FMDV in the viral cycle.

Acknowledgements

We thank Steve Pauszek for help with sequencing analysis and Kathy Apiccelli for help with graphic work.

References

Andreev, D.E., Fernandez-Miragall, O., Ramajo, J., Dmitriev, S.E., Terenin, I.M., Martinez-Salas, E., Shatsky, I.N., 2007. Differential factor requirement to assemble translation initiation complexes at the alternative start codons of foot-and-mouth disease virus RNA. RNA 13 (8), 1366–1374.
Arhel, N.J., Charneau, P., 2009. Bisarsenical labeling of HIV-1 for real-time fluorescence microscopy. Methods Mol. Biol. 485, 151–159.
Baxt, B., Morgan, D.O., Robertson, B.H., Timpone, C.A., 1984. Epitopes on foot-and-mouth disease virus outer capsid protein VP1 involved in neutralization and cell attachment. J. Virol. 51 (2), 298–305.
Belsham, G.J., 1992. Dual initiation sites of protein synthesis on foot-and-mouth disease virus RNA are selected following internal entry and scanning of ribosomes in vivo. Embo J. 11 (3), 1105–1110.
Cao, X., Bergmann, I.E., Fullkrug, R., Beck, E., 1995. Functional analysis of the two alternative translation initiation sites of foot-and-mouth disease virus. J. Virol. 69 (1), 560–563.
Carrillo, C., Tulman, E.R., Delhon, G., Lu, Z., Carreno, A., Vagnozzi, A., Kutish, G.F., Rock, D.L., 2005. Comparative genomics of foot-and-mouth disease virus. J. Virol. 79 (10), 6487–6504.
Chinsangaram, J., Piccone, M.E., Grubman, M.J., 1999. Ability of foot-and-mouth disease virus to form plaques in cell culture is associated with suppression of alpha/beta interferon. J. Virol. 73 (12), 9891–9898.
Clarke, B.E., Sangar, D.V., Burroughs, J.N., Newton, S.E., Carroll, A.R., Rowlands, D.J., 1985. Two initiation sites for foot-and-mouth disease virus polyprotein in vivo. J. Gen. Virol. 66 (Pt 12), 2615–2626.
Das, S.C., Panda, D., Nayak, D., Pattnaik, A.K., 2009. Biarsenical labeling of vesicular stomatitis virus encoding tetracysteine-tagged m protein allows dynamic imaging of m protein and virus uncoating in infected cells. J. Virol. 83 (6), 2611–2622.

Please cite this article in press as: Piccone, M.E., et al., Introduction of tag epitopes in the inter-AUG region of foot and mouth disease virus: Effect on the L protein. Virus Res. (2010), doi:10.1016/j.virusres.2010.09.004

de los Santos, T., de Avila Botton, S., Weiblen, R., Grubman, M.J., 2006. The leader proteinase of foot-and-mouth disease virus inhibits the induction of beta interferon mRNA and blocks the host innate immune response. J. Virol. 80 (4), 1906–1914.
de los Santos, T., Diaz-San Segundo, F., Grubman, M.J., 2007. Degradation of nuclear factor kappa B during foot-and-mouth disease virus infection. J. Virol. 81 (23), 12803–12815.
de los Santos, T., Segundo, F.D., Zhu, J., Koster, M., Dias, C.C., Grubman, M.J., 2009. A conserved domain in the leader proteinase of foot-and-mouth disease virus is required for proper subcellular localization and function. J. Virol. 83 (4), 1800–1810.
Devaney, M.A., Vakharia, V.N., Lloyd, R.E., Ehrenfeld, E., Grubman, M.J., 1988. Leader protein of foot-and-mouth disease virus is required for cleavage of the p220 component of the cap-binding protein complex. J. Virol. 62 (11), 4407–4409.
Duque, H., LaRocco, M., Golde, W.T., Baxt, B., 2004. Interactions of foot-and-mouth disease virus with soluble bovine alphaVbeta3 and alphaVbeta6 integrins. J. Virol. 78 (18), 9773–9781.
George, M., Venkataramanan, R., Gurumurthy, C.B., Hemadri, D., 2001. The non-structural leader protein gene of foot-and-mouth disease virus is highly variable between serotypes. Virus Genes 22 (3), 271–278.
Grubman, M.J., Baxt, B., 2004. Foot-and-mouth disease. Clin. Microbiol. Rev. 17 (2), 465–493.
Hinton, T.M., Li, F., Crabb, B.S., 2000. Internal ribosomal entry site-mediated translation initiation in equine rhinitis A virus: similarities to and differences from that of foot-and-mouth disease virus. J. Virol. 74 (24), 11708–11716.
Hollister, J.R., Vagnozzi, A., Knowles, N.J., Rieder, E., 2008. Molecular and phylogenetic analyses of bovine rhinovirus type 2 shows it is closely related to foot-and-mouth disease virus. Virology 373 (2), 411–425.
House, C., House, J.A., 1989. Evaluation of techniques to demonstrate foot-and-mouth disease virus in bovine tongue epithelium: comparison of the sensitivity of cattle, mice, primary cell cultures, cryopreserved cell cultures and established cell lines. Vet. Microbiol. 20 (2), 99–109.
Jackson, R.J., Kaminski, A., 1995. Internal initiation of translation in eukaryotes: the picornavirus paradigm and beyond. RNA 1 (10), 985–1000.
Kaminski, A., Belsham, G.J., Jackson, R.J., 1994. Translation of encephalomyocarditis virus RNA: parameters influencing the selection of the internal initiation site. Embo J. 13 (7), 1673–1681.
Kirchweger, R., Ziegler, E., Lamphear, B.J., Waters, D., Liebig, H.D., Sommergruber, W., Sobrino, F., Hohenadl, C., Blaas, D., Rhoads, R.E., et al., 1994. Foot-and-mouth disease virus leader proteinase: purification of the Lb form and determination of its cleavage site on eIF-4 gamma. J. Virol. 68 (9), 5677–5684.
Kleina, L.G., Grubman, M.J., 1992. Antiviral effects of a thiol protease inhibitor on foot-and-mouth disease virus. J. Virol. 66 (12), 7168–7175.
Kong, W.P., Roos, R.P., 1991. Alternative translation initiation site in the DA strain of Theiler's murine encephalomyelitis virus. J. Virol. 65 (6), 3395–3399.
Kozak, M., 1989. The scanning model for translation: an update. J. Cell Biol. 108 (2), 229–241.
Lopez de Quinto, S., Martinez-Salas, E., 1998. Parameters influencing translational efficiency in aphthovirus IRES-based bicistronic expression vectors. Gene 217 (1–2), 51–56.
Lopez de Quinto, S., Martinez-Salas, E., 1999. Involvement of the aphthovirus RNA region located between the two functional AUGs in start codon selection. Virology 255 (2), 324–336.
Mason, P.W., Rieder, E., Baxt, B., 1994. RGD sequence of foot-and-mouth disease virus is essential for infecting cells via the natural receptor but can be bypassed by an antibody-dependent enhancement pathway. Proc. Natl. Acad. Sci. U.S.A. 91 (5), 1932–1936.
Medina, M., Domingo, E., Brangwyn, J.K., Belsham, G.J., 1993. The two species of the foot-and-mouth disease virus leader protein, expressed individually, exhibit the same activities. Virology 194 (1), 355–359.
Ohlmann, T., Jackson, R.J., 1999. The properties of chimeric picornavirus IRESes show that discrimination between internal translation initiation sites is influenced by the identity of the IRES and not just the context of the AUG codon. RNA 5 (6), 764–778.
Perlman, M., Resh, M.D., 2006. Identification of an intracellular trafficking and assembly pathway for HIV-1 gag. Traffic 7 (6), 731–745.
Piccone, M.E., Pacheco, J.M., Pauszek, S.J., Kramer, E., Rieder, E., Borca, M.V., Rodriguez, L.L., 2010. The region between the two polyprotein initiation codons of foot-and-mouth disease virus is critical for virulence in cattle. Virology 396 (1), 152–159.
Piccone, M.E., Rieder, E., Mason, P.W., Grubman, M.J., 1995a. The foot-and-mouth disease virus leader proteinase gene is not required for viral replication. J. Virol. 69 (9), 5376–5382.
Piccone, M.E., Sira, S., Zellner, M., Grubman, M.J., 1995b. Expression in *Escherichia coli* and purification of biologically active L proteinase of foot-and-mouth disease virus. Virus Res. 35 (3), 263–275.
Poyry, T.A., Hentze, M.W., Jackson, R.J., 2001. Construction of regulatable picornavirus IRESes as a test of current models of the mechanism of internal translation initiation. RNA 7 (5), 647–660.
Roberts, P.J., Belsham, G.J., 1995. Identification of critical amino acids within the foot-and-mouth disease virus leader protein, a cysteine protease. Virology 213 (1), 140–146.
Rudner, L., Nydegger, S., Coren, L.V., Nagashima, K., Thali, M., Ott, D.E., 2005. Dynamic fluorescent imaging of human immunodeficiency virus type 1 gag in live cells by biarsenical labeling. J. Virol. 79 (7), 4055–4065.
Sangar, D.V., Newton, S.E., Rowlands, D.J., Clarke, B.E., 1987. All foot and mouth disease virus serotypes initiate protein synthesis at two separate AUGs. Nucleic Acids Res. 15 (8), 3305–3315.
Strebel, K., Beck, E., Strohmaier, K., Schaller, H., 1986. Characterization of foot-and-mouth disease virus gene products with antisera against bacterially synthesized fusion proteins. J. Virol. 57 (3), 983–991.
Swaney, L.M., 1988. A continuous bovine kidney cell line for routine assays of foot-and-mouth disease virus. Vet. Microbiol. 18 (1), 1–14.
Tesar, M., Harmon, S.A., Summers, D.F., Ehrenfeld, E., 1992. Hepatitis A virus polyprotein synthesis initiates from two alternative AUG codons. Virology 186 (2), 609–618.
Tosh, C., Mittal, M., Sanyal, A., Hemadri, D., Bandyopadhyay, S.K., 2004. Molecular phylogeny of leader proteinase gene of type A of Foot-and-mouth disease virus from India. Arch. Virol. 149 (3), 523–536.
van Rensburg, H., Haydon, D., Joubert, F., Bastos, A., Heath, L., Nel, L., 2002. Genetic heterogeneity in the foot-and-mouth disease virus Leader and 3C proteinases. Gene 289 (1–2), 19–29.
Zuker, M., 2003. Mfold web server for nucleic acid folding and hybridization prediction. Nucleic Acids Res. 31 (13), 3406–3415.

Return to Table of Contents

Please cite this article in press as: Piccone, M.E., et al., Introduction of tag epitopes in the inter-AUG region of foot and mouth disease virus: Effect on the L protein. Virus Res. (2010), doi:10.1016/j.virusres.2010.09.004

Journal of Wildlife Diseases, 46(1), 2010, pp. 209–217

EXPERIMENTAL INFECTION OF *DIDELPHIS MARSUPIALIS* WITH VESICULAR STOMATITIS NEW JERSEY VIRUS

Carlos M. Trujillo,[1,3] Luis Rodriguez,[2] Juan D. Rodas,[1] and John Jairo Arboleda[1]

[1] Grupo Centauro, Escuela de Medicina Veterinaria, Universidad de Antioquia, AA 1226, Medellín, Colombia 57, South America

[2] Foreign Animal Disease Research Unit, ARS – USDA, Plum Island Animal Disease Center, Route 25, Orient, New York 11957, USA

[3] Corresponding author (email: cm.trujillot@hotmail.com)

ABSTRACT: Although vesicular stomatitis has been present for many years in the Americas, many aspects of its natural history remain undefined. In this study, we challenged five adult Virginia opossums (*Didelphis marsupialis*) with vesicular stomatitis New Jersey serotype virus (VSNJV). Opossums had no detectable antibodies against VSNJV prior to being inoculated with $10^{6.5}$ median tissue culture infective doses ($TCID_{50}$) of VSNJV by two routes; intraepithelial/subepithelial (IE/SE) inoculation and scarification in the muzzle (SM). Clinical response was monitored daily and animals were tested for viral shedding. All infected animals developed vesicles and ulcers on the tongue and inflammation of the nasal alar folds. Virus was isolated from esophagus-pharynx, nasal, and from ocular swabs and lesions samples. The failure to detect viremia in these animals indicates that a source other than blood may be required for transmission to insect vectors. Our results suggest that *D. marsupialis* could play a role in the maintenance of VSNJV outside of domestic animal populations and could provide a model to study vesicular stomatitis virus pathogenesis.

Key words: *Didelphis marsupialis*, host, opossum, vesicular stomatitis virus.

INTRODUCTION

Vesicular stomatitis (VS) is caused by several viruses in the genus *Vesiculovirus*, family *Rhabdoviridae*. This disease primarily affects domestic cattle, horses, and swine, but also has been observed infrequently in camelids, sheep, goats, and some wildlife species; humans can also become infected, producing an acute, febrile, influenza-like illness (Thorne et al., 1983; Letchworth et al., 1999; McCluskey and Mumford, 2000).

Outbreaks of clinical disease are associated with infection by two vesicular stomatitis virus (VSV) serotypes, New Jersey (VSNJV) and Indiana (VSIV), with VSNJV being the most-common cause of clinical cases in Colombia, South America. Although VSV has been the object of exhaustive studies, limited advances have been achieved in understanding its ecology and epidemiology. Therefore, investigations of the wild and domestic maintenance and transmission cycles of the virus are needed to identify potential vectors and reservoirs and their role in transmission and persistence of VSV in enzootic areas. In addition, it is also important to identify the ecologic conditions (vegetation, temperature, rainfall, and relative humidity, among others), that allow the maintenance and re-emergence of VSV in endemic areas.

Some wild herbivores utilize areas occupied by domestic livestock, but their role as possible reservoir hosts for VSNJV remains speculative (Hanson and Brandly, 1957, cited by Yuill 1981; Stallknecht and Erickson, 1986; Webb et al., 1987). Currently, the natural reservoir for the VSVNJ has not been identified, but neutralizing antibodies have been detected in numerous wildlife species in enzootic areas of Central America including anteater (*Tamandua tetradactyla*), common opossum (*Didelphis marsupialis*), two-toed sloths (*Choleopus hoffmani*), spider monkeys (*Ateles* spp.), spiny rats (*Proechimys semispinosus*), and fruit bats (*Artibeus* spp.), among others (Tesh et al., 1969; Rodriguez et al., 1990). Experimental subcutaneous inoculation of VSNJV and VSIV into wildlife species from Panama demonstrated rapid development of antibodies against these viruses in 13

species of rodents, two species of marsupials, two species of bats, two nonhuman primates, one species of rabbit, one species of edentate, and one carnivore species (Tesh et al., 1970). In the same study, age had a significant effect on susceptibility to both serotypes; adult mammals remained asymptomatic after a subcutaneous inoculation with VSV, while death resulted in sucking wild mice, hamsters, marmosets, opossums, and anteaters 2–4 days after a subcutaneous inoculation. These animals exhibited damages to the central nervous system, but vesicular lesions were not detected.

In Colombia, studies published by Zuluaga and Yuill (1979) and Arboleda et al. (2001) suggest that the common opossum is a good candidate to serve as a reservoir of VSV; it is abundant and usually has a high prevalence of VSV antibodies. This species also is highly adaptable to habitat changes related to human activity and could serve as a local source for VSV transmission to humans and domesticated animals.

Our objective was to determine experimentally if *D. marsupialis* could serve as a possible reservoir species, or amplifier host, of VSNJV.

MATERIALS AND METHODS

Six wild opossums, four males and two females (all adults), of approximately 1.5 kg, were captured using Tomahawk traps and a bait made of peanut butter, oatmeal flakes, and vanilla essence (Mills et al., 1995). The two females were nursing one, and three, suckling baby opossums; according to their size, young were about 1 mo old. All young were found inside the pouch and looked healthy. Animals were trapped on a farm 40 km to the north of the city of Medellín (Antioquia, Colombia) with approval from local authorities (Corporación Autónoma Regional de Antioquia). Before experimental infection, captured opossums were acclimated for 1 mo. Food consisting of a combination of fruits, eggs, and pet food concentrate and water were provided ad libitum. Opossums were kept in individual cages of 80× 40×60 cm and handled according to the University's committee regulations for animal experimentation.

Prior to experimental infection, animals were clinically examined and did not show any evidence of illness, metabolic abnormalities, or physiologic stress. Furthermore, they were tested for VSNJV and VSIV antibodies using the serum neutralization assay.

The VSNJV used in this study was obtained from the immunovirology group of the University of Antioquia (Dr. María T. Rugeles). The virus had been originally isolated from a clinically ill cow at the Instituto Colombiano Agropecuario. This virus was intracerebrally inoculated in suckling mice and identified through serum neutralization assay in BHK-21 cells (American Type Culture Collection [ATCC], Rockville, Maryland, USA). Subsequently, the virus was amplified through one passage in BHK-21 cells and titered on Vero cells (ATCC) reaching $10^{7.5}$ median tissue culture infective doses ($TCID_{50}$).

Animals were housed in individual cages covered with a fine insect screen to avoid contact with vectors. Animals were sedated with an intramuscular injection of ketamine (100 mg/kg) and xylazine (10 mg/kg) and injected with $10^{6.5}$ $TCID_{50}$ of VSNJV in 100 µl of Eagle's minimum essential medium (MEM) with Earle's salts (Sigma Chemical Company, St. Louis, Missouri, USA) supplemented with 1% heat-inactivated fetal bovine serum (FBS; Difco Laboratories, Detroit, Michigan, USA). Three males were inoculated by intraepithelial/subepithelial (IE/SE) route and identified as 1IE/SE, 2IE/SE, and 3IE/SE; a male and a female (lactating with three offspring) were inoculated by scarification in the muzzle (SM) and identified as 4SM (male) and 5SM (female); and a remaining female was mock inoculated with viral isolation media by the IE/SE route.

For the inoculation, the virus was applied 2.5 cm proximal to the apex of the tongue. For the SM inoculation, each opossum was pricked 20 times on the snout and an inoculum of 100 µl of the virus suspension was added over the lesion and left there for 10 min; remaining liquid was dried off with a sterile gauze. All animals were examined daily for vesicular lesions and bled prior to inoculation and at 0, 12, 24, 48, 72, 96, 120, and 144 hr postinoculation (PI). Approximately 1.5 ml of blood per animal was obtained through cardiac puncture. A portion of the sample was transferred to tubes with anticoagulant (EDTA 100 UI/ml) for viral isolation in BHK-21 cell cultures; the other portion of the sample was placed in tubes without anticoagulant for

VSNJV and VSIV antibody testing by serum neutralization.

Samples of vesicular lesions, esophagus-pharynx, nasal, ocular, and rectal mucosa were obtained using sterile swabs that were placed in 1.5 ml of transport media consisting of MEM supplemented with 2% FBS (Difco) and antibiotics (penicillin 1,000 U/ml, streptomycin 1 μg/ml, amphotericin B 2.5 μg/ml; Sigma). Swab samples were then stored at −70 C until they were processed. Urine and feces samples were collected from all the animals and were stored at −70 C in vials with 1.5 ml transport media. Samples of tonsils, submandibular ganglion, kidney, lung, spleen, liver, and brain were obtained at 21 days PI, after the animals were euthanized. Tissues were stored at −70 C in sterile plastic tubes with 5 ml of transport media.

For sample preparation for virus isolation, blood samples were thawed, mixed by vortex, and diluted 1:5 in MEM supplemented with 2% FBS. For swab samples, fluid from swabs was drained against the walls of the vials and swabs were discarded. Samples were then mixed by vortex and centrifuged at 1500 × G for 10 min at 4 C. Tissues were thawed, sliced in 3×3×3 mm cubes, placed in vials with 0.5 ml MEM supplemented with 2% of FBS, and macerated with sterile homogenizers. An additional 0.5 ml of medium was added and mixed by vortex, and tubes were centrifuged at 1500 × G for 20 min at 4 C. Urine and feces were thawed and mixed in vortex, diluted 1:10 in MEM supplemented with 2% FBS and 2% antibiotics, and then centrifuged at 12,000 × G for 20 min.

For virus isolation, 100 μl of the diluted sample (blood), supernatant (swab, feces/urine/tissue) was inoculated on 1-day-old monolayers of BHK-21 cells (2×10^5 cells/well) cultured in 24-well plates. Plates were incubated for 1 hr at 37 C with rocking every 10 min. After this time, inoculum was removed and replaced by 1 ml of fresh medium (MEM supplemented with 2% of FBS); inoculated cells were incubated at 37 C in 5% CO_2. Plates were subsequently observed at 24, 48, and 72 hr PI for cytopathic effect (CPE). Two passages in BHK-21 cells were done, and samples were considered negative if CPE was not observed. The $TCID_{50}$ for positive samples was determined in a 96-well plate following the protocol described by Rovozzo and Burke (1973) and Ballew (1992); viral titers were calculated by the method of Reed and Muench (1938).

Sera from opossums were tested by VSVNJ serum neutralization assay in 96-well plates as previously described by Arboleda et al. (2001). Briefly, sera were inactivated at 56 C for 30 min, and twofold dilutions were performed beginning with 1:4 up to 1:1,024. A challenge dose of 100 $TCID_{50}$ of each viral serotype (VSNJV and VSIV) in a volume of 50 μl were combined with equal volumes of each serum dilution. The mixture was allowed to incubate for 60 min at 37 C, and 100 μl was added to each of four wells in 96-well plates with BHK-21 cells (seeded 24 hr prior to testing). Plates were incubated at 37 C with 5% CO_2 and observed daily for 72 hr for CPE.

Cell controls (MEM and cell monolayers), test sera controls (diluted serum plus maintenance medium), as well as virus controls (MEM and viruses infecting cell monolayer) were included in each plate. A positive bovine serum, with a neutralizing titer of 4.05 $TCID_{50}$ (expressed as the reciprocal logarithm of the dilution) to both VSNJV and VSIV (kindly provided by Dr. Guillermo Suarez Restrepo, VECOL SA, Bogotá), and a negative opossum serum that had previously been shown to be negative for the presence of antibodies against VSNJV, were also included in each test as positive and negative controls, respectively, for the serum neutralization tests. Serum samples were considered positive if the antibody titer was ≥32 (Cuartas and Muñoz, 2003; Nunamaker et al., 2003)

In order to determine the susceptibility of the possum's offspring to VSNJV, two out of the three offspring from one of the females (5SM) were subcutaneously inoculated with $10^{6.5}$ $TCID_{50}$ of VSNJV in a 40-μl volume; a third one was used as a negative control. Inoculated animals were observed for 7 days.

RESULTS

Lesions or clinical signs (weakness, anorexia, diarrhea, and salivation) were not observed at 24 hr PI (Table 1). Two of the animals inoculated in the tongue had lesions at 48 hr PI, with loss of continuity in epithelium, and irregular borders, but without vesicles or blood. Other lesions were observed; on cheeks, with hemorrhage (ecchymoses and petechiae), but without any type of secretion. By 72 hr PI, all animals inoculated via IE/SE had lesions at the inoculation site with ulcers that extended farther than the region of inoculation. Further, the lateral tongue epithelium sloughed off, leaving a reddened superficial ulcer with ragged mar-

TABLE 1. Clinical monitoring of opossums infected with VSNJV.

Animal ID (via inoculation)[a]	Days postinfection (DPI)[b]								
	0.5	1	2	3	4	5	6	14	21
1 IE/SE ♂	−	−	++	+++++	+++++	+H	+H	CH	−
2 IE/SE ♂	−	−	+++++	+++++	+++++	+H	+H	CH	−
3 IE/SE ♂	−	−	+++++	+++++	+++++	+H			
4 SM ♂	−	−	−	+++	+++	+H	+H	CH	−
5 SM ♀	−	−	+	++++	+++	+H	+H	CH	−
Mock ♀	−	−	−	−	−	−	−	−	−

[a] IE/SE = intraepithelial/subepithelial; SM = inoculation by scarification in the muzzle; ♂ = male; ♀ = female.

[b] − = without typical signs of the illness; + = lesion beginning in inoculation site; ++ = beginning of vesicular laceration outside of the inoculation site; +++ = inflammation and erosion in nasal nostril; ++++ = inflammation and erosion in nasal nostril with nasal discharge; +++++ = injury widespread with loss of the epithelium of the tongue; +H = beginning of healing process; HC = complete healing.

gins (Table 1). Later, erosions with irregular borders became deeper and bloody, but no vesicles appeared (Fig. 1). Animals infected via SM had inflammation of the nasal alar folds with erosions on the nasal septum, and one of the opossum had abundant nasal serous discharge in both nostrils. By day 5 PI, the healing process of the lesions began, and no vesicles were detected. At days 14 and 21 PI, the lesions had healed completely, and the animals remained in good health.

The suckling young of the female infected by scarification (5SM) had a normal growth without any type of disease or lesions. The mock-inoculated female did not show any clinical, physiologic, or behavioral change during the 21 days of observation.

The identity of isolated viruses was confirmed by a virus neutralization test using a specific serum against VSNJV. All blood samples tested negative by virus isolation, but VSNJV was isolated from swabs obtained from the esophagus-pharyngeal tract of all five of five infected opossums. In IE/SE inoculated animals, virus was detected from days 1–5 PI, whereas in animals infected via SM, virus was not detected in the oral cavity until day 3 PI. Nasal swabs from four of the five infected opossums were positive by virus isolation. In one male (3IE/SE), virus was isolated from 12 hr until day 5 PI (Table 2); VSNJV was also isolated from 48 hr to day 5 PI from tongue lesions of animals infected via IE/SE (Table 2). Virus was isolated from ocular swabs from two opossums (5SM and 3IE/SE) on days 2 and 3 PI, respectively (Table 2). We did not detect the virus at the site of inoculation of the snout of opossums infected via SM, and we did not detect any other virus from day 6 through day 21 PI. All samples of urine and tissues from infected opossums were negative for virus isolation; VSNJV was isolated only from a single stool sample, taken from animal 2IE/SE on day 3 PI (Table 2).

We isolated VSNJV from samples collected from 12 hr until day 5 PI, with viral titers ranging from 1.0 to 5.75 $TCID_{50}$/ml. Highest viral titers were found in samples taken of esophageal-pharyngeal (5.25 $TCID_{50}$/ml) and nasal swabs (5.75 $TCID_{50}$/ml) from opossum 2IE/SE, samples which were obtained 24 hr PI before showing any clinical signs compatible with VSV infection (Table 3).

Samples obtained from animals inoculated via IE/SE had higher viral titers than those of animals that were infected via SM. Similarly, higher titers were found in samples that were taken between days 1 and 2 PI prior to the detection of lesions (Table 3).

Before the experimental infection, all opossums were negative for the presence

FIGURE 1. Lesion with loss of the epithelium extending towards the apex of the tongue.

TABLE 2. Viral isolation from samples of experimentally infected opossum with VSNJV.

Route[a]		ID/Isolation source[b]	Days postinfection (DPI)[c]								
			0.5	1	2	3	4	5	6	14	21
IE/SE	1 ♂	EP	−	+	+	+	+	−	−	−	−
		L	−	−	+	+	−	−	−	−	−
	2 ♂	EP	−	+	+	+	+	+	−	−	−
		N		+	+	+	+	−	−	−	−
		L	−	−	+	+	−	−	−	−	−
		F	−	−	−	+	−	−	−	−	−
	3 ♂	EP	−	+	+	+	+	+	−	−	−
		N	+	+	+	+	+	+	−	−	−
		L	−	−	+	+	+	+	−	−	−
		O	−	−	−	+	−	−	−	−	−
SM	4 ♂	EP	−	−	−	−	+	−	−	−	−
		N	−	−	+	+	−	−	−	−	−
	5 ♀	EP	−	−	−	+	+	+	−	−	−
		N	−		+	−	−	−	−	−	−
		L	−	−	+	−	−	−	−	−	−
		O	−	−	+	−	−	−	−	−	−
Mock ♀			−	−	−	−	−	−	−	−	−

[a] IE/SE = intraepithelial/subepithelial; SM = inoculation by scarification in the muzzle.

[b] ♂ = male; ♀ = female; EF = esophagus-pharyngeal swab; N = nasal swab; O = ocular swab; F = feces; L = lesions.

[c] − = virus not detected; + = virus isolated.

TABLE 3. Viral titers from samples of opossum infected with VSNJV.

Animal identification (inoculation via)[a]	Days postinfection (DPI)[b,c]							
	0.5	1	2	3	4	5	6	14	21
1 IE/SE ♂	ND	EP=2.0	EP=2.0 L=2.25	EP=2.0 L=2.0	EP=2.0	ND	ND	ND	ND
2 IE/SE ♂	ND	EP=5.25 N=5.75	EP=2.25 N=4.25 L=4.0	EP=3.25 N=4.0 L=2.75 F=3.0	EP=1.0 N=2.0	EP=1.0	ND	ND	ND
3 IE/SE ♂	N=2.25	EP=2.0N=2.25	EP=1.0 N=2.25 L=3.0	EP=2.25 N=2.25 O =2.25 L=2.0	EP=1.0- N=1.75 L=1.0	EP=2.0 N=1.0 L=1.0	ND	ND	ND
4 SM ♂	ND	ND	N=2.25	N=2.0	EP=2.0	ND	ND	ND	ND
5 SM ♀	ND	N=3.25	N=2.25 O =3.75 L=4.25	EP=1.0	EP=1.0	EP=1.0	ND	ND	ND
Mock ♀	ND	ND	ND	ND	ND	ND	ND	ND	ND

[a] IE/SE = intraepithelial/subepithelial; SM = inoculation by scarification in the muzzle; ♂ = male; ♀ = female.

[b] Viral titers expressed in $TICD_{50}$/0.1 ml.

[c] ND = virus not detected; EF = esophagus-pharyngeal swab; N = nasal swab; O = ocular swab; F = feces; L = lesions.

of antibodies to VSNJV and VSIV (titer <1.5 log correspondent to 1:32 dilution). All sera remained negative up to 48 hr PI. On day 3 PI, neutralizing antibodies were detected in three of the five infected opossums, with titers of 32. In general, at 5 days PI, all experimentally infected animals seroconverted, showing increasing titers throughout the experiment that reached >512 by 14 days PI (Table 4). Seroconversion was delayed in animals that were experimentally inoculated via SM. None of the three suckling opposums with VSVNJ had lesions, but they did seroconvert with antibody titers >128 (data not shown).

DISCUSSION

Results of this experimental infection demonstrate the susceptibility of the opossum, *Didelphis marsupialis*, to VSNJV through two different inoculation routes, IE/SE and SM. Our results were partially consistent with the ones reported by Tesh et al. (1970). We did not observe mortality or any signs of disease in suckling opposums, but we did observe infection with seroconversion between day 4 and 6 PI in adults. Because we detected antibodies in both challenged and negative control suckling opossums, we believe that passively transferred antibodies from the mother (5SM female) may have protected these progeny from viral effects.

Antibody titers were determined based on 100 $TCID_{50}$ of VSNJV. While this allowed for accurate detection of an antibody response, reported antibody titers cannot be directly related to regulatory positive thresholds. The Office International des Epizooties (OIE, currently World Organisation for Animal Health), protocol recommends using 1,000 $TCID_{50}$ for the serum neutralization assay for domestic animals (OIE, 2008).

Although virus was isolated from many samples, titers were normally lower than the inoculated dose. While this does not demonstrate significant amplification, virus

TABLE 4. Neutralizing antibodies titers from opossum infected with VSNJV by IE/SE and SM.

Animal identification[a]	Days postinfection (DPI)								
	0	1	2	3	4	5	6	14	21
1 IE/SE ♂	0.60[b]	0.60	0.91	1.20	1.50	2.11	2.61	2.71	2.71
2 IE/SE ♂	0.60	0.92	0.90	1.50	2.33	2.41	2.41	≥2.71	>3.01
3 IE/SE ♂	0.60	0.60	0.90	1.52	2.11	2.11			
4 SM ♂	0.60	0.60	1.22	1.20	1.20	1.50	1.82	2.11	2.71
5 SM ♀	0.60	1.20	1.20	1.50	1.52	1.80	2.11	2.63	>2.71
Mock ♀	0.60	0.60	0.60	0.60	0.60	0.60	0.60	0.60	0.60

[a] IE/SE = intraepithelial/subepithelial; SM = inoculation by scarification in the muzzle; ♂ = male; ♀ = female.

[b] Reciprocal logarithm of the serum dilution.

was detected at relatively high viral titers between days 2 and 6. This demonstrates both replication and the possibility that this species could serve as a source of infection for other susceptible host or vector species. In our work, viremia was never detected, which could indicate a localized rather than a systemic infection. This is similar to what has been previously shown in cattle and swine by Rodriguez et al. (1990) and Stallknecht et al. (2004), respectively, but is in contrast with previous studies by Arbeláez and Rocha (1984) and Arbeláez and Valbuena (1987), who demonstrated VSNJV in the blood of a bovine animal experimentally infected by the IE/SE route and by nasal instillation. In these experiments, however, the duration of this viremia was only 24 hr and, to date, these results have not been replicated in any subsequent studies. On the other hand, viremia has also been previously reported in young rodents (Cornish et al., 2001).

The inability to isolate VSV from the blood of experimentally infected wild animals has been previously shown by other investigators. Karstad and Hanson (1957) described the presence of fever and mouth lesions in three out of four deer infected via IE/SE and no viremia in the first 72 hr after PI. The experimental infection of two pronghorn antelope (*Antilocapra americana*) with VSNJV via IE/SE (Thorne et al., 1983, cited by Webb et al., 1987) produced similar results to the ones described in deer. We were also able to detect virus excretion through different routes, but never in blood samples; therefore, we propose that these sites could be a possible source of infection for mechanical vectors, a possibility that has been proposed by others in earlier investigations (Ferris et al., 1955; Mason, 1978; Mead et al., 2000).

The apparent incubation time of VSV in opossums experimentally infected through the routes used in this study was 48 hr, which is similar to the time described for cattle experimentally infected with VSNJV and VSIV (Mason, 1978; Yuill, 1981; Arbeláez and Rocha, 1984; Letchworth et al., 1999; Schmitt, 2002). The clinical signs, and the extension and kinetics of lesions observed in experimentally infected opossums, were similar to the ones described for bovine, equine, and porcine subjects when these were experimentally inoculated (Howerth et al., 2006). However, our marsupials did not show profuse salivation, vesicles, or lesions in the feet, as occurs in some of the other above-mentioned domestic mammals.

The two routes used for inoculation, IE/SE and SM, caused different lesions, with the IE/SE route being responsible for the most-severe clinical manifestations. This observation was confirmed in one of the infected animals, which had severe lesions not only at the inoculation site, but also developed lesions on the right cheek, located in a place distant from the inoculation site. In general, after 72 hr

PI, secondary vesicles were not observed in the five experimentally infected opossums.

From a clinical point of view, it was possible to establish the susceptibility of this species to experimental infection as well as its capacity of shedding the virus through several routes. To the best of our knowledge, this is the first report which shows that *D. marsupialis* could play a role in the epidemiology of the virus, and it leaves the door open for future studies about its use as an animal model for the infection and the illness. Even though *Sus scrofa* (domestic pig), a natural host for VSV infection, has also been used and proposed as a good model to study mechanisms of viral pathogenesis for this agent (Redelman et al., 1989), the opossum *D. marsupialis* may also be considered a good and convenient model, based on low sustainability expenses, high prolific capability, its abundance in tropic areas of the world where VSV is endemic, and its adaptability to be kept in farms under captivity or laboratory conditions (De Souza et al., 1992; Jaramillo et al., 1992; Cuartas and Muñoz, 2003). *Didelphis marsupialis* could become an excellent alternative to the domestic species in the investigation of routes of infection and dissemination of VSV under natural conditions and could help to experimentally test the real capacity of vectors in the transmission of this virus. These findings support the susceptibility of *D. marsupialis* to VSNJV and, because it is one of the species most abundantly found not only in the wilderness but also in peridomestic environments of tropical regions of Colombia, we propose that opossums could participate in the VS viral cycle. The opposum could not only serve as a host for different vectors in the forest, but also as an intermediary host for transmission of VSNJV to other susceptible animals such as pigs, cows, and horses in rural areas, through direct contact or by contamination of inanimate objects (fomites and vehicles).

ACKNOWLEDGMENTS

The authors are thankful for all of the support and help provided by the principal investigator (M. T. Rugeles) and the staff of the Laboratorio de Inmunovirología of our University (Universidad de Antioquia), V. H. Quiroz, L. Carrillo, and A. C. Galvis. This study was partially sponsored by the ICA-USDA, ARS Cooperative Agreement No. 58-1940-1-F128, "Understanding the Ecology of Vesicular Stomatitis in Endemic Areas of Colombia."

LITERATURE CITED

Arbeláez, G., and J. Rocha. 1984. Transmisión por contacto del virus de la estomatitis vesicular tipo New Jersey en bovinos. Revista ICA 19: 191–199.

———, and R. Valbuena. 1987. La instilación nasal como vía de infección experimental de estomatitis vesicular tipo Indina, en bovinos. Revista ICA 22: 59–64.

Arboleda, J. J., G. A. Restrepo, M. I. Wolff, J. F. Uribe, H. A. Bedoya, V. H. Quiroz, and S. Pérez. 2001. Ecoepidemiología de la estomatitis vesicular en un municipio cafetero de Antioquia. Revista Colombiana de Ciencias Pecuarias 14: 20–27.

Ballew, H. C. 1992. Neutralization. *In* Clinical virology manual, S. Specter and G. Lancz (eds.). Elsevier, New York, New York, pp. 229–241.

Cornish, T. E., D. E. Stallknecht, C. C. Brown, B. S. Seal, and E. W. Howerth. 2001. Pathogenesis of experimental vesicular stomatitis virus (New Jersey serotype) infection in the deer mouse (*Peromyscus maniculatus*). Veterinary Pathology 38: 396–406.

Cuartas, C., and J. Muñoz. 2003. Marsupiales, Cenoléstidos e Insectívoros de Colombia. Editorial Universidad de Antioquia, Medellín, 342 pp.

De Souza, M. G., E. L. Chaplin, N. Saltiel, F. A. Pacheco, and N. Santos. 1992. Utilizaáo do *Didelphis marsupialis* como animal de laboratorio. Pesquisa Agropecuária Brasileira 27: 213–216.

Ferris, D. F., R. P. Hanson, R. J. Dicke, and R. H. Roberts. 1955. Experimental transmission of vesicular stomatitis virus by diptera. Journal of Infectious Diseases 96: 184–192.

Hanson, R. P., and C. A. Brandly. 1957. Epizootiology of vesicular stomatitis. American Journal of Public Health 47: 205–209.

Howerth, E. W., D. G. Mead, P. O. Mueller, L. Duncan, M. D. Murphy, and D. E. Stallknecht. 2006. Experimental vesicular stomatitis virus infection in horses: Effect of route of inoculation and virus serotype. Veterinary Pathology 43: 943–955.

Jaramillo, S. O., H. L. Porras, and J. J. Herrera. 1992. Tesis, Contribución a la implementación

de *Didelphis marsupialis* como reservorio de *Leishmania chagasi* mediante infección experimental. Facultad de Medicina Veterinaria, Universidad de Antioquia, Medellín, 43 pp.

KARSTAD, L. H., AND R. P. HANSON. 1957. Vesicular stomatitis in deer. American Journal of Veterinary Research 68: 162–166.

LETCHWORTH, G. J., L. L. RODRIGUEZ, AND J. DEL C. BARRERA. 1999. Vesicular stomatitis. The Veterinary Journal 157: 239–260.

MASON, J. 1978. La epidemiología de la estomatitis vesicular. Boletín del Centro Panamericano de la Fiebre Aftosa 29–30: 13–33.

MCCLUSKEY, B. J., AND E. L. MUMFORD. 2000. Vesicular stomatitis and other vesicular, erosive, and ulcerative diseases of horses. Veterinary Clinics of North America: Equine Practice 16: 457–469.

MEAD, D. G., F. B. RAMBERG, D. G. BESSELSEN, AND C. J. MARÉ. 2000. Transmission of vesicular stomatitis virus (New Jersey serotype) between infected and non-infected black flies co-feeding on non-viremic deer mice. Science 287: 485–487.

MILLS, J. N., J. E. CHILDS, T. G. KSIAZEK, C. J. PETERS, AND W. M. VELLECA. 1995. Methods for trapping and sampling small mammals for virologic testing. US Department of Health and Human Services, Public Health Service, Centers for Disease Control and Prevention, Atlanta, Georgia, 61 pp.

NUNAMAKER, R. A., J. A. LOCKWOOD, C. E. STITH, C. L. CAMPBELL, S. P. SCHELL, B. S. DROLET, W. C. WILSON, D. M. WHITE, AND G. J. LETCHWORTH. 2003. Grasshoppers (Orthoptera: *Acrididae*) could serve as reservoirs and vectors of vesicular stomatitis virus. Journal of Medical Entomology 40: 957–963.

OFFICE INTERNATIONAL DES EPIZOOTIES (OIE). 2008. *In*: Manual of diagnostic tests and vaccines for terrestrial animals. http://www.oie.int/eng/normes/mmanual/A00025.htm. Accessed 19 August 2009.

REDELMAN, D., S. NICHOL, R. KLIEFORTH, M. VAN DER MAATEN, AND C. WHETSTONE. 1989. Experimental vesicular stomatitis virus infection of swine: Extent of infection and immunological response. Veterinary Immunology and Immunopathology 20: 345–361.

REED, J. L., AND H. MUENCH. 1938. A simple method of estimating fifty per cent endpoint. American Journal of Hygiene 27: 493–497.

RODRIGUEZ, L. L., S. D. VERNON, A. I. MORALES, G., AND J. LETCHWORTH. 1990. Serological monitoring of vesicular stomatitis New Jersey virus in enzootic regions of Costa Rica. American Journal of Tropical Medicine and Hygiene 42: 272–281.

ROVOZZO, G. C., AND C. N. BURKE. 1973. A manual of basic virological techniques. Prentice-Hall, Englewood Cliffs, New Jersey, 274 pp.

SCHMITT, B. 2002. Vesicular stomatitis. The Veterinary Clinics of North America: Food Animal Practice 18: 453–459.

STALLKNECHT, D. E., AND G. A. ERICKSON. 1986. Antibodies to vesicular stomatitis New Jersey type virus in a population of white-tailed deer. Journal of Wildlife Diseases 22: 250–254.

———, J. B. GREER, M. D. MURPHY, D. G. MEAD, AND E. W. HOWERTH. 2004. Effect of strain and serotype of vesicular stomatitis virus on viral shedding, vesicular lesion development, and contact transmission in pigs. American Journal of Veterinary Research 65: 1233–1239.

TESH, R., P. PERALTA, AND K. JOHNSON. 1969. Ecological studies of vesicular stomatitis virus I. Prevalence of infection among animals and humans living in an area of endemic VSV activity. American Journal of Epidemiology 90: 255–261.

———, ———, AND ———. 1970. Ecological studies of vesicular stomatitis virus: Results of experimental infection in Panamanian wild animals. American Journal of Epidemiology 91: 216–224.

THORNE, E. T., E. S. WILLIAMS, W. J. ADRIAN, AND C. M. GILLIN. 1983. Vesicular stomatitis in pronghorn antelope: Serologic survey and artificial infection. Proceedings of the 87th annual meeting of the US Animal Health Association, Las Vegas, Nevada, pp. 638–643.

WEBB, P. R., R. MCLEAN, G. SMITH, J. ELLENBERGER, B. FRANCY, T. WALTON, AND T. MONATH. 1987. Epizootic vesicular stomatitis in Colorado, 1982: Some observations on the possible role of wildlife populations in an enzootic maintenance cycle. Journal of Wildlife Diseases 23: 192–198.

YUILL, T. M. 1981. Vesicular stomatitis. *In* CRC handbook series in zoonoses, Section B, viral zoonoses. Vol. 1, J. H. Steele and G. W. Beran (eds.). CRC Press, Boca Raton, Florida, pp. 125–142.

ZULUAGA, F. N., AND T. M. YUILL. 1979. Estudios ecológicos de la estomatitis vesicular en Antioquia, Colombia. Boletín de la Oficina Sanitaria Panamericana 87: 389–404.

Received for publication 7 October 2008.

Return to Table of Contents

Veterinary Immunology and Immunopathology xxx (2010) xxx–xxx

Contents lists available at ScienceDirect

Veterinary Immunology and Immunopathology

journal homepage: www.elsevier.com/locate/vetimm

Short communication

Marked differences between MARC-145 cells and swine alveolar macrophages in IFNβ-induced activation of antiviral state against PRRSV

D. He[b], C. Overend[a], J. Ambrogio[a], R.J. Maganti[a], M.J. Grubman[c], A.E. Garmendia[a,*]

[a] Department of Pathobiology and Veterinary Science, University of Connecticut, 61 N. Eagleville Rd, Storrs, CT 06269, USA
[b] College of Veterinary Medicine, South China Agricultural University, Guangzhou 510642, China
[c] Plum Island Animal Disease Center, USDA, ARS, Greenport, NY 11944, USA

ARTICLE INFO

Article history:
Received 12 October 2009
Received in revised form 1 July 2010
Accepted 28 July 2010

Keywords:
Porcine reproductive and respiratory syndrome virus (PRRSV)
Interferon beta
Alveolar macrophage

ABSTRACT

The activation of antiviral activity induced by recombinant swine interferon beta (rswIFNβ) against PRRSV was comparatively examined in MARC-145 cells and porcine alveolar macrophages (PAMs). A dose–response analysis showed, in MARC-145 cells, that isolate Mo25544 was highly sensitive to rswIFNβ while a vaccine strain and isolate PDV130-9301 were resistant to different extents. In contrast, all three viruses were equally sensitive to rswIFNβ in PAMs even at the lowest dose of IFN utilized in the bioassays. To analyze potential differences in mechanisms of antiviral activation between these cells, treatment with 2-aminopurine (2-AP), an inhibitor of double-stranded RNA-dependent protein kinase (PKR), was performed in rswIFNβ-treated cells. Addition of 2-AP to rswIFNβ-primed MARC-145 cells restored replication of the Mo25544 isolate, and to some extent that of vaccine virus and PDV130-9301. In contrast, virus replication could not be rescued for any of the three viruses with 2-AP in rswIFNβ-treated PAMs. The differences in sensitivity of PRRSV to rswIFNβ as well as the effects of 2-AP strongly suggest that MARC-145 cells and PAMs utilize different rswIFNβ-associated antiviral pathways. Therefore, studies to understand virus-host cell interactions performed in MARC-145 cells require additional scrutiny when utilized as a host cell model for immunologic responses to PRRSV.

1. Introduction

Porcine reproductive respiratory syndrome (PRRS) is one of the most important viral diseases that negatively affect the swine industry worldwide (Keffaber, 1989; Murtaugh et al., 2002; Mengeling et al., 2003). The causative agent, porcine reproductive respiratory syndrome virus (PRRSV), is a member of the Arteriviridae family in the order Nidovirales. The virus genome is a positive sense single-stranded RNA, and the virion's nucleocapsid is covered by a lipid bilayer containing several viral proteins.

The virus–host relationship is unique, and can be characterized by a deficient innate immune response including poor induction of type I interferon (IFNα/β) (Albina et al., 1998), sub-optimal humoral and cellular immunity, and persistence of the virus for long periods post-infection (Horter et al., 2002; Meier et al., 2003). Effective control of PRRS remains elusive and underscores the need for in-depth studies to gain an insight into the mechanisms leading to such an inefficient host response.

The innate immune response, particularly regarding the modulation and activation of IFNα/β, is relevant to the understanding of host–virus interactions and the resulting immune response (Albina et al., 1998; Alexopoulou et al., 2001; Samuel, 2001). Mounting evidence shows that infection with PRRSV results in poor induction of IFNα critically affecting the ensuing adaptive responses with

* Corresponding author. Tel.: +1 860 486 3945; fax: +1 860 486 2794.
E-mail address: antonio.garmendia@uconn.edu (A.E. Garmendia).

0165-2427/$ – see front matter © 2010 Elsevier B.V. All rights reserved.
doi:10.1016/j.vetimm.2010.07.023

delayed IFNγ and neutralizing antibody production, leading to persistent infection (Albina et al., 1998; Buddaert et al., 1998; Bautista and Molitor, 1999; Aasted et al., 2002; Royaee et al., 2004; Xiao et al., 2004). *In vitro* infection of porcine alveolar macrophages (PAMs) (Genini et al., 2008), monocyte-derived dendritic cells (DCs) or lung DCs (Loving et al., 2006a) resulted in transcription of IFNβ. However, transcription of interferon-stimulated genes, including IFNα, was not upregulated which led to the assumption that IFNβ may be transcribed but not translated (Loving et al., 2006a) thus preventing downstream signaling events. However, the assumed lack of translation of IFNβ remains to be confirmed.

Previously, we have demonstrated the antiviral effects of recombinant IFNβ (rswIFNβ) against PRRSV (Overend et al., 2007) which is consistent with similar findings using IFNα (Lee et al., 2004). As shown with IFNα (Lee and Kleiboeker, 2005), our study also suggested differences in sensitivity to rswIFNβ among PRRSV isolates. MARC-145, an extensively used cell line in the studies of PRRSV-host cell interactions including type I IFN and type II IFN antiviral mechanisms, are of simian origin, and are likely not an appropriate model for such studies. Consequently, the present study was undertaken to define differences between MARC-145 cells and PAMs regarding type I IFN-induced activation. Differences between cell types in sensitivity to IFN type I and effects of 2-aminopurine (2-AP), an inhibitor of double-stranded RNA-dependent protein kinase (PKR), on viral replication are discussed.

Field isolate Mo25544 kindly provided by Dr. Steve Kleiboeker (University of Missouri), PDV130-9301 (NVSL, Ames, IO) and a vaccine virus (RespPRRS Boehringer Ingelheim Vetmedica, Inc., St Joseph, MO) were examined in the study. MARC-145 cells, passage 49–55, were used for bioassays, propagation and titration of viruses. The cells were cultured and maintained in Dulbecco's Modified Eagles Medium (DMEM) supplemented with 10% fetal bovine serum (FBS), 0.35% glucose, 2 mM L-glutamine, 2.5 μg/ml fungizone, 100 U/ml penicillin and 100 μg/ml streptomycin. Cells were kept at 37 °C in a humidified 5% CO_2 incubator.

Alveolar macrophages (PAMs) were collected by bronchioalveolar lavage from lungs of PRRSV-negative, 4–6-week-old pigs as previously described (Overend et al., 2007). The PAMs were resuspended in RPMI-1640 with 10% FBS, 2 mM l-glutamine, 1 μg/ml fungizone, 100 U/ml penicillin and 100 μg/ml streptomycin. Before use, the PAM were confirmed to be PRRSV-free by real time RT-PCR. For testing, the cells were plated at a density of 1×10^6 cells/well in 24-well culture plates. The PAM cultures were incubated for 24 h at 37 °C in a humidified 5% CO_2 incubator and washed once with RPMI-1640 complete media before use.

A recombinant replication-defective adenovirus expressing swine IFNβ (Ad5swIFNβ) was the source of rswIFNβ for the study (Chinsangaram et al., 2003). The recombinant virus was propagated in HEK-293 cells (ATCC) with DMEM media containing glucose, antibiotics and 5–10% FBS. Forty-eight to seventy-two hours post-infection (hpi), rswIFNβ-containing culture fluids were harvested. The media was centrifuged at 100,000 × *g* for 2 h. The resulting supernatant was acidified to pH 2.0 for 18–20 h at 4 °C and then neutralized to pH 7.2 and stored at −80 °C until further use. Culture fluids from control Ad5 virus (Ad5Blue)-infected HEK-293 cells were processed identically and used as a negative control.

Bioassays were performed as previously described by Overend et al. (2007). Briefly, MARC-145 cells or PAM were primed with concentrations of either rswIFNβ, ranging from 20 to 1000 U/well, or an equivalent dilution of Ad5Blue control culture supernatant and then incubated for 20 h. Cells were inoculated with PRRSV isolates at 1000 $TCID_{50}$/well. After 2 h of incubation and washing with serum-free media, media with 2% FBS was added to maintain the cells. Samples were harvested 48 hpi for titration in MARC-145 cells. The activity of rswIFNβ (Units/ml) was based on protection of MARC-145 cells (PD_{50}) from infection with a PRRSV isolate previously determined to be sensitive to rswIFNβ (Overend et al., 2007). The dilution giving 50% protection from infection to the cells was assessed a value of I U from which the titer of the stock preparation (U/ml) was calculated. Confluent MARC-145 cells or PAMs seeded in 24-well plates were primed with rswIFNβ diluted in serum-free DMEM and incubated for 20 h. The cells were inoculated with PRRSV isolates at 1000 $TCID_{50}$/well. After 2 h incubation and subsequent washes, media with 2% FBS, with or without 8 mM 2-AP, was added to maintain the cells. At 48 hpi supernatants and cell pellets were harvested and titrated in MARC-145 cells.

The activation of innate antiviral activity induced by rswIFNβ against PRRSV was comparatively examined in MARC-145 cells and PAMs. Marked differences between the cell types were revealed in the bioassays indicating that increased scrutiny is needed when performing assays in the MARC-145 cell model. The results in MARC-145 cells showed consistently that isolate Mo25544 was sensitive to rswIFNβ while the vaccine strain and the PDV130-9301 isolate were resistant, albeit to different extents (Fig. 1A). Though the vaccine virus was shown before to be sensitive to rswIFNβ in MARC-145 cells (Overend et al., 2007), a dose-dependent resistance was revealed in the present study when rswIFNβ was titrated. In contrast, all isolates tested (PDV130-9301, Mo25544, and vaccine virus) were completely sensitive to all the concentrations of rswIFNβ utilized in PAMs (Fig. 1B). Previous work has demonstrated that the antiviral effects on the cells are induced specifically by rswIFNβ as demonstrated by neutralization of antiviral activities by an anti-rswIFNβ monoclonal antibody (Overend et al., 2007). This study also showed that culture supernatants from HEK-293 cells infected with the empty Ad5 vector had no antiviral effect (Overend et al., 2007). Though type I IFNs are associated with an antiviral function against PRRSV (Lee et al., 2004; Loving et al., 2006a; Overend et al., 2007) the sensitivity of the virus to type I IFN is highly variable. The importance of sensitivity or resistance to type I IFN in the pathogenesis of PRRS remains to be determined. Also, the reasons for the observed differences in rswIFNβ-induced antiviral activation between these cells are presently unknown. A possible explanation is that the relative sensitivity of cells to IFN derived from the same species much greater than to heterologous IFN (Gifford, 1963; Moehring and Stinebring, 1970; Veomett

Please cite this article in press as: He, D., et al., Marked differences between MARC-145 cells and swine alveolar macrophages in IFNβ-induced activation of antiviral state against PRRSV. Vet. Immunol. Immunopathol. (2010), doi:10.1016/j.vetimm.2010.07.023

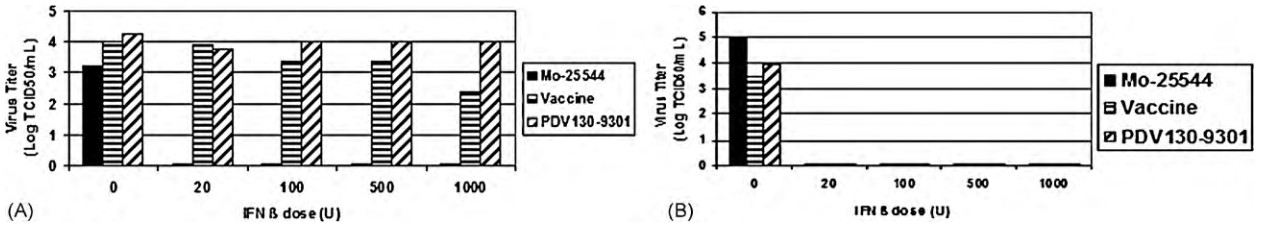

Fig. 1. Dose–dependent sensitivity of various PRRSV isolates to rswIFNβ in MARC-145 (A) cells or PAMs (B). Cells seeded in 24-well culture plates were primed with rswIFNβ at different concentrations (ranging from 20 to 1000 U/well in 100 μL media) and incubated for 20 h. The cells were then inoculated with the indicated isolates (1000 $TCID_{50}$/well) for 2 h. The cells were then rinsed and replenished with media containing 2% FBS. Culture fluids and cells were harvested 48 hpi for titration in MARC-145 cells. Each virus isolate was titrated directly in untreated MARC-145 cells to serve as positive controls and non-infected cells served as negative controls. Titers are in $TCID_{50}$/ml. Zero hour time point control samples (4th wash collected) contained no detectable virus (data not shown).

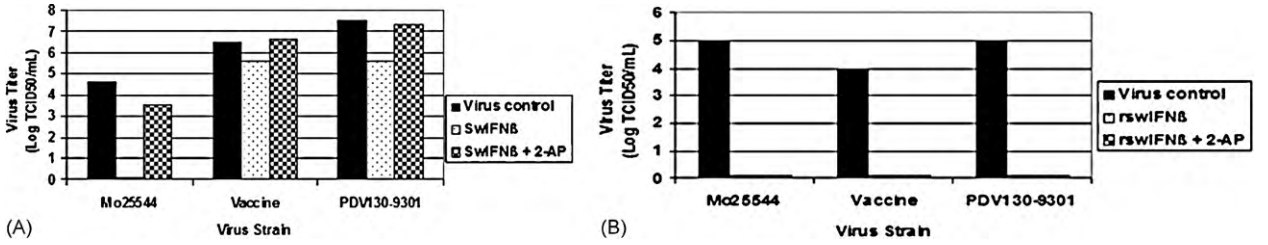

Fig. 2. Effect of 2-AP on PRRSV replication in rswIFNβ-primed MARC-145 cells or PAMs. Confluent MARC-145 cells (A) or PAMs (B) seeded in 24-well plates, were primed with rswIFNβ at 500 U and incubated for 20 h. Cells were challenged with the indicated isolates at 1000 $TCID_{50}$/well for 2 h. After rinsing, media containing 2% FBS, with or without 8 mM 2-AP was added. Culture fluids and cells were collected 48 hpi and titrated on MARC-145 cells. Titers are in $TCID_{50}$/ml. Zero hour time point control samples (4th wash collected) contained no detectable virus (data not shown).

and Veomett, 1979). Further investigation is required to acquire a better understanding of the observed effects on host cells in this system.

A previous study showed that PRRSV replication was inhibited by IFNγ and was partially recovered by addition of 2-AP (Rowland et al., 2001). These observations indicate that PKR is important in the antiviral response of MARC-145 cells against PRRSV. In the current study, the effect of 2-AP on virus replication in rswIFNβ-primed cells was markedly different between these two cells. Treatment of rswIFN β-primed and PRRSV-infected MARC-145 cells with 2-AP restored the replication of the rswIFN β-sensitive isolate (Mo25544), and to some extent those of the vaccine virus and the rswIFNβ-resistant isolate (PDV130-9301) (Fig. 2A). Thus, the results with MARC-145 cells are consistent with PKR being a mechanism of type I IFN-induced cell protection, specifically induced by rswIFNβ. In contrast, an identical treatment of rswIFN β-primed PAMs with 2-AP had no effect on the antiviral state induced resulting in failure to rescue replication of any of the viruses (Fig. 2B). These findings are consistent with a recent report that highlighted differences between poly I:C treated PAMs and peritoneal macrophages (PMs), exhibiting no induction of PKR in the former, and a profound expression in the latter (Loving et al., 2006b). Similarly, Gudmundsdottir and Risatti (2009) reported a lack of PKR expression in PAMs following PRRSV infection. At this point, it is unknown which interferon-stimulated genes are responsible for conferring the observed antiviral state against PRRSV in PAMs. However, while the specific mechanism of swIFNβ-induced protection in PAMs remains uncertain, this study indicates that PKR is not involved in establishing it.

A further understanding of the mechanisms of type I IFN suppression observed in PRRSV-infected animals (Albina et al., 1998; Buddaert et al., 1998), a phenomenon that is becoming increasingly accepted as a contributing mechanism in the virulence and pathogenesis of PRRS, is crucial to the development of effective control measures. Analysis of the differences in sensitivity to rswIFNβ in different cells, observed here, underscores the importance of utilizing appropriate, natural host cells when studying PRRSV. Despite challenges associated with utilizing primary cells versus established cell lines, doing so will provide relevant insights into potential mechanisms of virus/host cell interactions and immune evasion by PRRSV. In this study all the experiments were replicated at least three times utilizing PAMs from different animals with consistent results.

Conflict of interest

On behalf of all co-authors, the corresponding author affirms that there is no conflict of interest with this publication.

Acknowledgements

This work was supported by funds from the Specific Cooperative Agreement #58-1940-2-245 between the University of Connecticut and the USDA, ARS, the Hatch Multistate Integrated Control and Elimination of PRRS (NC229) Project CNS00860 and USDA Grant 20043520414267. The authors thank Dr. Lynn Rust formerly PI of the latter grant for helpful discussions and facilitation of this work.

Please cite this article in press as: He, D., et al., Marked differences between MARC-145 cells and swine alveolar macrophages in IFNβ-induced activation of antiviral state against PRRSV. Vet. Immunol. Immunopathol. (2010), doi:10.1016/j.vetimm.2010.07.023

References

Albina, E., Carrat, C., Charley, B., 1998. Interferon-alpha response to swine arterivirus (PoAV), the porcine reproductive and respiratory syndrome virus. J. Interferon. Cytokine Res. 18 (7), 485–490.

Alexopoulou, L., Holt, A.C., Medzhitov, R., Flavell, R.A., 2001. Recognition of double-stranded RNA and activation of NF-kappaB by toll-like receptor 3. Nature 413, 732–738.

Aasted, B., Bach, P., Nielsen, J., Lind, P., 2002. Cytokine profiles in peripheral blood mononuclear cells and lymph node cells from piglets infected in utero with porcine reproductive and respiratory syndrome virus. Clin. Diagn. Lab. Immunol. 9 (6), 1229–1234.

Bautista, E.M., Molitor, T.W., 1999. IFN gamma inhibits porcine reproductive and respiratory syndrome virus replication in macrophages. Arch. Virol. 144 (6), 1191–1200.

Buddaert, W., Van Reeth, K., Pensaert, M., 1998. In vivo and in vitro interferon (IFN) studies with the porcine reproductive and respiratory syndrome virus (PRRSV). Adv. Exp. Med. Biol. 440, 461–467.

Chinsangaram, J., Moraes, M.P., Koster, M., Grubman, M.J., 2003. Novel viral disease control strategy Adenovirus expressing alpha interferon rapidly protects swine from foot-and-mouth disease. J. Virol. 77 (2), 1621–1625.

Genini, S., Delputte, P.L., Malinverni, R., Cecere, M., Stella, A., Nauwynck, H.J., Giuffra, E., 2008. Genome-wide transcriptional response of primary alveolar macrophages following infection with porcine reproductive and respiratory syndrome virus. J. Gen. Virol. 89, 2550–2564.

Gifford, G.E., 1963. Studies on the specificity of interferon. J. Gen. Microbiol. 33, 437–443.

Gudmundsdottir, I., Risatti, G.R., 2009. Infection of porcine alveolar macrophages with recombinant chimeric porcine reproductive and respiratory syndrome virus: effects on cellular gene expression and virus growth. Virus Res. 145 (1), 145–150.

Horter, D.C., Pogranichniy, R.M., Chang, C.C., Evans, R.B., Yoon, K.J., Zimmerman, J.J., 2002. Characterization of the carrier state in porcine reproductive and respiratory syndrome virus infection. Vet. Microbiol. 86, 213–228.

Keffaber, K.K., 1989. Reproductive failure of unknown etiology. Am. Assoc. Swine Pract. Newsl. 1, 1–9.

Lee, S.M., Schommer, S.K., Kleiboeker, S.B., 2004. Porcine reproductive and respiratory syndrome virus field isolates differ in in vitro interferon phenotypes. Vet. Immunol. Immunopathol. 102 (3), 217–231.

Lee, S.M., Kleiboeker, S.B., 2005. Porcine arterivirus activates the NF-κB pathway through IκB degradation. Virology 342, 47–59.

Loving, C.L., Brockmeier, S.L., Sacco, R.E., 2006a. Differential type I interferon activation and susceptibility of dendritic cell populations to porcine arterivirus. Immunology 120, 217–229.

Loving, C.L., Brockmeier, S.L., Ma, W., Richt, J.A., Sacco, R.E., 2006b. Innate cytokine responses in porcine macrophage populations: evidence for differential recognition of double-stranded RNA. J. Immunol. 177, 8432–8439.

Meier, W.A., Galeota, J., Osorio, F.A., Husmann, R.J., Schnitzlein, W.M., Zuckermann, F.A., 2003. Gradual development of the interferon-gamma response of swine to porcine reproductive and respiratory syndrome virus infection or vaccination. Virology 309, 18–31.

Mengeling, W.L., Lager, K.M., Vorwald, A.C., Koehler, K.J., 2003. Strain specificity of the immune response of pigs following vaccination with various strains of porcine reproductive and respiratory syndrome virus. Vet. Microbiol. 93, 13–24.

Moehring, J.M., Stinebring, W.R., 1970. Examination of "species specificity" of avian interferons. Lett. Nat. 226, 360–361.

Murtaugh, M.P., Xiao, Z., Zuckermann, F., 2002. Immunological responses of swine to porcine reproductive and respiratory syndrome virus infection. Viral Immunol. 15, 533–547.

Overend, C., Mitchell, R., He, D., Rompato, G., Grubman, M.J., Garmendia, A.E., 2007. Recombinant swine beta interferon protects swine alveolar macrophages and MARC-145 cells from infection with porcine reproductive and respiratory syndrome virus. J. Gen. Virol. 88, 925–931.

Rowland, R.R., Robinson, B., Stefanick, J., Kim, T.S., Guanghua, L., Lawson, S.R., Benfield, D.A., 2001. Inhibition of porcine reproductive and respiratory syndrome virus by interferon-gamma and recovery of virus replication with 2-aminopurine. Arch. Virol. 146, 539–555.

Royaee, A.R., Husmann, R.J., Dawson, H.D., Calzada-Nova, G., Schmitzlein, W.M., Zuckermann, F.A., Lunney, J.K., 2004. Deciphering the involvement of innate immune factors in the development of the host response to PRRSV vaccination. Vet. Immunol. Immunopathol. 102, 199–216.

Samuel, C.E., 2001. Antiviral actions of interferons. Clin. Microbiol. Rev. 14, 778–809.

Veomett, M.J., Veomett, G.E., 1979. Species specificity of interferon action: maintenance and establishment of the antiviral state in the presence of a heterospecific nucleus. J. Virol. 31 (3), 785–794.

Xiao, Z., Batista, L., Dee, S., Halbur, P., Murtaugh, M.P., 2004. The level of virus-specific T-cell and macrophage recruitment is independent of virus load. J. Virol. 78, 5923–5933.

Return to Table of Contents

Please cite this article in press as: He, D., et al., Marked differences between MARC-145 cells and swine alveolar macrophages in IFNβ-induced activation of antiviral state against PRRSV. Vet. Immunol. Immunopathol. (2010), doi:10.1016/j.vetimm.2010.07.023

FOODBORNE PATHOGENS AND DISEASE
Volume 7, Number 4, 2010

DOI: 10.1089/fpd.2009.0372

Transcriptome Analysis of Genes Controlled by *luxS*/Autoinducer-2 in *Salmonella enterica* Serovar Typhimurium

Palmy R. Jesudhasan,[1] Martha L. Cepeda,[1] Kenneth Widmer,[1] Scot E. Dowd,[2] Kamlesh A. Soni,[1] Michael E. Hume,[1,3] James Zhu,[4] and Suresh D. Pillai[1]

Abstract

The enteric pathogen *Salmonella enterica* serovar Typhimurium uses autoinducer-2 (AI-2) as a signaling molecule. AI-2 requires the *luxS* gene for its synthesis. The regulation of global gene expression in *Salmonella* Typhimurium by *luxS*/AI-2 is currently not known; therefore, the focus of this study was to elucidate the global gene expression patterns in *Salmonella* Typhimurium as regulated by *luxS*/AI-2. The genes controlled by *luxS*/AI-2 were identified using microarrays with RNA samples from wild-type (WT) *Salmonella* Typhimurium and its isogenic *ΔluxS* mutant, in two growth conditions (presence and absence of glucose) at mid-log and early stationary phases. The results indicate that *luxS*/AI-2 has very different effects in *Salmonella* Typhimurium depending on the stage of cell growth and the levels of glucose. Genes with $p \leq 0.05$ were considered to be significantly expressed differentially between WT and *ΔluxS* mutant. In the mid-log phase of growth, AI-2 activity was higher (1500-fold) in the presence of glucose than in its absence (450-fold). There was differential gene expression of 13 genes between the WT and its isogenic *ΔluxS* mutant in the presence of glucose and 547 genes in its absence. In early stationary phase, AI-2 activity was higher (650-fold) in the presence of glucose than in its absence (1.5-fold). In the presence of glucose, 16 genes were differentially expressed, and in its absence, 60 genes were differentially expressed. Our microarray study indicates that both *luxS* and AI-2 could play a vital role in several cellular processes including metabolism, biofilm formation, transcription, translation, transport, and binding proteins, signal transduction, and regulatory functions in addition to previously identified functions. Phenotypic analysis of *ΔluxS* mutant confirmed the microarray results and revealed that *luxS* did not influence growth but played a role in the biofilm formation and motility.

Introduction

Quorum sensing, a form of cell-to-cell communication in bacteria, involves signaling molecules called autoinducers (AIs) through which bacteria respond to their environment based on their cell density (Pillai and Jesudhasan, 2006). Among the various quorum sensing systems (Whiteley *et al.*, 1999; Winzer and Williams, 2001; Sperandio *et al.*, 2003; Xavier and Bassler, 2003; Miller *et al.*, 2004) used by bacteria, the AI-2 system is used by both Gram-positive and Gram-negative bacteria and requires the *luxS* gene for the synthesis of the signaling molecule. AI-2, a derivative of 4,5-dihydroxy-2,3-pentanedione, has been found to exist in two interconvertible structures (Xavier and Bassler, 2005)—a furanosyl borate diester (2S,4S)-2-methyl-2,3,4-tetrahydroxytetrahydrofuran (*S*-THMF) in *Vibrio harveyi* (Chen *et al.*, 2002; Miller *et al.*, 2004) and a nonboronated form (2R,4S)-2-methyl-2,3,4-tetrahydroxytetrahydrofuran (*R*-THMF) in *Salmonella* Typhimurium (Miller *et al.*, 2004), a foodborne pathogen. *Salmonella* Typhimurium is known to detect and produce the cell signaling molecule AI-2, which is produced from *S*-adenosylmethionine by a three-enzymatic step reaction, of which the last step is catalyzed by *luxS*. AI-2 is known to regulate several key functions such as motility, biofilm formation, virulence, antibiotic production, and cell division in several pathogenic bacteria (Sperandio *et al.*, 1999, 2001;

[1]Food Safety and Environmental Microbiology Program, Departments of Poultry Science and Nutrition and Food Science, Texas A&M University, College Station, Texas.
[2]Medical Biofilm Research Institute, Lubbock, Texas.
[3]Food and Feed Safety Research Unit, Southern Plains Agricultural Research Center, Agricultural Research Service, U.S. Department of Agriculture, College Station, Texas.
[4]Plum Island Animal Disease Center, U.S. Department of Agriculture, Orient Point, New York.

Fong *et al.*, 2001, 2003; Lyon *et al.*, 2001; Miller *et al.*, 2002; McNab *et al.*, 2003).

LuxS has been identified in more than 55 species of bacteria including Gram-positive and Gram-negative bacteria (Surette and Bassler, 1999; Xavier and Bassler, 2003). Studies have shown that in *Salmonella* Typhimurium, *luxS* is responsible for the regulation of the *lsr* operon that helps in the internalization of AI-2. This has been hypothesized to be a mechanism to control AI-2 levels in the vicinity of a cell or to prevent AI-2 signaling by other bacterial species in its environment (Taga *et al.*, 2003). Recently it has been reported that in *Salmonella* Typhimurium, *luxS* is also responsible for virulence gene expression (Choi *et al.*, 2007) and polarization of the flagellar phase variation (Karavolos *et al.*, 2008). We have previously shown using microarray studies that AI-2 influenced virulence in *Salmonella* Typhimurium (Widmer *et al.*, 2007). We have also shown using proteomic analysis of *Salmonella* Typhimurium that AI-2 is responsible for a variety of cellular processes (Soni *et al.*, 2008).

In this study, global gene regulation by *luxS*/AI-2 in *Salmonella* Typhimurium was identified by comparing gene expression of *Salmonella* Typhimurium strain 87-26254 wild type (WT) and its isogenic *ΔluxS* mutant in two growth conditions at both mid-log and early stationary phase using microarrays. Genes regulated by AI-2 were identified by comparing gene expression in a *ΔluxS* mutant of *Salmonella* Typhimurium and *ΔluxS* mutant supplemented with cell-free supernatant of WT *Salmonella* Typhimurium. Phenotypic studies were conducted to examine the effects of *luxS* mutation on cell growth, motility, and biofilm formation.

Materials and Methods

Bacterial strains and growth conditions

The bacterial strain used in this study was *Salmonella* Typhimurium (accession no. 87-26254), a poultry isolate obtained from the National Veterinary Service Laboratory, Ames, IA. A *ΔluxS* mutant of this strain, designated PJ002 (*luxS*::*cat*), was subsequently generated in our laboratory (Widmer *et al.*, 2007). *Escherichia coli* no. 5, an environmental isolate, was used as a positive control for the AI-2 bioassays because of its ability to produce elevated levels of the AI-2 (Qin *et al.*, 2004). Strains of *Salmonella* Typhimurium (87-26254 and PJ002) and *E. coli* no. 5 were grown at 37°C in Luria–Bertani (LB) broth and LB broth plus 0.5% glucose. *V. harveyi* strain BB170 (*luxN*::Tn*5* sensor 1^-, sensor 2^+), a reporter used to determine AI-2 activity, was grown at 30°C with aeration in AI bioassay medium (Bassler *et al.*, 1993).

Preparation of cell-free supernatant

Overnight cultures of *Salmonella* Typhimurium (87-26254 and PJ002) grown in LB broth at 37°C were inoculated in 100 mL LB broth and in LB broth with 0.5% glucose (1:100) and grown at 37°C with shaking (250 rpm). Cell-free supernatants (CFS) were collected at different time points by removing the cells from the growth medium by centrifugation at 10,000 *g* for 2 min. The supernatants were then passed through 0.22 μm syringe filters (Corning®, Corning, NY) and stored at −20°C. CFS of *E. coli* no. 5 grown in fresh LB broth with 0.5% glucose was prepared from 3.5-h culture using the same procedure that was used for *Salmonella* Typhimurium.

Bioluminescence assay

Salmonella Typhimurium CFS obtained from both WT and mutant grown in LB broth and LB broth with 0.5% glucose were tested for the presence of AI-2 activity using the *V. harveyi* reporter strain BB170, which responds only to AI-2 (Surette and Bassler, 1998). Luminescence assays were performed as outlined elsewhere (Surette and Bassler, 1998). Luminescence was measured by quantifying light production of *V. harveyi* with a Wallac Victor 1420 multilabel counter (Perkin Elmer, Boston, MA). The ratios of the luminescence of the test samples (reporter strain with *Salmonella* Typhimurium CFS) to the control (reporter strain without CFS) were reported as relative AI-2 activity (fold induction).

Growth curves

Overnight cultures of WT and mutant grown at 37°C were inoculated (1:100) in fresh LB medium and fresh LB medium supplemented with 0.5% glucose. Two hundred microliters of the bacterial suspensions was added to each well of 96-well microtiter plate (Corning) and maintained for 8 h at 37°C in a Tecan plate reader (Tecan U.S. Research, Triangle Park, NC). Optical density at 600 nm of each sample was measured every 10 min. Before each measurement, the plate was shaken at low speed for 7 min to prevent settling of the culture. Sixteen wells were used for each treatment, and the experiment was repeated twice. Growth curves were generated in Excel (Microsoft, Redmond, WA) by plotting the average OD against time.

Swimming and swarming assay

The swimming and swarming motility assays were performed in LB broth (Difco) containing 0.3% and 0.5% agar, respectively, both in the presence and absence of 0.5% glucose. The overnight cultures of WT and mutant strains grown in LB broth were inoculated with sterile toothpicks in the center of swimming and swarming assay plates and incubated for 7 h at 37°C. The diameters of the motility halos were measured. At least five replicate plates were used for each condition, and statistical significance was calculated using Student's *t*-test.

Biofilm assay

The biofilm assay was performed in sterile round-bottom 96-well polystyrene plates (Nalge Nunc International, Rochester, NY) according to O'Toole and Kolter (1998) with some modifications. Overnight cultures of WT and mutant strains were diluted 1:100 in LB medium and LB medium supplemented with 0.5% glucose, and 100 μL of the aliquots was added to eight wells. The plates were incubated at 37°C for 36 h without shaking. After incubation, the suspension cultures were removed, and the plates were washed with distilled water. The biofilms were stained with 125 μL of 0.1% crystal violet (Fisher, Hanover Park, IL) per well for 15 min. The excess dye was removed by washing with distilled water. Dye associated with attached biofilms was dissolved in 200 μL of 95% ethanol, and 125 μL was transferred to an optically clear flat-bottom 96-well plate (Corning), and OD_{590} was measured.

Total RNA isolation

Overnight cultures of *Salmonella* Typhimurium WT and mutant strains were inoculated in LB broth and LB broth with

0.5% glucose at 37°C. Cells were grown in triplicate and harvested at mid-log and early stationary phase (3 and 7 h, respectively) for RNA extraction. Total RNA was isolated from the cultures using an RNeasy mini kit (Qiagen, Valencia, CA) according to the manufacturer's protocol. RNAprotect bacteria reagent (Qiagen) was added to the cultures to stabilize the RNA before isolation. The RNase-free DNase set (Qiagen) was used for on-column DNase digestion to remove residual genomic DNA. The quantity and quality of RNA were examined using a ND-1000 spectrophotometer (NanoDrop® Technologies, Wilmington, DE) and bioanalyser 2100 (Agilent Technologies, Palo Alto, CA), respectively.

cDNA synthesis and labeling

cDNA synthesis and purification were performed using "microbial RNA aminoallyl labeling" (ftp://ftp.jcvi.org/pub/data/PFGRC/pdf_files/protocols/M007.pdf), a standard operating procedure of The J. Craig Venter Institute (JCVI, formerly The Institute for Genomic Research). Ten micrograms of total RNA was used to synthesize cDNA using a random primer for reverse transcription (Invitrogen, Carlsbad, CA). Purified cDNAs from the WT and mutant were each labeled with Cy-3 mono-Reactive Dye and Cy-5 mono-Reactive Dye (GE Health Care, Piscataway, NJ) and were processed using a dye-swapping design. A total of 12 microarray slides were used for each time point. The 12 slides were divided as follows: four slides (technical replicates) were used for each of the three biological replicates. Each set of four slides had a different DNA sample. Among the four slides that used the same DNA, two slides had the same dye, and the dye was swapped for the other two. The labeling mixtures were purified using a QIAquick PCR purification kit (Qiagen).

Microarray hybridization, washing, and scanning

Salmonella Typhimurium LT2 genome microarrays (Versions 4) developed by JCVI and provided by the Pathogen Functional Genome Resource Center of the National Institutes of Health were used in this study. These arrays are 70 mer-oligo arrays consisting of 4504 open reading frames each in five replicate spots. Equal amounts of labeled cDNA from the treatment and control were used to hybridize the arrays. The labeled cDNA was hybridized following "hybridization of labeled cDNA probes" (ftp://ftp.jcvi.org/pub/data/PFGRC/pdf_files/protocols/M008.pdf), a standard operating procedure used at JCVI. The hybridization was carried out overnight at 42°C in a water bath using Corning hybridization chamber. After hybridization, the slides were washed and scanned using a GenePix 4100A scanner (Molecular Devices Corporation, Sunnyvale, CA) at 532 nm (Cy3 channel) and 635 nm (Cy5 channel), and the images were stored for further analysis.

Microarray data analysis

The data from three individual experiments (four slides per experiment including dye swap) were initially filtered for spot quality (signal uniformity, signal to background ratio, threshold intensity) using GenePix Pro 5.0 (Axon). Visually flagged spots as well as spots with a median signal value less than the sum of the local background median plus three standard deviations were omitted from analysis (Hegde *et al.*, 2000). Array data were normalized, and their statistical significance was evaluated using Acuity 4.0 (Molecular Devices). To identify genes differentially expressed between different treatment groups, a Student's *t*-test was performed and the false discovery rate was calculated using the Benjamini–Hochberg method (Benjamini and Hochberg, 1995) in Acuity. Genes with $p \leq 0.05$ were considered to be significantly expressed differentially between WT and *ΔluxS* mutant. The microarray data analysis procedures used in this study were fully minimum information about a microarray experiment compliant. The complete dataset and raw data are available at NCBI Gene Expression Omnibus database (accession no. GSE7558). Although a twofold cutoff is generally used for the analysis of microarray data, a less than twofold change in relative transcript levels can be biologically significant (Hughes *et al.*, 2000; Ichikawa *et al.*, 2000). Hence, genes that are significantly up- or downregulated with a lesser cutoff induction ratio have been included in Tables 2–5.

Supportive microarray studies

Genes identified in the microarray studies could be regulated either by *luxS* or AI-2. To identify the genes influenced by AI-2, another microarray study was conducted using the *ΔluxS* mutant (PJ002) with CFS from WT (wCFS) and mutant CFS (mCFS). The AI-2 activity of both wCFS and mCFS was measured using the AI-2 bioassay. Overnight culture of PJ002 was inoculated (1:100) in fresh LB broth with 10% of wCFS (treatment) and LB broth with 10% of mCFS (control) and grown at 37°C for RNA extraction. Cells were grown in triplicate and harvested after 3 h of growth. Total RNA was isolated from the cultures using an RNeasy mini kit (Qiagen) according to the manufacturer's protocol. Synthesis of cDNA, labeling, hybridizations, scanning of slides, and data analysis were performed using the same procedures as described above. Genes with $p \leq 0.05$ were considered to be significantly expressed differentially between wCFS and mCFS.

Quantitative real-time reverse transcriptase–polymerase chain reaction

Quantitative real-time polymerase chain reaction (PCR) was used to validate microarray results. Relative transcript levels of selected genes were measured using SYBR® Green PCR kit (Applied Biosystems) according to the manufacturer's recommendations. Aliquots from the same RNA samples (three biological replicates) used for microarray experiments were used for cDNA synthesis and subsequent quantitative real-time reverse transcriptase PCR (QRT-PCR). For each of the genes tested, primers were designed using Primer Express software (Applied Biosystems) to amplify products from 75 to 150 bp. 16S rRNA gene fragment was used as an internal control to normalize expression values. The reactions were performed on an ABI Prism 7900HT Sequence Detection System (Applied Biosystems) with the following cycle parameters: one cycle of 95°C for 10 min, followed by 40 cycles of 95°C for 15 sec and 60°C for 1 min. The difference (fold change) in the initial concentration of each transcript (normalized to 16S rRNA) with respect to the WT was calculated according to the comparative C_T method according to the $2^{-\Delta\Delta C_T}$ calculation (Livak and Schmittgen, 2001). A melting curve was completed following each reaction to confirm that no template-independent amplification was present.

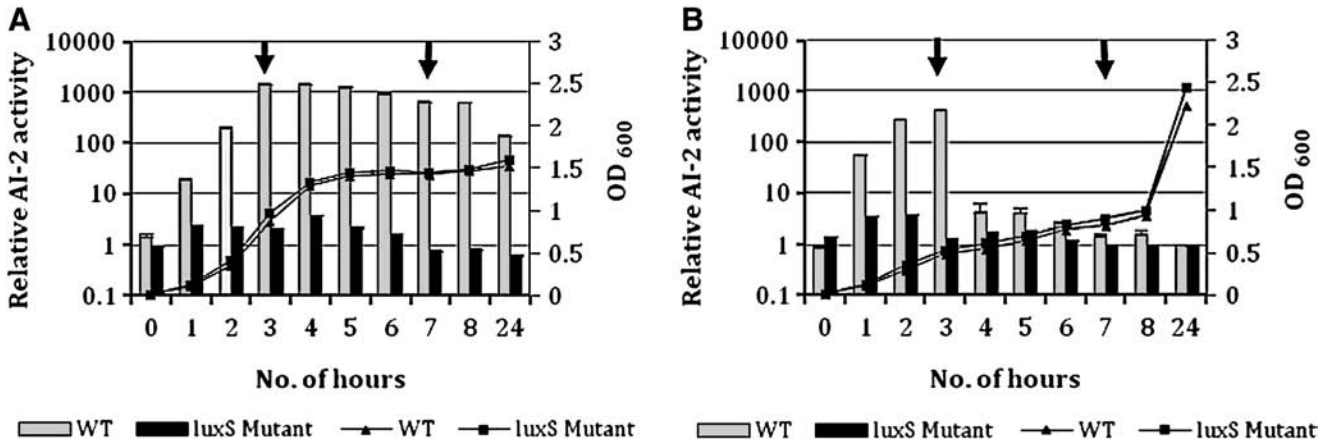

FIG. 1. Growth and autoinducer-2 (AI-2) activity of *Salmonella* Typhimurium wild type (WT) and its isogenic *ΔluxS* mutant (PJ002). (**A**) Luria–Bertani (LB) medium supplemented with glucose 0.5%; (**B**) LB medium without glucose. The assays were carried out in triplicate. Bars indicate AI-2 activity, and lines indicate growth. Each bar represents mean ± standard error of the mean of all the measurements. Arrows point to the time points at which samples were collected for RNA extraction.

Results

Bioluminescence assay

The bioluminescence bioassay used to check the AI-2 activity showed higher activity in WT in the presence of glucose (1500-fold) (Fig. 1A, B) in the mid-log phase (3 h) than in its absence (450-fold). In the early stationary phase (7 h), AI-2 activity was still high in the presence of glucose (650-fold) but was comparatively very low in the absence of glucose (1.5-fold). The *Salmonella* Typhimurium *ΔluxS* mutant PJ002 did not produce luminescence in both the presence and absence of glucose (Fig. 1A, B), confirming that the PJ002 strain does not produce AI-2 molecules in the absence of the *luxS* gene.

Effect of luxS *gene deletion on growth, motility, and biofilm formation in* Salmonella *Typhimurium*

Presence or absence of glucose did not affect the growth rates of both the *ΔluxS* mutant and its isogenic parent. Swimming and swarming motility was significantly ($p < 0.05$) reduced in the *ΔluxS* mutant strain compared with the WT (Fig. 2). Moreover, the mutant strain also formed less biofilm than the WT significantly ($p < 0.0001$) both in LB medium and LB medium supplemented with 0.5% glucose (Fig. 3). Significant inhibition in motility ($p < 0.05$) and biofilm formation ($p < 0.0001$) was observed in the WT in the presence of glucose (Figs. 2 and 3) due to catabolite repression. Microarray analysis revealed that in the absence of glucose, 27 of the 35 motility-related genes (Table 2) and 9 of the 13 biofilm formation–related genes (Table 3) were downregulated in the mid-log phase in the absence of both *luxS* and AI-2. Eleven motility-related genes and four biofilm formation–related genes had the same direction of regulation (downregulation) in both the microarray studies and the confirmatory microarray studies, indicating that these genes could be regulated by AI-2 (Tables 2 and 3).

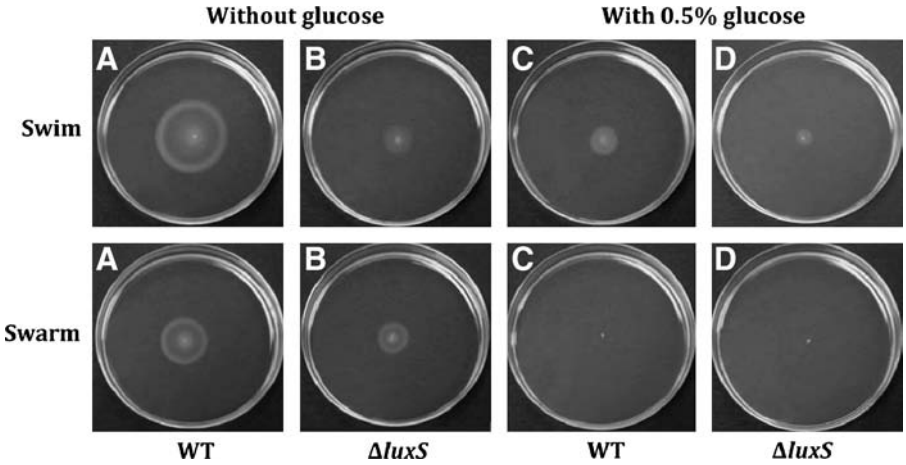

FIG. 2. Effect of *luxS* deletion on *Salmonella* Typhimurium motility. Swimming and swarming zones were measured 7 h after inoculating 0.3% and 0.6% LB agar plates, respectively, in both absence and presence of glucose (0.5%). Zone diameters (mean ± standard deviations; $n = 5$) are listed for each strain. The zone diameters for each strain in swimming motility (**A**) WT (30.5 ± 6.5), (**B**) *ΔluxS* (15.0 ± 1.6), (**C**) WT (13.2 ± 2.3), and (**D**) *ΔluxS* (10.7 ± 1.6); swarming motility (**A**) WT (22.7 ± 3.5), (**B**) *ΔluxS* (16.2 ± 1.5), (**C**) WT (0), and (**D**) *ΔluxS* (0) are shown. Mutant was deficient in motility both in the presence and absence of glucose.

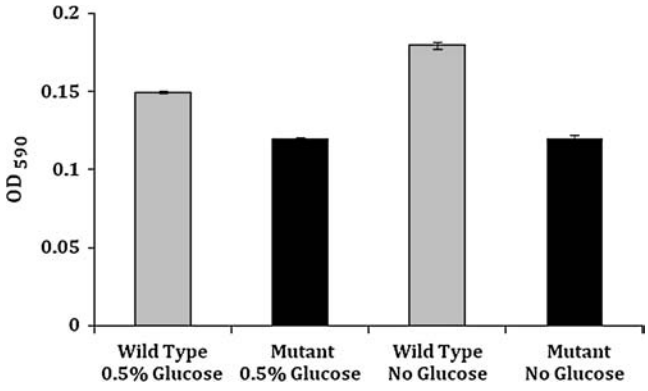

FIG. 3. Effects of *luxS* mutation and glucose on biofilm (mean OD ± SE; $p < 0.0001$, $n = 3$) formation in *Salmonella* Typhimurium. Biofilm assays were performed in 96-well plates, and eight wells were assigned for each strain and condition. Biofilms of WT and *ΔluxS* mutant were determined using crystal violet binding assay after 36 h of growth at 37°C in the presence and absence of glucose. Each bar represents mean ± standard error of the mean of all the measurements. Presence of glucose inhibited biofilm formation in WT. Mutant was deficient in biofilm formation both in the presence and absence of glucose.

Microarray identification of luxS*-regulated genes*

Differential expression of genes in LB medium without glucose was about 12% of the entire transcriptome (547 genes) at mid-log phase. This was substantially higher than differential regulation of genes (13 genes) in LB medium with glucose (Table 1). At early stationary phase, the gene modulation pattern was similar to that at mid-log phase with a higher number of genes differentially expressed in LB medium without glucose (60 genes) (data not shown) than in LB medium with glucose (16 genes) (Table 1). Of the 547 genes that were differentially regulated at mid-log phase in the absence of glucose, 217 were repressed and 330 were promoted (selected genes shown in Tables 2–6). After statistical analysis of the microarray data, the differentially expressed genes in the WT compared with the *ΔluxS* mutant were broadly categorized into functional groups based on the clusters of orthologous groups (Fig. 4). Genes in 21 functional categories were regulated by *luxS*/AI-2: unclassified genes (25 up and 8 down), enzymes of unknown function (17 up and 13 down), general function predicted (29 up and 23 down), secondary metabolite biosynthesis, transport, catabolism (2 up and 0 down), inorganic ion transport and metabolism (20 up and 15 down), lipid transport and metabolism (3 up and 9 down), coenzyme transport and metabolism (10 up and 8 down), nucleotide transport and

Table 1. List of Genes Differentially Regulated Between Wild Type (W) and *ΔluxS* Mutant (M) by *luxS*/Autoinducer-2 at Mid-Log and Early Stationary Phase in Luria–Bertani Broth with 0.5% Glucose in *Salmonella* Typhimurium

Genes	*Putative identification of JCVI database*	*Fold change mid-log W/M*	*Fold change early stationary W/M*
luxS	AI-2 production protein LuxS	5.1	5.4
fljB	Flagellin	2.7	2.5
intN	Integrase	2.2	–
fhuF	Ferric hydrozamate transport	2.0	–
pgsA	Phosphatidylglycerophosphate synthetase (CDP-1,2-diacyl-sn-glycero-3-phosphate phosphatidyl transferase)	2.0	–
pduO	Propanediol utilization: B12 related	−2.0	–
STM3772	Putative phosphotransferase system enzyme IIA	2.5	–
STM1669	Homology to invasin C of *Yersinia* intimin	−2.0	–
STM2617	Gifsy-1 prophage: similar to antiterminator Q	−2.1	–
STM1255	Putative ABC transporter periplasmic-binding protein	−2.2	–
dmsA	Anaerobic dimethyl sulfoxide reductase, subunit A	−2.2	–
glgB2	Maltooligosyl trehalose trehalohydrolase	−2.4	–
hscC	Putative heatshock protein, homolog of hsp70 in	−3.2	–
STM0293	Putative cytoplasmic protein	–	2.4
yfiD	Putative formate acetyltransferase	–	2.2
ynfK	Putative dethiobiotin synthase	–	2.1
focA	Putative FNT family, formate transporter (formate channel)	–	2.0
yccD	Putative cytoplasmic protein	–	2.0
STM3142	Putative ferrichrome-binding periplasmic protein	–	2.0
malM	Periplasmic protein of mal regulon	–	−2.0
STM3191	Putative arylsulfate sulfotransferase	–	−2.1
glxR	Tartronic semialdehyde reductase	–	−2.2
ynfM	Putative MFS familty transport protein	–	−2.4
STM3600	Putative sugar kinases, ribokinase family	–	−3.3
STM2358	Putative cytoplasmic protein	–	−2.2
STM3770	Putative phosphotransferase system enzyme IIC	–	−2.2
STM3257	Putative tagatose 6-phosphate kinase 1	–	2.7

Table 2. *Salmonella* Typhimurium Genes Involved in Motility That Are Regulated by *luxS*/Autoinducer-2 at Mid-Log Phase in the Absence of Glucose

Genes	*Putative identification of JCVI database*	*Fold change (W/M)*	*Fold change (wCFS/mCFS)*
Chemotaxis proteins			
Two-component system proteins			
cheA	Chemotaxis protein CheA	−1.3	1.0
cheB	Chemotaxis-specific methylesterase	1.3	−1.0
STM2314	Putative chemotaxis signal transduction protein	**3.5**	**1.1**
MCPs			
tcp	Methyl-accepting transmembrane citrate/phenol chemoreceptor	2.0	−1.0
STM3216	Putative methyl-accepting chemotaxis protein	**1.8**	**1.1**
trg	Methyl-accepting chemotaxis protein III	**2.1**	**1.1**
aer	Aerotaxis sensor receptor	2.5	−1.1
Flagellar assembly proteins			
Type III secretion			
fliH	Flagellar assembly protein H	**−2.1**	**−1.0**
fliO	Flagellar biosynthesis protein FliO	**−1.8**	**−1.0**
Motor/switch			
motA	Flagellar motor protein MotA	2.0	−1.0
motB	Flagellar motor protein MotB	2.1	−1.0
C-ring			
fliG	Flagellar motor switch protein G	**−2.3**	**−1.0**
fliN	Flagellar motor switch protein FliN	1.2	−1.0
M, S, P, and L rings			
flgA	Flagellar basal body P-ring biosynthesis protein FlgA	1.5	−1.0
Rod, hook, and filament			
flgB	Flagellar basal body rod protein FlgB	**−2.4**	**−1.1**
flgE	Flagellar hook protein FlgE	**1.3**	**1.1**
flgJ	Peptidoglycan hydrolase	**−2.1**	**−1.0**
flgK	Flagellar hook-associated protein FlgK	**2.2**	**1.1**
flgL	Flagellar hook-associated protein FlgL	**1.4**	**1.0**
fliD	Flagellar capping protein	**2.0**	**1.2**
fliK	Flagellar hook-length control protein	**1.2**	**1.0**
fljB	Flagellin	**−1.3**	**−1.0**
Regulation			
*flhC**	Regulator of flagellar biosynthesis, acts on class	1.4	−1.0
*flhD**	Regulator of flagellar biosynthesis, acts on class	1.3	−1.0
flgM	Anti-sigma28 factor FlgM	2.7	−1.1
Chaperones			
fliJ	Flagellar biosynthesis chaperone	**1.5**	**1.1**
Pilus system			
Fimbrial proteins			
fimA	Fimbrin	2.0	−1.0
fimD	Outer membrane usher protein precursor	−2.1	1.0
Putative motility			
lpfA	Long polar fimbrial protein A precursor	1.4	−1.1
stdC	Putative fimbrial chaparone	1.4	−1.0
cheM	Methyl-accepting chemotaxis protein II	**1.6**	**1.0**
stiA	Putative fimbrial subunit	1.2	−1.0
lpfE	Long polar fimbrial minor protein	1.2	−2.2
yifL	Putative outer membrane lipoprotein	1.2	−1.0
stbA	Putative fimbrial major subunit	**1.2**	**1.1**

Differentially regulated genes between wild type (w) and *ΔluxS* mutant (M) and between wild-type cell-free supernatants and *ΔluxS* mutant cell-free supernatants are listed. Genes that have the same direction of regulation in both W/M and wCFS/mCFS are regulated by AI-2 and are shown in bold.

wCFS, wild-type cell-free supernatants; mCFS, mutant CFS.

metabolism (6 up and 11 down), amino acid transport and metabolism (28 up and 15 down), carbohydrate transport and metabolism (31 up and 7 down), energy production and conversion (35 up and 4 down), posttranslational modification, protein turnover, chaperones (13 up and 5 down), intracellular trafficking and secretion (3 up and 6 down), cell motility (9 up and 1 down), cell wall/membrane biogenesis (8 up and 12 down), signal transduction mechanisms (25 up and 2 down), defense mechanisms (3 up and 3 down), cell cycle control, mitosis and meiosis (0 up and 2 down), replication, recombination, and repair (3 up and 17 down), transcription (38 up and 14 down), and translation (6 up and 37 down) (Fig. 4).

Table 3. *Salmonella* Typhimurium Genes Involved in Biofilm Formation That Are Regulated by *luxS*/Autoinducer-2 at Mid-Log Phase in the Absence of Glucose

Genes	*Putative identification of JCVI database*	*Fold change (W/M)*	*Fold change (wCFS/mCFS)*
csgA	Curlin major subunit, coiled surface structures cryptic	1.1	−1.1
csgC	Putative curli production protein	**1.2**	**1.0**
bcsA	Glycosyltransferase, probably involved in cell wall biogenesis	−1.8	1.0
bcsC	Endo-1,4-D-glucanase	**−1.8**	**−1.0**
yhjN	Putative cellulose synthase	**−1.6**	**−1.0**
fimA	Major type 1 subunit fimbrin (pilin)	2.0	−1.0
fimD	Outer membrane usher protein	−1.3	1.1
fimZ	Fimbrial protein Z, putative transcriptional regulator (LuxR/UhpA)	1.5	−1.1
fimW	Putative fimbrial protein	**1.4**	**1.0**
fimY	Putative regulatory protein	**1.3**	**1.1**
lpfA	Long polar fimbria	1.4	−1.1
lpfE	Long polar fimbrial minor protein	1.2	−2.2
yojN	Putative sensor/kinase in regulatory system	**1.6**	**1.1**

Differentially regulated genes between wild type (W) and *ΔluxS* mutant (M) and between wild-type cell-free supernatants and *ΔluxS* mutant cell-free supernatants are listed. Genes that have the same direction of regulation in both W/M and wCFS/mCFS are regulated by AI-2 and are shown in bold.

Table 4. *Salmonella* Typhimurium Genes Involved in Virulence Regulated by *luxS*/Autoinducer-2 at Mid-Log Phase in the Absence of Glucose

Genes	*Putative identification of JCVI database*	*Fold change W/M*	*Fold change wCFS/mCFS*
hha	Hemolysin expression modulating protein (involved in environmental regulation)	**1.9**	**1.0**
pagP	PhoPQ-activated gene	−1.4	1.3
mviM	Putative virulence factor	**2.2**	**1.3**
cobB	Putative nicotinate-nucleotide dimethylbenzimidazolephosphoribosltransferase, homolog of virulence factor	**1.6**	**1.2**
pagC	PhoP regulated: reduced macrophage survival	1.5	−1.8
hnr	Response regulator in protein turnover: mouse virulence	**−1.4**	**−1.3**
sirC	Regulation of invasion genes	**−2.3**	**−1.2**
virK	Virulence gene homologous sequence to virK in	−2.5	1.4
avrA	Putative inner membrane protein	1.4	−3.1
STM2868	Putative cytoplasmic protein	**−1.8**	**−2.1**
orgA	Putative flagellar biosynthesis/type III secretory pathway protein	**−1.7**	**−2.7**
prgI	Cell invasion protein cytoplasmic	**−1.4**	**−9.6**
hilD	Regulatory helix-turn-helix proteins, araC family	1.2	−3.3
hilA	Invasion genes transcription activator	**−2.0**	**−6.1**
sptP	Protein tyrosine phosphate	**−1.3**	**−5.9**
sicP	Chaparone, related to virulence	**−1.4**	**−5.0**
STM2880	Putative cytoplasmic protein	**−1.4**	**−2.9**
sipB	Cell invasion protein	1.3	−2.8
spaR	Surface presentation of antigen secretory proteins	**−1.5**	**−9.2**
invC	Surface presentation of antigen secretory proteins	**−1.5**	**−11.2**
invB	Surface presentation of antigen secretory proteins	**−1.4**	**−7.5**
invA	Invasion protein	**−1.6**	**−6.8**
invE	Invasion protein	**−1.4**	**−10.5**
ygdP	Putative invasion protein NTP pyrophosphohydrolase	**1.4**	**1.0**
fis	Site-specific DNA inversion stimulation factor	**−4.6**	**−1.0**
hfq	Host factor I for bacteriophage Q beta	**1.4**	**1.2**

Differentially regulated genes between wild type (W) and *ΔluxS* mutant (M) and between wild-type cell-free supernatants and *ΔluxS* mutant cell-free supernatants are listed. Genes that have the same direction of regulation in both W/M and wCFS/mCFS are regulated by AI-2 and are shown in bold.

Table 5. *Salmonella* Typhimurium Genes in lsr Operon That Are Regulated by luxS/Autoinducer-2 at Mid-Log Phase and Early Stationary Phases in Both the Absence and Presence of 0.5% Glucose

		Fold change W/M				
		LB broth		LB broth + glucose		
Genes	*Putative identification of JCVI database*	*Mid-log*	*Early stationary*	*Mid-log*	*Early stationary*	*Fold change wCFS/mCFS*
lsrA (ego)	Putative ABC-type sugar, aldose transport system, ATPase	1.7	2.0	1.4	−1.9	−1.1[a]
lsrB (yneA)	Putative ABC superfamily (peri_perm), sugar transport protein	2.2	2.7	–	1.1	−1.1[a]
lsrC (ydeY)	Putative ABC superfamily (membrane), sugar transport protein	2	2.3	1.1[a]	–	1.0[a]
lsrD (ydeZ)	Putative ABC superfamily (membrane), sugar transport protein	1.9	3.4	1.3	1.1	−1.1[a]
lsrE (STM4080)	Putative ribulose-5-phosphate 3-epimerase	1.3	2.0	–	–	1.1
lsrF (yneB)	Putative fructose-1,6-bisphosphate aldolase	1.5	2.1	−1.3[a]	−1.2	1.1
lsrG (yneZ)	Putative inner membrane protein	1.7	1.6	1.1	–	−1.1
lsrK (ydeV)	Putative sugar kinase	1.4	1.7	1.3	1.2	−1.0
lsrR (ydeW)	Putative transcriptional repressor	1.3[a]	1.3	1.2	–	−2.7

Differentially regulated genes between wild type (W) and *ΔluxS* mutant (M) and between wild-type cell-free supernatants and *ΔluxS* mutant cell-free supernatants are listed.
[a]$p > 0.05$.
LB, Luria–Bertani.

Validation of microarray results using QRT-PCR

To verify the microarray results, QRT-PCR was performed on a selected number of genes identified as *luxS*/AI-2-regulated, and the results are shown in Fig. 5. The magnitude of fold change was different in most of the genes when compared with that obtained using the microarray analysis. However, all of the genes used in this study had the same pattern of regulation (either up or down) as that of the microarray results. Multivariate analysis of the QRT-PCR results using JMP 6.0 (SAS Institute) showed a pairwise correlation coefficient of 0.933, to the microarray data ($p = 0.0021$).

Discussion

LuxS is involved in the production of AI-2, the cell–cell signaling molecule used by *Salmonella* Typhimurium. *luxS*/AI-2 is known to be involved in various cellular processes in *Salmonella* Typhimurium, but its influence on global gene expression has not been studied. This is the first study to report the impact of *luxS* mutation on the global gene regu-

Table 6. *Salmonella* Typhimurium Genes in *rbs* Operon That Are Regulated by *luxS*/Autoinducer-2 at Mid-Log Phase and Early Stationary Phases in Both the Absence and Presence of 0.5% Glucose

		Fold change W/M				
		LB broth		LB broth + glucose		
Genes	*Putative identification of JCVI database*	*Mid-log*	*Early stationary*	*Mid-log*	*Early stationary*	*Fold change wCFS/mCFS*
rbsA	ABC superfamily (atp_bind), D-ribose high-affinity transport protein	1.1	1.1[a]	–	1.1[a]	−1.1[a]
rbsB	ABC superfamily (peri_perm), D-ribose transport protein	2.0	–	–	–	1.1
rbsC	ABC superfamily (membrane), D-ribose high-affinity transport protein	−1.2[a]	1.2[a]	–	1.1[a]	1.0
rbsD	D-ribose high-affinity transport system membrane-associated protein	1.3[a]	–	–	1.1[a]	1.2
rbsK	Ribokinase	2.2	–	–	1.1[a]	1.2
rbsR	Transcriptional repressor for rbs operon (GalR/LacI family)	2.5	–	–	–	−1.1[a]

Differentially regulated genes between wild type (W) and *ΔluxS* mutant (M) and between wild-type cell-free supernatants and *ΔluxS* mutant cell-free supernatants are listed.
[a]$p > 0.05$.

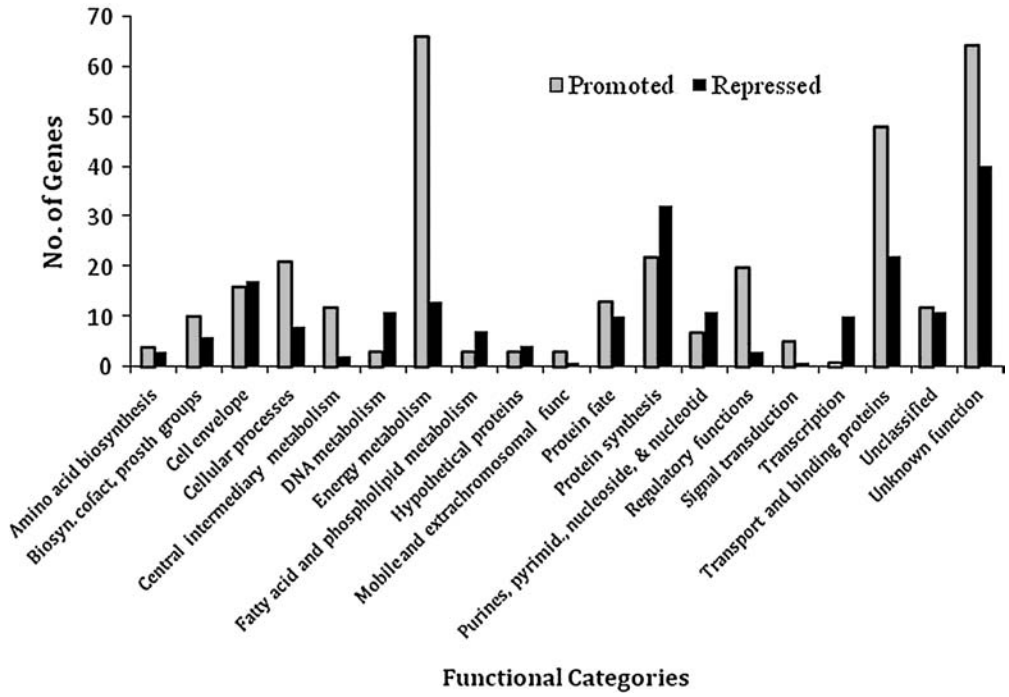

FIG. 4. Categories of genes regulated by *luxS*/AI-2. *luxS*/AI-2-regulated genes are grouped into functional categories based on the *Salmonella* Typhimurium genome annotation (http://cmr.jcvi.org/cgi-bin/CMR/shared/MakeFrontPages.cgi?page=geneattribute). The histograms represent the number of genes in each category promoted or repressed by *luxS* mutation in the mid-log phase in LB without glucose.

lation of *Salmonella* Typhimurium and to phenotypically characterize it based on growth, motility, and biofilm formation.

In this study, no difference in growth rates was observed between WT and *ΔluxS* mutant strains of *Salmonella* Typhimurium in LB with or without glucose supplementation (Fig. 1A, B). Similar observations were reported in *E. coli* K-12 (Wang *et al.*, 2005). However, Sperandio *et al.* (2001) reported that the growth rate of a *luxS* mutant of enterohemorrhagic *E. coli* O157:H7 (EHEC) was faster than its WT. In *Streptococcus pyogenes*, media-dependent growth defect was observed in *luxS* mutants (Lyon *et al.*, 2001). Results from our experiment suggest that *luxS*/AI-2 does not play a role in growth in *Salmonella* Typhimurium under the conditions tested.

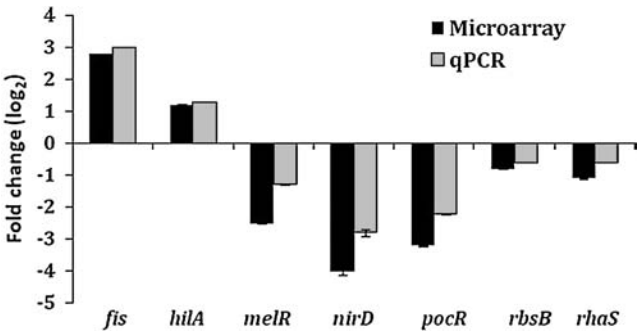

FIG. 5. Validation of microarray data of selected *luxS*/AI-2-regulated genes using real-time reverse transcriptase–polymerase chain reaction (PCR). The differences in expression of seven genes that are regulated by *luxS*/AI-2 in the mid-log phase in the absence of glucose were log_2 transformed and plotted against each other (microarray against reverse transcriptase–polymerase chain reaction).

WT *Salmonella* Typhimurium produced high levels of AI-2 in both log (1500-fold) and stationary (650-fold) phases in the presence of glucose (Fig. 1A). Earlier studies have reported that maximal AI-2 is produced between mid- and late log phases in the presence of glucose and that AI-2 activity is reduced with the onset of the stationary phase because of the depletion of glucose from the medium (Surette and Bassler, 1998, 1999). Contrary to what may be expected that higher levels of AI-2 result in a greater number of regulated genes, we only observed a small number of differentially expressed genes in *Salmonella* Typhimurium in the presence of glucose (Table 1). Of the total 4622 genes, only 13 were differentially expressed with 6 induced and 7 repressed. The minimal differential gene expression could be attributed to the abundance of glucose or catabolite repression (Wang *et al.*, 2005; Xavier and Bassler, 2005), suggesting that *Salmonella* Typhimurium uses cell signaling molecule for survival in glucose-limiting conditions.

In the absence of glucose, there was a 450-fold induction of AI-2 activity in the mid-log phase (Fig. 1B), but a large number of genes were differentially expressed. Other studies have also reported that AI-2 production is reduced in the absence of glucose (Surette and Bassler, 1998; Taga *et al.*, 2001; Wang *et al.*, 2005; Xavier and Bassler, 2005). Also, microarray analysis of *luxS*-dependent gene regulation in *E. coli* K-12 showed that more genes were differentially expressed in the absence of glucose (Wang *et al.*, 2005). We observed that 12% of the entire transcriptome was regulated with differential expression of genes in every set of clusters of orthologous groups at mid-log

phase (Fig. 4). Comparison of gene expression patterns at mid-log and early stationary phases showed that 31 genes had a biphasic response, which means that they were differentially expressed (either expressed or repressed) in both mid-log and stationary phases (data not shown).

Earlier studies have suggested that *luxS* plays an important metabolic function in the recycling of *S*-adenosyl homocysteine (Winzer *et al.*, 2002). In this study, we observed that among the genes that were regulated by *luxS*, genes encoding metabolism formed the largest group (Fig. 4). We also found that *luxS* not only plays a major role in metabolism but also regulates genes involved in other cellular processes in *Salmonella* Typhimurium (Fig. 4).

Flagellar biosynthesis in *E. coli* and *Salmonella* Typhimurium is regulated by more than 50 genes (Macnab, 1996), among which *flhDC* is the master regulator. In *Salmonella* Typhimurium, proteins MotA, MotB, FliG, FliM, and FliN have been identified as direct components of the rotary motor present in the cytoplasmic membrane and known to drive the bacterial flagellum (Macnab, 1996). In this study, among the genes that were differentially expressed (WT/*ΔluxS*), we observed downregulation of several key genes involved in motility including master regulator *flhDC* and components of the rotary motor *motA*, *motB*, *fliN*. Karavolos *et al.* (2008) reported that *luxS* affects flagellar phase variation in *Salmonella* Typhimurium. Studies in *E. coli* K-12 (Wang *et al.*, 2005) found no difference in motility between WT and *ΔluxS* mutant. In this study, phenotypic studies showed that *ΔluxS* mutant was less motile both in the presence and absence of glucose. Supportive microarray studies showed that among the motility genes that were downregulated, some were regulated by AI-2 (Table 2). Our observations indicate that both *luxS* and AI-2 influence motility in *Salmonella* Typhimurium.

Biofilms are considered as a developmental process as they are formed in steps that require intercellular signaling. Microarray studies showed that among the genes involved in biofilm formation that were differentially expressed (WT/*ΔluxS*), most were downregulated in the absence of *luxS*/AI-2 (Table 3). Prouty *et al.* (2002) reported that quorum sensing was important for full biofilm formation. They also reported that flagellar genes were important for biofilm formation and that fimbriae genes played a negative role in biofilm formation (Prouty *et al.*, 2002). In this study, microarrays comparing the differences in gene expression between *ΔluxS* mutant supplemented with WT CFS and *ΔluxS* mutant (wCFS/mCFS) showed similar direction of regulation in certain genes as in WT/*ΔluxS* mutant. Because AI-2 is present in both microarray studies, genes with a similar direction of regulation could be considered as influenced by AI-2. Phenotypic studies conducted to observe biofilm formation showed that, irrespective of the growth condition, biofilm formation was significantly less in the *ΔluxS* mutant (Fig. 3). Our microarray and phenotypic studies indicate that both *luxS* and AI-2 are involved in the biofilm process in *Salmonella* Typhimurium.

Cell–cell signaling and microbial pathogenesis are known to be closely linked (de Kievit and Iglewski, 2000), but their relationship in *Salmonella* Typhimurium is still unknown. Factor for inversion stimulation (*fis*) has been shown to be involved in DNA transcription, DNA replication at *oriC*, transposition, invasion of HEp-2 cells, and transcriptional activation and repression of several genes (Kelly *et al.*, 2004; Hirsch and Elliott, 2005a, 2005b). In pathogenic strains of *E. coli* and *Salmonella* Typhimurium, *fis* has been reported to modulate virulence gene expression (Kelly *et al.*, 2004). We observed that in the absence of glucose, *fis* showed a decreased WT/*ΔluxS* expression (−4.6-fold) at mid-log phase during which AI-2 is present (Table 4). In *E. coli*, it has been reported that *hha*, which encodes the regulator of the hemolysin operon and known to mediate environmental regulation of virulence factors in *Pseudomonas aeruginosa* (Whiteley *et al.*, 1999), was comparatively induced 11.1-fold in the presence of AI-2 (DeLisa *et al.*, 2001). Similarly, in this study we found that *hha* increased 1.9-fold in the presence of AI-2 at mid-log phase (Table 4). *fis* is a positive regulator of *hilA*, an activator of invasion genes, while *hha* is a negative regulator of *hilA*. *HilA* was found to be downregulated (twofold) at mid-log phase which could be due to the repression of *fis* and expression of *hha* (Table 4). This suggests that *luxS*/AI-2 regulates certain key virulence genes in *Salmonella* Typhimurium. None of the above mentioned genes (*fis*, *hha*, *hilA*) exhibited differential WT/*ΔluxS* expression at early stationary phase (data not shown). It must be noted that in the WT, AI-2 is present at mid-log phase (650-fold) and degraded or uptaken by cells at early stationary phase (1.5-fold) and hence AI-2 could be considered as the reason for the differential regulation of these genes at the mid-log phase. Further, microarray studies using *ΔluxS* mutant in the presence of CFS of WT *Salmonella* Typhimurium showed that key virulence genes were downregulated in the presence of AI-2. Higgins *et al.* (2007) have reported that the major AI-2 in *Vibrio cholerae* repressed the expression of virulence genes which is similar to the finding in this study that AI-2, the AI in *Salmonella* Typhimurium, represses the expression of its virulence genes.

In the WT, all the genes in the *lsr* operon were expressed at both mid-log and early stationary phases in the absence of glucose (Table 5). Significant induction of *rbsB* (periplasmic-binding protein), *rbsK* (cytoplasmic kinase), and *rbsR* (repressor) genes in the *rbs* operon were observed in the WT at mid-log phase (Table 6). Taga *et al.* (2001) and Xavier and Bassler (2005) found uptake of AI-2 even after the mutation of the *lsrB* gene, which is the receptor for AI-2 and therefore predicted the possibility of an alternative transport system. Recently, James *et al.* (2006) suggested the role of *rbsB* as a transporter of AI-2 in *Actinobacillus actinomycetemocomitans*. Interestingly, we observed that in contrast to the *lsr* operon that was induced at both time points, *rbsB*, *rbsK*, and *rbsR* were induced at mid-log phase when AI-2 was present and had no differential expression at early stationary phase when AI-2 had been degraded or uptaken by the cells (Fig. 1B). RbsB is known to be a LuxP and LsrB homolog (Taga *et al.*, 2001; James *et al.*, 2006). It is a part of the *rbs* operon that encodes six genes (*rbsD*, *rbsA*, *rbsC*, *rbsB*, *rbsK*, and *rbsR*) that form the ribose transport system (Iida *et al.*, 1984; Bell *et al.*, 1986). AI-2 synthesized by *luxS* is a ribose derivative, suggesting that the alternate transport system predicted (Taga *et al.*, 2001; Xavier and Bassler, 2005) could be the *rbs* transport system in *Salmonella* Typhimurium.

The microarray results were validated using QRT-PCR on a few selected genes. Though the magnitude of the fold change obtained using QRT-PCR was different from the microarray analysis, the direction of regulation was the same with a high correlation coefficient (0.93) (Fig. 5). The high degree of concordance between the QRT-PCR and microarray results, and

the use of multiple biological and technical replicates adds sufficient power to our analysis and confidence in these results.

Conclusions

The objective of this study was to examine the effect of *luxS*/AI-2 on global gene expression of *Salmonella* Typhimurium. Our results indicate that *luxS* and AI-2 are involved in the expression of genes that are related to motility, biofilm formation, virulence, translation, transcription, and other key cellular functions. The results show that AI-2 could play a vital role in the repression of key virulence-related genes in *Salmonella* Typhimurium.

Acknowledgments

This work was supported by Hatch grant H-8708 for the Texas AgriLife Research. We thank Bonnie L. Bassler for generously providing the *V. harveyi* BB170 reporter strains used in this study. DNA microarrays were obtained through National Institute of Allergy and Infectious Diseases (NIAID) Pathogen Function Genomics Resource Center, managed and funded by the Division of Microbiology and Infectious Disease, NIAID, National Institutes of Health, Department of Health and Human Services (DHHS), and operated by JCVI (formerly The Institute for Genomic Research).

Disclosure Statement

No competing financial interests exist.

References

Bassler BL, Wright M, Showalter RE, and Silverman MR. Intercellular signalling in *Vibrio harveyi*: sequence and function of genes regulating expression of luminescence. Mol Microbiol 1993;9:773–786.

Bell AW, Buckel SD, Groarke JM, *et al.* The nucleotide sequences of the rbsD, rbsA, and rbsC genes of *Escherichia coli* K12. J Biol Chem 1986;261:7652–7658.

Benjamini Y and Hochberg Y. Controlling the false discovery rate: a practical and powerful approach to multiple testing. J Royal Stat Soc B Meth 1995;57:289–300.

Chen X, Schauder S, Potier N, *et al.* Structural identification of a bacterial quorum-sensing signal containing boron. Nature 2002;415:545–549.

Choi J, Shin D, and Ryu S. Implication of quorum sensing in *Salmonella enterica* serovar typhimurium virulence: the luxS gene is necessary for expression of genes in pathogenicity island 1. Infect Immun 2007;75:4885–4890.

de Kievit TR and Iglewski BH. Bacterial quorum sensing in pathogenic relationships. Infect Immun 2000;68:4839–4849.

DeLisa MP, Wu CF, Wang L, Valdes JJ, and Bentley WE. DNA microarray-based identification of genes controlled by autoinducer 2-stimulated quorum sensing in *Escherichia coli*. J Bacteriol 2001;183:5239–5247.

Fong KP, Chung WO, Lamont RJ, and Demuth DR. Intra- and interspecies regulation of gene expression by *Actinobacillus actinomycetemcomitans* LuxS. Infect Immun 2001;69:7625–7634.

Fong KP, Gao L, and Demuth DR. luxS and arcB control aerobic growth of *Actinobacillus actinomycetemcomitans* under iron limitation. Infect Immun 2003;71:298–308.

Hegde P, Qi R, Abernathy K, *et al.* A concise guide to cDNA microarray analysis. Biotechniques 2000;29:548–550, 552–544, 556 passim.

Higgins DA, Pomianek ME, Kraml CM, *et al.* The major *Vibrio cholerae* autoinducer and its role in virulence factor production. Nature 2007;450:883–886.

Hirsch M and Elliott T. Fis regulates transcriptional induction of RpoS in *Salmonella enterica*. J Bacteriol 2005a;187:1568–1580.

Hirsch M and Elliott T. Stationary-phase regulation of RpoS translation in *Escherichia coli*. J Bacteriol 2005b;187:7204–7213.

Hughes TR, Roberts CJ, Dai H, *et al.* Widespread aneuploidy revealed by DNA microarray expression profiling. Nat Genet 2000;25:333–337.

Ichikawa JK, Norris A, Bangera MG, *et al.* Interaction of *Pseudomonas aeruginosa* with epithelial cells: identification of differentially regulated genes by expression microarray analysis of human cDNAs. Proc Natl Acad Sci USA 2000;97:9659–9664.

Iida A, Harayama S, Iino T, and Hazelbauer GL. Molecular cloning and characterization of genes required for ribose transport and utilization in *Escherichia coli* K-12. J Bacteriol 1984;158;674–682.

James D, Shao H, Lamont RJ, and Demuth DR. The *Actinobacillus actinomycetemcomitans* ribose binding protein RbsB interacts with cognate and heterologous autoinducer 2 signals. Infect Immun 2006;74:4021–4029.

Karavolos MH, Bulmer DM, Winzer K, *et al.* LuxS affects flagellar phase variation independently of quorum sensing in *Salmonella enterica* serovar typhimurium. J Bacteriol 2008;190:769–771.

Kelly A, Goldberg MD, Carroll RK, *et al.* A global role for Fis in the transcriptional control of metabolism and type III secretion in *Salmonella enterica* serovar Typhimurium. Microbiology 2004;150:2037–2053.

Livak KJ and Schmittgen TD. Analysis of relative gene expression data using real-time quantitative PCR and the 2(-Delta Delta C(T)) Method. Methods 2001;25:402–408.

Lyon WR, Madden JC, Levin JC, Stein JL, and Caparon MG. Mutation of luxS affects growth and virulence factor expression in *Streptococcus pyogenes*. Mol Microbiol 2001;42:145–157.

Macnab RM. Flagella and motility. In: *Escherichia coli and Salmonella: Cellular and Molecular Biology.* Neidhardt FC, Curtis III R, Ingraham JL, Lin ECC, *et al*. (eds.). Washington, DC: American Society for Microbiology Press, 1996, pp. 123–145.

McNab R, Ford SK, El-Sabaeny A, *et al.* LuxS-based signaling in *Streptococcus gordonii*: autoinducer 2 controls carbohydrate metabolism and biofilm formation with *Porphyromonas gingivalis*. J Bacteriol 2003;185:274–284.

Miller MB, Skorupski K, Lenz DH, Taylor RK, and Bassler BL. Parallel quorum sensing systems converge to regulate virulence in *Vibrio cholerae*. Cell 2002;110:303–314.

Miller ST, Xavier KB, Campagna SR, *et al. Salmonella* Typhimurium recognizes a chemically distinct form of the bacterial quorum-sensing signal AI-2. Mol Cell 2004;15:677–687.

O'Toole GA and Kolter R. Flagellar and twitching motility are necessary for *Pseudomonas aeruginosa* biofilm development. Mol Microbiol 1998;30:295–304.

Pillai SD and Jesudhasan PR. Quorum sensing: how bacteria communicate. Food Technol 2006;60:42–50.

Prouty AM, Schwesinger WH, and Gunn JS. Biofilm formation and interaction with the surfaces of gallstones by *Salmonella* spp. Infect Immun 2002;70:2640–2649.

Qin Y, Luo ZQ, and Farrand SK. Domains formed within the N-terminal region of the quorum-sensing activator TraR are required for transcriptional activation and direct interaction with RpoA from agrobacterium. J Biol Chem 2004;279:40844–40851.

Soni A, Jesudhasan PR, Cepeda M, *et al.* Autoinducer AI-2 is involved in regulating a variety of cellular processes in *Salmonella* Typhimurium. Foodborne Pathog Dis 2008;5:147–153.

Sperandio V, Mellies JL, Nguyen W, Shin S, and Kaper JB. Quorum sensing controls expression of the type III secretion gene transcription and protein secretion in enterohemorrhagic and enteropathogenic *Escherichia coli*. Proc Natl Acad Sci USA 1999;96:15196–15201.

Sperandio V, Torres AG, Giron JA, and Kaper JB. Quorum sensing is a global regulatory mechanism in enterohemorrhagic *Escherichia coli* O157:H7. J Bacteriol 2001;183:5187–5197.

Sperandio V, Torres AG, Jarvis B, Nataro JP, and Kaper JB. Bacteria-host communication: the language of hormones. Proc Natl Acad Sci USA 2003;100:8951–8956.

Surette MG and Bassler BL. Quorum sensing in *Escherichia coli* and *Salmonella* Typhimurium. Proc Natl Acad Sci USA 1998;95:7046–7050.

Surette MG and Bassler BL. Regulation of autoinducer production in *Salmonella* Typhimurium. Mol Microbiol 1999;31:585–595.

Taga ME, Miller ST, and Bassler BL. Lsr-mediated transport and processing of AI-2 in *Salmonella* Typhimurium. Mol Microbiol 2003;50:1411–1427.

Taga ME, Semmelhack JL, and Bassler BL. The LuxS-dependent autoinducer AI-2 controls the expression of an ABC transporter that functions in AI-2 uptake in *Salmonella* Typhimurium. Mol Microbiol 2001;42:777–793.

Wang L, Li J, March JC, Valdes JJ, and Bentley WE. luxS-dependent gene regulation in *Escherichia coli* K-12 revealed by genomic expression profiling. J Bacteriol 2005;187:8350–8360.

Whiteley M, Lee KM, and Greenberg EP. Identification of genes controlled by quorum sensing in *Pseudomonas aeruginosa*. Proc Natl Acad Sci USA 1999;96:13904–13909.

Widmer KW, Jesudhasan PR, Dowd SE, and Pillai SD. Differential expression of virulence-related genes in a *Salmonella enterica* serotype Typhimurium luxS mutant in response to autoinducer AI-2 and poultry meat-derived AI-2 inhibitor. Foodborne Pathog Dis 2007;4:5–15.

Winzer K, Hardie KR, Burgess N, *et al.* LuxS: its role in central metabolism and the *in vitro* synthesis of 4-hydroxy-5-methyl-3(2H)-furanone. Microbiology 2002;148:909–922.

Winzer K and Williams P. Quorum sensing and the regulation of virulence gene expression in pathogenic bacteria. Int J Med Microbiol 2001;291:131–143.

Xavier KB and Bassler BL. LuxS quorum sensing: more than just a numbers game. Curr Opin Microbiol 2003;6:191–197.

Xavier KB and Bassler BL. Regulation of uptake and processing of the quorum-sensing autoinducer AI-2 in *Escherichia coli*. J Bacteriol 2005;187:238–248.

Address correspondence to:
Suresh D. Pillai, Ph.D.
Food Safety and Environmental Microbiology Program
418B Kleberg Center
Departments of Poultry Science and Nutrition and Food Science
Texas A&M University
College Station, TX 77843

E-mail: spillai@poultry.tamu.edu

Return to Table of Contents

ANTIMICROBIAL AGENTS AND CHEMOTHERAPY, Jan. 2010, p. 452–459 Vol. 54, No. 1
0066-4804/10/$12.00 doi:10.1128/AAC.01435-08

Inhibition of B Virus (*Macacine herpesvirus* 1) by Conventional and Experimental Antiviral Compounds▽

P. W. Krug,[1]† R. F. Schinazi,[2] and J. K. Hilliard[1]*

Viral Immunology Center, Georgia State University,[1] and Laboratory of Biochemical Pharmacology, Department of Pediatrics, Emory University School of Medicine and Veterans Affairs Medical Center,[2] Atlanta, Georgia

Received 25 October 2008/Returned for modification 8 December 2008/Accepted 19 October 2009

B virus infection of humans results in high morbidity and mortality in as many as 80% of identified cases. The main objective of this study was to conduct a comparative analysis of conventional and experimental antiviral drug susceptibilities of B virus isolates from multiple macaque species and zoonotically infected humans. We used a plaque reduction assay to establish the effective inhibitory doses of acyclovir, ganciclovir, and vidarabine, as well as those of a group of experimental nucleoside analogs with known anti-herpes simplex virus activity. Four of the experimental drugs tested were 10- to 100-fold more potent inhibitors of B virus replication than conventional antiviral agents. Drug efficacies were similar for multiple B virus isolates tested, with variations within 2-fold of the median effective concentration (EC_{50}) for each drug, and each EC_{50} was considerably lower than those for B virus thymidine kinase (TK) mutants. We observed no differences in the viral TK amino acid sequence between B virus isolates from rhesus monkeys and those from human zoonoses. Differences in the TK protein sequence between cynomolgus and pigtail macaque B virus isolates did not affect drug sensitivity except in the case of one compound. Taken together, these data suggest that future B virus zoonoses will respond consistently to conventional antiviral treatment. Further, the considerably higher potency of FEAU (2′-fluoro-5-ethyl-Ara-U) than of conventional antiviral drugs argues for its compassionate use in advanced human B virus infections.

In its natural host, macaque monkeys, B virus (*Macacine herpesvirus* 1; *Simplexvirus*, *Herpesviridae*) causes lesions on epithelial surfaces (2, 33) and establishes reactivatable latent infection in sensory neurons (30, 37), like herpes simplex virus (HSV) in humans. B virus often results in severe pathogenesis, including paralysis, encephalitis, and in many cases, rapid death, following infection of humans (reviewed in reference 22). Nearly all reported cases of B virus zoonosis have been associated with individuals handling macaques during the course of research or technology development (33). Five fatalities, along with at least 23 cases in which the patient survived, have occurred in the past 20 years, underscoring that zoonotic infections remain a problem in the laboratory animal environment (7–9).

The CDC's B Virus Working Group currently recommends treatment of confirmed zoonotic infections with herpesvirus-specific antiviral drugs, including acyclovir (ACV) and ganciclovir (GCV) (10). Both agents in this class of compounds are phosphorylated to active form by virus-encoded thymidine kinase (TK). The resulting nucleoside triphosphate analog inhibits viral DNA replication by termination of chain elongation and by direct inhibition of herpesvirus DNA polymerase (24). While ACV is effective against B virus both in cell culture and in animal models (6), the dose required for 50% plaque reduction is more than 10-fold higher for B virus than for HSV type 1 (HSV-1) (38). GCV is twice as potent as ACV in B virus plaque reduction, yet the median effective concentration (EC_{50}) of GCV for B virus is almost 10 times higher than that for HSV-1 (38). In some, but not all, cases of zoonotic B virus infection, acyclovir and ganciclovir have proven to be effective at curtailing disease progression (7, 8). Zoonotic infections that have progressed to extensive central nervous system (CNS) involvement, including respiratory arrest, appear to be refractory to conventional antiviral intervention (12, 15; J. Hilliard, unpublished data).

Vidarabine (9-β-D-arabinofuranosyladenine [ara-A, or VDB]), an antiviral agent effective against HSV, may be useful for the treatment of early stages of zoonotic B virus infections, but it has not been used alone in previous cases. Prior to the use of ACV for treatment of HSV, intravenous VDB was used for treatment of encephalitic infections (34). In cell culture, it has been shown to be equally potent against B virus and HSV-1 (5). VDB does not require selective phosphorylation by the viral TK for activity (4); however, since VDB can be converted to its active form by host enzymes, it has potential toxicity in humans (29).

Experimental drugs effective in cell culture against HSV include the β-D-2′-fluoro-5-substituted arabinosyl pyrimidines FMAU (2′-fluoro-5-methyl-Ara-U) and FEAU (2′-fluoro-5-ethyl-Ara-U), both of which require phosphorylation by viral thymidine kinase for activation (19). FMAU and FEAU have potencies similar to that of ACV for inhibition of HSV-1 in cell culture, but FMAU has 10-fold greater potency than ACV against HSV-2 (19). Unfortunately, FMAU has been reported to be toxic to humans at elevated doses used for cancer chemotherapy (1, 13); FMAU can be incorporated into uninfected cell DNA by host DNA polymerase, suggesting the basis of its

* Corresponding author. Mailing address: Viral Immunology Center, Georgia State University, P.O. Box 4118, Atlanta, GA 30302. Phone: (404) 413-6560. Fax: (404) 413-6569. E-mail: jhilliard@gsu.edu.

† Present address: Plum Island Animal Disease Center, Agricultural Research Service, United States Department of Agriculture, Orient Point, NY.

▽ Published ahead of print on 26 October 2009.

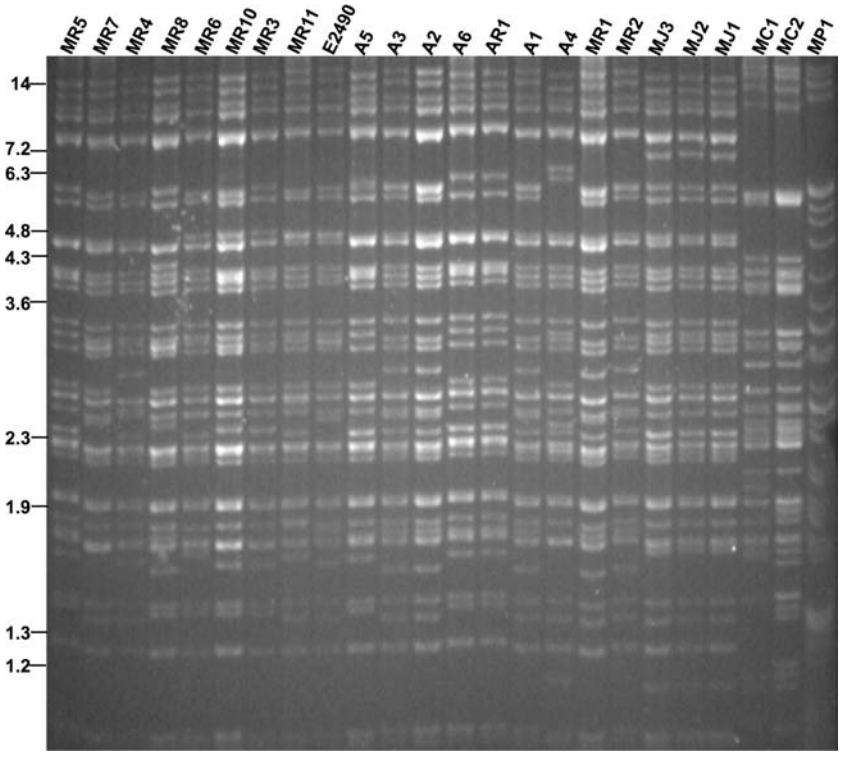

FIG. 1. Confirmation of B virus isolate genotype by RFLP. Viral DNA was digested with the SalI restriction enzyme and was separated on a 0.8% agarose gel. MR, rhesus macaque isolate; E2490, prototype laboratory strain; A, human isolate; MJ, Japanese macaque isolate; MC, cynomolgous macaque isolate; MP, pigtail macaque isolate. Size markers are indicated in kilobase pairs and reflect the positions of BstEII-digested lambda DNA fragments.

toxicity *in vivo* (11). FEAU has been shown to be a selective inhibitor of HSV DNA synthesis in cell culture (7), but its toxicity in humans has not been investigated. Other β-D-2′-fluoro-5-substituted arabinosyl pyrimidines, such as FMAC (2′-fluoro-5-methyl-Ara-C) and FBrAC (2′-fluoro-5-bromyl-Ara-C), have been synthesized and tested against HSV (17, 32; R. F. Schinazi, unpublished results). No information on FBrAC toxicity is known.

The goal of this study was to determine the general variability of drug susceptibility and the efficacy of a class of experimental antiviral agents by using a panel of B virus isolates from multiple macaque species and humans. The results presented here suggest that B virus isolates in the wild are susceptible to antiviral agents that require the viral TK for activity. Further, our findings that specific experimental nucleoside analogs are appreciably more effective than conventionally used antiviral agents at blocking B virus replication suggest that these drugs may benefit the treatment of high-morbidity human cases.

MATERIALS AND METHODS

Cells and viruses. African green monkey kidney (Vero) cells (ATCC CCL-81) were obtained from the American Type Culture Collection (Manassas, VA) and propagated in Dulbecco's modified Eagle's medium (DMEM; Mediatech) supplemented with 7% fetal bovine serum (FBS) (Invitrogen, Carlsbad, CA). Infections were done using DMEM supplemented with 1% FBS. All B virus plaque reduction assays were performed under biosafety level 3 conditions acceptable at the time of these experiments performed in compliance with the 4th edition of the *Biosafety in Microbiological and Biomedical Laboratories*. B virus infections for viral DNA purification and virus stock production were done under biosafety level 4 conditions, as mandated by the 5th edition of *Biosafety in Microbiological and Biomedical Laboratories* (28a) for propagating and handling B virus.

The E2490 reference strain of rhesus macaque B virus was originally obtained from R. N. Hull, Eli Lilly Research Laboratories (Indianapolis, IN), and passage 72 was used. All other wild-type viruses used in this study were diagnostic isolates obtained from the NIH's NCRR-supported National B Virus Resource Center, Georgia State University, Atlanta, GA. Restriction endonuclease digestions of these isolates' viral genomes are shown in Fig. 1.

The TK mutants were generated by cotransfection of NaI gradient-purified E2490 viral DNA with plasmids containing the TK gene with either a deletion (pBVΔTK) or a premature stop codon (pBVTKstop) into rabbit skin cells (ATCC CCL-68) (Fig. 2A) (technique described in reference 27). For pBVTKstop, a SpeI linker containing stop codons in all frames (catalog no. 1061; New England Biolabs) was inserted into the BglII site of pBVTK. Dilutions of the subsequent transfection stocks were plated on Vero cells, and individual plaques were screened by PCR and Southern hybridization. After three (BVΔTK) or four (BVTKstop) rounds of plaque purification, one plaque with no evidence of wild-type virus was chosen as the representative mutant of each virus for preparation of stocks.

The DNA sequence of both viral mutants was confirmed by sequencing. Confirmation of the deletion and stop codon insertion using PCR is shown in Fig. 2B. The parent virus PCR amplimer is 1,143 bp (Fig. 2B, lane 1). The deletion from ApaI to BspEI removes a 759-bp fragment, resulting in a 384-bp amplimer (lane 2). The insertion of the stop codon linker into the BglII site results in a 1,157-bp amplimer (lane 4) that, when cut with SpeI, yields 856-bp and 301-bp fragments (lane 3). Manipulation of these drug-resistant TK_{null} viruses is restricted to a biosafety level 4 laboratory in accordance with the Georgia State University Institutional Biosafety Committee and the Office of Biotechnology Activities at the National Institutes of Health.

Antiviral compounds. Acyclovir (ACV), ganciclovir (GCV), and vidarabine (VDB) were purchased from Sigma (St. Louis, MO). The compounds 1-(2-fluoro-5-methyl-beta-D-arabinofuranosyl)uracil (FMAU), 1-(2-deoxy-2-fluoro-beta-D-arabinofuranosyl)-5-ethyluracil (FEAU), 1-(2-deoxy-2-fluoro-beta-D-arabinofuranosyl)-5-bromylcytosine (FBrAC), and 1-(2-deoxy-2-

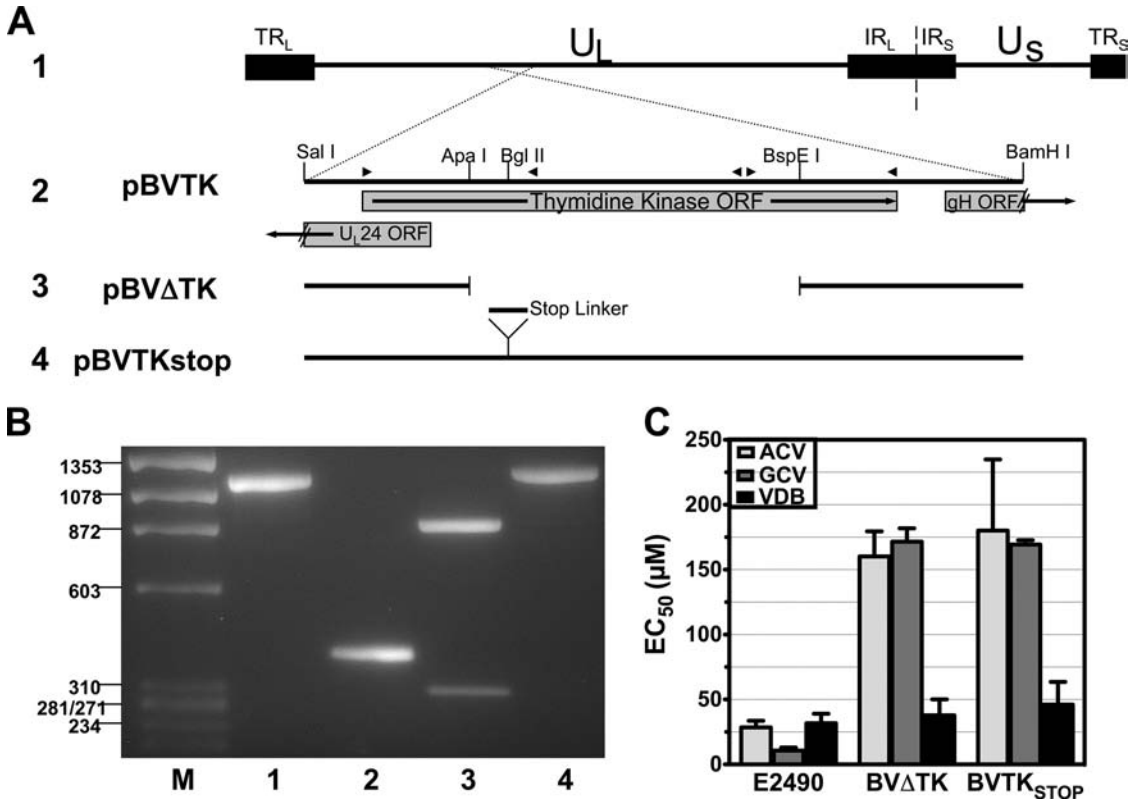

FIG. 2. Design and confirmation of recombinant B virus harboring mutations in thymidine kinase. (A) Overview of TK mutant construction: 1, orientation of the B virus genome; 2, BamHI–SalI fragment containing the complete TK open reading frame; 3, ApaI–BspEI collapse of pBVTK, deleting 754 amino acids from the center of TK; 4, stop codon linker insertion into the BglII site to prematurely stop TK translation. (B) Confirmation of mutants by PCR. Lanes: M, ϕX174/HaeIII marker; 1, E2490; 2, BVΔTK; 3, BVTKstop PCR product cut with SpeI; 4, BVTKstop (uncut). (C) Antiviral sensitivities of E2490, BVΔTK, and BVTKstop versus acyclovir, ganciclovir, and vidarabine. Error bars indicate standard deviations of three replicates.

fluoro-beta-D-arabinofuranosyl)-5-methylcytosine (FMAC) were synthesized in one of our laboratories (R.F.S.).

Plaque reduction assay. Confluent monolayers of Vero cells in 12-well microplates were infected with approximately 200 PFU of virus and incubated at 37°C with twofold serial dilutions of antiviral drug. After 1 h, the inoculum was removed and replaced with medium containing 1% methylcellulose and antiviral drug. Control wells did not contain antiviral drugs. The cells were fixed in 100% methanol 40 h after infection and were stained with Giemsa stain. Plaques were visually inspected and counted using a dissecting microscope. The number of plaques at each drug concentration was plotted versus the log of the drug concentration, and the slope of the regression line in the linear range was determined. The amount of drug required to reduce the number of plaques by 50% from those in the control wells (EC_{50}) was calculated from the equation of the regression line. Each drug was tested against each isolate at least twice in replicate wells, and the EC_{50} was calculated as an average value. Cytotoxicity in Vero cells for all the compounds was determined previously using a 3-(4,5-dimethyl-2-thiazolyl)-2,5-diphenyl-2H-tetrazolium bromide (MTT) assay. None of the compounds were cytotoxic when evaluated up to 10 μM (data not shown).

Viral DNA analysis. Viral DNA was isolated from infected cells by the method of Poffenberger and Roizman (23). Restriction digests were separated on 0.8% agarose gels. Each PCR amplification of the TK gene from rhesus, Japanese macaque, cynomolgus, and human B virus isolates was performed with primers 5′-CCAACGCTCCGTAAAACCG-3′ and 5′-ACCATCTTTATTGCGCCAG G-3′. Amplimers were purified after extraction from 1% agarose gels, and both strands were sequenced using an automated sequencer, model 377 (Applied Biosystems), with the primers given above and three internal primers, 5′-AAG ATCGTGTCCTCGATCTC-3′, 5′-GAGATCGAGGACACGATCTT-3′, and 5′-CACCTGAGCGCTGGCCATTG-3′. Because PCR amplification of the pigtail macaque B virus TK gene was not possible with the rhesus macaque-based PCR primers, restriction fragments containing the pigtail macaque B virus TK gene were cloned. These plasmids were subcloned, and the pigtail B virus TK gene was then sequenced using vector-specific primers and two internal gene-specific primers, 5′-AAGATCGTGTCCTCGATCTC-3′ and 5′-GAGATCGAG GACACGATCTT-3′. Sequence alignment was performed using MegAlign, version 4.03 (DNAStar, Madison, WI), with the Jotun Hein algorithm.

RESULTS

Characterization of the virus panel. One of the goals of this work was to examine the variability of drug potency and susceptibility for multiple B virus isolates from macaques and humans. We chose a large panel of B virus isolates from various species of macaques, as well as human isolates; many of the viruses were isolated recently and have been maintained at 3 or fewer passages. To verify the genotype and observe the genetic variability of the B virus isolates, we performed restriction fragment length polymorphism (RFLP) analysis with SalI restriction endonuclease (Fig. 1). Numerous polymorphisms were observed, similar to those noted in a previous study of multiple isolates from cynomolgus macaques (31). It is also noted that the seven B virus isolates from human zoonoses were genotyped as rhesus B virus. B virus isolates from cynomolgus monkeys and pigtail macaques had restriction profiles distinct from those of isolates from rhesus macaques, as previously reported by others (25). Recently, sequencing and RFLP analysis of PCR amplimers demonstrated specific characteristics that distinguish B virus isolates from Japanese and

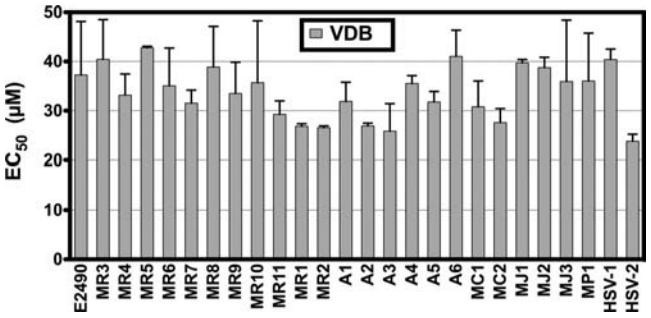

FIG. 3. Vidarabine sensitivities of B virus isolates. Plaque reduction assays were performed, and the 50% effective concentration (EC_{50}) of the drug against each isolate was determined. Each bar corresponds to the mean EC_{50}; error bars, standard deviations. Each isolate was tested against the drug in at least two independent experiments.

rhesus macaques (21). Our results show that Japanese macaque B virus RFLP patterns were very similar to those from rhesus macaque virus isolates, yet these isolates had distinct RFLPs generated by digestion with SalI (Fig. 1) and other restriction endonucleases (data not shown).

In order to determine if a B virus isolate was resistant to ACV or GCV, we created two thymidine kinase-defective B viruses as controls (Fig. 2). These viruses were 6-fold more resistant to ACV and 16-fold more resistant to GCV than the wild-type parental strain.

Sensitivity of B virus isolates to vidarabine. As previously reported (5), B virus and HSV-1 have similar sensitivities to VDB in cell culture, suggesting the hypothesis that the reason B virus is less sensitive to ACV and GCV than HSV is due to variation in the viral TKs, not the viral DNA polymerases. To detect differences in the B virus DNA polymerases, the sensitivities of the B virus isolates to VDB were determined by a plaque reduction assay. The rationale for the use of VDB was to determine whether mutations affecting the viral DNA polymerase might be present, since these mutations could potentially result in an observed resistance to drugs that require phosphorylation by the viral TK and may be mistakenly attributed to a partial or total loss of TK function.

We found that all rhesus isolates had very similar sensitivities to VDB (mean EC_{50}, 34.3 μM; range, 26.5 to 40.4 μM) (Fig. 3). As expected, the mean VDB sensitivities of the BVΔTK and the BVTKstop mutants were similar to those of the rhesus isolates (37.8 μM and 46.1 μM, respectively) (Fig. 2C). While the possibility of mutations in the viral DNA polymerase that do not affect the sensitivity of VDB cannot be completely ruled out, these results indicate that the DNA polymerase genes in these isolates are similar, suggesting that the large differences observed with TK-activated antiviral agents would likely be due to variations in the viral TK.

Sensitivities of B virus isolates to acyclovir and ganciclovir. Fatalities following zoonotic infections from 1987 to 1997 occurred despite pharmacologic intervention with ACV and/or GCV. To rule out the possibility that the fatality-associated viruses were strain variants that were "naturally" resistant to these antiviral agents, we determined the sensitivities of our panel of B virus isolates to these antivirals using plaque reduction assays. As controls, the TK_{null} mutants were used to determine a standard for completely resistant virus.

Our results for ACV and GCV (Fig. 4) were similar to those of previously published studies for rhesus B virus (38). The EC_{50} for each drug against each isolate was within a 2-fold difference of the mean sensitivity of all isolates from rhesus monkeys and humans (33.2 μM; range, 19.3 to 45.7 μM). The sensitivities of Japanese macaque, cynomolgus monkey, and pigtail macaque B virus isolates to ACV and GCV were very similar to those of the human and rhesus B virus isolates, suggesting that future human infections with these B virus genotypes could be treated with these antivirals. Because the drug sensitivities of the isolates did not approach the levels of the TK_{null} mutants (Fig. 2C), our results indicate that the isolates in this panel have wild-type antiviral drug sensitivity; however, it is possible that the variability observed in this assay could be due to minor differences in the TK genes.

Experimental drugs. While ACV and GCV have been shown to be effective in some cases of B virus zoonosis, the prognosis for patients is bleak once clinical signs indicate entry of B virus into the CNS. In order to discover more-efficacious B virus antiviral agents, we tested a panel of experimental compounds with known activity against HSV. FMAU and FEAU were found to be approximately 100 times more potent than conventional drugs (Fig. 5, upper panel). FMAC and FBrAC had approximately 10 times greater potency than ACV (Fig. 5, lower panel). Each of these agents requires the viral TK for activation, indicating that either they are activated with higher efficiency by TK or their phosphorylated forms are

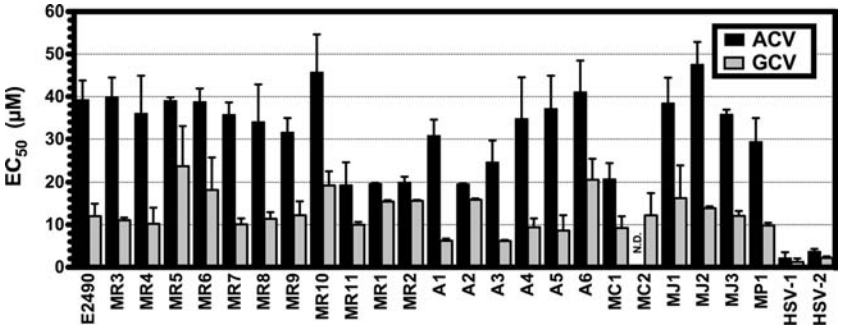

FIG. 4. Sensitivities of B virus isolates to conventional antivirals. Plaque reduction assays were performed, and the 50% effective concentration (EC_{50}) of each drug against each isolate was determined. Each bar corresponds to the mean EC_{50}; error bars, standard deviations. Each isolate was tested against each drug in at least two independent experiments. N.D., not done.

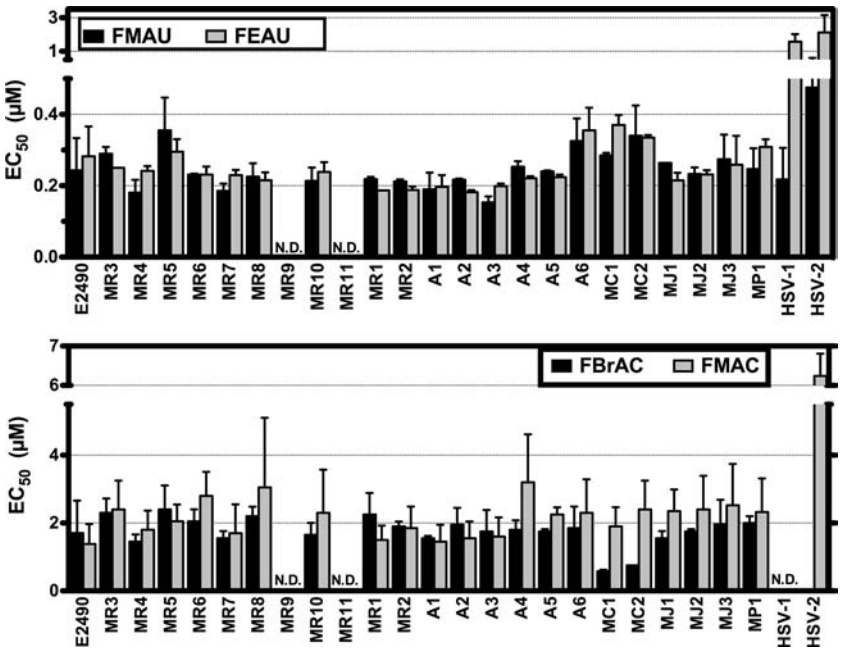

FIG. 5. Sensitivities of B virus isolates to experimental antivirals. Plaque reduction assays were performed, and the 50% effective concentration (EC_{50}) of each drug against each isolate was determined. Each bar corresponds to the mean EC_{50}; error bars, standard deviations. Each isolate was tested against each drug in at least two independent experiments. N.D., not done.

recognized by the viral DNA polymerase with higher affinity than the triphosphate forms of ACV or GCV. These data demonstrate that a more-efficacious panel of B virus antiviral agents exists within the class of 2′-fluoro-5-substituted arabinosyl pyrimidines.

Thymidine kinase heterogeneity. Most of the B virus isolates had similar sensitivities to each drug, with a range less than 2-fold from the mean. It is possible that the observed variation between these isolates is due to minor differences at the amino acid level in the viral proteins that can confer resistance to nucleoside analogs (TK or DNA polymerase). To determine whether apparent functional mutations existed in TK, the TK open reading frame (ORF) was sequenced from rhesus, Japanese macaque, cynomolgus monkey, pigtail macaque, and human B virus isolates.

Striking conservation between B virus TK ORFs from rhesus macaque, Japanese macaque, and human isolates was observed; one nucleic acid substitution was present in 8 of 22 of these isolates, but the difference did not affect the amino acid sequence. Cynomolgus monkey-derived B virus isolates have seven unique TK amino acid differences from rhesus and pigtail macaque B virus isolates (Fig. 6), and these differences may underlie the increased sensitivity of the cynomolgus isolates to FBrAC (Fig. 5, lower panel). While 27 unique amino acid differences were present in the pigtail macaque B virus isolate relative to rhesus and cynomolgus monkey B virus TK (Fig. 6), the drug sensitivity of the pigtail macaque B virus fell into the range of the rhesus B virus isolates with all tested antiviral agents. We hypothesize that the observed amino acid differences are likely in domains that are not functional with respect to drug interaction, or alternatively, they are in functional domains that are sufficiently conserved to retain function.

Included in these studies were isolates from three humans and two rhesus macaques sampled during a cluster of zoonotic infections in Pensacola, FL (8). The three human isolates and two monkey isolates are designated A1, A2, A3, MR1, and MR2, respectively. While there were minor differences in drug sensitivity among these isolates, the DNA sequences of the TK ORF were identical (data not shown). Taken together, the similar drug sensitivity and identical TK sequence suggest that replication in the human host did not result in antiviral resistance in these B virus isolates.

DISCUSSION

These data provide support for the value of and choices for antiviral intervention against zoonotic B virus infections, extending data originally demonstrating the efficacy of conventional drugs that target viral DNA replication. The potential of 2′-fluoroarabinofuranosyl 5-substituted pyrimidine nucleosides is demonstrated for the first time; these data may serve as the basis of compassionate use when the onset of severe morbidity signals unlikely success with conventional therapeutic approaches, as learned from the five fatal cases in recent years. Our data further suggest that there is no immediate host pressure that induces drug susceptibility-related changes in B virus during human infection. Each isolate, whether isolated from a macaque or from a human, was similarly sensitive to the antiviral agents used in these studies, suggesting that time to treatment is a major factor in human survival.

The TK_{null} mutants had VDB sensitivities similar to those of the wild-type isolate panel, supporting the hypothesis that the increased requirements of ACV and GCV for B virus plaque reduction are due to the differences between B virus and HSV TKs. While most of the known functional domains of TK are identical between the rhesus B virus and HSV, it is tempting to

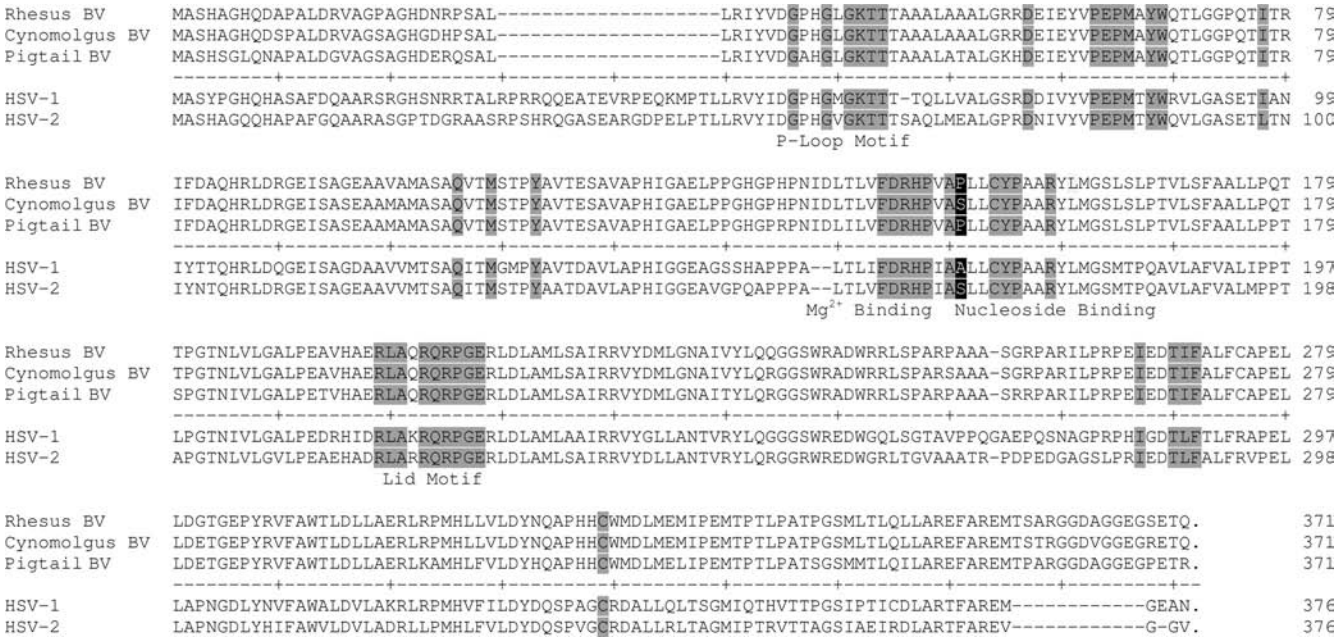

FIG. 6. Amino acid alignment of thymidine kinase sequences from three B virus genotypes, HSV-1, and HSV-2. Thymidine kinase open reading frames from the B virus strains E2490 (Rhesus BV), MC1 (Cynomolgus BV), and MP1 (Pigtail BV) were aligned using the Jotun Hein method. The thymidine kinase open reading frame from HSV-1 strain F and HSV-2 strain 333 were included for comparison. Shaded amino acids indicate identity with known functional domains.

speculate that the substitution of Pro150 in the B virus TK would place a kink in the nucleoside-binding domain that is not present in the same position in HSV TK (Ala168). Indeed, a change in the homologous amino acid in HSV-2 (Ser169) is responsible for the resistance of that virus to brivudin (BVdU) (35), and the same amino acid variation in the binding pocket is present in cynomolgus monkey B virus TK (Ser150). Zwartouw and colleagues (38) demonstrated the increased resistance of cynomolgus monkey B virus to BVdU almost 20 years ago. Site-directed mutagenesis and a structure-activity relationship analysis of B virus TK would be required to determine the roles of individual amino acids in the relative resistance of B virus to ACV and GCV.

B virus isolates from recent zoonotic infections demonstrated no variation in TK genes relative to isolates from rhesus macaques, and all appear similar to those from rhesus monkeys by restriction endonuclease profiles. These data validate a rhesus origin of B virus associated with these specific zoonoses. However, this is a small sample set, and it was noted that affected individuals had been working specifically with rhesus macaques. Thus, our data do not rule out the possibility that B virus from macaque species other than *Macaca mulatta* may share its pathogenic potential (25). Even so, B virus can be transmitted to nonmacaque monkeys (18, 36), and other macaques can harbor B virus acquired from rhesus monkeys (21, 25). Thus, regardless of the monkey species, if a monkey has been in contact with macaques, B virus should be presumed to be a hazard. Few cases previously reported in the literature have been associated with specific macaques (22); in fact, many affected individuals had histories of contact with multiple macaque species.

In each of the recent symptomatic cases of B virus zoonosis, treatment has consisted of acyclovir and/or ganciclovir (3, 9, 12, 16, 20). Of 11 infected individuals, 6 survived. The data presented here suggest that variable infection outcomes of antiviral therapy were not associated with virus mutations. It is possible that each individual had different host-dependent susceptibilities to B virus infection. Alternatively, since four of the five fatally infected individuals were not treated until severe neurological symptoms were detected, whereas three of the six survivors were hospitalized prior to the onset of acute neurological symptoms, the time for effective intervention may have been limited. This would underscore the importance of early identification of zoonotic disease, which can be generally accomplished early after infection for less than $300 worth of laboratory evaluations.

Zwartouw and colleagues (38) compared ACV and GCV against B virus in experimentally infected rabbits, observing 100% survival for the GCV-treated group for 5 months, compared to 33% survival for those treated with ACV. Interestingly, one of the patients from the Michigan cluster of human infections with B virus was given ganciclovir (5 mg/kg of body weight intravenously) twice daily, following a lack of success with ACV used at 15 mg/kg for 3 days, resulting in abatement of neurological symptoms and stabilization of cerebrospinal fluid antibody levels (12). In four other human cases, however, GCV was unable to reverse the fatal progression of disease (9, 17, 20), substantiating the need for more-efficacious antivirals for late-stage infection.

During the preparation of this article, a biochemical analysis of B virus TK was published, including some overlap with the present study (14). Our somewhat different approach was to determine if variability existed among wild isolates of B virus, hence our inclusion of many more virus strains, instead of just

three strains. Instead of characterizing the biochemical properties of B virus TK, we sought out compounds that had significantly greater efficacy in cell culture against a wide scope of B virus isolates, so that infectious-disease physicians would have more-powerful choices to treat cases of advanced human B virus infection. The creation of the TK_{null} mutant viruses as opposed to the production of recombinant protein allowed us to examine TK-mediated drug resistance in the context of viral infection. The authors of the previous study could not detect the phosphorylation of ACV or GCV with recombinant B virus TK; however, the increased resistance of the TK mutants to these drugs suggests that in cell culture infections, B virus TK does activate ACV and GCV.

Our studies indicate that a new, improved group of antiviral agents, 2′-fluoroarabinofuranosyl 5-substituted pyrimidine nucleosides, should be considered for therapeutic use to combat zoonotic B virus infection. Comprehensive analyses examining the cellular toxicity and effectiveness of a number of these compounds against HSV have been reported. FEAU has been shown to be the most selective anti-HSV antiviral in this class; it was not incorporated into uninfected cell DNA (17) and was 10-fold less toxic than ACV in cell culture (19). Other laboratories have demonstrated the *in vivo* safety of FEAU; no negative effects were reported in a monkey following six intravenous doses of FEAU at 30 mg/kg (7). Further work has demonstrated the *in vivo* safety and effectiveness of FEAU against simian varicella virus in African green monkeys (26), and analysis of FEAU in both a mouse model of HSV-2 (19) and a rabbit model of HSV-1 (28) has also demonstrated safety and effectiveness. In view of the impressively low doses required to inhibit B virus replication, FEAU should be considered as a compassionate-use treatment for human cases in which there is progressive or severe morbidity.

ACKNOWLEDGMENTS

We thank David Katz and Ludmila Perelygina for helpful comments during the preparation of the manuscript.

This work was supported in part by NIH grants P40 RR05162 (J.K.H.) and 2P30-AI-50409 (R.F.S.), the Georgia Research Alliance, and the Department of Veterans Affairs.

REFERENCES

1. **Abbruzzese, J. L., S. Schmidt, M. N. Raber, J. K. Levy, A. M. Castellanos, S. S. Legha, and I. H. Krakoff.** 1989. Phase I trial of 1-(2′-deoxy-2′-fluoro-1-beta-D-arabinofuranosyl)-5-methyluracil (FMAU) terminated by severe neurologic toxicity. Invest. New Drugs **7:**195–201.
2. **Anderson, D. C., R. B. Swenson, J. L. Orkin, S. S. Kalter, and H. M. McClure.** 1994. Primary Herpesvirus simiae (B-virus) infection in infant macaques. Lab. Anim. Sci. **44:**526–530.
3. **Artenstein, A. W., C. B. Hicks, B. S. Goodwin, Jr., and J. K. Hilliard.** 1991. Human infection with B virus following a needlestick injury. Rev. Infect. Dis. **13:**288–291.
4. **Balzarini, J., and E. De Clercq.** 1990. 9-Beta-D-arabinofuranosyladenine 5′-monophosphate (araAMP) is converted directly to its antivirally active 5′-triphosphate form by 5-phosphoribosyl-1-pyrophosphate (PRPP) synthetase. Biochem. Biophys. Res. Commun. **173:**781–787.
5. **Boulter, E. A., and D. P. Grant.** 1977. Latent infection of monkeys with B virus and prophylactic studies in a rabbit model of this disease. J. Antimicrob. Chemother. **3**(Suppl. A)**:**107–113.
6. **Boulter, E. A., B. Thornton, D. J. Bauer, and A. Bye.** 1980. Successful treatment of experimental B virus (Herpesvirus simiae) infection with acyclovir. Br. Med. J. **280:**681–683.
7. **Centers for Disease Control.** 1989. B virus infections in humans—Michigan. MMWR Morb. Mortal. Wkly. Rep. **38:**453–454.
8. **Centers for Disease Control.** 1987. B-virus infection in humans—Pensacola, Florida. MMWR Morb. Mortal. Wkly. Rep. **36:**289–290, 295–296.
9. **Centers for Disease Control and Prevention.** 1998. Fatal Cercopithecine herpesvirus 1 (B virus) infection following a mucocutaneous exposure and interim recommendations for worker protection. MMWR Morb. Mortal. Wkly. Rep. **47:**1073–1076, 1083.
10. **Centers for Disease Control and Prevention.** 1995. Publication of guidelines for the prevention and treatment of B virus infections in exposed persons. MMWR Morb. Mortal. Wkly. Rep. **44:**96–97.
11. **Chou, T. C., X. B. Kong, M. P. Fanucchi, Y. C. Cheng, K. Takahashi, K. A. Watanabe, and J. J. Fox.** 1987. Synthesis and biological effects of 2′-fluoro-5-ethyl-1-beta-D-arabinofuranosyluracil. Antimicrob. Agents Chemother. **31:**1355–1358.
12. **Davenport, D. S., D. R. Johnson, G. P. Holmes, D. A. Jewett, S. C. Ross, and J. K. Hilliard.** 1994. Diagnosis and management of human B virus (Herpesvirus simiae) infections in Michigan. Clin. Infect. Dis. **19:**33–41.
13. **Fanucchi, M. P., B. Leyland-Jones, C. W. Young, J. H. Burchenal, K. A. Watanabe, and J. J. Fox.** 1985. Phase I trial of 1-(2′-deoxy-2′-fluoro-1-beta-D-arabinofuranosyl)-5-methyluracil (FMAU). Cancer Treat. Rep. **69:**55–59.
14. **Focher, F., A. Lossani, A. Verri, S. Spadari, A. Maioli, J. J. Gambino, G. E. Wright, R. Eberle, D. H. Black, P. Medveczky, M. Medveczky, and D. Shugar.** 2007. Sensitivity of monkey B virus (Cercopithecine herpesvirus 1) to antiviral drugs: role of thymidine kinase in antiviral activities of substrate analogs and acyclonucleosides. Antimicrob. Agents Chemother. **51:**2028–2034.
15. **Holmes, G. P., L. E. Chapman, J. A. Stewart, S. E. Straus, J. K. Hilliard, and D. S. Davenport.** 1995. Guidelines for the prevention and treatment of B-virus infections in exposed persons. The B Virus Working Group. Clin. Infect. Dis. **20:**421–439.
16. **Holmes, G. P., J. K. Hilliard, K. C. Klontz, A. H. Rupert, C. M. Schindler, E. Parrish, D. G. Griffin, G. S. Ward, N. D. Bernstein, T. W. Bean, et al.** 1990. B virus (Herpesvirus simiae) infection in humans: epidemiologic investigation of a cluster. Ann. Intern. Med. **112:**833–839.
17. **Kong, X. B., A. C. Scheck, R. W. Price, P. M. Vidal, M. P. Fanucchi, K. A. Watanabe, J. J. Fox, and T. C. Chou.** 1988. Incorporation and metabolism of 2′-fluoro-5-substituted arabinosyl pyrimidines and their selective inhibition of viral DNA synthesis in herpes simplex virus type 1 (HSV-1)-infected and mock-infected Vero cells. Antiviral Res. **10:**153–166.
18. **Loomis, M. R., T. O'Neill, M. Bush, and R. J. Montali.** 1981. Fatal herpesvirus infection in patas monkeys and a black and white colobus monkey. J. Am. Vet. Med. Assoc. **179:**1236–1239.
19. **Mansuri, M. M., I. Ghazzouli, M. S. Chen, H. G. Howell, P. R. Brodfuehrer, D. A. Benigni, and J. C. Martin.** 1987. 1-(2-Deoxy-2-fluoro-beta-D-arabinofuranosyl)-5-ethyluracil. A highly selective antiherpes simplex agent. J. Med. Chem. **30:**867–871.
20. **Nanda, M., V. T. Curtin, J. K. Hilliard, N. D. Bernstein, and R. D. Dix.** 1990. Ocular histopathologic findings in a case of human herpes B virus infection. Arch. Ophthalmol. **108:**713–716.
21. **Ohsawa, K., D. H. Black, R. Torii, H. Sato, and R. Eberle.** 2002. Detection of a unique genotype of monkey B virus (Cercopithecine herpesvirus 1) indigenous to native Japanese macaques (Macaca fuscata). Comp. Med. **52:**555–559.
22. **Palmer, A. E.** 1987. B virus, Herpesvirus simiae: historical perspective. J. Med. Primatol. **16:**99–130.
23. **Poffenberger, K. L., and B. Roizman.** 1985. A noninverting genome of a viable herpes simplex virus 1: presence of head-to-tail linkages in packaged genomes and requirements for circularization after infection. J. Virol. **53:**587–595.
24. **Reardon, J. E.** 1989. Herpes simplex virus type 1 and human DNA polymerase interactions with 2′-deoxyguanosine 5′-triphosphate analogues. J. Biol. Chem. **264:**19039–19044.
25. **Smith, A. L., D. H. Black, and R. Eberle.** 1998. Molecular evidence for distinct genotypes of monkey B virus (herpesvirus simiae) which are related to the macaque host species. J. Virol. **72:**9224–9232.
26. **Soike, K. F., T. C. Chou, J. J. Fox, K. A. Watanabe, and C. A. Gloff.** 1990. Inhibition of simian varicella virus infection of monkeys by 1-(2-deoxy-2-fluoro-1-beta-D-arabinofuranosyl)-5-ethyluracil (FEAU) and synergistic effects of combination with human recombinant interferon-beta. Antiviral Res. **13:**165–174.
27. **Tognon, M., E. M. Cattozzo, S. Bianchi, and M. G. Romanelli. G.** 1996. Enhancement of HSV-DNA infectivity, in Vero and RS cells, by a modified calcium-phosphate transfection technique. Virus Genes **12:**193–197.
28. **Trousdale, M. D., J. L. Law, F. A. Yarber, K. A. Watanabe, and J. J. Fox.** 1992. Evaluation of 1-(2′-deoxy-2′-fluoro-beta-D-arabinofuranosyl)-5-ethyluracil in a rabbit model of herpetic keratitis. Antiviral Res. **17:**157–167.

28a. **U.S. Department of Health and Human Services Public Health Service, Centers for Disease Control and Prevention, and National Institutes of Health.** 2007. Biosafety in microbiological and biomedical laboratories, 5th ed. Government Printing Office, Washington, DC. http://www.cdc.gov/OD/OHS/biosfty/bmbl5/BMBL_5th_Edition.pdf.

29. **Van Etta, L., J. Brown, A. Mastri, and T. Wilson.** 1981. Fatal vidarabine toxicity in a patient with normal renal function. JAMA **246:**1703–1705.
30. **Vizoso, A. D.** 1975. Recovery of herpes simiae (B virus) from both primary and latent infections in rhesus monkeys. Br. J. Exp. Pathol. **56:**485–488.

31. **Wall, L. V., H. T. Zwartouw, and D. C. Kelly.** 1989. Discrimination between twenty isolates of herpesvirus simiae (B virus) by restriction enzyme analysis of the viral genome. Virus Res. **12:**283–296.
32. **Watanabe, K. A., U. Reichman, K. Hirota, C. Lopez, and J. J. Fox.** 1979. Nucleosides. 110. Synthesis and antiherpes virus activity of some 2′-fluoro-2′-deoxyarabinofuranosylpyrimidine nucleosides. J. Med. Chem. **22:**21–24.
33. **Weigler, B. J.** 1992. Biology of B virus in macaque and human hosts: a review. Clin. Infect. Dis. **14:**555–567.
34. **Whitley, R. J., and C. A. Alford.** 1981. Antiviral agents: clinical status report. Hosp. Pract. (Off. Ed.) **16:**109–121.
35. **Wild, K., T. Bohner, G. Folkers, and G. E. Schulz.** 1997. The structures of thymidine kinase from herpes simplex virus type 1 in complex with substrates and a substrate analogue. Protein Sci. **6:**2097–2106.
36. **Wilson, R. B., M. A. Holscher, T. Chang, and J. R. Hodges.** 1990. Fatal Herpesvirus simiae (B virus) infection in a patas monkey (Erythrocebus patas). J. Vet. Diagn. Invest. **2:**242–244.
37. **Zwartouw, H. T., and E. A. Boulter.** 1984. Excretion of B virus in monkeys and evidence of genital infection. Lab. Anim. **18:**65–70.
38. **Zwartouw, H. T., C. R. Humphreys, and P. Collins.** 1989. Oral chemotherapy of fatal B virus (herpesvirus simiae) infection. Antiviral Res. **11:**275–283.

Return to Table of Contents

AUTHOR INDEX

AUTHOR INDEX

AUTHOR INDEX

AUTHOR INDEX